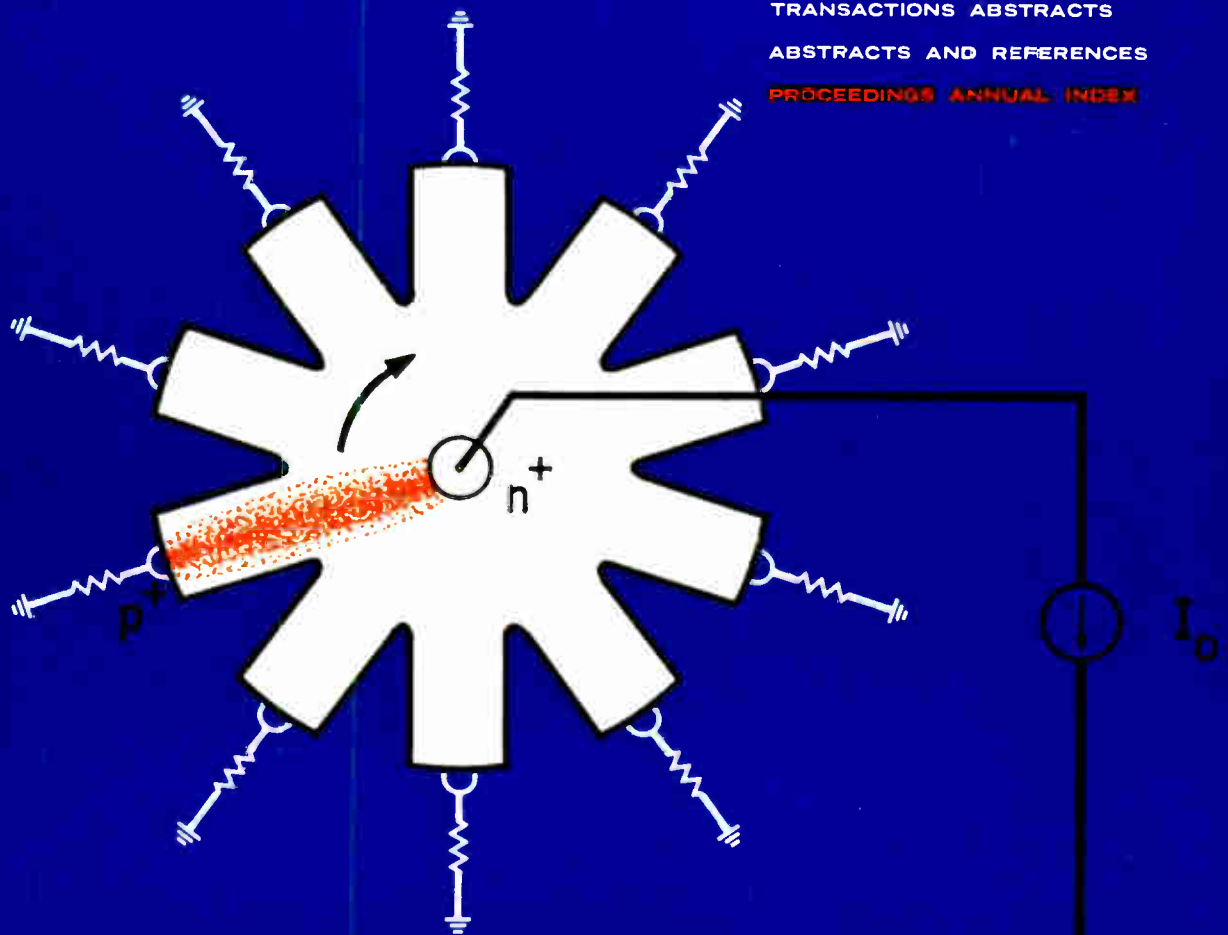


december 1962
the
institute
of
radio
engineers

Proceedings of the IRE

in this issue

DOUBLE INJECTION DIODES
SEMICONDUCTOR PLASMA DEVICE
BROAD-BAND FM DEMODULATOR
SOLID-STATE DISPLAY DEVICE
THIN-FILM CRYOTRON CIRCUITS
LONG-DISTANCE TROPOSPHERIC CIRCUITS
TRANSACTIONS ABSTRACTS
ABSTRACTS AND REFERENCES
PROCEEDINGS ANNUAL INDEX



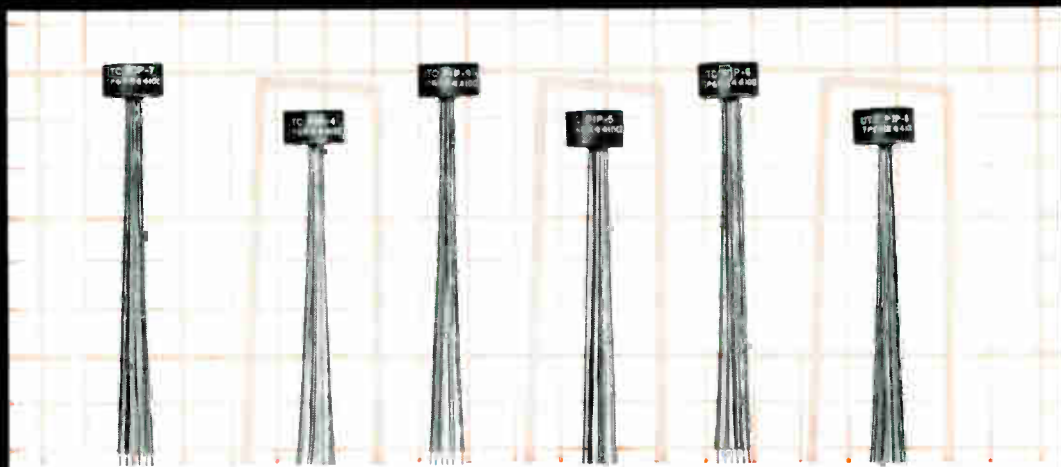
PLASMAS IN SEMICONDUCTORS: Page 2428





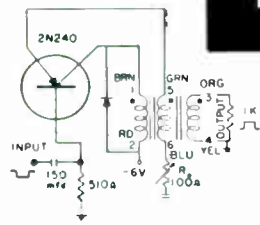
NEW PIP SERIES

ULTRAMINIATURE TRANSISTOR PULSE TRANSFORMERS



UNITS SHOWN ACTUAL SIZE—IMMEDIATE DELIVERY FROM STOCK

TRANSISTOR TEST CIRCUIT



All units individually checked and adjusted, in transistor circuit illustrated, to parameters in table.

DEFINITIONS

Amplitude: Intersection of leading pulse edge with smooth curve approximating top of pulse.
Pulse width: Microseconds between 50% amplitude points on leading and trailing pulse edges.
Rise Time: Microseconds required to increase from 10% to 90% amplitude.
Overshoot: Percentage by which first excursion of pulse exceeds 100% amplitude.
Droop: Percentage reduction from 100% amplitude at specified time after 100% amplitude point.
Backswing: Negative swing after trailing edge as percentage of 100% amplitude.

- RUGGED—COMPLETELY METAL CASED
- Manufactured & Guaranteed to MIL-T-21038B
- 5/16" Dia. x 3/16" Ht.; Wt. 1/20 oz.
- Ratios—4:4:1 and 5:3:1
- Anchored leads, withstands 10 lb. pull test
- Printed circuit use, plastic insulated leads
- Can be suspended by leads or clip mounted

Type No.	APPROX. DCR, OHMS			BLOCKING OSCILLATOR PULSE					COUPLING CIRCUIT CHARACTERISTICS						
	1-Brn 2-Rd	3-Org 4-Yel	5-Grn 6-Blu	Width μ Sec.	Rise Time	% Over Shoot	Droop %	% Back Swing	P Width μ Sec.	Volt Out	Rise Time	% Over Shoot	Droop %	Back Swing	Imp. in/out*
RATIO 4:4:1 MIL TYPE TP6RX4410CZ															
PIP-1	.18	.20	.07	.05	.02	0	0	37	.05	9	.018	0	0	12	50
PIP-2	.47	.56	.17	.1	.025	0	0	25	.1	8	.02	0	0	5	50
PIP-3	1.01	1.25	.37	.2	.03	2	0	15	.2	7	.035	0	0	5	100
PIP-4	1.5	1.85	.54	.5	.05	0	0	15	.5	7	.06	0	0	0	100
PIP-5	2.45	3.1	.9	1	.08	0	0	14	1	6.8	.15	0	0	5	100
PIP-6	3.0	3.7	1.1	2	.10	0	0	15	2	6.6	.18	0	2	10	100
PIP-7	4.9	6.05	1.8	3	.20	0	0	14	3	6.8	.20	0	2	10	100
PIP-8	8.0	9.7	2.9	5	.30	0	0	3	5	7.9	.22	0	13	25	200
PIP-9	13.1	15.9	4.7	10	.35	0	5	12	10	6.5	.4	0	15	20	200
PIP-100	Transistor pulse transformer kit, consisting of PIP-1 thru PIP-9 in plastic case.														
RATIO 5:3:1 MIL TYPE TP6RX5310CZ															
PIP-10	.55	.41	.15	.1	.01	0	0	20	.1	8	.01	0	0	5	140/50
PIP-11	2.9	2.2	.82	1	.02	4	4	6	1	6.6	.05	0	6	12	280/100
PIP-12	9.4	7.1	2.6	5	.05	0	12	12	5	8	.09	2	12	25	560/200

* Input winding leads Brn-Rd (1-2); output winding leads Org-Yel (3-4); leads Grn-Blu (5-6) open.

AND CUSTOM BUILT UNITS TO YOUR SPECS.

Write for catalog for full details on these and 1000 other stock items



UNITED TRANSFORMER CORP.

150 VARICK STREET, NEW YORK 13, N.Y.

PACIFIC MFG. DIVISION, 3630 EASTHAM DRIVE, CULVER CITY, CALIF.
 EXPORT DIVISION, 13 EAST 40th STREET, NEW YORK 18, N.Y. CABLES: "ARLAR"

December, 1962

published monthly by The Institute of Radio Engineers, Inc.

Proceedings of the IRE®

contents

	Poles and Zeros	2417	
	George W. Bailey, Executive Secretary	2418	
	Scanning the Issue	2419	
	Message from the President, Patrick E. Haggerty	2420	
PAPERS	Double Injection Diodes and Related DI Phenomena in Semiconductors, <i>Nick Holonyak, Jr.</i> ..	2421	
	The Madistor—A Magnetically Controlled Semiconductor Plasma Device, <i>I. Melngailis and R. H. Rediker</i>	2428	
	Design and Performance of a Broad-Band FM Demodulator with Frequency Compression, <i>C. L. Ruthroff and W. F. Bodtmann</i>	2436	
	A Solid-State Display Device, <i>Stephen Vando</i>	2445	
	Correction to "Higher-Order Temperature Coefficients of the Elastic Stiffnesses and Compliances of Alpha-Quartz," <i>R. Bechmann, A. D. Ballato, and T. J. Lukaszek</i>	2451	
	Switching Speed and Dissipation in Fast, Thin-Film Cryotron Circuits, <i>Norman H. Myers</i>	2452	
	Properties of 400 Mcps Long-Distance Tropospheric Circuits, <i>J. H. Chisholm, W. E. Morrow, Jr., B. E. Nichols, J. F. Roche, and A. E. Teachman</i>	2464	
	CORRESPONDENCE	The Use of a Paraboloidal Reflector of Small Focal Ratio as a Low-Noise Antenna System, <i>I. J. K. Pauliny-Toth, I. R. Shakeshaft, and R. Wielebinski</i>	2483
		Effect of Mirror Alignment in Laser Operation, <i>J. F. Ready and D. L. Hardwick</i>	2483
		Electro-Optic Properties of Zinc Selenide, <i>Richard W. McQuaid</i>	2484
	On Power Dissipation in Semiconductor Computing Elements, <i>Robert W. Keyes</i>	2485	
	A Method of Switching Persistent Currents in Superconducting Coils, <i>M. D. Bonfeld</i>	2485	
	Varactor Frequency Doubler from 11.5 Gc to 23 Gc, <i>M. Uenohara, R. L. Rulison, and C. H. Bricker</i> ..	2486	
	An Electronically Variable Delay Line, <i>J. W. Kluser</i>	2487	
	Tunnel Diode Audio-Frequency Noise, <i>M. D. Burkhard and E. F. Sidor</i>	2487	
	Focused Side Pumping of Laser Crystal, <i>K. Tomiyasu</i>	2488	
	Efficiency of a Multiple Ellipses Confocal Laser Pumping Configuration, <i>D. L. Fried and P. Eltgroth</i> ..	2489	
	A 35.5 kMc Parametric Amplifier, <i>George W. Fitzsimmons</i>	2490	
	Two Results in the Preliminary Design of Optimum Linear Systems, <i>S. H. Durrani</i>	2490	
	Low-Frequency Circuit Relations as Developed from Field Theory, <i>Anthony J. Ferraro</i>	2491	
	Single-Sideband Modulation and Reception of Light at VHF, <i>C. F. Buhner and L. R. Bloom</i>	2492	
	Breakdown Voltage of GaAs Diodes Having Nearly Abrupt Junctions, <i>H. Kressel, A. Blicher, and L. H. Gibbons, Jr.</i>	2493	
	The O-Type Backward-Wave Oscillator Frequency Pushing, <i>Ichiro Sakuraba</i>	2493	
	Determination of Depletion Layer Thickness at Indium-Germanium Contacts with No Applied Voltage, <i>D. P. Sanders and E. S. Schlegel</i>	2494	
	WWV and WWVH Standard Frequency and Time Transmissions, <i>National Bureau of Standards</i> ..	2494	
	Prediction of Rise Time in Junction Transistors, <i>P. E. Kolk</i>	2495	
	Simplified Calculation of Unabsorbed Field Intensity on Overseas Transmission Circuits, <i>Hans J. Albrecht</i>	2495	
	Parameters of a Piezoelectric Crystal, <i>R. Bechmann and A. D. Ballato</i>	2496	
	A General Expression for the Output of a Dicke-Type Radiometer, <i>John Knight</i>	2497	
	An Expansion for Log-Periodic Functions, <i>W. J. Welch</i>	2498	
	Autocorrelation by Magnitude of the Difference, <i>T. A. Martin</i>	2499	
	Synchronous Wave Amplification in the Quadrupole Pump, <i>K. Kakizaki</i>	2500	
	Resonant Frequency Shift Phenomenon in Parametric Amplifiers and Harmonic Generators that Use Current Driven Nonlinear Capacitors, <i>G. C. Lowe</i>	2501	
	Measurement of Effective Susceptibility of Magnetic Inks, <i>H. J. Kump</i>	2502	
	Minimum-Power FM Reception Using Frequency Feedback, <i>Robert E. Heitzman</i>	2503	
	A Method of Measurement and Display of Probability Functions of Ergodic Random Processes by Orthogonal Series Synthesis, <i>A. A. Wolf and J. H. Dietz</i>	2503	
	Reflection Cavity Maser with Large Gain Bandwidth, <i>A. H. Nagy and G. E. Friedman</i>	2504	
	The Sifting Property of a Common Function, <i>Harry Urkowitz</i>	2505	
	A Low-Impedance Maxwell Bridge for Measuring Toroidal Magnetic Materials from 1 ke to 100 ke, <i>A. L. Rasmussen and R. C. Powell</i>	2505	
	Spurious Responses in Microwave Garnet Devices, <i>R. Blau, E. Sullivan, and M. Skrill</i>	2506	
	A Note on the Radiation Resistance and Field Strength of a Large Loop Antenna, <i>E. J. Martin, Jr.</i> ..	2507	
	Optimum Cross-Correlation Radar System, <i>Robert H. MacPhie</i>	2508	
	An Interesting Black Box Problem Solved by a Noise Measurement, <i>R. B. Goldner</i>	2509	
	Electron Ray Tracing, <i>R. H. Lee</i>	2509	
	Interesting Behavior of VA-99 as a Millimeter-Wave Amplifier, <i>K. Ishii, D. E. Schumacher, and K. R. Kelly</i>	2510	

COVER

The growing importance of plasma effects in semiconductors is typified by the magnetically rotated plasma switching device described in the article on page 2428.

continued

	A New Method to Find the Roots of a Fourth-Order Equation, <i>Kurt H. Haase</i>	2510
	Systematic Matrix Inversion by Signal-Flow Graph, <i>Jean-Paul Jacob</i>	2511
	A DC-Pumped Amplifier Using Space-Periodic Magnetic Field, <i>T. Wessel-Berg and K. Blötekjær</i>	2513
	A New Precision Low-Level Bolometer Bridge, <i>Q. V. Davis</i>	2514
	An Unexpected Effect in an Experimental Transverse Wave Tube, <i>K. Blötekjær, B. Målsnes, and A. Nordbotten</i>	2514
	Microwave Measurement of Conductivity and Dielectric Constant of Semiconductors, <i>B. R. Nag and S. K. Roy</i>	2515
	Reciprocal Ferrite Phase-Shifter Measurements, <i>Max J. Schindler</i>	2516
	Hilbert Transforms and Positive-Real Functions, <i>R. W. Newcomb</i>	2516
	Selectivity and Sensitivity in Functional Blocks, <i>W. E. Newell</i>	2517
	The Majority Decision Element as a Null Detector, <i>Robert C. Sommer</i>	2518
	Some Combinations of Noise Signals, <i>Kenneth Abend</i>	2518
	Bounds on the 3-Positions Experimental Integral, <i>Kenneth Abend</i>	2519
	On the Two-Generator Method (e_n, i_n) of Noise Characterization, <i>Harry F. Cooke</i>	2520
	3-Display System, <i>A. A. Goldberg</i>	2521
	"Egg Crate" Reflector Surface for Large Paraboloids, <i>E. O. Willoughby</i>	2521
	Origin of the Word "Radio," <i>E. F. Goodenough</i>	2522
	Function Generator for $Y = AX^3 + BX^2 + CX + D$, Employing the Galvanomagnetic Effects in Semiconductors, <i>S. Kataoka and H. Yamada</i>	2522
	Frequency Dependence of the Equivalent Series Resistance of Varactor Diodes and its Effect on Parametric Amplification, <i>L. D. Braun</i>	2523
	A Stability Chart for Linear Discrete Systems, <i>E. I. Jury</i>	2524
REVIEWS	Books:	
	"Introduction to Radar Systems," by Merrill I. Skolnik, <i>Reviewed by I. L. McNally</i>	2527
	"Control System Theory: Feedback Engineering," by G. Lago and L. M. Benningfield, <i>Reviewed by A. M. Hopkin</i>	2527
	"Microminiaturization: Proceedings of the AGARD Conference," G. W. A. Dummer, Ed., <i>Reviewed by Robert A. Gerhold</i>	2527
	"The Age of Electronics," Carl F. J. Overhage, Ed., <i>Reviewed by Robert M. Bowie</i>	2528
	"Linear Vacuum-Tube and Transistor Circuits," by A. J. Cote, Jr., and J. B. Oaks, <i>Reviewed by Ian O. Ebert</i>	2528
	"The Dynamics of Automatic Control Systems," by E. P. Popov, <i>Reviewed by George S. Axelby</i>	2529
	"Physical Electronics," by C. L. Hemenway, R. W. Henry, and C. Caulton, <i>Reviewed by C. W. Carnahan</i>	2530
	Recent Books.....	2530
	Scanning the TRANSACTIONS.....	2531
ABSTRACTS	Abstracts of IRE TRANSACTIONS.....	2532
	Announcement: Abstracts and References to be Discontinued.....	2538
	Abstracts and References.....	2539
	Translations of Russian Technical Literature.....	2552
INDEX	1962 PROCEEDINGS OF THE IRE INDEX.....	Follows page 2552
IRE INTERNATIONAL NEWS	Current IRE Statistics.....	14A
	Calendar of Coming Events and Authors' Deadlines.....	14A
	Current IRE Standards Available.....	15A
	Professional Group News.....	24A
	Programs:	
	Millimeter and Submillimeter Conference.....	24A
	9th National Symposium on Reliability and Quality Control.....	28A
DEPARTMENTS	Contributors.....	2525
	IRE People.....	36A
	Industrial Engineering Notes.....	32A
	Meetings with Exhibits.....	8A
	Membership.....	44A
	News—New Products.....	42A
	Positions Open.....	76A
	Positions Wanted by Armed Forces Veterans.....	85A
	Professional Group Meetings.....	57A
	Section Meetings.....	50A
	Advertising Index.....	127A

BOARD OF DIRECTORS, 1962
 *P. E. Haggerty, *President*
 A. M. Angot, *Vice President*
 *T. A. Hunter, *Vice President*
 *Ernst Weber, *Vice President*
 *S. L. Bailey, *Treasurer*
 *Haraden Pratt, *Secretary*
 *T. F. Jones, Jr., *Editor*
 *R. L. McFarlan, *Senior Past President*
 *L. V. Berkner, *Junior Past President*

1962
 A. B. Bereskin (R4)
 M. W. Bullock (R6)
 A. B. Giordano (R2)
 A. N. Goldsmith
 *D. E. Noble

W. G. Shepherd
 G. Sinclair
 B. R. Tupper (R8)

1962-1963
 M. R. Briggs (R3)
 W. B. Bruene (R5)
 E. F. Carter
 D. K. Reynolds (R7)
 L. C. Van Atta
 F. K. Willenbrock (R1)

1962-1964
 G. K. Teal
 G. A. Wootton

*Executive Committee Members

EXECUTIVE SECRETARY
 George W. Bailey
 John B. Buckley, *Chief Accountant*
 Laurence G. Cumming, *Field Secretary*
 Richard M. Ember-on, *Professional Groups Secretary*
 Joan Kearney, *Assistant to the Executive Secretary*
 Emily Sirjane, *Office Manager*

ADVERTISING DEPARTMENT
 William C. Copp, *Advertising Manager*
 Lillian Petranek, *Assistant Advertising Manager*

EDITORIAL DEPARTMENT
 Alfred N. Goldsmith, *Editor Emeritus*
 Thomas F. Jones, Jr., *Editor*
 E. K. Gannett, *Managing Editor*
 Helene Frischauf, *Associate Editor*
 W. Reed Croone, *Student Affairs Sec'y*

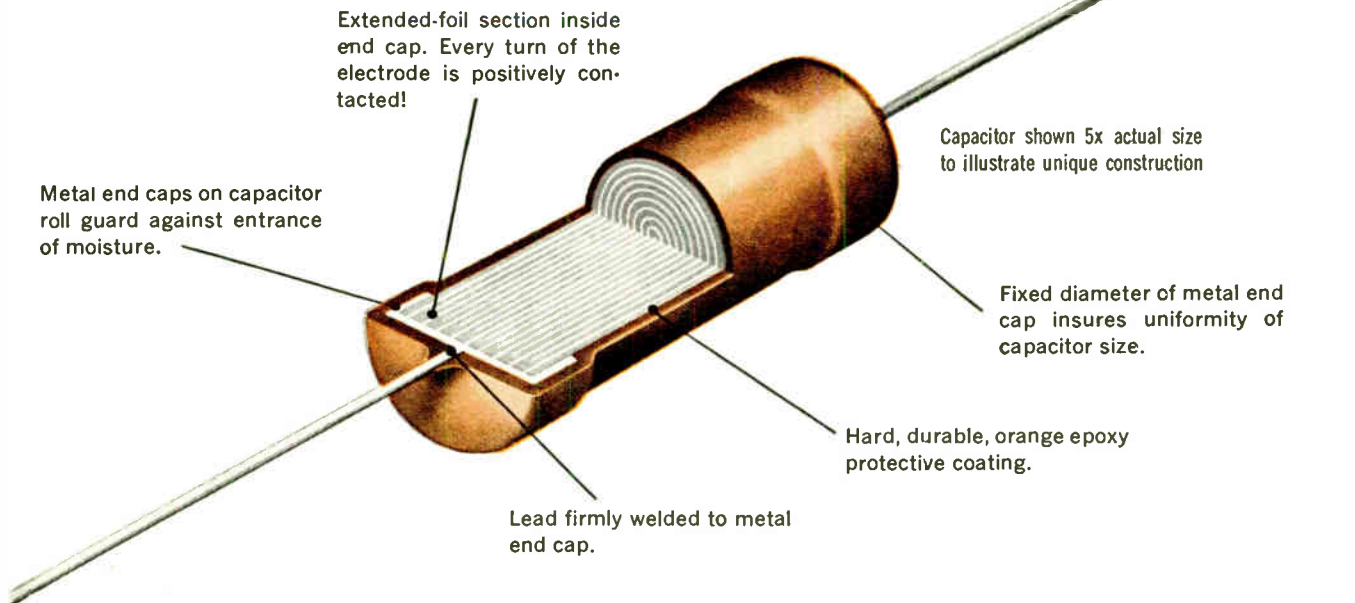
EDITORIAL BOARD
 T. F. Jones, Jr., *Chairman*
 A. H. Waynick, *Vice Chairman*
 E. K. Gannett
 D. W. Martin
 J. D. Ryder
 D. B. Sinclair
 Kiyoo Tomiyasu
 J. G. Truxal



PROCEEDINGS OF THE IRE, published monthly by The Institute of Radio Engineers, Inc., at 1 East 79 Street, New York 21, N. Y. Cable Address: IRADENGS
 Manuscripts should be submitted in triplicate to the Editorial Department. Correspondence column items should not exceed four double-spaced pages (illustrations count as one-half page each). Responsibility for contents of papers published rests upon the authors, and not the IRE or its members. All republication rights, including translations, are reserved by the IRE and granted only on request. Abstracting is permitted with mention of source.
 Thirty days notice is required for change of address. Price per copy: members of The Institute of Radio Engineers, one additional copy, \$1.25; non-members, \$2.25. Yearly subscription price: members \$9.00, one additional subscription \$13.50; public libraries and colleges \$13.50; non-members in United States, Canada, and U. S. Possessions \$18.00; abroad \$19.00. Second-class postage paid at Menasha, Wisconsin, under the act of March 3, 1879. Acceptance for mailing at a special rate of postage is provided for in the act of February 28, 1925, embodied in Paragraph 4, Section 412, P. L. and R., authorized October 26, 1927. Printed in U.S.A. Copyright © 1962 by The Institute of Radio Engineers, Inc.

New from Sprague!

PACER® FILMITE® 'E' CAPACITORS



Multi-advantage Construction in a Low-cost Film Capacitor!

MINIFIED SIZE—

Rating for rating, Pacer Capacitors are almost one-third the size of conventional paper or paper-film tubulars, making them ideally suited for transistorized circuitry and other space-saving applications where small size with dependability is an important consideration.

BEST POSSIBLE NON-INDUCTIVE SECTION—

Metal end caps over extended foil sections assure non-inductive capacitors, since all turns of the electrode are contacted beyond question.

IMPROVED HUMIDITY RESISTANCE—

End caps act as effective moisture barriers. Capacitor sections are further protected by hard, durable, orange epoxy coating.

UNIFORMITY OF SIZE—

Unlike other epoxy-coated units, the end caps on Pacer Capacitors assure the rigid fixed diameters needed for use with automatic insertion equipment. The two smallest sizes are identical with resistor and diode sizes, making them especially suitable for 'cordwood' packaging.

For complete technical data on Pacer Capacitors, write for Engineering Bulletins 2066 and 2067 to Technical Literature Service, Sprague Electric Co., 235 Marshall Street, North Adams, Massachusetts.

SPRAGUE COMPONENTS

CAPACITORS

TRANSISTORS

MAGNETIC COMPONENTS

RESISTORS

MICRO-CIRCUITS

INTERFERENCE FILTERS

PULSE TRANSFORMERS

PIEZOELECTRIC CERAMICS

PULSE-FORMING NETWORKS

TOROIDAL INDUCTORS

HIGH TEMPERATURE MAGNET WIRE

CERAMIC-BASE PRINTED NETWORKS

PACKAGED COMPONENT ASSEMBLIES

FUNCTIONAL DIGITAL CIRCUITS

ELECTRIC WAVE FILTERS



'Sprague' and '®' are registered trademarks of the Sprague Electric Co.

Jesse Taub, Joseph Tardi, and Harvey Hindin of our Applied Electronics Department describe the results of a theoretical and experimental study of band-pass filters having minimum mid-band insertion loss. Standing-wave ratios and time delay variations are also improved using these designs. The interesting results should suggest many other applications to the reader.

How to Reduce Filter Insertion Loss

The design and performance of band-pass filters that have a lower insertion loss than the maximally flat or Tchebycheff designs for a given 3-db bandwidth and skirt selectivity are described. This low insertion loss is particularly important when the 3-db bandwidth is narrow (2 percent or less). Other useful properties such as low SWR and flat time delay are also described.

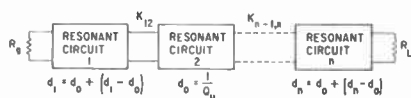


FIGURE 1. COUPLED-CIRCUIT REPRESENTATION OF BAND-PASS FILTER

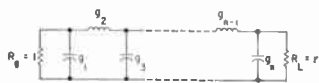


FIGURE 2. LOW-PASS PROTOTYPE FILTER

Most band-pass filters can be represented by a set of coupled resonant circuits (Figure 1) that can be converted to a low-pass prototype filter¹ (Figure 2) having element values (g_i). Cohn² has shown that, if all (g_i) values chosen for a given skirt-selectivity requirement are equal, the filter will have the minimum possible mid-band insertion loss for the unloaded resonator Q 's (Q_{ii}) that are used. A design procedure for equal-element filters has been developed at AIL³ that gives the coupling coefficient (K) and decrement (d) values (in terms of g_i) that are necessary to achieve a given selectivity. This procedure is valid for both lossy and lossless resonant circuits. The design theory and data for filters having from two to eight coupled resonators are given. This design has been used at AIL to markedly reduce the mid-band insertion loss of filters previously designed for a maximally flat and Tchebycheff amplitude versus frequency response. Other characteristics such as input SWR and time-delay distortion also have been improved.

Figure 3 shows one such filter, which has four coupled resonant circuits. Each resonator was formed from quarter-wave sections of helical coaxial transmission line¹ and had unloaded Q 's in the vicinity of 400. The filter was designed for a center frequency of 60 Mc, a 3-db bandwidth of 710 kc, and a 60-db skirt bandwidth of 4 Mc.

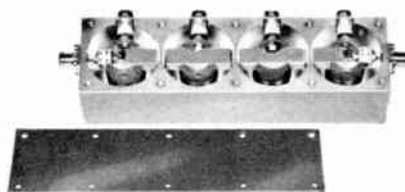


FIGURE 3.

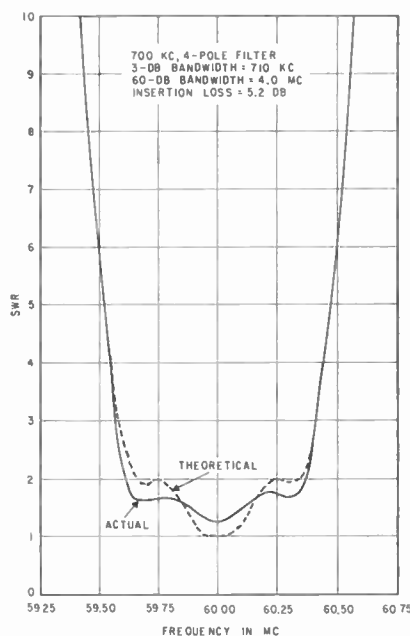


FIGURE 4. SWR OF FOUR-RESONATOR EQUAL-ELEMENT FILTER

The measured amplitude versus frequency response of this filter was in close agreement with the theoretical equal element response.⁴ The mid-band insertion loss was 5.2 db. The same filter designed on a maximally flat basis would have yielded a mid-band loss of 7 db (this estimate of loss was made with the aid of reference 5).

Figure 4 shows an input SWR at mid-band of less than 1.20; the SWR is under 2 over a good portion of the filter pass band. This result is in agreement with the theoretical curve (Figure 4). The measured mid-band SWR's of

comparable maximally flat filters are usually over 1.5. Therefore, we believe that the equal-element design also may prove useful where low SWR pass bands are important. The need for low SWR's occurs: (1) when filters are used in conjunction with transistor IF amplifiers and (2) to reduce "pulling" effects when used directly at the outputs of microwave oscillators.

The time delay versus frequency of equal-element filters has been analyzed for from two to eight resonators; for example, the delay for a four-resonator filter was found to be flat within ± 10 percent over 80 percent of the pass band. This flatness is useful when the filter must faithfully pass pulse modulation.

The theoretical and experimental results clearly indicate that equal-element filter designs can improve insertion loss, SWR, and time delay characteristics in many applications when compared to the more conventionally used maximally flat and Tchebycheff responses.

If more information is desired on this subject, the authors will be glad to supply it.

A complete bound set of our sixth series of articles is available on request. Write to Harold Hechtman at AIL for your set.

REFERENCES

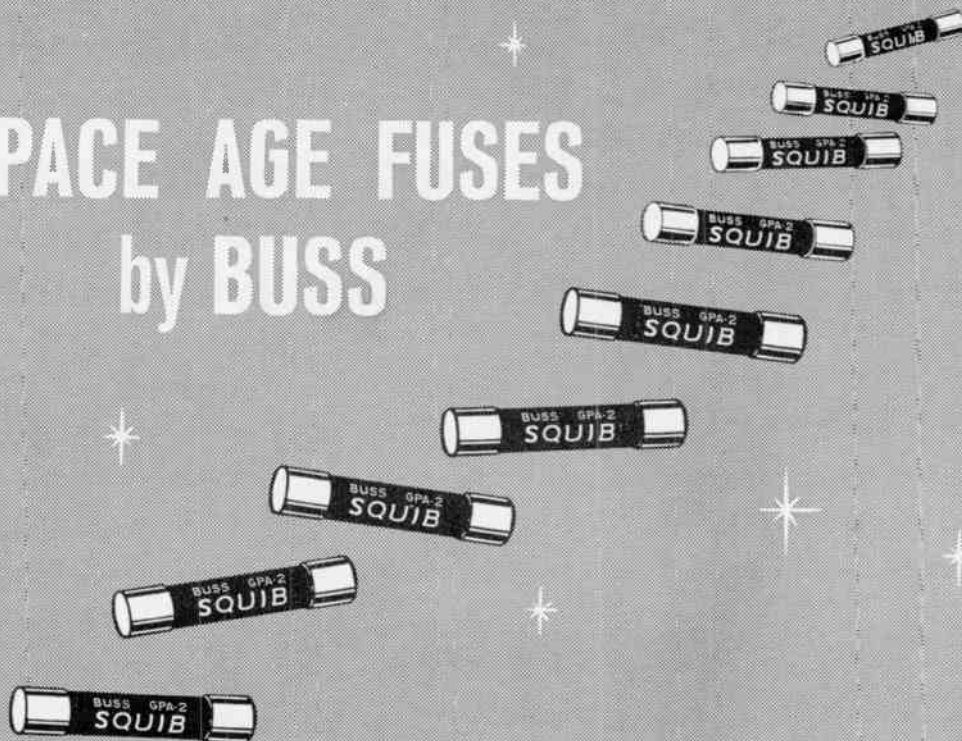
1. S. B. Cohn, "Direct-Coupled-Resonator Filters," Proc. IRE, Vol. 45, p. 187-196, February 1957.
2. S. B. Cohn, "Dissipation Loss in Multiple-Coupled-Resonator Filters," Proc. IRE, Vol. 47, p. 1312-1348, August 1959.
3. J. J. Taub, "Design of Minimum Loss Band-Pass Filters," Memorandum 38, Airborne Instruments Laboratory, May 1962.
4. W. W. McAlpine and R. O. Schildknecht, "Coaxial Resonators with Helical Inner Conductor," Proc. IRE, Vol. 47, p. 2099-2104, December 1959.
5. E. G. Fubini and E. A. Guillemin, "Minimum Insertion Loss Filters," Proc. IRE, Vol. 47, p. 37-41, January 1959.



AIL/
DIVISION

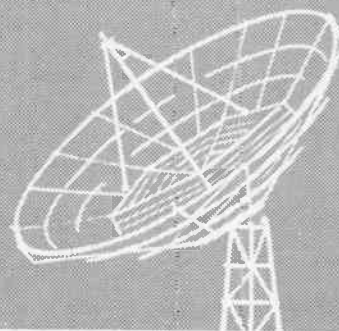



SPACE AGE FUSES by BUSS



Especially designed for
Squib Circuitry

*Another outstanding
development by the
makers of BUSS fuses.*



 The space-age speeded the need for Squib circuitry—and to meet the need for protection and control of such circuits, BUSS engineers worked closely with the engineers who design and produce Squib circuits.

The result is a line of BUSS Squib fuses that have the needed electrical characteristics and are almost unbelievably accurate and dependable.

If you, too, should have a special problem in electrical protection . . . you can save engineering hours by turning to BUSS where the facilities of the world's largest fuse research laboratory and its staff of engineers are always at your service.

And don't overlook the complete line of BUSS fuses for your day in and day out protection needs . . . whatever your electrical protection needs—turn first to BUSS—it pays.

BUSS

BUSSMANN MFG. DIVISION

MAKERS OF THE COMPLETE LINE OF
FUSES OF UNQUESTIONED HIGH QUALITY

McGraw-Edison Co. • St. Louis 7, Mo.

News from Bell Telephone Laboratories

WE'RE "FINGERPRINTING" VOICES...TO FIND BETTER WAYS OF TRANSMITTING THEM

Acoustics scientists at Bell Telephone Laboratories study voices to learn how one voice differs from all others, what makes yours instantly recognizable to friends and family, and what the elements of a voice are that give it the elusive qualities of "naturalness."

To enable us to examine speech closely, we devised a method of making spectrograms of spoken words. We call them voiceprints. They are actual pictures of sound, revealing the patterns of voice energy. Each pattern is distinctive and identifiable. They are so distinctive that voiceprints may have a place, along with fingerprint and handwriting identification, as an important tool of law enforcement.

The shape and size of a person's mouth, throat and nasal cavities cause his voice energy to be concentrated into bands of frequencies. The pattern of these bands remains essentially the same despite modifications which may result from loss of teeth or tonsils, the advancement of age, or attempts to disguise the voice.

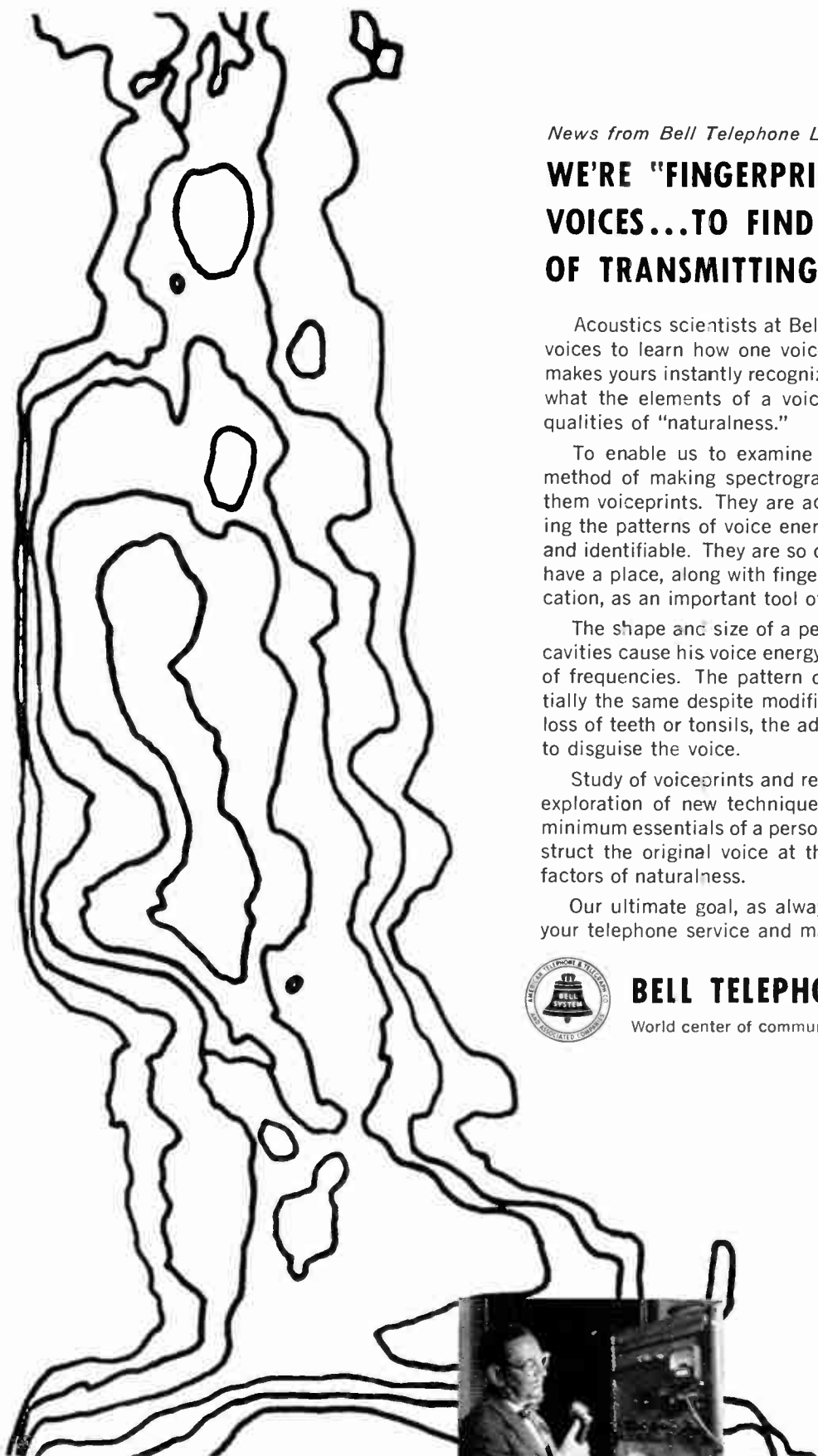
Study of voiceprints and recognition factors is part of our exploration of new techniques to extract and transmit the minimum essentials of a person's voice and from these reconstruct the original voice at the receiving end, retaining its factors of naturalness.

Our ultimate goal, as always, is to learn how to improve your telephone service and make it a better value.



BELL TELEPHONE LABORATORIES

World center of communications research and development



Word Picture. This is a picture of the spoken word "you." By analyzing the sound with a Spectrograph, the Laboratories' Lawrence G. Kersta makes a print of the word in graph form. Graph shows frequency, time taken, and intensity used in making speech sound.





Pathfinder II's printer
imprints give operators
accurate real time prop-
agation information. (Printer
is in right foreground)

PATHSOUNDER II: COMPLETE MILITARY FREQUENCY MANAGEMENT

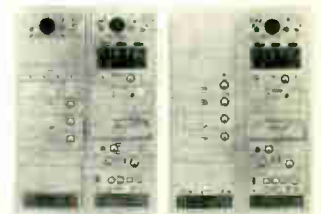
PATHSOUNDER II, the outgrowth of G/A's ionosphere sounder system now in world-wide use, provides the communicator with accurate propagation information for frequency management. Example: Complete propagation information can be obtained for all possible paths of a 10 station network in less than three minutes.

Specifically designed for *military* use, PATHSOUNDER II provides:

- Mil components, construction and packaging.
- Freedom from interference and overloading with an electronically tuned preselector and a new phase-corrected IF filter.
- Maximum reliability with an integrated solid state power supply and a new solid state control unit.
- An electrostatic printer which automatically delivers permanent ionograms of high quality (5 shades of gray scale) in fifteen seconds.

Your request for technical details on this equipment is welcome.

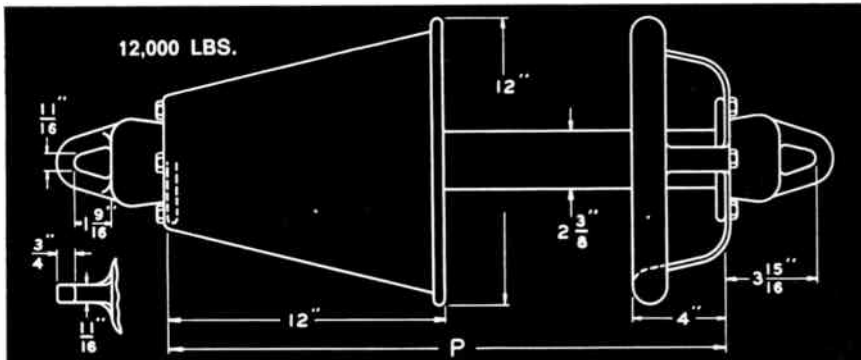
974 COMMERCIAL STREET, PALO ALTO, CALIF. / DAVENPORT 1-4175 (AREA CODE 415)



We have opportunities for
qualified antenna and com-
munications engineers. An
equal opportunity employer.

LAPP HEAVY-DUTY ANTENNA INSULATORS

...in all these standard sizes to save you time and money

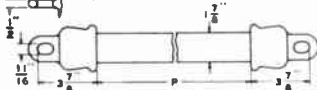


No. 9171, without ring or shield, for most high-strength applications. Standard "P" dimensions: 12, 16, 20, 24, 30 inches.

No. 9172, with two grading rings to raise voltage at which corona starts, and to distribute voltage to reduce heating of porcelain. Standard "P" dimensions: 20, 24, 30 inches.

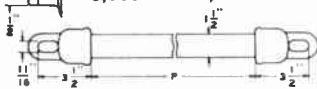
No. 9173, with corona ring and rain shield, preferred for vertical installations. Standard "P" dimensions: 24 and 30 inches.

9,000 and 10,500 LBS.



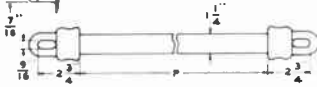
No. 43812 in porcelain (rated at 9,000 lb. average ultimate strength) or No. 43813 in steatite (10,500 lbs.), in standard "P" dimensions of 12, 14, 16, 20 inches.

6,000 and 7,000 LBS.



No. 43810 in porcelain (rated at 6,000 lb. average ultimate strength) or No. 43811 in steatite (7,000 lbs.), in standard "P" dimensions of 10, 12, 14, 16 inches.

4,000 and 5,000 LBS.



No. 43808 in porcelain (rated at 4,000 lb. average ultimate strength) or No. 43809 in steatite (5,000 lbs.), in standard "P" dimensions of 8, 10, 12, 14 inches.

FLASHOVER AND RADIO RATINGS

WET FLASHOVER 60 ~ KV eff.				RADIO RATING KV eff.		
"P" Inches	All except No. 9172 No. 9173	No. 9172	No. 9173	All except No. 9172 No. 9173	No. 9172	No. 9173
8	45			21		
10	54			22		
12	62			23		
14	70			24		
16	77			24		
20	88	88		25	34	
24	96	96	60	27	37	34
30	108	108	108	28	40	38

Steatite Insulators will have the same Flashover but twice the Radio Rating.

Lapp

WRITE for Bulletin 301-R.
Lapp Insulator Co., Inc.,
238 Sumner Street, LeRoy, N. Y.



**Meetings
with Exhibits**

As a service both to Members and the industry, we will endeavor to record in this column each month those meetings of IRE, its sections and professional groups, which include exhibits.

Δ

January 30-February 1, 1963

Fourth Winter Convention on Military Electronics, Ambassador Hotel, Los Angeles, Calif.

Exhibits: Mr. Philip Diamond, Philip Diamond Enterprises, 14921 Ventura Blvd., Sherman Oaks, Calif.

February 8-15, 1963

Third International Symposium on Quantum Electronics, UNESCO Bldg. & Parc d'Exposition, Paris, France

Exhibits: M. Foucoult, Federation Nationale des Industries Electroniques, 23 rue de Lubeck, Paris 16, France

March 25-28, 1963

International Radio & Electronics Show and IRE International Convention, New York Coliseum and Waldorf-Astoria Hotel, New York, N.Y.

Exhibits: Mr. William C. Copp, IRE Advertising Dept., 72 West 45th St., New York 36, N.Y.

April 17-19, 1963

SWIRECO (Southwestern IRE Conference & Electronic Show), Dallas Memorial Auditorium, Dallas, Texas

Exhibits: Mr. Hal Copeland, 810 Wilson Bldg., Dallas 1, Texas

May 13-15, 1963

NAECON (National Aerospace Electronics Conference), Biltmore Hotel, Dayton, Ohio

Exhibits: IRE Dayton Office, 1414 E. Third St., Dayton, Ohio

May 20-22, 1963

National Telemetering Conference, Albuquerque, N.M.

Exhibits: Mr. F. G. McGavock, F. G. McGavock Associates, 3820 E. Colorado Blvd., Pasadena, Calif.

May 21-23, 1963

Spring Joint Computer Conference, Cobo Hall, Detroit, Mich.

Exhibits: Mr. A. D. Meacham, American Data Processing, Inc., Detroit, Mich.

May 27-28, 1963

Seventh National Conference on Product Engineering & Production, Boston, Mass.

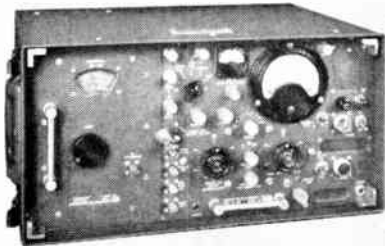
Exhibits: Mr. C. W. Watt, Raytheon Co., Lexington, Mass.

(Continued on page 10-A)

THE ONLY SIMPLE FORMULA FOR

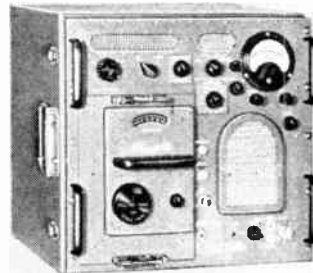


INTERFERENCE MEASUREMENTS



LOW FREQUENCY • Model NF-105

14 KC-1000 MC



HIGH FREQUENCY • Model NF-112

1000 -15,000 MC

**ENTIRE
FREQUENCY
RANGE**

14 KC-15 KMC

Through years of hard field use Model NF-105 has acquired an outstanding reputation as a noise and field intensity meter for the frequency range from 150 kilocycles to 1000 megacycles. The versatility of this instrument has now been expanded through the introduction of a new tuning unit extending its coverage down to 14 kilocycles. What is more, this unique measuring equipment has been joined by Model NF-112 which covers the frequency range from 1000 to 15,000 megacycles. The same simplicity, accuracy and speed of operation and reliability of performance which made Model NF-105 so successful have been designed into Model NF-112. Each instrument uses an impulse generator as its calibrator; each combines in one basic unit the components common to all frequency ranges, including the power supply, calibrator, attenuators and metering circuits. All frequency determining components and circuits are contained in plug-in tuning units. Model NF-112, incidentally, uses one single antenna for the entire range from 1000 to 10,000 megacycles. **You save considerably in SIZE, WEIGHT and COST by letting these two instruments do your entire interference measuring job from 14 KC all the way up to 15,000 MC.**

Approved for testing under Specifications MIL-I-11748, MIL-I-16910A, MIL-I-6181D, Category A and MIL-I-26600, Category A.
For complete technical information, send for Catalog 614. Plan to attend our next seminar on interference instrumentation. Details upon request.



EMPIRE DEVICES, Inc.
AMSTERDAM, NEW YORK • VICTOR 2-8400

MANUFACTURERS OF: FIELD INTENSITY METERS • DISTORTION ANALYZERS • IMPULSE GENERATORS • COAXIAL ATTENUATORS • CRYSTAL MIXERS

THE *New* SENSITIVE RESEARCH CREST VOLTMETER

Measures...

**POSITIVE PEAK*
TRUE RMS**

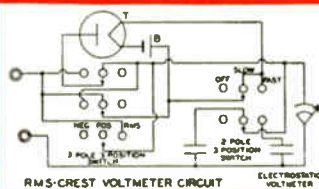
and
NEGATIVE PEAK



MODEL CRV
and MULTIPLIER

RANGES	Basic instrument 0-1 Kilovolt. External multipliers available up to 100 Kilovolts.
ACCURACY	Model CRV 1% of full scale for RMS and for peaks of 10 per second or faster.
SCALE LENGTH	5.2 inch hand drawn mirrored scale.
INPUT IMPEDANCE	RMS = 10,000 megohms and 25 micro microfarads. Positive Peak = 10,000 megohms & 15 micro microfarads. Negative Peak = 10,000 megohms & 15 micro microfarads.
MULTIPLIERS	Accuracy 1%. Capacitor divider type for AC or pulsed DC. (Not steady state D.C.) Input Impedance capacitive — Varies with the full scale range used from .001 mfd. to .000025 mfd.
PHYSICAL DIMENSIONS	Basic instrument 13¼" x 7½" x 6½" 12" x 9" x 27½" for 50 KV range multiplier. Proportionate in height with range of multipliers.
AVAILABILITY	Portable for horizontal use. Panel mounted on special order.

Inquiries Invited



Symbol of Quality

SENSITIVE RESEARCH INSTRUMENT CORPORATION

NEW ROCHELLE, N. Y.

ELECTRICAL INSTRUMENTS OF PRECISION SINCE 1927



(Continued from page 8A)

June 4-6, 1963

Armed Forces Communications & Electronics Show, Sheraton Park Hotel, Washington, D.C.

Exhibits: Mr. William C. Copp, 72 West 45th St., New York 36, N.Y.

July 22-26, 1963

Fifth International Conference on Medical Electronics, Liege, Belgium

Exhibits: Dr. L. E. Flory, RCA Laboratories, Princeton, N.J.

August 20-23, 1963

WESCON (Western Electronics Show & Conference), Cow Palace, San Francisco, Calif.

Exhibits: Mr. Don Larson, WESCON, 1435 La Cienega Blvd., Los Angeles, Calif.

September 9-11, 1963

Seventh National Convention on Military Electronics, Shoreham Hotel, Washington, D.C.

Exhibits: Mr. Leland D. Whitlock, 5614 Greentree Rd., Bethesda, Md.

September 30-October 2, 1963

Canadian Electronics Conference, Toronto, Ont., Canada

Exhibits: IRE Canadian Electronics Conference, 1819 Yonge St., Toronto 7, Ont., Canada

October 1-3, 1963

National Symposium on Space Electronics & Telemetry, Fontainebleau Hotel, Miami Beach, Fla.

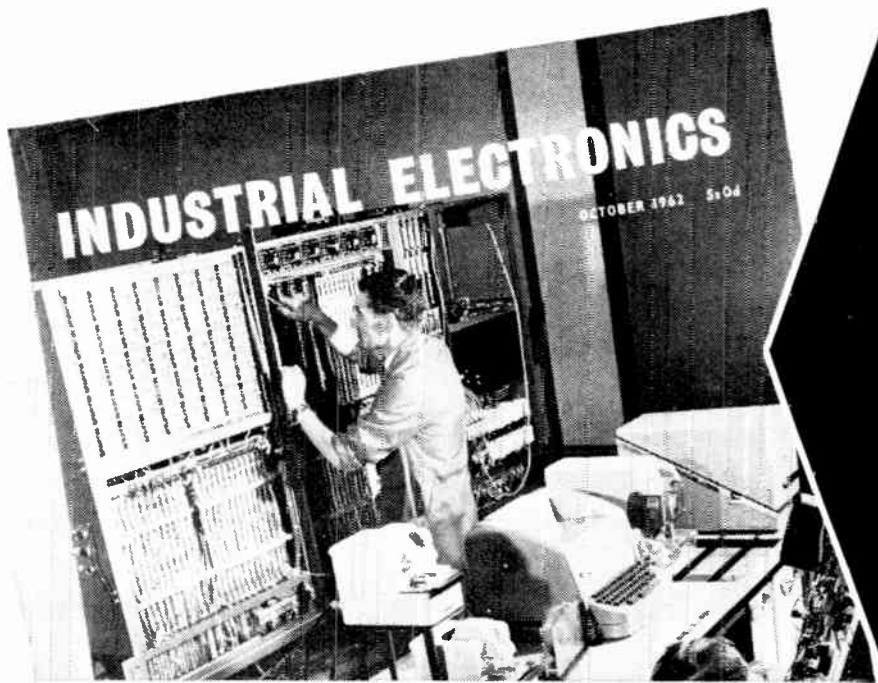
Exhibits: Mr. Charles H. Doersam, Jr., Instruments for Industry, Inc., 101 New South Rd., Hicksville, L.I., N.Y.

October 7-9, 1963

Ninth National Communications Symposium, Hotel Utica & Utica Municipal Auditorium, Utica, N.Y.

Exhibits: Mr. R. E. Gaffney, General Electric Co., Light Military Electronics Dept., Utica, N.Y.

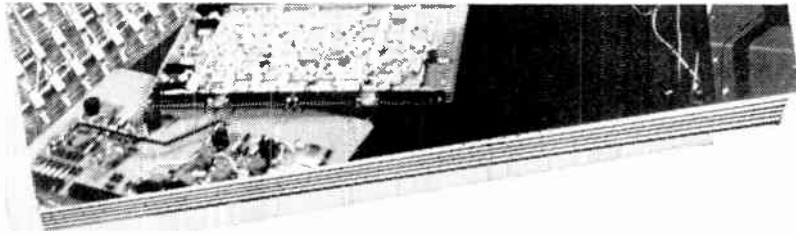
Note on Professional Group Meetings: Some of the Professional Groups conduct meetings at which there are exhibits. Working committeemen on these groups are asked to send advance data to this column for publicity information. You may address these notices to the Advertising Department and of course listings are free to IRE Professional Groups.



HERE!

is the information
wanted today by the
electronics
manufacturing and
user industries

The *NEW* British monthly for the soaring industrial applications of electronics



INDUSTRIAL ELECTRONICS will meet the rapidly rising demand for information on the practical applications of electronics in all branches of industry.

It will show how electronic techniques can cut costs, increase productivity, improve quality. It will spotlight new advances and applications, describing new products and equipment from manufacturers all over the world. INDUSTRIAL ELECTRONICS is a development of Electronic Technology; building on the unique experience of that internationally known journal, it will provide a vital service for production executives, works managers, buyers and directors—helping them to meet ever-increasing competition.

**MAKE SURE
OF YOUR
FIRST COPY
TODAY!**

To: British Publications Inc. 30 East 30th St., New York 22, N.Y.
Enter my own subscription to INDUSTRIAL ELECTRONICS for:—
12 months (12 issues) \$4.50, 36 months (36 issues) \$17.00.
Check M.O. for \$ enclosed.

Name _____
Address _____
City _____
Zone _____ State _____ PRO. IRE

**INDUSTRIAL
ELECTRONICS**

The widest, most practical
coverage of today's needs
PLUS the established authority
of 'Electronic Technology'
Published monthly from October 1962

The advent of integrated circuits demands new approaches to circuit and system designs. The new Motorola MECL* logic circuits are designed around the properties of integrated circuits rather than those of individual components, therefore capitalizing on the advantages of this new technology.

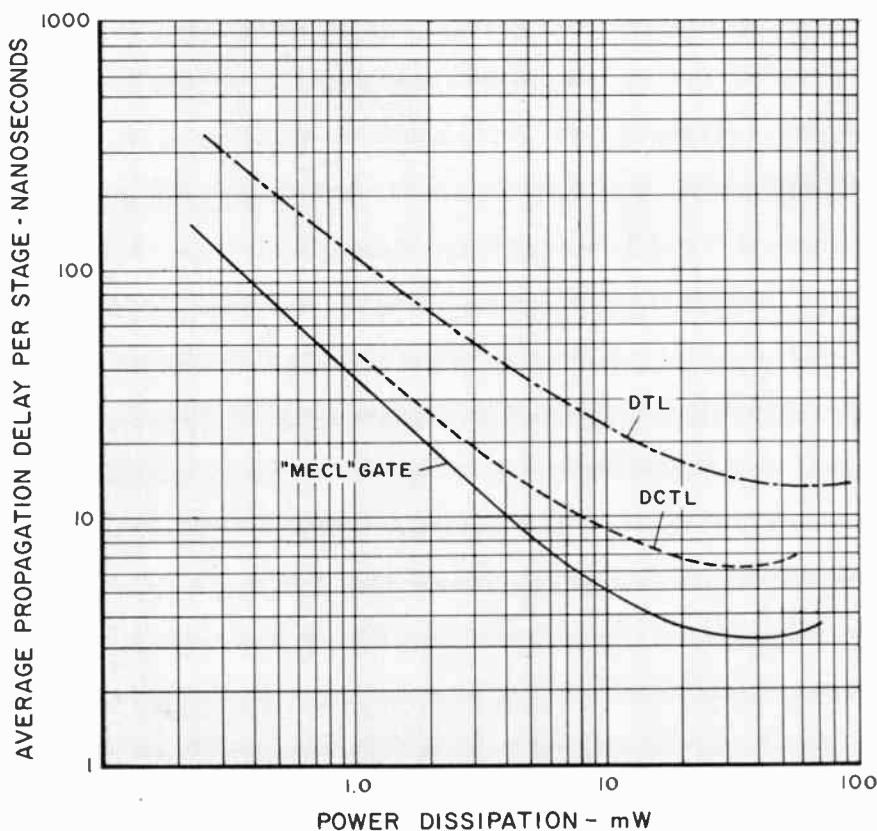
Motorola MECL Circuits...For 3rd Generation Integrated Circuit Computers

Integrated circuits offer the computer industry a new and powerful tool for satisfying the demand for space-age computer designs of ever-increasing complexity. They not only provide solutions for the widely publicized requirements of reduced size and weight, improved reliability and, eventually, lower costs, but new circuits developed by Motorola's Semiconductor Products Division operate at higher speed and with lower power than standard transistor circuits.

These benefits cannot be achieved merely by taking circuits designed for use with discrete components and translating them into integrated circuit form. Such redesign does not provide all of the improvements possible with this new technology. For, just as the transistor required a departure from tube circuit design, so the unique characteristics of integrated circuits benefit from a design approach specifically geared to their particular advantages and limitations.

For example, the inherent properties of integrated circuits provide greater freedom for circuit design than is apparent at first glance. In designing integrated circuits for large-scale production, transistors should be considered as no more expensive than diodes, and diodes, in turn, as no more expensive than passive elements. This, to some degree, will free the circuit designer from the economic restrictions of present techniques.

On the other hand, the present state of the integrated circuit art also presents some limitations. Among these are: 1) inherent parasitic coupling between components through a common semiconductor substrate; 2) restricted ranges of component values, and 3) limitations on individual component tolerances.



Speed versus power-dissipation comparison between three practical forms of computer logic designs illustrates the higher speed capability and lower power consumption of MECL circuits.

Taking into account both the additional design freedoms and limitations of the integrated circuits art, Motorola Semiconductor engineers developed an advanced form of logic circuitry, called MECL circuits, which we believe is superior to any other circuit presently available — whether made from discrete components or integrated circuits. The series consists of an OR-NOR gate, a flip-flop, and a half-adder — all the ingredients for the arithmetic portion of even the most complex digital computer.

Design Considerations

Motorola MECL circuits were the result of exhaustive research of all major logic configurations from a standpoint of integrated circuit compatibility. In every comparison, the current-mode logic approach demonstrated indisputable performance superiority over such commonly used forms as DTL (diode-transistor logic) and DCTL (direct-coupled transistor logic) circuits.

*MECL — trademark of Motorola Inc.

It eliminates, for example, the parameter of transistor storage time as a speed-limiting factor¹ — thus extending the maximum potential circuit speed beyond the limits of other logic forms.

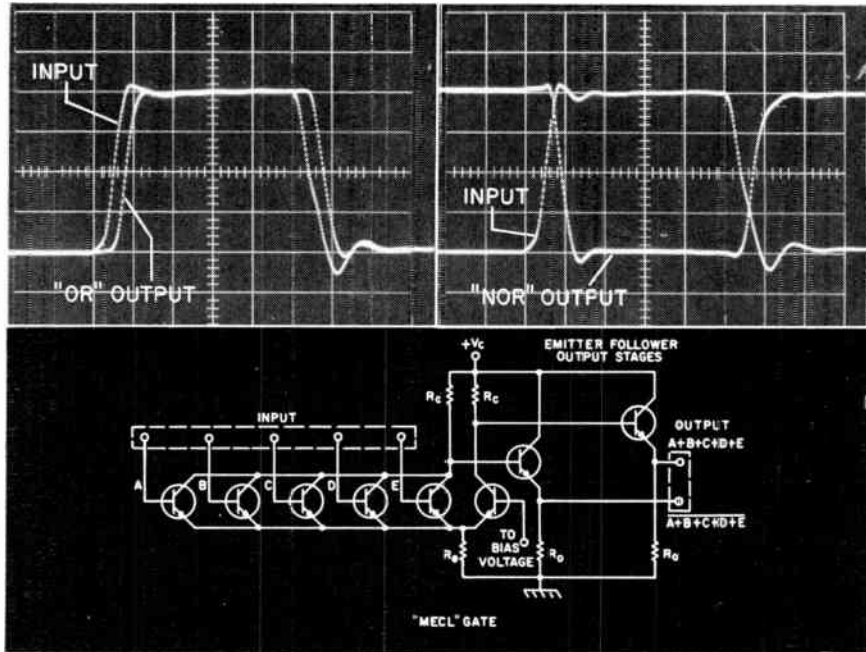
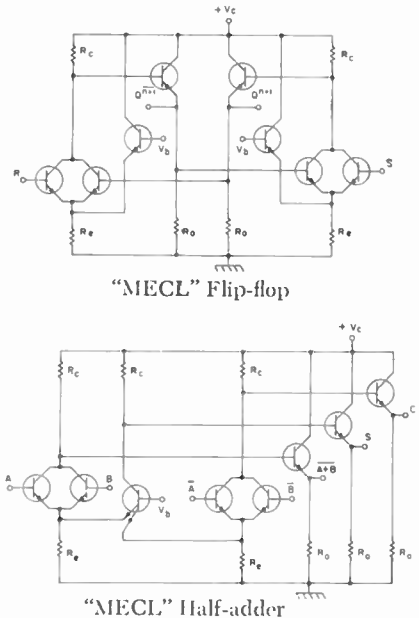
It is uniquely tolerant of component values¹. Absolute values of resistors are relatively unimportant so long as proper ratios between circuit resistances is maintained. This is highly compatible with integrated circuit processes where absolute parts values are difficult to achieve, but where resistance ratios can be held to very close tolerances.

It is non-critical of transistor parameters, maintains constant power supply loading, has unexcelled DC stability, and contributes to high noise immunity¹ — factors that greatly influence performance reliability.

In fact, the only area in which the basic current-mode approach suffered by comparison with other logic forms, was in the relatively large number of transistors it requires. While this has been a major economic deterrent, preventing the widespread adoption of current-mode logic with discrete components, it becomes an insignificant factor in the cost of integrated circuits.

MECL Circuit Advantages Over DTL and DCTL

The dynamic advantages of MECL circuits over other forms of logic are apparent from an examination of the input-output characteristics shown in conjunction with the schematic diagram of the gate circuit.



"OR" and "NOR" outputs of a typical Motorola "MECL" gate circuit show transient response times in the order of 3.5 nanoseconds with a fan-out of 1. (Horizontal scale = 10 nsec Div., Vertical scale = 0.2 V/Div.)

- **High Speed Operation** — Delay time of less than 5 nanoseconds per stage. Circuit speed is increased not only by the elimination of the storage time limitation, but also by the high inherent feedback in the circuit which greatly reduces input capacitances, and by the low impedance of the common-emitter nodes which lessens the deteriorating effects of parasitic and lead capacitances.

- **High Logic Capability** — The direct signal and its complement are both available from the same gate. The availability of both direct and complementary outputs from the same circuit provides a simplification of the overall logic. This not only reduces the number of stages required, but further increases system speed by eliminating the propagation delay associated with such extra stages.

- **Large Fan-In and Fan-Out Capability** — For greater logic power. Fan-in capability is high because of the high input impedance resulting from the large amount of feedback provided by the common emitter resistance. Fan-out capability is high because of the low output impedance of the emitter follower circuit. With a fan-out of 12, a propagation delay of only 5.5 usec can be achieved. Each additional loading stage adds only about 0.25 nsec to the total delay.

- **Low Noise and Crosstalk** — High input and low output impedances of MECL circuits greatly reduce both

inductive and capacitive cross talk between adjacent signal lines. Noise generated in power supply and ground lines is minimized due to the constant-current requirements of this logic family.

- **Fewer Interconnecting Problems** — The simultaneous availability of complementary signals reduces interconnecting problems by a factor of 2 or more. Utilization of a ten-pin header provides additional inputs as compared to eight-pin headers.

Speed-Power Range

Ultra-high-speed MECL logic circuits are being made available as standard components with a typical propagation delay of only 4 nanoseconds. Standard circuits for operation at lower speeds are rated at 100 nanoseconds with less than 1 mw power dissipation. Applications requiring intermediate speeds will be met by "custom-designed" MECL circuits.

Further information about Motorola MECL logic circuits can be obtained by writing Motorola Semiconductor Products Inc., Technical Information Department, 5005 East McDowell Road, Phoenix 8, Arizona.

¹Techniques Of Current-Mode Logic Switching — W. D. Rochr, Motorola Semiconductor Products Inc., *Electronic Design*, September 13, 1962



Current IRE Statistics

(As of October 31, 1962)

Membership—99,948
 Sections*—111
 Subsections*—35
 Professional Groups*—29
 Professional Group Chapters—304
 Student Branches†—242

* See November, 1962 issue for a list.
 † See October, 1962 for a list.

Calendar of Coming Events and Authors' Deadlines*

1962

- Dec. 4-6: FJCC (Fall Joint Computer Conf.), Sheraton Hotel, Philadelphia, Pa.
 Dec. 6-7: 13th Nat'l Conf. on Vehicular Communications, Disneyland Motel, Anaheim, Calif.

1963

- Jan. 8-10: Millimeter and Submillimeter Conf., Cherry Plaza Hotel, Orlando, Fla.
 Jan. 21-24: 9th Nat'l Symp. on Reliability and Quality Control, Sheraton Palace Hotel, San Francisco, Calif.
 Jan. 30-Feb. 1: 4th Winter Convention on Military Electronics, Ambassador Hotel, Los Angeles, Calif.
 Feb. 11-15: 3rd Internat'l Symp. on Quantum Electronics, UNESCO Bldg., Paris, France.
 Feb. 20-22: Internat'l. Solid State Circuits Conf., Sheraton Hotel and Univ. of Pa., Phila., Pa.
 Mar. 25-28: IEEE International Convention, Coliseum and Waldorf-Astoria Hotel, New York, N. Y.
 Apr. 10-11: 4th Symp. on Engrg. Aspects of Magnetohydrodynamics, Univ. of California.
 Apr. 16-18: Symp. on Optical Masers, New York, N. Y.
 Apr. 17-19: (Southwestern IRE Conf. and Elec. Show), Dallas Memorial Auditorium, Dallas, Tex.
 Apr. 17-19: Internat'l Nonlinear Magnetism (INTERMAG) Conf., Shoreham Hotel, Washington, D. C.
 Apr. 24-26: 7th Region Tech. Conf., San Diego, Calif.
 May 2-3: 4th Nat'l Symp. on Human Factors in Elec. Marriott Twin Bridges Motel, Washington, D. C.
 May 7-9: Electronic Components Conf., International Inn, Washington, D. C.
 May 13-15: NAECON (Nat'l Aerospace Electronics Conf.), Dayton, Ohio.
 May 17-18: Symp. on Artificial Control of Biology Systems, Univ. of Buffalo, School of Med., Buffalo, N. Y.
 May 20-22: Nat'l Symp. on Microwave Theory and Techniques, Miramar Hotel, Santa Monica, Calif. (DL*:

* DL = Deadline for submitting abstracts.

(Continued on page 15A)

IEEE MERGER NEWS

The Joint Merger Committee, acting in behalf of the Board of Directors of AIEE and IRE, is currently engaged in working out the many details of the IEEE organization. While this work is in process, it is most important that the functions of Committees and other organizational units of the IRE and AIEE should not be interrupted. To assure continuity in these activities, IRE President Haggerty and AIEE President Teare have sent letters to all committee and subcommittee personnel of the two societies requesting their continued service in their present posts until such time as the IEEE Board of Directors issues further instructions.

PGBTR CHICAGO CONFERENCE PAPERS SOLICITED

The 1963 Chicago Spring Conference on Broadcast and Television Receivers is planned for June 18-19, 1963, and will be held at the O'Hara Inn, Chicago, Ill. Papers are sought that would be of particular interest to those in the home entertainment radio and television industry. Of special interest are papers dealing with new products, and with new concepts of component and circuit design.

The deadline for receipt of papers is February 15, 1963. Potential authors are asked to submit a 50-100 word summary including title of the paper, and name, company affiliation and position of the author. Papers should be limited to approximately 2500 words and the presentation to twenty minutes. The papers should be submitted to Mr. Morman Parker, Papers Committee, Motorola, Incorporated, 9401 West Grand

Avenue, Franklin Park, Ill.

Authors will be notified of the selection of papers early in March, 1963. Biographical information will be requested at that time, but complete papers will not be required until the time of presentation. Since it is expected that all the papers will be published in the IRE TRANSACTIONS ON BROADCAST AND TELEVISION RECEIVERS, authors will be expected to supply, before presentation, a transcript suitable for such submission.

TELSTAR EXCHANGE BETWEEN IRE AND ITU

On October 4, 1962, the IRE and the International Telecommunication Union broadcasted telephone discussions via the Telstar satellite. Scientists at the National Symposium on Space Electronics and Telemetry, Hotel Fontainebleau, Miami Beach, Fla., and officials of the International Telecommunication Union, ITU Building, Geneva, Switzerland, took part in the exchange from 10:34 to 10:55 A.M., Eastern Standard Time. The following were participants:

George Jacobs, Chief Frequency Division, Voice of America.

Arthur Rudolph, Assistant Director for Systems Engineering, NASA; and National Chairman of the IRE National Symposium on Space Electronics and Telemetry.

Lloyd V. Berkner, Past President, IRE.
 Warren H. Chase, Past President, IEEE.

Manohar B. Sarwate, Deputy Secretary General, ITU.

Nicolai Krasnosselski, Chairman, International Frequency Registration Board, ITU.

John H. Gayer, Vice-Chairman, International Frequency Board, ITU.



Participants of the Reliability Training Conference held on September 24-28, 1962 in Princeton, N. J. Included (left to right) are Paul Darnell, speaker on Telstar Reliability; Dr. Dirk van der Reyden, Course Instructor; Stanley Zwerling, Vice Chairman of the Conference; and Herman Wuerffel, recipient of the PGRQC Award for Outstanding Contributions to the Field of Reliability.

CURRENT IRE STANDARDS

Please order by number from IRE Headquarters, 1 E. 79 St., N. Y. 21, N. Y. A 20 per cent discount will be allowed on order for 100 or more copies mailed to one address.

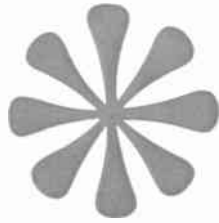
Standard	Cost
48 IRE 2., 11, 15.S1 Standards on Antennas, Modulation Systems, and Transmitters: Definitions of Terms, 1948.	\$0.75
48 IRE 2.S2 Standards on Antennas: Methods of Testing, 1948. Adopted by ASA. (ASA C16.11-1949, R 1961.)	\$0.75
53 IRE 2.S1 Standards on Antennas and Waveguides: Definitions of Terms, 1953. Reprinted from the December, 1953, PROCEEDINGS.	\$0.75
55 IRE 2.S1 Standards on Antennas and Waveguides: Definitions for Waveguide Components, 1955. Reprinted from the September, 1955, PROCEEDINGS.	\$0.25
59 IRE 2.S1 Standards on Antennas and Waveguides: Waveguide and Component Measurements, 1959.	\$0.75
Reprinted from the April, PROCEEDINGS.	\$0.75
53 IRE 3.S2 Standards on American Recommended Practice for Volume Measurements of Electrical Speech and Program Waves, 1953. Adopted by ASA. (ASA C16.5-1954.)	\$0.50
Reprinted from the May, 1954, PROCEEDINGS.	\$0.50
56 IRE 3.S1 Standards of Audio Systems and Components: Methods of Measurement of Gain, Amplification, Loss, Attenuation, and Amplitude-Frequency-Response, 1956 Adopted by ASA. (ASA C16.29-1957.)	\$0.80
Reprinted from the May, 1956, PROCEEDINGS.	\$0.80
58 IRE 3.S1 Standards on Audio Techniques: Definitions of Terms, 1958. Reprinted from the December, 1958, PROCEEDINGS.	\$0.60
50 IRE 4.S1 Standards on Circuits: Definitions of Terms in Network Topology, 1950. Reprinted from the January, 1951, PROCEEDINGS.	\$0.50
53 IRE 4.S1 Standards on Circuits: Definitions of Terms in the Field of Linear Varying Parameter and Nonlinear Circuits, 1953. Reprinted from the March, 1954, PROCEEDINGS.	\$0.25
60 IRE 4. S1 Standards on Circuits: Definitions of Terms for Linear Signal Flow Graphs, 1960. Reprinted from the September, 1960, PROCEEDINGS.	\$0.25
60 IRE 4.S2 Standards on Circuits: Definitions of Terms for Linear Passive Reciprocal Time Invariant Networks, 1960. Reprinted from the September, 1960, PROCEEDINGS.	\$0.50
51 IRE 6.S1 Standards on Electroacoustics: Definitions of Terms, 1951. Reprinted from the May, 1951, PROCEEDINGS.	\$1.00
52 IRE 7.S2 Standards on Gas-Filled Radiation Counter Tubes: Methods of Testing, 1952. Reprinted from the August, 1952, PROCEEDINGS.	\$0.75
57 IRE 7.S2 Standards on Electron Tubes: Definitions of Terms, 1957. Reprinted from the derived 1957, PROCEEDINGS.	\$1.00
62 IRE 7.S1 Standards on Electron Tubes: Methods of Testing, 1962. Reprinted from the September, 1962, PROCEEDINGS.	\$2.50
56 IRE 8.S1 Standards on Electronic Computers: Definitions of Terms, 1956. Reprinted from the September, 1956, PROCEEDINGS.	\$0.60
59 IRE 8.S1 Standards on Static Magnetic Storage: Definition of Terms, 1959. (Adopted by ASA. (ASA C16.35-1962.)	\$0.50
Reprinted from the March, 1959, PROCEEDINGS.	\$0.20
43 IRE 9.S1 Standards on Facsimile: Temporary Test Standards, 1943	\$0.20
56 IRE 9.S1 Standards on Facsimile: Definitions of Terms, 1956. Adopted by ASA. (ASA C16.30-1957.)	\$0.60
Reprinted from the June, 1956, PROCEEDINGS.	\$0.60
55 IRE 10.S1 Standards on Industrial Electronics: Definitions of Industrial Electronics Terms, 1955. Reprinted from the September, 1955, PROCEEDINGS.	\$0.50
53 IRE 11.S1 Standards on Modulation Systems: Definitions of Terms, 1953. Reprinted from the May, 1953, PROCEEDINGS.	\$0.50
58 IRE 11.S1 Standards on Information Theory: Definitions of Terms, 1958. Reprinted from the September, 1958, PROCEEDINGS.	\$0.50
54 IRE 12.S1 Standards on Radio Aids to Navigation: Definitions of Terms, 1954. Adopted by ASA. (ASA C16.26-1955.)	\$1.00
Reprinted from the February, 1955, PROCEEDINGS.	\$1.00
59 IRE 12.S1 Standards on Navigation Aids: Direction Finder Measurement, 1959. Reprinted from the August, 1959, PROCEEDINGS.	\$1.00
60 IRE 13.S1 Standards on Nuclear Techniques: Definitions for the Scintillation Counter Field, 1960. Reprinted from the August, 1960, PROCEEDINGS.	\$0.60
49 IRE 14.S1 Standards on Piezoelectric Crystals, 1949, Adopted by ASA. (ASA C83.3-1951. R 1954 R 1961.)	\$0.80
Reprinted from the December, 1949, PROCEEDINGS.	\$0.60
57 IRE 14.S1 Standards on Piezoelectric Crystals—The Piezoelectric Vibrator: Definitions and Methods of Measurement, 1957. Reprinted from the March, 1957, PROCEEDINGS.	\$0.60
58 IRE 14.S1 Standards on Piezoelectric Crystals: Determination of the Elastic, Piezoelectric and Dielectric Constants—The Electromechanical Coupling Factor, 1948. Reprinted from the April, 1958, PROCEEDINGS.	\$0.75
61 IRE 14.S1 Standards on Piezoelectric Crystals: Measurements of Piezoelectric Ceramics, 1961. Adopted by ASA. (ASA C 16 C 83.24-1962.)	\$0.70
Reprinted from the July, 1961, PROCEEDINGS.	\$0.70
55 IRE 15.S1 Standards on Pulses: Methods of Measurements of Pulse Quantities, 1955. Adopted by ASA. (ASA C16.28-1956.)	\$0.60
Reprinted from the November, 1955, PROCEEDINGS.	\$0.60

Calendar of Coming Events and Authors' Deadlines*

(Continued from page 1-1)

- Jan. 15, 1963. Dr. I. Kaufman, Space Tech. Labs. Inc., 1 Space Pk., Redondo Beach, Calif.
- May 26-28: Spring Joint Computer Conf., Washington Hilton Hotel, Washington, D. C.
- May 27-28: 7th Nat'l Conf. on Product Engrg. and Production, Boston, Mass.
- June 4-5: 5th Nat'l Radio Frequency Interference Symp., Bellevue-Stratford Hotel, Philadelphia, Pa.
- June 11-13: Nat'l Symp. on Space Electronics and Telemetry, Los Angeles, Calif.
- June 19-21: Joint Automatic Control Conf., Univ. of Minnesota, Minneapolis, Minn.
- July 9-11: 1963 PAGAP Internat'l Symp., NBS, Boulder, Colo.
- July 22-26: 5th Internat'l. Conf. on Medical Electronics, Liege, Belgium.
- Aug. 20-23: WESCON (Western Elec. Show and Conf.) Cow Palace, San Francisco, Calif.
- Aug. 27-Sept. 4: 2nd Congress, Internat'l Fed. of Automatic Control, Basle, Switzerland.
- Sept. 9-11: 7th Nat'l Conv. on Military Electronics, Shoreham Hotel, Washington, D. C.
- Sept. 18-19: 12th Annual Industrial Electronics Symp., Michigan State Univ., East Lansing, Mich.
- Sept. 24-27: Internat'l. Telemetering Symp., London, England.
- Sept. 30-Oct. 2: Canadian Electronics Conf., Toronto, Ontario, Canada.
- Oct. 1-3: 8th Annual Symp. on Space Electronics, Miami Beach, Fla.
- Oct. 7-9: 9th Nat'l Communications Symp., Utica, N. Y.
- Oct. 21-23: East Coast Conf. on Aerospace and Navigational Electronics (ECCANE), Baltimore, Md.
- Oct. 28-30: Nat'l Electronics Conf., McCormick Pl., Chicago, Ill.
- Oct. 29-31: 10th Annual Meeting PGNS and Internat'l Symp. on Plasma Phenomena and Measurements, El Cortez Hotel, San Diego, Calif.
- Oct. 31-Nov. 1: 1963 Electron Devices Meeting, Sheraton Park Hotel, Washington, D. C.
- Nov. 4-6: NEREM (Northeast Research and Engrg. Meeting), Boston, Mass.
- Nov. 11-13: Radio Fall Meeting, Hotel Syracuse, Syracuse, N. Y.
- Nov. 10-14: 9th Annual Conf. on Magnetism and Magnetic Materials, Chalfonte-Haddon Hall, Atlantic City, N. J.
- Nov. 12-14: Fall Joint Computer Conf., Las Vegas Conv. Center, Las Vegas, Nev.
- Nov. 18-20: 16th Annual Conf. on Engrg. in Biology and Medicine, Lord Baltimore Hotel, Baltimore, Md.
- Dec. 5-6: 14th Nat'l Conf. on Vehicular Communications.
- Feb. 13-14: Internat'l Solid State Circuits Conf., Sheraton Hotel and Univ. of Pa., Philadelphia, Pa.
- Mar. 23-26: IEEE Internat'l Conv., Coliseum and Waldorf-Astoria, New York, N. Y.

* DL = Deadline for submitting abstracts.



Zero Failures in Over a Million Tube Hours

a proven new high in reliability for frame grid tubes

**AMPEREX, largest manufacturer of frame grid tubes,
announces two 10,000-hour Premium Quality tubes, types 6922M and 7737M,
with specified failure rates exceeding the reliability requirements of
Mil Specs MIL-E-1/1168A and MIL-E-1/1451 respectively.**

In a stringent four-year reliability testing program, the AMPEREX 6922M twin triode, designed for use in radar, oscilloscopes, computers, broadband amplifiers and critical airborne applications, achieved a failure rate of 0.10%/1000 hours for inoperatives and 0.17%/1000 hours for total failures. 2860 tubes were each tested for 1000-hour periods for a total of 2,860,000 tube hours.

DATA: TYPE 6922M: $G_m=12,500 \mu\text{mhos}$ at 15 ma.; Amplification Factor=53, AFR=1.0%/1000 hours; Mechanical Outline T-6½, 9-pin miniature, maximum height 1½".

The 7737M, a ruggedized, non-microphonic version of the JAN 6688, was similarly tested. This Premium Quality pentode was designed for critical airborne applications, coaxial cable amplifiers and video and broadband IF amplifiers in communications and radar equipment. In 1962, the 7737M achieved a failure rate of zero %/1000 hours for inoperatives and 0.75%/1000 hours for total failures.

DATA: TYPE 7737M: $G_m=16,500 \mu\text{mhos}$ at 13 ma.; Amplification Factor=33, AFR=1.0%/1000 hours; Mechanical Outline T-6½, 9-pin miniature, maximum height 1½".

The 6922M and 7737M are available in production quantities, with specified failure rates, to MIL Specs MIL-E-1/1168A and MIL-E-1/1451 respectively. To guarantee the Specified Failure Rates, the military specifications require test procedures using one acceptance figure for a cumulative total of 250 tubes resulting from 5 successive samplings of 50 tubes each, and another acceptance figure for the individual 50-tube samplings. This procedure, employing the unusually large quantities of tubes in both the individual samplings and the total cumulative samplings, guarantees the statistical significance and accuracy of the result. Results achieved in 10,000-hour life tests of individual lots of both tube types enable us to guarantee the reliability and specify the failure rates of these tubes.

The complete story of this unparalleled achievement in tube reliability is available in a new brochure: "Guaranteed Reliability with AMPEREX Premium Quality Frame Grid Tubes." This new brochure describes the production techniques used in the manufacture of AMPEREX frame grid tubes and presents a detailed analysis of how AMPEREX conceived and conducted these reliability tests and life studies. Write for your free copy to: AMPEREX Electronic Corporation, Special Purpose Tube Department, 230 Duffy Avenue, Hicksville, Long Island, New York.

IN CANADA: PHILIPS ELECTRON DEVICES LTD., 116 VANDERHOOF AVENUE, TORONTO 17, ONTARIO





CURRENT IRE STANDARDS

Please order by number from IRE Headquarters, 1 E. 79 St., N. Y. 21, N. Y. A 20 per cent discount will be allowed on order for 100 or more copies mailed to one address.

	<i>Standard</i>	<i>Cost</i>
58	IRE 15. TRI IRE Technical Committee Report: Methods for Testing Radiotelegraph Transmitters (Below 50 MC). Reprinted from the January, 1959, PROCEEDINGS	\$0.60
61	IRE 15.S1 Standards on Radio Transmitters: Definitions of Terms, 1961. Reprinted from the February, 1961, PROCEEDINGS	\$0.25
49	IRE 16.S1 Standards on Railroad and Vehicular Communications: Methods of Testing, 1949. Adopted by ASA. (ASA C16.18-1951, R 1961.) Reprinted from the December, 1949, PROCEEDINGS	\$0.50
47	IRE 17.S1 Standards on Radio Receivers: Methods of Testing Frequency-Modulation Broadcast Receivers, 1947. Adopted by ASA. (ASA C16.12-1949, R 1961, with supplement C16.12a.)	\$0.50
48	IRE 17.S1 Standards on Radio Receivers: Methods of Testing Amplitude-Modulation Broadcast Receivers, 1948. Adopted by ASA. (ASA C16.19-1951, R 1961.)	\$1.00
49	IRE 17.S1 Tests for Effects of Mistuning and for Downward Modulation. 1949 Supplement to 47 IRE 17.S1. Reprinted from the December, 1949, PROCEEDINGS	\$0.25
51	IRE 17.S1 Standards on Radio Receivers: Open Field Method of Measurement of Spurious Radiation from Frequency Modulation and Television Broadcast Receivers, 1951. Reprinted from the July, 1951, PROCEEDINGS	\$0.50
52	IRE 17.S1 Standards on Receivers: Definitions of Terms, 1952. Reprinted from the December, 1952, PROCEEDINGS	\$0.60
55	IRE 17.S1 Standards on Radio Receivers: Method of Testing Receivers Employing Ferrite Core Loop Antennas, 1955. Reprinted from the September, 1955, PROCEEDINGS	\$0.50
60	IRE 17.S1 Standards on Television: Methods of Testing Monochrome Television Broadcast Receivers, 1960. Adopted by ASA. (ASA C16.13-1961.) Reprinted from the June, 1960, PROCEEDINGS	\$1.00
53	IRE 19.S1 Standards on Sound Recording and Reproducing: Methods of Measurement of Noise, 1953. Reprinted from the April, 1953, PROCEEDINGS	\$0.50
53	IRE 19.S2 Standards on Sound Recording and Reproducing: Methods for Determining Flutter Content, 1953. Adopted by ASA. (ASA Z57.1-1954.) Reprinted from the March, 1954, PROCEEDINGS	\$0.75
58	IRE 19.S1 Standards on Recording and Reproducing: Methods of Calibration of Mechanically-Recorded Lateral Frequency Records, 1958. Adopted by ASA. (ASA S4.1-1960.) Reprinted from the December, 1958, PROCEEDINGS	\$0.60
51	IRE 20.S1 Standards on Pulses: Definitions of Terms—Part I, 1951. Reprinted from the June, 1951, PROCEEDINGS	\$0.50
51	IRE 20.S2 Standards on Transducers: Definitions of Terms, 1951 Reprinted from the August, 1951, PROCEEDINGS	\$0.50
52	IRE 20.S1 Standards on Pulses: Definitions of Terms—Part II, 1952. Reprinted from the May, 1952, PROCEEDINGS	\$0.50
58	IRE 20.S1 Index to IRE Standards on Definitions of Terms, 1942-1957. Reprinted from the February, 1958, PROCEEDINGS	\$1.00
59	IRE 20.S1 Standards on Methods of Measuring Noise in Linear Twoports, 1959. Reprinted from the January, 1960, PROCEEDINGS	\$0.75
51	IRE 21.S1 Standards on Abbreviations of Radio-Electronic Terms, 1951. Reprinted from the April, 1951, PROCEEDINGS	\$0.50
57	IRE 21.S1 Standards on Letter Symbols and Mathematical Signs, 1958. (Reprinted 1957.) Reprinted from the August, 1957, PROCEEDINGS	\$0.60
57	IRE 21.S2 Standards on Reference Designations for Electrical and Electronic Equipment, 1957. Reprinted from the November, 1957, PROCEEDINGS	\$0.70
57	IRE 21.S3 Standards on Graphical Symbols for Semiconductor Devices, 1957. Reprinted from the December, 1957, PROCEEDINGS	\$0.60
55	IRE 22.S1 Standards on Television: Definitions of Color Terms, 1955. Reprinted from the June, 1955, PROCEEDINGS	\$0.60
50	IRE 23.S2 Standards on Television: Methods of Measurement of Time of Rise, Pulse Width, and Pulse Timing of Video Pulses in Television, 1950. Reprinted from the November, 1950, PROCEEDINGS	\$0.75
50	IRE 23.S3 Standards on Television: Methods of Measurement of Electronically Regulated Power Supplies, 1950. Reprinted from the January, 1951, PROCEEDINGS	\$0.75
54	IRE 23.S1 Standards on Television: Methods of Measurement of Aspect Ratio and Geometric Distortion, 1954. Adopted by ASA. (ASA C16.23-1954, R 1961.) Reprinted from the July, 1954, PROCEEDINGS	\$0.60
55	IRE 23.S1 Standards on Television: Definitions of Television Signal Measurement Terms, 1955. Reprinted from the May, 1955, PROCEEDINGS	\$1.00
58	IRE 23.S1 Standards on Television: Measurement of Luminance Signal Levels, 1958. Adopted by ASA. (ASA C16.31-1959.) Revision of Part I 50 IRE 23. S1 Reprinted from the February, 1958, PROCEEDINGS	\$0.60
60	IRE 23.S1 Standards on Television: Measurement of Differential Gain and Differential Phase, 1960. Adopted by ASA. (ASA C16.33-1961.) Reprinted from the February, 1960, PROCEEDINGS	\$0.60
60	IRE 23.S2 Standards on Video Techniques: Measurement of Resolution of Camera Systems, 1961. Adopted by ASA. (ASA C16.34-1962.) Revision of Part II 50 IRE 23. S1 Reprinted from the March, 1961, PROCEEDINGS	\$0.50

PLANS IN PROGRESS FOR
IEEE WINTER GENERAL MEETING

The first IEEE Winter General Meeting will be held in New York, N. Y., on January 27-February 1, 1962. Technical sessions will be held at the Statler Hilton and New Yorker Hotels, as well as at the Coliseum, the site of the second Electrical Engineering Exhibition. Approximately 138 sessions are to be organized by technical committees in each of the AIEE's six technical divisions. More than 600 Transactions and Conference papers are expected to be programmed for the meeting.

Rooms have been set aside at both the Statler Hilton and New Yorker Hotels, for members and guests attending the meeting. Letters of request for reservations should be sent to the hotel selected, specifically referring to the AIEE meeting.

In addition to the technical sessions, the IEEE Winter General Meeting Committee is planning social activities for the benefit of all participants in the meeting. An informal tea will be held before the formal program begins, on Sunday, January 27, in the ballroom of the Statler Hilton Hotel. The perennial Smoker will be held on Tuesday evening, January 29, in the Grand Ballroom of the Statler Hilton Hotel. Requests for tickets should be sent to AIEE Smoker Committee, 345 East 47 St., New York, N. Y., accompanied by checks made payable to that Committee. The price is \$11.50 per ticket. The Annual Dinner Dance and Reception is scheduled for Thursday night, January 31. Advance reservations and ticket requests at \$15 each may be sent to John V. Cadden, I. V. Jochem, Inc., 18 Lindsley Ave., West Orange, N. J. Checks should be made out to "Special Account, Secretary, AIEE."

A program of inspection trips is being prepared, including trips to Radio City Music Hall, Western Electric Co., Consolidated Edison Company's System Operator's Office, *The New York Times*, James Forrestal Research Center, United Nations General assembly, Bell Telephone Laboratories, Consolidated Edison Company's Indian Point Generating Station, Picatinny Arsenal, New York Stock Exchange, Public Service Electric and Gas Company's Seawen Generating Station, International Business Machines Corp., Holophane Light and Vision Co., and Brookhaven National Laboratories.

Plans are being made by the Ladies Entertainment Committee for an interesting week of events for the ladies attending the Meeting. On Tuesday evening, January 29, a dinner with entertainment will be held in the Penn Top of the Statler Hilton Hotel, and a tour through Helena Rubinstein's Salon is planned for Wednesday, January 30.

Members of the 1963 IEEE Winter General Meeting Committee are: W. G. Vieth, Chairman; J. G. Dorse, Vice Chairman; W. T. Rea, Vice President District 3 and Budget Coordinator; H. T. Marex, Representative, Technical Operations Department; J. J. O'Connor, Chairman, Public Relations Committee; W. G. Cheney, General Session; R. E. Briesemeister, Hotel Accommodations; F. C. Reed, Jr., Registration; P. Zarakas, Inspection Trips; T. W. Bartlett and R. T. Weil, Jr., Student Assistants; J. D. Thuerk, Smoker; H. W. Grissler, Dinner Dance; Mrs. R. W. Gillette, Ladies Events.

How to stop voltage transients and diode failures

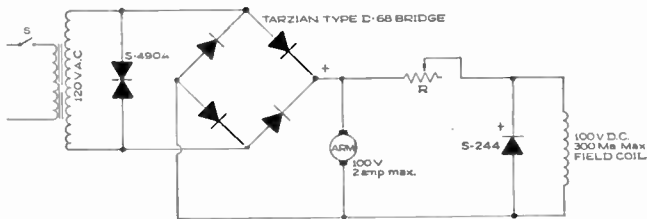
Any circuit that is switched can generate high voltage spikes of harmful amplitude to semiconductor devices. Sarkes Tarzian voltage transient suppressors (Klipvolts) offer an economical, efficient solution.

One recurrent problem that suppressors solve is encountered when switching is at the primary of a transformer. Magnetizing currents are interrupted, causing a voltage spike many times the steady state value of secondary voltage. The result is failure of voltage sensitive devices in the circuit.

Transient voltage spikes of very short time duration often

escape detection by instruments of normal sensitivity. Spikes occurring in control circuits where oscillation or "ringing" can occur are also hard to find. These transients can often be the reason for circuit problems that seem to have no obvious cause.

Standard Tarzian suppressors can handle discharge currents as high as 430 amperes (43,000 ampere load current in a three-phase circuit). Special types can be custom-designed for any practical rating. The diagrams shown here represent actual applications in which Klipvolt suppressors have been used. Your circuit is probably well within their wide range of application.

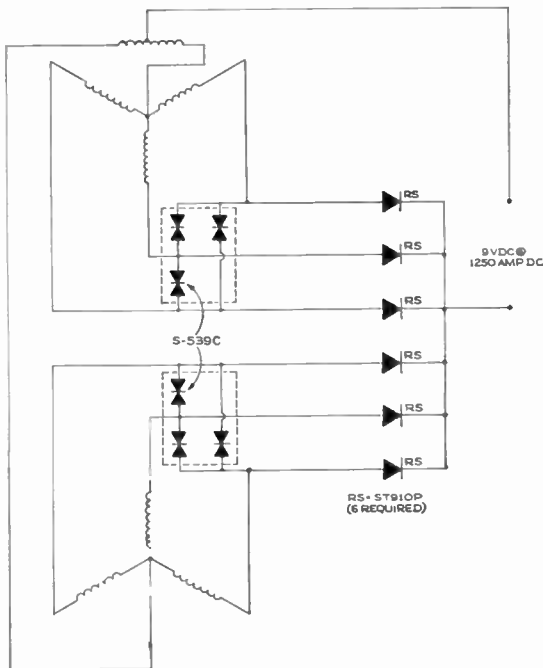


Transient Voltages in Motor Speed Control Rectifier (Fig. 1)

Problem: D-68 bridge rectifier assembly with 400V diodes is used to supply DC to controlled speed DC motor. Switching is accomplished at primary of an isolation transformer. Random switching causes intermittent rectifier failures. Tests show transients to 600V without suppression.

Solution: Use S-490A non-polarized Klipvolt across transformer secondary. Use S-244 Klipvolt across the motor field coil to limit transient spikes to less than 150V.

Result: Rectifier failure eliminated.

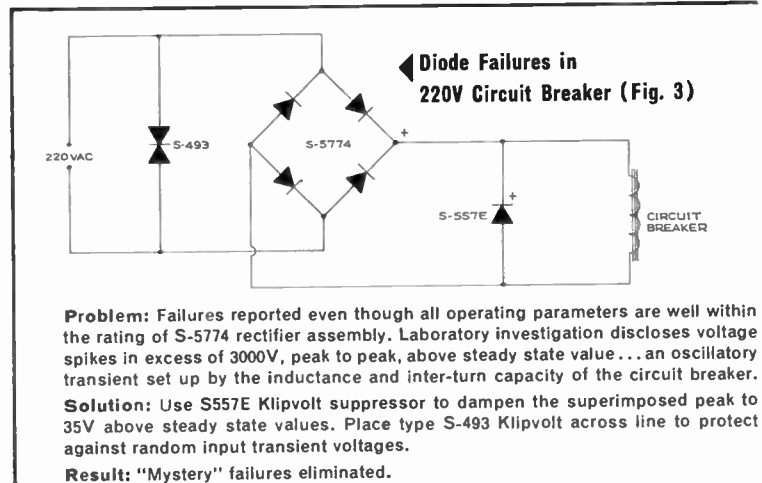


Voltage Transients in Electroplater (Fig. 2)

Problem: Three-phase center tap and six-phase star connections causing transient voltages several times the steady state peak value at the secondary... in excess of 200V.

Solution: Connect an S-539C suppressor across the secondary to reduce transients to below 100V. Use 100 PIV rated diodes instead of 300 PIV ratings.

Result: Substantial cost saving on heavy current diodes.



Diode Failures in 220V Circuit Breaker (Fig. 3)

Problem: Failures reported even though all operating parameters are well within the rating of S-5774 rectifier assembly. Laboratory investigation discloses voltage spikes in excess of 3000V, peak to peak, above steady state value... an oscillatory transient set up by the inductance and inter-turn capacity of the circuit breaker.

Solution: Use S557E Klipvolt suppressor to dampen the superimposed peak to 35V above steady state values. Place type S-493 Klipvolt across line to protect against random input transient voltages.

Result: "Mystery" failures eliminated.

TYPICAL TARZIAN KLIPVOLT SUPPRESSORS

POLARIZED				NON-POLARIZED			
Type	Max DC Volts	Max PIV	Peak Dischg. Amperes	Type	Max RMS Volts	Max PIV	Peak Dischg. Amperes
S-550	27	45	5.5	Single Phase			
S-550L	27	45	430	S-487	35	50	2.5
S-554	135	225	5.5	S-490A	140	200	4.5
S-554L	135	225	430	S-492L	210	300	180
S-556	189	315	5.5	S-493	400	280	2.5
S-556L	189	315	430	Three Phase			
S-557E	216	360	65	S-539C	50	35	13.5
				S-544L	210	300	180



SARKES TARZIAN, Inc.

World's Leading Manufacturers of TV and FM Tuners • Closed Circuit TV Systems • Broadcast Equipment • Air Trimmers • FM Radios • Magnetic Recording Tape • Semiconductor Devices
SEMICONDUCTOR DIVISION • BLOOMINGTON, INDIANA
 Canadian Licensee: Marsland Engineering Limited • 350 Weber Street North, Waterloo, Ontario

CURRENT IRE STANDARDS

Please order by number from IRE Headquarters, 1 E. 79 St., N. Y. 21, N. Y. A 20 per cent discount will be allowed on order for 100 or more copies mailed to one address.

<i>Standard</i>	<i>Cost</i>
61 IRE 23.S1 Standards on Video Techniques: Definitions of Terms Relating to Television, 1961. Supplement to S5 IRE 23. S1 Reprinted from the July, 1961, PROCEEDINGS.	\$0.50
45 IRE 24.S1 Standards on Radio Wave Propagation: Definitions of Terms Relating to Guided Waves, 1945.	\$0.20
50 IRE 24.S1 Standards on Wave Propagation: Definitions of Terms, 1950. Reprinted from the November, 1950, PROCEEDINGS.	\$0.60
55 IRE 26.S1 Standards on Graphical and Letter Symbols for Feedback Control Systems, 1955. Reprinted from the November, 1955, PROCEEDINGS.	\$0.25
55 IRE 26.S2 Standards on Terminology for Feedback Control Systems, 1955. Reprinted from the January, 1956, PROCEEDINGS.	\$0.50
61 IRE 27.S1 Standards on Radio Interference: Methods of Measurement of Conducted Interference Output to the Power Line from FM and Television Broadcast Receivers in the Range of 300 KC to 25 mc, 1961. Adopted by ASA. (ASA C16.25-1962.) Reprinted from the September, 1961, PROCEEDINGS.	\$0.60
56 IRE 28.S1 Standards on Letter Symbols for Semiconductor Devices, 1956. Reprinted from the July, 1956, PROCEEDINGS.	\$0.50
56 IRE 28.S2 Standards on Solid-State Devices: Methods of Testing Transistors, 1956. Reprinted from the November, 1956, PROCEEDINGS.	\$0.80
58 IRE 28.S1 Standards on Solid-State Devices: Methods of Testing Point-Contact Transistors for Large-Signal Applications, 1958. Reprinted from the May, 1958, PROCEEDINGS.	\$0.70
60 IRE 28.S1 Standards on Solid-State Devices: Definitions of Semiconductor Terms, 1960. Reprinted from the October, 1960, PROCEEDINGS.	\$0.50
60 IRE 28.S2 Standards on Electrostatographic Devices, 1961. Reprinted from the March, 1961, PROCEEDINGS.	\$0.50
61 IRE 28.S1 Standards on Solid-State Devices: Definitions of Terms for Nonlinear Capacitors, 1961. Reprinted from the August, 1961, PROCEEDINGS.	\$0.25
61 IRE 28.S2 Standards on Solid-State Devices: Measurement of Minority-Carrier Lifetime in Germanium and Silicon by Method of Photoconductive Decay. Reprinted from the August, 1961, PROCEEDINGS.	\$0.60
62 IRE 28.S1 Standards on Solid-State Devices: Definitions of Superconductive Electronics Terms, 1962 Reprinted from the April, 1962, PROCEEDINGS.	\$0.25
61 IRE 30.RP1 IRE Recommended Practices on Audio and Electroacoustics: Loud Speaker Measurements. Reprinted from the October, 1961, PROCEEDINGS.	\$0.60

PAPERS SOLICITED FOR SAN DIEGO SYMPOSIUM

The Third Annual San Diego Symposium for Biomedical Engineering will be held on April 22-24, 1963, in conjunction with the IRE 7th Region Technical Conference on April 24-26, 1962. The two meetings will take place in the same location. Technical sessions on Monday and Tuesday will be arranged by the San Diego Symposium for Biomedical Engineering for SDSBE registrants only; those on Thursday and Friday will be arranged by the IRE for IRE registrants only; the Wednesday sessions will be the result of a cooperative effort by the two Program Committees to arrange sessions which will be comprehensive and of outstanding value to both groups. Although registration for the two meetings will be separate, registrants for either will be welcome at the Wednesday sessions.

As in the past, the theme of the SDSBE will be interdisciplinary cooperation. Papers are hereby solicited in:

- (1) Medicine and biology where advances have been made possible by techniques or equipment of the physical sciences and engineering;
- (2) The physical sciences and engineering, as applied to medicine and biology.

Papers describing work inspired by presentations at these SDSBE or similar sym-

posia, or resulting from personal contacts made through them are particularly invited. Workers in the field of biomedical engineering who can offer papers describing significant progress, or real potential, which has not been reported elsewhere, are urged to send a title and summary to the Program Committee immediately to assist us in planning.

Prospective speakers must send full-length drafts of their papers by December 15, 1962 to John H. McLeod, Chairman, Program Committee, 8484 La Jolla Shores Drive, La Jolla, Calif. These drafts may be preliminary; an opportunity to update, modify, and/or correct them will be given before publication. But all material to be covered in the final version must be covered to approximately the same degree, and all tables and illustrations must be included. Only by careful consideration of such a complete draft can the reviewers (one each from the life sciences, the physical sciences, and the Program Committee) determine the relative merits of the competing papers.

Speakers will be selected and notified by the first week in February, 1963. Final versions of their drafts must be in the hands of the Publication Committee not later than March 14, 1962. The Committee will work from these drafts and submit galley proofs for approval, no further work will be required of authors.

POLYTECHNIC SYMPOSIUM ON OPTICAL MASERS

The Thirteenth Annual Polytechnic International Symposium, devoted to "Optical Masers," will be held in New York, N. Y., on April 16-18, 1963. The Symposium will attempt a comprehensive integration of the physics and technology bearing directly on the discovery, theory, and application of maser phenomena at optical and infrared frequencies. Prospective authors are invited to submit papers no later than December 15, 1962. Specific topics proposed to be included are as follows:

Quantum Electrodynamics and Related Topics in Physics: Dispersion, coherence; radiative corrections, stimulated emission, thermodynamical implications, photon-photon scattering; bearing on and tests of general relativity, interactions with gravitational fields.

Materials: Solid, liquid and gaseous systems; spectroscopy, optical properties, crystal growth, nonlinear effects, magneto-optic and electro-optic effects.

Optical Maser Configurations: High efficiency optics, resonant structures, traveling wave structures, modal phenomena.

System Considerations: Communications, radar, astronomy, medicine, instrumentation, industrial processes, phonon modulation.

The 1963 Symposium is organized by the Microwave Research Institute of the Polytechnic Institute of Brooklyn in cooperation with the IRE, AIEE and Optical Society of America. It is co-sponsored by the Air Force Office of Scientific Research, the Office of Naval Research and the Army Research Office.

In keeping with tradition, the Symposium will endeavor to serve the two-fold purpose of providing both a review of the present state of research in the optical maser field and a forum for discussion of recent outstanding advances of interest to engineers, chemists, and physicists involved in laser research and development. The program will comprise both invited and a limited number of contributed papers and will conclude with a round-table discussion. Further information may be obtained from Professors L. Bergstein, W. Kahn or G. Oster, Co-chairmen of the Symposium Committee. Correspondence should be addressed to Symposium Committee, Polytechnic Institute of Brooklyn, 55 Johnson St., Brooklyn 1, N. Y.

JTAC REPRINTS AVAILABLE

The IRE Joint Technical Advisory Committee has reprinted copies of Session 29 of the IRE International Convention Record.

Session 29, sponsored by PGMH and PGREI, was a panel on "Electromagnetic Compatibility—Its Significance to Our Survival." Members of the panel and their papers were as follows: "Basic Issues of Spectrum Conservation," D. G. Fink; "Spectrum Pollution," R. P. Gifford; "The Cost of Radio Frequency Interference," F. L. Ankenbrandt; and "System Electromagnetic Compatibility—DOD's Approach to the Problem," J. A. McDavid.

The reprints may be obtained free of charge from: JTAC Secretary, IRE Headquarters, 1 E. 79 St., New York 21, N. Y.

IS THERE ANY OTHER
ECM OSCILLATOR
 THAT CAN MATCH THE
50%+ EFFICIENCY OF G.E.'S...



SURE.
 G.E.'S...



DON'T BE REPETITIOUS!

I'M NOT. THEY'RE TWO DIFFERENT
 G-E **VTMS**. BOTH HAVE THE **HIGHEST EFFICIENCY**
 (PLUS LIGHTEST WEIGHT AND HIGHEST
 POWER OUTPUT) EVER AVAILABLE for ECM power oscillators.

They differ only in frequency output. Matched into a system, they can sweep the entire range between 2.6 and 3.2 gigacycles in as little as one nanosecond.

Here are some specs on these two VTMs that bear comparison to other ECM oscillation methods:

Power output.....	.75 watts min.
Frequency.....	ZM-6046: 2.6-2.9gc
	ZM-6047: 2.9-3.2gc
Input capacitance.....	.40 picofarads
Weight.....	6.8 lbs.
Max. dimensions.....	5.5 x 4.6 x 3.8 inches
Efficiency.....	50% min.

Of course, these are only two from a large VTM selection. General Electric was first to introduce practical VTMs and remains the leader in this field. Its VTMs have been proven in major ECM programs. Development has been supported by all the service arms, and G.E. is continually bringing new types out of development and into the factory. Well worth checking their sales office. For any electronically-swept oscillator application (250 mc upward), General Electric VTMs ought to get first consideration...

...BY CONTACTING
 ONE OF THE
 SALES OFFICES LISTED BELOW,
 IF YOU'LL PARDON
 THE REPETITION.



ELECTRONICS

INCLUDING IGNITRONS, HYDROGEN
 THYRATRONS, MAGNETRONS, METAL-
 CERAMIC TETRODES, TWT's, HIGH-

POWER DUPLEXERS, HIGH-POWER WAVEGUIDE FILTERS, KLYSTRONS AND THERMI-
 ONIC CONVERTERS. FOR INFORMATION ON THESE PRODUCTS, WRITE SECT. 265-21,
 POWER TUBE DEPT., GENERAL ELECTRIC CO., SCHENECTADY, N. Y. OR TELEPHONE
 TODAY: SCHENECTADY, N. Y. FRanklin 4-2211 (Ext. 5-3433) • WASHINGTON, D. C. EXecutive 3-3600 • DAYTON, OHIO Baldwin 3-7151 • LOS ANGELES, CALIF. BRadshaw 2-8566
 SYRACUSE, N. Y. 652-5102 • CHICAGO, ILL. SPring 7-1600 • CLIFTON, N. J. GRegory 3-6387 • NEW YORK, N. Y. WIsconsin 7-4065 • ORLANDO, FLA. GArden 4-6280

GENERAL ELECTRIC

POWER TUBE DEPARTMENT

265-21

WINTER INSTITUTE ON AUTOMATIC CONTROL

The University of Florida, Gainesville, Fla., is presenting the Second Graduate Winter Institute on Optimum and Adaptive Control System Theory on February 18-22, 1963. The Institute is sponsored by the Engineering and Industrial Experiment Station of the University's College of Engineering. Industry, University and Government representatives are invited to attend this tutorial conference on automatic control. Each participant must have at least a bachelor's degree in any of the fields of engineering or in physics, and an adequate background in control systems either practical or academic.

Registration fee for the Institute is \$100.00. To facilitate proper planning for the program it is necessary that registration forms be sent no later than January 15, 1963 to: Division of General Extension, Florida Institute for Continuing University Studies, Seagle Building, Gainesville, Fla. Since a special ladies program is being planned, delegates should indicate on the registration form if they plan to bring their wives.

The lecturers at the conference are: Dr. Michael Athanassiades, Professor Jens G. Balchen, Dr. John E. Bertram, Professor J. F. Coales, Dr. Pieter Eykhoff, Professor I. Flügge-Lotz, David L. Mellen, Professor Bernard Widrow, and Professor Olle I. Elgerd.

Dr. Athanassiades received the B.S.E.E., M.S.E.E., and Ph.D. degrees from the University of California. At present, he is on the staff of the M.I.T. Lincoln Laboratory, conducting research in the field of optimal control theory with application to minimum time, minimum fuel and minimum energy systems. He is a member of IRE, AIEE, Phi Beta Kappa, Eta Kappa Nu, and Sigma Xi. His lectures will cover the following topics:

Exposition of the Maximum Principle and Hamilton-Jacobi Theory

Derivation of Necessary Conditions on Optimal Control for Minimum Time, Minimum Fuel, and Minimum Energy Criteria

Design of High-Order Real-Pole Bang-Bang Control Systems

Minimum Time Control of Oscillatory Plants

Design of Second Order Minimum-Fuel Systems

Design of Minimum Time, Minimum Fuel, and Minimum Energy Self-Adjoint Systems.

Professor Balchen is Head Professor of the Division of Automatic Control at the Technical University of Norway, Trondheim. He received the Diploma Degree from this University in 1949, and the M.S. degree from Yale University. Currently, he is leading a research program at the Technical University in the general field of optimum control of multivariable processes. His other activities include membership on the Executive Council of the International Federation of Automatic Control. His lectures at the Winter Institute will concentrate on the following two areas:

Optimal Control of Multivariable Processes

Determination of System Dynamics by Use of Adjustable Models.

Dr. Bertram received the B.S.E.E. degree from Washington University in 1952, and the M.S. and Sc.D. degrees from Columbia University in 1955 and 1958, respectively. He is Manager of Control Systems Research at the International Business Machines Corporation. The object of his lectures is to present a tutorial discussion of the problem of stochastic optimal control. To motivate the topic, several stochastic optimal control problems with physical origin will be outlined. After classifying these problems, a mathematical formulation of the stochastic optimization problem will be presented. A discussion will follow of some sample problems where the stochastic and optimization can be treated separately.

Professor Coales received his formal education at Cambridge University, England, where he is presently in charge of the Control Group in the Engineering Department. He has engaged in research on radio direction finding, ultra-short wave radar, computers, and all phases of control. He is a member of the Executive Committee of the National Physical Laboratory, and is a consultant on research and development, particularly in the field of automation, to a number of large industrial groups. His lectures will cover the topics of fast-time predictor systems and the application of nonlinear filters and self-adjusting models to control systems.

Dr. Eykhoff received the B.S. and M.S. degrees in electrical engineering from the Technological University in Delft, The Netherlands, and the Ph.D. degree from the University of California, Berkeley. He is a member of the faculty of the Technological University, in charge of a research group studying the problem of parameter estimation, and building a special type of analog computer for simulating the nonstationary stochastic type of signals that occur in many of these estimation problems. He is a member of the IRE, AIEE, Sigma Xi, Royal Dutch Institute of Graduated Engineers, and International Association for Analog Computation. He will devote his lecture series to the problem of system identification. A critical review of the variety of methods proposed to achieve estimation of system parameters will be given, as well as an exposition of the work being done at Delft.

Dr. Flügge-Lotz received the Diplom-Ingenieur degree in engineering mechanics in 1929, and the Ph.D. degree in engineering in 1929, from the Technical University of Hannover, West Germany. She joined the staff of Stanford University in 1949, where she presently is Professor of Aeronautical Engineering and Engineering Mechanics, lecturing and conducting research in fluid mechanics and control. She is a member of IRE and Sigma Xi, and an Associate Fellow of IAS. Her lecture topics will comprise:

Ideal and Realistic Contactors (Relays)—their use in feedback control systems for improving stability and performance

General Behavior of Systems in the Neighborhood of Switching points—systems with and without zeros in the plant transfer function, controlled and uncontrolled chatter, design suggestions for third order systems

Relation Between Optimal and Con-

tactor Control—Pontryagin's maximum principle and contactor control, difficulty of expressing the time-dependent control function as function of the phase variables, approximate switching functions which lead to near optimum performance.

Dr. Widrow received the B.S., M.S., and Ph.D. degrees from the Massachusetts Institute of Technology. He is an Associate Professor of Electrical Engineering, engaged in research and teaching in systems theory, control theory, adaptive logic, and adaptive control systems. He is also President of Memistor Corporation, Mountain View, Calif., and a member of AIEE, IRE, and Sigma Xi. He will lecture on the topic of "Pattern Recognition and Adaptive Control."

Dr. Elgerd received the B.S.E.E. and Diploma Degree from the Royal Institute of Technology, Stockholm, and the D.Sc. degree from Washington University. He is responsible for the Graduate Control and Simulation Program at the University of Florida, and is a consultant to the Inertial Guidance and Control Group of The Martin Company and Aerospace Corporation. He is a member of the Swedish Society of Engineers and Architects, IRE, AIEE, and Sigma Xi.

Mr. Mellen received the B.S.A.E. and M.S.A.E. degrees from Iowa State University. He is associated with Minneapolis-Honeywell Company, as a Project Manager for the guidance and control system for a special test vehicle. He is an Associate Fellow of the Institute of Aerospace Sciences. His lecture will discuss "The Development and Flight Test of an Adaptive Flight Control System for the X-15 Vehicle."

NATIONAL PGPEP CONFERENCE

The IRE Professional Group on Product Engineering and Production, with the cooperation of its Boston chapter, will hold the 7th National Conference on Product Engineering and Production at the Continental Hotel, Cambridge, Mass., May 27-28, 1963.

The program for the Conference will cover advanced production techniques, micro-miniature system and product design, and product designs to meet world-wide competition. As a special feature, there will be a Product Design Competition. The products accepted for the competition will be on special display.

The Program Chairman is Jack Staller of Sylvania Electronic Systems, Needham Heights, Mass. The General Chairman for the Conference is Chan Watt of The Raytheon Company, Lexington, Mass.

SYMPOSIUM RECORD AVAILABLE

A Record of the papers presented at the 1962 National Symposium on Space Electronics and Telemetry, held on October 2-4, 1962 in Miami Beach, Fla., was printed and available for sale at the Symposium.

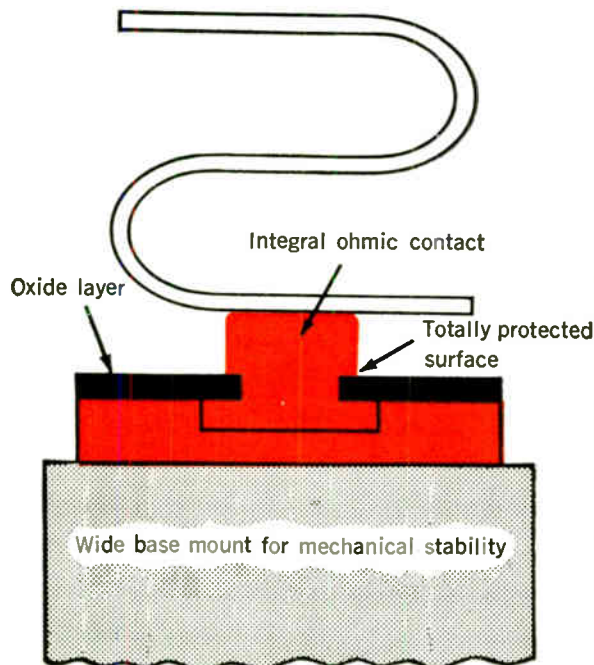
A limited number of copies are available for sale at IRE Headquarters at \$12.50 each. Orders will be filled on a first-come, first-served basis.

Send your check to IRE Headquarters, 1 E 79 St., New York 21, N. Y. for a copy of the *Symposium Record*.

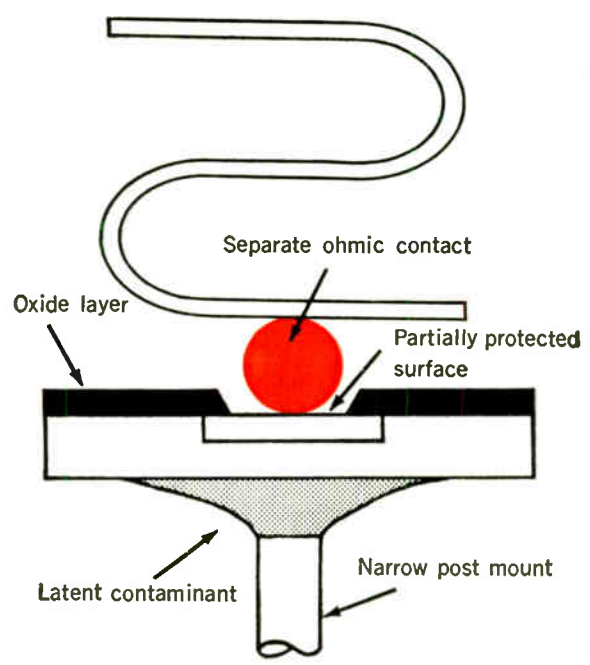


300°C NANOSECOND DIODE

THE INSIDE STORY OF UNIPLANAR* VS. MULTI-PART CONSTRUCTION



RAYTHEON/RHEEM UNIPLANAR* DIODE



CONVENTIONAL PLANAR MULTI-PART DIODE

UNIPLANAR* construction boosts silicon diode reliability

Uniplanar* one-piece construction, produced at Raytheon/Mountain View (formerly Rheem Semiconductor), brings a major improvement to silicon planar diode reliability. This is demonstrated by a 300°C storage capability, unequalled shock and vibration resistance, and more uniform electrical characteristics.

The result of Raytheon/Rheem Uniplanar* construction is a one-piece unit that can't shake loose or become misaligned. The entire chip assembly, including ohmic contact, is formed by a single process. This technique permits positive

surface passivation of the entire junction area. A high level of uniformity is achieved, since ohmic contacts are chemically formed thousands at a time.

300°C storage is obtained because, for the first time, it is possible to exclude the latent contaminants introduced by multi-part assembly techniques.

Uniplanar* construction is available at no extra cost in such types as 1N914, 1N916, 1N3064, and 1N251. For further information, please contact the nearest Raytheon Field Office.

* Exclusive one-piece planar construction from Raytheon/Mountain View (formerly Rheem Semiconductor).



PROFESSIONAL GROUP NEWS

At its meeting on October 16, 1962, the IRE Executive Committee approved the following chapter: PG on Broadcast and Television Receivers—Indianapolis Chapter.

SWIRECO CALL FOR PAPERS

The fifteenth annual Southwestern IRE Conference and Electronics Show, SWIRECO, will be held in Dallas, Texas, April 17-19, 1963. The event is also the Region 6 IRE Meeting. Principal sessions tentatively scheduled are Geophysics; Space Electronics, including communications and propagation; Electronic Systems and Applications; and Bionics. Technical papers are sought in any of the various specialties of Electronics. A student paper competition is also planned. Abstracts of approximately 300 words should be sent to the Technical Program Chairman, Al Mitchell, Graduate Research Center of the Southwest, P. O. Box 8478, Dallas 5, Texas. All abstracts must be received prior to January 15, 1963, and acceptance notices will be provided within 30 days.

The technical program, as well as SWIRECO's 275-booth trade exposition will be held in Dallas Memorial Auditorium. Dr. A. E. Salis, head of the Electrical Engineering Department of Arlington State

College, Arlington, Texas, is General Chairman of the Conference. Technical Program Committee members are G. B. Gibson, Electrical Systems Branch, N.A.S.A., Manned Spacecraft Center, Houston; Dr. A. W. Straiton, Defense Research Laboratory, University of Texas, Austin; Dr. F. E. Brooks, Temco Aerosystems Division of Ling-Temco-Vought, Incorporated, Dallas; and Dr. W. Hughes, Chairman, Electrical Engineering Department, Oklahoma State University, Stillwater, Oklahoma.

Complete information on exhibits and attendance is available from Hal Copeland, Swireco Manager, The Hal Copeland Co., 810 Wilson Building, Dallas 1, Texas.

ELECTROCHEMICAL SOCIETY CALL FOR PAPERS

The Symposium on Thin Films for Electronic Application, sponsored jointly by the Electronics, Electric Insulation, and Electrothermics and Metallurgy Divisions, will be held in Pittsburgh, Pa., April 15-18, 1963. The objectives of the Conference are to present a current picture of the status of thin film technology and to encourage the exchange of information on thin film research and development activities.

Papers are solicited on all aspects of thin film technology having electronic applica-

tion. Papers can be organized, for example, along the lines of materials (metals, insulators, semiconductors) and combinations thereof (*i.e.*, cermets); techniques for thin film deposition, monitoring and testing; materials for specific application (*i.e.*, magnetic, dielectric, superconducting, tunneling); properties of thin films (experimental and theoretical); ageing effects in thin films; compatibility of thin films with other thin films and various substrates; devices and integrated circuits employing thin films.

Three copies each of a 75 word abstract and a 500-1000 word extended abstract should be sent to Society Headquarters, 30 East 42 St., New York, N. Y., not later than December 14, 1962. If there are any questions concerning the Symposium, please contact any of the Committee Members mentioned below. Late news papers of a short (5-10 minute) duration describing recent research results are also desired. Three copies of late news paper abstracts should be submitted to any of the Committee Members no later than March 15, 1963.

The Committee Members are Henry S. Sommers, Jr., RCA Laboratories, David Sarnoff Research Center, Princeton, N. J.; Peter White, IBM Corporation, Thomas J. Watson Research Center, P. O. Box 218, Yorktown Heights, N. Y.; David Vermilyea, General Electric Co., Research Laboratory, P. O. Box 1088, Schenectady, N. Y.; Arnie Lesk, Motorola Semiconductor Division, 5005 East McDowell Rd., Phoenix, Ariz.

Millimeter and Submillimeter Conference

CHERRY PLAZA HOTEL, ORLANDO, FLA., JANUARY 7-10, 1963

The Millimeter and Submillimeter Conference, under sponsorship of the Orlando Section of the IRE, will be held January 7-10, 1963, in the Egyptian Room of the Cherry Plaza Hotel, Orlando, Fla. It should be noted that the Conference has been extended to January 7 to permit presentation of some 56 papers. Advance registration arrangements may be made by mailing \$5.00 before December 21, 1962, to: H. L. Bassett, Registration Chairman, Millimeter and Submillimeter Conference, Martin Company—MP-75, Orlando, Fla.

A Conference Digest, consisting of abstracts of the program papers, will be distributed at no cost to each registrant. One issue of the IRE TRANSACTIONS ON MICROWAVE THEORY AND TECHNIQUES will be devoted to Conference papers and will serve as the Conference record.

J. W. Dees is the General Chairman of the Conference and J. J. Gallagher is the Program Chairman. The program of the Conference will be as follows:

Monday Afternoon, January 7

Introductory Remarks and Opening Address: *W. Arbuckle, Chairman, IRE Orlando Section, Radiation, Inc., Orlando, Fla.; J. W. Dees, Chairman, Millimeter and Sub-*

millimeter Conference, Martin Company, Orlando, Fla.

Opening Address: "State of the Art—Background and Recent Developments," *Dr. P. D. Coleman, Department of Electrical Engineering, University of Illinois, Urbana, Ill.*

Session I—Millimeter and Submillimeter Transmission Lines

Moderator: *Georg Goubau, USAERDL, Fort Monmouth, N. J.*

"The H-Guide Concept, a Method for Low-Loss Transmission at MM Waves," *F. J. Tischer, Ohio State University, Columbus, Ohio. (Invited)*

"A Low Loss Waveguide System and Components," *A. P. King, Hughes Aircraft Company, Culver City, Calif. (Invited)*

"Transmission Methods for Short Millimeter Waves," *F. Sobel, M. Cohn, M. King, and J. Wiltsch, Electric Communication, Inc., Timonium, Md.*

"Millimeter Transmission by Oversize and Shielded-Beam Waveguides," *G. R. Valenzuela, Carlyle Barton Lab., Johns Hopkins University, Baltimore, Md.*

"Investigations on a Beam Waveguide for Optical Frequencies," *G. Goubau and J. R. Christian, USAERDL, Fort Monmouth, N. J.*

Session II—Resonant Structure and Quasi-Optical Techniques

Moderator: *Yardley Beers, National Bureau of Standards, Boulder, Colo.*

"Experimental Study of Spherical Mirror Fabry-Perot Resonators," *R. W. Zimmerer, National Bureau of Standards, Boulder, Colo. (Invited)*

"Design Problems and Performance of Millimeter Wave Fabry-Perot Reflector Plates," *H. Welling and H. G. Andresen, USAERDL, Fort Monmouth, N. J.*

"Quasi-Optical Techniques for Millimeter Wave Transmission," *R. G. Fellers, University of South Carolina, Columbia, S. C. (Invited)*

"Submillimeter Components using Oversize Quasi-optical Waveguides," *J. J. Taub, H. Hindin, and M. L. Wright, Airborne Instruments Lab., Deer Park, N. Y.*

"Lens Systems for Millimeter Wave Antennas," *M. A. Kott, Carlyle Barton Lab., Johns Hopkins University, Baltimore, Md.*

"Optical and Quasi-Optical Transmission Techniques and Component Systems for Millimeter Wavelengths," *R. H. Garnham, Royal Radar Establishment, Great Malvern, Worcester, England.*

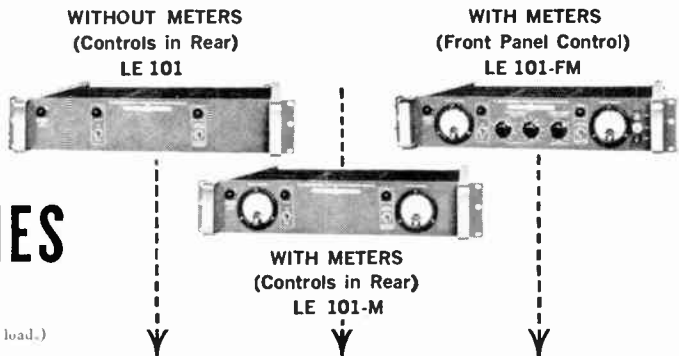
Only Lambda offers:

Environment-engineered power supplies

mass-produced at Competitive Prices

**NEW
LE SERIES**

DC OUTPUT
(Regulated for line and load.)



0-36 VDC	5 Amp	LE 101	\$420	LE 101-M	\$460	LE 101-FM	\$470
0-36 VDC	10 Amp	LE 102	525	LE 102-M	565	LE 102-FM	575
0-36 VDC	15 Amp	LE 103	595	LE 103-M	635	LE 103-FM	645
0-36 VDC	25 Amp	LE 104	775	LE 104-M	815	LE 104-FM	825
0-18 VDC	8 Amp	LE 105	425	LE 105-M	465	LE 105-FM	475
0- 9 VDC	10 Amp	LE 109	430	LE 109-M	470	LE 109-FM	480

Plus THESE FEATURES:

- All solid state
- Completely protected
- Adjustable automatic current limiting
- Continuously variable
- Remotely programmable over entire range
- Constant voltage/constant current
- Wide input frequency and voltage range
- Convection cooled—no blowers
- 50°C ambient
- Guaranteed 5 years

CONDENSED TENTATIVE DATA

REGULATED VOLTAGE:

Regulation

(line and load) Less than .05 per cent or 8 millivolts (whichever is greater). For input variations from 105-135 VAC and for load variations from 0 to full load.

Transient Response

(line) Output voltage is constant within regulation specifications for any 15 volt line voltage change within 105-135 VAC.

(load) Output voltage is constant within 25 MV for load change from 0 to full load or full load to 0 within 50 microseconds of application.

Remote Programming 50 ohms/volt constant over entire voltage range.

Ripple and Noise Less than 0.5 millivolt rms.

Temperature Coefficient Less than 0.015%/°C.

AC INPUT: 105-135 VAC; 45-66 CPS and 320-480 CPS in two bands selected by switch.

OVERLOAD PROTECTION:

Thermal Thermostat, reset by power switch, thermal overload indicator light front panel.

Electrical:

External Overload

Protection Adjustable, automatic electronic current limiting.

METERS: Ruggedized voltmeter and ammeter to Mil-M-10304B specifications on metered models.

PHYSICAL DATA:

Mounting Standard 19" rack mounting.

Size LE 101, LE 105, LE 109 3½" H x 19" W x 16" D
 LE 102 5¼" H x 19" W x 16" D
 LE 103 7" H x 19" W x 16½" D
 LE 104 10½" H x 19" W x 16½" D

SEND FOR COMPLETE DATA ON LE SERIES



LAMBDA ELECTRONICS CORP.

515 BROAD HOLLOW ROAD • HUNTINGTON, L. I., NEW YORK • 516 MYRTLE 4-4200

Western Regional Office: 230 North Lake Avenue, Pasadena, California • Phone: Code 213, MUrray 1-2544
 New England Regional Office: 275 Boston Post Road, Marlboro, Massachusetts • Phone: Code 617, HUNtley 5-7122
 Middle Atlantic District Office: 515 Broad Hollow Road, Huntington, L. I., New York • Phone: Code 516, MYrtle 4-4200
 Southeastern Region: W. A. Brown & Associates, Inc., Engineering Representatives
 Orlando, Fla. • Fort Lauderdale, Fla. • Huntsville, Ala. • Alexandria, Va. • Winston-Salem, N. C.

Tuesday, January 8

Session III—Millimeter Components

Moderator: *L. L. Bertran, FXR, Inc., Woodside, N. Y.*

"TE₀₁ Mode Components in the 3 MM Region," *Alan J. Simmons, TRG Inc., East Boston, Mass.* (Invited)

"A Range of 2 and 1 Millimetre Waveguide Components," *R. Meredith and G. H. Preece, Royal Radar Establishment, Great Malvern, Worcester, England.*

"Resonant Cavity Type Mode Transducer and Mode Filter for the Circular TE₀₂ Mode," *S. Shimada, Hitachi, Central Research Laboratory, Kokubunji, Tokyo, Japan.*

"A Simple Grating System for Millimeter and Submillimeter Wavelength Separation," *K. B. Mallory and R. H. Miller, Stanford University, Stanford, Calif.; P. A. Szente, Instituto Tecnológico de Aeronautica, Sao Paulo, Brazil.*

"Design of Some New T-Band Components," *P. Wolfert, Sylvania Electronic System-Central, Buffalo, N. Y.*

"An Automatic Swept-Frequency Smith Chart Plotter," *Ir. F. C. deRonde, Philips Research Laboratories, Eindhoven, Netherlands.*

"Magnetic Materials for Millimeter Wave Applications," *P. Rodrique, Sperry Microwave Electronics Company, Clearwater, Fla.* (Invited)

"Millimeter Resonance Isolators Utilizing Hexagonal Ferrites," *G. R. Harrison, D. R. Taft, and L. R. Hodges, Jr., Sperry Microwave Electronics Company, Clearwater, Fla.*

"Development of Gaseous Switching Devices at a 3.2-MM Wavelength," *J. D. Woermbke, T. M. Nelson, and S. D. Schreyer, Westinghouse, Baltimore, Md.*

"Status Report on International Millimeter Waveguide Flange Standards," *Tore N. Anderson, Budd-Stanley Company, Inc., Syosset, N. Y.*

Tuesday Afternoon

Session IV—Millimeter Techniques and Measurements

Moderator: *D. D. King, Electronic Communications, Inc., Timonium, Md.*

"Microwave Type Bolometer for Submillimeter Wave Measurements," *J. F. Byrne and C. E. Cook, Motorola Inc., Riverside, Calif.*

"A Measurements System for 50-90 Gc," *M. W. Long and J. C. Butterworth, Georgia Institute of Technology, Atlanta, Ga.*

"A Relative Amplitude and Phase Plotter for Millimeter Wave Fields," *P. Wolfert and T. Schiller, Sylvania Electronic System-Central, Buffalo, N. Y.*

"A Measurement of Detector Impedance at Millimeter and Submillimeter Wavelengths," *K. B. Mallory and R. H. Miller, Stanford University, Stanford, Calif.; P. A. Szente, Instituto Tecnológico de Aeronautica, Sao Paulo, Brazil.*

"Frequency Stabilization of a Millimeter BWO," *R. Kopeck, Sylvania Electronic System-Central, Buffalo, N. Y.*

"A Frequency Lock System for Millimeter Wave Klystrons," *H. Welling and H. G. Andresen, USAERDL, Fort Monmouth, N. J.*

"Detection of Microwave Radiation from the Re-Entry Plasma," *D. Keren,*

RCA, Burlington, Mass.

"Millimeter Radar Techniques for Studying Plasma Effects Associated with Hypersonic Velocity Projectiles," *P. E. Robillard, H. M. Musal and R. I. Primich, General Motors Corp., Santa Barbara, Calif.*

"Millimeter Wavelength Focussed Probes and Focussed Resonant Probes for Use in Studying Ionized Wakes behind Hypersonic Velocity Projectiles," *R. I. Primich and R. A. Hayami, General Motors Corp., Santa Barbara, Calif.*

"A Narrow-Bandwidth Heterodyne Detection System for Millimeter Wave Measurements," *S. Okamura, T. Okoshi, and S. Kawakami, University of Tokyo, Tokyo, Japan.*

"Millimeter Single-Sideband Generators," *W. P. Ernst and A. Skislaw, Princeton University, Princeton, N. J.*

"Some Quantum Considerations for Submillimeter and Optical Communications," *D. P. Harris and W. R. Ramsay, Lockheed Missiles and Space Company, Palo Alto, Calif.*

Tuesday Evening Session

Moderator: *To be announced.*

This Session will be held open for possible Russian participation and/or for post deadline papers which represent unusual current interest, major achievements or advances in the field of millimeter and submillimeter technology.

Wednesday, January 9

Session VA—Millimeter Sources

Moderator: *Howard Scharfman, Spencer Laboratory, Raytheon Company, Burlington, Mass.*

"Conventional Reflex Klystron and Magaetron Short MM Waves," *Th. I. Splenger and G. H. Plantina, Phillips Research Laboratories, Eindhoven, Netherlands.* (Invited)

"Magnetic Field Reflex Klystrons and Frequency Multipliers for Millimeter Wave Generation," *E. A. Ash, Standard Telecommunication Laboratories Ltd., Harlow, Essex, England.*

"The Generation of High-Pulsed Power at Millimeter Wavelengths Using the Ubitron," *R. M. Phillips, General Electric Company, Palo Alto, Calif.*

"Production of Submillimeter Waves by Bunched, Relativistic Electrons," *K. B. Mallory and R. H. Miller, Stanford University, Stanford, Calif.; P. A. Szente, Instituto Tecnológico de Aeronautica, Sao Paulo, Brazil.*

"Bunching of an Electron Beam by Deflection Modulation," *J. R. Baird and P. D. Coleman, Ultramicrowave Group, University of Illinois, Urbana, Ill.*

"The Laddertron—A New Millimeter Wave Power Oscillator," *K. Fujisawa, Osaka University, Toyonaka, Osaka, Japan.*

"New Types of Millimeter Wave Tubes with Ladder Structures," *S. Aoi, S. Nakajima, Y. Arai and R. Higashi, Oki Electric Industry Company, Ltd., Tokyo, Japan.* (Invited)

"Two Classes of Interaction Circuits for Millimeter Wave Generation and Amplification," *D. C. Buck, Westinghouse, Elmira, N. Y.*

"A Racetrack Microtron for Millimeter and Submillimeter Wave Generation," *H. Froelich and E. Brannen, University of*

Western Ontario, London, Canada.

"Crossed-Field Frequency Multiplier Interaction," *J. B. Thomas, Raytheon Company, Burlington, Mass.*

Wednesday Afternoon

Session VB—Millimeter Sources

Moderator: *Howard Scharfman, Spencer Laboratories, Raytheon Company, Burlington, Mass.*

"Cerenkov Radiation in Anisotropic Ferrites," *F. J. Rosenbaum and P. D. Coleman, Ultramicrowave Group, University of Illinois, Urbana, Ill.*

"A 1-Watt CW-Backward Wave Oscillator for the 50-75 Gc Band," *R. T. Schumacher, Varian Associates, Palo Alto, Calif.*

"Wide Tuning Range Swept Oscillator Sources for 48-110 Gc," *J. A. Noland, W. R. Day, and L. Sandstrom, Sperry Rand Corp., Gainesville, Fla.*

Session VI—Millimeter Masers

Moderator: *Frank S. Barnes, University of Colorado, Boulder, Colo.*

"Extension of the Laser-Pumped Ruby Maser to Millimeter Wavelengths," *D. P. Devor, Hughes Research Laboratories, Malibu, Calif.* (Invited)

"Multiple Quantum Effects at Millimeter Wavelengths," *R. H. Pantell and R. G. Smith, Stanford University, Stanford, Calif.* (Invited)

"Stimulated Emission in the Submillimeter Region," *R. J. Strain and P. D. Coleman, Ultramicrowave Group, University of Illinois, Urbana, Ill.*

"Packaged Tunable Traveling-Wave and a Maser Radiometry for the 8 MM Band," *F. R. Arams, B. Peyton, J. Baris, and J. Franceschini, Airborne Instruments Laboratory, Deer Park, N. Y.*

"Generation of MM-Waves by Multiple Quantum Transitions," *H. G. Andresen, USAERDL, Fort Monmouth, N. J.*

"Millimeter Wave Generation by Non-linear Quantum Susceptibility," *D. P. Akitt, R. J. Strain, and P. D. Coleman, Ultramicrowave Group, University of Illinois, Urbana, Ill.*

Wednesday Evening Banquet

Toastmaster: *H. E. Webber, Director, Advanced Technology, The Martin Company, Orlando, Fla.*

Speaker: *P. A. Siple, Scientific Advisor, U. S. Army Research Office, Arlington, Va.*

Thursday, January 10

Session VII—Harmonic Generation and Detection Techniques

Moderator: *J. M. Richardson, National Bureau of Standards, Boulder, Colo.*

"Backward Diodes for Low-Level Millimeter Wave Detection," *C. A. Burrus, Bell Telephone Laboratories, Holmdel, N. J.* (Invited)

"A Universal Wall-Current Detector," *Ir. F. C. deRonde, Phillips Research Laboratories, Eindhoven, Netherlands.*

"Millimeter Wave Harmonic Generators, Mixers and Detectors," *F. L. Wentworth, J. D. Rodgers, J. W. Dozier, and M. Cohn, Electronic Communications, Inc., Timonium, Md.*

"Harmonic Generation by Electron Beam Virtual Bunching with Sweep Modu-

To Contractors and Subcontractors
on U. S. Government Projects

Western Electric offers high reliability diodes, transistors and magnetrons

- Western Electric's Laureldale, Pennsylvania, plant is now in its tenth year of producing semiconductor devices of ultra-high quality and reliability for government applications.
- Devices designed by a resident Bell Telephone Laboratories group have performance standards exceeding specification requirements which are based on MIL-S-19500B.
- Mechanized production facilities and a comprehensive statistical quality control program assure uniformity and contribute to obtaining ultimate process capabilities.
- For further information on Western Electric-Laureldale electron devices and magnetrons . . .

Telephone — Area Code 215 — 929-5811

LAURELDALE PLANT
MAKER OF ELECTRON PRODUCTS



lation," *G. T. Flesher, General Motors Corp., Santa Barbara, Calif.*

"Harmonic Generation and Detection Theory with Field Emission Cathodes," *G. T. Flesher, General Motors Corp., Santa Barbara, Calif.; E. Brannen, University of Western Ontario, London, Canada*

"An In-Line Harmonic Generator," *E. G. Wessel, University of Colorado, Boulder, Colo.; R. J. Strain, University of Illinois, Urbana, Ill.*

Session VIII—Millimeter Receivers— Radiometry—Propagation

Moderator: *E. W. Richter, RCA, Burlington, Mass.*

"Superheterodyne Radiometers for Use at 70 Gc and 140 Gc," *R. Meredith, F. L. Warner, Royal Radar Establishment, Great Malvern, Worcester, England. (Invited)*

"High Sensitivity 100 to 300 Gc Radio-M. Cohn, F. L. Wentworth, and J. C. Wiltse, *Electronic Communications, Inc., Timonium, Md. (Invited)*

"Radiometry in the Submillimeter Region," *R. A. Williams and W. S. C. Chang, Ohio State University, Columbus, Ohio.*

"Factors Affecting Earth-Satellite Millimeter Wavelength Communications," *A. W. Straiton and C. W. Tolbert, University of Texas, Austin, Tex. (Invited)*

"A Submillimeter Superheterodyne Receiver," *J. Cotten, Electronic Communications, Inc., Timonium, Md.*

Thursday Afternoon

Session IX—Millimeter Spectroscopy and Resonance Phenomena

Moderator: *G. Heller, MIT Lincoln Laboratory, Lexington, Mass.*

"Recent Millimeter Wave Experiments in Solids," *G. Heller, MIT Lincoln Laboratory, Lexington, Mass. (Invited)*

"A Submillimeter Interference Spectrometer" *W. K. Rivers, Jr. and M. S. Spiel, Georgia Institute of Technology, Atlanta, Ga.*

"Spectroscopic Techniques in the Millimeter Region," *J. J. Gallagher, Martin Company, Orlando, Fla.*

Session X—Open Discussions

Moderator: *Benjamin Lax, MIT Lincoln Laboratory, Lexington, Mass.*

Panel: *M. W. P. Strandberg, MIT, Department of Physics, Cambridge, Mass.; H. Motz, Oxford University, Oxford, England; W. P. Ayres, Melabs, Palo Alto, Calif.; C. B. Wharton, General Dynamics Corp., San Diego, Calif.*

The papers presented at this Conference will encompass a wide variety of new ideas on millimeter wave generation, applications, and techniques. This session will be open for further discussion of these ideas and for a general exchange of information on millimeter topics. In addition, the following topics will be open for discussion: Application of High Magnetic Fields to Millimeter Problems; Millimeter Pulse Work; Future Trends in Millimeter and Submillimeter Technology.

9th National Symposium on Reliability and Quality Control

SHERATON-PALACE HOTEL, SAN FRANCISCO, CALIF., JANUARY 22-24, 1963

The Ninth National Symposium on Reliability and Quality Control, sponsored by the IRE Professional Group on Reliability and Quality Control, AIEE, ASQC, and EIA, will be held at the Sheraton-Palace Hotel, San Francisco, Calif., on January 22-24, 1963. The program of the Symposium is as follows:

Tuesday, January 22

Session 1—Keynote Address and Panel Response

"Current Management Reliability Objectives," *Lysle A. Wood, Vice President, General Manager, Boeing Aero-Space Division.*

Panel Response

Moderator: *J. M. Bridges, Director, Office of Electronics, ODDR&E.*

Session 2A—General Management

Moderator: *L. W. Ball, Boeing, Aero-Space Division.*

"The Management and Engineering Approach to Product Quality," *A. V. Feigenbaum, General Electric Company.*

"System Worth and Incentive Contracts," *W. C. Fredrick, ARINC Research Corporation.*

"Incentive Contracts and Product Assurance," *E. F. Dertinger, Raytheon Company.*

"The Role of the Buyer in Reliability," *R. T. Dewey, Boeing, Aero-Space Division.*

Session 2B—Research and Training

Moderator: *E. J. Nucci, Office of Engineering Management, ODDR&E.*

"Future Needs in Research and Training," *M. M. Tall, Radio Corporation of America.*

"Reliability Physics (The Physics of Failure)," *D. R. Earles, AVCO Corporation and Mary F. Eddins, AVCO Corporation.*

"Systems Reliability Engineering Graduate Program," *T. L. Regulinski, Wright-Patterson AFB, Air Force Institute of Technology.*

"A Proposal Curriculum for Reliability Engineering," *H. C. Jones, University of Maryland.*

Tuesday Afternoon

Session 3A—Program Management

Moderator: *R. G. Gibson, Lockheed Missiles and Space Company.*

"Military Customers Management of Quality Control and Reliability Programs," *Comdr. R. W. Smiley, Bureau of Naval Weapons.*

"Parts Oriented Reliability Program Problems," *C. S. Bartholomew, The Boeing Company.*

"Reliability—Small Companies—Space Subsystems," *M. D. Johnson, Santa Barbara Research Center.*

"The Computer Reliability Report," *I. R. Whiteman, C-E-I-R, Inc.*

Session 3B—Systems Analysis

Moderator: *L. S. Gephart, Lockheed Missiles and Space Company.*

"The Reliability of Repairable Systems," *G. Nagy, Goodyear Aircraft Corporation.*

"An Easy Design Method of Having Highest Systems Reliability," *M. Sasaki, Defense Academy, Japan.*

"A Realistic Measure of Spacecraft Reliability," *G. R. Grainger, W. E. Faragher, and L. L. Philipson, Planning Research Corporation.*

"Bureau of Ships Maintainability Specification," *Jacob Sacks and Gerald Margulies, Bureau of Ships, Navy Department.*

Wednesday, January 23

Session 4A—Electronic Parts

Moderator: *Herbert E. Morrison, Litton Systems, Inc.*

"Building Blocks of Reliable Circuits and Systems," *Donald J. Hamman, Battelle Memorial Institute.*

"Component Parts Reliability Programs at USASRD," *J. W. Gruol, U. S. Army Signal Research and Development Laboratory, Fort Monmouth, N. J.*

"The Development of a Selective Degradation Screen for Detecting Potentially Unreliable Silicon Transistors," *Albert Fox and C. H. Zierdt, Jr., General Electric Company.*

"Separation of Accelerated Failure



**20 CPS TO 200 KC
ULTRA STABLE "AUDIO"
SWEEPING OSCILLATOR**

**KAY
Sona-Sweep MODEL M
141-C**

- Sweep audio frequencies high-Q filters, tape recorders.
- Ultra-stable narrow frequency sweeps 20 cps to 200 kc.
- 200 cps to 200 kc in single frequency sweep.
- Both linear and logarithmic sweeps plus manual sweep control.
- Built-in audio detector.
- Fixed and variable pulse type markers.

New Alignment Technique

The Sona-Sweep Model M adapts the accepted techniques of r-f swept frequency alignment to audio and ultrasonic (e.g., tape recorder) bandpass measurements and adjustments. In addition, the highly stable response curve developed by the Model M and the parallel display provided by its manual control, give easier, more accurate checks of high Q filters and sharp slope devices.

Detecting At Audio

A major disadvantage of previous sweeping oscillator techniques for use at audio frequencies has been the difficulty of obtaining a clean envelope response. Usually, no single audio frequency detector covers the octaves of the full audio range. Often, too, the large bypassing necessary slows down detector response so as to make it inaccurate for changing (swept) conditions. To eliminate this difficulty, a synchronous detector has been provided, giving adequate bypassing down to about 200 cps.

Single Trace With Markers

A clean, detected envelope of audio frequency bandpass characteristics clearly defines amplitude vs frequency. The increase in trace intensity provided by the detected signal (rather than by a diffused a-f pattern) makes it much easier to view the response characteristics and to monitor any adjustments of the circuit under test. The sharp pulse type markers provided by the Model M precisely and clearly define critical points along the trace.

Model M — A Complete System

The Model M provides a complete measurement system, including—logarithmic, linear

and manual sweeps, or a calibrated c-w signal; sharp, "crystal," pulse type frequency markers and precision step attenuator.

Variable Center Frequencies

The Model M is a double heterodyne sweep generator employing three crystal controlled oscillators. Either linear or log sweeps are available with center frequencies continuously variable between 20 cps and 200 kc. The swept output is blanked during retrace time, providing a zero-voltage base line. To eliminate phasing adjustments, a sawtooth voltage, synchronized with the swept output, is available to drive the X-axis of the scope.

Varied Sweep Rates

For checking high-Q circuits and low frequency response characteristics, variable rep rates down to 0.2 cps are available. This wide choice of rep rates, continuous to 25 cycles, plus a 30 cycle lock, permits selection of the optimum rep rate which gives an accurate response display of the circuit being tested, plus ease of viewing on the scope screen.

Varied Sweep Widths

Sweep widths are continuously variable from 20 cps to 200 kc. In each of three steps — 2 kc, 20 kc, 200 kc—new modulating circuits are switched in to provide maximum stability in each range.

Logarithmic Sweeps

A nominally logarithmic sweep, most useful for studying audio and video low pass circuits, provides an expanded view of the low frequency end, while showing overall frequency characteristics.

Manual Sweep

A manually controlled swept output provides a means of varying cw signal in synch with the oscilloscope display. The manual control covers the same frequency range to which the Model M is set for electronic sweeping. It can be used to examine response characteristics in detail, or in response to cw and near cw conditions. When the Sona-Sweep is used with an electronic counter and accurate voltmeter, it can perform all the checks where cw is preferred. In addition, it can utilize the counter and its scope synchronization feature to frequency calibrate the oscilloscope display.

High Level Output

The Model M delivers a high level output of 5 volts rms into 600 ohms over the entire frequency range. The built-in, precision step attenuator provides up to 59 db of attenuation in discrete steps. An additional 6 db of variable attenuation is provided. Output is flat within ± 0.5 db.

SPECIFICATIONS

Center Frequency Range: 20 cps to 200 kc. Continuously variable.

Sweep Width — Three ranges: 20 cycles to 2 kc., 200 cycles to 20 kc., 200 cycles to 200 kc.

Sweep Output And Repetition Rates:

Sawtooth for horizontal deflection of scope trace. Low impedance output, approx. 3 V pp.

a. Fixed at 30 cps in Line-Lock mode.
b. Variable 0.2 to 25 cps for logarithmic sweep.

c. Three continuously variable linear ranges: 0.2 cps to 1 cps, 1 cps to 5 cps, 5 cps to 25 cps.

Output Level: 5 volts rms into 600 ohms.

Flatness: ± 0.5 db over widest sweep.

Markers: (Optional): Ten crystal pulse type markers, positioned at customer specified frequencies; e.g., 200 cycles, 500 cycles, 1 kc, 2 kc, 5 kc, 20 kc, 50 kc, 100 kc and 200 kc.

Markers designated for use at wide sweep (200 kc) are not applicable to other sweep widths. Specify whether for wide (200 kc) or narrow (less than 20 kc).

Calibrated CW Output: 20 cps to 200 kc.

Built-In Attenuator: Switchable steps, 3 db, 6 db, 10 db, 20 db, 20 db, plus 6 db variable.

Power Supply: Input approximately 220 watts. 117 volts ($\pm 10\%$), 60 cps B+ electronically regulated.

Dimensions: 19 $\frac{3}{8}$ " x 10 $\frac{7}{8}$ " x 16 $\frac{1}{2}$ ".

Price:

\$1295.00 f.o.b. factory \$1425.00 f.a.s. N.Y.

\$17.00 ea. for markers \$19.00 ea. for markers

Weight: 57 lbs.

KAY ELECTRIC COMPANY

Dept. I-12 • MAPLE AVE., PINE BROOK, MORRIS COUNTY, N. J. • Capital 6-4000

Modes in Semiconductors, *W. D. Rowe, Sylvania Electronic Systems.*

Session 4B—Fabrication and Assembly

Moderator: *D. A. Hill, Hughes Aircraft Company.*

"The Impact of Reliability of Manufacturing," *J. Fernbach, International Business Machines.*

"Human Reliability Production Auditing," *D. Meister, General Dynamics/Astronautics.*

"Analysis of In-Plant Component Failure," *R. P. Caldarone, Mary Lou Wolf, and J. W. Dzimianski, Westinghouse Electric Corporation.*

"Criteria for Solder Joints—Metallurgical Completeness," *J. D. Keller, Martin Marietta Corporation.*

Wednesday Afternoon

Session 5A—Electronic Parts

Moderator: *Clifford C. Peterson, Motorola, Inc., Western Military Electronics Center.*

"Life Performance Observations on Corning Oxide Resistors," *Lawrence D. Hines, Corning Glass Works.*

"Reliability of Printed Wiring Cordwood Modules," *Thomas S. Gore, Jr. and Weldon V. Lane, U. S. Army Signal Research and Development Laboratory, Fort Monmouth, N. J.*

"Failure Analysis of Potted Electronic Modules," *Burton S. Levin, Re-Entry Systems Department, General Electric Company.*

"Safeguarding Dense Electronic Packages from Human Error," *Dr. Melvin Freitag and H. G. Frankland, Ryan Electronics/Ryan Aeronautical Company.*

Session 5B—Inspection and Screening

Moderator: *W. N. Lamb, Bendix Pacific Corporation.*

"Manufacturing Reliability," *B. L. Lubelsky, Lockheed Missiles and Space Company.*

"Infrared Techniques Enhance Electronic Reliability," *Ricardo Vanzetti, Raytheon Company.*

"Sequential Three-Way Classification of Lot Quality," *J. A. Lecher and H. Ginsburg, Westinghouse Research Laboratories.*

"Weibull Tables for Bio-Assaying and

Fatigue Testing," *H. P. Goode, and John H. K. Kao, Cornell University.*

Session 5C—Statistics

Moderator: *J. T. Koppenhaver, N.A.S.A.*

"Using Transfer Functions in Reliability Prediction," *I. Bosinoff, Sylvania Electronic Systems.*

"Exact Truncated Sequential Tests," *L. A. Aroian, Reliability Staff, Space Technology Laboratories.*

"Monte Carlo: Reliability Tool for Design Engineers," *F. Harris and J. Myers, Aerospace Division, Hughes Aircraft Company.*

"Reliability Models in Space Systems Planning and Decision-Making," *G. H. Sandler, Major Systems Division, Radio Corporation of America.*

Thursday, January 24

Session 6A—Design Review

Moderator: *E. F. King, University of California, Los Angeles.*

"Effective Design Review Administration," *J. Y. McClure, General Dynamics Corporation.*

"Component Part Failure Rate Curve Considerations," *Daniel A. Adams, International Business Machines Corporation.*

"Reliability Assurance for Custom Testers," *B. O. Allen and W. W. Westman, Sandia Corporation.*

"Reliability Evaluations by Computer Simulation," *E. Veitsch and G. Ashendorf, Radio Corporation of America.*

Session 6B—Quality Assurance

Moderator: *J. Condon, N.A.S.A.*

"How to Select Optimum Burn-in Duration for Parts," *R. H. Norris, General Electric Company.*

"Case History—Quality Engineering in Action," *E. H. Nielsen, Minneapolis-Honeywell Regulator Company.*

"Reliability Takes Part in a Vendor Rating Program," *L. G. Rado, Cannon Electric Company.*

"Some Pitfalls of the Weibull Distribution," *Paul Gottfried and H. R. Roberts, Booz-Allen.*

Session 6C—Mechanical Aspects of Electronic Design

Moderator: *John de S. Coutinho, Grum-*

man Aircraft Engineering Corporation.

"System Design for Reliability," *Henry F. Katzenstein, Solid State Radiations, Inc.*

"Design, Reliability and Commercial Automatic Pilots," *R. H. Wagner, Sperry Phoenix Company.*

"Environmental Chamber System Engineering," *A. R. Saltzman, U. S. Saltzman, U. S. Naval Air Development Center.*

"Process Control and Reliability," *Walter H. Friedlander, Collins Radio Company.*

Thursday Afternoon

Session 7A—Design Testing

Moderator: *W. Cox, Northrop Corporation.*

"Reliable Systems Versus Automatic Testing," *Alan D. Swain, Sandia Corporation.*

"Sequential Testing of Electronics Systems," *W. F. Mikhail and J. H. Bailey, International Business Machines Corporation.*

"A Controlled Study of Automated Testing Techniques," *Philip R. Oyerly and Dewey C. King, ARINC Research Corporation.*

"Limitations of Plans Designed to Demonstrate Minimum Life with High Confidence," *Benjamin Epstein, Consultant, Palo Alto, Calif., and Andrew C. Gorski, Autometrics Division, North American Aviation, Inc.*

Session 7B—Maintenance and Operation

Moderator: *F. L. Ankenbrandt, Brig. Gen., USAF (Ret.) Radio Corporation of America.*

"Relationship of Apollo Program Reliability to an Integrated System Checkout Plan," *James E. Sloan, N.A.S.A.*

"Reliability Approach to the Spare Parts Problem," *G. H. Ebel and Andrew J. Lang, Fairchild Camera and Instrument Corporation.*

"On the Proper Preventive Maintenance," *H. H. Cho, Laboratory for Electronics, Inc.*

"A Practical Approach to Maintainability Prediction," *G. T. Harrison, Jr., ARINC Research Corporation.*

"A Procedure for System Maintainability Testing," *B. L. Retterer and R. A. Miles, RCA Service Company.*

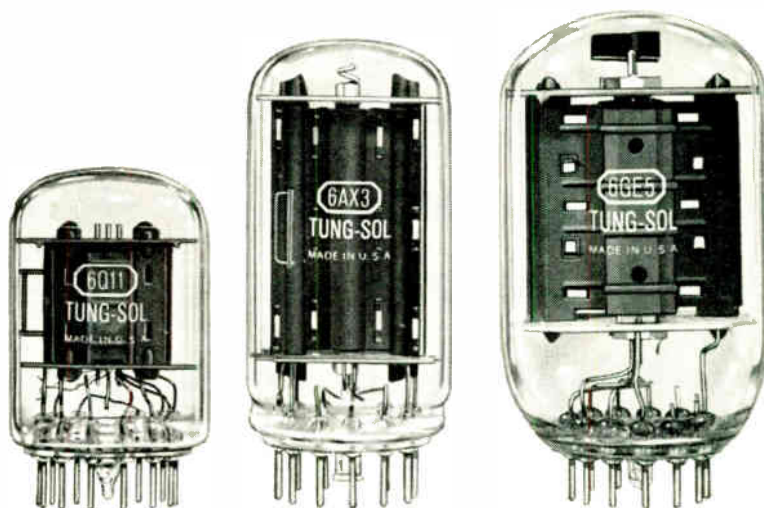
Higher Performance Standards With Improved Reliability...

Tung-Sol compactrons provide several advantages that can contribute to lower costs and improved performance. For example, the increased number of pins permit greater heat dissipation. As a result, compactrons run cooler with higher reliability than conventional tubes. The exhaust tubulation is situated between the pins so that broken tips rarely occur. This also permits the use of top

caps for very high voltage designs. In addition, the compactron design readily lends itself to combining multiple tube elements within a single envelope.

Compactrons require less space on the chassis or printed circuit boards, less height than conventional tubes, less air cooling volume per function. More space between pins improves element isolation, allows higher voltage ratings, simplifies printed circuit and chassis design.

Tung-Sol compactrons are available in production volume for numerous circuit requirements, including radio, tv, hi-fi and stereo, controls and instrumentation equipment. Write for Tung-Sol compactron data file which includes the following types: 6AX3, 6GE5, 6Q11, 12AX3, 12GE5, 8149, 8150 and 1AJ2. Other types will soon be available and special designs will be considered. Tung-Sol Electric Inc., Newark 4, N.J. TWX: NK193.

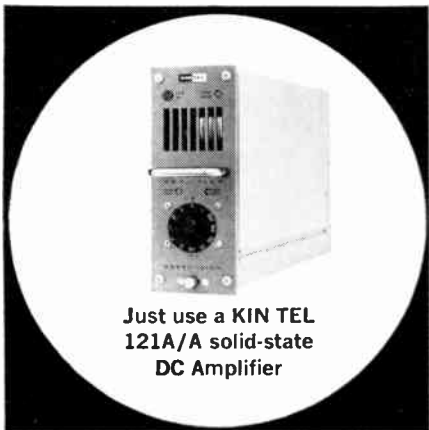


TUNG-SOL COMPACTRONS

 **TUNG-SOL®**



accurate
amplification
of low-level
signals from
DC to
beyond 200 kc?



Just use a KIN TEL
121A/A solid-state
DC Amplifier

The KIN TEL 121A/A is a non-inverting amplifier with response from DC to beyond 200 kc. It has fixed gains of 0, +1, +10, +20, +30, +50, +100, +200, +300, +500, and +1000, and a control that adjusts any fixed gain from X1 to X2.2. Amplification is stable within 0.01%, accurate within 0.1% for all gains other than +1 (0.2% accuracy at +1), linear within 0.005% for outputs up to ± 15 volts DC with loads of 200 ohms or more. Input impedance is greater than 10 megohms (less than 500 pf to 50 kc); output impedance is less than 0.3 ohm and 50 μ h. Frequency response is flat within 0.25% to 2 kc, within 4% to 10 kc, within 3 db to 200 kc. Drift is less than ± 2.0 μ v equivalent input for over 40 hours at +1000 gain. Equivalent input noise at +1000 gain is 3 μ v peak-to-peak in a 20-cps band, 3 μ v RMS in a 50-kc band. Output capability is ± 15 volts into 200 ohms, ± 100 ma into 10 to 100 ohms. Amplifier fits standard KIN TEL cabinets and modules. Price \$1000.

Representatives in all major cities



5725 Kearny Villa Road, San Diego 12, Calif.
Phone 277-6700 (Area Code 714)



Industrial Engineering Notes*



PETITION TO FCC FOR CHANNELS 14 AND 15

The Federal Communications Commission will be asked today to assign ultra high frequency television channels 14 and 15 to two-way, land mobile radio services to relieve frequency congestion "seriously impairing" communications of public safety agencies, health services, and industry.

The request will be made in a petition to be filed with the FCC exclusively by the Land Mobile Communications Section of the Electronic Industries Association.

TV viewers on channels 14 and 15, the petition emphasized, would be protected against interference by forbidding mobile systems to operate within the coverage area of existing channel 14 or 15 television stations.

"Many of the individual radio services within the Safety and Special Services group are presently suffering highly crowded conditions that have required stacking 20-30 users on the same frequency in the same area, seriously impairing the effective use of their land mobile radio communications," the petition declared.

William J. Weisz, EIA Land Mobile Section Chairman and Vice President of the Communications Division of Motorola Inc., said the most seriously affected area of the country is Los Angeles where as many as 50 systems are packed into the same frequency.

"Many communities, moreover, cannot set up needed additional public safety radio systems without prohibitively sacrificing communications efficiencies," Mr. Weisz said. "Lack of frequencies is seriously hampering police and fire departments, emergency services, highway maintenance and other local government operations, transportation, and essential business and industrial communications."

Channels 14 and 15, the petition pointed out, "are presently being very sparsely used in the United States, with only three stations in operation on Channel 14 and five in operation on Channel 15."

ASSOCIATION ACTIVITIES

EIA's brochure to interest and guide high school and first-year college students in taking advantage of career opportunities in the electronics industry is expected to be available for distribution in about two weeks, Educational Coordinating Committee Chairman Ben Edelman (Western Electric Co.) said last week. Mr.

Edelman said the brochure, printed in three colors, "dramatically highlights a history of accomplishment in electronics and pictures an array of opportunities for career fulfillment in our industry." A key section, he pointed out, will tell students what they should do to prepare themselves for careers ranging from skilled electronics plant worker to administrator or scientist. Distribution plans are being worked out with national organizations of educators and arrangements will be made for EIA member-companies to make copies available to schools in their area, Mr. Edelman said. Single copies will be sent without charge from EIA to school administrators, guidance counsellors, and science and mathematics teachers. Bulk orders from schools will be filled at a special price, he said, and member-companies will be offered the publication, in quantity, at a charge which will only partially recapture printing costs. The brochure, "Electronics—Your Chance To Shape the Future," was prepared under the supervision of the Educational Coordinating Committee in cooperation with the IRE.

GOVERNMENTAL AND LEGISLATIVE

Dissemination of scientific and technical information generated by Government agencies has become a national problem and can no longer be handled on an agency-by-agency basis, according to Dr. Jerome B. Wiesner, Director of the Office of Science and Technology. More than 35 Government departments and agencies carry on scientific and technical information activities and each must tailor its information system to its mission under separate legislative authority, Dr. Wiesner told the Senate Reorganization Subcommittee at hearings on shortcomings in dissemination of information. He called for an interlocking system of agency information activities overseen by the Federal Council for Science and Technology and operating under policy guidance of the Office of Science and Technology. Deputy Defense Secretary Roswell Gilpatrick acknowledged a deficiency in technical information assistance in the Defense Department and recommended that a single director be established to handle information collection and dissemination. He pointed out, however, that the key issue is the relative value of a centrally controlled information center. Referring to the Gilpatrick recommendation, Subcommittee Chairman Hubert Humphrey (D., Minn.) said he would urge DOD to consult key committees of Congress on the establishment of "something like a defense information agency." With a centralized agency, he said, the Pentagon will remain "choked with data it cannot digest."

(Continued on page 35A)

* The data on which these Notes are based were selected by permission from *Weekly Reports*, issues of October 1, 8, 15, and 22, 1962, published by the Electronic Industries Association, whose helpfulness is gratefully acknowledged.



Allen-Bradley Hot Molded Resistors prove their complete reliability in the brilliant success of Telstar

Type TR 1/10 Watt

Type CB 1/4 Watt

Type EB 1/2 Watt

Type GB 1 Watt

Type HB 2 Watts

ALLEN BRADLEY HOT MOLDED RESISTORS ARE AVAILABLE IN ALL STANDARD EIA RESISTANCE VALUES AND TOLERANCES

Allen Bradley Co., 222 W. Greenfield Ave., Milwaukee 4, Wis. • In Canada: Allen-Bradley Canada Ltd., Galt, Ontario

ALLEN-BRADLEY
QUALITY ELECTRONIC COMPONENTS
World Radio History

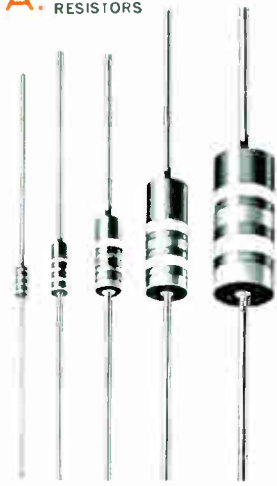
■ In their latest engineering achievement, the Telstar satellite, Bell Telephone Laboratories took a bold new design approach that emphasized the use of high reliability components with virtually total elimination of redundancy. All apparatus packages for Telstar were built "in-house" by Bell Labs, and they were carefully designed and tested for long life. Thus, the use of A-B Type CB (1/4 watt) and Type EB (1/2 watt) hot molded resistors for this important project *clearly* acknowledges their ability to meet the most severe operating conditions.

Allen-Bradley resistors are made by a unique hot molding process—developed and used exclusively by A-B—which assures such uniform and stable characteristics that their performance is accurately predictable in service . . . and they are completely free from catastrophic failures.

You can obtain this same outstanding performance *only* when you insist on A-B fixed resistors. For full details on the complete line of A-B *quality* electronic components, please write for Publication 6024, today.

The satellite Telstar was designed and built by American Telephone & Telegraph Co.'s Bell Telephone Laboratories, and AT&T paid for the cost of launching by NASA.

A. HOT MOLDED RESISTORS



C. PRECISION METAL GRID RESISTORS



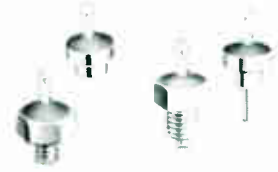
E. HOT MOLDED POTENTIOMETERS TYPE J AND TYPE K



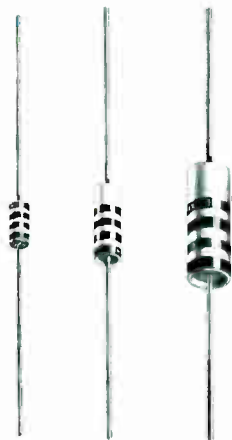
G. FERRITES AND CERAMIC MAGNETS



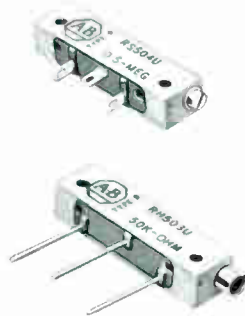
H. FEED-THRU AND STAND OFF CAPACITORS



B. HERMETICALLY SEALED RESISTORS



D. ADJUSTABLE FIXED RESISTORS



F. HOT MOLDED POTENTIOMETERS TYPE G AND TYPE L



I. HIGH FREQUENCY LOW-PASS FILTERS



J. HIGH TEMPERATURE CAPACITORS



They're all A-B quality... your assurance of utmost reliability and peak performance

A. EXCLUSIVE HOT MOLDED RESISTORS are conservatively rated. Stable and uniform characteristics assure superior performance. No known instance of catastrophic failure. Rated 1/10, 1/4, 1/2, 1, and 2 watts at 70°C. Values to 22 meg. Tol: ±5, 10, and 20%.

B. HOT MOLDED SOLID RESISTORS, hermetically sealed in ceramic tubes, remain stable. Rated 1/8, 1/3, and 1 watt. Res. to 22 meg.

C. PRECISION RESISTORS—Metal Grid Construction. Non-inductive. Tol: ±0.1, 0.25, 0.5, and 1.0%. TC: ±25 PPM/°C. Rated 1/4, 1/2, and 1 watt at 100°C.

D. ADJUSTABLE FIXED RESISTORS. Resistance element and terminals hot molded into integral

unit with insulated mounting base. Stepless adjustment. Non-inductive. Remains fixed in "set" position. Watertight. Rated 1/4 watt at 70°C. Values to 2.5 meg. Tol: ±10 and 20%

E. TYPE J POTENTIOMETERS. Solid, hot molded resistance element. Smooth, quiet control which improves with long life. Compact. Rated 2.25 watts at 70°C. Values to 5 meg.

TYPE K POTENTIOMETERS. Same as the above but rated 1 watt at 125°C; 2 watts at 100°C; and 3 watts at 70°C.

F. TYPE G POTENTIOMETERS are miniature controls with solid molded resistance element. Only 1/2" diam. Smooth control—also improves with age. Rated 1/2 watt at 70°C. Values to 5 meg.

TYPE L POTENTIOMETERS are similar to Type G but rated 1/2 watt at 100°C. Can be used up to 150°C with reduced "load."

G. FERRITES in a wide range of "items," such as flared rings, quarter rounds, U cores, E cores, cup cores, toroids, etc., can be supplied for a very large variety of applications. Consistently uniform magnetic characteristics. Contact us for complete information on A-B ceramic permanent magnets having a high energy-to-weight ratio.

H. FEED-THRU AND STAND-OFF CAPACITORS. Discoidal design eliminates all parallel resonance effects at 1000 Mcps and less. Standard values 470 mmf ±20% and 1000 mmf GMV. Special

values from 6.8 mmf to 1500 mmf. Rated to 500 v DC max.

I. HIGH FREQUENCY LOW-PASS FILTERS for eliminating undesired radiation in the range from 100 to 8000 Mcps. Effective filtering actually increases with frequency over a wide band. Attenuation to 75 db and more. Ratings to 500 v, and to 5 amp DC or low frequency AC current.

J. HIGH TEMPERATURE CAPACITORS. Ceramic disc type—encapsulated in ceramic case—for use where reliability and superior performance are important. For continuous operation at 500 v in 150°C ambient. Values from 2.2 to 3300 mmf. Tol: ±5, 10, and 20%.

10-G2-E

ALLEN-BRADLEY

**QUALITY
ELECTRONIC
COMPONENTS**

Allen-Bradley Co., 222 W. Greenfield Avenue, Milwaukee 4, Wisconsin • In Canada: Allen-Bradley Canada Ltd., Galt, Ontario

World Radio History

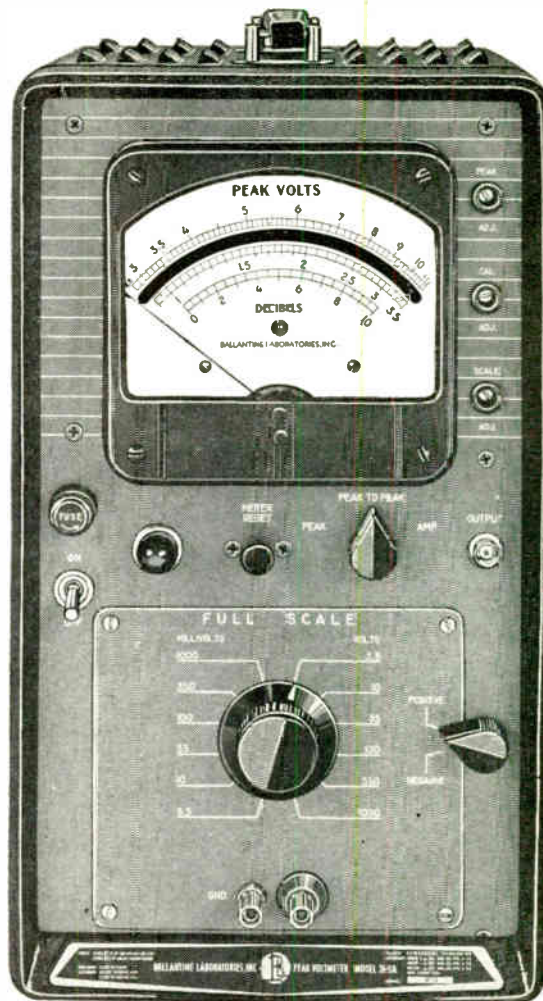
(Continued from page 32A)

Budget Bureau Director David Bell, reviewing his agency's plans to ease the information problem, said he would encourage the use of computers to handle the information "explosion." They would be used, he said, for both collection and interchange of data. (Editor's Note: During his testimony, Dr. Wiesner summarized the information tasks of Federal agencies. A limited number of copies of the summary is available from the Marketing Services Department, EIA Headquarters.) **President Kennedy last week named 13 top-level business, professional, and labor figures as incorporators of the company to own and operate the nation's space communications satellite system.** The group will set up the corporate framework of the multi-million-dollar firm, arrange for stock offerings, and serve as the Communications Satellite Corporation's board of directors until it appoints a permanent board. The Communications Satellite Act, passed by Congress and signed by the President August 31, provides that the corporation shall be owned half by the public and half by communications carriers. The profit-making firm will be regulated by existing Government communications rulings. No representatives of the electronics or communications industries were named to the group. The appointees, who must be confirmed by the Senate were: Edgar F. Kaiser (Kaiser Industries); David M. Kennedy (Board Chairman, Chicago's National Bank and Trust Co.); Philip L. Graham (Publisher, Washington (D. C.) Post); Sidney Weinberg (director of several companies including Continental Ca. Co., General Electric Co., Ford Motor Co., B. F. Goodrich Co., and Van Raaite Co.); Bruce G. Sundlun (partner in Washington law firm of Amram, Hahn & Sundlun); Byrne L. Litschgi (partner in Tampa law firm of Coles, Himpes & Litschgi); and Beardsley Graham (President, Spindletop Research Inc.). Also, Leonard Woodcock (Vice President, United Automobile, Aircraft and Agricultural Workers of America); Sam Harris (with New York law firm of Strasser, Spiegelberg, Fried & Frank); George J. Feldman (Counsel and Vice President, Masten Co., Inc., and engaged in private law practice in Boston, Washington, and New York); Leonard E. Marks (partner in law firm of Cohn and Marks in Washington); John T. Connor (President, Morek & Co.); and George L. Killion (President, American President Lines). The Federal Communications Commission already has established a new Office of Satellite Communications in its Common Carrier Bureau to handle regulatory functions of space communications common carriers. **A second round of tests of television-for-a-fee transmissions was authorized for Denver by the Federal Communications Commission last week.** The FCC granted the Gotham Broadcasting

(Continued on page 70A)

BALLANTINE VOLTMETER model 305A

Price \$415.



**MEASURES
PEAK**

**OR PEAK-TO-PEAK PULSES
AS SHORT AS 0.5 μ s**

**... at pulse rates as low as 5 pps ... voltages
of 1 mV to 1000 V**

Also measures **COMPLEX WAVEFORMS** having fundamental of 5 cps to 500 kc with harmonics to 2 Mc.

ACCURACY is 2% to 5% OF INDICATED VOLTAGE, depending upon waveform and frequency.

SCALE is the usual Ballantine log-voltage and linear db, individually hand-calibrated for optimum precision.

INPUT IMPEDANCE is 2 meg, shunted by 10 pF to 25 pF.

Write for brochure giving many more details

— Since 1932 —



BALLANTINE LABORATORIES INC.

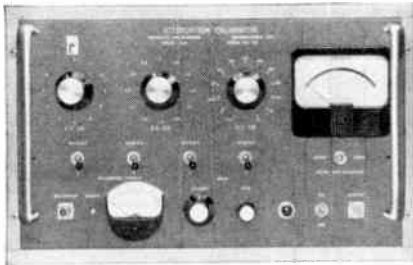
Boonton, New Jersey


CHECK WITH BALLANTINE FIRST FOR LABORATORY AC VACUUM TUBE VOLTMETERS, REGARDLESS OF YOUR REQUIREMENTS FOR AMPLITUDE, FREQUENCY, OR WAVEFORM. WE HAVE A LARGE LINE, WITH ADDITIONS EACH YEAR. A-50V AC AND DC AG INVERTERS, CALIBRATORS, CALIBRATED WIDE BAND AF AMPLIFIER, DIRECT-READING CAPACITANCE METER, OTHER ACCESSORIES. ASK ABOUT OUR LABORATORY VOLTAGE STANDARDS TO 1,000 MC.






ATTENUATION CALIBRATOR



STILL THE BEST

after **10**
YEARS



For 10 years the  Model BA-5 Attenuation Calibrator has been the most precise, the most advanced instrument on the market for measuring rf and microwave attenuation. It is still the only commercial instrument designed specifically for that purpose using the audio substitution technique.

The  BA-5 is versatile. It is the only instrument needed for attenuation measurements with the  Single Channel System and it is also a basic component in the  Dual Channel System. Each method has a direct dynamic range of 35 db. With perfect auxiliary equipment the  Single Channel System is capable of accuracies of ± 0.02 db/10 db or ± 0.02 db, whichever is greater. In practical production test installations, average system accuracy is ± 0.1 db/10 db or ± 0.1 db, whichever is greater. Even in production testing the  Dual Channel System is capable of accuracies of $\pm 0.02/10$ db or ± 0.01 db, whichever is greater. The range of either system can be extended to 55 db with partial rf substitution with only a slight deterioration in accuracy.

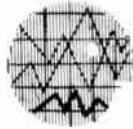
Write for complete specifications on the  BA-5. For detailed information on the techniques of insertion loss measurements, request  Application Notes 1 and 4.



**WEINSCHTEL
ENGINEERING**

GAITHERSBURG, MARYLAND
TEL: AREA CODE 301; 948-3434
TWX: 301-926-3730

SANTA MONICA, CALIFORNIA
631 WILSHIRE BOULEVARD
TWX: 213-879-0490



IRE People



Daniel G. Dow (S'53-M'57) has been promoted to Manager of Tube Research at Varian Associates' Tube Division. He be responsible for all basic research in microwave tubes and devices.

Prior to this new appointment, he was a Senior Scientist in Varian's Central Research Laboratory, where he was involved in investigation of microwave applications of plasma devices and in laser research.

From 1953 to 1955 he was a Project Officer in the Electron Tube Branch at Wright Air Development Center, Dayton, Ohio, responsible for research and development of microwave tubes.

From 1955 to 1958 he was a Research Assistant at Stanford University, where he was engaged in research on high power traveling wave tube techniques.

Before joining Varian in 1961, he was a member of the electrical engineering faculty at California Institute of Technology. He also served as a consultant to the physics laboratory of the Hughes Research Laboratories.

A native of Ann Arbor, Michigan, Dr. Dow received the B.S. degree in engineering physics and the M.S. degree in electrical engineering from the University of Michigan. He received the Ph.D. degree in electrical engineering from Stanford University, Calif. He holds several patents in the field of microwave devices and has published technical papers on microwave tubes, plasma physics and solid state devices.



Donald H. Ellis (M'60) has been named Section Head, Airborne Systems Equipment, at Dynatronics, Inc., Orlando, Fla. Prior to his new appointment, he was a senior project engineer responsible for design and development of airborne telemetry components and systems. He headed a study program which led to the development of advanced system techniques for aerospace PCM telemetry and supervised the development of a major PCM telemetry subsystem for Saturn. Other experience includes responsibility for various guidance and data system projects for both ground and airborne applications.

Mr. Ellis received the B.E.E. degree from Clemson College and did graduate work at M.I.T. He is Chairman of the Orlando Section of the IRE Professional Group on Space Electronics and Telemetry.



Sherman M. Fairchild (M'52), Founder and Board Chairman, was elected to the newly created post of Chairman of the Executive Committee of Fairchild Camera and Instrument Corp.

Mr. Fairchild founded what is now Fairchild Camera and Instrument Corpo-

ration in 1920, with the production of an aerial camera designed around his invention of an extremely fast and efficient between-the-lens shutter which made accurate aerial photography possible for the first time. In addition to the aerial camera shutter, developments conceived and sponsored by him include the cabin airplane, the folding wings airplane, wing slots and flaps, hydraulic brakes and landing gear for aircraft, the cargo airplane and the flight-analyzer camera.

He was a Director of Pan American World Airways from 1928 to 1956. He has been a Director and member of the Executive Committee of International Business Machines since 1925, and a Director of Giannini Controls Corp., since 1948. He currently is Chairman of the Board of Fairchild Stratos Corporation.



Richard R. Fidler (S'50-A'52-M'57) has been appointed an Assistant Director of Engineering at the Eastern operation of Sylvania Electronic Systems, a division of Sylvania Electronic Products



Inc. He will be in charge of the operation's information processing organization which is engaged in advanced systems analysis, through production of a variety of electronic products and systems.

Since 1960, he has served as Manager of the Advanced Systems Laboratory, Needham, Mass. He joined Sylvania in 1956 as Engineer-in-Charge of the data processing phase of an early anti-missile missile program. Previously he was a staff member of the Massachusetts Institute of Technology's Lincoln Laboratory, Lexington, and was a Project Manager for the Laboratory-for-Electronics, Boston.

Mr. Fidler received the B.A. degree in physics from Gettysburg College, and the B.S. degree in electrical engineering from M.I.T. He served as a radar technician in the U. S. Navy, during World War II and the Korean conflict.



Beardsley Graham (S'39-A'41-SM'47) President of Spindletop Research, Inc., Lexington, Kentucky, was named by President Kennedy as an incorporator of the Satellite Communications Corporation.



(Continued on page 38A)

New from Sprague!

2N2095

TO-31 CASE



2N2098

TO-9 CASE



Investigate these Power Amplifiers for your VHF Communications Needs!

CHECK THESE KEY PARAMETERS:

$P_d @ 25^\circ\text{C case}$	1 W
BV_{CBO}	30 V
BV_{CEO}	15 V
f_T	1 Kmc
$PG @ 160 \text{ Mc}$	7 db
C_{ob}	8 pF
$r_b^1 C_c$	60 nsec

Sprague's ECDC technology, proven in the 2N2100 nanosecond film memory driver, has been extended to amplifier or oscillator transistors covering a wide range of VHF communications applications. The ECDC process combines the benefits of electrochemical and diffusion technology to provide today's best combination of electrical characteristics for maximum circuit efficiency.



For complete engineering data, write for Engineering Bulletins 30,409 and 30,414 to Technical Literature Service, Sprague Electric Company, 235 Marshall Street, North Adams, Massachusetts.

SPRAGUE COMPONENTS

TRANSISTORS

CAPACITORS

MAGNETIC COMPONENTS

RESISTORS

MICRO-CIRCUITS

INTERFERENCE FILTERS

PULSE TRANSFORMERS

PIEZOELECTRIC CERAMICS

PULSE-FORMING NETWORKS

TOROIDAL INDUCTORS

HIGH TEMPERATURE MAGNET WIRE

CERAMIC-BASE PRINTED NETWORKS

PACKAGED COMPONENT ASSEMBLIES

FUNCTIONAL DIGITAL CIRCUITS

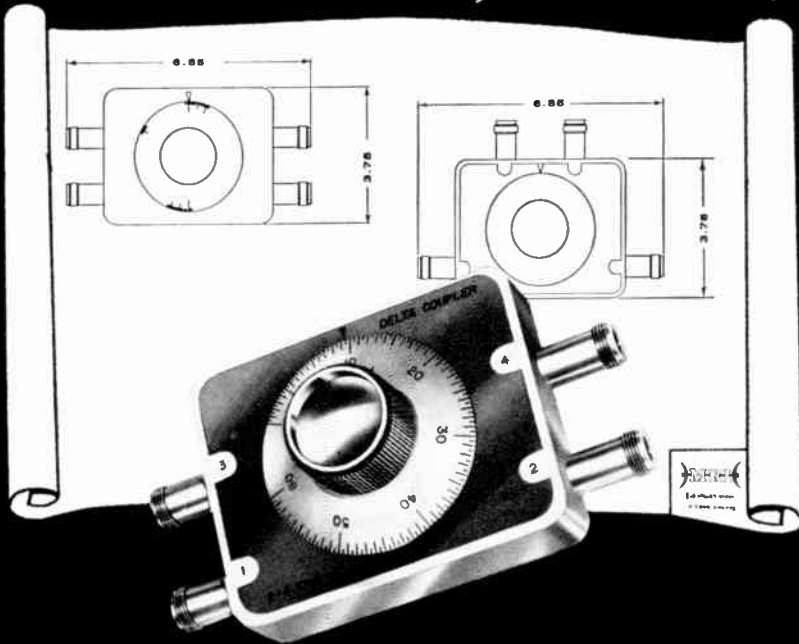
ELECTRIC WAVE FILTERS



"Sprague" and "®" are registered trademarks of the Sprague Electric Co

NEW from

MRI



DUAL-FUNCTION DELTA-COUPPLERS

This unique instrument is a broadband precision calibrated directional coupler which is adjustable from 5 to 70 db and may also be used as a precision variable attenuator over these ranges. Accuracy of the delta coupler is assured to within ± 1 db of absolute attenuation over the specified frequency range and is displayed on a direct reading dial. Maximum power handling capability of this unit is 200 watts. Other features include low VSWR, low insertion loss, and high directivity. The coupler is available in the following frequency ranges:

AVAILABLE IN FOUR FREQUENCY RANGES

Configuration	Model No.	Frequency Range (mc)
	C99 1270001	500 - 1000
	C99 2270001	2000 - 4000
	C99 1270002	1000 - 2000
	C99 3270001	4000 - 8000

Complete specifications available on request.



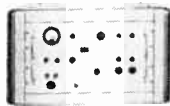
Ferrite Isolators



Antennas



Subsystems



"L" Band ATC and DME Transponder Test Sets

MRI

MICRO-RADIONICS, INC.
Formerly Kearfott Microwave Division
14844 OXNARD STREET, VAN NUYS, CALIFORNIA
STate 6-1760 TWX: VNYS 5451



IRE People



(Continued from page 38A)

Richard Hodgson (M'47-SM'51), Executive Vice President of Fairchild Camera and Instrument Corporation, has been named President. He joined Fairchild Camera in June, 1955. He was one of the organizers of Chromatic Television Laboratories, Inc., and was President of the firm when he joined Fairchild.



His association with the military dates back to 1942, when he was a research staff member of M.I.T.'s Radiation Laboratory working on microwave radar developments. In 1944 he was assigned to the Office of the Secretary of War as an expert consultant on radar. During this period he also served as civilian radar advisor to General Hoyt B. Vandenberg. He also was a consultant to the Department of the Air Force in 1952 and 1953, advising on the organization of the research and development program as part of a three-man advisory group headed by Lt. Gen. James H. Doolittle. This work led to the establishment of the Air Research and Development Command.

He has been a Director of Television Development for Paramount Pictures Corporation; Assistant Treasurer of Allen B. Du Mont Laboratories; Head of the Engineering Management Division of Brookhaven National Laboratory, A.E.C.; a senior change board engineer for Lockheed Aircraft Corporation and a manufacturing and process economic analyst for Standard Oil Company of California.



Rudolf E. Kalman (S'53-A'55-M'61) a staff scientist at the Martin Company's Research Institute for Advanced Study (RIAS), was named by the Maryland Academy of Sciences as the State's Outstanding Young Scientist of 1962. He was cited for his "outstanding contributions to fundamental research in differential equations as applied to automatic control, and specifically for his discovery of the duality principle in control theory." He receives an engraved plaque bearing the citation and a \$500 cash grant.

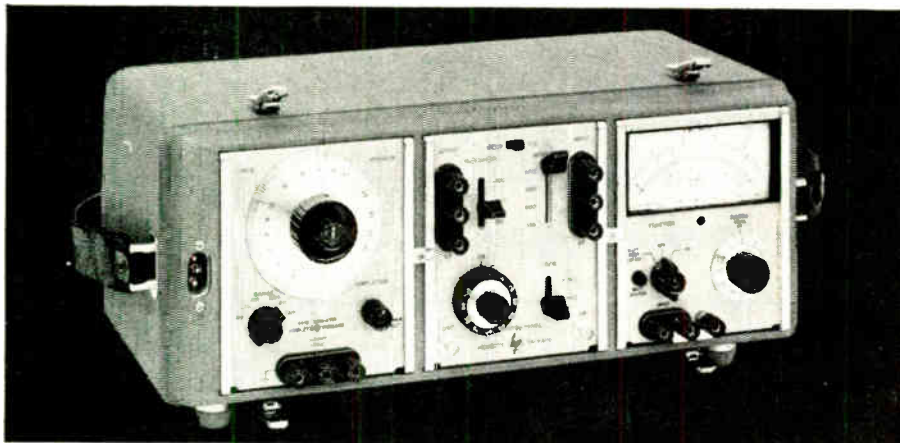
Before joining the staff of RIAS, he was employed by DuPont Corporation and International Business Machines Research Laboratory.

Dr. Kalman was born in Budapest and educated in the United States at the Massachusetts Institute of Technology, where he obtained both the B.S. and M.S. degrees in electrical engineering. He received the Ph.D. degree at Columbia University in 1957. Before joining the staff of RIAS, Dr. Kalman was employed by DuPont Corporation and International Business Machines Research Laboratory.



(Continued on page 40A)

SIMPLIFY communications maintenance



**NEW
portable
test set
measures
gain,
attenuation,
frequency
response**

SPECIFICATIONS

The new **hp** 3550A Portable Test Set, designed specifically for transmission system testing, is especially useful for alignment and maintenance of multichannel communication systems. It incorporates a 5 cps to 560 kc oscillator with fully floating output, a 1 mv to 300 v 5 cps to 2 mc voltmeter, and attenuator and impedance matching networks to individually match the oscillator and voltmeter to 135, 600 and 900 ohm lines.

The solid state instruments are housed in a compact case with a splash-proof cover, and both the oscillator and voltmeter operate from internal rechargeable batteries or from an ac line. The three instruments may be used separately in or out of the case.

The oscillator provides flat frequency response and excellent amplitude and frequency stability. The highly accurate voltmeter provides a db scale for easy measurement -72 to $+52$ dbm. The attenuator and impedance matching unit includes calibrate features to eliminate insertion loss. Oscillator and voltmeter batteries recharge during ac operation.

Check the specifications for the remarkable versatility and convenience of this test set, then contact your **hp** representative or call direct for a demonstration on your bench or in the field.

Frequency Range:	OSCILLATOR (⊕ H07-204B)
Dial Accuracy:	5 cps to 560 kc, 5 ranges
Frequency Response:	$\pm 3\%$
Output Impedance:	$\pm 3\%$ into rated load
Output:	600 ohms
Distortion:	10 mw (2.5 v rms) into 600 ohms, 5 v rms open circuit, completely isolated
Hum and Noise:	Less than 1%
Temperature Range:	Less than 0.05%
	-20° to $+50^{\circ}$ C
	VOLTMETER (⊕ 403B)
Range:	0.001 to 300 v rms full scale; -72 to $+52$ dbm
Frequency Range:	5 cps to 2 mc
Accuracy:	0° C to 50° C, within $\pm 2\%$ of full scale from 10 cps to 1 mc, within $\pm 5\%$ of full scale from 5 to 10 cps and 1 to 2 mc (on 300 v range, accuracy is $\pm 10\%$ from 1 to 2 mc; AC-21A 10:1 Divider Probe allows measurements to 300 v in the 1 to 2 mc range with an accuracy of $\pm 5\%$; 0° C to -20° C, $\pm 8\%$ of full scale from 5 cps to 2 mc
Nominal Input Impedance:	2 megohms, shunted by approximately 40 pf on 0.001 v to 0.03 v ranges, 20 pf on 0.1 v to 3 v ranges, 15 pf on 10 to 300 v ranges
DC Isolation:	Signal ground may be ± 500 v dc from external case
Noise:	Less than 4% of full scale on 1 mv range, 3% on other ranges
Attenuation:	ATTENUATOR/PATCH PANEL
Accuracy:	110 db in 1 db steps
	10 db section, error less than ± 0.125 db at any step, dc to 100 kc; less than ± 0.25 db, 100 kc to 1 mc.
	100 db section, error less than ± 0.25 db at any step up to 70 db, less than ± 0.5 db above 70 db, from dc to 100 kc; less than ± 0.5 db up to 70 db, less than ± 0.75 db above 70 db, 100 kc to 1 mc
Impedance:	600 ohms
Input and Output:	50 cps to 560 kc; balance better than 40 db; frequency response ± 0.5 db, 50 cps to 560 kc; impedance, 135, 600, 900 ohms center tapped. Input includes 10K bridging impedance; insertion loss, less than 0.75 db at 1 kc; maximum level $+10$ dbm (2.5 v into 600 ohms)
	GENERAL
Power:	Voltmeter and oscillator each use a power supply of 4 rechargeable batteries (furnished, 40 hr. operation per recharge [20 hours at -20° C], up to 500 recharging cycles). Automatic recharging during ac operation
Dimensions:	8 $\frac{3}{8}$ " high, 19 $\frac{1}{4}$ " wide, 13 $\frac{3}{4}$ " deep. Weight 30 $\frac{1}{2}$ lbs.
Price:	\$990.00

Data subject to change without notice. Price f.o.b. factory.



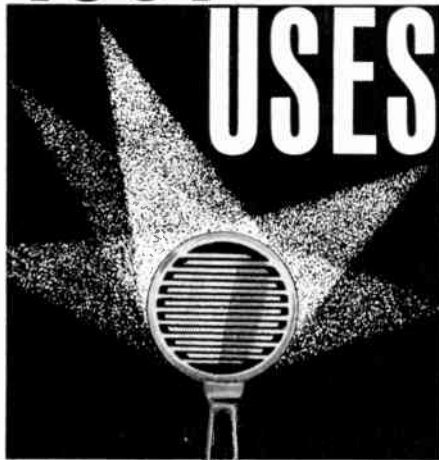
HEWLETT-PACKARD COMPANY

1501 Page Mill Road, Palo Alto, California, Area Code 415, DA 6-7000
Sales and service representatives in all principal areas; Europe, Hewlett-Packard S. A., 54-54bis Route des Acacias, Geneva; Canada, Hewlett-Packard (Canada) Ltd., 8270 Mayrand Street, Montreal

8090

1001

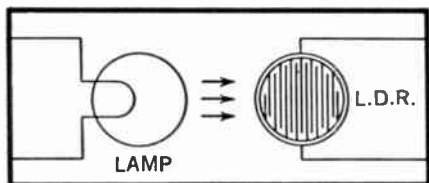
USES



FERROXCUBE LIGHT DEPENDENT RESISTOR CONTROLS CURRENT FLOW AS LIGHT INTENSITY VARIES

Let your creativity run wild with this one . . . The Ferroxcube LDR is a light dependent resistor offering a resistance ratio of 25,000 to 1 for a light intensity change from total darkness to 1,400 foot candles.

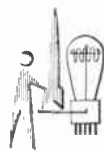
Interesting? Here's low-cost (as low as 25¢, depending upon quantity), compact (smaller than a dime), automatic control that can serve as a relay, a potentiometer of ultra-quiet characteristics and high resolution, or as a gain limiter. Use it in TV receiver design, toys, computers, and wherever else light control is feasible.



TRY IT! Order a LDR-1A Engineering Kit—includes 4 LDR's and complete technical data—only \$10.00. Send check or money order to . . .



FERROXCUBE
CORPORATION OF AMERICA/SAUGERTIES, N.Y.



NEWS New Products



Broadband Random Noise Generator

General Microwave Corp., 155 Marine St., Farmingdale, N. Y., announces the availability of the Model 503 broadband random noise generator. The Model 503 is designed for the rapid measurement of noise figure over the frequency range of from 1 to 500 mc, and features a variable excess noise output from 0 to 19 db. The noise power generated results from the action of two diodes operating in their temperature-limited regions, and is a direct function of the diodes' dc plate current.



Since this current depends upon the power supplied to the diodes' filaments, a well-regulated dc filament supply is employed to ensure a stable and hum-free output. The plate supply is similarly well-regulated.

The noise output, variable from 0 to 19 db, is indicated on a logarithmically calibrated meter, direct reading in decibels of noise figure.

The noise output is accurate to ± 0.5 db over the frequency range and at any point on the meter scale. The VSWR measured at the output jack from 3 to 500 mc is 1.2 maximum, and 1.5 maximum from 1 to 3 mc. Price is \$350.00. Delivery is from stock.

Thermistor Probes

Yellow Springs Instrument Co., Box 106, Yellow Springs, Ohio, announces the availability of a new form of its precise thermistor family. The precise thermistors are mounted in 2-inch Teflon® probes which can be formed to any configuration required by the user with just finger pressure. A stiffening wire in the heat sealed Teflon® tube may be bent with finger pressure to any required shape and the entire probe then assumes that shape. Two #32 tinned copper wire leads insulated from each other by a smaller Teflon® tube ex-

tend one-inch beyond the probe body. The probes, like the thermistors, follow identical resistance-temperature curves to within $\pm 1\%$ over most of their -80 to $+150^\circ\text{C}$ useable span. Each probe is accompanied by numerical charts indicating resistance to each degree of centigrade temperature and curves indicating tolerances both as a % resistance and as a maximum indicated temperature variation if the probes are used in measurement circuits. A family of probes with base resistances at 25°C of 100 ohms, 300 ohms, 10K, 30k, and 100K is provided.



Probes are part of the 44000 precise thermistor group. Prices are below \$8.00 each in 1-9 quantities with discounts in quantity. Deliveries in small quantities are from stock, larger quantities within 30 days.

Trimpot Data Sheet

New technical data sheet on Daystrom 301 Series Squaretrim® subminiature trimming potentiometers provides complete specifications covering these $\frac{1}{2}$ " square adjustable potentiometers. With a range of 10 ohms to 65 kilohms, operating temperature range of -55 to 150°C , a power rating of 1 watt in still air (i.e., without the use of a heat sink), and meeting or exceeding all applicable MIL specs, the bottom-pin potentiometers in the Daystrom Squaretrim 301 Series are used for the delicate adjustment of computer, control, telemetering, missile, and other critical military and industrial electronic circuits.

In addition to actual-size photographs, the technical data sheet contains detailed electrical, mechanical, and environmental specifications on the 301 Series. Modification possibilities are also shown. Complete engineering drawings, power rating curve, and circuit diagram are given.

Copies of the Squaretrim 301 Series Technical Data Sheet may be obtained by writing Daystrom, Incorporated, Potentiometer Div., Archbald, Pa.

(Continued on page 110-A)

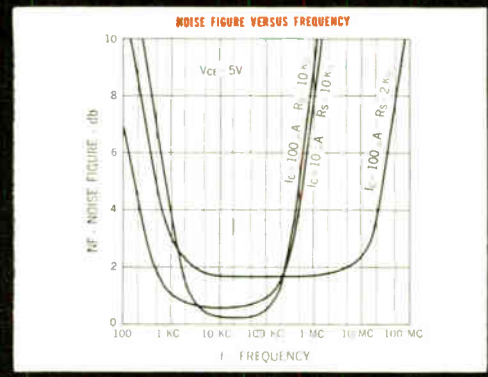
High DC Gain, High Voltage Amplifiers!

**30 minimum h_{FE}
at very low current:
 $I_C = 1\mu A$.**

60 V minimum LV_{CEO}

**low current f_T :
15 mc minimum
at $I_C = 50\mu A$;
Low Noise Figure:
3 db maximum
at $I_C = 10\mu A$
1.8 db typical.**

		2N2484		2N2483			
Symbol	Characteristic	Min.	Typ. Max.	Min.	Typ. Max.	Units	Test Conditions
LV_{CEO}	Collector-Emitter Voltage	60		60		Volts	$I_C = 10mA$ $I_B = 0$
h_{FE}	DC Current Gain	30					$I_C = 0.001mA$ $V_{CE} = 5.0V$
h_{FE}	DC Current Gain	100	500	40	120		$I_C = 0.01mA$ $V_{CE} = 5.0V$
h_{FE}	DC Current Gain	150		60			$I_C = 0.5mA$ $V_{CE} = 5.0V$
h_{FE} (-55°C)	DC Current Gain	20		10			$I_C = 0.01mA$ $V_{CE} = 5.0V$
NF	Noise Figure ^(note 1)	1.8	3.0	2.0	4.0	db	$I_C = 0.01mA$ $V_{CE} = 5.0V$
NF	Noise Figure ^(note 2)	1.8	3.0	2.0	4.0	db	$I_C = 0.01mA$ $V_{CE} = 5.0V$
C_{ob}	Output Capacitance		6.0		6.0	pf	$I_E = 0$ $V_{CB} = 5.0V$
f_T	Gain Bandwidth Product	15		12		mc	$I_C = 50\mu A$ $V_{CE} = 5.0V$ $f = 1$ mc



Note 1— $R_s = 10K\Omega$; Power Bandwidth of 15.7 kc with 3 db points at 10 cycles and 1Q kc.
Note 2— $f = 1kc$; $R_s = 10K\Omega$; Power Bandwidth of 200 cps.

Now available from FAIRCHILD

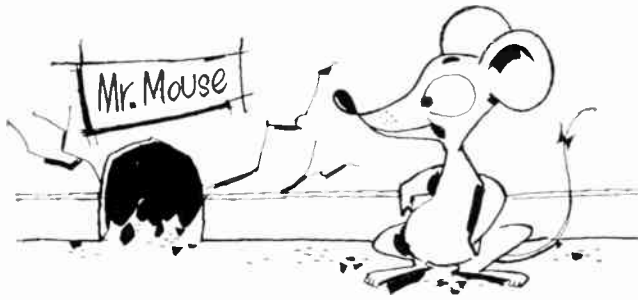
2N2484: A general purpose low level amplifier featuring high DC gain and f_T at low collector current. These advantages, plus a low broad band noise figure,⁽¹⁾ make the 2N2484 ideal for general purpose amplifiers as well as satellite and space probe applications. The Fairchild PLANAR* process provides extremely high stability and reliability in a military temperature environment.

2N2483: Has similar characteristics, except for h_{FE} ratings. Both 2N2483 and 2N2484 are packaged in JEDEC TO-18. A data sheet covering both devices is available.

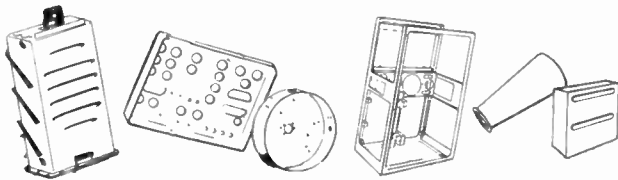
FAIRCHILD
SEMICONDUCTOR
545 WHISMAN RD., MOUNTAIN VIEW, CALIF. • YORKSHIRE 8-8161 • TWX: 415 969-9165
A DIVISION OF FAIRCHILD CAMERA AND INSTRUMENT CORPORATION

*PLANAR: a patented Fairchild process.

Special Purpose Housing



AMERICAN ALUMINUM Custom-Crafts to Your Exact Needs



American Aluminum's 50 year old specialty is manufacturing aluminum enclosures and related shapes for the electrical-electronics industry. Our experienced engineers will design your special purpose housings, chassis, racks, panels and other formations or they will carry on from a blueprint and finish anything you start.

Join our long list of satisfied customers. You can rely on us for the utmost in precision where today's more exacting standards are met. The American Aluminum team will meet your specific needs with unsurpassed craftsmanship plus exceptional service and cooperation.

**SEND US YOUR BLUEPRINTS
PUT YOUR PROBLEMS IN CAPABLE
AND LONG EXPERIENCED HANDS**

COMPLETE FABRICATING FACILITIES FOR
Deep Drawing, Heat Treating, Spinnings, Assembly,
Brake Work, Stampings, Anodizing, Welding
Finishing

Complete die making facilities
Stock dies on hand for many shapes
Complete inspection facilities

Our new WIEDEMAN TURRET PUNCH PRESS will
insure time and money saving benefits for you.

Write today for complete literature on the
services of American Aluminum



AMERICAN ALUMINUM COMPANY

Manufacturers of Aluminum Products
for Industry since 1910

230 Sheffield Street, Mountainside, New Jersey



Membership



The following transfers and admissions
have been approved and are now ef-
fective:

Transfer to Senior Member

Adachi, S., Sendai, Japan
Bittman, L. R., Lutherville, Md.
Bolz, R. A., Yonkers, N. Y.
Brand, F. A., Elberon, N. J.
Calvert, R. B., Brookville, Pa.
Campbell, R. E., Benson, Ariz.
Cheney, C. L., Wichita, Kan.
Chow, C. K., Wayne, Pa.
Daniels, R. E., Downers Grove, Ill.
Durrani, S. H., Albuquerque, N. M.
Epprecht, G. W., Baden AG, Switzer-
land
Gabor, A., Port Washington, L. I.,
N. Y.
Glaze, G. O., Hollywood, Calif.
Howell, M., Somerdale, N. J.
Kalman, R. E., Baltimore, Md.
Lane, J. F., Lexington, Mass.
Lathrop, R. C., USAF Academy, Colo.
Lyman, R. C., Monroeville, Pa.
MacNichol, E. F., Jr., Baltimore, Md.
McLeod, J. S., Washington, D. C.
Olson, A. E., Eureka, Calif.
Radcliffe, A. J., Jr., Orlando, Fla.
Raible, R. W., Little Rock, Ark.
Rausch, R. H., Dewitt, N. Y.
Renner, R. N., Los Angeles, Calif.
Reyling, G. F., Portola Valley, Calif.
Say, D. L., Brookville, Pa.
Scott, A. C., Madison, Wis.
Spilker, J. J., Jr., Palo Alto, Calif.
Stephan, A., Pomona, Calif.

Tilley, A. E., La Habra, Calif.
Truxall, F. W., Columbus, Ohio
Vuilleumier, R. F., Santa Monica,
Calif.
Wickstrom, S. T., Skokie, Ill.
Wiseman, S. D., Littleton, Colo.
Worthington, D. T., Rome, N. Y.
Zimet, M. M., New York, N. Y.

Admission to Senior Member

Allison, E., San Pedro, Calif.
Babeock, L. E., Framingham Centre,
Mass.
Barabasci, S., Rome, Italy
Bennett, W. R., Jr., New Haven,
Conn.
Bonham, W. E., Warren, Ariz.
Crawford, H. D., Stillwater, Okla.
David, F. E., Lutherville, Md.
Davis, D. E., Garland, Tex.
Dinhobel, F., Akron, Ohio
Eichbaum, B. R., Maple Glen, Pa.
Gaetano, A. F., Los Gatos, Calif.
Gallagher, J. J., Orlando, Fla.
Hemel, A., Chicago, Ill.
Hess, G. K., Jr., Patrick AFB, Fla.
Hollway, D. L., Sydney, N.S.W.,
Australia
Mayburg, S., Bayside, L. I., N. Y.
Moshier, R. F., Ann Arbor, Mich.
Muss, D. R., Pittsburgh, Pa.
Nakahara, Y., Tokyo, Japan

(Continued on page 46A)

AUTOMATIC SIGNAL TRACKING BANDPASS FILTER

SERIES 450 VARIES ITS CENTER FREQUENCY AS SIGNAL CHANGES

With bandpass continuously adjust-
able from 2.5 to 100 cps via a panel
knob, this electronic signal chaser
improves signal/noise ratio of analog
signals that either drift or change
frequency as a function of time.
Signal frequency can vary from 100
cps to 120 kc — the Series 450 Filter
tracks it, automatically, with S/N
improvement up to 38 db. Lost signal
momentarily? No problem. The 450 has a memory — searches to re-acquire
the signal.



Output is the frequency itself, multiplied times 1, 10 or 100. Optional ac-
cessories include a dc analog of the input signal frequency, wide-band detector
to extract intelligence from the tracked signal, and a pilot acquisition con-
trol to permit phase-locking to an external pilot frequency until the signal
itself reaches that frequency.

WRITE TO: *Interstate* ELECTRONICS CORPORATION

707 East Vermont Ave. • Anaheim, California • Phone 714-772-2222
(A subsidiary of Interstate Engineering Corporation)

NATIONWIDE REPRESENTATIVES

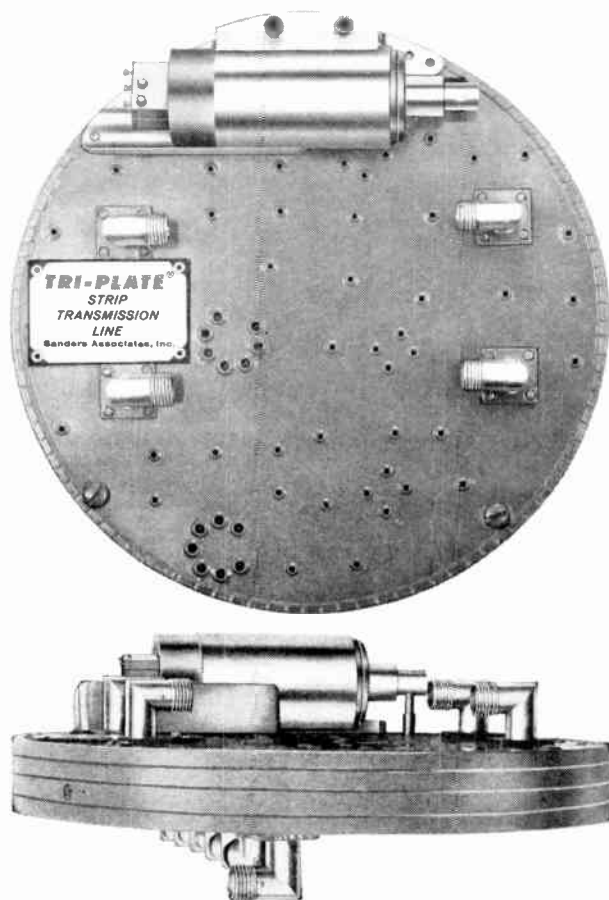
ANOTHER *Interstate* SOLID-state INSTRUMENT

Microwave, semiconductor and fast switching circuits with high density packaging, that heretofore have been thought impractical or impossible to build because of their bulk or complexity, are now successfully produced in TRI-PLATE Strip Transmission Line. □ In breadboarding, packaging and quantity production, what the

concept of strip transmission promised, TRI-PLATE techniques deliver — they've made the concept a practical reality! □ TRI-PLATE circuitry provides packaging versatility to solve the most difficult problems. The broadband mono-pulse front end for S-band shown below contains nine hybrid rings, three channel step attenuators, three bal-

anced mixers and six internally mounted 1N831 diodes in a multi-layer package of less than 17 cubic inches. Engineered to conform to the customer's space and size requirements, it measures just 5¾" in diameter and is less than 5/8" thick. This is but one example of how TRI-PLATE circuitry makes possible high density packaging which would

Compact packages made possible with Tri-Plate[®] techniques



be impossible to achieve with conventional coaxial or waveguide techniques. □ To help you speed the time from design to breadboard to prototype to production with known characteristics, there are more than 600 TRI-PLATE Modules — including over 150 TRI-PLATE Mounts for standard and advanced semiconductor devices — available from Sanders. They let you test new circuit ideas — no matter how different or daring — with speed, ease and economy.

You can go from paper schematics to functioning circuits in just minutes to evaluate new design concepts. □ And a system designed in TRI-PLATE Modules can be produced in quantity as an Integrated TRI-PLATE Package, with performance equal to if not better than that of the modular prototype, and with great savings in size and weight.

□ For more information about Strip Transmission Line and how TRI-PLATE Products have made it a practical reality, for the latest literature — including specifications and prices — or for consultation regarding your specific requirements, write to Sanders Associates, Inc., Microwave Products Department, Nashua, New Hampshire.

® REG. T.M.; EXTENSIVE PATENT COVERAGE. SANDERS ASSOCIATES, INC.

CREATING NEW DIRECTIONS IN ELECTRONICS
SANDERS TRI-PLATE[®] STRIP TRANSMISSION LINE 

Large production gives you low prices!
— that's why...

Over 100 O.E.M.s
have standardized
on

AMPERITE

Thermostatic DELAY RELAYS

2 to 180 Seconds

Actuated by a heater, they operate on A.C., D.C., or Pulsating Current.

Hermetically sealed. Not affected by altitude, moisture, or climate changes. SPST only—normally open or closed.

Compensated for ambient temperature changes from -55° to $+80^{\circ}$ C. Heaters consume approximately 2 W. and may be operated continuously. The units are rugged, explosion-proof, long-lived, and—inexpensive!

TYPES: Standard Radio Octal, and 9-Pin Miniature . . . List Price, \$4.00.

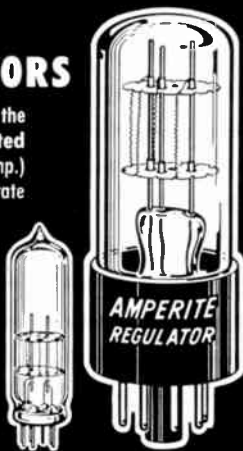
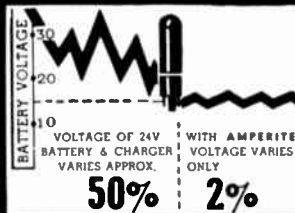


Also — Amperite Differential Relays: Used for automatic overload, under-voltage or under-current protection.

PROBLEM? Send for Bulletin No. TR-81

BALLAST REGULATORS

Amperite Regulators are designed to keep the current in a circuit automatically regulated at a definite value (for example, 0.5 amp.) . . . For currents of 60 ma. to 5 amps. Operate on A.C., D.C., or Pulsating Current.



Hermetically sealed, they are not affected by changes in altitude, ambient temperature (-50° to $+70^{\circ}$ C.), or humidity . . . Rugged, light, compact, most inexpensive List Price, \$3.00.

Write for 4-page Technical Bulletin No. AB-51

AMPERITE

561 Broadway, New York 12, N. Y. . . . CAnal 6-1446
In Canada: Atlas Radio Corp., Ltd., 50 Wingold Ave., Toronto 10



Membership

(Continued from page 41A)

Nontura, K. C., Riviera Beach, Fla.
Oberlin, R. P., Phoenix, Md.
Panagakos, A., Albuquerque, N. M.
Renna, N., Jr., Baltimore, Md.
Reverdin, D. L., Paris, France
Rice, W. M., Timonium, Md.
Riggs, L. S., El Segundo, Calif.
Silverman, J. H., Wickliffe, Ohio
Slotnick, D. L., Baltimore, Md.
Tonning, A., Oslo, Norway
Yabroudy, G. A., Farmingdale, L. I., N. Y.

Transfer to Member

Briscoe, H. R., Jr., Chattanooga, Tenn.
Chapelaine, A. J., Jr., Suitland, Md.
Clisch, D. F., Ottawa, Ont., Canada
Depew, H. H., Valley Center, Kan.
Eisenstein, N., Rego Park, L. I., N. Y.
Faiola, A. R., Mamaroneck, N. Y.
Gibbs, L. C., Los Angeles, Calif.
Goldberg, S. D., Melrose, Mass.
Hilsdale, F. A., Los Angeles, Calif.
Howland, R. L., Tucson, Ariz.
Kaya, P., Den Haag, Netherlands
Knox, W. E., Jr., Anchorage, Alaska
Richardson, R. G., Minneapolis, Minn.
Sarris, R. A., Baltimore, Md.
Schwell, O., Ottawa, Ont., Canada
Shook, W. A., Seattle, Wash.

Admission to Member

Abbott, D. W., Baltimore, Md.
Ahlstrom, E. R., Neptune, N. J.
Allen, C. L. D., Falls Church, Va.
Allen, P. D., London, England
Allen, P. E., Livermore, Calif.
Allison, L. J., Cincinnati, Ohio
Anderson, R. J., Stockton, Calif.
Anderson, R. B., Huntsville, Ala.
Ashcroft, R. T., Webster, N. Y.
Aslin, H. K., Livermore, Calif.
Band, J. T., Newport Beach, Calif.
Barham, D. J., Portsmouth, Va.
Bartlow, B. B., Stoneham, Mass.
Baxter, R. H., Albuquerque, N. M.
Beck, J. B., Fayetteville, N. Y.
Bhat, R. A., Madras, India
Bodker, J. R., Jr., Independence, Ohio
Boyce, G. D., San Ysidro, Calif.
Bracey, M. F., Zaria, Northern Nigeria
Brown, B. F., Stillwater, Okla.
Brown, C. W., Woodland Hills, Calif.
Bruce, M. E., Binghamton, N. Y.
Buchowski, R. A., Wheeling, Ill.
Burns, R. W., Garden Grove, Calif.
Campbell, K. A., Winnipeg, Man., Canada
Caprio, J. R., Buffalo, N. Y.
Chapman, H. W., Brooklyn, N. Y.
Clark, W. M., Charleston, S. C.
Conrad, E. E., Bethesda, Md.
Corlew, C. L., New York, N. Y.
Crowley, W. M., Neptune, N. J.
Daugherty, B. R., Springfield, Va.
Dawes, D. L., South Lincoln, Mass.
Dearden, J. R., Oreland, Pa.
Dempsey, J. L., Chicago, Ill.
Dillon, H. C., Dallas, Tex.
Dimitrios, P. P., Franklin Park, Ill.
Doering, J. W., Torrance, Calif.
Dolan, J. L., Green Bank, W. Va.
Donahue, D. C., Red Bank, N. J.
Donkin, T. R., Northport, L. I., N. Y.
Duff, D. R., Lexington, Ky.
Durr, W. F., Anaheim, Calif.
Durschinger, J. A., Baltimore, Md.
Evans, J. J., Garden Grove, Calif.
Fickey, C. J., Searsdale, N. Y.
Filek, L. T., Joliet, Ill.

Fitins, V., Langhorne, Pa.
Flink, J. H., Flushing, L. I., N. Y.
Fousef, V. L., Lancaster, Calif.
Fox, C. E., Jr., Washington, D. C.
Fredkin, E., Maynard, Mass.
Gates, F. K., Tiburon, Calif.
Gatto, P. R., Philadelphia, Pa.
Gee, E., East Palo Alto, Calif.
Gilbert, J. H., Baltimore, Md.
Gillin, H. C., E. Pepperell, Mass.
Grafton, F. M., Upper Montclair, N. J.

Grantham, W. L., Langley Field, Va.
Grierson, J. K., Ottawa, Ont., Canada
Gunter, G. H., Whippany, N. J.
Haab, W. G., Garden Grove, Calif.
Hale, D. C., Maywood, Ill.
Hall, S. R., Baltimore, Md.
Hanson, H. A., Lutherville Timonium, Md.
Harding, M. C., Redwood City, Calif.
Harper, J. C., Anaheim, Calif.
Harraly, D. J., Wayland, Mass.
Henry, J. L., Tulsa, Okla.
Hensel, C. L., Baltimore, Md.
Hersh, D. H., Lee's Summit, Mo.
Hietrich, H. A., Reading, Pa.
Hicks, M. C. L., Victoria, Australia
Higier, T., Washington, D. C.
Hill, C. F., San Diego, Calif.
Holland, W. R., Tulsa, Okla.
Holmes, A. S., Cobham, Surrey, England

Holmgren, G. L., Dallas, Tex.
Howard, S. D., Hawthorne, Calif.
Huey, G. J., Fort Wayne, Ind.
Ingle, R. K., Stanhope, N. J.
Ingram, R. D., Baltimore, Md.
Jarvis, P. C., Lakewood, Calif.
Johnsen, O. H., Paris, France
Julik, A. G., Gardena, Calif.
Jull, G. W., Ottawa, Ont., Canada
Kaplan, A. A., San Jose, Calif.
Karp, A., Los Angeles, Calif.
Kebbell, T. A., Stevenage, Hertfordshire, England

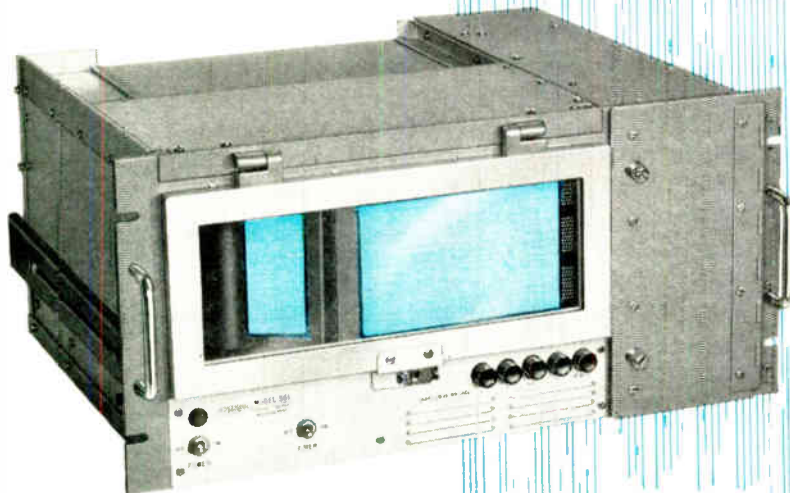
Keener, G. R., Lacey Springs, Ala.
Kemmner, B. L., Dallas, Tex.
Kesler, D. F., Playa Del Rey, Calif.
Kinton, I. H., Camden, N. J.
Kluek, M. H., Roswell, N. M.
Kraybill, A. V., Riverside, Ill.
Kusuda, Z., Takatsuki, Osaka, Japan
Lange, A. C., Oak Park, Ill.
Lawrence, W. G., Los Angeles, Calif.
Lecanliar, B. L., Montreal, Que., Canada

Levine, R., Canoga Park, Calif.
Light, E. J., New York, N. Y.
Long, J. D., No. Hollywood, Calif.
Lovell, R. T., Wilmington, Del.
Lule, M. J., Port Washington, L. I., N. Y.
Manger, R. F., Dayton, Ohio
McGee, J. L., Morton Grove, Ill.
McGowan, A. J., Buffalo, N. Y.
McKeever, J. E., Beaumont, Tex.
McKown, D. C., Chino, Calif.
McPherson, F. S., Gardena, Calif.
Meyer, A. U., Orange, N. J.
Miller, E. L., Los Angeles, Calif.
Miller, R. D., Silver Spring, Md.
Moore, G. T., Palo Alto, Calif.
Moreno, A. L., Sao Paulo, Brazil

Morgan, H. K., Philadelphia, Pa.
Morguloff, D., Dallas, Tex.
Mullen, J. H., Bridgeton, Mo.
Nagel, D. O., Dallas, Tex.
Nicelli, V., Milano, Italy

(Continued on page 48A)

New SANBORN 30-channel EVENT RECORDER

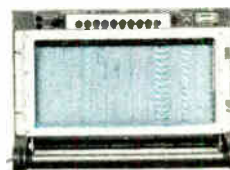


only 8 $\frac{3}{4}$ " high, with solid-state plug-in writing control: \$2050 complete

- Compact portable case or rack mounts in 8 $\frac{3}{4}$ " of panel space
- Meets MIL-I-26600/2 Class 1B RFI Spec.
- Choice of 6 solid-state plug-in Writing Controls
- Simple front-loading of 4.07" wide, 300-foot charts, built-in paper take-up
- Solid-state pulse generator and power supply
- Confidence: under worst combination of low line voltage and short duration signals, probability of marking exceeds 99%
- Response to events as short as 1.3 ms
- Constant trace intensity at all speeds
- Self-cleaning, reversible styli replaceable individually or in groups of 30; stylus pressure automatically maintained
- 4 pushbutton-selected chart speeds, 1 to 100 mm/sec.; remote controlled chart speeds available on special order
- Signal return isolated from chassis (1 megohm min.)

This economical new 30-channel operations monitor provides immediate, permanent recording of on-off events on dry, electro-sensitive charts — using "pulsed writing" for maximum clarity and economy of power. Six different interchangeable, plug in 10-channel solid-state Writing Control cards are available to match your signal voltage and recording requirements. Included are types which operate with logic levels between +6 and +40 volts or -6 and -40 volts. Also, "precision types" for monitoring low level signals are available with adjustable threshold or balanced input (with respect to signal return). Model 361 system, for rack mounting or portable case, is 8 $\frac{3}{4}$ " x 19" wide x 14 $\frac{1}{2}$ " deep, weighs approx. 50 lbs. Complete 30-channel system, with either +6 v to +40 v or -6 v to -40 v Writing Control, is \$2050 F.O.B. Waltham, Mass. Prices with other Writing Controls on request.

FOR UP TO 120 CHANNELS of on-off recording, Model 360 uses 16" wide, 450-foot charts; has 9 standard and 9 optional additional speeds; takes only 14" of panel space complete with integral cooling system. Solid-state plug-in Writing Control cards described above are optional. Model 360 120-channel Recorder alone, \$3900; prices with various Writing Controls on request.



Call your nearby Sanborn Sales-Engineering Representative for complete specifications and application assistance. Offices throughout the U.S., Canada and foreign countries.

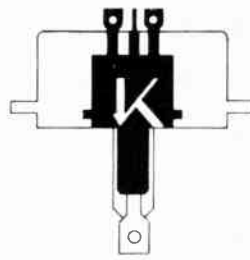
INDUSTRIAL DIVISION
SANBORN COMPANY

WALTHAM 54, MASSACHUSETTS
A Subsidiary of Hewlett-Packard Company

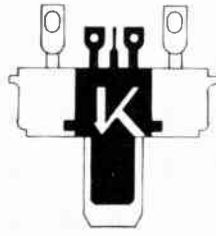
KEARFOTT

KEARFOTT power transistors average 30% lighter, 50% smaller and occupy 50% less mounting surface. **NEW** modified TO-10 hermetically sealed case and improved internal construction provide miniaturized **GERMANIUM PNP POWER** devices with ratings up to **120V @ 15 AMPS** (our #KPG2000). We are also a **DEPENDABLE SOURCE** for the following devices with ratings up to **200V @ 3AMPS**: 2N538 through 2N540A, 2N1202, 2N1203, 2N1326, 2N1438, 2N1466, 2N1501, 2N1502, 2N1504/10. Also available in TO-13 cases: 2N143/13, 2N156, 2N158, 2N158A, 2N1437, 2N1465.

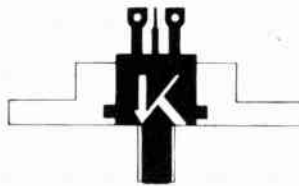
The following **DISTRIBUTORS** stock these devices: Carter Assoc. Inc., Scottsdale, Arizona; Cramer Electronics, Inc., Newton, Mass.; Hollywood Radio & Electronics, Hollywood, California; Solid State Specialist, Mountain View, California; Terminal-Hudson Electronics, New York City; Valley Electronics, Inc., Towson, Maryland. Write Kearfott Division, General Precision, Inc., Little Falls, New Jersey or 437 Cherry Street, West Newton, Massachusetts. These devices are designed, manufactured and life tested by **KEARFOTT SEMICONDUCTOR CORP.**, West Newton, Mass.



TO-36



MT-7



TO-3



TO-10



RO-28-1

Note how little volume and space are required by Kearfott's Transistors

GENERAL PRECISION AEROSPACE **KEARFOTT DIVISION**
LITTLE FALLS, NEW JERSEY
GENERAL PRECISION, INC.



Membership

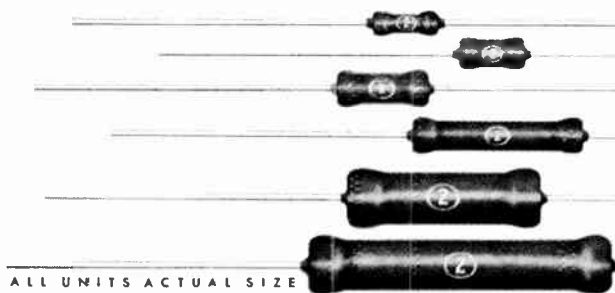


(Continued from page 163)

- Nicholson, B. F., Chesham, Bucks, England
- Norris, T. P., San Diego, Calif.
- Oberbeck, R. W., Loring AFB, Me.
- Orang, H. S., Ankara, Turkey
- Orme, J. E., Vancouver, B. C., Canada
- Papp, J., Washington, D. C.
- Patterson, R. E., Kansas City, Mo.
- Phillips, C. C., Lewisville, N. C.
- Phillips, W. A., Houston, Tex.
- Phillips, W. E., Lubbock, Tex.
- Pierick, K. R., Manhattan Beach, Calif.
- Pilling, D. E., Sepulveda, Calif.
- Poletsky, R., St. Louis, Mo.
- Pruitt, W. B., Clearwater, Fla.
- Puckette, S. C., Bellaire, Tex.
- Ramaswamy, V., Evanston, Ill.
- Ramsey, W. R., Prairie Village, Kan.
- Reids, W. A., Cherry Hill, N. J.
- Rieh, D. V., Grand Rapids, Mich.
- Robeck, R. H., Mountaine-side, N. J.
- Roberts, G. E. C., Stevenage, Hertfordshire, England
- Rombach, J. C., Santa Monica, Calif.
- Rorick, W. G., Cedar Rapids, Iowa
- Rubi, F. A., Scottsdale, Ariz.
- Sanders, J. B., Garland, Tex.
- Sanders, W. H., Menlo Park, Calif.
- Sandgate, J. H., Elmwood Park, Ill.
- Schindler, E., Bern, Switzerland
- Schuchman, R., San Diego, Calif.
- Schwieger, C. W., San Diego, Calif.
- Shatas, R. A., Redstone Arsenal, Ala.
- Sheerin, R. R., So. Hingham, Mass.
- Shelton, P. L., Crownsville, Md.
- Shepard, W. M., Herndon, Va.
- Shepherd, J. T., Rochester, Kent, England
- Shultz, J. D., Santa Monica, Calif.
- Simbi, M. S., Needham, Mass.
- Slaughter, R. P., Tulsa, Okla.
- Stocum, T. R., Jr., Encino, Calif.
- Smith, H. D., Del Mar, Calif.
- Smith, R. E., Dallas, Tex.
- Spicer, J. A., Littlefield Park, Ariz.
- Stannard, S. A., Windsor, Ont., Canada
- Stueker, H. T., Fort Worth, Tex.
- Sutherland, E. A., Mountain View, Calif.
- Sykes, R. C., Canoga Park, Calif.
- Takahira, A., Boulder, Colo.
- Takashima, B. T., West Los Angeles, Calif.
- Terpening, L. E., Irving, Tex.
- Terra, J. M., Peabody, Mass.
- Thompson, F. H., Washington, D. C.
- Thompson, J. C., Annapolis, Md.
- Tinckra, C. P., Mountain View, Calif.
- Toot, A. B., Dayton, Ohio
- Tootchan, G. D., Upper Darby, Pa.
- Tripathi, J. N., Bangalore, India
- Uher, G. T., Mountain View, Calif.
- Udovin, B. A. C., Ventura, Calif.
- Unger, F. G., Wakefield, Mass.
- Vergato, J. A., Pittsfield, Mass.
- Watson, A. C., Jr., Phoenix, Ariz.
- Webster, G. E., Park Ridge, Ill.
- Welp, L. L., Davenport, Iowa
- Welsh, W. G., Sr., Burbank, Calif.
- Westlake, J. H., Calgary, Alta., Canada
- Whittaker, J. L., Granada Hills, Calif.
- Willbur, D. E., Chadwick, N. Y.
- Wilkins, C. H., Warner Robins, Ga.
- Williams, A. J., Indian River City, Fla.
- Williams, D. R., Norman, Okla.
- Williams, W. R., Utica, N. Y.
- Woll, E. J., Jr., Fort Huachuca, Ariz.
- Woolam, A. E., China Lake, Calif.
- Wu, W. L. S., San Diego, Calif.
- Wynne, W. T., Willow Grove, Pa.
- Yee, E. L., Los Angeles, Calif.
- Zebell, R. A., San Jose, Calif.

(Continued on page 503)

our stock answer is



YES!

ALL AXIAL LEAD BLUE JACKET RESISTORS

in 1, 2, 3, 5, 7 and 10-watt power ratings are carried in factory stock for immediate delivery. Place your order now with your nearest Sprague District Office or Sales Representative.

Key Sprague Industrial Distributors carry most popular ratings in local stocks.

S P R A G U E S A L E S O F F I C E S

Ariz.	Phoenix, Sprague Electric Co., 3550 N. Central Ave., 279-5435	Mo.	St. Louis, Sprague Electric Co., 3910 Lindell Blvd., JE 5-7239
Cal.	Los Angeles, Sprague Electric Co., 12870 Panama St., UP 0-7531 or EX 8-2791	N. J.	Camden, Sprague Electric Co., 545 Cooper St., WO 6-1776
	San Francisco, W. J. Purdy of Calif., 312 7th St., UN 3-3300	N. M.	Albuquerque, Bowen & Carlberg Co., 2228A San Mateo Blvd., N.E., AM 5-1579
Colo.	Denver, R. G. Bowen Co., Inc., 721 S. Broadway, RA 2-4641	N. Y.	New York, Sprague Electric Co., 50 E. 41st St., OR 9-1195
D.C.	Washington, Sprague Electric Co., 2321 Wisconsin Ave., N.W., 338-7911		Great Neck, William Rutt, Inc., 123 Middle Neck Rd., HU 2-8160
Fla.	Clearwater, Sprague Electric Co., 1152 Cleveland St., 446-3119	N. C.	Winston-Salem, Sprague Electric Co., 928 Burke St., 722-5151
Ill.	Chicago, Sprague Electric Co., 5942 W. Montrose Ave., MU 5-6400	Ohio	Chagrin Falls, Sprague Electric Co., 24 N. Main St., CH 7-6488
Mass.	North Adams, Sprague Electric Co., Marshall St., 664-4411		Dayton, Sprague Electric Co., 224 Leo St., BA 3-9187
	Newton, Sprague Electric Co., 313 Washington St., WO 9-7640	Tex.	Dallas, Sprague Electric Co., 3603 Lemmon Ave., La 1-9971
Mich.	Detroit, ABM Sales Co., 10114 Puritan Ave., UN 2-1300	Utah	Salt Lake City, R. G. Bowen Co., Inc., 463 E. 3rd St., S., EM 3-4528
Minn.	Minneapolis, H. M. Richardson & Co., Inc., 9 E. 22nd St., FE 6-4078	Wash.	Seattle, Sprague Electric Co., 4601 Aurora Ave., ME 2-7761

*For application engineering assistance write:
Marketing Dept., Resistor Division, Sprague Electric Co., Nashua, New Hampshire.*

SPRAGUE COMPONENTS

RESISTORS	INTERFERENCE FILTERS	HIGH TEMPERATURE MAGNET WIRE
CAPACITORS	PULSE TRANSFORMERS	CERAMIC-BASE PRINTED NETWORKS
MAGNETIC COMPONENTS	PIEZOELECTRIC CERAMICS	PACKAGED COMPONENT ASSEMBLIES
TRANSISTORS	PULSE-FORMING NETWORKS	FUNCTIONAL DIGITAL CIRCUITS
MICRO CIRCUITS	TOROIDAL INDUCTORS	ELECTRIC WAVE FILTERS



*Sprague' and '®' are registered trademarks of the Sprague Electric Co.



Membership

(Continued from page 18A)

Admission to Associate

Aaron, P. D., Port Washington, L. I., N.Y.
 Arnold, R. E., Copley, Ohio
 Barisone, G. L., Birmingham, Mich.
 Patchler, R. C., Melrose Park, Pa.
 Bernard, M. Y., Paris, France
 Boon, C. E., Rantoul, Ill.
 Calapini, J. G., Chicago, Ill.
 Courtney, W. F., Thompsonville, Conn.
 Crozier, P. W., Rockland, Mass.
 Duncan, M. A., Torrance, Calif.
 Elbert, H. F., Sarasota, Fla.
 Feaster, J. L., Kirkwood, Mo.
 Friedman, M., Chicago, Ill.
 Grunauer, D. R., Brooklyn, N. Y.
 Gugelman, C. O., Seattle, Wash.
 Hild, A. C., Baltimore, Md.
 Hulbert, J. A., Willowdale, Ont., Canada
 Humphrey, W. G., Jr., So. Hamilton, Mass.
 Imam, M. Z., Karachi, Pakistan
 Jones, C. R., Winston-Salem, N. C.
 Keyes, R. E., Scotch Plains, N. J.
 Klemm, H. K., Port Washington, L. I., N. Y.
 Korein, J., New York, N. Y.
 Lauro, L. G., Torino, Italy
 Light, E. J., New York, N. Y.
 Lynn, W. V., Detroit, Mich.
 MacLaren, K. D., Winnipeg, Man., Canada
 Maguire, J. T., Draut, Mass.
 Mahmood, K., Kabul, Afghanistan
 Mangold, D. W., Eau Gallie, Fla.
 Martinez, J. L., Mendoza, Argentina
 Matter, D. J., Racine, Wis.
 McKnight, R. W., Troy, N. Y.
 Messick, R. L., North Canton, Ohio
 McGarry, D., Oyster Bay, L. I., N. Y.
 Michell, F. R., Fort Bliss, Tex.
 Miller, J. V., Redwood City, Calif.
 Mitchell, J. E., Jr., Washington, D. C.
 Omureali, M. S., Ankara, Turkey
 Parada, P. C. C., Caracas, Venezuela
 Peters, H. S., St. Charles, Ill.
 Potrat, B. M., Baltimore, Md.
 Richter, L. D., Baltimore, Md.
 Ryan, J. A., Longmeadow, Mass.
 Smith, B. R., Burlington, Iowa
 Sujanani, H. H., Cotabato City, Philippines
 Salazar, C. C., Ciudad, Guatemala
 Spaulding, H. E., Easton, Pa.
 Thomas, J. R., Fairview, Mass.
 Tucker, L. F., Englewood, Colo.
 Uhl, N. P., Silver Spring, Md.
 Van Lehn, J. D., Cambridge, Ohio
 Voelker, C. G., Towson, Md.
 Wessel, H. U., Deerfield, Ill.
 Yamaguchi, T. D., Los Angeles, Calif.
 Yoshino, T., Tokyo, Japan
 Zeller, I. R., No. Massapequa, L. I., N. Y.



Section Meetings

ATLANTA

"Systems Equipment Engineering," M. C. Wright, Western Electric Co.; 9/28/62.

BEAUMONT-PORT ARTHUR

"GEMINI, Man-In-Space-Project," W. B. Evans, NASA; Two movies with paper; 9/18/62.

"Production Flow Stations in Lake Maracaibo, Venezuela," P. S. Phillips, Sun Pipe Line Co.; 10/16/62.

BENELUX

International Symposium on Information Theory; 9 3-7/62.

BINGHAMTON

"Telstar—An Experiment in Satellite Communications," J. R. Githens, Bell Telephone Labs.; Joint with AIEE; 9/24 62.

BYFALO-NIAGARA

Tour of Sylvania Home & Commercial Electronics Div.; 9/22/62.

CLEVELAND

"Problems of Manned Space Flight," T. Black, NASA; 5/10/62.

"A Voice for Mercury," F. E. Demaree, Bell System Training School; 9 13/62.

DALLAS

"Telstar," R. W. Hatch, Bell Telephone Labs.; 9/25 62.

EMPORIUM

"The Great Barrier Reefs of Australia," J. W. Wells, Cornell University; 9 11/62.

ERIE

Tour of WSEE Television Studios, E. Zellefrow; Joint with AIEE; Ladies Night; 9 11/62.

"Design and Application of Crystal Filters," D. Bednarski, Biley Electric Co.; "Toroidal Inductors: Design Considerations and Specifications," W. Trudnowski; Forbes and Wagner Co.; 10 3 62.

FORT HAVEN

"Range Instrumentation for the X-15 Rocket Program," J. Conley, USAF; 10/2/62.

FORT WAYNE

"Recent Development in Relays," L. D. DeLalio, Filters, Inc.; 10/18/62.

FORT WORTH

"FM Multiplex Systems for Stereophonic Transmission and Reception," C. L. Griggs, Trinity Broadcasting Co., KJLH AM-FM; 10 9 62.

INDIANAPOLIS

Tour of U. S. Naval Avionics Facility; Joint with AIEE; Film "The USNAFI Story"; 9/13/62.

KANSAS CITY

"A Linear Computer for Time and Distance," K. L. Morton, Western Electric; 9/10/62.

LITTLE ROCK

"Sub-Carrier Operation of FM Broadcasting Stations," O. Alagood and J. Elder; Radio Station KMMK-FM; Film "Music In Motion"; 10/15 62.

LOS ANGELES

"Space Exploration and Baseball," F. Adler, Hughes Aircraft Co.; Joint meeting hosted by Southern Sub-Section; 9/27/62.

MOBILE

Tour of WKRG-TV Transmitter Facility, H. Skelton; 4/27/62.

"Human Factors in Engineering," H. Berridge, Air Proving Ground Eglin AFB; 5/24/62.

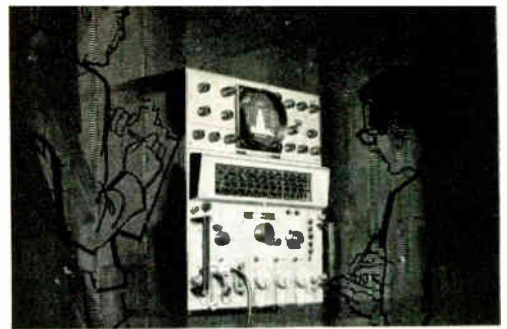
"PERT (Program Evaluation and Review Techniques)," W. Fundinger, Mobile Air Materiel Area (Air Force); 6/28/62.

"Telstar," R. Gudgen, Southern Bell Tel. & Tel.; 9/27/62.

NEW YORK

Panel on Information Retrieval, M. Kochen, IBM Research Center; M. M. Flood, University of Michigan; H. P. Luhn, Consultant; R. Kirsch, Nat'l Bureau of Standards; J. Tukey, Bell Tel. Labs.; 10/3/62.

(Continued on page 54A)



Panoramic SPECTRUM ANALYZER

SPA-4a

SPECIFICATION HIGHLIGHTS

FREQUENCY RANGE: 10 mc to 44,000 mc in 8 bands, (selected by push-button operated band switch).

FREQUENCY ACCURACY: Scale calibrations $\pm 1\%$ or ± 1 mc, whichever is larger.

GUARANTEED MINIMUM SENSITIVITIES

RANGE (mc)	SENSITIVITY* (dbm)
10 to 420	-100 to -110
350 to 1000	-95 to -105
910 to 2200	-105 to -110
1980 to 4500	-100 to -105
4500 to 10880	-100 to -110
10880 to 18000	-95 to -105
18000 to 26500	-85 to -95
26500 to 44000	-75 to -90

*minimum measurable signal

DISPERSION (2 separate swept I.o.'s): wideband adjustable up to 70 mc (greater dispersions optional), narrow-band 0-5 mc.

I-F BANDWIDTH: Adjustable continuously from 1 kc to 80 kc.

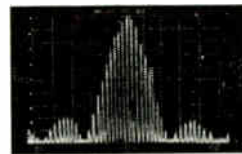
AMPLITUDE SCALE CALIBRATIONS: Linear, 40 db Log, and Power (square law).

SWEEP RATE: Continuously adjustable from 1 cps to 60 cps; synchronized from line or external source; or free running plus provision for Sweep Rate Calibration.

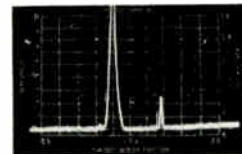
FREQUENCY MARKERS: Two calibrated ranges: 0 to ± 40 mc and 0 to ± 3 mc.

Marker Modulation input range, 10 kc - 2 mc, for additional marker pips with frequency spacing determined only by external modulating signal generator frequency.

AUXILIARY OUTPUTS: Synchroscope. Detected signal envelope with 60 db gain. X, Y, and Z axis outputs also provided.



Typical SPA-4a screen photograph showing spectrum of pulsed signal. Here, individual sidebands are clearly resolved.



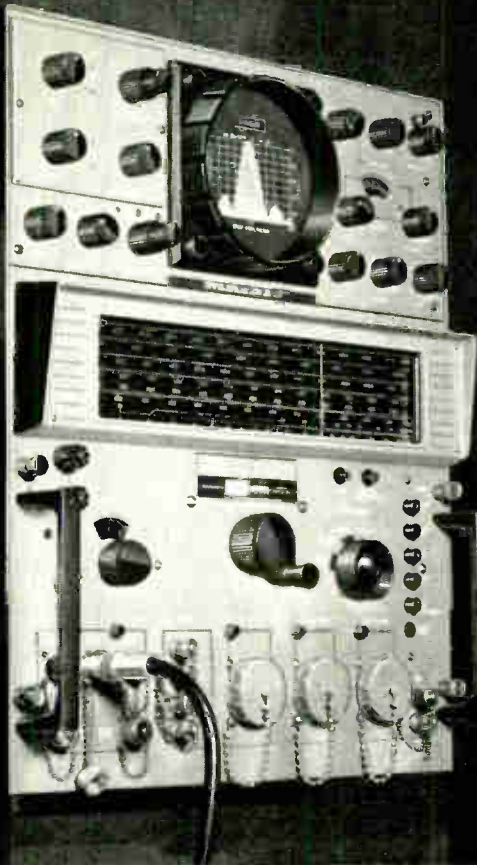
Wide spurious-free dynamic range of SPA-4a shown at left. Larger signal 15 db above full scale log. Smaller signal is -43 db from larger.

Electronic Engineers & Physicists

Expansion program opens new opportunities. Interesting work on advanced instrumentation projects . . . excellent working and living environment. Contact **Mr. A. E. Rodger**, Singer Metrics Division, Singer Manufacturing Company, 915 Pembroke St., Bridgeport 8, Conn.



Panoramic* SPECTRUM ANALYZER
SPA-4a 10 mc to 44,000 mc
 WITH ONE TUNING HEAD



STILL UNMATCHED

IN BROAD RANGE SENSITIVITY — WITH PROVEN RELIABILITY

PROVIDES RAPID, ACCURATE RF thru MICROWAVE ANALYSIS

You can count on *sensitivity of at least* -100 dbm in S or X band, -85 dbm in K band... typically, signals 5 to 10 db weaker can be analyzed with the SPA-4a. (See complete sensitivity table on facing page).

SPA-4a's unmatched performance is due to its many advanced design features. For example, the simply used, directly calibrated tuning head with push-button band selection includes not two but *three* stabilized, low FM local oscillators. The highest frequency l.o. covers the 4.5-11 mc band on fundamentals. The four internal broad band input mixers (1 coax and 3 waveguide) provide exceptional response.

High uniform sensitivity, low residual distortion and fewer l.o. harmonics provide displays with a wide spurious-free dynamic range. These SPA-4a characteristics have enabled it to handle many heretofore difficult applications such as narrow pulsed signal analysis and broad band, low level measurements such as in distortion tests and RFI monitoring. With its low residual FM and selectivity adjustable to 1 kc, the SPA-4a also finds important application in narrow band signal studies which require resolution of closely spaced frequencies and a high order of analyzer stability.

ADDITIONAL OUTSTANDING FEATURES

- Extremely bright traces on 5" CRT with 3 calibrated level scales, linear, 40 db log, and power.
- Adjustable I-F bandwidth facilitates setting of optimum selectivity for all types of signals.
- Synchroscope output provides detected and amplified signal input for external scope.
- Marker Modulation enables precise narrow band dispersion calibrations by means of sideband pips.
- Well-shielded, modular construction. Convenient access to all parts.
- Low down-time due to careful construction (using MIL spec's as guide) and vigorous quality control.

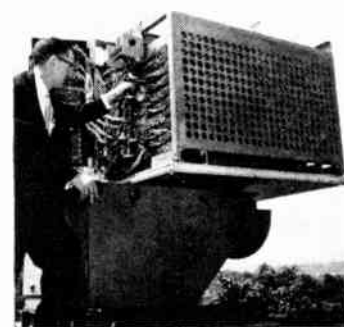
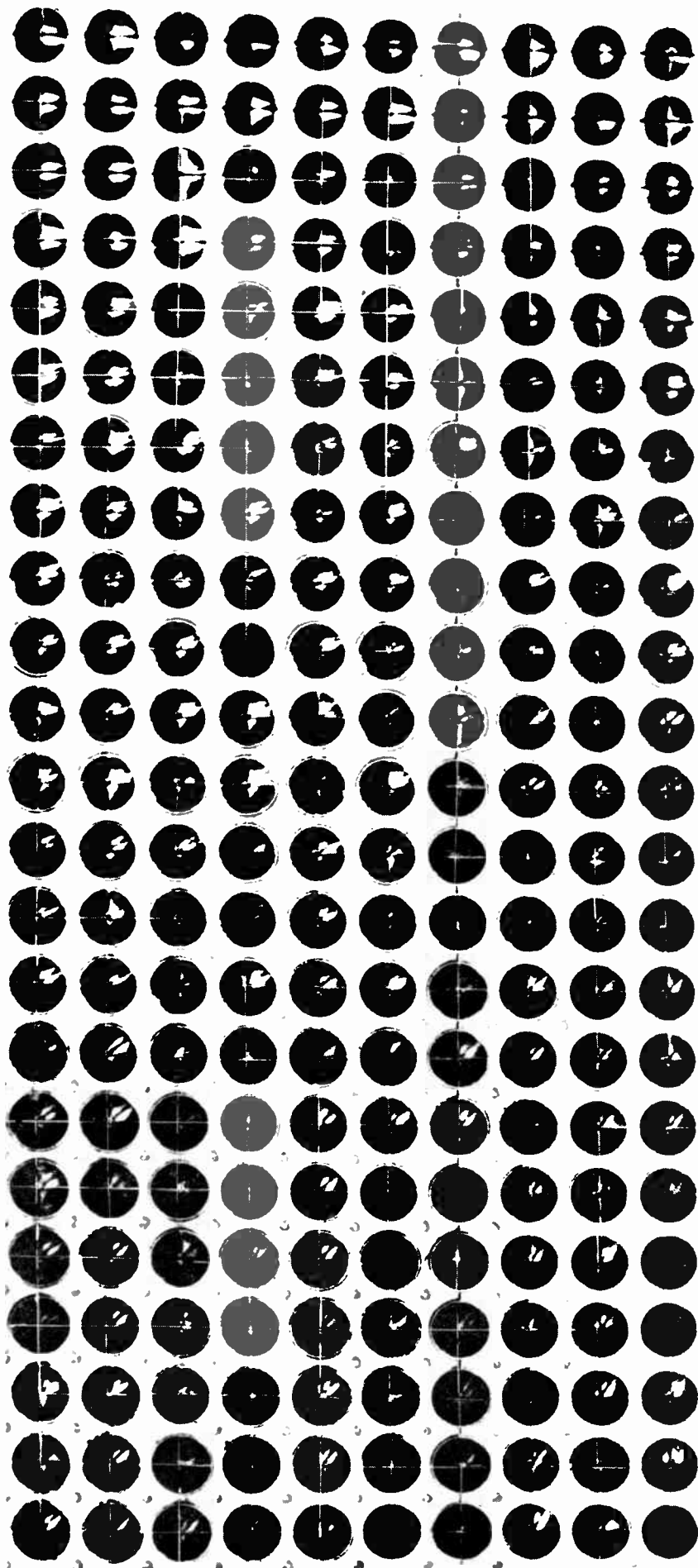
FIELD PROVEN, HUNDREDS NOW SUCCESSFULLY USED

- Pulsed signal analysis; power points, lobe widths, irregular pulsing.
- Monitoring of AM, FM, PM communication channels.
- Malfunction study, e.g., parasitics, carrier shifts, etc.
- Noise and RFI investigations.
- Distortion analysis; harmonic, intermodulation, etc.
- Calibration and maintenance of signal sources.

Channel your microwave spectrum analysis problems to the Panoramic SPA-4a — get the quick, guaranteed-reliable answers now obtained from hundreds in operation (see facing page for specification highlights). A quarter-century of spectrum analyzer experience assures you of engineered quality you can count on. Why not get complete information? Write, wire or phone today for the SPA-4a comprehensive 8-page technical bulletin and new catalog digest.



* A TRADEMARK OF THE SINGER MANUFACTURING COMPANY



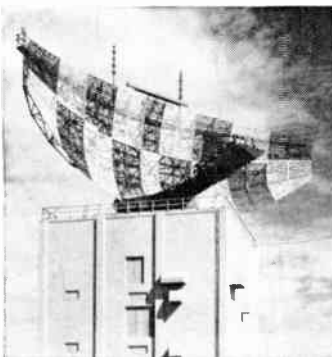
PHASED PLANAR ARRAY forms multiple scanning radar beams. G.E.'s even newer, more efficient **MOSAR** array scans the sky millions of times each second to generate at low cost as many independently steered receive beams as needed.

RADAR

Sweeping advances in aerospace technology have caused radar targets to vary widely in size, range and altitude, speed and acceleration. Resulting radar design problems are further intensified by electronic jamming and the need for decoy discrimination, creating a continuous demand for increased capabilities.

General Electric has anticipated this challenge with steady improvements in transmitter and receiver performance, mechanical design, and signal processing. Low-noise parametric amplifiers and masers extend effective range while new pulse compression techniques improve target range discrimination. Antenna structures are built to increasingly closer tolerances for reduced side-lobes and precise angular positioning. Coherent integrators provide both velocity resolution and high signal-to-noise ratios, combining with side-lobe cancellers to diminish the effect of radio interference.

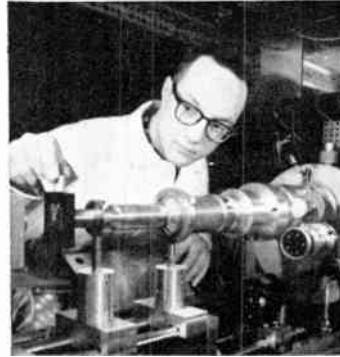
Such developments are reflected in a broad range of radars produced by General Electric and installed in virtually every major country in the Free World—radars that include the FPS-50 surveillance giant for the Air Force's BMEWS, the High Power Acquisition Radar (HIPAR) for the Army's Improved Nike-Hercules System, and the Marine Corps' high-mobility TPQ-10.



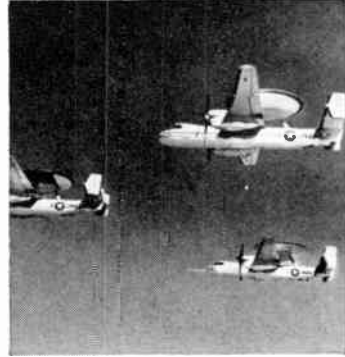
GROUND BASED FPS-24 search radar is one of the largest and most modern radars in the Semi-Automatic Ground Environment (SAGE) air defense network. Designed for the U.S. Air Force, it will detect supersonic high-altitude aircraft at long range.



STABILIZED ANTENNA for the U.S. Navy's SPS-30 shipboard radar is actuated in roll and pitch by a unique dual ball-screw drive. The precision, electro-formed organ-pipe scanner permits long-range, high-accuracy search and height-finding capability.



OPTICAL PROCESSOR uses oil-film storage to analyze high-resolution radar returns in real time. Over one million integrations can be performed simultaneously by this processor to determine range, velocity, and acceleration for multiple targets.

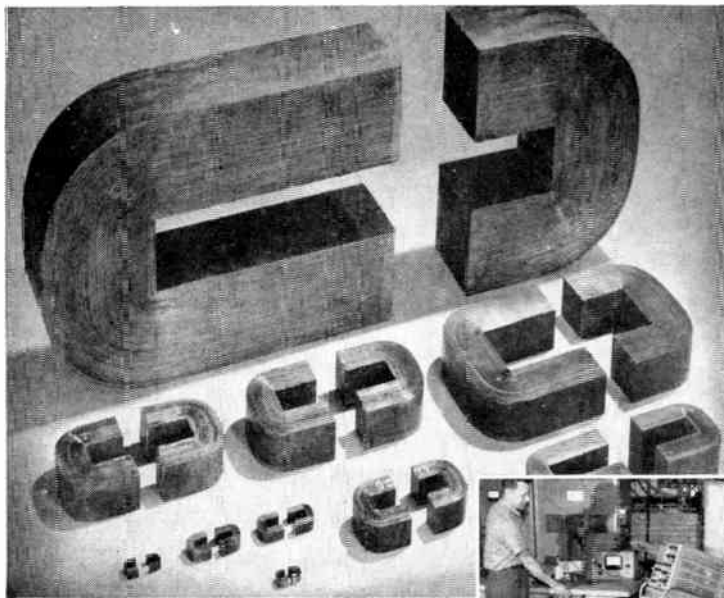


AIRBORNE APS-96 will afford increased detection capabilities for fleet early warning as well as contribute to the control of intercept aircraft. This advanced radar is currently under flight test aboard the U.S. Navy Grumman-built Hawkeye.

Progress Is Our Most Important Product

GENERAL  ELECTRIC

AEROSPACE AND DEFENSE GROUP



Arnold Pulse Transformer Cores are individually tested under actual pulse conditions

The inset photograph above illustrates a special Arnold advantage: a 10-megawatt pulse-testing installation which enables us to test-prove pulse cores to an extent unequalled elsewhere in the industry.

For example, Arnold 1 mil Silectron "C" cores—supplied with a guaranteed minimum pulse permeability of 300—are tested at 0.25 microseconds, 1000 pulses per second, at a peak flux density of 2500 gauss. The 2 mil cores, with a guaranteed minimum pulse permeability of 600, receive standard tests at 2 microseconds, 400 pulses per second, at a peak flux density of 10,000 gauss.

The test equipment has a variable range which may enable us to make special tests duplicating the actual operating conditions of the transformer. The pulser permits tests at .05, .25, 2.0 and 10.0 microsecond pulse duration, at repetition rates varying anywhere from 50 to 1000 pulses per second.

This is just another of Arnold's facilities for better service on magnetic materials of all description. ● Let us supply *your* requirements.

Here's technical data on **ARNOLD SILECTRON CORES**



Bulletin SC-107 A contains design information on Arnold Tape Cores wound from Silectron (grain-oriented silicon steel). It includes data on cut C and E cores, and uncut toroids and rectangular shapes. Sizes range from a fraction of an ounce to more than a hundred pounds, in standard tape thicknesses of 1, 2, 4 and 12 mils.

Cores are listed in the order of their power-handling capacity, to permit easier selection to fit your requirements, and curves showing the effect of impregnation on core material properties are included.

4102

ADDRESS DEPT. P-12.



ARNOLD

SPECIALISTS in MAGNETIC MATERIALS

THE ARNOLD ENGINEERING COMPANY, Main Office: MARENGO, ILL.
BRANCH OFFICES and REPRESENTATIVES in PRINCIPAL CITIES



Section Meetings

(Continued from page 50A)

NORTH CAROLINA

"College Achievement and Progress in Management," D. L. Grant, American Tel. & Tel. Co.; 9/26/62.

NORTHERN NEW JERSEY

"Fundamentals of Future Electronics," T. Carver, Princeton University; 9/12/62.

OKLAHOMA CITY

"Automation and Control of Atoka Pipeline Pumping Stations," F. Rodesney, Benham Engineering Co.; Joint with AIEE; 9/25/62.

PRINCETON

"Electron Beam Drilling, Milling and Welding," R. Bakish, Electronics and Alloys, Inc.; 10/9/62.

ROCHESTER

"Optical Masers: Principles, Practices and Potentialities," C. Alley, Univ. of Rochester; 9/26/62.

"Facsimile Is It Analogue or Digital?," J. L. Wheeler, Xerox Corp., Inc.; 10/11/62.

SACRAMENTO

"Satellite Communications with emphasis on Telstar," J. W. Fitzwilliams, Bell Tele. Labs.; Joint with AIEE; 9/27/62.

"Direct Energy Conversion," J. J. W. Brown, General Electric Co.; Joint with AIEE; 10/11/62.

SALT LAKE CITY

"Your Future With IEEE," D. K. Reynolds, Univ. of Washington; Joint with AIEE; 9/28/62.

SCHENECTADY

"Technical Aspects of Telstar," J. A. Murray, Bell Tele. Labs.; 10/16/62.

SEATTLE

Student Prize Papers Contest; 4/10/62.

"Report on Travel and Communications in Europe," T. R. Hewitt; Pacific Northwest Bell Tele.; Retired; 5/10/62.

"Miniaturization Philosophy for the Entertainment Section of Electronics," J. R. de Miranda, Philips Industries; 8/28/62.

"Stanford Linear Accelerator," K. Willson, Stanford Linear Accelerator Center; 9/20/62.

SHREVEPORT

"VORTAC, Discussion & Inspection," E. S. Turner and P. Patterson, Federal Aviation Agency; 10/2/62.

SOUTH BEND MISHAWAKA

"Electronics in the Oil Industry," G. Mully, Gulf Oil; 9/27/62.

SOUTH CAROLINA

"Maintenance Data Analysis—A Tool To Reliability," H. A. Voorhees, Western Electric Co.; 9/28/62.

TOLEDO

Annual Fall Dinner Meeting; 9/13/62.

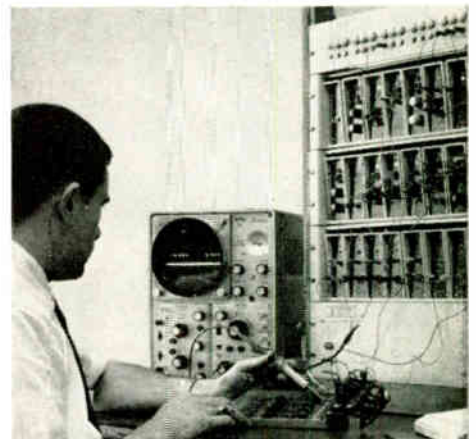
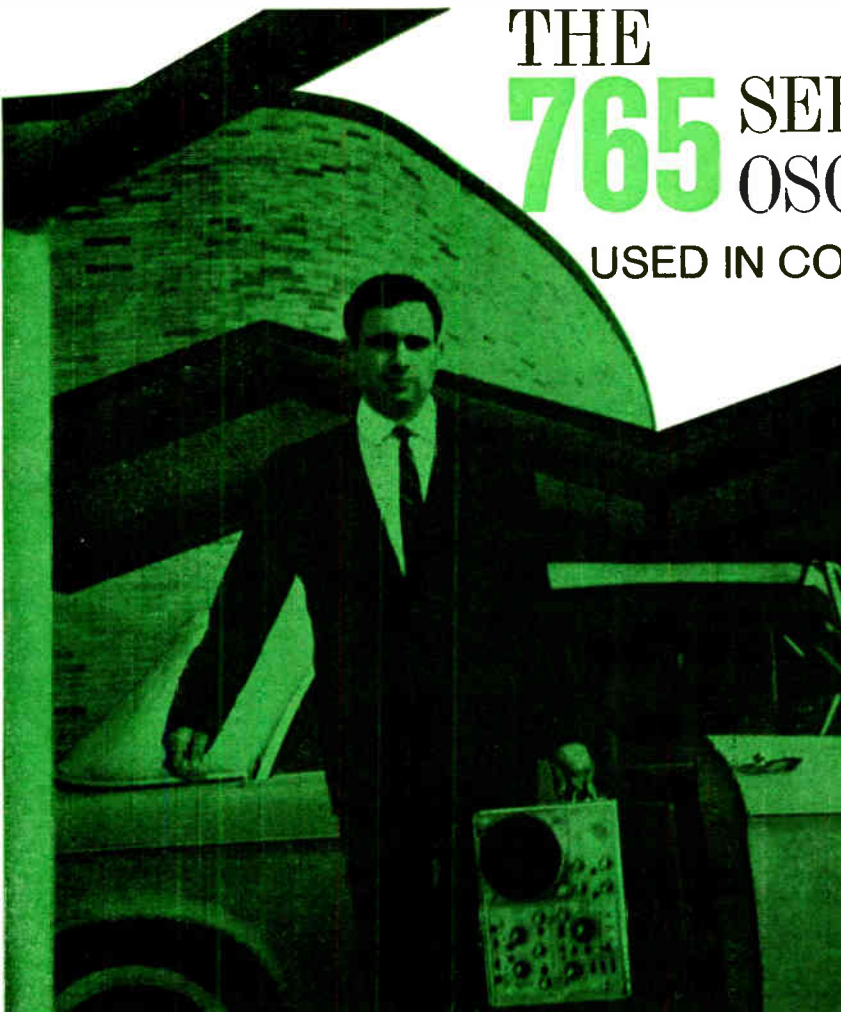
TUCSON

Tour of facilities of Kitt Peak National Observatory; 6/28/62.

(Continued on page 50A)

THE 765 SERIES OSCILLOSCOPES

USED IN COMPUTER CHECKOUT



The need for professional, laboratory-type high-frequency oscilloscopes—easily transported in the lab or in the field—was one of the design parameters that prompted the development of Du Mont's new, solid-state, light-weight 765 series of oscilloscopes. A 5 mv/cm sensitivity at 25 Mc, a 14.8 nsec risetime, together with dual-beam capabilities are part of the specifications which are incorporated.

An example of the use of this new, highly-portable scope is illustrated by Mr. David Denniston, sales engineer of Digital Equipment Corporation, Maynard, Massachusetts, who utilizes it in the field and in his laboratory to periodically check and maintain computer modules manufactured by the firm. The compactness and light weight features enable Mr. Denniston to readily transport his Du Mont 766 bench type high frequency scope in his car. As a result, there is no need to depend upon a customer's oscilloscope. He knows that the instrument he uses is correctly calibrated and that field test measurements are valid.

THREE VERSIONS—The 765 Series comes in three different mechanical configurations to meet user requirements. The 765 PortaScope* for real portability. The 766 Bench Version. The 767 Rack Mounted version only 7-inches high.

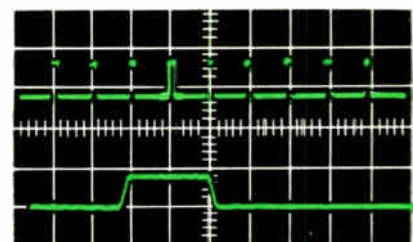
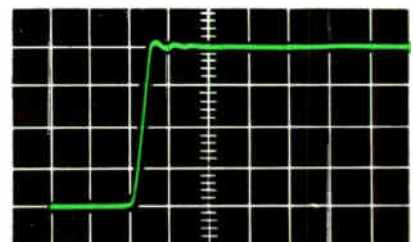
* T.M.

7"



TYPE 767 OSCILLOSCOPE
—shortest (only 7" high) rack-mount, high-frequency oscilloscope available.

- Ten times more sensitive (5 mv/cm) at 25 Mc.
- Silicon solid-state circuitry
- Flexibility of dual plug-in circuits driving CRT directly
- Smallest high-frequency oscilloscope available
- Three versions—for bench, portable or rack use.



Upper oscillogram displays how a 3 nsec risetime looks on a 765 Series Oscilloscope when using a Type 76-01 Single-Channel Plug-In. Rapid switching transients are easily "captured" to establish necessary corrective measures on system under test. Sweep rate is 10 nsec/cm as provided by a Type 74-03 Time Base Plug-In. Below: Type 74-13 Dual Time Base Delaying Sweep Plug-In provides a strobe to select a particular pulse or trace sector (as depicted by brightened pulse), and enables its expansion for detailed investigation. Used with Type 76-02 Dual Channel Plug-In, expanded trace can be studied simultaneously as shown in lower trace.

GET ON BOARD THE NEW, GROWING DU MONT. Too opportunities for oscilloscope and other instrument engineers. Engineering openings also in storage tubes, multiplier phototubes. Tube sales engineers, district sales and engineers for mobile, and closed-circuit television engineers and sales engineers. Write or call George Vetan, Industrial Relations, Prescott 3-2000.

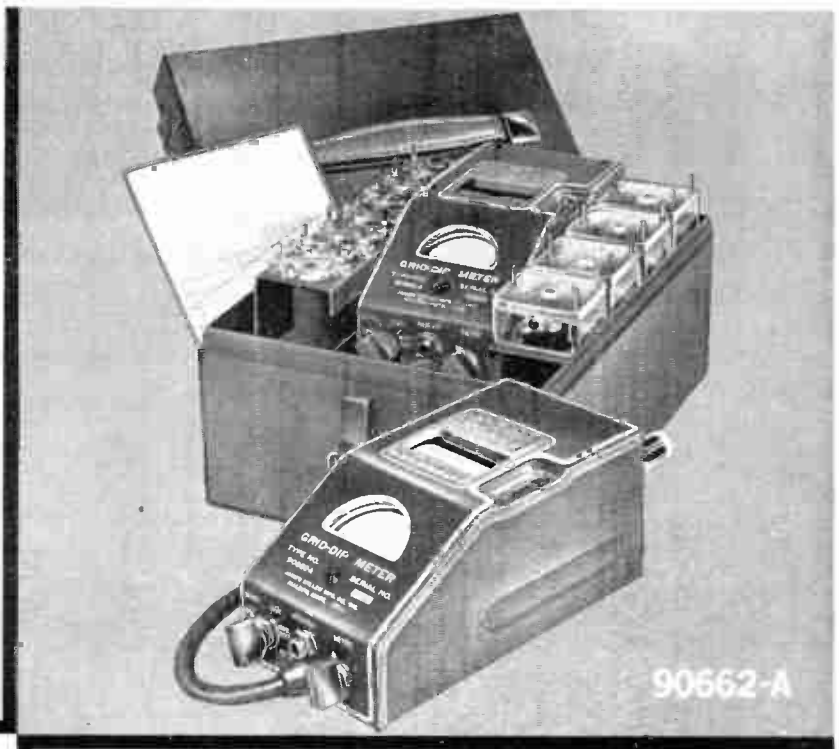


ALLEN B. DU MONT LABORATORIES
DIVISIONS OF

FAIRCHILD CAMERA AND INSTRUMENT CORPORATION 750 BLOOMFIELD AVENUE, CLIFTON, N.J.

Designed for

 Application



**NO. 90662-A INDUSTRIAL
 GRID DIP METER**

225 kc. to 300 mc. Hand calibrated $\pm 0.5\%$. Rugged 1-milliamper meter with transistor d. c. amplifier for maximum sensitivity. Transistor modulator. Silicon rectifiers. Convenient single-unit one-hand operation. Eleven individual coils with form-fitting molded covers. Complete in carrying case.

JAMES MILLEN MFG. CO., INC.
MALDEN
MASSACHUSETTS

on-time delivery of emergency and prototype

BENDIX

connector needs. 8 Stocking Facilities

Specify the new Bendix Products

AVNET

contact Avnet for best service

on-time delivery of Sperry Semiconductors

AVNET

8 Stocking Facilities, Coast to Coast.

Specify the new Sperry Products

SPERRY

contact Avnet for best service



Section Meetings

(Continued from Jan. 54)

TULSA

"Air Traffic Control Facilities at Tulsa Municipal Airport," W. Plummer, FAA; "Radar Facilities at Tulsa Airport," R. Allen, FAA; Tour of Spartan Electronic School; Tour of new Airport Control Tower Facilities; Tour of Radar Installation at Tulsa Municipal Airport; 9-29-62.

TWIN CITIES

"Looking at Patents," S. R. Peterson; Meyers & Peterson; Joint with AIEE; 9-25-62.
 "Miniaturization," C. Wellard, American Components, Inc.; Joint with AIEE; 10-11-62.

VIRGINIA

"Microwave Phototubes," B. J. McMurtry, Sylvania Elec. Prod., Inc.; 9-28-62.
 "Automation in Color Sorting," J. Ward, Specialties, Inc.; 10-12-62.

WESTERN MASSACHUSETTS

"The Cytotron: The Ultimate in Micro-miniaturization?," B. R. Shepard, General Elec. Co.; 9-25-62.

WICHITA

"The Effects of Acoustical Noise on Electronic Equipment," G. C. Cassidy, The Boeing Co.; 5-31-62.

WINNEPEG

General Business Meeting; 9-28-62.

SUBSECTIONS

BUSINESS SYSTEMS

"Seismic Instrumentation and its Application to the Detection of clandestine Nuclear Explosions," A. Vigil, United Electro Dynamics; "The Seismological Observator, Tonto Nat'l Forest, Arizona," P. Klasky, United Electro Dynamics; 9-12-62.

CAUSKILL

"Opportunities from the Shakeout in Electronics," C. Edgar, Senior Security Analyst; C. M. Losh, Rhodes and Co.; 10-9-62.

MERRIMACK VALLEY

"An Undergraduate Level Educational Program in Semiconductor Electronics," R. B. Adler, MIT; 9-21-62.

PANAMA CITY

"The Bateman Theory of Human Audition," J. D. Grandine, United Research Associates, Inc.; 9-25-62.

PUEBLO

"Residential Acoustics," J. J. Martinet, Western Electric Co.; 9-11-62.

SOUTHERN

"Space Exploration & Baseball," F. Adler, Hughes Aircraft Co.; 9-27-62.

WESTERN NORTH CAROLINA

"Manufacturing Processes Celanese Plant," S. Finch, Celanese Plant; Tour of Celanese Plant; 9-28-62.

REQUIRED

Excellence In Receiver Selectivity With Minimum Component Population

SOLUTION:

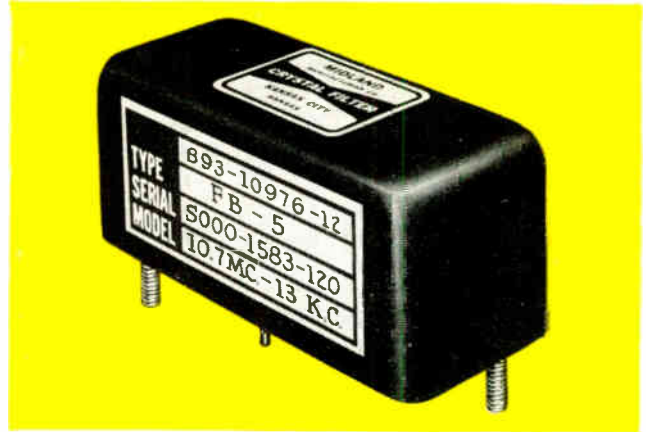
1 Midland filters with guaranteed ultimate discrimination of more than 100 db with 60db/3db BWR < 1.8 2 A low cost stock filter with virtually no insertion loss

FACT

Midland crystal filters are the result of exact design methods and real production knowhow.

Facts are facts and filters are Midland's business. Their filter and crystal engineering skills and facilities assure the user of top reliability and performance. * This is Midland's Type FB-5 crystal filter produced by the tens of thousands — the only sure proof of production ability. It is an 8 pole — 6 zero precision network that incorporates no added dissipative elements in inband ripple control. Result: Superior selectivity with essentially no midband insertion loss. A quality production component with immediate delivery. Engineering Bulletin NBS-103 is available detailing complete technical information. Prices on request.

* Write for Midland's capabilities and facilities brochure, "Midland — in microspect".



SPECIFICATIONS

Center Freq: 10.7 MC \pm 375 CPS
 Bandwidth @ 6 db.: 13.0 KC Min. — 13.8 KC Max.
 60 db/6 db BWR: 1.8 Max.
 100 db/6 db BWR: 2.2 Max.
 Ultimate Attenuation: 105 db. Min., 8 MC to 14 MC
 Midband Insertion Loss: 0.5 db. Nominal, 1 db. Max.
 Inband Ripple: 0.5 db. Nominal, 0.8 db. Max.
 Operating Temp. Range: -55° C to $+90^{\circ}$ C
 Zin/Zout Req: 1100 OHMS \pm 5% in parallel with adjustable capacitor 0-5 picofarads.
 Dimensions: 2 $\frac{3}{8}$ " L x 1" W x 1 $\frac{32}{32}$ " H



MANUFACTURING COMPANY
 Division Pacific Industries, Inc.
 3155 Fiberglas Road Kansas City 15, Kansas

Professional Group Meetings

AEROSPACE AND NAVIGATIONAL ELECTRONICS

Akron—September 18

"Survey of Solid State Devices," Dr. Lawrence J. Giacometto, Michigan State University, East Lansing, Mich.

New York—June 14

Business meeting and tour of Bendix Plant.

ANTENNAS AND PROPAGATION MICROWAVE THEORY AND TECHNIQUES

Philadelphia—September 19

"Semiconductor Diode Switch, Limiter and Duplexer Advances at Diamond Fuse Laboratories," Robert Garver, Diamond Ordnance Fuse Laboratories.

"Early Adventures in Microwave Research," Dr. George Southworth, Bell Telephone Laboratories (Retired).

Toronto—September 24

"The Nature of the Moon's Surface," Dr. B. A. MacRae, University of Toronto.

AUDIO

Cleveland—May 24

"New Techniques in Stereophonic Recording for Multiplex," Kenneth R. Hamann, Cleveland Recording Company, 1515 Euclid Ave., Cleveland, Ohio.

Philadelphia—September 28

"A System of Electrostatics Recording," Robert Kerr, E. I. DuPont of Nemours and Company, Wilmington, Del.

AUTOMATIC CONTROL

Los Angeles—May 8

"Hydrofoils," R. Smyth and J. M. Johnson, Douglas Aircraft Company, Santa Monica, Calif.

New York—May 22

"Hall Effect Devices as Applied to Control Systems," Donald Leibowitz, General Precision Aerospace Group, Little Falls, N. J.

New York—April 25

"Information Theory Applied to Bionics and Biology," Jack D. Cowan, M. I. T.

BIO-MEDICAL ELECTRONICS

Cleveland—September 19

"Graduate Education in Biomedical

(Continued on page 58A)

on-time delivery of Microdot Connectors and Cable

AVNET

8 Stocking Facilities,
Coast to Coast

Specify the new Microdot Products

MICRODOT

contact Avnet for best service

on-time delivery of standard

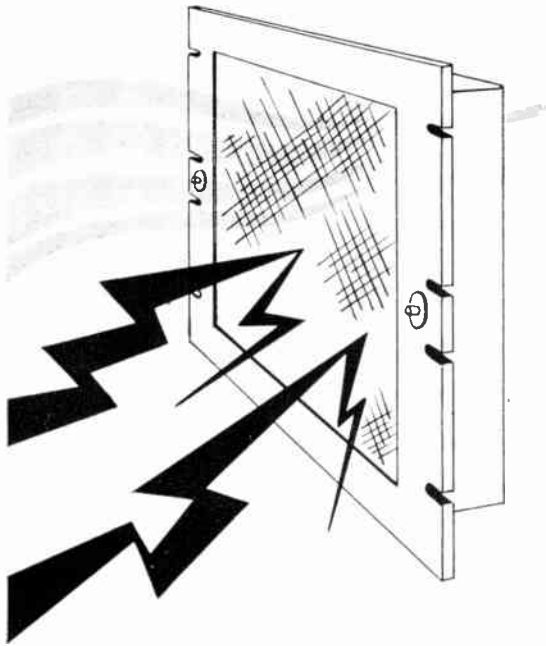
SEMICONDUCTORS

and hard to get items.

Specify the new semiconductors

AVNET

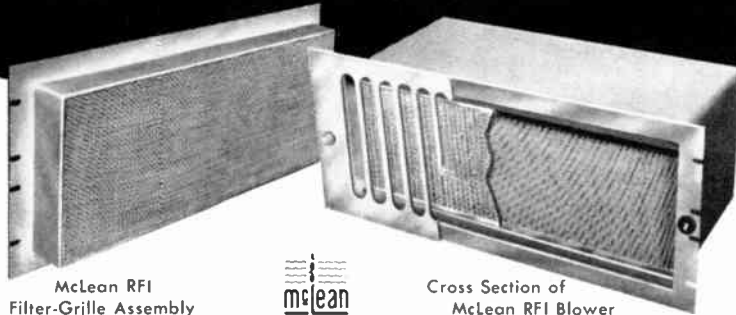
contact Avnet for best service



**FILTERED
COOLING AIR
IN!...**

**RFI
OUT!**

**WITH
NEW McLEAN
RFI BLOWERS!
AND FILTER-GRILLE ASSEMBLIES**



McLean RFI
Filter-Grille Assembly



Cross Section of
McLean RFI Blower

Now McLean makes it possible for you to pressurize radio shielded electronic cabinets with cool, filtered air without opening the "envelope" to RF interference.

These new McLean RFI blowers and filter-grille assemblies have been government-approved for RFI performance in accordance with MIL-I-6181D — meeting or exceeding all requirements including susceptibility, generation and shieldability. This development is one of many by McLean engineers designed to assure reliability of electronic equipment. **WRITE TODAY** for further information.

McLEAN
ENGINEERING LABORATORIES

World Leader in Packaged Cooling

P.O. Box 228, Princeton, New Jersey

Phone: Area Code 609 WAlnut 4-4440 TWX 609-799-0245



SEND FOR
NEW 44-PAGE
CATALOG

Or Our
NEW MIL-SPEC
BLOWER
CATALOG

**Professional
Group Meetings**

(Continued from page 57A)

Engineering," Dr. J. H. U. Brown, National Institutes of Health, Bethesda 14, Md.

Rochester — October 2

"Electronic Analogs of the Human Ear," Professor Josef Zwislocki, Syracuse University, Syracuse, N. Y.

Rochester — July 17-18

"Conference on Data Acquisition and Processing in Biology and Medicine."

CIRCUIT THEORY

Los Angeles — September 18

"Spaceborne Computers for Now and Later," Ladimer J. Andrews, Aerospace Corporation, El Segundo, Calif.

"Integrated Switching Circuit Using Transistor Coupled Logic," James L. Buie, Pacific Semiconductors, Inc., El Segundo, Calif.

CIRCUIT THEORY

INFORMATION THEORY

Omaha-Lincoln — September 4

"Kickoff: Thirteenth Annual Professional Registration Class," Richard Kessler, NW Bell, Omaha, Neb., Joseph A. Rogers, Westinghouse Elevators, Omaha, Neb.

COMMUNICATIONS SYSTEMS

Northern New Jersey — September 18

"Data Communications Using the Telephone Systems," W. O. Fleckenstein, Bell Telephone Laboratories, Holmdel, N. J.

COMMUNICATIONS SYSTEMS

VEHICULAR COMMUNICATIONS

Omaha-Lincoln — September 25

"The New Six Trunk Line Concentrator-Identifier for Telephone Answering Service," Merle Laughlin, Western Electric, Omaha, Neb.

Tour, Western Electric Manufacturing Floor.

Omaha-Lincoln — September 20

"Telstar and Satellite Communications," Glen H. Sanders, Northwestern Bell Telephone Company, Omaha, Neb.

Philadelphia — May 21

"Sequential Coding," George C. Hennesy, RCA, Camden, N. J.

Philadelphia — April 24

"Department of Defense World Wide Communications Systems," Raymond Lazinski, Philco Corporation, Philadelphia, Pa.

(Continued on page 60A)

How Important is Experience?

When you select a microwave spectrum analyzer, remember that Polarad is the pioneer. In fact, we have had more experience in designing, building, and helping engineers apply microwave spectrum analyzers than all of our competitors combined . . . several times more. We wrote the only textbook in the field — in its fifth printing now. (Write for one — it's free.)

So What? Why should it matter to you that we have the most experience? Does experience really count? We think it does. In fact, we believe it is the **most important factor in your final decision**. Let us tell you why.

Every circuit in a Polarad spectrum analyzer is a second- or third-generation design. That means:

- refinements that make it more precise and stable.
- sophistications that make it more versatile and useful.
- revisions that make it more reliable and economical.
- updating that assures state-of-the-art capability.

On the other side of the coin is what experience spares you. You know the kind of thing we mean:

- subtle surprises . . . the mixer, or other circuit that isn't there, just when you need it. (All Polarad Spectrum Analyzers are furnished **complete**.)
- inconveniences . . . like the hard-to-read

scale, the oversensitive control, or the awkward panel arrangement.

- weak links . . . the causes of sudden failure right in the middle of an important test.

Everyone is plagued by these things . . . and only experience — **properly applied to the evolution and elaboration of a design** — ever eliminates all of them.

To sum up, when you buy a Polarad spectrum analyzer, you benefit in two ways: you get the **most** instrument for your money; and you get the accumulated experience of thousands of engineers, in many hundreds of installations all over the world. No one else can offer you that much.

Call your Polarad Field Engineer for positive proof.



Newest in a Distinguished Family — the Model SA-84 WA Extended-Range Spectrum Analyzer

Extended Frequency Range: 10 MC-63,680 MC in a single self-contained instrument! Extended Dispersion Range: 25 KC to well over 80 MC (to 100 MC on special order!) Highest Sensitivity ever offered in this class of spectrum analyzer!

Wide-Range Variable Resolution: 1 KC-80 KC! Many other features: 0.01% Crystal-controlled markers over entire frequency range . . . log-linear display . . . (up to 36 db calibrated log display) accurate IF attenuator . . . full 5" usable display.

HAVE YOU MADE
RESERVATIONS YET?



Polarad's new "Project Mohammed" is now bringing the "Mountain" (our new Mobile Microwave Calibration Laboratory) to "Mohammed" (your microwave instruments). Be sure to take advantage of this opportunity to have your gear checked — at your doorstep. Save weeks of delay and needless expense. Call your Polarad field engineer for details and schedules!

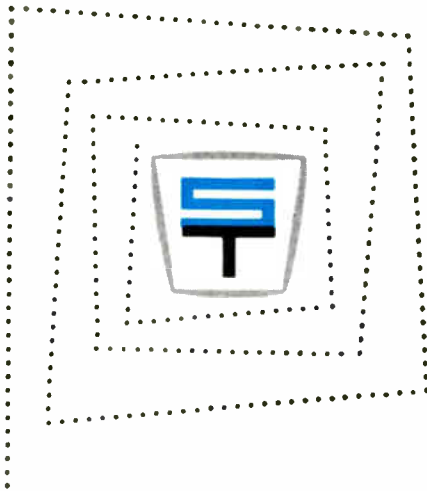
POLARAD

Polarad Electronics Corporation

World Leader in
Microwave Instrumentation
43-20M 34th Street

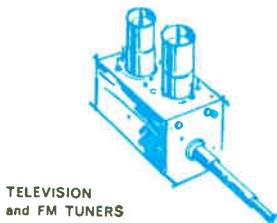
Long Island City 1, New York

PRACTICAL INGENUITY IN ELECTRONICS

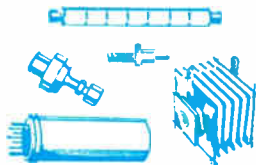


What is it? You might call it a philosophy... an idea... a principle.

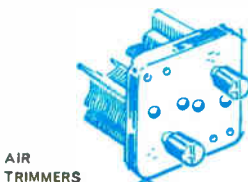
What does it mean? Technical excellence, reliability, performance—combined with sensible pricing. On this philosophy rests the enviable Tarzian reputation for customer satisfaction. Too, it has earned for Sarkes Tarzian, Inc. recognition as the producer of "the world's finest tuner for the world's finest sets". You'll also find this same practical ingenuity in all of these electronic products from Tarzian:



TELEVISION
and FM TUNERS



SEMICONDUCTOR DEVICES



AIR
TRIMMERS



BROADCAST
EQUIPMENT



MAGNETIC TAPE



FM RADIOS and
AM/FM RADIOS

Electronic Products of Tomorrow ... TODAY



SARKES TARZIAN INC

east hillside drive • bloomington, indiana • edison 2-7251

Professional Group Meetings

(Continued from page 58A)

COMPONENT PARTS

Los Angeles—September 10

"Problems and Solutions in Darnell Specifications," Leo Jacobson, Angstrom Precision, Inc., Los Angeles, Calif.

New York—May 14

"Production of Reliable Transistors," J. Hillman, General Instrument.

"Transistor Failure Mechanisms," C.H. Zierdt, Jr., Semiconductor Products Dept., General Electric Company, Syracuse, N. Y.

New York, Northern New Jersey,
Long Island—April 25

"Radio Interference Through Design Practice," S. Burrano, Burrano Associates, Inc., Westwood, N. J.

"Radio Interference Letters," M. Furst, R. F. Interonics, Oceanside, N. Y.

ELECTRON DEVICES

Albuquerque-Los Alamos—September 26

"Some Devices We Would Like to Have," Dr. Bennett L. Basore, Dikewood Corporation, Albuquerque, N. Mex.

New York Metropolitan Area—June 7

"Masers for Amplifying and Generating Microwaves and Light," Frank R. Arams, Airborne Instrument Laboratory.

New York Metropolitan Area—May 31

"High-Power Microwave Tubes," Thomas D. Sege, Sperry Gyroscope Company.

New York Metropolitan Area—May 24

"Unconventional Free-Electron Devices," Dr. Gerhard Weibel, General Telephone and Electronics Laboratories.

New York Metropolitan Area—May 17

"Microwave Tunnel Diode Oscillators," Dr. Fred Sterzer, RCA Tube Division.

New York Metropolitan Area—May 10

"Varactor Multipliers in Microwave Power Sources," Dr. R. P. Rafuse, Massachusetts Institute of Technology.

ELECTRONIC COMPUTERS

Long Island—May 1

"Grumman Aircraft's Computation Facility," G. Fogee, Grumman Aircraft, Bethpage, N. Y.

"Combined Analog-Digital Simulation at Grumman," A. Burns, Grumman Aircraft, Bethpage, N. Y.

(Continued on page 62A)

NEW VALUE PACKAGE

Sampling sweep and sampling dual-trace plug-in units with the Tektronix Type 561A Oscilloscope

• illuminated internal graticule • rectangular ceramic crt

This new low-drift sampling system is as easy to operate as a conventional oscilloscope — but with sensitivity and bandwidth possible only through sampling.



HERE'S WHAT YOU CAN DO WITH THIS SAMPLING SYSTEM:

- 1 Measure millivolt wide-band signals with either 0.4-nsec risetime sampling channel. Time-measurement range extends to 100 microseconds.
- 2 Trigger internally from A and B signals. Matched internal delay lines in both channels assure accurate time comparisons.
- 3 Display repetitive signals on 15 calibrated equivalent sweep rates from 0.2 nsec/cm to 10 μ sec/cm, accurate within 3%. Magnifier provides 10X sweep expansion . . . time per dot remains the same for digital readout (with auxiliary equipment).
- 4 Measure millivolt signals in the presence of a ± 1 -volt dc component by means of a dc-offset voltage, monitorable at the front panel.
- 5 Reduce time jitter and amplitude noise, if needed, on the more sensitive vertical ranges and faster sweep rates by means of a smoothing control.
- 6 Show X-Y (lissajous) patterns, observe single or dual-trace displays, add signals algebraically.
- 7 Change the signal-source impedance without affecting the dot transient response.
- 8 Vary sweep delay through 100 nanoseconds.
- 9 Drive X-Y plotters or similar readout accessories.
- 10 Select calibrated vertical sensitivities from 2 to 200 mv/div.
- 11 Choose signal probes for higher input impedances, various attenuations.

TYPE 561A CHARACTERISTICS

UNIQUE CRT • 5-inch rectangular ceramic-envelope tube • Illuminated no-parallax internal graticule on high quality parallel-ground plate-glass face • Controllable graticule lighting—for convenient trace photography • Monaccelerator design and 3.5-KV accelerating potential — for a bright, sharply-defined trace of small spot size •

OTHER FEATURES Improved regulated power supplies • Regulated dc heater supply • Z-axis input • Amplitude calibrator with 18 steps from 0.2 mv to 100 v • Operation from 105 v to 125 v or 210 v to 250 v, 50 to 400 cps.

TYPE 561A Oscilloscope	\$470
(without plug-ins)	
TYPE 3S76 Dual-Trace Sampling Unit . .	\$1100
TYPE 3T77 Sampling Sweep Unit	\$650
Probes:	
Type P6032 Cathode-Follower Probe . .	\$160
Type P6034 Miniature Passive Probe . .	\$35
(10X attenuation)	
Type P6035 Miniature Passive Probe . .	\$35
(100X attenuation)	

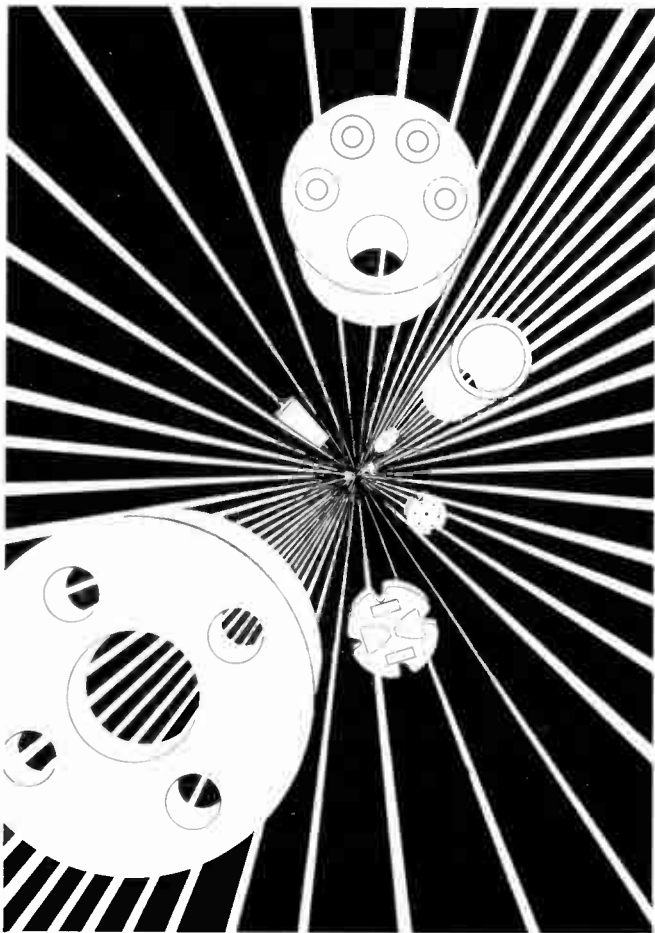
U. S. Sales Prices, f.o.b. Beaverton, Oregon

The Type 561A also accepts other plug-ins for differential, multi-trace, and wide-band applications, plus the two latest which provide high sensitivity, wide-band, dual-trace operation combined with calibrated sweep delay.

For a demonstration—please call your Tektronix Field Engineer.

Tektronix, Inc. P. O. BOX 500 • BEAVERTON, OREGON / Mitchell 4-0161 • TWX-503-291-6805 • Cable: TEKTRONIX

Tektronix Field Offices are located in principal cities throughout the United States. Please consult your Telephone Directory.
 Tektronix Canada Ltd: Field Offices in Montreal, Quebec • Toronto (Willowdale) Ontario.
 Tektronix International A. G., Terrassenweg 1A, Zug, Switzerland • Overseas Distributors are located in 27 countries and Honolulu, Hawaii.



Ceramics to infinity

Wesgo capability can provide an endless number of shapes and forms in quality high alumina ceramics for your most demanding applications.

Dense, vacuum-tight Wesgo alumina ceramics, with up to 99.5% Al_2O_3 , are strong, hard and abrasion resistant. They offer high thermal conductivity, exceptional chemical inertness and superior electrical properties at microwave frequencies—even at high temperatures.

Wesgo ceramics are available in sizes and shapes to meet your individual specifications. Manufacturing is to tight dimensional tolerances; parts are of uniform density, free from internal and surface defects. All are quality controlled to meet unparalleled performance standards.

Write today for a brochure describing these premium ceramics or Wesgo's precious metal brazing alloys

WESGO — Where Quality is the Chief Consideration



WESTERN GOLD & PLATINUM COMPANY

Dept. P, 525 Harbor Blvd., Belmont, California
LYell 3-3121 Area Code 415

786c

Sub-Miniature Indicator Lights Conform to applicable Military Specifications.

Mount from FRONT of Panel in 15/32" Clearance Hole

NEON

Assemblies with Built-in Resistor
(A patented DIALCO feature—U.S. Pat. No. 2,421,321)

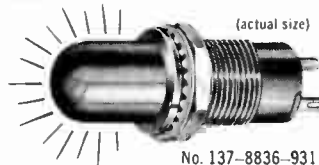
Conform to MS25257... Accommodate T-2 Neon Glow Lamps: Type NE-2D (MS25252)

is recommended for general service on 105-125 volts AC or DC. The High Brightness type NE-2J (not MS) may be used on 110-125 volts AC only.

Features: Stovepipe lens molded of high-heat plastic gives 180° light spread; available in choice of signal colors... Two terminals... Rugged construction; phenolic insulation of Mil. Spec. grade... Anti-rotation (locking) features prevent rotation of unit while being tightened to panel... For complete data request Brochure L-159C.



T-2



(actual size)

No. 137-8836-931

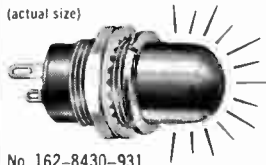
INCANDESCENT

Assemblies conform to MS25256

Accommodate T-1-3/4 Incandescent bulb with midget flanged base, in voltages ranging from 1.3 to 28 (the 6 V. and 28 V. conform to MS25237).

For complete data request Brochure L-156E.

Samples on Request—at Once—No Charge



No. 162-8430-931



T-1 3/4

DIALCO

PILOT LIGHTS

"The Eyes of Your Equipment"



Foremost Manufacturer of Pilot Lights

DIALIGHT
CORPORATION

60 STEWART AVE., BROOKLYN 37, N.Y. • Area Code 212, HYacinth 7-7600



Professional Group Meetings

(Continued from page 694)

Long Island—February 6

"Nanosecond Pulse Circuits for Nuclear Instrumentation," Dr. Robert Sugarman, Brookhaven National Laboratory.

Long Island—December 6

"The Navigation System for Polaris Submarines," Joseph Caligiuri, Sperry Gyroscope Company, Marine Division.

Santa Ana—September 27

"Functionally Interconnected Logic," Jack Pariser, Hughes Aircraft Company, Fullerton, Calif.

San Francisco—September 25

"The HCM-202 Thin Film Computer," A. S. Fukin, Hughes Aircraft Company, Los Angeles, Calif.

ENGINEERING MANAGEMENT

Buenaventura—September 25

"The Presidential Order on Organized Groups of Federal Employees," John MacCauley, Head, Employee Relations Division.

(Continued on page 613)



100 kW CW

1.7-2.4 Gc

FOR DEEP SPACE COMMUNICATIONS

Varian Associates' new VA-858 CW amplifier klystron offers the highest known power in S-band for deep-space communications. Developed by the same team of engineers who brought the industry the highest power in X-band, the VA-858 is conservatively rated at 100 kW, and in actual continued operation has delivered in excess of 175 kW. The VA-858 is available in four models. Tubes can be tuned for high gain, high efficiency, or wide bandwidth. With suitable stagger tuning, a 3 db bandwidth of 20 Mc can be achieved, with a power gain of 50 db. Tuning range of each tube is 150 Mc below 2 Gc, and 200 Mc above 2 Gc. Small size of the tube is ideal for antenna mounting.

If your deep-space or satellite project requires such exemplary tubes, Varian has (or can design) the tube for you. Write Tube Division.

CHARACTERISTICS	SYNCH TUNED	HIGH EFF. TUNED	BRDAD-BAND TUNED
Power Output (kW)	103	122	122
Drive Power (mW)	35	350	1000
Gain (db)	65	55	51
Efficiency (%)	35	41	41
Bandwidth, 3 db (Mc)	8.5	15	21
Beam Voltage (kVdc)	35	35	35
Beam Current (Adc)	8.5	8.5	8.5

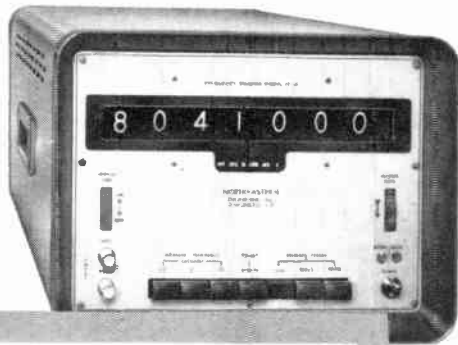


VARIAN associates
TUBE DIVISION • Palo Alto 2, Calif.

MICROWAVE TUBE GROUP

PALO ALTO TUBE DIVISION • BOMAC DIVISION • S-F-D LABORATORIES, INC. • SEMICON ASSOCIATES, INC. • VARIAN ASSOCIATES OF CANADA, LTD. • SEMICON OF CALIFORNIA, INC.

NORTHEASTERN FIRST AGAIN!



1 MC Transistorized Counter with pushbutton ease!

Northeastern's Model 15-30 features simple and fast pushbutton selection; easy thumb-action controls for display time and counting cycle. Gated counting, in-line nixie readout and self-check features included.

Frequency Stability 1 part in 10^7 per week
Frequency Range 10 cps to 1 MC

Standard Output Frequencies
1, 100 cps; 10, 100 KC and 1 MC

Max. Period Measurement Frequency . . 100 KCS

Period Range
10 μ sec. to 10^4 sec. (10^6 with standard output frequencies)

Maximum Resolution 1 μ sec. between pulses

Input Voltage 250 MV to 100 V Max. RMS

Power 115 VAC 60 cycle, 40 VA

Size 12" wide, 9" high, 17" deep

PRICE \$1550.00

NORTHEASTERN

ENGINEERING INCORPORATED

AFFILIATE OF ATLANTIC RESEARCH CORPORATION

DEPT. 2 R MANCHESTER, NEW HAMPSHIRE

Employment Opportunities Open At All Levels



Ask To See The Difference!

Now! A REALLY STABLE 10 μ V DC MICRO-VOLT AMMETER!

ULTRA-SENSITIVE DC
MICRO-VOLT-AMMETER

10 μ V-1 KV, mid-zero; 10 μ A-1mA, mid-zero;
.np. Imp., 1-100 meg; DC Output, 2.5V @ 1mA;
Basic Accy, Volts-1%, Amperes-2%.

Model MV-07C \$495.00

MILLIVAC Instruments, Inc.

1100 Altamont Ave., Schenectady, N. Y.

Professional Group Meetings

(Continued from page 62.1)

Seattle—April 5

"Technology's Role in the Growth Explosion," Ralph H. Miner, Lockheed Missiles and Space Company, Sunnyvale, Calif.

Seattle—March 16

"How to Achieve Individual Income Tax Savings," Durwood L. Alkire, Touche, Ross, Bailey & Swart, Certified Public Accountants, Seattle, Wash.

ENGINEERING WRITING AND SPEECH

Los Angeles—September 18

"The Application of Technical Communications," Russell Broman, P. R. Broman Company.

Northern New Jersey—September 25

"Printing and Duplicating Processes for the Engineer," Eli Fuchs, Raritan Arsenal (U. S. Army), Metuchen, N. J.

INDUSTRIAL ELECTRONICS

Omaha-Lincoln—September 26

"Long Range System Planning," Henry C. Samplers, Omaha Public Power District, Omaha, W. E. Miller, OPPD, System Planning Engineering, Omaha, Neb.

INFORMATION THEORY

San Francisco—September 27

"Data Communication Through Binary Superposition Channels," Dr. William H. Kautz, Stanford Research Institute, Menlo Park, Calif.

INSTRUMENTATION

Los Angeles—May 15

"Temperature Measurements in Extreme Environments," L. B. Gardner, for Edwin N. Kaufman, Litton Industries.

Los Angeles—March 20

"New Techniques for Measuring Nutating Antenna Parameters," Samuel Rosen, Rantec Corporation, Calabasas, Calif.

Philadelphia—September 18

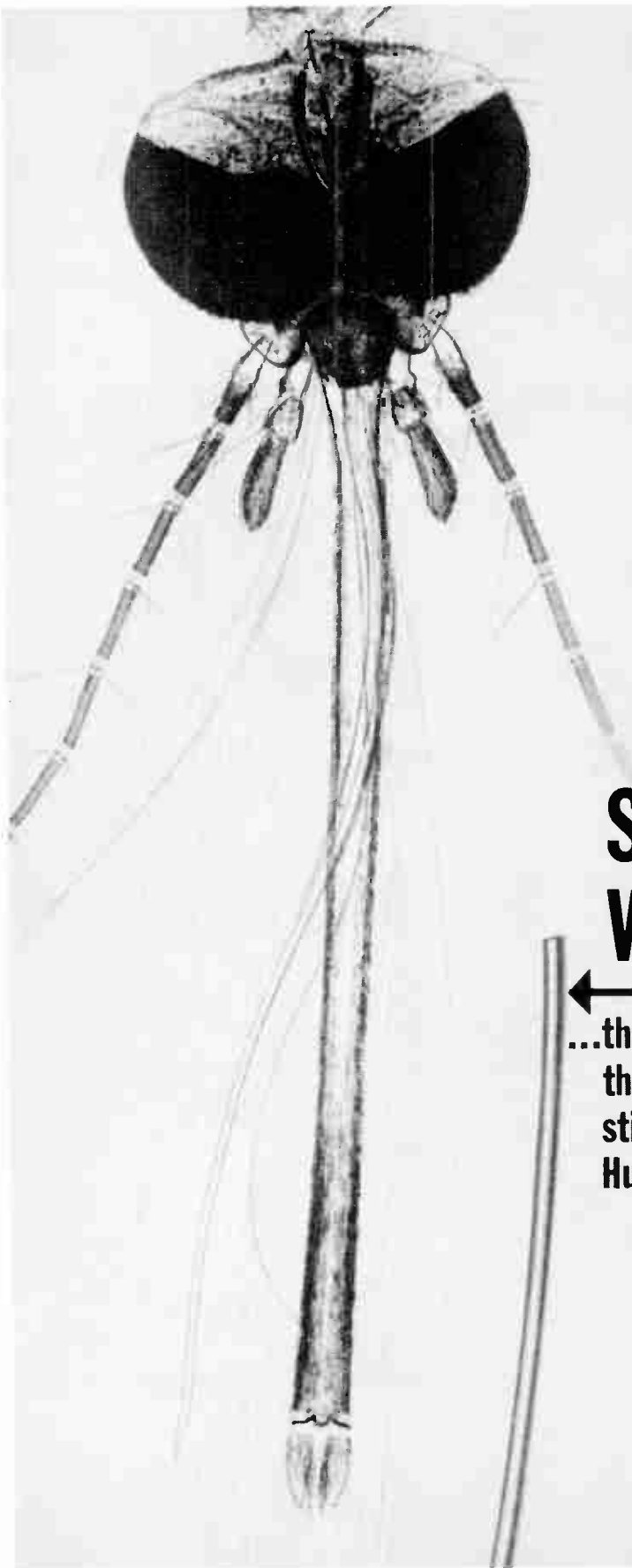
"Accuracy," Earl F. Gard, Frankford Arsenal, Philadelphia, Pa.

MICROWAVE THEORY AND TECHNIQUES

Boston—September 27

"Advances in Microwave Solid-State Devices," Frank A. Brand, USASRD, Fort Monmouth, N. J.

(Continued on page 68A)



Nature has given the mosquito a proboscis that measures 0.0031 of an inch at its widest point. Nickel makes it possible to produce tubing that's much finer.

How fine? The tubing pictured here—drawn by the Superior Tube Co.—has an outside diameter of 0.0019 of an inch, a wall thickness of 0.00065 of an inch and an inside diameter of 0.0004 of an inch!

But the smallest tube ever made is still much finer. The fact is, that nickel tubing has been drawn down to 0.00061 outside diameter and 0.000036 inside diameter. *That's really fine!*

SMALL WONDER

←
...that tubing finer
than a mosquito's
stinger calls for a
Huntington Alloy!

Tiny tubing like this is just one example of how you can get Huntington Alloys in any form or size you may want, right down to the fine sizes produced by specialists in strip wire and tubing. In commercial production, Huntington high-nickel alloys are made in tube forms from 0.010 inch outside diameter to the giant welded cylinders used in paper-making machinery. They're also available in wire and strip forms. And in all the other various shapes and sizes needed for electronic applications.

Perhaps a Huntington high-nickel alloy can help you solve one of your electronic problems? Write for the informative booklet, "Huntington Alloys for Electronic Uses." It will give you a convenient reference on the properties, available forms and typical applications of these alloys.

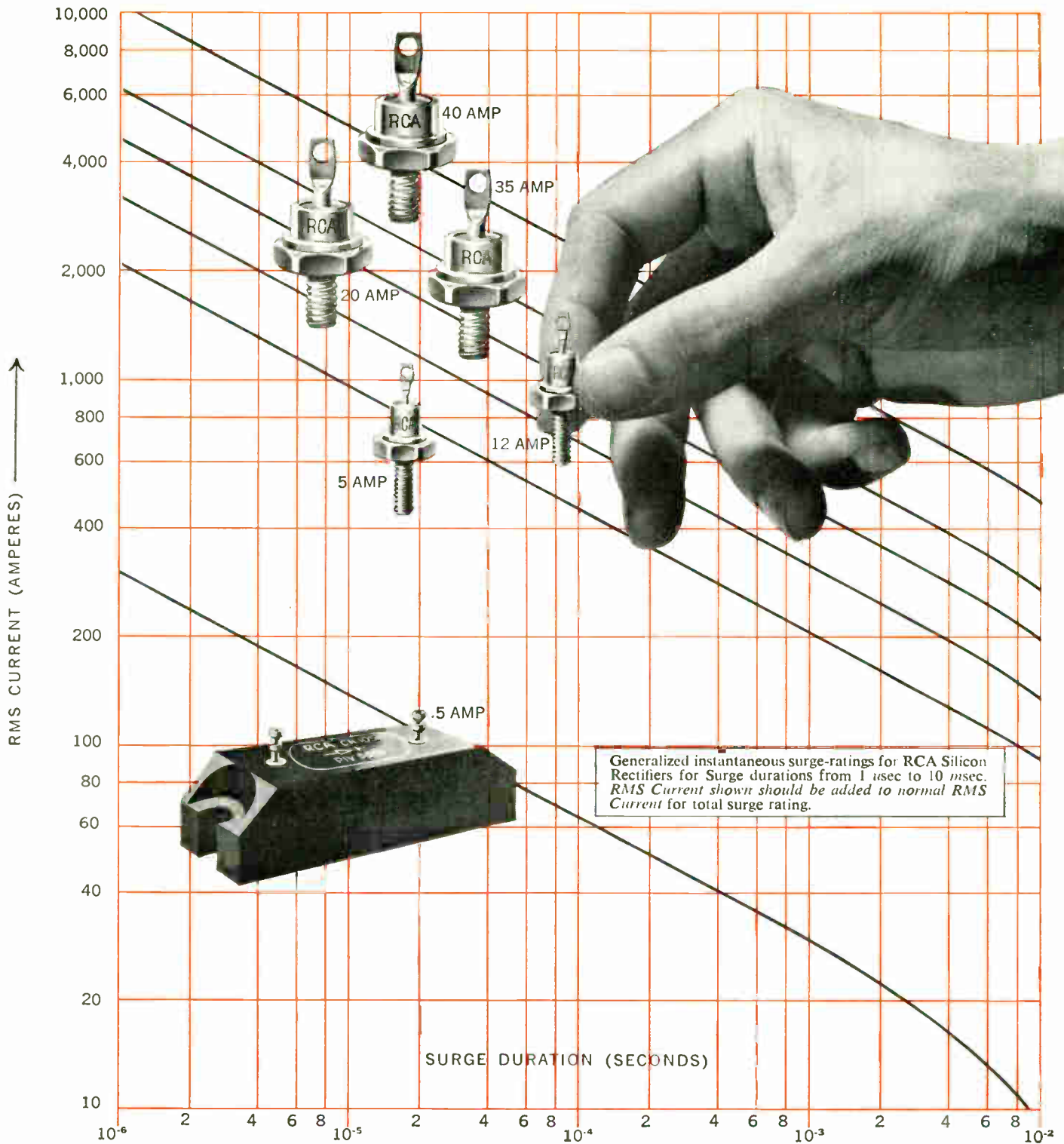
HUNTINGTON ALLOYS



HUNTINGTON ALLOY PRODUCTS DIVISION

THE INTERNATIONAL NICKEL COMPANY, INC.

HUNTINGTON 17 • WEST VIRGINIA



Here's New Assurance of Extra Performance... in Every RCA Silicon Rectifier You Specify

Now you can design rectifier circuits with much greater assurance with RCA Silicon Diffused-Junction Rectifiers, because you have *complete* surge information. Check the surge value for the conditions you must meet and you'll find the right RCA rectifier for the job.

RCA Silicon Rectifiers can withstand temporary current overloads hundreds of times higher than average current rating.

Here are some of the features of RCA Silicon Rectifiers that make this quality possible:

- Diffused Junction Process...extremely tight characteristics limits

- Each package designed to meet the stringent environmental and mechanical requirements of today's military and industrial power equipment
- Extra-high-strength zirconium-alloy mounting stud
- Unique internal heat sink assures union of pellet and contact to eliminate high-current hot spots
- Thermal fatigue cycling tests — the best

- assurance for long and dependable service
- Every unit is dynamically tested prior to shipment

Call your RCA Representative for complete information. For your copy of the RCA Application Note, SMA-4, write to RCA Semiconductor and Materials Division, Commercial Engineering, Section 1T-12, Somerville, N. J.

AVAILABLE THROUGH YOUR RCA DISTRIBUTOR

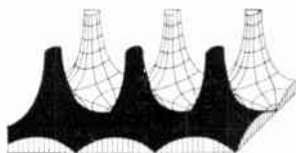


THE MOST TRUSTED NAME IN ELECTRONICS

Proceedings of the IRE



Poles and Zeros



Abstracts and References.
See page (2538) for announcement of the greatest importance to users of *Abstracts and References*.

International. An international subcommittee comprised of Dr. R. L. McFarlan, Chairman, IRE International Committee, Professor Alexander Bereskin, Director, Region 4, and Professor Adolfo Di Marco, Chairman, Buenos Aires Section, toured eight countries of Latin America this summer. They sought to determine steps which the IRE should take to improve communications with, and meet the professional society needs of, engineers and scientists in the radio, electronic, and electrical industries. In Venezuela, Brazil, Argentina, Chile, Peru, Ecuador, Colombia, and Mexico, they visited nine universities, six factories, and four government laboratories. IRE sections exist in Rio de Janeiro (Dr. Joao A. Wiltgen, Chairman), Buenos Aires (see above), Chile (Julio del Rio, Chairman), and Colombia (Professor Werner Westphal, Chairman). The Buenos Aires Section is the largest in South America and the first to be established outside North America. Good potential for formalizing activities into a section or subsection was found in Venezuela, Uruguay, Peru, Sao Paulo, and Colombia. The Mexico City Section of the AIEE will absorb and serve IRE members upon merger. Colleges and universities visited were satisfactorily equipped and staffed to award the B.S. degree. Although few are giving the Master's or Doctor's degree in engineering, several are planning to expand staff and facilities and activate graduate programs in the near future. Throughout the visit, the Committee found enthusiasm, plans, and progress. Latin America can be expected to move ahead with the IEEE.

Who Reads PROCEEDINGS? Students do! As of this writing, 75% of renewals of student membership and 33% of new student members are paying \$9 dues instead of the basic \$5 fee in order to receive PROCEEDINGS.

Literacy and Technology. As the last issue of the PROCEEDINGS OF THE IRE goes to press, it seems fitting to fix this point in time and thereby establish a perspective view of the future. Your Editor undertook a bit of research and came up with the following, which sheds some light on our potential and responsibilities as we become members of the IEEE: At the dawn of recorded history—about 4000 B.C.—there were about 150,000 people in the known world who could read and write. This number doubled on a 950-year cycle until the end of the Middle Ages. The invention of printing, the compass, the technique of sailing into the wind, and other technical and humanistic advances established both need and desire for literacy. The doubling time dropped to about 100 years. Further technical, governmental, and medical advances created

the "population explosion" of Malthus and the doubling time in the early 1800's became 50, then 40, then 30 years, and now 20 years. There are presently about 1.5 billion literates in the world. The rate of creation of literature and knowledge has followed closely the rate of increase of literacy. General printed material is doubling today about every 20 years. The Harvard University Library is doubling in numbers of books and pamphlets every 20 to 25 years. Note that this means that Harvard will buy as many books in the next 25 years as they have purchased in the last 300 years! The M.I.T. Library, being oriented toward technical literature, is smaller than that of Harvard, but is doubling on a 10 to 15 year cycle. The number of pages of technical papers is said to be doubling every 15 years. Dr. Werner Von Braun says that knowledge of space science is doubling every 7 years. PROCEEDINGS OF THE IRE pages of editorial material has doubled every 11 years for over 40 years, and the TRANSACTIONS pages output has doubled every three years over the last decade! IRE membership has, on the average, doubled every seven years for four decades. This is truly a remarkable era in the history of mankind, and we IRE'ers can be proud of our contributions thereto.

End of an Era. During the next 40 years *there will be as many man years of literacy as there has been in all of man's past history*. It is reasonable to expect almost proportional creativity and progress, as summed over all spheres of activity. Extrapolation of trends indicate that the world will be essentially 100% literate at the turn of the century. The next 40 years is truly "the end of an era" during which the progress of mankind has "exploded" as a chain reaction among technology, mass education, and population growth. After the year 2000 A.D. the number of literates will increase, not percentage-wise, but only as the population increases.

Beginning of a New Era. When one era ends, another must begin. The new era is already taking form in many nations of the world. The United States, Canada, Western Europe, Russia, Japan, and Australia, for example, are almost totally literate at this moment. If the explosion of progress is to continue (if progress is to continue to accelerate), we must raise the level of the average per capita education—and this means to press every man to achieve his personal saturation level in education. It means more, better, and more efficient schools, colleges and graduate programs. To our field of Electrical Science and Engineering, it means greatly expanded Ph.D. programs and, in addition, development of "another layer on the cake"—large and strong post-doctorate programs which will stress study and research at the highest level in an academic atmosphere. Our colleagues in Chemistry, Physics, and Biology have sizable post-doctorate programs already underway. IEEE faces a new and tremendous challenge in helping our profession fulfill its responsibilities to society.—T.F.J.



George W. Bailey

Executive Secretary

In recognition of his eighteen years of continuous devoted and dedicated service, the Board of Directors of The Institute of Radio Engineers, on behalf of its members, bestows on George W. Bailey, Executive Secretary of the Institute, a Distinguished Service Award in this year of 1962.

George W. Bailey has given unstintingly of his time, his effort, his thought, and his consistent devotion to duty during that period.

He has planned many of the administrative and operational procedures of the Institute while overcoming many anticipated or unforeseen difficulties and obstacles.

He has developed policies of wide scope, worked out details of procedures, and skillfully, and with unswerving determination, implemented and successfully carried them out.

He has won the admiration and respect of the membership of the Institute, its Officers and Directors, and its correspondents as well as the esteem and cooperation of leading governmental and industrial representatives.

He has created a great tradition of effectiveness and personal standing for his office as Executive Secretary, and has established valuable guidelines for those holding a like office.

On this occasion of the year of the Fiftieth Anniversary of the Institute, the Board of Directors and Officers of The Institute of Radio Engineers, on behalf of its members, hereby unanimously express their personal esteem and official approval of his unusual and valuable accomplishments and of his major and lasting contributions to the welfare of the Institute.

The foregoing resolution was adopted by the IRE Board of Directors at its meeting on October 17, 1962. Upon the formation of The Institute of Electrical and Electronics Engineers in January, 1963, Dr. Bailey will serve as Executive Consultant.

Scanning the Issue

Double Injection Diodes and Related DI Phenomena in Semiconductors (Holonyak, p. 2421)—Recent work on double injection phenomena in insulators has shown that when the injection level is increased beyond a certain threshold, the material exhibits negative resistance. This work has opened up a new area of study which promises to be of major importance in the immediate future. This paper and the one that follows give ample evidence why. The first paper presents a considerable amount of new experimental data on double-injection negative-resistance phenomena in gallium arsenide, silicon, and germanium *p-i-n* diodes, and in particular describes many device possibilities inherent in this work. Among them are a new low-voltage regulator in a voltage range not presently available in zener diodes, a method of fabricating a memory array of noninteracting elements on a single substrate, a new class of photosensitive diodes, and higher power microwave *p-i-n* switching elements. In addition to these specific device developments, this work makes a notable contribution to a subject of rapidly growing importance, namely, plasma effects in semiconductors.

The Madistor—A Magnetically Controlled Semiconductor Plasma Device (Melngailis and Rediker, p. 2428)—Plasma effects in semiconductors, prominently mentioned in the preceding paper, once again take the center of the stage. And once again the existence of a negative resistance region in a suitably designed diode at high injection levels is crucial to the operation of the devices under consideration. In the present paper an important new element is added, that of controlling the position of the plasma inside the material by means of an externally applied magnetic field. The result is a new class of devices which the authors call "madistors." Novel dual-base and multiple-base structures are described in which the plasma, and hence the output current, can be magnetically switched from one base contact to another to form bistable flip-flops and multicontact stepping switches. Other important types of madistors include a four-terminal amplifier with an isolated input, and a variable gain transistor. It is noteworthy that in all of these applications the magnetic fields required is only about 10 gauss.

Design and Performance of a Broad-Band FM Demodulator with Frequency Compression (Ruthroff and Bodtmann, p. 2436)—In the course of developing an extremely sensitive receiving system for the Project Echo communication satellite experiments, the designers utilized an old but almost-forgotten technique of applying negative feedback to an FM receiver in order to improve its operating threshold. However, there remained considerable uncertainty as to how and where the threshold improvement set in, largely because of the nonlinear nature of the problem and the associated difficulty of describing and analyzing it mathematically. In spite of this difficulty, a theory for predicting the threshold was developed and published in the PROCEEDINGS last January. The present companion paper reduces the theory to practice and offers interesting experimental verification of the predicted threshold improvement. In addition, the authors provide a timely description of a demodulator intended for an intercontinental satellite communication system capable of

handling television or telephone service.

Solid-State Display Device (Yando, p. 2445)—By combining certain unique properties of piezoelectric and electroluminescent materials, a new method of scanning has been developed for solid-state displays. The display device consists of a thin, flat panel of piezoelectric material supporting an electroluminescent layer. Voltage pulses, applied to a few electrodes on the periphery of the panel, produce elastic impulses which, as they travel across the piezoelectric panel, are accompanied by localized electric fields generated by piezoelectric action. These fields interact with the EL layer to produce light. The configuration and size of the lighted area can be controlled by the mode of application and relative timing of the input voltage pulses to produce oscilloscope patterns or television-type displays. The simplicity of the structure and the novelty of the scanning method will make this development of interest to many individuals concerned with new ideas in the solid-state device and display field.

Switching Speed and Dissipation in Fast, Thin-Film Cryotron Circuits (Meyers, p. 2452)—The development of faster cryotron circuits has progressed to a point where it becomes feasible to consider circuit time constants in the nanosecond rather than the microsecond range. Simplifying assumptions concerning switching speed and heat generation which were adequate for analyzing slower circuits are no longer valid. The detailed properties of the components themselves produce effects which at higher speeds can no longer be ignored. While it has been generally recognized that these limitations exist, there has been no detailed analysis of the phenomena involved nor computation of the delay times produced. This paper deals theoretically with these factors and provides valuable and new calculations of the expected high-speed switching behavior of film cryotrons. As such it will be of high interest to cryogenic, magnetic amplifier, and computer engineers, as well as switching theoreticians.

Properties of 400 Mcps Long-Distance Tropospheric Circuits (Chisholm, *et al.*, p. 2464)—This paper presents the results of an extensive program of UHF tropospheric propagation research to explore the feasibility of extending the range of transhorizon communications systems beyond 400 miles to possibly 800 miles. As a result of more than 16,000 hours of measurements, a great deal of information was gathered for a distance range where existing data was meager. The measurements are valuable in their own right and are additionally interesting because they provide some results which do not seem to be indicated by present theoretical models or by extrapolation of data for shorter ranges. Systems engineers will be especially interested in the performance reported for 120-foot antennas at a 600-mile range.

Annual Index (Follows page 2552)—During this year approximately 600 technical papers and letters appeared in the pages of the PROCEEDINGS. The 1962 annual index for the PROCEEDINGS, containing listings by subject and by author, appears at the end of the editorial section of this issue. The index to the IRE INTERNATIONAL CONVENTION RECORD will appear next month.

Scanning the Transactions appears on page 2531.

Message from the President

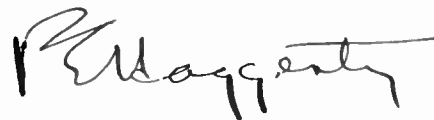
Fellow Members of IRE:

It has been my privilege to serve you as your President during this the Fiftieth and the last year of our society in its present form. A very large part of my duties for you this year have been concerned with the establishment of the IEEE, whose creation you have supported overwhelmingly by vote and deed. All of us, in working for the establishment of the IEEE, have done so with a single aim—to bring into being a professional society superior to either of its component parts. IRE has been an excellent organization, and it has served its members well, but we, the members of IRE, are joining with the members of AIEE so that we may have an improved institute even better able to serve our profession and the greater society of which we are all a part.

Let's remember that after the first of the year we are not members of IRE any more but members of IEEE, and that it is the fact of the consolidation of our two large societies which gives us this new opportunity to create a better society. But, it is also a fact of that consolidation that we bring together two large groups of engineers whose methods of operation and traditions have been somewhat different, and that now we will be working together in a new environment with new methods of operation, different in many respects from those in either of the predecessor societies. A little patience and a lot of common sense will make the first year or two of transition much smoother. It will take a few years to gain all the benefits from our consolidation, but if we work toward this during 1963, I know we will find the most difficult problems of transition out of the way by the end of the year. We are extraordinarily fortunate to have as the first President of the consolidated society the extremely competent Dr. Ernst Weber, and surely in Mr. Donald Fink we have found a man whose background capabilities and qualities are exactly those needed by the IEEE's General Manager. No professional society could expect finer leadership, but even, with such leadership, IEEE can be no stronger than we, its members, make it.

As for me, I look back on the tasks of this Golden Anniversary year with humility because there is still so much to be done, and yet with pride in the accomplishments you let me share.

Sincerely,



P. E. Haggerty
President

Double Injection Diodes and Related DI Phenomena in Semiconductors*

NICK HOLONYAK, JR.†, SENIOR MEMBER, IRE

Summary—Experimental studies of double injection (DI) negative resistance phenomena in GaAs, Si, and Ge are presented. V-I characteristics, switching, trapping, and photosensitivity properties of GaAs DI $p-i-n$ diodes, fabricated by diffusion and alloying processes on semi-insulating crystals and in other cases fabricated via epitaxial processes with Cu-doped i regions, are described. Similar studies and data are presented on Si DI $p-i-n$ diodes prepared via diffusion and/or alloying processes. Silicon DI $p-i-n$ diodes are described which have been doped with various deep level impurities such as Au, Zn, Cd, or Co and which, depending upon the kind and concentration of deep level impurities, display a wide range of behavior including useful photosensitivity, switching, and voltage regulation properties. Brief mention is made of Ge DI $p-i-n$ diodes fabricated on n -type crystals counter-doped with Cu, Fe, Ni, Co, or Mn. A comparison is made between experimental results and current theories of double injection effects. As might be expected, existing theories do not completely account for the experimental situation, *e.g.*, breakdown to constant voltage in certain units and phenomena which seem closely related to plasma effects. In addition to various practical implications, including possibilities for a noninteracting diode negative resistance matrix, low voltage regulator diodes, photosensitive charge-storage diodes, and higher power microwave switching $p-i-n$ diodes, the significance of deep level doping and possible and actual effects (*e.g.*, secondary switching effects) on epitaxial Si devices are described. The use of DI phenomena for study of deep level impurities and their properties is made apparent as well as the further possibilities inherent in Hall's now 12 year-old $p-i-n$ diode.

INTRODUCTION

AS POINTED OUT by Hall¹ over ten years ago, current in the forward direction in a $p-i-n$ diode is carried by recombination of electrons and holes which are injected from either side into a relatively thin, neutral i region. In $p-i-n$ structures consisting of semi-insulating² (si) intermediate regions of large dimensions relative to a diffusion length, current (low-level) can be carried in the forward direction in large part by space-charge-limited-emission processes. At higher current levels, as indicated by Lampert,^{3,4} beyond

a certain threshold voltage double injection can result in a significant increase in lifetime in the i region (or si region) and cause the diode to exhibit negative resistance, as in effect, the i region becomes conductivity modulated. Earlier, Stafeev⁵⁻⁷ and co-workers predicted and presented experimental confirmation, at low temperatures, of the existence of a negative resistance in "long" Ge diodes in which single carrier injection increased lifetime. Still earlier Tyler⁸ observed a switching effect at low temperatures in Fe-doped Ge which can be satisfactorily explained by Stafeev's work, or now perhaps better by Lampert's model and the experimental results and interpretations which are presented below. Finally, Melngailis and Rediker⁹ have obtained experimental results on InSb "long" diodes at low temperatures which in general confirm Stafeev's theories, and Holonyak, *et al.*,¹⁰ have presented experimental evidence confirming some of the main features of Lampert's model.

In this paper we shall describe room temperature experimental results on GaAs, Si, and Ge $p-i-n$ (or $p-si-n$) diodes which extend the work described above and which also bring to light a number of problems not adequately resolved by any of the current theories. A number of the practical implications and new applications made possible by this work are discussed also. In the interest of convenience, and because his theory fits our experiments reasonably well, we shall describe our results below mainly in terms of Lampert's model.

DOUBLE INJECTION

Lampert considers double injection in an insulator (semi-insulator, which can be assumed to be in the form of a $p-i-n$ diode) with an assumed acceptor recombination level E_R somewhat below the Fermi level so that at equilibrium electrons fill the level. He assumes

* Received July 20, 1962; revised manuscript received September 29, 1962. This work was partially supported by the Electronics Research Directorate, Air Force Cambridge Research Center, Contract No. AF 19(604)-6623. Much of the material of this paper was presented at the IRE-AIEE Solid State Device Research Conference, University of New Hampshire, Durham, N. H.; July 9-11, 1962.

† Advanced Semiconductor Laboratory, Semiconductor Products Department, General Electric Co., Syracuse, N. Y.

¹ R. N. Hall, "Power rectifiers and transistors," *Proc. IRE*, vol. 40, pp. 1512-1518; November, 1952. U.S. Patent No. 2,994,018; July 26, 1961.

² C. H. Gooch, C. Hilsum and B. R. Holeman, "Properties of semi-insulating GaAs," *J. Appl. Phys.*, vol. 32, pp. 2069-2073; October, 1961.

³ M. A. Lampert, "The role of injecting contacts in photoconductors," *J. Phys. Chem. Solids*, vol. 22, pp. 189-197; December, 1961.

⁴ M. A. Lampert, "Double injection in insulators," *Phys. Rev.*, vol. 125, pp. 126-141; January, 1962.

⁵ A. A. Lebedev, V. I. Stafeev and V. M. Tuchkevich, "Some properties of gold-doped germanium diodes," *Soviet Phys.—Tech. Phys.*, vol. 1, pp. 2071-2080; October, 1957.

⁶ V. I. Stafeev, "Modulation of diffusion length as a new principle of operation of semiconductor devices," *Soviet Phys.—Solid State*, vol. 1, pp. 763-768; December, 1959.

⁷ V. I. Stafeev, "Photoconductivity in semiconductor diodes induced by carrier lifetime changes," *Soviet Phys.—Solid State*, vol. 3, pp. 1829-1833; March, 1962.

⁸ W. W. Tyler, "Injection breakdown in iron-doped germanium diodes," *Phys. Rev.*, vol. 96, pp. 226-227; October, 1954.

⁹ I. Melngailis and R. H. Rediker, "Negative resistance InSb diodes with large magnetic field effects," *J. Appl. Phys.*, vol. 33, pp. 1892-1893; May, 1962.

¹⁰ N. Holonyak, Jr., S. W. Ing, Jr., R. C. Thomas and S. F. Bevacqua, "Double injection with negative resistance in semi-insulators," *Phys. Rev. Lett.*, vol. 8, pp. 426-428; June 1, 1962.

further that the hole capture cross section σ_p is considerably larger than the electron capture cross section σ_n of the recombination centers. When sufficient voltage is applied so as to inject electrons and holes into the insulator, a "recombination barrier" prevents holes (because of low lifetime, and diffusion length shorter than the i -region length W) from contributing appreciably to the current. Hence, initially only a small space-charge-limited-emission electron current is observed. At a critical threshold voltage V_{th} such that the hole transit time across the insulator (or i region) is of the order of the low-level hole lifetime, meaning holes can traverse the i region before recombining, the current increases through a negative resistance region until the voltage attains a minimum value,

$$V_M \sim (\sigma_n/\sigma_p)V_{th}, \quad (1)$$

at which point begins the "semiconductor regime." At the onset of the negative resistance region holes, first near the p region, depopulate the recombination centers of electrons and tend to fill the centers with holes, so that finally for each arriving electron one hole is annihilated and

$$\tau_{p, \text{high}} \approx \tau_{n, \text{high}} \approx \frac{1}{\bar{v}_p \sigma_n N_R}. \quad (2)$$

In other words, the hole lifetime increases from

$$\tau_{p, \text{low}} \approx \frac{1}{\bar{v}_p \sigma_p N_R} \quad (3)$$

to $\tau_{p, \text{high}}$. As more current is applied this phenomenon sweeps across the insulator and in effect converts the insulator into a semiconductor, just as though the N_R acceptor levels were actually donors and contributed N_R electrons to the conduction band. At this point, according to Lampert's model, the diode begins to exhibit positive resistance. The assumption is made on theoretical grounds that the current increases as a power of voltage, presumably in accordance with older theories of space-charge-limited emission. As will be seen below, experimental observations at moderate current levels do not necessarily support the last assumption above, nor do they necessarily support (1) for the minimum voltage after switching.

EXPERIMENTAL PROCEDURE

Many of the effects described above and other related effects have been observed in semi-insulating GaAs² (10^5 to 10^7 ohm-cm), in epitaxially grown GaAs p - si - n diodes¹¹ in which the si region is copper-doped, in high purity Si doped with Au ($\sim 10^5$ ohm-cm) and n -type Si counter-doped with deep levels such as Au, Zn,

Cd, or Co, and in n -type Ge counter-doped with Cu, Fe, Ni, Co, or Mn. P - i - n (or p - si - n) diodes were fabricated on these materials by conventional alloying processes, combinations of diffusion and alloying of junctions, and by all-diffusion procedures.¹² Various measurements were performed on the diodes including examination of the V-I characteristics, change in V-I characteristics as a function of illumination, photoresponse as a function of wavelength (to determine E_R where possible), some pulse and diode recovery measurements, and some qualitative aspects of magnetic effects.

DOUBLE INJECTION IN GaAs

The V-I characteristic of a typical GaAs p - si - n diode is shown in Fig. 1 with 1) the diode in room light and 2) the diode illuminated with a microscope lamp. The diode whose characteristic is shown in Fig. 1 consists of a thin Mn-diffused degenerate p region in a mesa configuration on a si GaAs substrate. A ball-alloyed tin dot on the $p+$ region gives rise to a reverse-biased tunnel junction which acts as the "ohmic" contact to the mesa $p+$ region. Near the mesa, on semi-insulating (si) GaAs, another tin dot forms the $n+$ region of the p - si - n diode. In diodes fabricated in this manner frequently another $n+$ region, and a second p - si - n diode with a common $p+$ region, is formed by alloying the mesa structure down on a metal plate with an alloy doped with tin.

The V-I characteristic shown in Fig. 1 is much as would be expected from Lampert's model. Other similar units, depending upon si -region thickness, have exhibited maximum pre-breakdown voltages of over 200 and ratios of minimum to maximum voltages as low as 0.25. Measurements of diode breakdown voltages and diode thicknesses indicate fields at breakdown near 2000 v/cm, clearly much less than the fields required for conventional avalanche or for tunneling. As is evident from traces 1) and 2) in Fig. 1, an applied potential of the order of one volt is required before the barriers at either end of the diode are lowered sufficiently to allow appreciable injection. Curve A) of Fig. 2 shows that the unit of Fig. 1 displays a space-charge-limited pre-breakdown current almost proportional to V^2 . Curve B) of Fig. 2 shows the prebreakdown V-I characteristic of another unit (Zn-doped $p+$ region and some copper contamination of the si GaAs) which obeys the I^2 dependence.

The V-I trace labeled 2) in Fig. 1 shows that illumination tends to lower the breakdown voltage, *i.e.* light tends to move the diode toward the semiconductor regime. Light tends also to increase the pre-breakdown current as would be expected if traps play a role in governing the magnitude of the space-charge-limited current. It should be mentioned that the light sensitivity of these diodes, and similar diodes in Si and Ge, is much

¹² Planar diffused, epitaxial Au-doped double injection diodes were supplied by T. R. Selig and C. O. Hull.

¹¹ N. Holonyak, Jr., D. C. Jilison and S. F. Bevacqua, "Halogen vapor transport and growth of epitaxial layers of intermetallic compounds and compound mixtures," in "Metallurgical Society Conferences," John Wiley and Sons, Inc. (Interscience Div.), New York, N. Y., vol. 15, pp. 49-59; 1962.

greater in the forward than in the reverse direction. This suggests many interesting applications, including devices with photoluminescent or other optical inputs and double injection negative resistance outputs.

At low currents in GaAs one frequently sees a hysteresis loop on the V - I curve retrace, where again the device tends to stay in the semiconductor regime. This is thought to be due to secondary traps or levels which are not accounted for in Lampert's model but which are known to exist in the experimental structures. This is evident in the light sensitivity of the space-charge-limited pre-breakdown current and is evident also from units of the type shown in Fig. 3 in which the diode switches a second time through a negative resistance region (at higher currents) down to a second voltage "minimum." These data show that many levels may take part in the operation of double injection diodes. Some levels may legitimately take part in causing a change in lifetime and switching; others may better play the role of traps.

Measurements of the photoresponse of these diodes all lead to a sharply increasing signal output in the range from 0.5 to 0.8 eV, in spite of the fact that the infrared source intensity in this range decreases monotonically. Hence, these measurements are taken as giving a reasonable estimate of the energy E_R . Most *si* GaAs used in these measurements lead to a value of 0.7 to 0.75 eV (below the conduction band) for E_R , consistent with previous estimates of the level which is responsible for *si* GaAs.² Mn-doped units give a value nearer to 0.6 eV. In some units a second level occasionally is observed near 1.0 eV, a level perhaps due to heat treating or contamination effects incurred in diode fabrication.

For a GaAs double injection diode with side-by-side $p+$ and $n+$ regions on one surface, as described previously, and with an applied magnetic field oriented to deflect hole current deeper into the crystal wafer, a field strength of ~ 5 kG shifts the entire V - I trace to higher voltages, to roughly double those with no field. A somewhat lesser shift is observed with reversed magnetic field. In both cases the shape of the V - I characteristic is preserved. According to Lampert's model,^{3,4} the breakdown voltage and minimum voltage are dependent on the length of the *i* or *si* region. Thus, deflecting the current path and changing recombination properties, particularly near the surface, with magnetic field can account for much of the high magnetic sensitivity of these diodes.

Before describing the results obtained on Si, we should remark that selected GaAs *p-si-n* diodes grown by epitaxial procedures with Cu-doped *si* regions¹¹ exhibit double injection negative resistances at low temperatures. These diodes typically exhibit room temperature space-charge-limited currents proportional to voltage to a power 2.5 to 3.5,¹¹ but exhibit no negative resistance (unless cooled). This might be expected since many copper levels are relatively close to the band edges and are

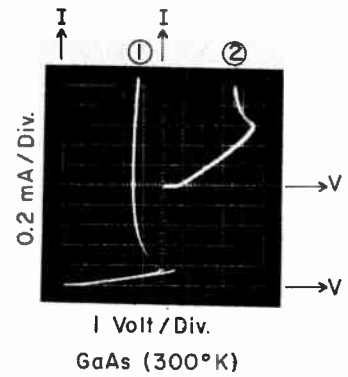


Fig. 1—Double injection negative resistance *p-i-n* (*p-si-n*) diode fabricated on semi-insulating GaAs. Mn-diffused $p+$ region Sn-alloyed $n+$ region; 1) Diode in room light, 2) Diode illuminated with microscope lamp.

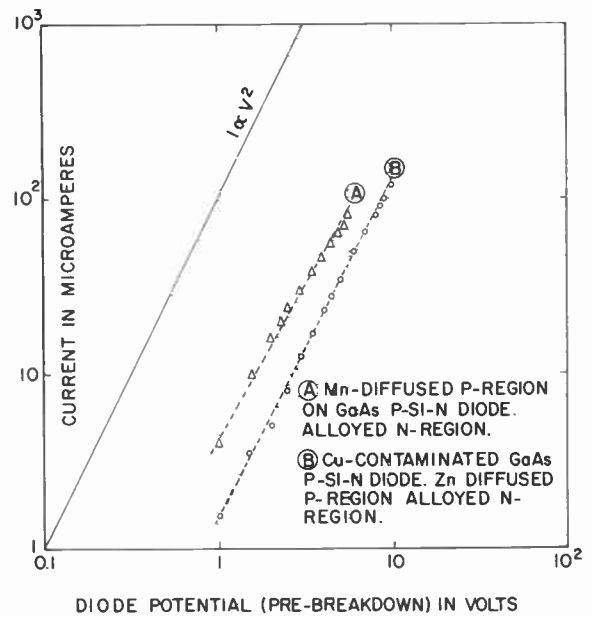


Fig. 2—Pre-breakdown SCL, V - I characteristics of GaAs *p-i-n*, double injection negative resistance diodes: A) Mn-diffused $p+$ region (814°C, 40 min, 6 mg Mn, 5 mg As), Sn-alloyed $n+$ region; B) Zn-diffused $p+$ region (760°C, 14 min, 4 mg Zn, 5 mg As), Sn-alloyed $n+$ region.

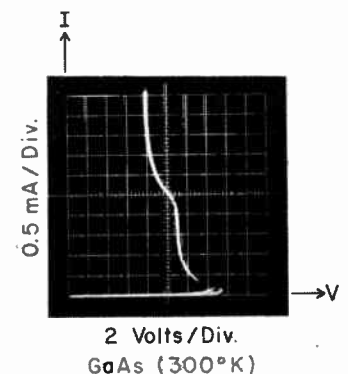


Fig. 3—Double injection negative resistance *p-i-n* diode fabricated on semi-insulating GaAs (Monsanto V-456), Zn-diffused p -region (760°C, 14 min, 4 mg Zn, 6 mg As), Sn-alloyed $n+$ region

easily ionized thermally. The V-I characteristics and structure observed in these diodes (at low temperatures) are varied and complicated, and frequently exhibit multiple switching and trapping effects as well as unexpected oscillations (even in regions in which the V-I characteristic has positive slope).

DOUBLE INJECTION IN SILICON

Much of what has been said above concerning GaAs double injection diodes applies in a general sense to Si units. For example, Fig. 4 shows the V-I plots of three silicon double injection diodes in the low current region below breakdown. Since the diodes represented by curves A) and B) are planar passivated units, they perhaps most indicate the true state of affairs in double injection. That is, these units are not plagued with variable surface conditions and, just as GaAs, exhibit a SCL current proportional to V^2 up to a point reasonably close to breakdown. The fields in the *si* region at breakdown in Si, again like GaAs, lie in the range from 10^3 to 10^4 v/cm.

Figs. 5 and 6 (next page) show the characteristics of two somewhat different Au-doped Si double injection diodes. The diode of Fig. 5 was fabricated by allowing $p+$ and $n+$ regions on opposite sides of relatively high purity Si which was melt-doped with Au (final resistivity $\sim 10^2$ ohm-cm). Fig. 6 is the characteristic of a planar-epitaxial $p+n$ $n+$ -diode¹² in which the initial n -region resistivity was ~ 1 ohm-cm and was compensated (by diffusion) to high resistivity with $\sim 2 \times 10^{16}$ Au atoms/cm³. The light sensitivity of the first unit in the forward direction is evident [trace 2]. Both units switch through the negative resistance region to a region of lower voltage which tends to hold constant over a very large current range, and in neither case tends to show a current increase (in the "semiconductor regime") proportional to V^2 (or V^3) at moderate current levels. Rather, the behavior in this region is much like the constant voltage region of a gas tube, and like a gas tube suggests that these diodes would be useful for voltage regulation in the range from 1 to 5 volts, which are typical voltages observed in various experimental units.

The magnitude of the constant voltage following breakdown appears to be more a function of the deep center (Au) doping concentration than of σ_n/σ_p and is consistent with recent work of Gibbons and Reddi¹³ on high-field breakdown in Au-doped silicon in the absence of double injection. The fact that the voltage after breakdown is dependent upon concentration of deep levels is perhaps better illustrated by the V-I characteristics of Fig. 7, which were taken on a unit fabricated on 100 ohm-cm n -type Si counter-doped to higher resistivity with Co. The diode of Fig. 7 switches through the negative resistance region to a voltage typical of that of a normal forward-biased silicon p - i - n diode.

In this case no V^2 (or V^3) SCL current dependence is observed following breakdown (semiconductor regime). Because of the weak background donor doping in a 100 ohm-cm n -type crystal, in the example of Fig. 7 we can not be certain that the deep levels responsible for double injection switching are due to Co, or other contaminating impurities or complexes introduced during diffusion of Co into the diode wafer. Nevertheless, the fact remains that double injection switching occurs in lightly doped, Co-diffused n -type samples from the higher voltage SCL region down to the voltage of the usual forward-biased p - i - n diode. Complete switching of the type described implies that (1) does not properly account for the behavior of DI diodes possessing a low concentration of deep level impurities. Finally, in Fig. 7 we see from the leads to a V-I characteristic which resembles that of the usual p - i - n diode.

Not all deep levels which might be selected for double injection diodes give equal or equivalent behavior. For example, higher light sensitivity in Si units may be obtained with a multilevel impurity like Zn (or Co) which is introduced into the lattice in concentration just over half of that of the background shallow donor concentration [5]. Fig. 8 shows the V-I characteristics of a double injection diode prepared on 0.25 ohm-cm n -type Si-doped by diffusion with Zn to approximately 2×10^{16} atoms/cm³. The V-I characteristics were traced with a 60 \sim signal and on the ascending portion of the signal gave the trace labeled 1), and on the descending portion the trace labeled 2). The effects of trapping are clear. If the tracing signal is allowed to drive the diode in the reverse (and forward) direction, increasing the signal magnitude results in an increased breakdown voltage, consistent with the fact that reverse bias helps to empty traps. Light (optical injection) causes the diode to switch all the way to the characteristic of a normal forward-biased p - i - n diode, and eliminates all signs of trapping. Comparable Au-doped units are not as light-sensitive, do not usually switch down very far in voltage, and do not exhibit as extensive trapping effects. Higher voltage (thicker) Zn-doped Si double injection diodes display a very noisy and erratic behavior near breakdown, perhaps attributable to fluctuation phenomena again involving traps, or due to deep level oscillator-like phenomena which are not too clearly understood.^{14,15}

Infrared photoresponse measurements (forward bias) on Au-doped Si units give a strong signal output in the range from 0.46 to 0.68 eV and indicate the level E_R at or near 0.55 eV, as expected from the known Au acceptor level in Si. Similar measurements on Zn-doped Si units give an increasing output signal in the range from 0.55 to 0.8 eV, which is the range in which the Zn levels (acceptor levels) are known to lie. Measurements on Co-doped units indicate a Co acceptor level at or near

¹³ J. F. Gibbons and V. G. K. Reddi, "Electrical Breakdown Phenomena in Gold-Doped Silicon," presented at IRE-AIEE Solid State Device Res. Conf., University of New Hampshire, Durham; July 9-11, 1962.

¹⁴ N. Holonyak, Jr., to be published.

¹⁵ R. D. Larrabee and M. C. Steele, "Oscillator—new type of semiconductor oscillator," *J. Appl. Phys.*, vol. 31, pp. 1519-1523; September, 1960.

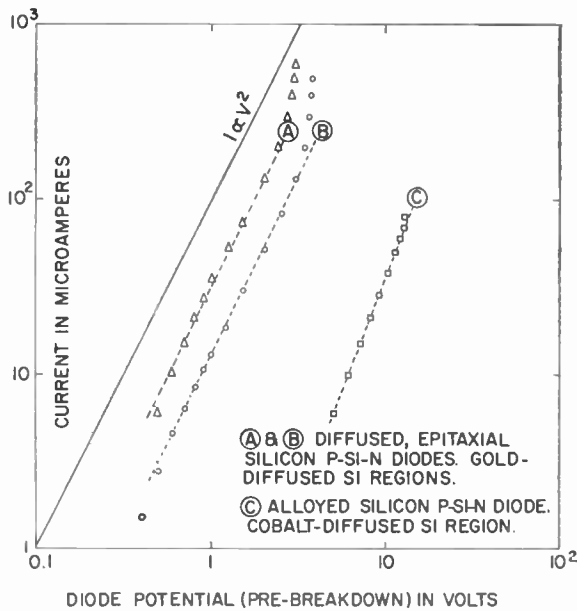


Fig. 4—Pre-breakdown SCL, V-I characteristics of Si *p-i-n* double injection negative resistance diodes: A) and B) diffused, epitaxial *p-si-n* diodes, Au-diffused *si* regions ($\sim 2 \times 10^{16}$ Au atoms/cm³); C) Al-B, Au-Sb alloyed *p-si-n* diode, Co-diffused *si* region.

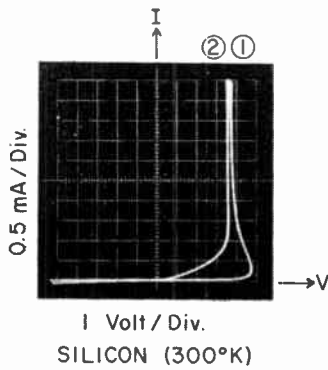


Fig. 5—Alloyed (Al-B, Au-Sb) double injection *p-i-n* diode fabricated on melt-doped (Au) Si: 1) Diode in room light, 2) Diode illuminated with microscope lamp (light injection).

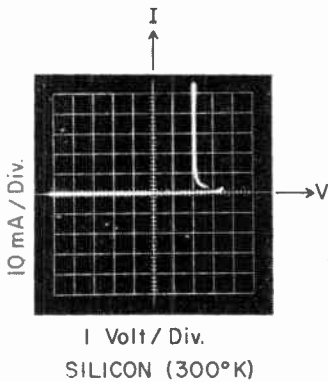


Fig. 6—Diffused, epitaxial *p-i-n* double injection diode in which the *i* region was originally *n*-type and was counter-doped by diffusion with Au ($\sim 2 \times 10^{16}$ atoms/cm³).

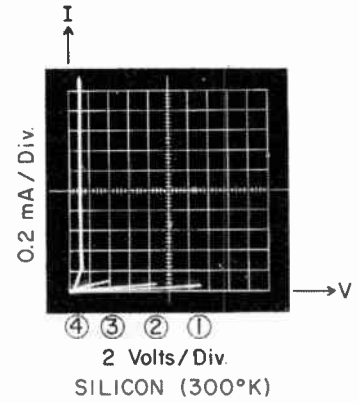


Fig. 7—Alloyed (Al-B, Au-Sb) double injection *p-i-n* diode fabricated on 100 ohm-cm *n*-type Si into which Co was diffused at 1130°C: 1) V-I characteristic in room light; 2), 3) and 4) V-I characteristics when diode is successively more heavily illuminated; 4) Diode completely turned on.

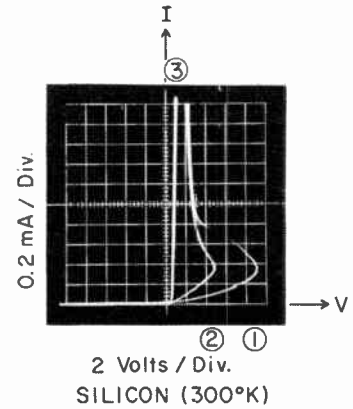


Fig. 8—Alloyed (Al-B, Au-Sb) double injection *p-i-n* diode fabricated on 0.25 ohm-cm *n*-type Si into which Zn was diffused at 1150°C: 1) and 2) V-I characteristics in room light, 60-tracing signal; 3) Diode illuminated and turned on (light injection).

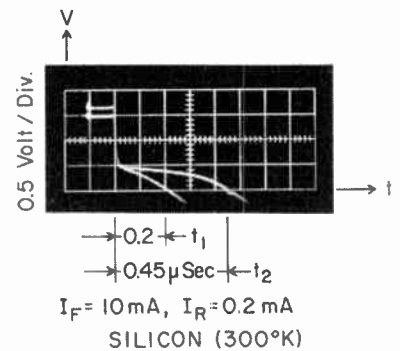


Fig. 9—Alloyed (Al-B, Au-Sb) double injection (Zn counter-doped) *p-i-n* diode forward recovery characteristic (Tektronix S Unit): t_1) Diode in room light, t_2) Diode illuminated.

0.5 eV above the valence band. On some units a broadened response is observed near the band edge and perhaps indicates a deep level near the valence band edge. Since Co-doped DI diodes in many respects resemble Zn-doped units and also have high photoresponse, it is reasonable to expect Co to display a many-level behavior in Si. Because it has been possible to counter-dope less than 5 ohm-cm *n*-type Si to over 10^4 ohm-cm with Co, we estimate that Co (in lapped wafers) has a solubility of near 10^{15} atoms/cm³ at 1200°C.

Double injection diodes possess several interesting switching properties. Pulse turn-on measurements performed on GaAs units indicate that a feed-through signal is observed immediately upon application of the pulse signal and is followed by diode turn-on at a delayed time proportional to the hole transit time across the *si* layer. If the pulse voltage applied to the diode is increased, correspondingly shorter transit times and turn-on times are observed. For silicon double injection diodes of the type shown in Fig. 6 taken from a lot of nominally 5 V (dc) breakdown and *si* thickness ~ 0.5 mils, an estimate of hole transit time t_p and low-level hole lifetime τ_p gives

$$t_p \sim \frac{W^2}{\mu V} \sim 10^{-9} \text{ sec} \sim \tau_p. \quad (4)$$

If we assume hole thermal velocities of 10^7 cm/sec, from (3) and the known Au concentration of $\sim 2 \times 10^{16}$ atoms/cm³ $\sigma_p \approx 5 \times 10^{-15}$ cm², which is in fairly good agreement with previous estimates of the hole capture cross section of Au centers in Si.

The recovery properties of a highly photosensitive Zn counter-doped Si double injection diode (Fig. 8) are shown in Fig. 9. The recovery characteristics of Fig. 9 were taken with a Tektronix S Unit set to deliver a forward bias current of 10 ma and to withdraw a recovery current of a constant magnitude 0.2 ma. The two traces shown exhibit the forward voltage on the diode, at 10 ma bias and at 0.2 ma bias, for the diode in room light and for the diode illuminated with a microscope lamp. The point at which the forward voltage goes to zero following switching from forward to reverse current is a measure of the recovery time. An initial forward voltage of 1.65 V and a recovery time $t_1 = 0.2 \mu\text{sec}$ corresponds to the case of the diode in room light, and 1.5 V initial forward voltage and recovery time $t_2 = 0.45 \mu\text{sec}$ corresponds to the case of the diode illuminated with a microscope lamp.

This example shows that illumination causes the diode to operate in the longer lifetime condition of the semiconductor regime, and more than doubles the recovery time. As is evident, careful doping with a properly selected deep level leads to strong photoeffects, which obviously offer a number of attractive practical possibilities. For example, it is possible to make a double injection diode with a negligibly small negative resist-

ance region which can be operated as a photosensitive charge-storage diode.¹⁶ Also, since deep level impurities help reduce lifetime at low current levels, they should in turn help suppress the recovery "tail" on charge-storage diodes.

DOUBLE INJECTION IN GERMANIUM

In the case of Ge, because of its relatively narrow bandgap, the question may be raised whether double injection negative resistances are possible at room temperature. Successful (300°K) experimental double injection diodes have been prepared by alloying *p+* and *n+* regions on *n*-type Ge wafers which have been counter-doped with Fe, Cu, Co, Ni, or Mn. The behavior of these diodes is in some respects like that observed in GaAs and Si units. Diodes fabricated on wafers counter-doped with Fe, Cu, Ni, or Co (concentration roughly half that of the shallow donor concentrations) exhibit switching from the point of breakdown all the way, or near, to the voltage of a conventional forward-biased Ge junction. A typical characteristic of a Cu-doped unit is shown in Fig. 10.

Depending upon wafer thickness and possibly the nature of the *n*-region alloy, some Ge units (Fe-doped and Cu-doped) have been fabricated with breakdowns over 200 V and such that roughly from zero bias to half that at breakdown (forward bias) a saturation current is observed. (Impedance levels greater than 10^6 ohms are observed, *i.e.*, ~ 0.1 ma @ 100 V.) This coupled with the high photosensitivity and high breakdown voltage observed in some units has prompted Rediker,¹⁷ and later Hall,¹⁸ to suggest that these diodes may actually be a form of *p-n-p-n* switch. For example, if shallow gettering of deep level impurities occurs when the *p+* dot is alloyed to the wafer, a structure consisting of *p+* region, gettered *n* region, deep level counter-doped

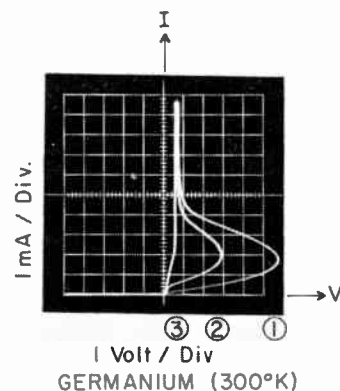


Fig. 10—Ge double injection diode (0.3 ohm-cm Ge compensated with Cu to 10 ohm-cm): 1), 2) and 3) Diode successively more heavily illuminated, 3) Diode turned on.

¹⁶ J. L. Moll, S. Krakauer and R. Shen, "P-N junction charge-storage diodes," *Proc. IRE*, vol. 50, pp. 43-53; January, 1962.

¹⁷ R. H. Rediker, private communication.

¹⁸ R. N. Hall, private communication.

region, and finally $n+$ region will result, and the anomalous behavior is quickly explained (*i.e.*, saturation current). For wafers doped with the faster diffusing impurities (Cu and Ni) this explanation may apply in some cases. However, it fails to adequately account for those units in which high percentages of deep level impurities (Fe and Cu) are included in both $p+$ and $n+$ alloys to suppress out-diffusion of deep level impurities from the counter-doped wafers during alloying of $p+$ and $n+$ regions. Also 20 to 30 different units made with a wide range of alloys (p and n) have been sectioned, and in no case has it been possible to make clear-cut identification of any junctions other than those created by the p and n alloy dots. Further, some room temperature negative resistances have been observed on Zn counter-doped crystals, crystals in which diffusion and gettering of Zn is highly improbable because of the small diffusion constant of Zn. These units, it should be mentioned, can be fabricated apparently only when an n -type alloy dot having a thyristor-like¹⁹ property is used. This would mean that these particular diodes are perhaps better explained by Stafeev's work rather than by Lampert's double injection model, which, however, does apply to some extent at the current level at which the n contact becomes a good emitter.

From a practical point of view, to some degree it does not matter whether double injection diodes or $p-n-p-n$ diodes are being discussed. Both obviously have many equivalent electrical properties. Both are in a sense "double injection" diodes. In a $p-n-p-n$ diode the end p and n regions double inject (holes from one end, electrons from the other) and when switching occurs and the middle junction switches to forward bias, the charge level in both center base regions is raised to high levels. A double injection diode after switching also exhibits a high charge level in the center region (because of lifetime change).

A difference in the two is the fact that in the high impedance OFF-region the $p-n-p-n$ switch exhibits a saturation current, whereas in wider bandgap materials double injection diodes exhibit a SCL current. Another difference (not particularly true of Si or GaAs or necessarily true of Ge) is the fact that a double injection diode does not in all cases switch down all the way to the voltage of one forward-biased conventional junction. In terms of photosensitivity, the double injection diode enjoys considerable potential for more interesting behavior (than a $p-n-p-n$ switch) because of dependence upon deep impurity levels for operation.

CONCLUSIONS

Although studies of double injection diodes are relatively new, it is already possible to draw a number of

important conclusions concerning this area of work. Double injection phenomena obviously are useful for study of SCL currents and deep levels as well as oscillator-like effects.¹⁴ The negative resistance effects which are observed have immediate practical significance. For example, because double injection diodes can be built on extremely high resistivity substrates (10^6 to 10^7 ohm-cm in GaAs), possibilities exist for building noninteracting switching arrays in matrix form on a single crystal. Because of their exceptionally high forward bias photosensitivity, DI diodes offer a number of attractive light or infrared applications, as well as applications involving electrically driven, light-producing inputs which are used to drive DI diodes used as output elements (electronic relays). The post-breakdown constant voltage behavior of Si DI diodes offers an immediate practical application as a voltage regulator element at voltages lower than can be attained via conventional avalanche regulator diodes.

Whereas design of a $p-i-n$ diode formerly was not regarded as critically dependent upon the detailed properties of the i region, now other significant design parameters (kind and concentration of deep levels) are evident, which can be useful or harmful—but nevertheless must be considered. In a useful sense, designing with deep impurity levels can lead to possible means of improving or changing the operation of charge-storage diodes, *e.g.*, make them light-sensitive. Graded diffused junctions or junctions on epitaxial regions cannot have their speeds of operation increased arbitrarily by doping to high concentrations with Au, as is often attempted in current practice. If a high enough Au concentration is diffused into a graded junction (Si), the junction transition region becomes counter-doped (compensated) to a high resistivity and to a low lifetime (at low levels), which in turn leads to a double injection negative resistance characteristic if the width of the compensated region is greater than the hole diffusion length. A similar and troublesome problem of this type can occur in epitaxial diodes and transistors in which excessive amounts of Au are diffused to kill lifetime. This can lead to secondary switching in a transistor driven into saturation.

In spite of the rather extensive theoretical and experimental information and the practical implications which already are evident in double injection studies, a number of problems still remain. The theoretical models now available do not adequately account for the constant voltage property observed in Si and in some GaAs under conditions of double injection at moderate current levels. This may well be a plasma effect, which would be consistent with the observation of oscillator-like phenomena in certain DI diodes.¹⁴ The theories now available do not adequately account for impurity concentration effects, and switching down to the level of one forward-biased standard $p-n$ junction in DI diodes lightly doped with deep levels. Trapping phenomena,

¹⁹ G. W. Mueller and J. Hilibrand, "The 'thyristor'—a new high-speed switching transistor," IRE TRANS. ON ELECTRON DEVICES, vol. ED-5, pp. 2-5; January, 1958.

which are evident in a number of experimental diodes, as yet have not been examined sufficiently in DI theoretical work. Although deep level impurities have been extensively studied in Ge and Si, we find now that this work is incomplete and are finding, particularly in Si, significant new deep level impurities such as Co. The study of deep levels and their effects in GaAs and other compounds has barely begun and requires considerable attention before the full implications of DI in GaAs and the compound semiconductors can be assessed.

ACKNOWLEDGMENT

The author is particularly indebted to S. F. Bevacqua for assistance in most of this work. For assistance in portions of this work he would like to thank also C. V. Bielan, F. A. Carranti, D. K. Hartman, B. G. Hess, S. W. Ing, Jr., S. J. Lubowski, R. E. Morrison, T. P. Sylvan, and R. C. Thomas. He is grateful to T. R. Selig and C. O. Hull for supplying planar diffused, epitaxial Si DI diodes and to R. N. Hall, R. E. Halsted, A. L. McWhorter, and R. H. Rediker for helpful discussions.

The Madistor—A Magnetically Controlled Semiconductor Plasma Device*

I. MELNGAILIS†, MEMBER, IRE, AND R. H. REDIKER†, SENIOR MEMBER, IRE

Summary—The madistor is a new active device which makes use of the effects of a magnetic field on an injection plasma in a semiconductor. The formation of an injection plasma has been observed in *p*-type InSb at temperatures below 100°K as donor traps become saturated by electrons injected through a forward biased *n*⁺*p* junction. In an appropriately designed *n*⁺*pp*⁺ diode, the saturation of traps and the subsequent increase in electron lifetime bring about an abrupt decrease of base resistance, and a negative resistance region is observed in the current-voltage characteristic. Because of the high mobility of electrons in InSb (5×10^5 cm²/vsec) the plasma can be appreciably deflected and deformed by transverse magnetic fields of the order of 10 gauss. The possibility of controlling the position of a plasma inside a solid by means of a magnetic field can be utilized in a number of different types of madistors in which the input circuit is isolated from the output.

The operation at 77°K of four types of InSb madistors has been studied. The first makes use of a specially designed *n*⁺*pp*⁺ diode mounted in the air gap of a small ferromagnetic-core electromagnet. A small change in the electromagnet winding current produces a magnetic field at the diode and causes a larger change in diode current. Typically an increase in mmf of 200-ma turns produces an additional magnetic field intensity of 5 gauss which decreases the diode current by 10 ma. Four-terminal amplifiers and switching circuits using these madistors have been built and simple feedback oscillators have indicated power gain at frequencies up to 450 kc. In the second type of madistor a magnetic field of about 10 gauss switches the output current of a specially designed dual-base diode from one base contact to the other. Because of the negative resistance characteristic, the magnetic field can be removed and the current in suitable structures will remain in the contact to which it had been switched. Switching times of 2 to 3 μsec have been measured

for these bistable flip-flops. A third type includes devices with a multiplicity of base contacts in which the injection plasma and hence the output current is magnetically switched in sequence from one base contact to the next. A disc-shaped InSb device with an injecting contact at the center and "ohmic" contacts along the periphery has been operated as a stepping switch. In transistor-like structures, which make up a fourth madistor type, the magnetic field effects on the emitter injection plasma are used to control the collector current and hence the transistor current gain.

INTRODUCTION

ACTIVE SEMICONDUCTOR DEVICES which make use of the interaction of a magnetic field with the current in a semiconductor have been extensively investigated in the past. Hall-effect amplifiers [1], [2] as well as amplifiers based on the magneto-resistance effect [3]–[6] have been described. Devices have been built [7], [8] based on the Suhl effect [9] in which both minority and majority carriers are deflected by a magnetic field toward one surface of the semiconductor. The effect of magnetic field on the current at high forward injection levels in germanium diodes has been explored by Karakushan and Stafeev [10], [11] and has been ascribed by them to the reduction in the effective mobility and the increased path length of minority carriers in a magnetic field. Because of these two phenomena the ratio L/d , where L is the diffusion length and d is the base thickness of the diode, is decreased and the conductivity modulation of the base region which is present at these high injection levels is reduced.

All the devices described above require magnetic fields of the order of thousands of gauss to produce an

* Received August 1, 1962; revised manuscript received, September 26, 1962. Operated with support from the U. S. Army, Navy, and Air Force. A preliminary report of this work was presented at the IRE-AIEE Solid State Device Research Conference, University of New Hampshire, Durham, N. H., July 9–11, 1962.

† Massachusetts Institute of Technology Lincoln Laboratory, Lexington, Mass.

appreciable effect in the semiconductor output circuit, and hence have been limited in their application. A new mechanism for magnetically controlled semiconductor devices is provided by the possibility of producing a localized injection plasma by saturating traps in a semiconductor [12] and of controlling the position of the plasma by means of a magnetic field. Such active devices have been named madistors (*magnetic deflection of an injection plasma produced by saturating traps*). The operation of InSb madistors at 77°K will be described in this paper. In these devices an appreciable effect is produced in the semiconductor output circuit by magnetic fields of the order of 10 gauss.

Several types of madistors will be described in detail. The diode madistor is a four-terminal device with electromagnet input and a specially designed diode¹ output in which feedback is eliminated by suitable construction of the output circuit. Deflection of the plasma can also be utilized in various dual- or multi-base madistors in which the plasma is switched between contacts. Dual-base madistors can be designed so the magnetic field is necessary to maintain the current at the desired base contact, or they can be designed so that the magnetic field can be removed after switching. In the transistor madistor the current amplification of the transistor output is modulated by the magnetic field.

MAGNETOINJECTION IN INSB

The Injection Plasma

The formation of an injection plasma has been observed [12] in *p*-type InSb at temperatures below 100°K as donor traps become saturated by electrons injected through a forward biased *p-n* junction. For low injection levels as a consequence of trapping, electron lifetimes in *p*-type InSb at 77°K are as short as 5×10^{-10} sec [13], [14], while the lifetime of holes in the same material is about 10^{-6} sec. However, if a large number of electrons are injected into a *p*-type crystal from a forward biased *n⁺p* junction, or by a strong light source, the traps eventually become saturated and the electron lifetime increases [12]. In an *n⁺pp⁺* diode with the *p*-base of the order of 1 mm thick there is little conductivity modulation in the base at low forward currents (<0.2 a/cm²) because trapping limits the diffusion length of injected electrons to about 10^{-3} cm. At higher forward currents more electrons are injected into the base, the traps become saturated first near the junction, and a region of relatively long electron lifetime (10^{-7} – 10^{-6} sec) and high conductivity is formed. Fig. 1 illustrates an injection plasma inside of which the electron diffusion length is of the order of a millimeter and the base resistance is conductivity modulated, while outside the plasma the electron diffusion length is its original value, about 10^{-3} cm, and conductivity modu-

¹ Diodes, transistors, etc., which are specially designed for use in madistors will be called magnetodiodes, magnetotransistors, etc.

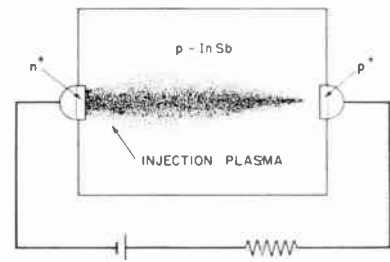


Fig. 1—Injection plasma in an *n⁺pp⁺* InSb diode.

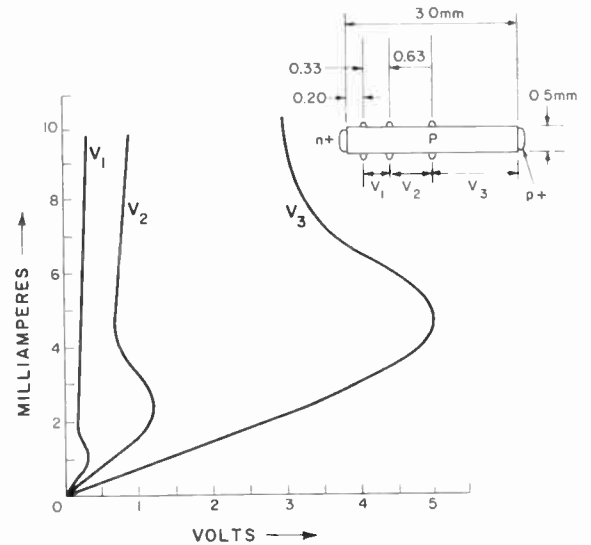


Fig. 2—Potential probe measurements along the base region of a bar-shaped *n⁺pp⁺* InSb diode at 77°K. The abscissa is the voltage across different portions of the base region. The ordinate is the diode current.

lation is negligible. As the current is increased, the injection plasma penetrates deeper into the base until it extends to the *p⁺* contact.

The formation of the injection plasma can produce a negative resistance region in the forward current-voltage characteristic of diodes if the diode characteristic is determined by the bulk resistance of the base. Stafeev [15] has shown that a negative resistance results from a “self-multiplication” of carriers in the base as carrier lifetime increases with increasing injection level. An increase of lifetime reduces the resistivity of the base and enhances injection from the *p-n* junction which in turn produces a further lifetime increase, etc.

The longitudinal growth of the plasma region can be observed as the diode current is increased, by probing the potential along the side of a bar-shaped base and noting the propagation of the negative resistance down the base. The results of such an experiment are shown in Fig. 2. The “breakdown” point does not occur at a critical value of current density or electric field in the base, but rather seems to depend on the density of injected carriers. The small-signal conductance between probes on opposite sides of the bar was also measured as a function of diode current. As the diode current was increased the conductance increased first in regions close

to the p - n junction, while no change was observed between probes farther along the bar. At higher currents the conductance change propagated down the length of the bar toward the ohmic contact. Traps in the base can be also saturated by injecting carriers with light. With sufficient light intensity the conductance of the base can be increased sufficiently to eliminate the negative resistance characteristic. The increase of carrier lifetime in the base with increased injection level can also be noted by observing the reverse recovery transient of diodes initially biased in the forward direction.

All the above experiments indicate the validity of the injection plasma model in explaining the negative resistance in n^+pp^+ InSb diodes. As expected, the negative resistance becomes more pronounced as the length of the base and the resistivity of the InSb are increased. In all devices to be described here such a negative resistance exists² and is crucial to the operation of some of these devices.

Magnetic Effects on I-V Characteristic of n^+pp^+ InSb Diodes

The forward current-voltage characteristics of an InSb n^+pp^+ diode are shown in Fig. 3 for different magnetic fields perpendicular to the direction of current flow. The diode dimensions are shown in the inset of Fig. 3. In the portion of the I-V characteristic following the negative resistance the application of magnetic fields perpendicular to the direction of current flow greatly increases the forward resistance of the diode.

The effect of the magnetic field is to deflect the injected carriers, resulting in a displacement and deformation of the plasma. In a bar-shaped base region the plasma is deflected toward the surface, where carrier lifetime is shorter than inside the bulk. This reduces the number of added carriers in the base and increases the base resistance. For diodes with a small p^+ contact and a base region of sufficiently large cross section so that the plasma is far removed from the surface, the increase of resistance results mainly from a deflection of the plasma away from the p^+ contact. Because of the high mobility of electrons in InSb (5×10^5 cm²/vsec) these effects become important at small magnetic fields. If the diode of Fig. 3 is operated with a quiescent magnetic field of 55 gauss and the load line as shown, the application of 5 additional gauss reduces the current by 8 ma.

Suhl Effect in p -Type InSb

In order to demonstrate deflection of the injection plasma by magnetic fields, we have made measurements similar to those originally made by Suhl and Shockley in germanium [9]. The inset of Fig. 4 shows the sample configuration. A constant forward current of 11 ma

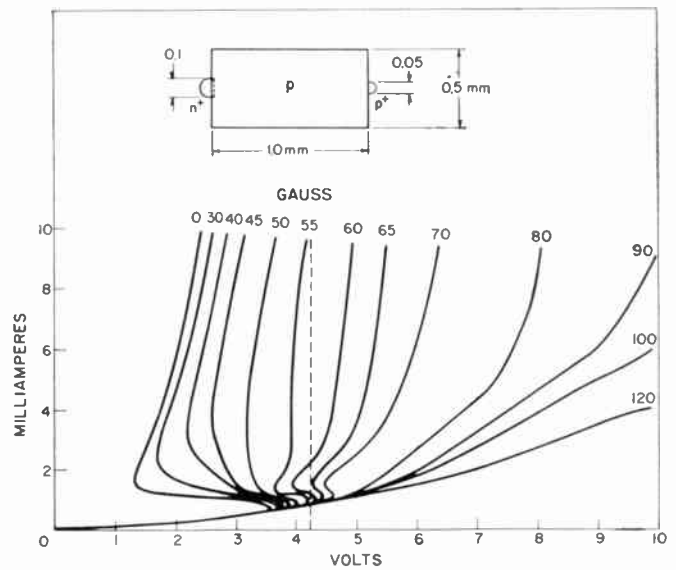


Fig. 3—Effect of magnetic field perpendicular to the current flow on the forward current-voltage characteristic of an n^+pp^+ InSb diode at 77°K. The diode dimensions are shown in the inset.

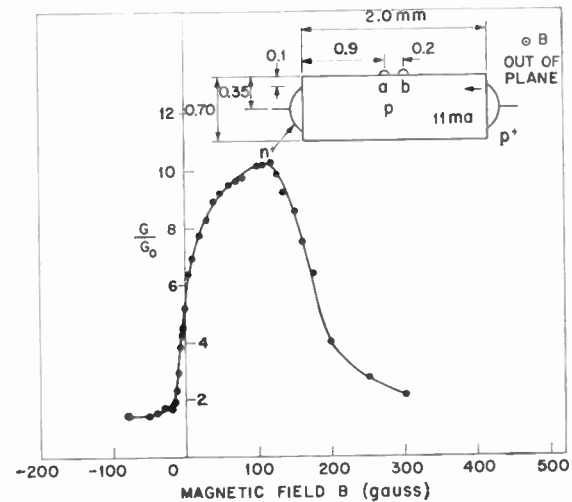


Fig. 4—Conductance measured at 77°K between surface probes as a function of transverse magnetic field. G_0 is conductance between probes with no minority carrier injection in the base. The sample geometry is shown in inset.

was passed through the diode, and the conductance between two closely spaced probes a and b was measured by means of a small 1000-cps ac signal, while varying the transverse magnetic field. With two-carrier conduction the Hall voltage is minimized because both holes and electrons are deflected toward the same surface, reducing a buildup of charge, and the plasma undergoes an angular displacement. The plot in Fig. 4 shows first an increase of conductance with positive magnetic field, as the plasma is deflected towards probe b , followed by a decrease as the plasma is deflected past probe a and the carriers recombine at the surface before reaching the region between the probes. The magnitudes of field required for the Suhl effect are comparable to the mag-

² Madistors have been fabricated with appropriate choice of semiconductor resistivity and geometry which do not have a negative resistance region. These have been described in I. Melngailis, *et al.* [16]. They will not be discussed in this paper.

nitudes that cause the magnetic effect in diode characteristics (Fig. 3).

THE DIODE MADISTOR

The possibility of controlling the position of a plasma inside a solid by means of small magnetic fields can be utilized in a number of different devices. Among the advantages of such devices is isolation of the input circuit from the output, which greatly simplifies attendant circuitry.

Fig. 5 shows an artist's representation of a diode madistor with a magnetodiode in the air gap of an electromagnet. The assembly is mounted on a standard TO-5-type transistor header (diameter 0.25 in). The output characteristics of such a diode madistor are illustrated in Fig. 3. Neglecting the reluctance of the ferromagnetic core, typically a change of 200 ma-turns produces a change of 5 gauss in the 0.5 mm air gap and a change of about 10 ma in output diode current.

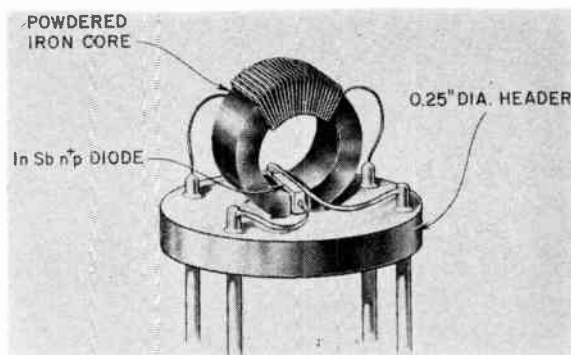


Fig. 5—Artist's sketch of an experimental diode madistor, showing diode mounted in the air gap of ferromagnetic toroid.

The return lead from the diode is passed through the air gap parallel to the diode in order to prevent the flux due to the diode current from linking the input coil. This reduces feedback due to inductive coupling.

Magnetodiode Design and Fabrication

Provided the carrier mobility is maintained at a high value, the magnetic sensitivity is higher for InSb n^+pp^+ diodes with higher resistivity base regions. This is expected because in higher resistivity material the effect of the conductivity modulation due to the injection plasma will be larger, and the deflection and deformation of the plasma by the magnetic field will increase the diode resistance to a larger value. Base regions with resistivity between 20 and 100 ohm-cm at 77°K have been used.

Also as expected from the plasma model, the magnetic sensitivity is greater in InSb n^+pp^+ diodes with longer base regions, because for the same deflection angle the transverse displacement of the plasma increases with distance away from the injecting contact. However, increasing the base length also increases power dissipation and can cause excessive heating. To

maintain the magnetic sensitivity at a reduced power level the size of contacts must be scaled down as the base length is reduced. The maximum power dissipation in the diode of Fig. 3 for the loadline shown is about 40 mw. This diode has a base region 1 mm long and p^+ ohmic contact 0.05 mm in diameter. With further miniaturization the power level may be further reduced.

The rectifying n^+ contacts were made by alloying to the base region indium spheres containing a small percentage of tellurium. Indium spheres with a small percentage of zinc were alloyed to the base region for the p^+ ohmic contacts. After alloying, the surfaces were etched with a mixture of hydrofluoric, nitric, and acetic acids (1:2:2). This was followed by an electrolytic etch using a 0.1 normal KOH solution.

Electromagnet Design

Diode madistors have been built by mounting diodes either inside small air-core solenoids (about 3 mm diameter) or in air gaps cut in small ferromagnetic toroids. The air-core solenoids are to be preferred if absolute linearity of response is desired and hysteresis and eddy current losses cannot be tolerated. With ferromagnetic toroids the magnetic field is more easily limited to the volume of the InSb diode mounted in the air gap, and the reluctance of the magnetic circuit is smaller than the reluctance of an equivalent air-core solenoid. Fewer ampere turns are thus required to produce a given magnetic field (B) at the diode, and the inductance of the input coil is reduced.

To select a suitable material for the toroids, the magnetic properties of various ferrite, ceramic and powdered iron cores were measured at liquid nitrogen temperature. High-frequency powdered iron cores³ showed almost no changes in their permeability, losses, and frequency response from room temperature down to 77°K. Because of their low losses and superior frequency characteristics they are considered most suitable at present although their permeability (about 30) is somewhat lower than desired. Preliminary measurements on high permeability ferrites and ceramics in most cases show a large decrease in permeability, especially at the low magnetic fields of interest, between room temperature and 77°K, and their losses are much greater than those of powdered iron cores.

Electrical Characterization of the Diode Madistor

The small-signal behavior of a diode madistor [Fig. 6(a)] can be described by linear four-terminal network equations:

$$V_1 = z_{11}I_1 + z_{12}I_2, \quad (1)$$

$$V_2 = z_{21}I_1 + z_{22}I_2, \quad (2)$$

where V and I denote small alternating voltages and currents. It is useful to define the following low-fre-

³ Arnold Engineering Co., Marengo, Ill.

quency parameters at a given operating point:

$$r_m = \left(\frac{\partial v_2}{\partial i_1} \right)_{i_2}, \tag{3}$$

$$r_d = \left(\frac{\partial v_2}{\partial i_2} \right)_{i_1}. \tag{4}$$

The parameter r_m determines the circuit gain and can be called transresistance; r_d is the slope of the diode characteristic. The corresponding impedances can be represented to a first approximation as

$$z_m = \frac{r_m}{1 + \frac{j\omega}{\omega_{cm}}}, \tag{5}$$

$$z_d = r_d \left(1 + \frac{j\omega}{\omega_{cd}} \right) = z_{22}, \tag{6}$$

where ω_{cm} and ω_{cd} are cutoff frequencies. The diode impedance z_d has an inductive term because it is limited by the conductivity modulation in the base which causes the current to lag the voltage. The transimpedance z_m has a capacitive term because of the time required for the injection plasma to readjust after the application of the input current which produces the magnetic field. Thus the output voltage lags the input current. The measured frequency variation of z_m and z_d in the cutoff range, however, is more gradual than 6 db per octave,⁴ and the above representation is only a first-order approximation to the true frequency response.

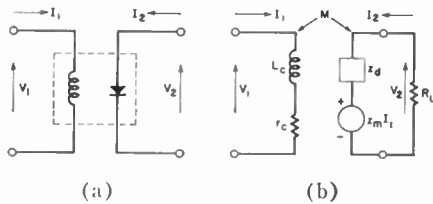


Fig. 6—(a) Madistor four-terminal network notation. (b) Small-signal equivalent circuit of madistor.

Taking into account the mutual inductance M between the input and output circuits,⁵

$$z_{21} = z_m \pm j\omega M, \tag{7}$$

$$z_{12} = \pm j\omega M. \tag{8}$$

Using the notation developed above, the four-terminal network equations become

$$V_1 = (r_c + j\omega L_c)I_1 \pm j\omega M I_2, \tag{9}$$

$$V_2 = \left[\frac{r_m}{1 + \frac{j\omega}{\omega_{cm}}} \pm j\omega M \right] I_1 + r_d \left(1 + \frac{j\omega}{\omega_{cd}} \right) I_2, \tag{10}$$

where r_c and L_c are the coil resistance and inductance, respectively.

Fig. 6(b) shows an equivalent circuit corresponding to (1) and (2). Typical values of the parameters for present diode madistors are

- $r_c = 0.8\Omega$
- $L_c = 2 \times 10^{-4}h$
- $M = 10^{-8}h$
- $r_m = 150\Omega$
- $\omega_{cm} = 3 \times 10^5 \text{ sec}^{-1}$
- $r_d = 30\Omega$
- $\omega_{cd} = 3 \times 10^6 \text{ sec}^{-1}$

With these values the approximate input impedance Z_i can be calculated as

$$Z_i = \frac{V_1}{I_1} = r_c + j\omega L_c \left[1 \pm \frac{Mr_m}{L_c(r_d + R_L)} \frac{1}{1 + \frac{j\omega}{\omega_{cm}}} \right], \tag{11}$$

where R_L is the load resistance. The last term in (11) represents the feedback due to inductive coupling. For the parameter values listed above

$$\frac{Mr_m}{L_c r_d} = 2.5 \times 10^{-4};$$

hence the feedback term in (11) is negligible and the madistor can be considered a unilateral active device.

The approximate current and voltage amplification, and power gain obtained from (1) and (2) are then, respectively,

$$\frac{I_2}{I_1} = \frac{r_m}{r_d + R_L} \frac{1}{1 + \frac{j\omega}{\omega_{cm}}}; \tag{12}$$

$$\frac{V_2}{V_1} = \frac{r_m R_L}{(r_d + R_L)r_c} \frac{1}{\left(1 + \frac{j\omega L_c}{r_c} \right) \left(1 + \frac{j\omega}{\omega_{cm}} \right)}; \tag{13}$$

$$\frac{P_{out}}{P_{in}} = \frac{r_m^2 R_L}{r_c(r_d + R_L)^2} \frac{1}{1 + \frac{\omega^2}{\omega_{cm}^2}}. \tag{14}$$

Although the frequency response of the voltage amplification is limited by the L/r ratio of the input coil, the frequency response of the current and power gain is determined only by the response of the diode. The frequency response of the coil, however, can be compensated in the input circuit.

A simple current feedback oscillator [Fig. 7(a)] was built for the purpose of determining the maximum frequency of oscillation. The alternating current through the diode was fed back to the input coil by means of a capacitor. Since the biasing circuits are isolated with high inductance chokes, the ac equivalent circuit shown

⁴ F. W. Sarles, private communication.

⁵ The sign of the coupling term depends on the direction of the coil winding with respect to the diode circuit.

in Fig. 7(b) can be used for small signals. The condition for instability of this loop is

$$\frac{r_m}{1 + \frac{\omega^2}{\omega_{cm}^2}} > r_c + r_d. \quad (15)$$

The highest oscillation frequency which has been obtained with present diode madistors is 450 kc.

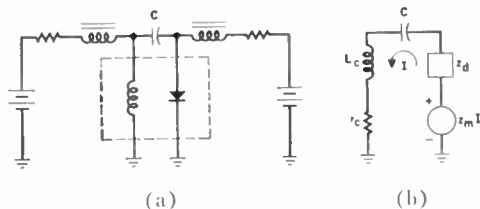


Fig. 7—(a) Madistor current-feedback oscillator. (b) Small-signal equivalent circuit of oscillator in (a).

DUAL-BASE MADISTORS

Besides the simple diode structure, effects of a magnetic field on the injection plasma can be used in structures with additional contacts. Fig. 8 shows the dual base madistor, a structure with a single n^+ rectifying contact on one end of a p -type InSb base and two p^+ ohmic contacts on the opposite end. A forward current I_0 from a constant-current source is passed through the n^+p junction. If the p^+ contacts are sufficiently far apart a plasma can be established between the n^+p junction and one of the p^+ contacts, as shown, leaving a region near the other p^+ contact in the high-impedance state. This is possible because the large change of lifetime between the inside of the plasma and surrounding regions confines injected carriers to a fairly discrete region and prevents their diffusion throughout the base. Once a plasma has been established between the n^+p junction and one p^+ contact, the voltage across the base drops because of the bistable current-voltage characteristic associated with the formation of an injection plasma, and the voltage is too low to cause injection breakdown between the n^+p junction and the other p^+ contact. Thus most of the current I_0 always passes through one of the p^+ contacts. If, however, a magnetic field is applied perpendicular to the plane of the figure with appropriate polarity, the plasma, and hence the current, can be deflected to the other p^+ contact. Upon removing the magnetic field the plasma remains in its new position and a magnetic field of opposite polarity is required to return it to the original p^+ contact. Fig. 9 shows the current in one of the p^+ contacts as a function of the magnetic field. The bistable switching cycle is shown for two values of total current I_0 . With $I_0 = 3.8$ ma the switching field in either direction is about 7 gauss. The transition from one state to the other is sufficiently abrupt so that with suitable magnetic bias the dual-base madistor of Fig. 9 can be switched by magnetic fields of less than 0.5 gauss. (The earth's magnetic field is 0.6 gauss.)

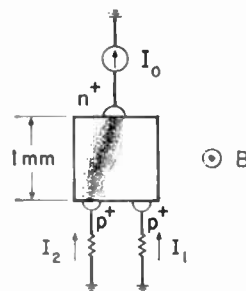


Fig. 8—Bistable dual-base madistor with plasma between the n^+p junction and one of the p^+ contacts.

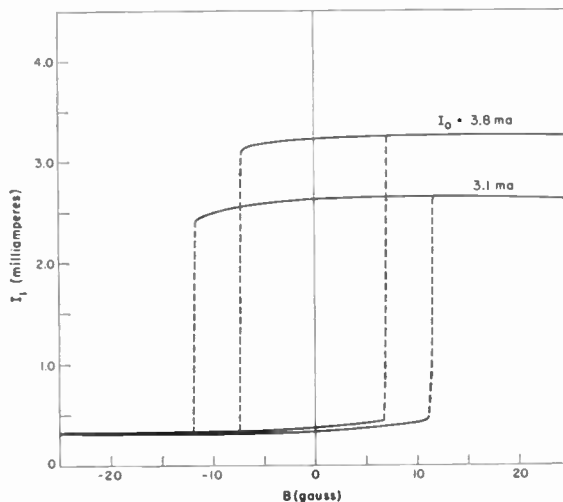


Fig. 9—Current in one base contact of the dual-base madistor of Fig. 8 as a function of transverse magnetic field for two values of total current I_0 . The data were taken at 77°K.

Madistor flip-flops have been built by mounting dual-base structures in air gaps of powdered iron toroids and their switching speed has been measured by applying alternate positive and negative current pulses to the core winding. The current rise (and fall) time is an inverse function of the amplitude of the switching pulse. With a pulsed magnetic field of twice the value of the critical dc field the current rises with a time constant of about 2 μ sec in present flip-flop circuits. The mechanisms determining the transfer speed of the plasma are under investigation at present. In suitably designed units the output of one bistable madistor can be used as input to a next flip-flop stage.

As the n^+p junction current I_0 is increased, the injection plasma increases in size and at a critical value of I_0 encompasses both p^+ contacts. The current I_0 then divides evenly between these two contacts. In this case a transverse magnetic field merely concentrates more of the carriers on one side of the base, thereby creating an unbalance in the currents in the two "ohmic" contacts. Fig. 10 shows a plot of this current difference as a function of transverse magnetic field for different values of I_0 . In the dual-base madistor of Fig. 10 the spacing between the p^+ "ohmic" contacts is smaller than that in Fig. 8 so that the critical value of I_0 at which the

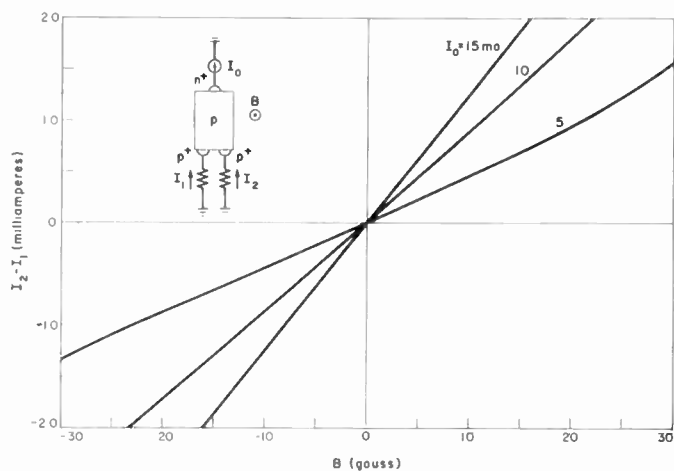


Fig. 10—Base current difference ($I_2 - I_1$) of linear dual-base madistor at 77°K as a function of magnetic field for different values of total current I_0 .

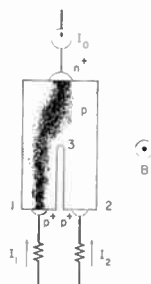


Fig. 11—Dual-base madistor with longitudinal slit separating the two base regions.

madistor switches from bistable to linear operation is reduced.

Because of its relatively linear response at small fields, the device of Fig. 10 may have some applications of its own. However, the bistable operation range can be extended to higher currents by cutting a longitudinal slit in the middle of the base region, as shown in Fig. 11. This reduces diffusion between the regions near the two p^+ contacts and the plasma is confined to either one or the other branch. Bistable switching of the plasma between the branches is accomplished in the same manner as in the dual-base structure of Fig. 8.

MADISTOR STEPPING SWITCH

The mode of operation demonstrated by dual-base madistors can be extended to more complex configurations with additional p^+ "ohmic" contacts. A particularly interesting application is the stepping switch shown in Fig. 12. Here an n^+ contact alloyed in the center of a disc is surrounded by ten branches each with a p^+ contact.

Most of the current I_0 passes through the branch which contains the plasma, while all others remain in the high-impedance state. A magnetic field perpendicular to the plane of the disc deflects the plasma to the adjacent branch. By adjusting the amplitude and time

duration of the magnetic field the plasma can be advanced by any number of branches and the current output stepped any desired number of p^+ contacts. Ring-counter operation can be achieved by applying magnetic field pulses of appropriate magnitude to advance the plasma one branch per pulse.

If the magnetic field is left at a constant value equal to or larger than the minimum switching field, the plasma will continue to rotate around the circle from contact to contact. Fig. 13 is an oscilloscope trace of the current in one branch of a preliminary eight-branch device with a rotating plasma. A pulse appears each time the plasma passes the branch under observation. The rotation rate increases as the magnetic field is increased. For the preliminary stepping switch of Fig. 13, 60 μ sec per revolution was required for the maximum steady magnetic field (65 gauss) at which the plasma stayed well defined.

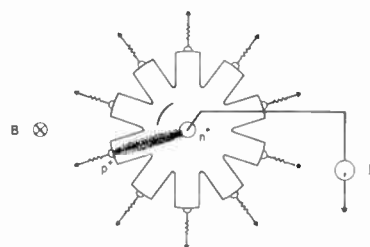


Fig. 12—Madistor stepping switch with centrally located n^+p junction surrounded by ten branches with p^+ contacts.

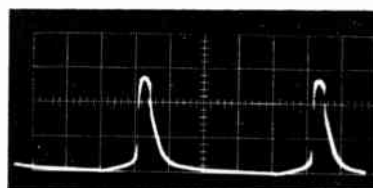


Fig. 13—Current as a function of time in one branch of circular eight-branch stepping switch at 77°K with a constant magnetic field of 40 gauss applied perpendicular to the plane of the switch. The vertical scale is 1 ma per division, and the horizontal scale is 20 μ sec per division.

TRANSISTOR MADISTOR

Magnetic deflection of the injection plasma can also be used to control collection of minority carriers by reverse biased n^+p junctions. For example, in specially constructed n^+pn^+ transistors,⁶ the emitter forward current produces a plasma in the base and minority carriers from the plasma are collected by the reverse biased collector. A transverse magnetic field can deflect the plasma either away from or toward the collector, depending on the transistor configuration, and thereby cause an increase or decrease in the collector current. Fig. 14 shows a plot of the common base current ampli-

⁶ Initial experiments on transistors were performed on units made by H. Hemeke of Texas Instruments, Dallas, Tex., and supplied through the courtesy of the U. S. Naval Ordnance Laboratory. Because of the very thin base regions in these units the magnetic effects were significantly smaller than those shown in Fig. 14.

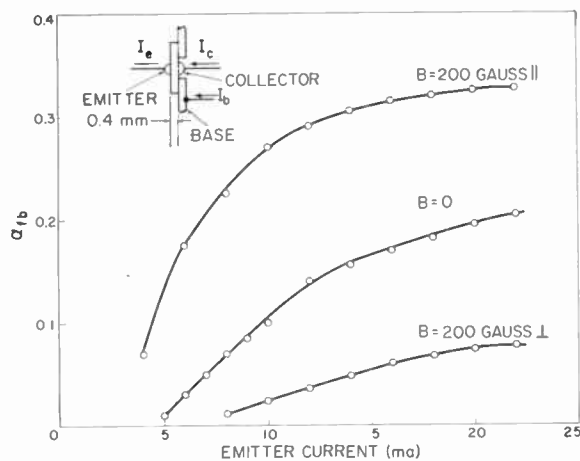


Fig. 14—Common base current amplification α_{fb} as a function of emitter current. The three curves correspond to 0 magnetic field, 200 gauss perpendicular to collector-emitter axis and 200 gauss parallel to collector-emitter axis. The InSb transistor shown in the inset was operated at 77°K.

cation ($\alpha_{fb} \equiv [\partial I_c / \partial I_e]_{V_c}$) as a function of emitter current for the transistor shown in the inset of Fig. 14. This transistor consists of a p -type InSb wafer with concentrically alloyed emitter and collector dots and a ring-shaped p^+ base contact surrounding the collector. At emitter currents below 5 ma α_{fb} is very small because traps in the base region prevent injected electrons from reaching the collector. As the emitter current is increased and traps become saturated, electrons are able to traverse the base, and α_{fb} increases.

Also shown in Fig. 14 is the common base current amplification for magnetic field parallel and for magnetic field perpendicular to the axis connecting the center of the emitter and collector junctions. A transverse magnetic field deflects the injection plasma away from the collector thereby reducing α_{fb} . A longitudinal magnetic field reduces the radial carrier diffusion and has a focusing effect on the injection plasma. Since concentration of the plasma increases the number of carriers which are able to reach the collector, α_{fb} is enhanced by fields parallel to the emitter current.

Magnetically controlled minority carrier collection as illustrated by Fig. 14 can be used with various different device geometries with one or more collectors, and preliminary tests indicate the possibility of achieving very large magnetic sensitivities. In addition, transistor structures like the one in Fig. 14 may be useful in quantitative studies of trapping phenomena and magnetic effects in InSb.

CONCLUSIONS

We have demonstrated that under suitable conditions a discrete plasma can be formed in a semiconductor by the injection of minority carriers from a forward biased junction and that the position of the plasma can be controlled by small magnetic fields, provided carrier mobilities are high. While this principle has been demonstrated for p -type InSb at 77°K, no fundamental obsta-

cle limits such a process to InSb alone. A compound semiconductor may be found with a wider energy gap and hence a higher operating temperature, which has both sufficiently high carrier mobilities and the necessary trapping centers (either inherent or artificially introduced) that can be saturated by the injected carriers.

We have described devices which make use of the effects of a magnetic field on the injection plasma and have demonstrated their operation as four terminal amplifiers with an isolated input, as flip-flops, as stepping registers, and as variable gain transistors. These devices are of particular interest because of their simplicity and because of the small (≈ 10 gauss) magnetic fields necessary for operation. The same structures can be used in many additional circuit applications, for example, in choppers, modulators, or digital gaussmeters. Other special purpose structures which use the principles developed above should further extend the application range. The response speed ($\approx 2 \mu\text{sec}$) of madistors is limited by minority carrier processes involved in the displacement of the plasma; hence, some improvement may be possible by scaling down dimensions of the devices and reducing lifetimes.

ACKNOWLEDGMENT

The authors wish to thank L. J. Belanger and M. L. Barney for fabricating the madistors and F. W. Sarles for valuable discussions on circuit applications. We are indebted to A. J. Strauss for supplying the p -type InSb.

REFERENCES

- [1] I. M. Ross and N. A. C. Thompson, "An amplifier based on the Hall effect," *Nature*, vol. 175, p. 518; March 19, 1955.
- [2] H. J. Thuy, "Der galvanomagnetische Verstärker," *Arch. elektr. Übertragung*, vol. 8, pp. 269-278; June, 1954.
- [3] A. Aharoni, E. H. Frei and G. Horowitz, "New active circuit element using the magnetoresistive effect," *J. Appl. Phys.*, vol. 26, pp. 1411-1415; December, 1955.
- [4] M. Green, "The gaussistor, a solid state electronic valve," *IRE TRANS. ON ELECTRON DEVICES*, vol. ED-3, pp. 133-141; July, 1956.
- [5] D. A. Kleinman and A. L. Schawlow, "Corbino disk," *J. Appl. Phys.*, vol. 31, pp. 2176-2187; December, 1960.
- [6] S. F. Sun, "Oscillators by means of a magnetoresistance effect," *Proc. IRE*, vol. 50, pp. 1484-1493; June, 1962.
- [7] M. Madelung, L. Tewordt, and H. Welker, "Zur Theorie der magnetischen Sperrschicht in Halbleitern," *Z. Naturforsch.*, vol. 10a, pp. 476-488; 1955.
- [8] E. Weisshaar, "Magnetische Sperrschichten in Germanium II," *Z. Naturforsch.*, vol. 10a, pp. 488-495; 1955.
- [9] H. Suhl and W. Shockley, "Concentrating holes and electrons by magnetic fields," *Phys. Rev.*, vol. 75, pp. 1617-1618; May 15, 1949.
- [10] E. I. Karakushan and V. I. Stafeyev, "Magnetodiodes," *Soviet Phys. Solid State*, vol. 3, pp. 493-498; September, 1961.
- [11] E. I. Karakushan and V. I. Stafeyev, "Large area magnetodiodes," *Soviet Phys. Solid State*, vol. 3, pp. 1476-1482; January, 1962.
- [12] I. Melngailis and R. H. Rediker, "Negative resistance InSb diodes with large magnetic-field effects," *J. Appl. Phys.*, vol. 33, pp. 1892-93; May, 1962.
- [13] R. N. Zitter, A. J. Strauss and A. E. Attard, "Recombination processes in p -type indium antimonide," *Phys. Rev.*, vol. 115, pp. 266-273; July 15, 1959.
- [14] R. A. Laff and H. Y. Fan, "Carrier lifetime in indium antimonide," *Phys. Rev.*, vol. 121, pp. 53-62; January, 1961.
- [15] V. I. Stafeyev, "Modulation of diffusion length as a new principle of operation of semiconductor devices," *Soviet Phys. Solid State*, vol. 1, pp. 763-768; December, 1959.
- [16] I. Melngailis, A. R. Calawa and R. H. Rediker, "Magnetodiode effects in InSb," *Bull. Phys. Soc.*, vol. 7, p. 88; January, 1962.

Design and Performance of a Broad-Band FM Demodulator with Frequency Compression*

C. L. RUTHROFF†, MEMBER, IRE, AND W. F. BODTMANN‡

Summary—This paper contains a discussion of several major problem areas concerning the design, construction, systems application and threshold improving properties of the Frequency Compression Demodulator.

A complete description of an experimental broad-band demodulator is presented. This demodulator is intended for use in an intercontinental satellite communication system and is suitable for either television or telephone service.

Circuit details, performance data, and a measured comparison with FM are presented.

I. INTRODUCTION

THE WORK described in this paper has been motivated by the attractive possibilities of high quality broad-band communications via orbiting satellites, either active or passive. Considering the large expense involved in orbiting a satellite as well as other factors such as reliability and long life it is not difficult to grasp the importance of reducing the amount of RF power radiated by the satellite. The Frequency Compression Demodulator (FCD) makes a power reduction possible by its improved operating threshold relative to conventional FM receivers.

The first application of negative feedback to an FM receiver was made by Chaffee.¹ Chaffee made a careful experimental study of many of the properties of the demodulator and he and Carson² evolved a theory describing the performance above the threshold region.

A frequency compression demodulator was used in the NASA Project Echo satellite communications experiment.³ That experiment afforded the first well-documented experimental evidence that the threshold of an FM receiver can indeed be improved by the use of negative feedback.

The equations describing the operation of the FCD in the threshold region are nonlinear and have yielded no exact solution to date. This fact and the fact that threshold phenomena are basically subjective and difficult to describe mathematically make the theoretical approach very difficult. In spite of these difficulties Enloe⁴ has presented a theory which predicts the

threshold in terms of the noise bandwidth of the demodulator. Measurements on several demodulator configurations including the one described here are in excellent agreement with his theory.

In this paper a broad-band FCD is described in detail. The initial design was directed toward a satellite communications system capable of acceptable television transmission or several dozen telephone channels. The baseband bandwidth⁵ was chosen to be 1 Mc. This is the minimum bandwidth required to meet the initial television objective and is small enough that excessive transmitted power or ground station antenna size is not required.

II. DISCUSSION OF THRESHOLD EFFECTS

It is customary to describe the behavior of an FM receiver in the threshold region by curves such as shown in Fig. 1. These curves show the relationship between the input Carrier-to-Noise power ratio, CNR, at RF to the baseband output Signal-to-Noise power ratio, SNR. Above the point marked "FM Threshold" the relationship is linear and is described by the expression

$$S/N_0 = 3M^2C/N_i \quad (1)$$

where,

S = Signal power output for sine wave signal

N_0 = Noise power output in baseband

C = Carrier power input at RF

N_i = Noise power input at RF in a band equal to twice the baseband

FM Modulation Index M

$$= \frac{\text{Peak sine wave deviation in cps}}{\text{Baseband bandwidth in cps}}$$

Below the point marked "FM Threshold" the curve departs from linearity. While the rms S/N_0 are as shown, the subjective effects of this threshold are not described accurately by this curve.

The threshold in an FM receiver is caused by the noise peaks exceeding the carrier amplitude at the input to the frequency detector. Each time a noise peak exceeds the carrier amplitude an impulse in frequency

* Received June 12, 1962; revised manuscript received September 26, 1962.

† Bell Telephone Laboratories, Inc., Holmdel, N. J.

¹ J. G. Chaffee, "Application of negative feedback to frequency modulation systems," *Bell Sys. Tech. J.*, vol. 18, pp. 404-437; July, 1939.

² J. R. Carson, "Frequency modulation—theory of the feedback receiving circuit," *Bell Sys. Tech. J.*, vol. 18, pp. 395-403; July, 1939.

³ C. L. Ruthroff, "FM demodulators with negative feedback," *Bell Sys. Tech. J.*, vol. 40, pp. 1149-1156; July, 1961.

⁴ L. H. Enloe, "Decreasing the threshold in FM by frequency feedback," *Proc. IRE*, vol. 50, pp. 18-30; January, 1962.

⁵ The baseband bandwidth corresponds to the 3-dB bandwidth of the open-loop amplitude response. The feedback is within 3 dB of a constant value over this band.^{1,2,4}

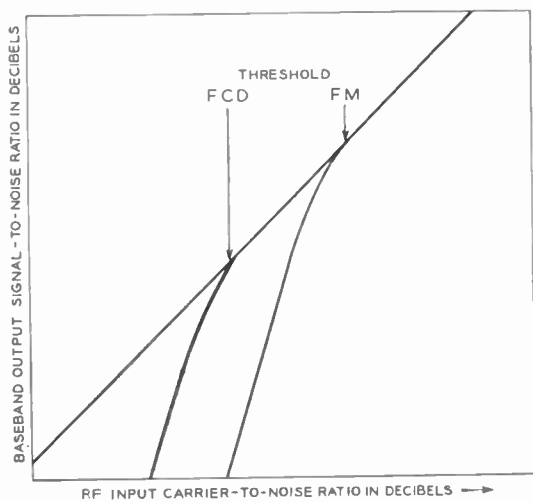


Fig. 1—Threshold curves.

occurs.^{6,7} The frequency detector converts this into an impulse in amplitude and the receiver output is the response of the output filter to the impulse. The contribution of these impulses to the output rms noise power is described by Fig. 1. Because the noise appears as a random sequence of impulses the subjective effect depends upon the nature of the signals being received. For example, if the application is a single audio channel the impulses occur as sharp pops to the ear. These pops are very disturbing and subjectively the circuit degrades much more rapidly than indicated by Fig. 1. There is a similar effect in a television picture. Each impulse appears as a black or white spot on a scanning line, the length of the spot being determined by the impulse response of the output filter. For the single audio or video channel then, operation at CNR's below the threshold is generally unsatisfactory even though Fig. 1 may show a respectable output SNR.

A third application is that of multiplexing many audio channels on one carrier by frequency division. For such a signal, the energy in each noise impulse is shared by all of the channels and no distinct pops are heard. By invoking the central limit theorem it can be seen that the noise in each channel tends to become Gaussian and Fig. 1 applies with reasonable accuracy.

In all of these applications the behavior of the receiver is adequately described by the curve above the point marked "FM Threshold." The improvement in threshold afforded by the FCD consists of extending the linear behavior to a lower CNR as shown in Fig. 1. When this demodulator is used, the effects described above begin in the region marked "FCD Threshold." Above this point the demodulator behavior is described by (1). The difference, in decibels, between the points

marked "FM Threshold" and "FCD Threshold" is the threshold improvement. An objective of the demodulator design is to maximize the threshold improvement.

III. FREQUENCY COMPRESSION DEMODULATOR—GENERAL DESCRIPTION

A simplified block diagram of the demodulator is shown in Fig. 2. It contains all of the components necessary in a conventional FM receiver and, in addition, the output is connected to the voltage-controlled local oscillator (VCO) to complete the negative feedback connection. The phase of the feedback is such that the VCO frequency tends to follow the frequency of the input signal thereby reducing the FM modulation index in the mixer output. The result is a reduction of the modulation index of the IF signal relative to the index of the RF signal and is, of course, negative feedback. If the RF index is M , the IF index is M/F , where F is the feedback factor. Since the IF index is small, the IF noise bandwidth can be made smaller than the RF bandwidth and an improvement in threshold can be expected relative to the threshold obtained using conventional FM in the same RF bandwidth. As Enloe has shown the threshold depends upon the closed-loop bandwidth which is, of course, related to the IF bandwidth.

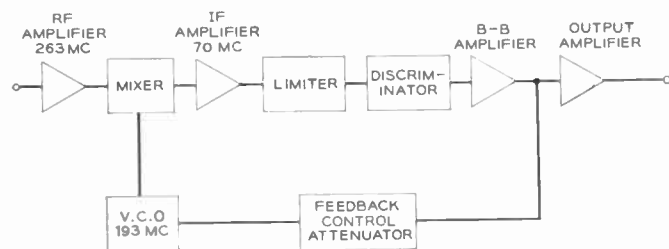


Fig. 2—Block diagram: Frequency Compression Demodulator.

The large number of components in the feedback loop makes the feedback design difficult, especially when the desired baseband bandwidth is quite large. Also in this design there are two restrictions not normally found in feedback design. Superposition does not hold in the intermediate frequency circuits and, as Enloe has shown,⁴ the allowable IF filter responses are severely limited. In addition, the threshold depends upon the closed-loop bandwidth of the circuit. Therefore, we not only want large feedback but we want it with a small closed-loop bandwidth. This is discussed in more detail in a later section.

The approach for the present design calls for a single-pole filter in the IF amplifier and a single pole in the baseband amplifier. All other components are made as broad-band as possible to minimize delay or non-minimum phase shift. Any nonminimum phase shift increases the closed-loop bandwidth and decreases the threshold improvement. There is a simple lead network in the baseband amplifier to obtain some phase correction.

⁶ G. Granlund, "Interference in Frequency Modulation Reception, M.I.T. Res. Lab. of Electronics, Cambridge, Mass., R. L. E. Rept. no. 42; January 20, 1949.

⁷ S. O. Rice, "Properties of a sine wave plus random noise," *Bell Sys. Tech. J.*, vol. 27, pp. 109-157; January, 1948.

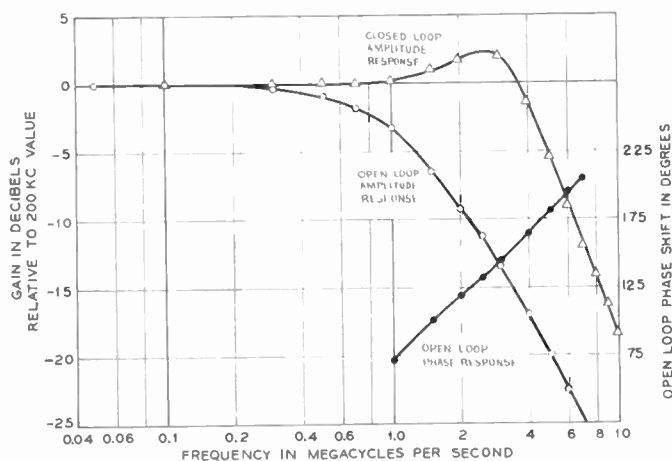


Fig. 3—Amplitude and phase responses of FCD.

IV. EXPERIMENTAL RESULTS

A. Feedback Conditions

As discussed in Section I the baseband bandwidth was chosen to be 1 Mc. It is desirable to have full feedback over the whole baseband, otherwise the IF spectrum will have large components at high frequencies and the distortion will be large. Therefore, the open-loop amplitude response is adjusted to be 3 db down at 1 Mc relative to the response at 50 kc. The single-pole IF filter is 3 db down at ± 1.75 Mc. The open-loop amplitude response consists of the responses of the IF filter, the baseband lead network, and a single-pole filter in the baseband amplifier. The baseband filter has a 3-db bandwidth of about 1.36 Mc giving the measured open-loop amplitude response of Fig. 3. The open-loop phase shift is the sum of the minimum phase shift corresponding to the amplitude response plus a delay term. The delay term describes the phase shift of all the other components in the feedback loop. These include the VCO, Mixer, Limiter, and Discriminator, all of which have been designed to be broad-band, and hence contribute very little to the amplitude response. The equivalent delay is about 38 nsec. The open-loop phase response is also given in Fig. 3. Shown also is the measured closed-loop amplitude response for 12 db of feedback. The baseband measurements were made with low-level sinusoidal signals. The open-loop responses were measured from the VCO input to the baseband amplifier output with a 263-Mc carrier input at normal level into the RF amplifier. The closed-loop amplitude response was measured from the baseband input to an FM transmitter (not shown) to the output of the baseband amplifier. The amplitude responses can also be measured by adding broad-band noise to the carrier at the input to the RF amplifier and measuring the power spectra at the baseband amplifier output with the loop closed or open. This type of measurement gives results identical to those of Fig. 3. The closed loop noise bandwidth, determined by graphically integrating the closed-loop amplitude response of Fig. 3, is approximately 6.7 Mc.

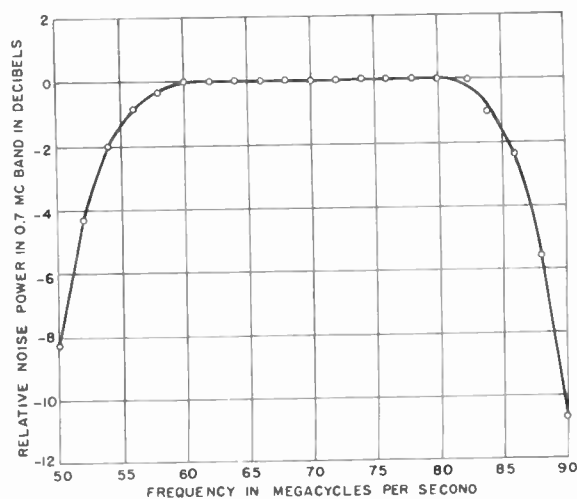


Fig. 4—Power spectrum of IF noise generator.

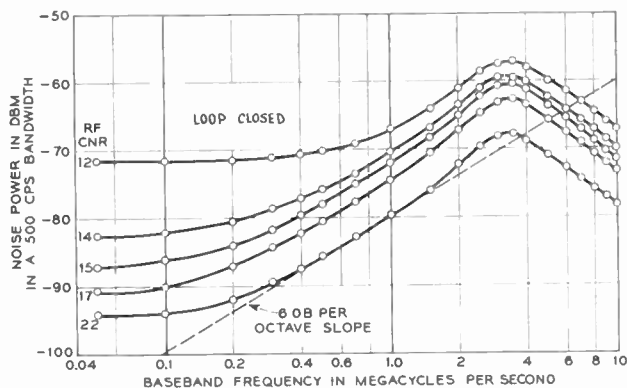


Fig. 5—Baseband output power spectra vs input CNR.

B. Threshold Performance

All threshold measurements were made using a noise generator consisting of two high-gain broad-band IF amplifiers in tandem. Care was taken to insure that the noise peaks were not clipped. The output spectrum of the noise generator is shown in Fig. 4 and is substantially flat over a 20-Mc band.

In all of the threshold measurements the input CNR is referred to a 2-Mc bandwidth. This bandwidth was chosen arbitrarily and is equal to the corresponding double sideband AM bandwidth. The input CNR is measured in all instances at the input to the RF amplifier.

1. Output Noise Density: Fig. 5 is a family of measured output noise spectra plotted for various input CNR as a function of baseband frequency. The loop was closed for this measurement. A 6 db-per-octave slope has been added for convenience. In a conventional FM receiver the output at the higher frequencies would follow the dashed line which represents the well-known "triangular" spectrum. The rising character of the spectra near 3 Mc is due to the closed-loop amplitude response; in fact, the closed-loop amplitude response can be obtained by adding a negative slope of 6 db per octave to the spectrum of Fig. 5 for a CNR = 22 db.

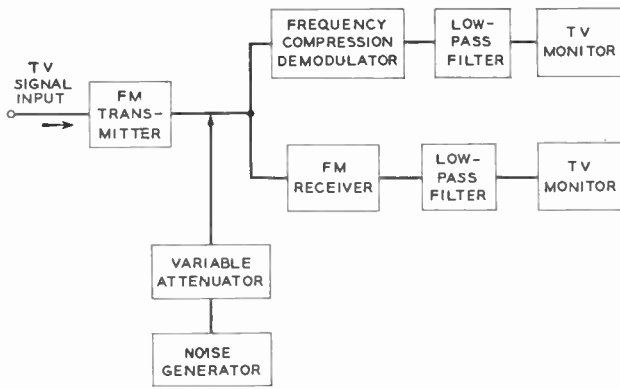


Fig. 6—Threshold comparison circuit.

In addition to the response at higher frequencies which is determined by the closed-loop amplitude response, the noise density at the lower frequencies departs substantially from that of a "triangular" spectrum. This phenomenon also occurs in conventional FM. It is caused by the noise impulses described in Section II. The impulses occur at random and have a flat amplitude spectrum which fills in the noise spectrum at the lower frequencies. As the CNR is decreased in the threshold region the number of impulses increases rapidly and the spectrum tends to fill in more quickly. Inspection of Fig. 5 indicates that this effect begins to be substantial when the CNR in the 2-Mc band is near 14 db. This can be interpreted as the beginning of the threshold region as described in connection with Fig. 1. This number should be compared with the threshold measurements on a television signal, described in the next section.

2. Television Comparison Experiment: In order to demonstrate conclusively that this demodulator has an improved threshold behavior for television relative to that of conventional FM, a comparison circuit, shown in Fig. 6, was set up which compares the performance of conventional FM and the FCD when demodulating the same input signal. In this experiment, a band-limited television signal is frequency modulated with a peak deviation of 9 Mc. Wide-band noise is added to this signal from the generator of Fig. 4. A conventional FM receiver and the FCD each demodulate this signal and the outputs are displayed on identical television monitors.

The input television signal was passed through a maximally flat envelope delay two-pole low-pass filter with a response 3 db down at 2 Mc. The two output baseband filters are identical maximally flat envelope delay two-pole low-pass filters whose response is down 3 db at 1 Mc. The IF filter in the FM receiver is a double-tuned bandpass filter centered at 70 Mc with a 3-db bandwidth of 18 Mc;⁸ the measured response of which is shown in Fig. 7.

⁸ The choice of filter shape and bandwidth is a matter of judgment. The configuration used is believed to be a reasonable compromise between threshold and distortion performance.

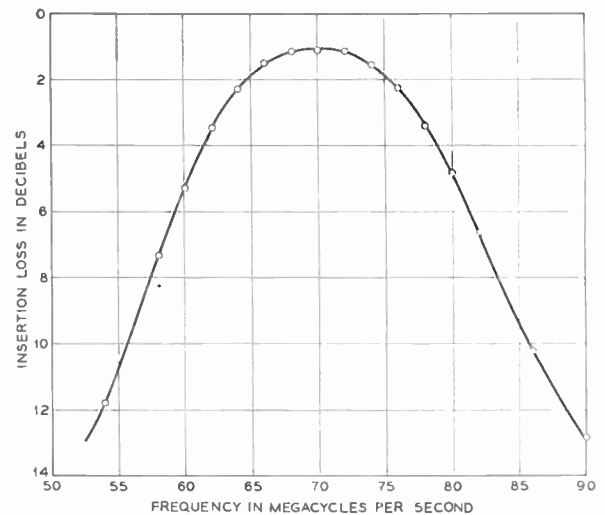


Fig. 7—Measured input amplitude response of FM receiver.

The experiment was arranged so that any desired CNR could be set up by adjusting a single attenuator and the television monitors examined for threshold effect.

The photographs of Figs. 8 and 9 were made for various CNR's and show the nature of the threshold. The exposure time covers two frames which accounts for the slight blurring of the motion in Fig. 9. The signal for Fig. 9 was taken off the air while that for Fig. 8 was taken from a pattern generator with no interlace.

For large CNR's the pictures are identical as indicated by the pictures labelled $C/N = \infty$. For the frames labelled $C/N = 19$ db and $C/N = 20$ db, an appreciable number of impulses appear on the pictures from the conventional receiver while there are no impulses on the picture from the FCD. For a $C/N = 14$ db the picture from the conventional receiver is severely degraded while the picture from the FCD is beginning to show impulses. The threshold improvement of the FCD is seen to be about 5–6 db.

It is of interest to note that the threshold of the FM receiver is beginning at a $C/N \approx 19$ db in a 2-Mc band. This is a $C/N \approx 10$ db in the filter bandwidth of 18 Mc which demonstrates that the FM receiver is working properly.

3. Distortion Measurements and Multiplex Performance: In order to describe the performance of the receiver for use with telephone multiplex signals it is necessary to have a measure of signal-to-distortion as well as signal-to-noise ratios. Some preliminary distortion measurements have been made and are presented in Fig. 10. For these measurements the telephone multiplex signal is simulated by a band of random noise. The power spectrum of the noise generator used for this signal is depicted in Fig. 11. The noise generator is arranged to modulate the FM transmitter with a prescribed rms frequency deviation. The demodulator output power in a 500-cycle band centered at 1 Mc is meas-

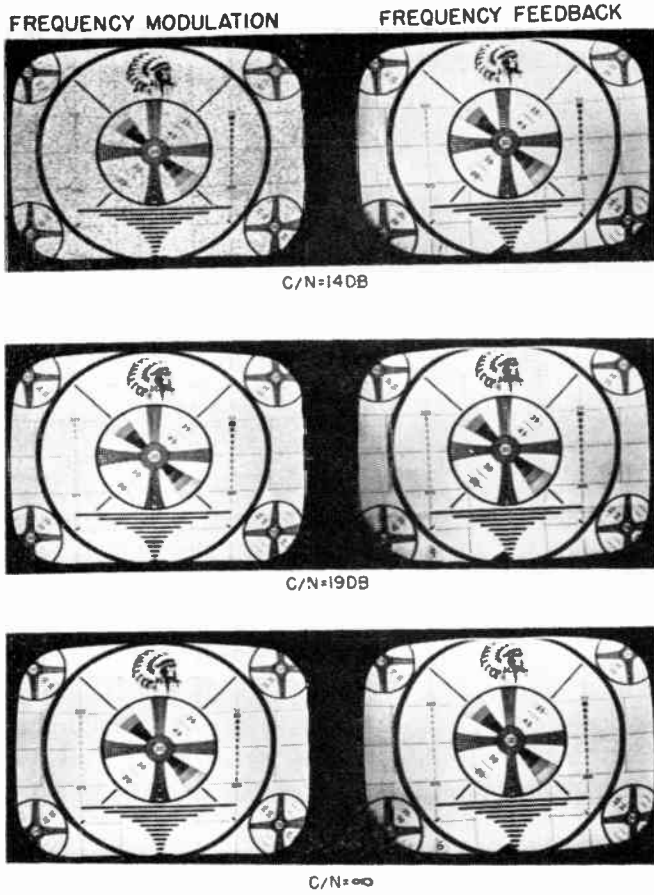


Fig. 8—Television comparison experiment—test pattern.

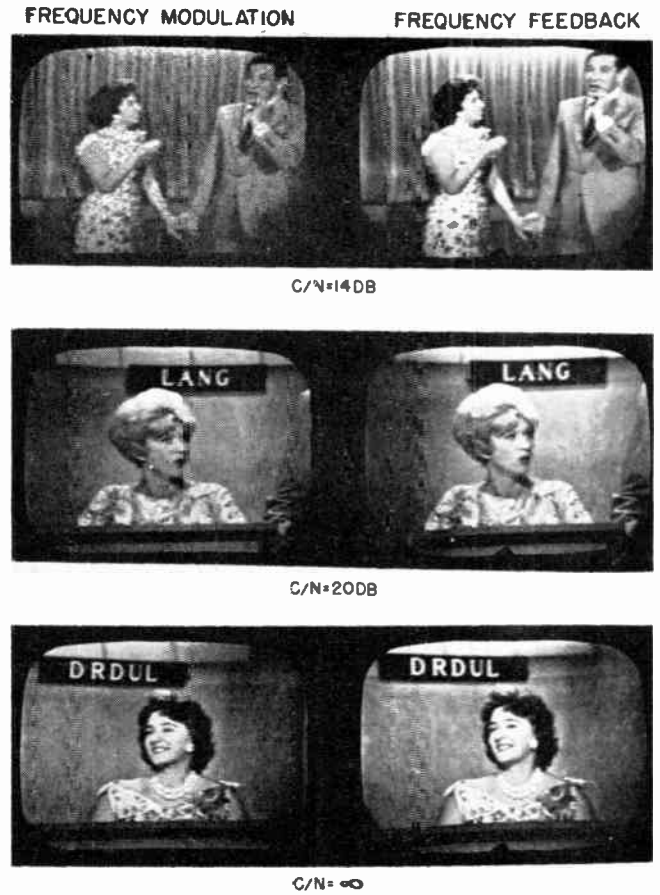


Fig. 9—Television comparison experiment—off-the-air.

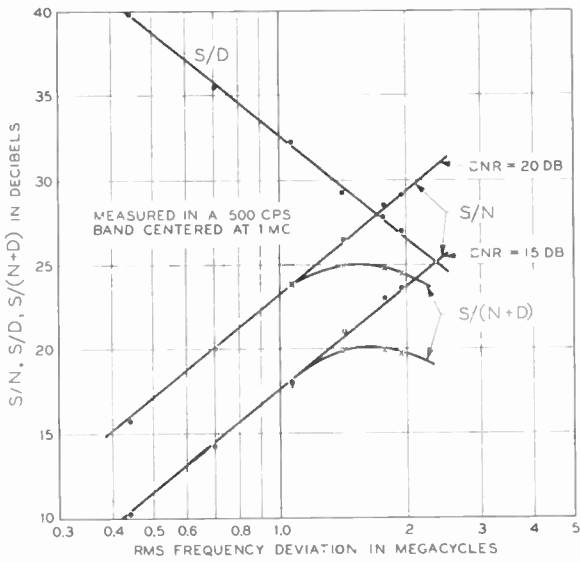


Fig. 10—Measured S/N and S/D performance.

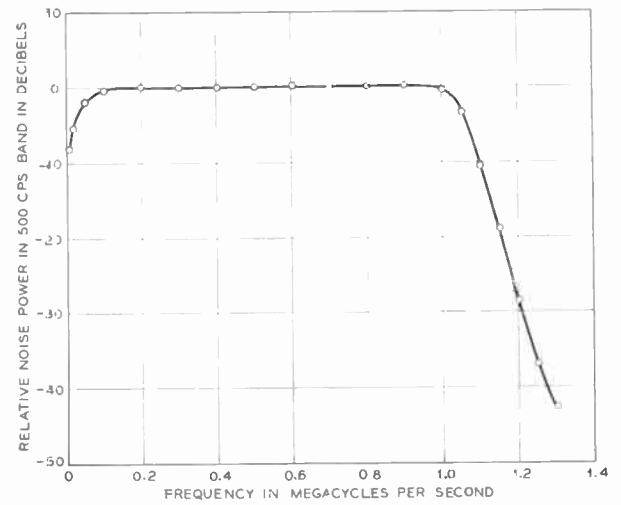


Fig. 11—Power spectrum of baseband noise generator.

ured. This power is denoted signal power or S . Then a narrow-band rejection filter is placed between the noise generator and the FM generator. This filter removes the input power in the region of 1 Mc. Another power measurement which consists of distortion and noise power is made in the demodulator output, and is denoted $N+D$. When the baseband noise generator is disconnected completely from the FM transmitter a measurement of noise power N is made. The data of Fig. 10 was taken in this manner.

For a CNR of 20 db the distortion and noise contributions add approximately on a power basis. This is not true for a CNR of 15 db because for a CNR of 15 db the noise power contributes substantially to the total deviation. The abscissa of Fig. 10 indicates only that part of the total deviation due to signal whereas the total distortion power is a function of the total deviation. The total noise and distortion power should be, and is, greater than the sum of the noise and distortion products obtained by measuring them separately. It should be noted that a similar result is also true for a conventional FM receiver operating in the threshold region.

Another item of interest in connection with Fig. 10 is that the S/D curve slants downward at 6 db per octave indicating that the distortion is predominantly second order. Since simple theory predicts third-order distortion the existing second-order distortion is not believed inherent in the demodulation process. The second-order distortion has been traced to the nonlinear frequency-voltage characteristic of the VCO, which has nonlinearity consistent with the measured distortion. This result implies that the use of a more linear VCO will result in substantially improved performance with respect to signal-to-distortion performance. Work presently in progress is aimed at reducing the distortion in the VCO and improving the demodulator performance.

Although the results presented in Fig. 10 must be regarded as preliminary, it is still of interest to ask what performance is to be expected in an application involving a single-sideband telephone multiplex signal. Using the data of Fig. 10 and noting that pre-emphasis will improve the noise performance of the top channel by approximately 4 db, the demodulator will handle 240 channels with zero-level noise of 41 dba⁹ in the top channel at a CNR = 15 db.

V. CIRCUIT DESCRIPTION

The circuit of the voltage-controlled oscillator (VCO) is shown in Fig. 12. The center frequency is 193 Mc and the modulation is applied to the varactor diodes D_1

and D_2 . DC is applied to provide a suitable bias for the varactors and to provide a frequency adjustment. The sensitivity of the VCO is about 30 Mc/volt so care has been taken to provide a stable bias voltage, hence the reference diode.

The open-loop gain of the receiver is directly proportional to the VCO sensitivity. For this reason it is desirable to operate the varactors near zero bias where maximum sensitivity is obtained. Two factors which operate against this requirement are, 1) the Q of the varactors and 2) the amplitude of the RF voltage appearing across the varactors:

- 1) Diffused silicon varactors have excellent Q near zero bias and in this instance a bias of 0.3 v dc was selected.
- 2) The amplitude of the RF voltage across the varactors must be small enough so that the diodes do not conduct in the forward direction. The power output of the VCO is thereby limited, and because this power drives the mixer it affects the loop gain.

A compromise between these conflicting factors was made by operating at a low dc bias and including a single broad-band gain stage between the VCO and mixer. The gain stage also acts as a buffer and supplies about 5 cw to drive the mixer. The gain is 6 db and the bandwidth greater than 200 Mc.

The network in series with the input serves the dual purpose of preventing excessive loading on the oscillator tank circuit by the input source, and of shaping the phase response of the input circuit. The second function is of particular importance since the VCO is in the feedback loop. An equivalent circuit for baseband frequencies is shown in Fig. 13. The capacitor C represents the parallel combination of varactors D_1 and D_2 , and is a part of the oscillator tank circuit. The value of the resistor $R=180\Omega$ was chosen as the minimum value required to prevent excessive tank circuit loading by the input circuit. The inductance L was chosen to minimize the envelope delay at baseband. The delay at zero frequency is 2.66 nsec with L as shown. With L omitted the delay is 9.05 nsec.

The 1-pf capacitor in the input lead (Fig. 12) resonates with the $0.78 \mu\text{h}$ inductor at 193 Mc. Finally, with the element values shown, the Q is low enough so that no serious amplitude modulation results when the VCO frequency is swept over a 20-Mc band.

The VCO drives the amplifier and mixer of Fig. 14. A balanced mixer is used and every effort was made to make it broad-band to minimize the effect of its delay on the feedback loop. Transformers T1 and T2 are broad-band devices of a type previously described.¹⁰

The output transformer T3 is single-tuned with the turns ratio adjusted to match the input of the IF amplifier. It has a $Q \approx 1$.

⁹ For a discussion of dba see A. J. Aikens and D. A. Lewinski, "Evaluation of message circuit noise," *Bell. Sys. Tech. J.*, vol. 39, pp. 879-909; July, 1960.

¹⁰ C. L. Ruthroff, "Some broad-band transformers," *PROC. IRE*, vol. 47, pp. 1337-1342; Aug., 1959.

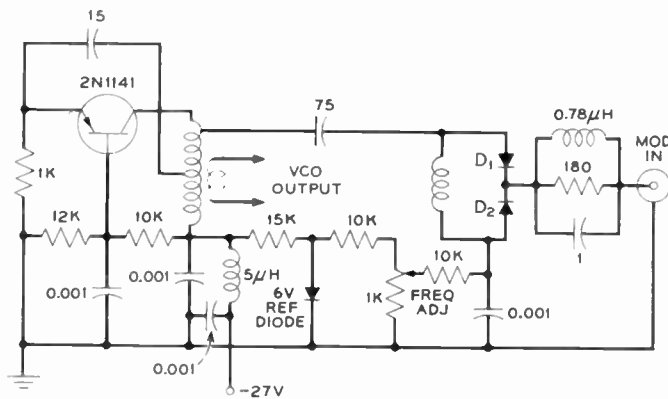
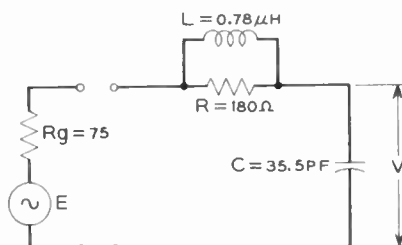


Fig. 12—VCO schematic.



$$\frac{V}{E} = \frac{Q + j\gamma}{Q - \left(\frac{R+Rg}{Rg}\right)\gamma^2 + j(1+Q)\gamma}$$

$$\gamma = \frac{\omega}{\omega_0}$$

$$\omega_0 = \frac{1}{RgC}$$

$$Q = \frac{R}{\omega_0 L}$$

Fig. 13—VCO: baseband equivalent input circuit

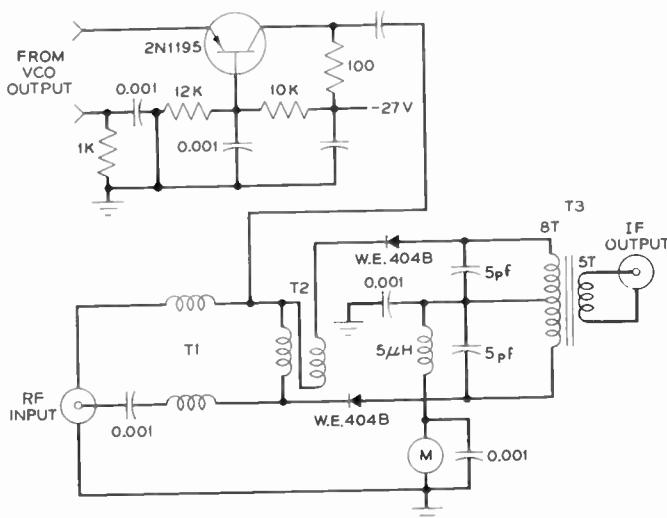


Fig. 14—Mixer schematic.

The circuit schematic for the IF amplifier, limiter, and discriminator is shown in Fig. 15. The IF amplifier has a single-pole resonant circuit on the collector side of transistor Q_1 . The center frequency is 70 Mc and the 3-db bandwidth 3.5 Mc.

The purpose of the limiter is to reduce the amplitude modulation present in the signal at the output of the IF amplifier. This particular limiter¹¹ was selected because of its excellent limiting efficiency; approximately 30 db of effective amplitude-modulation suppression is obtained with an insertion loss of 8 db in a single stage. This performance is obtained with a low impedance level which results in a broad bandwidth and small delay.

The amplifier following the limiter raises the limiter output level to a value suitable for driving the discriminator. The gain is about 11 db and the bandwidth in excess of 250 Mc. An amplifier of this type is described in another article by Ruthroff & Bodtmann;¹² the transformers T4 are described elsewhere by Ruthroff, Fig. 3.¹⁰

The discriminator is a conventional balanced type with one diode reversed to provide a single-ended output. The circuit has been made as broad as possible, consistent with reasonable gain, to reduce loop delay. The tuned circuits resonate at 50.8 and 96.4 Mc respectively and have a loaded $Q=3$.

Care must be taken to reduce the phase shift in the discriminator output circuit. This requirement conflicts with the necessity of reducing the IF carrier amplitude to prevent overloading the baseband amplifier. In the present design, the solution was to insert the 2250-pf capacitor across the output as shown in Fig. 15. The capacitor reduces the IF carrier amplitude to a manageable value and also forms a part of the single-pole baseband filter.

The baseband amplifier schematic is given in Fig. 16. The transistors are experimental types having alpha cutoff frequencies above 2000 Mc. Several functions are performed by this amplifier.

- 1) It supplies broad-band, low delay gain in the feedback loop.
- 2) Low-frequency shaping is accomplished by making all series-coupling capacitors very large except one which is 4 μf. This insures a slow roll-off at low frequencies and satisfies the stability criterion.
- 3) A lead network is included in the first interstage for phase correction.
- 4) A 140-Mc trap is included to reduce the second harmonic of the IF frequency and prevent overloading of the amplifier.

¹¹ C. L. Ruthroff, "Amplitude modulation suppression in FM systems," *Bell Sys. Tech. J.*, vol. 37, pp. 1023-1046; July, 1958.

¹² W. F. Bodtmann and C. L. Ruthroff, "A wide band transistor IF amplifier for space and terrestrial repeaters using grounded base transformer-coupled stages," to be published.

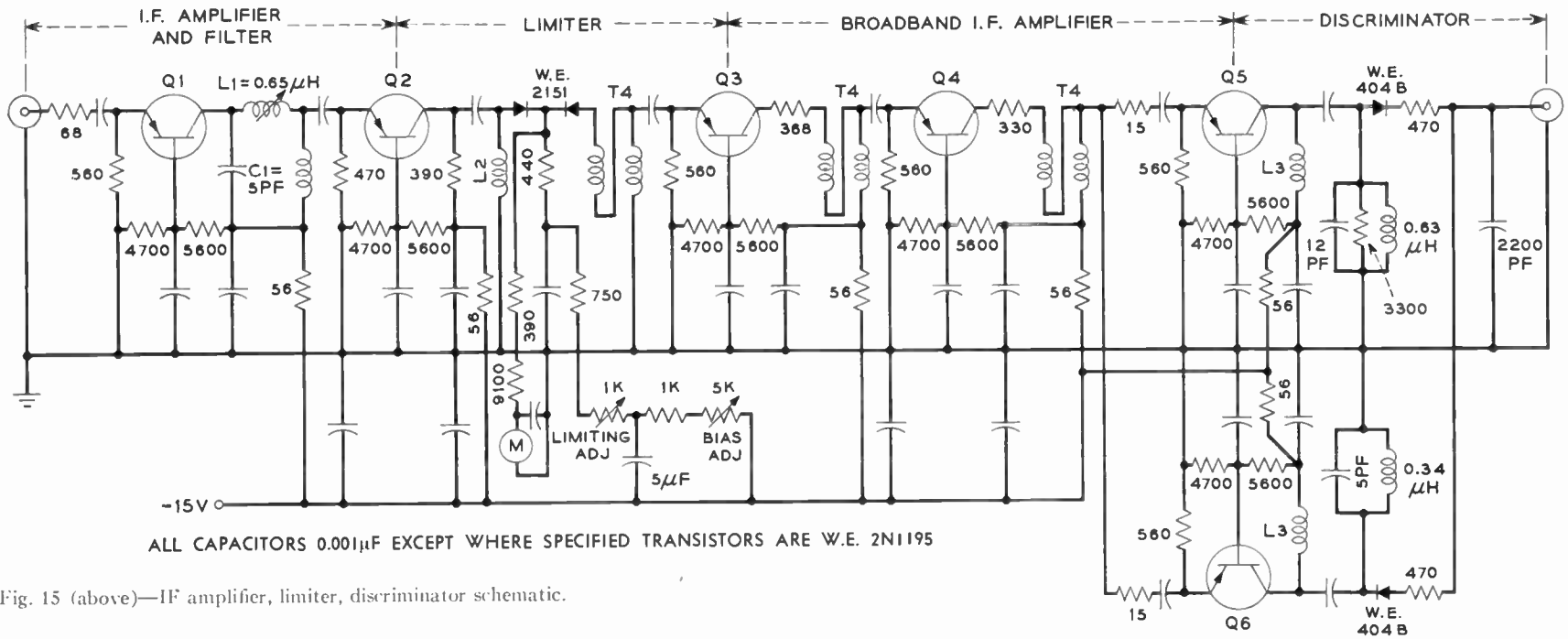
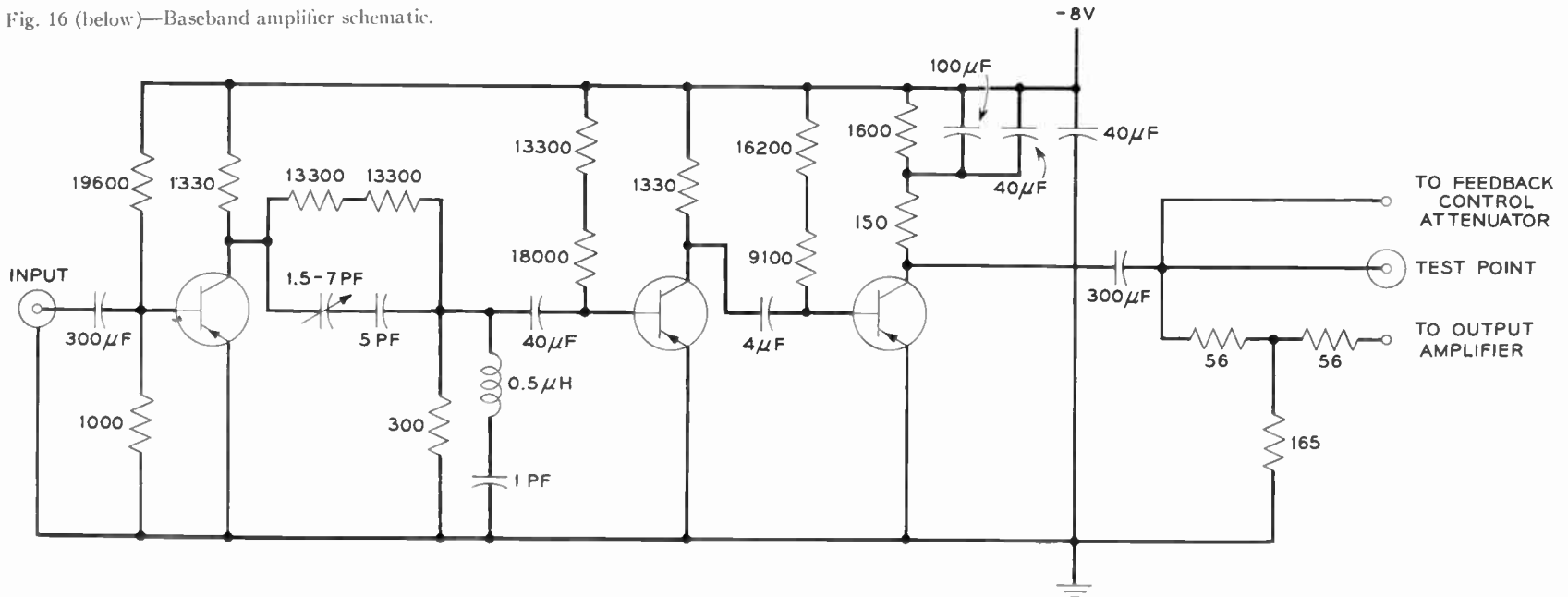


Fig. 15 (above)—IF amplifier, limiter, discriminator schematic.

Fig. 16 (below)—Baseband amplifier schematic.



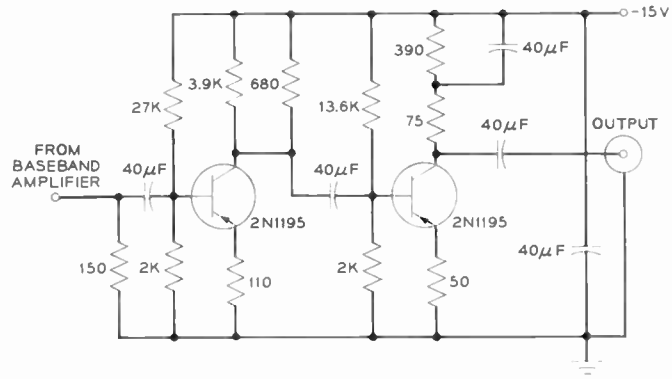
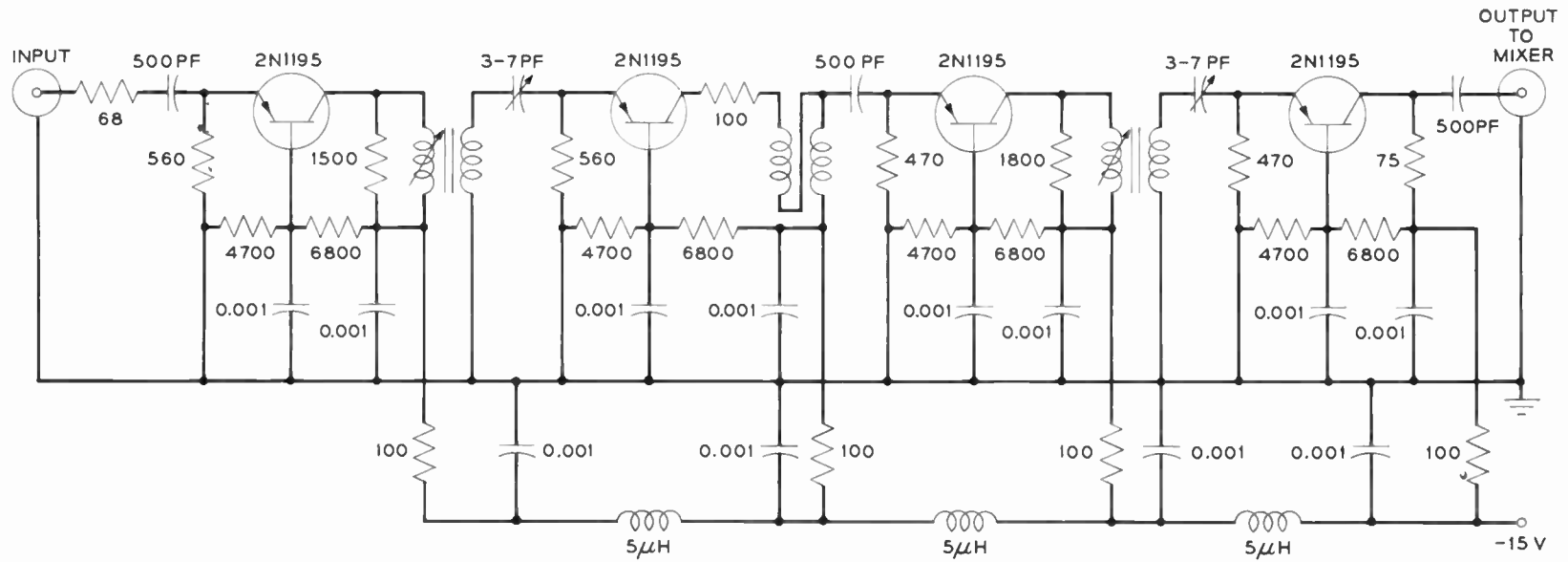


Fig. 17 (above)—Output amplifier schematic.

Fig. 18 (below)—RF amplifier schematic.



The final component in the feedback loop is the feedback control attenuator. This is a specially designed unit which has a total physical length between input and output of one inch. It contributes negligible delay to the loop and is used to change the feedback in fixed steps.

An output amplifier is provided to isolate the feedback loop from the load and to raise the baseband output signal to a suitable level. The schematic is shown in Fig. 17.

The principal function of the RF amplifier (Fig. 18) is to reject the noise power at the image frequency. This is accomplished by two double-tuned stages separated by a broad-band interstage. The broad-band stage increases the stability of the amplifier. The amplitude response is flat to ± 0.25 db over a 20-Mc band centered at 263 Mc. The input impedance is 75Ω .

SUMMARY AND CONCLUSIONS

The Frequency Compression Demodulator which has been described has a measured threshold improvement relative to a conventional FM demodulator of about 5-6 db. The threshold occurs when the RF carrier-to-

noise power ratio is 14 db in a 2-Mc band. Intended for use in a satellite communications system, the FCD is capable of handling a television picture of the quality indicated in Figs. 8 and 9, or alternatively, a telephone multiplex signal with a maximum of about 240 telephone circuits.

Insofar as broad-band applications are concerned, the major stumbling block in the way of getting further threshold improvement, or extending the baseband bandwidth, is the delay around the feedback loop. The many types of components in the feedback loop contribute to this delay and make the design difficult for large feedback. Considerable effort will need be made on all components in order to realize demodulators with baseband bandwidths of 5 or 10 Mc. The deleterious effect of the loop delay can be emphasized by noting that if the only phase shift were the minimum phase associated with the open-loop amplitude response of Fig. 3, a further improvement in threshold of about 2 db would be realized in the present demodulator.

In a real way, then, the performance is limited by the skill of the designers and the state of the art of the various components in the feedback loop.

A Solid-State Display Device*

STEPHEN YANDO†

Summary—A solid-state display device based on a new principle is described. The device consists of a thin, flat panel of piezoelectric material supporting an electroluminescent layer. Voltage pulses, applied to a few electrodes on the periphery of the panel, introduce traveling elastic waves into the piezoelectric material. Electric fields which accompany the waves interact with the electroluminescent layer to produce a localized "spot" of illumination. The position of the spot is controlled by varying the relative timing of the pulses to produce either a raster or an oscilloscope pattern. Means for continuously modulating the light intensity of the spot are also described.

INTRODUCTION

WITH THE ADVENT of electroluminescent (EL) layers as simple area sources of light came the expectation that a thin-panel solid-state replacement for the cathode ray tube might eventually be devised. For this to be realized some suitable means had to be found for creating localized and controllable electric fields in the plane of an electroluminescent

phosphor layer. Various means have been proposed for subdividing EL phosphor layers into elementary areas and for exciting them sequentially.^{1,2} As the number of display elements increases, such methods become increasingly difficult to carry out because they result in intricate and costly structures as well as complex electronic drive apparatus. This limits the application of these devices to a few specialized areas. To compete effectively with the cathode ray tube in most applications, a solid-state display must be simple in structure and must be operable with relatively simple electronic drive circuitry.

A new solid-state display device of low structural complexity has been made by combining certain unique properties of piezoelectric and electroluminescent materials. When elastic impulses are propagated across a thin panel of piezoelectric material, localized electric

* Received December 14, 1961; revised manuscript received August 22, 1962.

† General Telephone and Electronics Laboratories, Inc., Bayside, N. Y.

¹ J. A. Rajchman, G. R. Briggs, and A. W. Lo, "Transfluxor controlled electroluminescent display panels," *Proc. IRE*, vol. 46, pp. 1808-1824; November, 1958.

² E. A. Sack, "ELF—a new electroluminescent display," *Proc. IRE*, vol. 46, pp. 1694-1699; October, 1958.

fields are produced on the panel surface through the direct piezoelectric effect. These fields interact with an EL phosphor layer in contact with the piezoelectric surface to produce light. The configuration and size of the lighted area can be controlled by the mode of application and relative timing of input voltages applied to a few electrodes along the panel boundary.

SOME PROPERTIES OF PIEZOELECTRIC CERAMICS

Lead zirconate-titanate is a ceramic material that can be polarized and rendered piezoelectric. It can be used in the display panel because, in addition to its strong piezoelectric behavior, it can be obtained readily in a variety of shapes and sizes. Before the principles of the display device are discussed, some properties of piezoelectric ceramics will be reviewed.

In general, polycrystalline ferroelectric materials such as lead zirconate-titanate become permanently polarized when subjected to strong electric fields at elevated temperatures. In this state the material becomes anisotropic in its physical and electrical properties and exhibits strong piezoelectric behavior. To describe the electromechanical properties, a convention has been adopted for piezoelectric materials consisting of a right-handed coordinate system whose axes are designated 1, 2 and 3 where the 3 direction represents the direction of the polarizing field.

When the polarized ceramic material of Fig. 1(a) is subjected to a positive electric field, *i.e.*, the same polarity as the original polarizing field, as in Fig. 1(b), a positive strain or extension results in the 3 direction and a negative strain results in the transverse 1 and 2 directions. The magnitudes of these strains are given by the piezoelectric coefficients d_{33} , d_{31} and d_{32} , respectively. By virtue of the symmetry of this effect, a negative field produces the opposite strains shown in Fig. 1(c).

Like all true piezoelectric materials, polarized lead zirconate-titanate also possesses the direct piezoelectric effect. When a positive or tensile stress is applied in the 3 direction, a positive field is developed in the same direction. A positive field in the 3 direction is also obtained when a negative or compressive stress is applied in the 1 or 2 direction. The magnitudes of these fields per unit applied stress are defined by the piezoelectric coefficients g_{33} , g_{31} and g_{32} respectively.

SURFACE FIELDS IN A PIEZOELECTRIC STRIP

The piezoelectric properties of polarized ceramic are utilized as shown in Fig. 2 to produce a localized electric field on the surface of the ceramic strip. The structure illustrated in Fig. 2 is a flat, thin polarized ceramic strip with a metallic ground-plane electrode covering the entire back side and an input electrode near the lower edge on the front side. The upper and lower edges of the ceramic are joined to a suitable absorbing material such as lead which rapidly attenuates any incident elastic waves. This structure functions as a terminated electromechanical transmission line in which an elec-

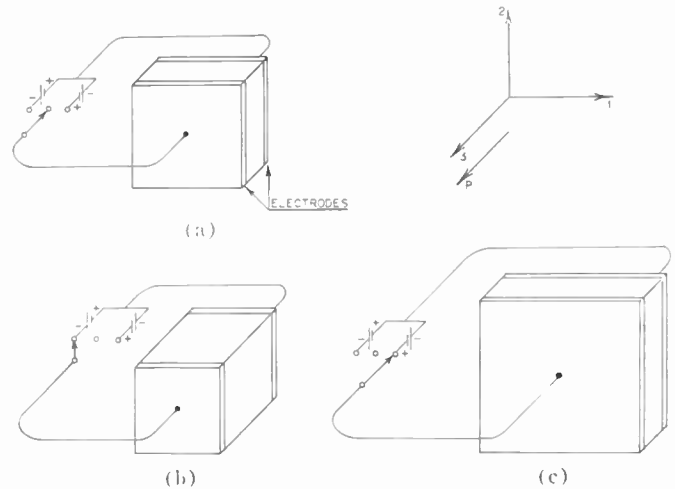


Fig. 1—Mechanical response of polarized lead zirconate-lead titanate to applied fields parallel to the direction of polarization.

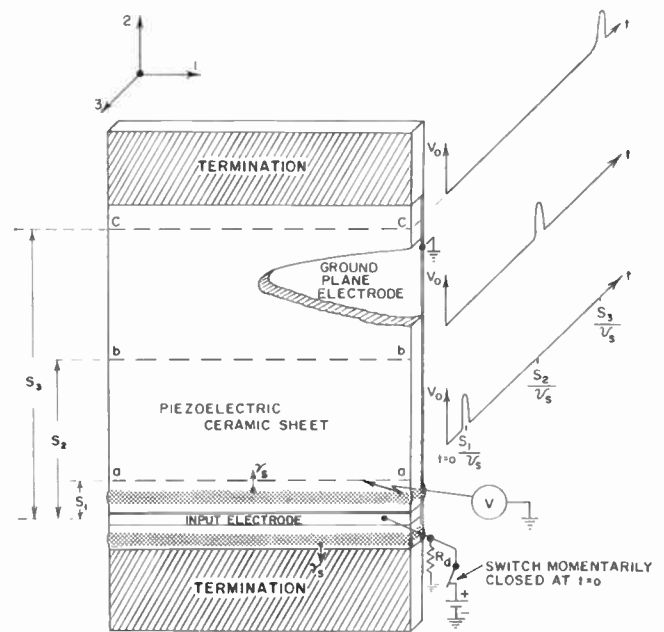


Fig. 2—Surface field produced by a single elastic pulse.

trical input signal is converted into a pair of elastic pulses traveling up and down the line, respectively. Because the propagation takes place in a piezoelectric medium, an electric field caused by the direct piezoelectric effect accompanies the elastic wave pulse.

As shown in Fig. 2, a single elastic pulse is produced by the momentary application of the indicated positive voltage to the input electrode. Under the influence of this excitation the ceramic material experiences a rapid contraction in the 3 direction, a rapid expansion in the 2 direction, followed by a relatively slow expansion in the 1 direction. Only the rapid expansion in the 2 direction produces a significant elastic wave. As the material expands in the 2 direction a narrow zone of pressure, which is proportional to the rate of change of the strain, builds up at the upper and lower edges of the strained input

region. These narrow zones of pressure move in the + and - directions, respectively, at the characteristic propagation velocity of sound v_s in the medium. The wave traveling in the negative 2 direction is absorbed in the lower termination. The wave traveling in the positive 2 direction traverses the piezoelectric ceramic strip with relatively small loss and is absorbed in the upper termination. As the elastic wave propagates up the ceramic strip, the compression resulting in the 2 direction as the wave passes any point results in a positive output voltage in the 3 direction by virtue of the transverse piezoelectric output coefficient g_{32} . If a voltage probe is placed on the surface of the ceramic strip along the lines a , b and c , pulses will be observed at times s_1/v_s , s_2/v_s and s_3/v_s , respectively, as the elastic wave passes.

No significant elastic wave is produced by the slow discharge of the input electrode through resistor R_d , since the resultant rate of change of strain is proportionately small.

SURFACE FIELDS DUE TO SUPERIMPOSED ELASTIC

The surface electric field configuration attained with the arrangement shown in Fig. 2 is in the form of a traveling line. The possibilities for employing such a field configuration in a display are very limited. A more useful arrangement may be obtained through the use of two oppositely-directed elastic waves. Mutual wave reinforcement causes an output electric field maximum whose position along the ceramic strip can be controlled by the relative timing of the two inputs.

Fig. 3 shows an electromechanical transmission line identical to that of Fig. 2 except for the addition of a second input electrode. Positive input voltages momentarily applied to both input electrodes at time $t=0$ cause a pair of pulses of compression to be radiated from each electrode; one directed toward the termination and the other across the piezoelectric strip. The pulses directed into the terminations are absorbed, while pulses directed across the ceramic strip traverse its length to the opposite termination without serious attenuation. These waves are represented at a time when they are approaching the center of the strip. The associated electric fields can be detected by a voltage probe placed on the surface of the ceramic strip. If a voltage probe is placed anywhere along line a , two positive voltage pulses will be observed; one at time s_1/v_s when the impulse from the lower electrode passes, and another at the later time s_3/v_s when the impulse from the upper input electrode passes. All along line b only one pulse of double amplitude passes. Along this line the impulses from both electrodes arrive simultaneously, and as a result the mechanical pressures reinforce one another causing an enhanced electrical output. As previously stated, this line of voltage maximum can be made to occur anywhere along the strip by controlling the relative timing of the application of the input voltages. Such a field configuration extends the possibilities

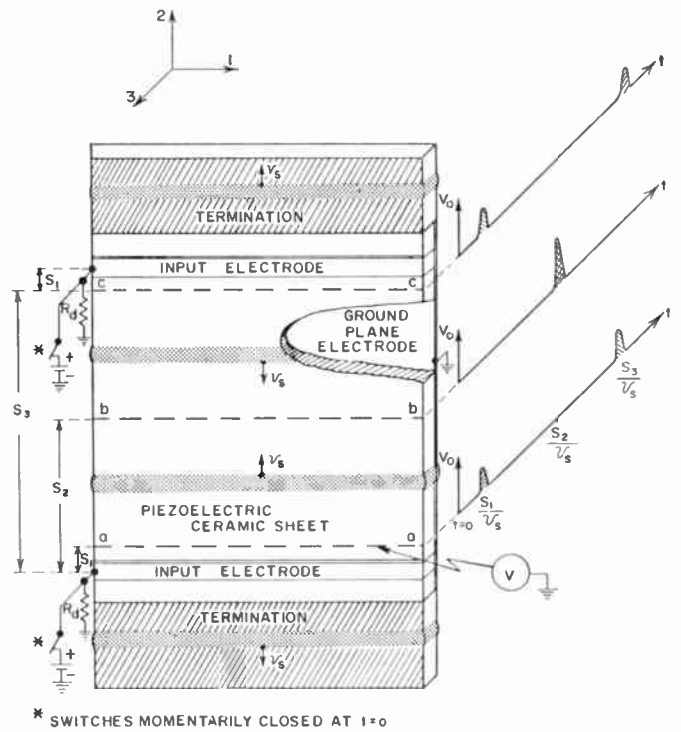


Fig. 3—Surface fields produced by two simultaneously launched elastic pulses.

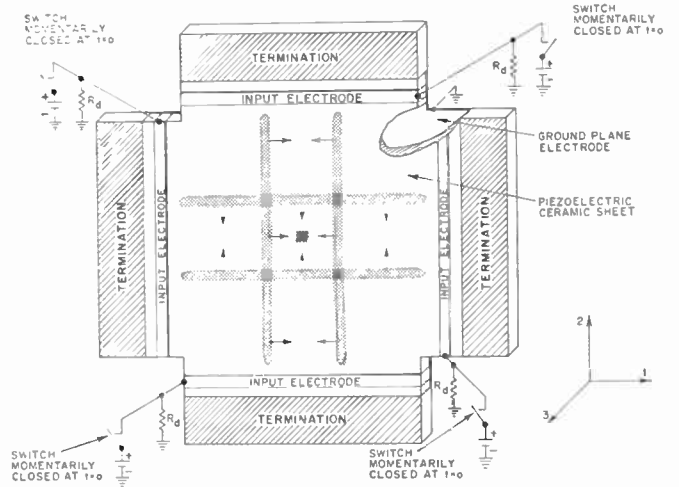


Fig. 4—Surface fields produced by four simultaneously launched elastic pulses.

for display devices, but to be of greatest general use surface fields in the form of a voltage "spot" rather than a voltage line are necessary.

Fig. 4 shows a structure capable of forming and controlling such a voltage spot. The configuration is an electromechanical transmission line capable of launching and sustaining the propagation of two pairs of elastic waves; one in the positive and negative 1 direction, and the other in the positive and negative 2 direction. These waves are represented at a time when they are approaching the center of the sheet. If all four inputs are

applied simultaneously, as shown in Fig. 4, the four resulting elastic waves intersect at the center of the piezoelectric sheet. The central elementary volume is simultaneously subjected to compressive stresses by the four waves. Each of these stresses produces an electric field in the 3 direction and they are additive. Consequently a probe on the central element detects a single pulse whose magnitude is four times greater than that caused by a single wave. Voltages twice that of a single wave appear at points of secondary intersection, while all other elements exhibit four pulses of unit amplitude spaced in time. By appropriately timing the application of the four input voltages with respect to one another the voltage spot can be made to appear at any point on the surface of the ceramic sheet.

In order to prevent the occurrence of ambiguous intersections, the applications of succeeding pulses must be delayed until the preceding elastic waves have traversed the display area. Such a restriction limits to several thousand points per second the rate at which information can be displayed. This rate is inadequate for video transmission systems such as television where the picture elements must be displayed at a peak rate of approximately six million elements per second. For such applications a fast-moving voltage spot analogous to the spot of a cathode ray electron beam is required.

PRODUCTION OF A MOVING VOLTAGE SPOT

A high-speed moving voltage spot can be generated at the intersection of two orthogonal elastic impulses propagating within a piezoelectric ceramic sheet. Fig. 5 shows a construct which is able, when the indicated switches are momentarily closed, to create two elastic impulses with their associated electric fields in the piezoelectric ceramic sheet; one is propagated to the right in the positive 1 direction, and the other downward in the negative 2 direction. At their point of intersection the ceramic element is subjected to simultaneous compressive stresses in the 1 and 2 directions, thereby causing the output field to be twice that of the single-wave field. A probe on the surface of the piezoelectric ceramic sheet would detect a voltage pulse at the time this intersection passes. In Fig. 5 the excitation is applied to both input electrodes at $t=0$. As a result, both elastic waves start out at the same instant and their point of intersection moves on the 45° diagonal at an apparent velocity of $\sqrt{2}$ times the velocity of propagation sound v_s within the ceramic medium. An important feature is that this apparent velocity is a function of the angle between the elastic waves, and hence, is easily adjustable.

By delaying the application of voltage to input electrode I with respect to that of electrode II, as shown in Fig. 6, the point of intersection of the elastic waves can be displaced from the central diagonal by an amount proportional to this delay. In this manner a voltage spot can be made to scan the entire area of the ceramic sheet in a series of closely-spaced parallel lines.

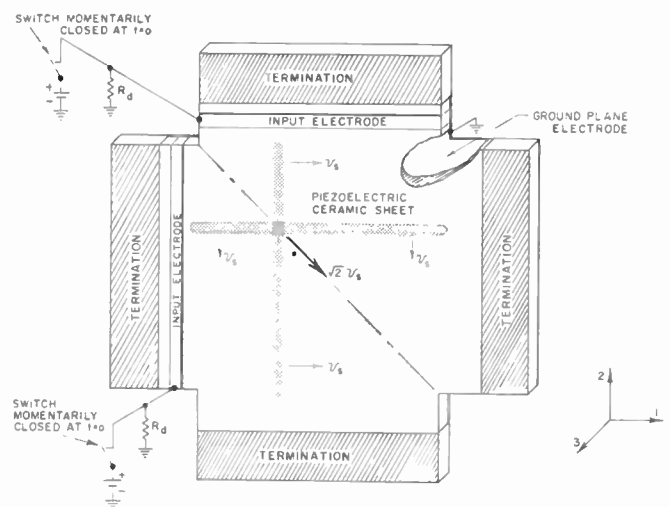


Fig. 5—Surface fields produced by two simultaneously launched orthogonal elastic pulses.

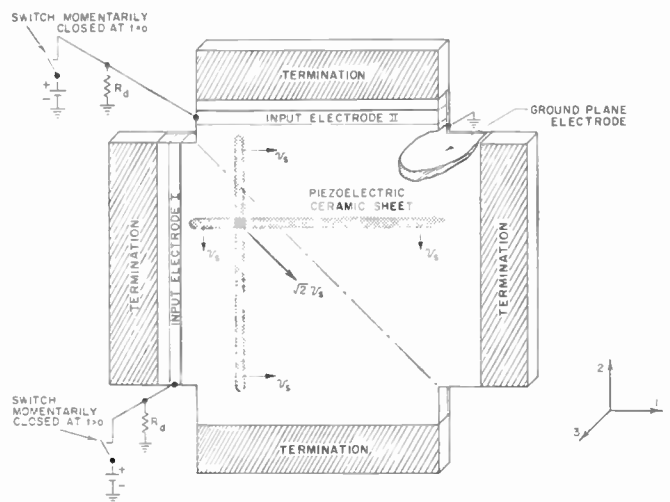


Fig. 6—Displacement of diagonal of intersection by delay of one input pulse.

PRODUCTION OF ELECTROLUMINESCENCE AND SUPPRESSION OF BACKGROUND

A solid-state display device can be constructed by applying an electroluminescent layer to the surface of the ceramic sheet. Interaction with the changing electric field of the voltage spot will produce an emission whose brightness is given by the exponential relationship³

$$B = e^{-\frac{a}{\sqrt{2}}} + b, \quad (1)$$

where B is the average brightness in foot-lamberts, v is the peak-pulse voltage, and a and b are constants which are related to the phosphor, the electroluminescent cell construction, and the pulse width of the excitation.

Because of this exponential brightness characteristic,

³ T. J. Sloyan, "Electroluminescent Emission Under Pulse Excitation," presented at IRE-AIEE Solid-State Device Research Conf., Cornell University, Ithaca, N. Y.; June 17-19, 1959.

the light emission at the voltage spot is much greater than that produced at the secondary intersections. As a result, a display of single points and simple waveforms is clearly visible against the background. When complex patterns and images are displayed, the trace is weakened by excessive time sharing of the light-emitting spots. A much higher degree of nonlinearity is therefore necessary if the trace is to be visible above the background.

Nonlinear resistances have been used to improve the contrast ratio of various electroluminescent displays.⁴⁻⁶ To satisfy the requirement of contrast improvement in this panel, a special polycrystalline cadmium-sulphide nonlinear resistance layer was developed. Such layers have demonstrated an ability to retain their nonlinear behavior for pulse excitations of less than 0.1- μ sec duration, and to carry pulsed current densities in excess of 40 amperes in². These properties are essential if background suppression is to be achieved under the 1.0- μ sec pulse excitation provided by the present piezoelectric displays.

MODULATION OF VOLTAGE SPOT

When the cadmium-sulphide nonlinear resistance layer and an EL phosphor layer are applied to the piezoelectric ceramic sheet of Fig. 5, it becomes feasible to video modulate the scanning voltage spot. Fig. 7 shows a cross section of such a multilayered structure taken through the voltage spot and along the central diagonal of Fig. 5. In Fig. 7 this voltage spot is represented by the equivalent voltage generator V_p with its internal impedance Z_p . This source acts between the top and bottom surfaces of the ceramic sheet and travels with the elastic waves at the indicated velocity. A modulation source V_m is connected between the ground plane electrode and the transparent top electrode. This source is seen to be effectively in series with the piezoelectric voltage source V_p and the nonlinear resistance and electroluminescent phosphor layers. The magnitude of the modulating voltage is adjusted to one-half the magnitude of the voltage spot. Thus the peak applied voltage at this point will be $3/2 V_p$, while everywhere else it will not exceed V_p . The relatively thick nonlinear resistive layer is a poor conductor at low voltages, but becomes highly conductive as the applied voltage exceeds V_p . As a result, excitation of the electroluminescent phosphor layer takes place only at the spot. In this manner a modulated light emission will be obtained as the spot scans the electroluminescent layer. Another

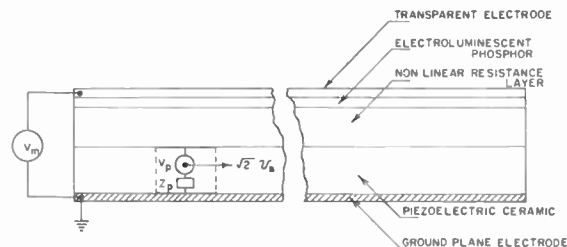


Fig. 7—Cross section of piezoelectric display panel.

important benefit is obtained through the use of the nonlinear resistance layer. Because it is considerably thicker than the EL layer, this layer reduces the load capacitance presented to the modulation source and results in a proportionate saving of modulation power.

A DISPLAY FOR HALF-TONE IMAGES

By employing the principles and structures described previously, a device for displaying pictorial images can be achieved. Fig. 8 represents a piezoelectric display device having this potential. A composite electroluminescent-nonlinear resistance layer with transparent electrode is applied over the image display area. In the manner previously shown, two orthogonal elastic waves are used to obtain a high-speed scanning voltage spot. Discharge devices S_1 and S_2 apply saw-tooth voltages of horizontal line frequency to the two input electrodes. By appropriate timing, the successive discharges of S_1 and S_2 will produce a series of voltage spots that will completely scan the raster area in a series of closely spaced horizontal lines. A typical velocity of propagation in the ceramic is about 3600 meters per second. This results in a spot speed of 5100 meters per second. Such a scanning speed results in a rectangular raster whose diagonal is thirteen inches. It will be recalled that this is not a fixed size, since the speed of the spot can be altered by adjusting the angle between the intersecting waves. The number of picture elements which can be displayed on one line will remain constant, however, since the spot size will increase in proportion to the line length. The modulation voltage applied to the panel is in the form of a video-modulated pulse train. The pulse width would normally be equal to the pulse width generated by the sweeping voltage spot. In current displays this pulse width is approximately 1 μ sec. By reinforcing the voltage spot as it scans the raster, a video-modulated line of light will be produced. A series of such modulated lines will make up a complete frame.

As a result of the experimental work to date, piezoelectric solid-state displays of the 4-input type shown in Fig. 4, and up to 5 inch \times 5 inch in size have been constructed. Circuits have also been built for automatically timing the injection of successive waves onto the panel, making possible the display of normal oscilloscope patterns. Fig. 9 is a photograph of a lissajous figure on a

⁴ D. H. Mash, "An electroluminescent digital indicator with a silicon carbide coding matrix," *J. Sci. Instr.*, vol. 37, pp. 47-50; February, 1960.

⁵ B. Kazan and F. H. Nicoll, "An electroluminescent light-amplifying picture panel," *Proc. IRE*, vol. 43, pp. 1888-1897; December, 1955.

⁶ J. Matarese and M. S. Wasserman, "Crossed-Grid Electroluminescent Panel Displays with Sequential and Random Access," presented at IRE Electron Devices Meeting, Washington, D. C.; November 15, 1959.

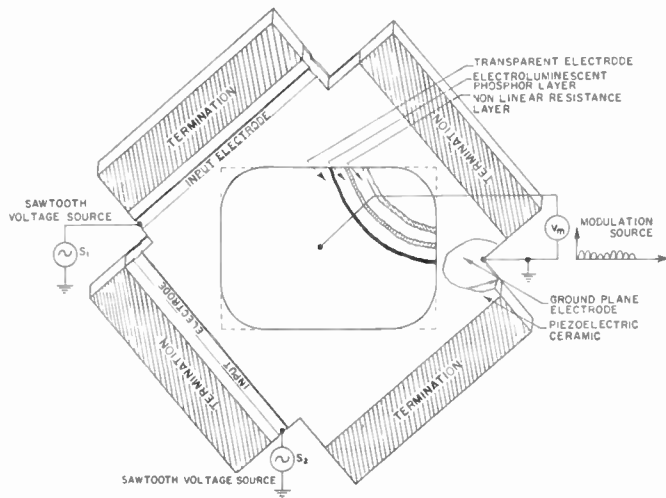


Fig. 8—Piezoelectric display for pictorial images.

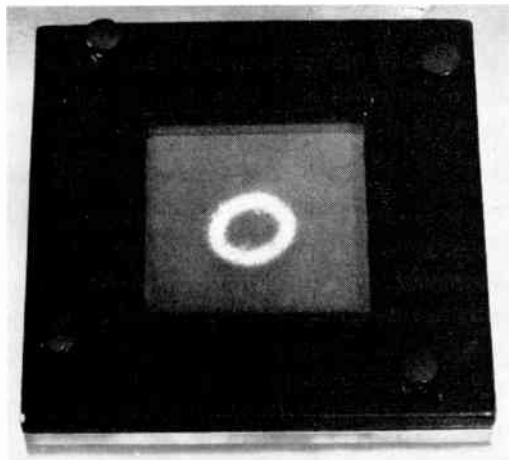


Fig. 9—Lissajous figure resulting from 1000-cps X and Y signals.

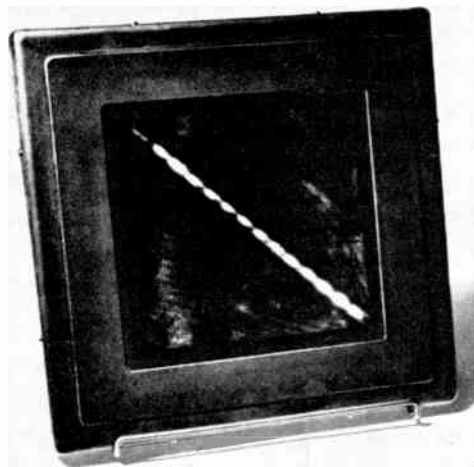


Fig. 10—Dot pattern resulting from 540-kc intensity modulation.

2½ inch × 2½ inch display which employs a nonlinear resistance layer in series with the electroluminescent layer. This figure is a familiar circle where the X and Y inputs are 1000-cps sinusoidal signals. The trace brightness is approximately 0.25 foot lambert and the effective spot size is 140 mils. As is evident from the photograph, the complete suppression of all background illumination has been achieved by the addition of the nonlinear resistance layer.

An earlier 5 inch × 5 inch display without a nonlinear resistance layer, but arranged for application of a modulating voltage, is shown in Fig. 10. The dot pattern results when a 540-kc signal modulates a voltage spot moving at approximately 0.2 inch per microsecond. The voltage spot is formed by two orthogonally intersecting elastic waves as shown in Fig. 5, and the modulating voltage is applied in the manner indicated in Fig. 7. Dot patterns have been obtained for modulation frequencies as high as 1.25 Mc. In this panel, modulation is restricted to the area of the scanning line because the large load capacitance associated with the entire display area would be too difficult to drive. As will be shown, the capacitance presented to the modulation source can be materially reduced through the introduction of a nonlinear resistance layer. This layer will also result in the elimination of the background illumination evident in Fig. 10.

CAPABILITIES OF THE PIEZOELECTRIC DISPLAY

Brightness and Contrast Ratio

To realize the full potentialities of the piezoelectric device as a practical display will require the use of a nonlinear resistance layer in series with the electroluminescent phosphor layer. As has been previously indicated, this layer will significantly improve the contrast ratio and will reduce the video power requirement in television-type displays.

A typical electroluminescent layer for use in this device will have a capacitance of approximately 3500 μμf/in². Such a lamp would have a brightness under a pulse excitation of 1-μsec duration of

$$B = 0.01fe^{-123/\sqrt{v}} + 8.1 \text{ (foot-lamberts),} \quad (2)$$

where v=peak pulse voltage (volts) and f=pulse repetition rate (pulses/sec).

A suitable polycrystalline CdS plastic-embedded nonlinear resistance layer to complement the operation of the electroluminescent layer would be approximately 38 mils thick and will have a capacitance of approximately 115 μμf/in². Its incorporation will result in a thirty-fold reduction in the capacitive loading on the modulation source. The nonlinear current response of such a layer is typically

$$I = 2.1(10^{-13})I^{5.2} \text{ amperes/in}^2. \quad (3)$$

Such a nonlinear current, which varies from approximately 5 ma/in² for $V=100$ volts to 23 amperes/in² for $V=500$ volts, makes possible a great contrast improvement even with pictorial images where the suppression level is two-thirds of the magnitude of modulated voltage spot. If in Fig. 8 the voltage spot is 333 volts, the peak modulation voltage 166 volts and the scanning rate 30 frames/sec, the image produced at the resulting 500-volt drive would have a brightness of 0.13 foot lambert and a contrast ratio better than 10 to 1 on practically all subject matter. Even for the worst possible case of a single black dot on a white background, the indicated contrast ratio would be 3.4 to 1.

Resolution

The spot size of the piezoelectric display is controlled by many factors including the angle of intersection of the elastic waves, the velocity of propagation of sound within the piezoelectric ceramic, the thickness of the ceramic plate, and the response of the electroluminescent and nonlinear resistive layers. Spot size will be defined by that diameter where the outer brightness is 1/30th of the center brightness. With orthogonally-intersecting elastic waves and using the materials presently available, the minimum attainable spot size is approximately 0.080 inch. When related to the 0.2 inch per microsecond scanning velocity of the voltage spot, such an aperture represents a capability for the display of a 1.25-Mc signal. This estimate is supported by the 540-ke trace shown in Fig. 10, where the dot pattern is obviously larger than the spot size.

Video Power Requirements

The video power requirement of the piezoelectric display

is basically controlled by the capacitance of the nonlinear resistive layer and the operating voltage of the electroluminescent layer. As indicated previously, a peak drive of 500 volts is required with presently available techniques and materials. This drive would be composed of a 333-volt voltage spot and a peak modulation voltage of 166 volts. Taking into account the capacitance of all three layers, the input capacitance at the modulation terminal will be approximately 110 $\mu\text{mf/in}^2$. If an efficient peaking circuit⁷ is used, the indicated peak video power requirement is 5.7 watts/sq in for a 1-Mc bandwidth. For practically all pictures, however, the power requirement should not exceed about 2 watts/in². Although this figure is high it nevertheless should soon be possible to display video signals of 1-Mc bandwidth in the Laboratory. In the future, as improved layers become available and as improved methods for driving the display are developed, significant reductions in the video power requirement should result.

ACKNOWLEDGMENT

The author wishes to express his appreciation to Drs. B. E. Bartels and A. L. Solomon for their early and continued support of the program, to S. Talesnick for his design of the electronic system for operating the display, to R. Zitta for his invaluable assistance in fabricating and evaluating the display, and to F. Pallilla and W. Zloczower for preparing some of the materials used in the construction of the device.

⁷L. Schupak, "A High-Gain Video Amplifier Peaking Circuit," RCA, Industry Service Lab., Rept. No. LB-996; October 20, 1955.

CORRECTION

R. Bechmann, A. D. Ballato, and T. J. Lukaszek, authors of "Higher-Order Temperature Coefficients of the Elastic Stiffnesses and Compliances of Alpha-Quartz," which appeared on pages 1812-1822 of the August, 1962, issue of PROCEEDINGS, have called the following to the attention of the *Editor*.

On page 1817 in Table VI, "Values for the Temperature Coefficients of the Stiffnesses for Alpha-Quartz at 50°C According to Mason [16], 1951," the values given for $T_{c_{\lambda\mu}}^{(1)}$ refer to 20°C and have been calculated from the values given by Mason for 50°C. For the values of

$T_{c_{\lambda\mu}}^{(1)}$ at 50°C see [16].

Also, in Table VI, the following typographical errors are corrected: $T_{c_{33}}^{(2)} = -187 \cdot 10^{-9}/(^{\circ}\text{C})^2$ instead of $-182 \cdot 10^{-9}/(^{\circ}\text{C})^2$ and $T_{c_{33}}^{(3)} = -410 \cdot 10^{-12}/(^{\circ}\text{C})^3$ instead of $410 \cdot 10^{-12}/(^{\circ}\text{C})^3$.

On page 1817 in Table IX, $T_{s_{11}}^{(3)}$ should be $38.3 \cdot 10^{-12}/(^{\circ}\text{C})^3$ instead of $147 \cdot 10^{-12}/(^{\circ}\text{C})^3$ and $T_{s_{12}}^{(3)}$ should be $-1460 \cdot 10^{-12}/(^{\circ}\text{C})^3$ instead of $-2287 \cdot 10^{-12}/(^{\circ}\text{C})^3$, due to an erroneously omitted term.

Also on page 1817 in Table X, $T_{s_{13}}^{(2)} = -2110 \cdot 10^{-9}/(^{\circ}\text{C})^2$ instead of $-2100 \cdot 10^{-9}/(^{\circ}\text{C})^2$.

Switching Speed and Dissipation in Fast, Thin-Film Cryotron Circuits*

NORMAN H. MEYERS†, SENIOR MEMBER, IRE

Summary—As thin-film cryotron circuits become faster, the detailed properties of the components themselves have an increasing effect on over-all circuit operation. When a cryotron switches from the superconducting to the resistive state in a fast circuit, its inductive characteristics can change enough to add appreciable delay and dissipation to its driving circuit. The inductive and resistive transition of the component can be accompanied by diamagnetic hysteresis and by eddy-current-damping effects, which add to dissipation and further delay the switching of the component. These component and circuit effects are complex and interrelated, but considerable insight is gained by analyzing separately various portions of the general behavior.

INTRODUCTION

CONSIDERABLE interest exists at present in the development of evaporated, thin-film, superconducting, computer components and circuits. Among the potential advantages of this type of circuitry are high speed, small size, low power dissipation, low cost, logical simplicity, reliability, and the possibility of automated batch fabrication.

From the viewpoint of the circuits engineer, the speed and power dissipation of components and circuits are two of the more interesting and fundamental properties. In previous studies of these properties it usually has been assumed that the components, the thin-film cryotrons, can be switched instantaneously compared with the circuit switching time. Furthermore, it also has been assumed that the only heat generated in circuit operation is that associated with the transfer of current from one inductive path, suddenly switched resistive, to another parallel superconducting path. These assumptions are adequate for analysis of relatively slow circuits with time constants in the microsecond range or longer.

However, with the advent of the in-line cryotron and superconducting alloy films it becomes feasible to think in terms of nanosecond circuit time constants. As the circuits are speeded up, new effects, associated with the more detailed operation of the components themselves, become significant contributors to delay and dissipation. It is the purpose of this paper to define and appraise some of the more important effects of the cryotrons themselves upon circuit operation at higher speeds.

When a cryotron gate switches from the super to normal state, all of the inductances of the component

change. These inductance changes delay the current transfer process in the circuit which is driving the cryotron and causing its gate to change state. This delay in current transfer also brings about increased dissipation in the circuit driving the cryotron. The increased delay and dissipation occur irrespective of whether the cryotron is initially superconducting and driven resistive, or initially resistive and driven superconducting.

The total stage delay, made up partly of current-transfer time in the driving circuit and partly of component switching time, is minimized by biasing the cryotron as close as possible to its resistive transition and by employing the largest permissible supply current. However, practical considerations set upper limits on supply and bias currents. The effects of cryotron inductance changes upon stage delay and dissipation are not negligible in fast circuits even when the optimum supply and bias currents are utilized.

Switching of the cryotron gate film can be accompanied by diamagnetic hysteresis in the gate material itself, particularly at temperatures well below the critical temperature. This phenomenon can generate appreciable heat in the gate under certain conditions. However, hysteresis may be eliminated (or at least minimized) by learning to control the grain structure of evaporated films.

Furthermore, as the gate changes state, eddy currents are induced within the normal portion of the gate itself by the motion of the phase boundary between the normal and superconducting portions. The effects of these eddy currents are to damp the motion of the phase boundary and to generate heat within the gate undergoing switching.

Difficulty is encountered in analyzing the eddy currents because the structure of the intermediate state in a film undergoing switching is not well understood. Furthermore, there is still considerable question as to what criterion governs the onset of phase transition in a film subjected to an applied field while carrying an appreciable current.

Pippard's treatment of eddy-current-damped, phase boundary propagation in a semi-infinite superconductor can be applied to the case of a cryotron gate film. Such an approach is a vast over-simplification. However, it is useful in demonstrating the qualitative nature of the interaction between component and circuit.

The current transfer process in the driving circuit, the inductance change in the driven cryotron, and the eddy-

* Received May 1, 1962; revised manuscript received, September 6, 1962. The work described in this paper was supported by the Bureau of Ships, U. S. Navy.

† Harvard Business School, Boston, Mass. Formerly with International Business Machines Corp., Thomas J. Watson Research Center, Yorktown Heights, N. Y.

current effects in the driven cryotron are all interrelated and can not really be treated independently. Consequently, the general problem is very complex but considerable insight can be obtained by examining certain portions of the general problem while neglecting other portions. This is the approach followed in the present paper.

Rationalized mks units are used throughout the present paper.

CRYOTRON CONTROL INDUCTANCE CHANGE

Consider a single, thin-film cryotron consisting of a superconducting control and ground plane (with relatively high critical field) and a superconducting gate, (with lower critical field), all insulated from one another by thin dielectric layers. Either the more familiar crossed-film cryotron [1] or the more recent in-line cryotron [2], as shown in Fig. 1, suffices for the present discussion.

It is well-known that resistance may be caused to appear in the gate by application of current to the control. The control characteristic for small gate current, typical of pure gate material near its critical temperature with trimmed edges [3], is as shown in Fig. 2. Because the control and gate width W is several orders of magnitude greater than the total thickness of the structure T , the magnetic field produced by the control current is very nearly equal to the control current divided by the width.

In order for resistance to appear in the gate, the magnetic field produced by control current must penetrate the gate material. As this happens the self-inductance of the control changes from a relatively low value to a higher value [4]. This is shown in Fig. 3 by a plot of flux linking the control λ_c vs control current i_c . As the field penetrates the gate at the critical control current I_c , the flux abruptly rises to a higher value. This is an involved and intriguing process.

Actually the field penetration conceivably could precede the appearance of resistance. The experimental fact that resistance appears abruptly at a certain critical field in a film with trimmed edges does not guarantee that the flux changes abruptly at the same field strength. However, experiments indicate that penetration depth is not a strong function of applied field [5] up to values very near the resistive critical field. Hence, it is plausible to assume that the flux change in a dc field occurs sharply at the resistive critical field of a trimmed film.

The source of control current supplies energy as the switching occurs. Some of the energy is stored in the magnetic field, some is converted into internal energy within the material itself, and some is converted to eddy current heat. If the process is constrained to occur very slowly the energy converted to Joule heat through the mechanism of eddy currents is negligible. As the control current is raised from zero to I_c the flux builds up from zero to λ_1 along the line 01 in Fig. 3. The per unit length energy supplied by the control current source and stored

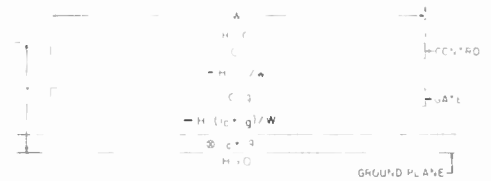


Fig. 1—End view of an in-line cryotron (distorted scale; actually $W \gg T$).

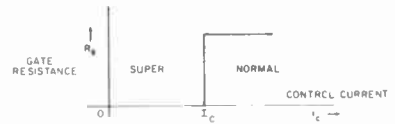


Fig. 2—Gate resistance as a function of control current.

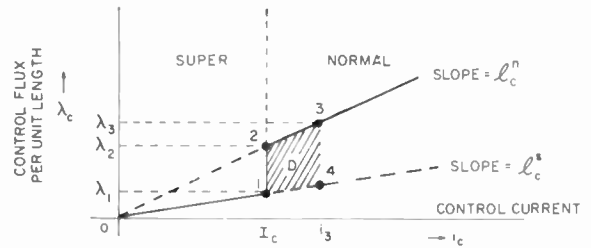


Fig. 3—Cryotron control inductance characteristic.

in the form of magnetic field energy and kinetic energy of superelectrons [4] is

$$\int_0^{\lambda_1} i_c d\lambda_c = \frac{1}{2} \lambda_1 I_c = \frac{1}{2} l_c^s I_c^2 = E_{11}, \tag{1}$$

where l_c^s is the per unit length control self-inductance with the gate superconducting.

Now if the flux slowly increases from λ_1 to λ_2 , the current source supplies an amount of energy equal to the rectangular area to the left of path 12 in Fig. 3.

$$\int_{\lambda_1}^{\lambda_2} i_c d\lambda_c = (\lambda_2 - \lambda_1) I_c = (l_c^n - l_c^s) I_c^2 = E_{12}, \tag{2}$$

where l_c^n is the per unit length control self-inductance with the gate fully normal.

At point 2 the energy stored in the field is simply

$$\frac{1}{2} \lambda_2 I_c = \frac{1}{2} l_c^n I_c^2 = E_{22}. \tag{3}$$

Eq. (3) assumes that the stored energy associated with the magnetic field is a "state function" [6] of the variables λ_c and i_c and is independent of the past history of these variables. Thus the increase in stored field energy as the system moves from point 1 to point 2 is

$$\Delta E = E_{22} - E_{11} = \frac{1}{2} (l_c^n - l_c^s) I_c^2. \tag{4}$$

This increase in stored field energy is only half of the energy supplied by the control current source, as seen by comparing (2) and (4). The other half of the supplied energy is absorbed by the gate material itself, in the form of stored internal energy, as the gate switches from

the superconducting to normal state. Thus, as the system moves slowly from point 1 to point 2 at essentially constant current,

$$E_{12} = \Delta E + \Delta E \quad (5)$$

Supplied by current source Stored in field Stored internally in gate material.

The interpretation expressed in (5) is in contradiction with that given by Buck [7]. According to Buck, half of the energy supplied is lost in Joule heat associated with eddy currents while the other half is analogous to a latent heat. If Joule heating accounted for half of the energy supplied during the magnetic switching of a superconductor into the resistive state it would never be possible to achieve reversible field-induced transitions [8]. Hysteresis always would accompany the switching process. Experimentally, this is not found to be the case.

One way to see that (5) is reasonable is as follows: First, recognize that the internal energy density at a particular temperature in the normal state f^n exceeds the internal energy density in the super state f^s by an amount related to the bulk critical field of the gate material H_{cb} [8]. The internal energy referred to here is that which exists in the absence of magnetic field. Thus,

$$f^n - f^s = \frac{\mu_0}{2} H_{cb}^2, \quad (6)$$

where μ_0 is the permeability of free space. The latent heat absorbed isothermally when superconductivity is destroyed in a magnetic field [8], [9] is neglected as it will be throughout the rest of this paper.¹ Consequently, it should be correct to equate the increase in internal energy as expressed in circuit terms by (4) to the internal energy density difference of (6) multiplied by the gate volume. For a unit length of gate material

$$\Delta E = \frac{1}{2}(I_c^n - I_c^s)I_c^2 = \frac{\mu_0}{2} H_{cb}^2 W d, \quad (7)$$

where W is the gate width and d is the gate thickness.

Expressions have been derived [4] for the inductance parameters of the structure of Fig. 1 in terms of the dimensions and material properties. The presently pertinent result is

$$I_c^n - I_c^s = \frac{\mu_0}{W} \left(d - 2\beta^{-1} \tanh \left(\frac{\beta d}{2} \right) \right), \quad (8)$$

where β is the reciprocal penetration depth of the superconducting gate material at the temperature in question.

Substituting (8) into (7) and rearranging

$$\left(\frac{I_c}{W} \right)^2 = H_{cb}^2 \left(1 - 2(\beta d)^{-1} \tanh \left(\frac{\beta d}{2} \right) \right)^{-1}. \quad (9)$$

¹T. H. Cheng has suggested in a private communication that latent heat may not be negligible in the switching of a thin gate film.

Since I_c is the critical control current (not the critical current of the gate film) and W is much larger than T , I_c/W is the critical field of the gate film. Therefore, (9) is just London's result for the critical field of a film in terms of the critical field of the bulk material [10].

The point to be emphasized is that the energy balance expressed in (5) is completely compatible with London's picture of the switching of a thin film under the influence of an applied magnetic field.

Returning now to Fig. 3 one can see that the system moves along line 23 as the control current is increased beyond I_c . In this process all of the energy supplied by the current source is stored in the magnetic field,

$$\int_{\lambda_2}^{\lambda_3} i_c d\lambda_c = \frac{\lambda_3 i_3 - \lambda_2 I_c}{2} = \frac{1}{2} I_c^n (i_3^2 - I_c^2). \quad (10)$$

If the control current is slowly reduced to zero, the energy flows just described are essentially reversible and everything returns to the initial state.

EFFECT ON CIRCUIT SPEED

The change of cryotron control inductance, as the gate switches, can have an appreciable effect on the speed of a cryotronic circuit. For purposes of further discussion consider the simple flip-flop circuit of Fig. 4. The loop shown in Fig. 4(a) contains three in-line cryotrons of the type shown in Fig. 1. Two of these are input cryotrons with their gates in the loop. They serve the function of causing current to transfer from leg to leg in the loop as their controls are energized with suitable signal currents. The third cryotron has its control in series with leg 2 and permits the loop to drive another circuit. All three cryotrons are assumed to be identical.

If the cryotron gate resistance is small compared with the characteristic impedance of the thin-film transmission line connecting cryotrons, which is usually the case in practice, the transient behavior of the circuit can be understood in terms of lumped resistance and inductance parameters alone [11]. The capacitances among controls, gates, connection lines, and ground plane may be neglected in this case. Fig. 4(b) shows an equivalent, lumped network suitable for a preliminary analysis of the transient behavior of the flip-flop. It includes no bias lines for the cryotrons and neglects the mutual inductance between each control and its associated gate.

At time zero, input cryotron 1 is assumed fully resistive and is therefore characterized by resistance (R) and gate self-inductance L_{g1} . Input cryotron 2 is assumed superconducting, so it is characterized by the different gate self-inductance L_{g2} . Inductances L_1 and L_2 account for the connection lines among components on their respective sides of the loop. Initially all of the supply current is assumed to flow in leg 1 so

$$i_1(0) = I_s \quad \text{and} \quad i_2(0) = 0. \quad (11)$$

Consequently, the output cryotron of leg 2 is superconducting and is characterized by the control self-induct-

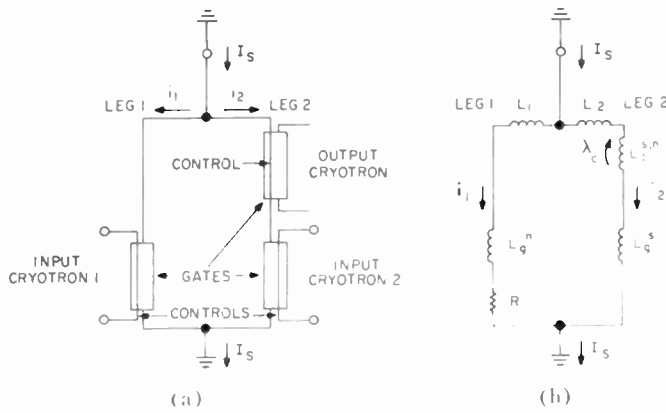


Fig. 4—Flip-flop with in-line cryotrons. (a) Schematic. (b) Equivalent network.

ance with the gate in the superconducting state L_c^s .

Starting from the prescribed initial conditions, the current in leg 2 will simply build up exponentially from zero toward the final value I_s . However, this process continues unaltered only until the critical control current of the output cryotron is reached. The time t_{01} required is

$$t_{01} = \frac{L_{t^*}}{R} \ln \left(\frac{I_s}{I_s - I_c} \right), \tag{12}$$

where L_{t^*} is the total loop inductance with the output cryotron superconducting

$$L_{t^*} = L_1 + L_2 + L_{g^n} + L_{g^s} + L_c^s. \tag{13}$$

Once i_2 has reached I_c the process becomes more interesting. If one takes Fig. 3 literally, the current i_2 cannot increase further until the cryotron control flux has built up from λ_1 to λ_2 . Actually, Fig. 3 is a reasonable representation of the cryotron behavior only for very slow operation such that eddy current effects are negligible. For faster operation the switching of the gate is retarded by eddy currents induced in the normal portion. In order for the field applied to the gate to overcome the eddy currents and drive the switching process to completion it is necessary for the control current to increase as the penetration progresses and the flux builds up.

For the moment let us take Fig. 3 literally. It is a constraint upon the loop equations such that currents i_1 and i_2 must remain constant until the cryotron control flux reaches λ_2 . During this interval

$$i_1 = I_s - I_c \tag{14}$$

$$i_2 = I_c. \tag{15}$$

Since the currents are constant there is no voltage drop across any of the inductances in the loop except the output cryotron control. The voltage e across a varying inductance L is made up of two parts

$$e = \frac{d\lambda}{dt} = \frac{d}{dt}(Li) = L \frac{di}{dt} + i \frac{dL}{dt}. \tag{16}$$

Even though the current is constant the output cryotron control can generate a back voltage while its inductance is increasing.

The loop voltage equation during the cryotron switching interval is simply

$$(I_s - I_c)R = I_c \frac{dL_c}{dt}. \tag{17}$$

Those familiar with magnetic amplifier operation will see an analogy here. A constant voltage governs the rate of flux change in a square-loop material. Separating variables and integrating yields the component switching time, the time required for the flux to build up in the control from λ_1 to λ_2 at the critical control current.

$$t_{12} = \frac{L_c^n - L_c^s}{R} \times \frac{I_c}{I_s - I_c}. \tag{18}$$

The so-called "stage delay" t_{02} is the time from the first appearance of full resistance in the gate of the input cryotron until the output gate is fully switched. Hence

$$t_{02} = t_{01} + t_{12} = \frac{L_{t^*}}{R} \ln \left(\frac{I_s}{I_s - I_c} \right) + \left(\frac{L_c^n - L_c^s}{R} \right) \left(\frac{I_c}{I_s - I_c} \right). \tag{19}$$

It is instructive to put some typical numbers into (19). In the Appendix the per unit length inductances are evaluated for film thicknesses, material properties, and a width typical of those currently encountered in practice. If the cryotrons are all one inch long

$$L_c^n = 2.37 \times 10^{-10} \text{ h,}$$

$$L_c^s = 1.94 \times 10^{-10} \text{ h,}$$

$$L_c^n - L_c^s = 0.434 \times 10^{-10} \text{ h,}$$

$$L_{g^n} = 1.05 \times 10^{-10} \text{ h,}$$

$$L_{g^s} = 0.978 \times 10^{-10} \text{ h.}$$

If the loop of Fig. 4 is taken as 1 inch wide, 2 inches long, and the connections are striplines of the same width as the cryotrons, the connection inductances are

$$L_1 = 1.68 \times 10^{-10} \text{ h,}$$

$$L_2 = 0.838 \times 10^{-10} \text{ h.}$$

Consequently, the total loop inductance with the output gate superconducting is

$$L_{t^*} = 6.48 \times 10^{-10} \text{ h.}$$

Assuming that the gate is indium, 0.009 inch wide, and 6000 Å thick, the gate resistance at liquid helium temperature is about

$$R = 0.11 \text{ ohm.}$$

Typical current values might be

$$I_s = 0.40 \text{ a,}$$

$$I_c = 0.25 \text{ a.}$$

Using these values, the results are

$$t_{01} = 5.78 \text{ nsec,}$$

$$t_{12} = 0.66 \text{ nsec,}$$

$$t_{02} = 6.44 \text{ nsec.}$$

In this example the extra delay due to the control inductance change of the output cryotron is better than 10 per cent of the total stage delay. The effect is not negligible and rises as I_s is reduced toward I_c . For I_c unchanged, but $I_s = 0.30 \text{ a}$,

$$t_{01} = 10.6 \text{ nsec,}$$

$$t_{12} = 1.97 \text{ nsec,}$$

$$t_{02} = 12.6 \text{ nsec.}$$

The component delay has risen to better than 15 per cent of the stage delay.

Thus far the results relating to stage delay are interesting but overly simplified. The effects of bias current, gate current, and mutual inductive coupling have been neglected completely. Actually, these quantities are significant, as will be shown in the next section.

INFLUENCE OF BIAS AND SUPPLY CURRENT ON STAGE DELAY

Examination of (19) suggests that the stage delay can be reduced either by increasing the supply current I_s , so as to drive the cryotron harder, or by biasing the cryotron close to its transition, so as to effectively reduce the critical control current I_c . However, practical considerations limit the maximum permissible values of supply and bias currents.

In order to understand these limitations it is necessary to consider the current gain characteristic of a biased, in-line cryotron. The structure of Fig. 1 may be biased by applying dc current to a second control line of width W placed parallel to and directly above (but insulated from) the first control line. For convenience, the positive direction of bias current i_b is defined as parallel to the positive direction of control current i_c and gate current i_g . Because the width of the structure W is many times its total height T , one unit of bias current has the same effect on the gate as one unit of control current. This has been verified experimentally by A. E. Brenne-²

The in-line cryotron has an incremental current gain G greater than unity only over a portion of its gain characteristic [2]. The high gain condition exists with gate current flowing opposite to the resultant of the control and bias currents. Therefore, Fig. 5 is drawn with $-i_g$

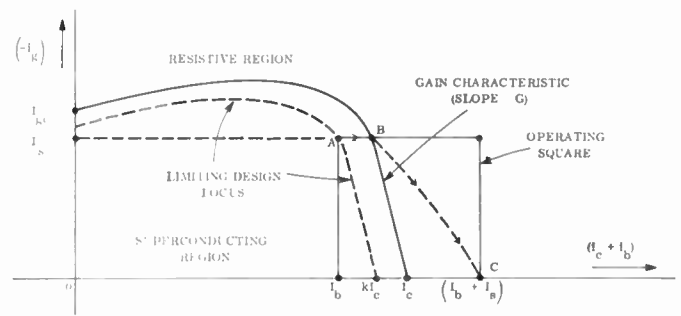


Fig. 5—Operation of a biased, in-line cryotron on its gain characteristic.

as the ordinate and the resultant $i_c + i_b$ as the abscissa. As shown, the current gain curve is a locus separating the region in which the gate is superconducting from the region in which the gate is resistive.

In any practical application of cryotronic circuits, it will be necessary to supply the working current I_s to a large number of switching circuits from a single current source in a serial manner. Therefore, if one circuit is to drive another, the maximum gate or working current in one stage is the same as the maximum control current signal applied to the next stage. This means that a given cryotron must operate within a square of size I_s on its gain diagram, as indicated in Fig. 5.

Initially, the output cryotron is biased in the superconducting state at point A of Fig. 5. The currents at this point are

$$\begin{aligned} i_g &= -I_s, \\ i_b &= I_b, \\ i_c &= 0. \end{aligned} \tag{20}$$

As the control current begins to grow toward I_s the state of the cryotron moves toward point B. Actually, inductive coupling between the control and gate circuits causes the gate current to increase somewhat, but this effect will be neglected in the interests of simplicity. At point B the gate switches to the resistive state. Thereafter the gate current is transferred to an alternate superconducting path as the control current continues to increase toward I_s . Thus, the state of the cryotron moves from point B to point C along some path like the one shown dotted in Fig. 5.

Note that point A must lie within the superconducting region even when the cryotron is carrying full gate current and that point C must lie within the resistive region even in the absence of gate current. Clearly, this is not possible unless the cryotron has an incremental current gain greater than unity.

If the same supply and bias currents are applied to a large number of cryotronic circuits, point A will remain fixed for all components involved. However, the incremental current gain G and the critical value of the combined bias and control currents I_c will vary from one component to another. In addition, any temperature rise caused by the combined dissipation of a large num-

² A. E. Brenne-²mann, Private communication.

ber of circuits operating on a common substrate will have the effect of moving the gain characteristic inward. Consequently, point *A* must be sufficiently far away from the average gain characteristic to allow for these irreproducibilities and operating variations among components.

In other words, one cannot bias a cryotron barely inside its gain curve because of some uncertainty as to where the gain curve is located. The dotted curve in Fig. 5, which roughly parallels the actual gain curve, is a limiting design locus which allows for the variations in cryotron gain. Point *A* must lie on or within this design locus.

As the operating square in Fig. 5 becomes larger and point *A* moves along the dotted locus, a condition of maximum I_c is reached. This occurs when the dotted locus has a slope of unity at point *A*. Beyond this condition, a further increase in I_s calls for an even greater decrease of I_b so that point *C* begins moving to the left rather than further to the right.

In a practical case, one finds that the maximum permissible supply current I_s is something like 80 per cent of the critical gate current I_{gc} . A typical cryotron gain curve might have a critical control current I_c roughly double the critical gate current I_{gc} and an incremental gain G of about 4. At present it does not seem safe to expand the design locus beyond 90 per cent of the gain curve.

Therefore, for illustrative purposes,

$$\begin{aligned} I_c &= 0.8I_{gc}, \\ I_c &= 2I_{gc}, \\ I_b &= kI_c - (I_s/G) = 1.6I_{gc}. \end{aligned} \quad (21)$$

The effect on stage delay of the considerations just discussed now can be examined. While the cryotron moves from point *A* to point *B*, all inductances remain constant. Furthermore, it will be assumed that the bias and gate currents also remain constant. The time required for control current to grow exponentially to the new critical value is given by the expression

$$t_{01} = \frac{L_l^*}{R} \ln \left\{ \frac{I_s}{I_s - [I_c - I_b - (I_s/G)]} \right\}. \quad (22)$$

This control current build-up time should be compared with that expressed in (12). The influence of bias and gate current is to reduce the effective value of critical control current and thereby reduce t_{01} .

At point *B* the gate undergoes a phase change. During the component switching time t_{12} , all currents will be assumed to remain constant. However, all self- and mutual inductances of the biased, in-line cryotron undergo the changes indicated in the Appendix. Consequently, the loop voltage equation in the circuit driving the cryotron changes from (17) to the new expression,

$$\{I_s - [I_c - I_b - (I_s/G)]\} R = \frac{d\lambda_c}{dt}, \quad (23)$$

where λ_c is the resultant flux linking the control line. From the Appendix we have

$$\frac{d\lambda_c}{dt} = -I_s \frac{1}{2} \frac{\Delta l}{\Delta l} + [I_c - I_b - (I_s/G)] \frac{\Delta l}{\Delta l} + I_b \frac{\Delta l}{\Delta l}. \quad (24)$$

The quantity Δl is equal to the increase of control self-inductance.

The first term on the right side of (24) arises from the change of mutual inductance between the control and gate. It is negative because the gate current flows in the antiparallel direction, as mentioned in connection with Fig. 5. Similarly, the second term on the right side of (24) stems from the change of control self-inductance while the final term is associated with the change of mutual inductance between the control and bias lines.

The combination of (23) and (24) yields a new expression for the component switching time t_{12} .

$$t_{12} = \frac{\Delta l}{R} \left\{ \frac{I_c - I_s(1/2 + 1/G)}{I_s(1 + 1/G) + I_b - I_c} \right\}. \quad (25)$$

Eq. (25) does not reduce to (18) in the absence of bias current and with infinite incremental gain. This is a consequence of the fact that gate current and mutual coupling between control and gate were neglected in formulating (18). The inductive effect of antiparallel gate current is to hasten the component switching.

Some practical limits on supply and bias currents have been discussed in connection with Fig. 5 and expressed in (21). Introducing these limits into (22) and (25) yields the following delay times:

$$\begin{aligned} t_{01} &= 1.69 \text{ nsec}, \\ t_{12} &= 0.92 \text{ nsec}, \\ t_{02} &= 2.61 \text{ nsec}. \end{aligned}$$

The component delay in this case is about 35 per cent of the total stage delay.

If the supply current is reduced to $0.6I_{gc}$ and the bias current is increased according to (21), the delay times become

$$\begin{aligned} t_{01} &= 2.39 \text{ nsec}, \\ t_{12} &= 1.53 \text{ nsec}, \\ t_{02} &= 3.92 \text{ nsec}. \end{aligned}$$

Now the component delay is 39 per cent of the total stage delay. Clearly, the component delay under discussion is not a negligible effect.

Eqs. (22) and (25) show that the component delay must become a larger fraction of the total stage delay as supply current is decreased from the maximum practical value. The denominator of the bracketed term in each equation is the same and it tends to vanish as I_s approaches $(1-k)I_c$. Hence, each bracketed term increases without bound as I_s decreases. Naturally, the logarithmic expression for t_{01} increases less rapidly with increasing argument than the expression for t_{12} .

OTHER FACTORS AFFECTING DELAY

The situation is actually worse than the simple calculations made thus far indicate, particularly for very high speed circuits. For one thing, eddy currents tend to increase the component delay. Secondly, the component delay must be multiplied directly by the number of output cryotrons irrespective of which side of the loop they are in and irrespective of whether they are driven from super to normal or vice versa, as will be demonstrated later. In a typical logical stage there may be four or more output cryotrons. Thirdly, the component delay is independent of the cryotron length if all cryotrons are identical. This stems from the fact that only the output cryotron inductances enter into t_{12} and these are proportional to length as is the resistance of the driving cryotron.

In order to attain high circuit speeds one attempts to lengthen the cryotrons without lengthening the loop. This reduces t_{01} without altering t_{12} and thus makes the component delay a larger fraction of the stage delay. Another method of attaining high speed circuits is to reduce the thickness of the insulating films in order to reduce the inductances. This will also reduce t_{01} without altering the component delay. The reason is that the inductance change which appears in t_{12} depends only upon the gate film thickness and not on the insulation thickness, as shown in (8). Since the current gain of the cryotron depends directly on the gate thickness at a given temperature it is not permissible to reduce the gate thickness in an effort to cut down the component delay.

It was pointed out earlier that a certain amount of energy must be supplied by the source of control current in order to switch the gate. The component delay depends on how rapidly the source can supply this energy. The internal impedance level of the control current source governs directly the power to the cryotron control. For example, at a fixed current level I , the power carried by a transmission line of characteristic impedance Z is I^2Z . Consequently, the component delay can be expected to be appreciably greater when the cryotron is driven by other low impedance circuitry than when it is switched by a signal from a high impedance source, such as a 50-ohm transmission line. Therefore, care should be taken not to assume that the results of switching speed measurements made on thin superconducting films are directly indicative of attainable component speeds in thin-film circuits.

EFFECT ON DISSIPATION

The inductive changes of the output cryotron also have an effect on the joule heat generation in the resistive gate of the input cryotron.

For the moment, bias current, gate current, and mutual inductance in the output cryotron again will be neglected. The energy converted to heat in the gate of the input cryotron of Fig. 4, in an arbitrary time in-

terval t_a to t_b , is

$$E_{ab} = \int_{t_a}^{t_b} i_1^2 R dt. \tag{26}$$

Evaluating the heat generated in each of the three time intervals of the current transfer process

$$E_{01} = \frac{1}{2} L_t^s I_c (2I_s - I_c), \tag{27}$$

$$E_{12} = (L_c^n - L_c^s) I_c (I_s - I_c), \tag{28}$$

$$E_{23} = \frac{1}{2} L_t^n (I_s - I_c)^2, \tag{29}$$

where the subscripts 0, 1, 2 and 3 refer to points on the state diagram of Fig. 3 and it is assumed that $i_3 = I_s$.

The total dissipation expression may be simplified by recognizing that

$$L_t^n - L_t^s = L_c^n - L_c^s. \tag{30}$$

The result is

$$E_{03} = E_{01} + E_{12} + E_{23} \\ = \frac{1}{2} L_t^s I_s^2 + \frac{1}{2} (L_c^n - L_c^s) (I_s^2 - I_c^2). \tag{31}$$

The first term on the right-hand side of (31) is the dissipation that would come about even in the absence of inductance change. The second term is the extra dissipation that results from the inductive switching of the output cryotron.

Using the same parameter values as before with $I_s = 0.4$ a and $I_c = 0.25$ a, the first term amounts to 5.18×10^{-11} joules while the second term is 0.21×10^{-11} joules. Thus, the extra dissipation due to the control inductance change is less than 4 per cent of the total heat generation.

If bias and gate currents are taken into account, as at point B in Fig. 5, then the result is,

$$E_{03} = \frac{1}{2} L_t^s I_s^2 \\ + \frac{1}{2} (L_c^n - L_c^s) (I_s - I_c') (2I_b + I_c'), \tag{32}$$

where

$$I_c' = I_c - I_b - (I_s/G) = (1 - k) I_c. \tag{33}$$

Using the typical supply and bias current limits of (21) one finds that the extra dissipation in the gate of the driving cryotron, due to inductive changes in the output cryotron, amounts to about 17 per cent of the total joule heat generated. This is not a negligible effect. However, as shown by (32) and (33), this extra dissipation vanishes as the supply current is reduced toward $(1 - k) I_c$ and the so-called "overdrive" disappears.

Inductive changes have less effect on dissipation than upon stage delay. This is true because the current in the gate of the driving cryotron has diminished appreciably from its initial value before the inductance of the output cryotron begins to change.

HYSTERESIS LOSS

In addition to joule heating, there can be another type of dissipation in a cryotron gate which also is re-

lated to the change of control inductance during switching. Not all gate films exhibit reversible transitions. Some have hysteresis in their gate resistance vs control current characteristics as shown in Fig. 6(a). Concurrently, there probably is hysteresis in the control flux vs control current characteristic as shown in Fig. 6(b), although this has not yet been observed, directly. As with any hysteresis phenomenon, the area inside the loop in Fig. 6(b) is the energy converted to heat in the material per traversal of the loop. One can readily evaluate this energy per unit length of gate.

$$E_h = \frac{1}{2}(l_c^n - l_c^*) (I_c^2 - I_d^2). \quad (34)$$

The size of the hysteresis loop depends on the grain structure of the film and hence upon the film thickness and temperature of the substrate during evaporation [12]. For a particular film the loop width varies with temperature. Fig. 7 shows some experimental values of the critical field for increasing field H_c and the critical field for decreasing field H_d as a function of reduced temperature for a typical indium gate film.³ This particular film was 4500 Å thick and exhibited sharp transitions at both H_c and H_d .

Using the same values for control inductance as before, one can obtain a rough estimate of how much energy loss is involved. Fig. 8 is a plot of the energy dissipation per cycle of operation per inch of gate length as a function of reduced temperature. A cycle of operation involves two current transfers. For purposes of comparison, twice the dissipation due to a single current transfer (in the absence of gate film hysteresis and output cryotron inductance changes) is shown by the upper horizontal line in Fig. 8. This line was calculated from the first term of (31) using $I_s=0.4$ a. It is not strictly correct since the supply current and loop inductance would vary somewhat with temperature. Similarly, twice the extra dissipation due to the control inductance change of the output cryotron [calculated from the second term of (31)] is shown by the lower horizontal line in Fig. 8.

One can see that gate film hysteresis loss may become appreciable below a reduced temperature of 0.9 and can be as high as 50 per cent of the total loss at a reduced temperature of 0.6. However, means may well be found to control the grain structure of films so as to greatly reduce hysteresis loss.

ENERGY FLOW IN A MULTIPLE CONTROL CRYOTRON

The energy flowing into the control terminals of a cryotron during the switching of its gate, in the absence of bias current and gate current, has been examined in detail. In addition, bias has been shown to have an important effect on stage delay. Consequently, the energy flow in a two-control cryotron undergoing switching will be evaluated next.

³ The author is indebted to A. E. Brennemann for this data (private communication).

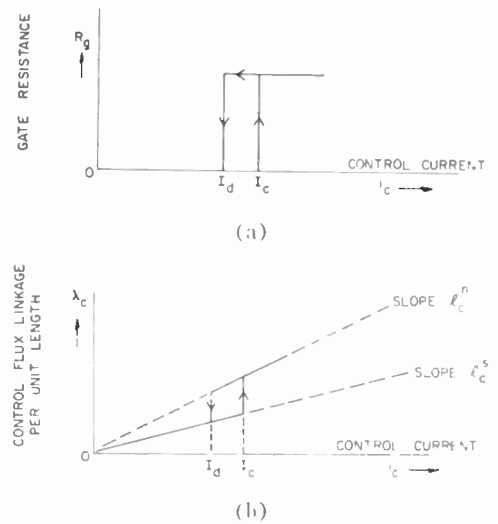


Fig. 6—Hysteresis in cryotron gate material. (a) Effect of hysteresis on gate resistance (small gate current). (b) Effect of hysteresis on control flux.

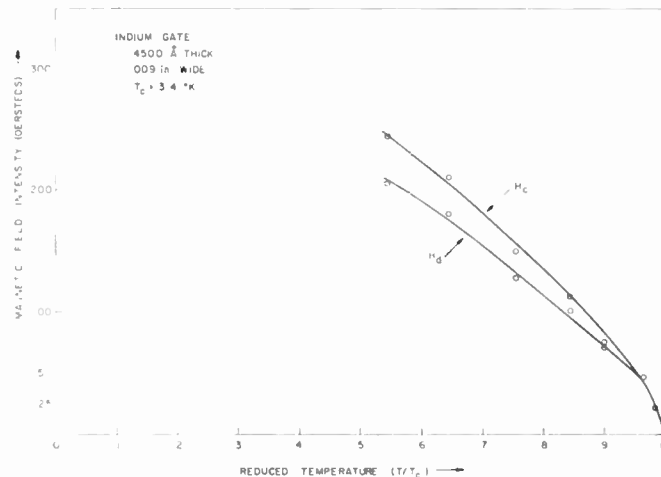


Fig. 7—Magnetic hysteresis in cryotron gate film as a function of reduced temperature.

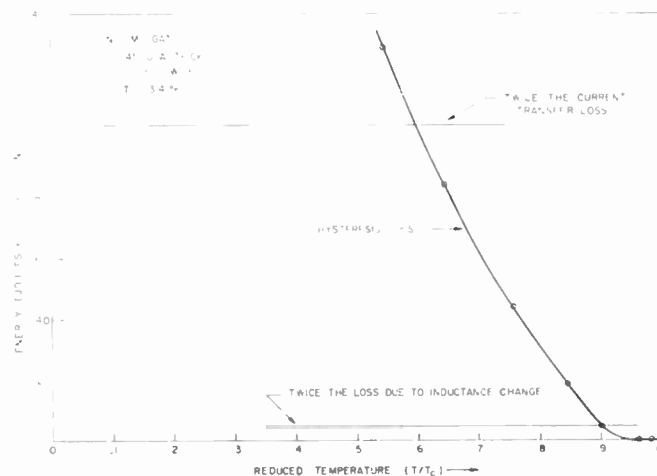


Fig. 8—Cryotron gate hysteresis loss as a function of reduced temperature.

Unfortunately, it will not be possible to take gate current into account. The reason is that the switching of a gate film in the presence of both gate current and applied field is not understood fully. The film tends to break up into an intermediate state of uncertain structure. Efforts to write free-energy equations on the basis of the classical London model lead to results which do not agree with experiment.⁴ Therefore, gate current will be neglected in the present analysis.

When the gate of a double control cryotron changes state the inductance matrix is altered in an interesting way [4].

$$[I^{n1} - I^n] = \Delta L \begin{bmatrix} (\Delta L_0/\Delta L) & \frac{1}{2} & \frac{1}{2} \\ \frac{1}{2} & 1 & 1 \\ \frac{1}{2} & 1 & 1 \end{bmatrix}. \quad (35)$$

The quantities ΔL and ΔL_0 are expressed in the Appendix in terms of dimensions and properties of materials. The first row and column of the matrix relate to the gate, the second to the control, and the third to the bias line. The self-inductance of the gate is clearly an exception to an otherwise orderly pattern. The quantity $\Delta L_0/\Delta L$ approaches 1/3 for gate thicknesses large compared with a penetration depth, vanishes for a gate thickness of three penetration depths, and is negative below three penetration depths. This unusual behavior will not cause problems in the present analysis because the gate current is assumed zero.

Two modes of operation of the cryotron under discussion are possible. The device may be biased in the superconducting state and driven resistive by a signal current in its control or, conversely, it may be biased in the resistive state and driven superconducting by a signal which opposes the bias.

In the first mode, it is assumed that the cryotron is biased at point 1 of Fig. 9 by a current $-I_{b1}$ in its bias line and is driven resistive by a current $-I_c + I_{b1}$ in its control line. Further assume that these currents are held constant during the switching.

The energy input at each set of terminals during switching can be evaluated by carrying out the integration.

$$\text{Energy input} = \int_{\lambda^n}^{\lambda^n} i d\lambda. \quad (36)$$

Furthermore, the change in stored field energy is readily evaluated from the inductance matrix since the energy is a state function [6] of the independent currents and flux linkages.

One finds that the net energy input again is twice the increase in stored field energy. The other half is converted into internal energy in the material. Part of the net energy input comes from the bias current source while the rest comes from the signal control current

source. Each source supplies a fraction of the total energy which is equal to the fraction of the critical control current which it carried during switching. Fig. 10 shows schematically the flow of energy in the structure as a result of super to normal switching.

If the gate is biased in the resistive state, as at point 2 in Fig. 9, and then driven superconducting by an opposing signal in its control, the situation is somewhat different. Both the field and the material give up energy so one might expect to find some of it coming out on the signal line. This might be advantageous but does not happen.

During the normal-to-super transition the bias line carries a negative current $-I_{b2}$ while the control carries a positive current $I_{b2} - I_c$. The unit of inductance change is $-\Delta L$ for a normal-to-super transition. The resulting energy flow is shown in Fig. 11. The arrows take care of the directions of energy flow so that ΔL is still a positive quantity.

If point 2 of Fig. 9 is as far into the normal region as point 1 is into the super region; *i.e.*, $I_{b2} - I_c = I_c - I_{b1}$; then just as much energy must be put into the cryotron control terminals to drive it normal-to-super as to drive it super-to-normal. The energy given up by the field and gate material plus the energy put in at the control terminals during the normal-to-super transition

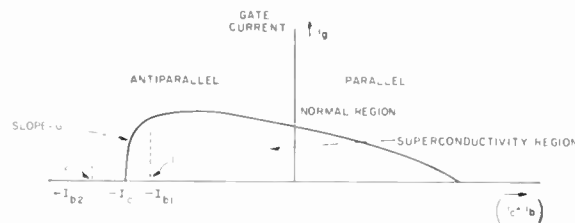


Fig. 9—Typical gain curve of an in-line cryotron.

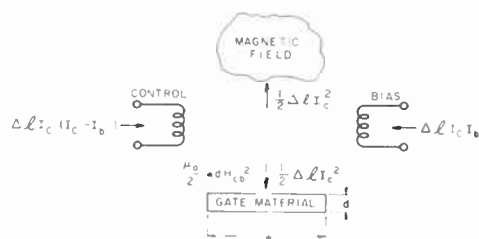


Fig. 10—Energy flow in two-control cryotron switched super-to-normal (no gate current).

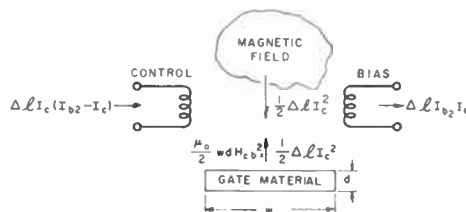


Fig. 11—Energy flow in two-control cryotron switched normal-to-super (no gate current).

⁴ Perhaps the more sophisticated Ginzburg-Landau theory can be employed to resolve this difficulty.

all emerges at the bias terminals and is fed back into the bias-current source.

The energy flow depicted in Figs. 10 and 11 is the reason that an output cryotron delays the driving circuit, irrespective of which leg of the circuit the cryotron is in and irrespective of whether it is driven super-to-normal or vice versa.

The operation shown in Fig. 11 suggests that some sort of an amplifier is possible. More energy comes out on the bias line than is put in on the control line. The field and material must then be "recharged," ready for the next cycle of operation.

EDDY CURRENTS

Thus far, eddy currents in the gate have been neglected. They cause additional switching delay and additional dissipation. One can obtain an idea of their effect by imagining the control of the cryotron of Fig. 1 to be subjected to a step of current of amplitude i_3 , where i_3 is larger than I_c as indicated in Fig. 3. Gate current, bias, and mutual coupling are to be neglected.

The cryotron moves instantaneously from point zero to point four of Fig. 3. The gate has had no time to switch so the flux has not increased beyond $I_c i_3$. Now, with the current constant at i_3 the flux builds up from point 4 to point 3 at a rate governed by the eddy currents until the system comes to rest at point 3. The stored field energy and internal energy of the gate material are the same as though the current had been increased slowly and the system had followed path 0123. However, the energy supplied by the current source in the case of the step exceeds that supplied during a slow build-up by the shaded area D . Consequently, D must represent the heat generated through the mechanism of eddy currents:

$$D = \frac{1}{2}(I_c^n - I_c^s)(i_3^2 - I_c^2). \tag{37}$$

Pippard [13] has studied in detail the propagation of a magnetic field through a semi-infinite superconducting solid. The surface field is assumed greater than the bulk critical field, penetration effects in the superconducting region are neglected, and a phase boundary between the normal and superconducting regions propagates into the superconductor with the field at this boundary equal to the bulk critical field.

According to Pippard's result, the time required for the boundary to propagate a distance x is

$$t = \mu_0 \sigma (x/2z)^2 \tag{38}$$

where σ is the conductivity in the normal phase and z is a function of the driving field such that

$$\sqrt{\pi} z \operatorname{Erf}(z) \exp(z^2) = \left(\frac{i_3}{I_c} - 1\right). \tag{39}$$

Expanding the left side of (39) in a power series one can show that

$$2z^2 \approx \frac{i_3}{I_c} - 1, \tag{40}$$

for

$$\frac{2}{3}z^2 \ll 1. \tag{41}$$

Subject to this approximation, the time of (38) becomes

$$t \approx \frac{\mu_0 \sigma}{2} x^2 \left(\frac{i_3}{I_c} - 1\right)^{-1}. \tag{42}$$

It is crude at best to apply these results to evaporated gate films. Penetration effects are not negligible. Critical fields are not constant but are known to increase toward infinity with diminishing thickness. Furthermore, the structure of the intermediate state probably is very complex and not much like Pippard's laminar model, particularly for thinner films. However, eddy currents undoubtedly play a role in the magnetic switching of gate films and application of the elementary theory to this problem sheds light on the nature of the operation.

Since the gate of a cryotron in the absence of gate current is subjected to an equal field on each face, it seems proper to consider two phase boundaries propagating toward the center with each one traveling a distance $x=d/2$, where d is the total thickness. Thus, one can perhaps estimate the order of magnitude of gate film switching time t_s from Pippard's theory as

$$t_s = \frac{\mu_0 \sigma d^2}{8} \left(\frac{i_3}{I_c} - 1\right)^{-1}. \tag{43}$$

Just to obtain a feeling for the order of magnitude of time involved, assume the same typical parameter values as before; namely,

$$\begin{aligned} i_3 &= 0.4 \text{ a,} \\ I_c &= 0.25 \text{ a,} \\ d &= 6000 \text{ \AA,} \\ \sigma &= (6 \times 10^{-10} \text{ ohm} - m)^{-1}. \end{aligned}$$

Substituting these values into (43) gives

$$t_s = 0.16 \text{ nsec.}$$

Such a short time seems completely negligible at first glance. Note, however, that t_s approaches infinity as i_3 falls toward I_c . In circuit operation the cryotron is not driven by a step from a current source. Instead, switching begins as soon as i_3 reaches I_c and the driving current i_3 may not rise appreciably above I_c during switching.

It is important to understand the relationship between the eddy current switching time t_s and the component switching time t_{12} calculated earlier. An expression for the component delay was derived on the basis of a quasi-static representation of the cryotron which neglected

eddy currents. The resulting delay was found to vary inversely with the internal impedance of the energy source causing the cryotron to switch. This component delay vanishes as the driving source becomes a current source with infinite internal impedance.

On the other hand, considering eddy currents, it becomes apparent that there is actually a delay t_s associated with the switching of the cryotron even when it is driven by a current source. In other words, the component switching time is adequately represented by the expression for t_{12} when the cryotron is driven by a very low impedance source and the switching is slow compared with t_s . As the impedance of the driver is raised, the component delay does not tend to vanish as the expression for t_{12} indicates but rather approaches t_s as a lower limit. Thus the effect of eddy currents is always to add to the component switching time and to set a lower limit on this delay.

INDUCTANCE CHANGE AND EDDY CURRENTS

In general, the retarding effects of inductance change and eddy currents should be treated simultaneously rather than separately.⁵ An approximate solution to the combined problem is very enlightening.

Consider the time interval during which the gate is changing state. Assume that the control current of the output cryotron in the circuit of Fig. 4(b) increases linearly with time at a rate proportional to the overdrive $I_s - I_c$. Thus

$$i_2 = I_c + \left(\frac{I_s - I_c}{a}\right)t, \tag{44}$$

where a is an unknown constant.

In addition, assume that the location of each interphase boundary is proportional to time. Therefore,

$$x = vt, \tag{45}$$

where v is some constant but unknown velocity.

These two assumptions, (44) and (45), are found to be compatible with Pippard's treatment of the eddy current constraint. Substituting them into (42)⁶ gives a relationship between a and v which is independent of time. The component switching time t_{12}' can, therefore, be expressed in terms of a . The result is

$$t_{12}' = \frac{d}{2} \left(\frac{\mu_0 \sigma a}{2K}\right)^{1/2}, \tag{46}$$

where

$$K = \frac{I_s - I_c}{I_c}. \tag{47}$$

⁵ This was first pointed out by Dr. W. B. Ittner, III in a private communication.

⁶ In (42), i_3 has been used for control current in order to agree with Fig. 3. In the present analysis, i_2 is used for control current to agree with Fig. 4(b).

During the switching interval, the control current is no longer constant and the loop voltage equation becomes [from Fig. 4(b)],

$$(I_s - i_2)R = L \frac{di_2}{dt} + L_c \frac{di_2}{dt} + i_2 \frac{dL_c}{dt}, \tag{48}$$

where

$$L = L_1 + L_2 + L_g^u + L_g^s. \tag{49}$$

The control inductance L_c changes during the switching interval by an amount which is small compared with the inductance of the rest of the loop L . Hence, L_c may be treated as nearly constant and the first two terms on the right side of (48) may be combined.

In addition, assume that the amount of control current change during the switching interval is small compared with the initial value I_c .

Under these conditions, the circuit constraint yields another relationship between switching time and the constant a :

$$t_{12}' = \frac{L_c^u - L_c^s}{RK} \left(1 - \frac{L_c^s}{Ra}\right)^{-1}. \tag{50}$$

If a is very large compared with the circuit time constant, so that i_2 does not change during switching, (50) reduces to (18).

For a given value of K , (46) and (50) now can be solved simultaneously for a and t_{12}' . This is done graphically in Fig. 12 for $K=0.6$, a value corresponding to $I_s=0.4$ a and $I_c=0.25$ a. Note that the component switching time is more than double the value calculated earlier neglecting eddy currents. This strongly suggests that eddy currents must be taken into account in any effort to predict accurately the switching speeds of fast cryotronic circuits.

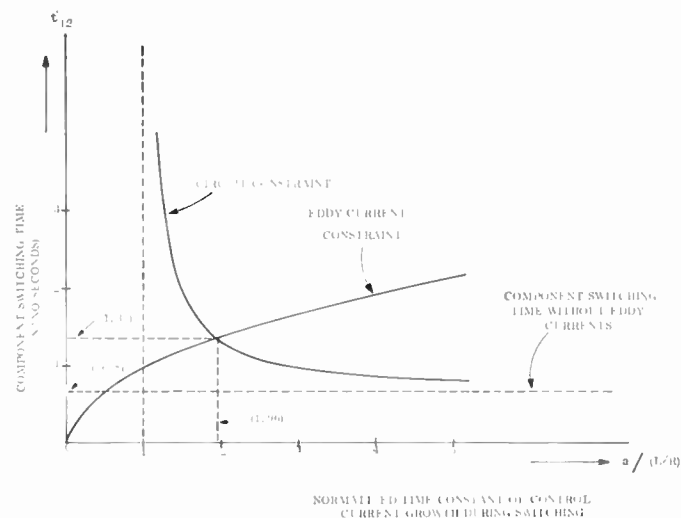


Fig. 12—Circuit and eddy current constraints on component switching time.

APPENDIX

This Appendix is intended to provide a ready reference for previously derived [4] inductance formulas applicable to a two-control, in-line cryotron. Typical dimensions and parameters are assumed in order to provide illustrative values.

The inductance matrix with the gate superconducting is

$$[L_s] = \frac{\mu_0}{\Pi} \begin{bmatrix} \textit{gate} & & & \\ (h_1 + b_0 + b_1) & (h_1 + b_0 + c_1) & & \\ (h_1 + b_0 + c_1) & (h_1 + h_2 + b_0 + b_2 + 2c_1) & (h_1 + h_2 + b_0 + 2c_1 + c_2) & \\ (h_1 + b_0 + c_1) & (h_1 + h_2 + b_0 + 2c_1 + c_2) & (h_1 + h_2 + h_3 + b_0 + b_3 + 2c_1 + 2c_2) & \end{bmatrix} \begin{matrix} \textit{gate} \\ \textit{control} \\ \textit{bias} \end{matrix}$$

where for convenience,

$$b_n (n = 1, 2, 3 \dots) = \beta_n^{-1} \coth \beta_n d_n,$$

and

$$c_n (n = 1, 2, 3 \dots) = \beta_n^{-1} \tanh (\beta_n d_n / 2).$$

The subscripts $n=0, 1, 2$ apply in sequence counting upward from the ground plane.

With the gate (conductor 1) in the normal state, the inductance matrix becomes

$$[L_{n1}] = \frac{\mu_0}{\Pi} \begin{bmatrix} \textit{gate} & & & \\ (h_1 + b_0 + d_1/3) & (h_1 + b_0 + d_1/2) & (h_1 + b_0 + d_1/2) & \\ (h_1 + b_0 + d_1/2) & (h_1 + h_2 + b_0 + b_2 + d_1) & (h_1 + h_2 + b_0 + d_1 + c_2) & \\ (h_1 + b_0 + d_1/2) & (h_1 + h_2 + b_0 + d_1 + c_2) & (h_1 + h_2 + h_3 + b_0 + b_3 + d_1 + 2c_2) & \end{bmatrix} \begin{matrix} \textit{gate} \\ \textit{control} \\ \textit{bias} \end{matrix}$$

Consequently, the change in inductance of the structure as a result of gate switching is

$$[L_{n1} - L_s] = \Delta I \begin{bmatrix} \textit{gate} & & \\ (\Delta I_g / \Delta I) & \frac{1}{2} & \frac{1}{2} \\ \frac{1}{2} & 1 & 1 \\ \frac{1}{2} & 1 & 1 \end{bmatrix} \begin{matrix} \textit{gate} \\ \textit{control} \\ \textit{bias} \end{matrix}$$

where

$$\Delta I = \frac{\mu_0}{\Pi} (d_1 - 2c_1)$$

$$\Delta I_g = \frac{\mu_0}{\Pi} \left(\frac{d_1}{3} - b_1 \right).$$

Assuming the following typical dimensions and parameters for illustrative purposes

$$\mu_0 = 4\pi \times 10^{-7} h/m$$

$$\Pi = 0.009 \text{ inch}$$

$$h_1 = h_2 = h_3 = 5000 \text{ \AA}$$

$$d_0 = d_1 = d_2 = d_3 = 6000 \text{ \AA}$$

$$\lambda_0 = \lambda_2 = \lambda_3 = 500 \text{ \AA}$$

$$\lambda_1 = 1500 \text{ \AA},$$

$$b_0 = b_2 = b_3 = 500 \text{ \AA}$$

$$b_1 = 1500 \text{ \AA}$$

$$c_0 = c_2 = c_3 = 500 \text{ \AA}$$

$$c_1 = 1446 \text{ \AA}.$$

Consequently,

$$[L_s] = 10^{-10} \frac{h}{\text{in}} \begin{bmatrix} \textit{gate} & \textit{control} & \textit{bias} \\ .978 & .970 & .970 \\ .970 & 1.94 & 1.94 \\ .970 & 1.94 & 2.78 \end{bmatrix} \begin{matrix} \textit{gate} \\ \textit{control} \\ \textit{bias} \end{matrix}$$

$$[L_{n1}] = 10^{-10} \frac{h}{\text{in}} \begin{bmatrix} \textit{gate} & \textit{control} & \textit{bias} \\ 1.05 & 1.19 & 1.19 \\ 1.19 & 2.37 & 2.37 \\ 1.19 & 2.37 & 3.21 \end{bmatrix} \begin{matrix} \textit{gate} \\ \textit{control} \\ \textit{bias} \end{matrix}$$

$$[L_{n1} - L_s] = 10^{-10} \frac{h}{\text{in}} \begin{bmatrix} \textit{gate} & \textit{control} & \textit{bias} \\ .0698 & .217 & .217 \\ .217 & .434 & .434 \\ .217 & .434 & .434 \end{bmatrix} \begin{matrix} \textit{gate} \\ \textit{control} \\ \textit{bias} \end{matrix}$$

ACKNOWLEDGMENT

The author wishes to acknowledge the stimulation of Dr. W. B. Ittner, III, Dr. H. Sobol, A. E. Brennemann, and T. H. Cheng.

REFERENCES

- [1] V. L. Newhouse, J. W. Bremer, and H. H. Edwards, "An improved film cryotron and its application to digital computers," *Proc. IRE*, vol. 48, pp. 1395-1404; August, 1960.
- [2] D. R. Young, "Recent developments in high speed superconducting devices," *Brit. J. Appl. Phys.*, vol. 12, pp. 359-000; August, 1961.
- [3] R. B. DeLano, Jr., "Edge effects in superconducting films," Office of Naval Res. Symp. Rept. No. ACR-50, Washington, D. C., May, 1960.
- [4] N. H. Meyers, "Inductance in thin-film superconducting structures," *Proc. IRE*, vol. 49, pp. 1640-1649; November, 1961.
- [5] D. Schoenberg, "Field dependence of λ ," in "Superconductivity," Cambridge University Press, Cambridge, England, 2nd ed., pp. 161-161; 1952.
- [6] D. C. White and H. H. Woodson, "State functions," in "Electromechanical Energy Conversion," John Wiley and Sons, Inc., New York, N. Y., pp. 38-55; 1959.
- [7] D. A. Buck, "A magnetically controlled gating element," *Proc. Eastern Joint Computer Conf.*, T-92, pp. 47-50; December 10-12, 1956.
- [8] D. Schoenberg, "Differences of thermodynamic functions," in "Superconductivity," Cambridge University Press, Cambridge, England, 2nd ed., pp. 56-58; 1952.
- [9] W. B. Ittner, III, "Superconducting to normal phase transition in tantalum," *Phys. Rev.*, vol. 111, pp. 1483-1487; September, 1958.
- [10] F. London, "Phase transition of thin superconducting films," in "Superfluids," Dover Publications Inc., New York, N. Y., vol. 1, 2nd ed., p. 130; October, 1960.
- [11] N. H. Meyers, "Electrical switching-speed considerations in a simple thin-film superconducting circuit," Project Lightning, Sixth Quart. Progress Rept. Armed Services Technical Information Agency (ASTIA), Washington, D. C., vol. 11, Appendix A, p. 107; October, 1960.
- [12] M. E. Behndt, R. H. Blumberg, and G. R. Giedd, "On the influence of aggregation on the magnetic phase transition of evaporated superconducting thin films," *IBM J. Res. & Dev.*, vol. 4, p. 184; April, 1960.
- [13] A. B. Pippard, *Phil. Mag.*, vol. 41, p. 243; 1950.

Properties of 400 Mcps Long-Distance Tropospheric Circuits*

J. H. CHISHOLM†, W. E. MORROW, JR.†, MEMBER, IRE, B. E. NICHOLS†, MEMBER, IRE,
J. F. ROCHE‡, MEMBER, IRE, AND A. E. TEACHMAN§, SENIOR MEMBER, IRE

Summary—Measurements are reported on beyond-the-horizon propagation losses at 400 Mcps. Data are given on the losses and their variations from 98 to 830 mi beyond the horizon. The transmission loss between isotropic antennas varies from about 190 db at 100 mi to about 300 db at 800 mi distance. Also described are measurements of frequency-selective fading, space diversity, and variations in the angle of arrival of the signals.

INTRODUCTION

BEGINNING IN 1953, the Massachusetts Institute of Technology Lincoln Laboratory has conducted an extensive program of UHF tropospheric propagation research designed to investigate the feasibility of long-range transhorizon communications systems. During the course of this program, measurements were obtained over paths ranging from 98 to 830 mi in length, utilizing a series of receiving sites along the eastern coastal region of the United States. In addition, a cooperative program was undertaken with the U. S. Naval Research Laboratory in which a shipborne receiving terminal was utilized to obtain over-

water measurements in the North Atlantic area by continuous measurements out to 734 mi for several days in the winter and summer seasons. It is believed that these data, which include more than 16,000 hr of measurements, have established a definite pattern of propagation characteristics at extreme ranges that were not indicated by current theoretical models or by extrapolation from existing data obtained by measurements over paths a few hundred miles in length. In addition to signal level measurements, a variety of experiments were performed to investigate the performance of large high-gain antenna systems and the limitations imposed by the long-range propagation mechanism pertinent to the design of tropospheric communications systems intended to operate over distances from 400 to possibly 800 mi.

TEST TRANSMISSION PATHS

Fig. 1 shows a map of the various paths over which measurements were made. The principal transmitting facilities were located at the M.I.T. Round Hill field station in South Dartmouth, Mass. The receiving site at Riverhead, L. I., N. Y., was operated jointly with RCA Laboratories. At Holmdel, N. J., the facilities were located at Bell Telephone Laboratories' Crawford Hill Site. At Red Bank, N. J., the installation was lo-

* Received November 29, 1961; revised manuscript received, August 6, 1962.

† Lincoln Laboratory, Massachusetts Institute of Technology, Lexington, Mass. Operated with support from the U. S. Army, Navy, and Air Force.

‡ Sylvania Electronics Systems Division, Amherst, N. Y.

§ Jansky and Bailey, Washington, D. C.

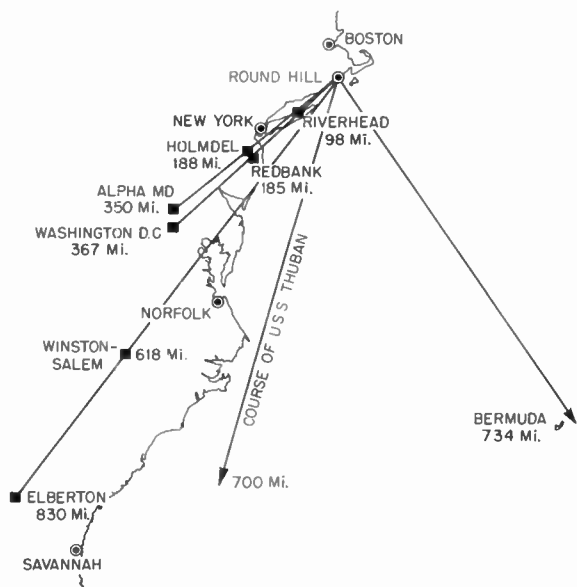


Fig. 1—Paths used for experimental UHF tropospheric propagation measurements. The transmitters were located at the M.I.T. Lincoln Laboratory Round Hill Field Station, S. Dartmouth, Mass.

ated at the U. S. Army Signal Corps' Coles Signal Laboratory. The Navy Department provided the U.S.S. *Achernar* for the summer overwater tests and the U.S.S. *Thuban* for the winter tests. Personnel and equipment for this joint program were provided by the Naval Research Laboratory and Lincoln Laboratory. In the latter part of the program, measurements were also made over a 640-mi path utilizing a developmental military communications system [AN/FRC-47(XD-1)] employing sites at Sauratown Mountain near Winston-Salem, N. C. and at Millstone Hill, Westford, Mass.

EQUIPMENT AND FACILITIES

A group of the antennas used for transmissions from Round Hill during the course of these experiments is shown in Fig. 2. In the center rear of this group is shown the 60-ft paraboloidal antenna which is steerable in elevation and azimuth. This antenna was connected to a 50-kw, 400-Mc CW klystron transmitter. The transmitting antennas were at heights varying from 60 to 113 ft above mean sea level and were oriented in a southeasterly direction over an open water foreground.

A view of the 28-ft and 60-ft diameter antennas at the Winston-Salem site is shown in Fig. 3. The 60-ft diameter antenna had a triple feed system which allowed the beams to be set at various angular positions by lateral and vertical movements of the feed assembly. A photograph of the moving assembly mechanism of this feed system is shown in Fig. 4.

The most distant receiving terminal was located at Elberton, Ga., which is about 830 mi from Round Hill. A view of this receiving site is shown in Fig. 5. The terrain in the foreground of the antenna has a downward slope resulting in an effective antenna height of approximately 150 ft above the average terrain in the first two miles in the direction of Round Hill.

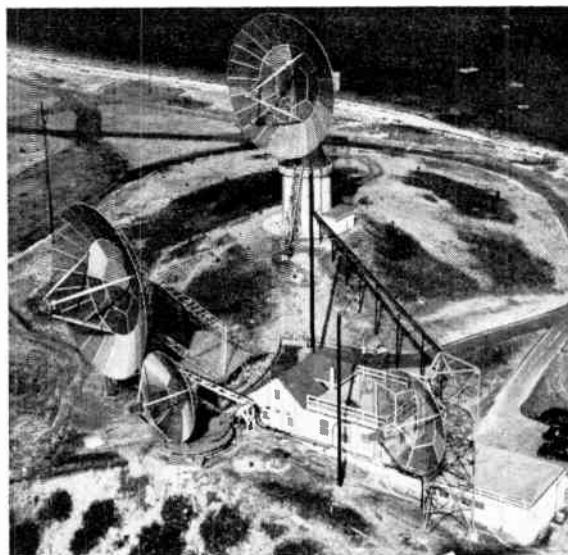


Fig. 2—The array of fixed and rotating antennas, 28 ft and 60 ft in diameter, which was used for UHF transmissions from M.I.T. Field Site at Round Hill, South Dartmouth, Mass.

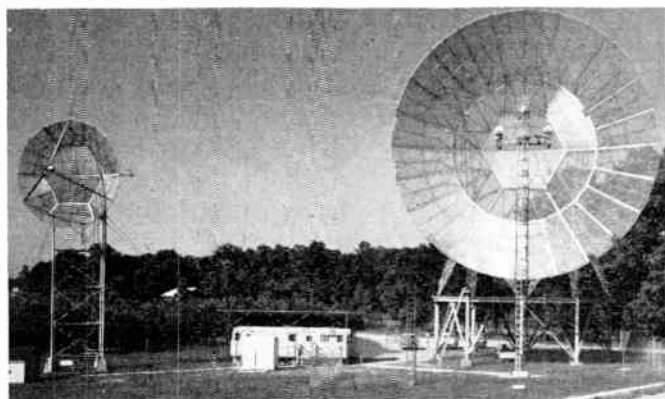


Fig. 3—Photograph of the Winston-Salem, N. C., receiving site showing the 28-ft and 60-ft diameter paraboloidal antennas.

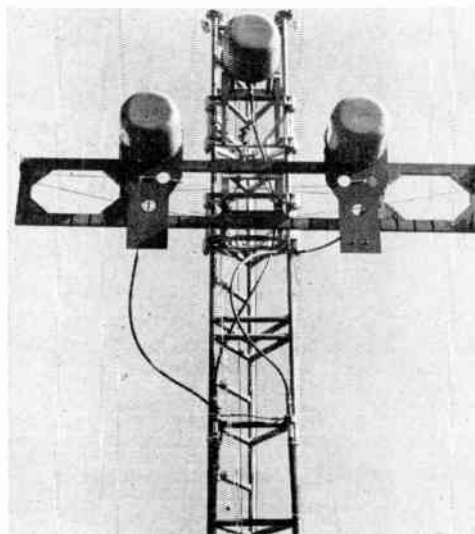


Fig. 4—Photograph of the triple feed assembly used at the Winston-Salem and Elberton receiving terminals. (The individual feeds and the horizontal supporting arm were adjustable from the ground by means of a cable and pulley system.)

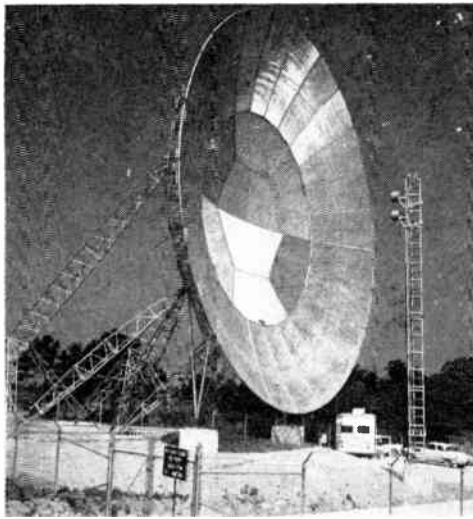


Fig. 5— Photograph of most distant receiving terminal located at Elberton, Ga.

A view of the receiving and recording equipment installed at Winston-Salem is shown in Fig. 6. Similar equipment was employed at the site located at Elberton Ga. Dual receiving facilities were incorporated in each terminal to permit simultaneous reception on either two separated antennas or two separate frequencies.

All the equipment was attended twenty-four hours a day, and calibrations were checked at hourly intervals. The block diagram of Fig. 7 shows a typical receiving system with signal level recording equipment. The recording equipment consisted of modified Gates signal level distribution recorders, Esterline Angus chart recorders, and Edin high speed chart recorders. Amplitude calibration was obtained from a laboratory-constructed, crystal-controlled signal generator which was highly stable in frequency and well shielded to permit calibration for extremely low signal levels. The over-all maximum frequency deviation for the transmitters and the receivers was generally less than 10 cps for periods of several hours, thus making it possible to use receivers with bandwidths of 100 cps.

Signal level distribution recorders were used in most instances. In some cases (particularly for weak signals), it was necessary to use Esterline Angus chart recorders with an integration capacitor connected across the AGC circuit. The time constant was variable from six to twelve seconds. Hourly median values were obtained from the signal level distribution recorders or scaled from the Esterline Angus charts in some cases of low signal level. Edin chart recorders, capable of recording up to 40 cps, were used to study short-term fading characteristics.

The transmissions from Sauratown Mountain to Millstone Hill at 399 Mc were made by means of 120-ft antennas and a 20- to 30-kw (CW) transmitter, which are components of the AN/FRC-47(XD-1) tropospheric scatter radio system. A view of the Millstone Hill terminal is shown in Fig. 8.

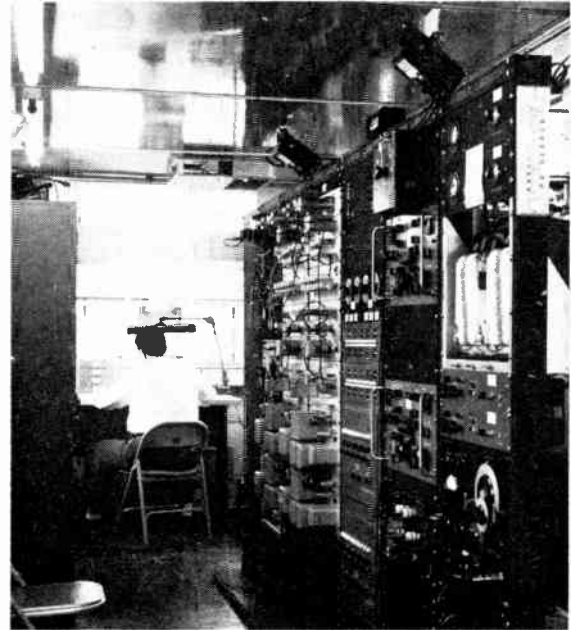


Fig. 6—View of dual receiving and recording equipment installed at the Winston-Salem site.

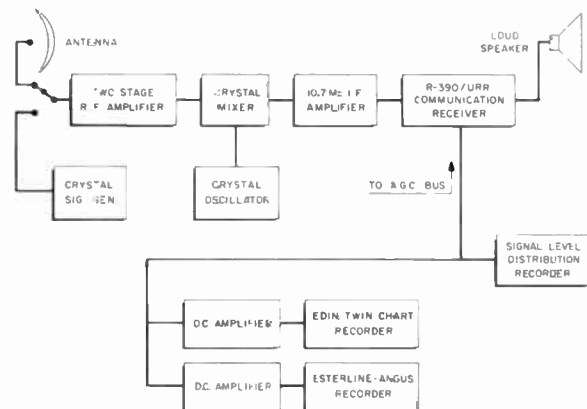


Fig. 7—Block diagram of signal level recording system.



Fig. 8—A view of the Millstone Hill, Westford, Mass., terminal of the AN/FRC-47(XD-1) tropospheric scatter system.

SIGNAL LEVEL AS A FUNCTION OF DISTANCE

One of the primary purposes of the program of measurements was to determine the attenuation of the signal strength as a function of distance from the transmitter. The levels of signals received over paths of 98 to 830 mi at 412 to 417 Mc have been analyzed to provide information which would indicate the limit of the range of communications systems, as well as provide information about the nature of the mechanism which might be useful to confirm or to indicate modifications of proposed theoretical models. In order that the results of these measurements may be presented in a convenient manner for both of these purposes, the data are shown in terms of equivalent path loss between isotropic antennas (assuming free space gains are realized) and also in terms of signal level relative to that which would be obtained under free space conditions.

System path loss is determined from the following relationship:

$$\text{path loss } L_p = \frac{P_T G_T G_R}{P_R}$$

where P_T is transmitter power (watts) G_T is the gain of the transmitting antenna referred to an isotropic radiator, and G_R is the gain of the receiving antenna referred to an isotropic radiator.

Results of measurements at 400 Mc for a yearly period over distances ranging from 98 to 618 mi are shown in Fig. 9 for a range of percentile values. Only the median value of signals received at the 830-mi distance is shown. These data indicate the following attenuation rates obtained from the yearly median values in the indicated range intervals:

Range (mi)	Attenuation rate (db/mi)
90-180	0.22
180-350	0.18
350-630	0.11
630-840	0.20

The increase in attenuation rate at distances beyond 600 mi indicates that highly reliable ground point-to-point communications systems intended to operate over paths much longer than 600 mi will become rapidly more expensive with increasing distance.

Several theoretical models predict decreases in the rate of attenuation with distance¹⁻³ rather than a constant rate of attenuation vs distance. The attenuation rate measured in these experiments for the range from 600 to 800 mi is almost twice that observed at the 400 to 600 mi range. These data indicate that extrapolation of levels obtained at shorter distances by curve fitting methods would predict signals substantially higher at distances in excess of 600 mi than the levels

¹ H. G. Booker and W. E. Gordon, "A theory of radio scattering in the troposphere," Proc. IRE, vol. 38, pp. 401-412; April, 1950.

² W. E. Gordon, "Radio scattering in the troposphere," Proc. IRE, vol. 43, pp. 23-28; January, 1955.

³ K. A. Norton, "Point-to-point radio relaying via the scatter mode of tropospheric propagation," IRE TRANS. ON COMMUNICATIONS SYSTEMS, vol. CS-4, pp. 39-49; March, 1956.

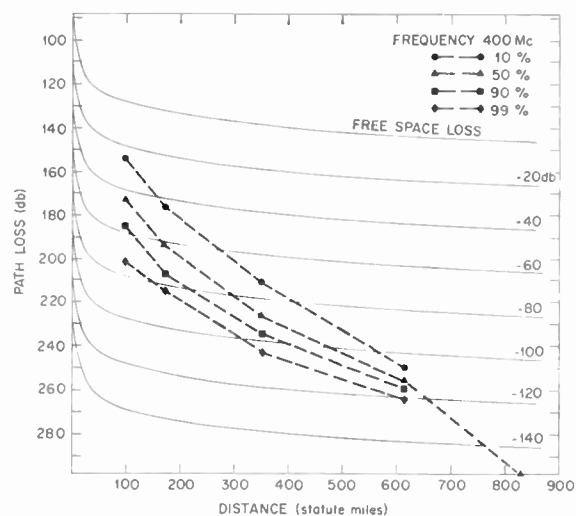


Fig. 9—Variation in signal level as a function of distance from the transmitter.

actually observed in these experiments. It is believed that further theoretical study and perhaps modifications of existing models will be required to predict adequately the propagation of radio signals at these extreme ranges.

A comparison of the signal level variation as a function of distance from the transmitter observed over water was made with the levels measured over land. The overwater data were obtained in a series of ship-to-shore measurements and are reported in more detail in a paper published in 1958 by Dinger *et al.*⁴ The comparison of the data obtained over a land path and over a water path is shown in Fig. 10. The squares connected by solid lines indicate the monthly median values for overland paths under wintertime conditions, and the closed circles indicate hourly medians of the overwater measurements for two round trips of shipborne measurements made in January and February, 1956. Although the general slope of the attenuation curves over both land and water are in fair agreement, the overwater paths indicate a signal level for these two runs which is about 6 db higher than that observed over land during the winter periods. The difference in the levels observed over water and the levels observed over land may be attributed in part to the difference in the foreground of the receiving antennas used on overland and overwater paths. In addition, the small size of the statistical samples resulting from two overwater runs out to 750 mi must be taken into consideration in evaluating the difference in observed signal strength on an overwater path vs the long-term data obtained on the overland paths. A third factor to be considered is the milder temperatures encountered at the more distant portions of the overwater path in the Gulf Stream region.

⁴ H. E. Dinger, W. E. Garner, D. H. Hamilton and A. E. Teachman, "Investigation of long-distance overwater tropospheric propagation at 400 MC," Proc. IRE, vol. 46, pp. 1401-1410; July, 1958.

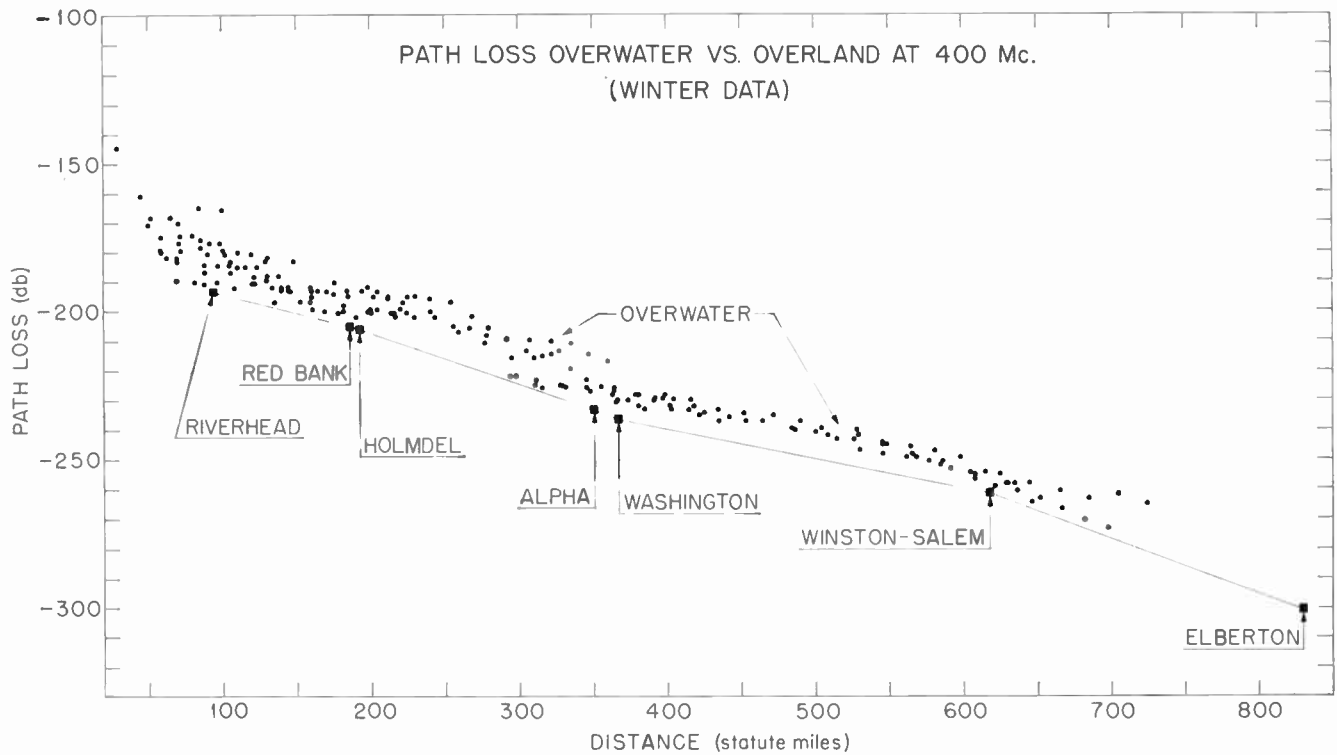


Fig. 10—Variation in signal level as a function of distance from the transmitter for overwater and overland paths under wintertime conditions.

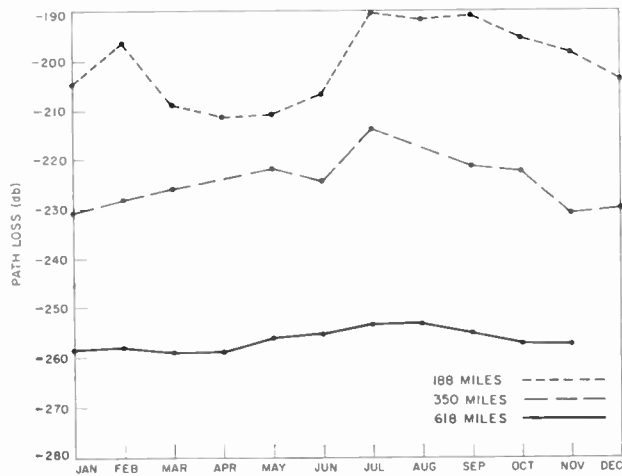


Fig. 11—Seasonal variation of monthly median values of signal level at 400 Mc.

One of the interesting features of the long-term measurements on the 618-mi path is the small seasonal variation as contrasted to the much larger variations observed over shorter paths. The cyclic seasonal variation of the signal levels is shown in Fig. 11 which shows the monthly median values of received signals observed at distances of 188, 350, and 618 mi over a complete seasonal cycle. It can be seen that the difference between maximum and minimum monthly median values is greatest at the shorter distances. At the greatest distance there is less than 6-db difference between the maximum and minimum monthly median values.

MONTHLY AND SHORT-TERM SIGNAL VARIATIONS

The distribution of hourly median values for an individual month also shows a definite variation with distance. The curves shown in Fig. 12 indicate the distributions of hourly median values of signal level received during January, 1956, over paths 98, 188, 350, and 618 mi in length. These distributions indicate a definite trend toward a smaller variation in the hourly median values between the 10 and 90 percentiles at 618 mi than that observed at 98 and 188 mi.

During the summer season, the differences between the hourly median values of signal level observed 10 per cent and 90 per cent of the time at 188 mi, compared to the variation observed at 618 mi, is even more marked as shown in the curves of Fig. 13. There is some evidence of enhanced conditions even at the longer 618-mi distance as indicated by the sharp upturn in the distribution curve between the 10 percentile and the 1 percentile values.

The signals received over distances far beyond the radio horizon were generally found to be Rayleigh distributed when sampling periods of about one hour's duration were used. Typical distributions of signals received over paths of 188, 350, and 618 mi are shown in Fig. 14. These data were obtained during the period 0500 to 0550 EST on January 23, 1957, which was a period representative of wintertime conditions. The effect of summertime enhancements are indicated in Fig. 15 which contains distributions of signals received during the month of June for paths of 188, 350, and 618

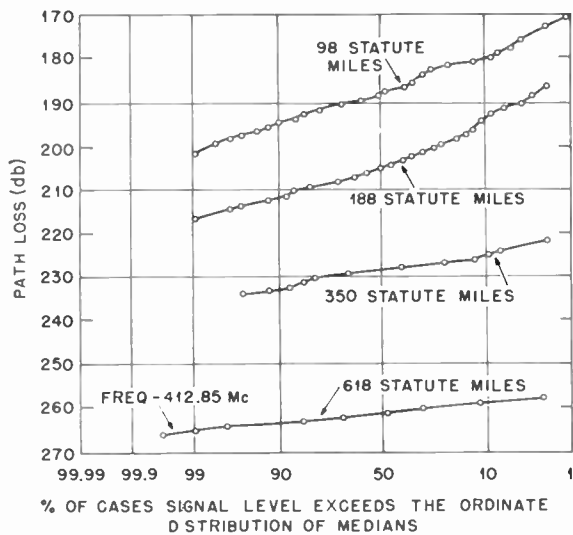


Fig. 12—Distributions of hourly median values observed at 400 Mc over paths 98 to 618 mi during a typical winter month.

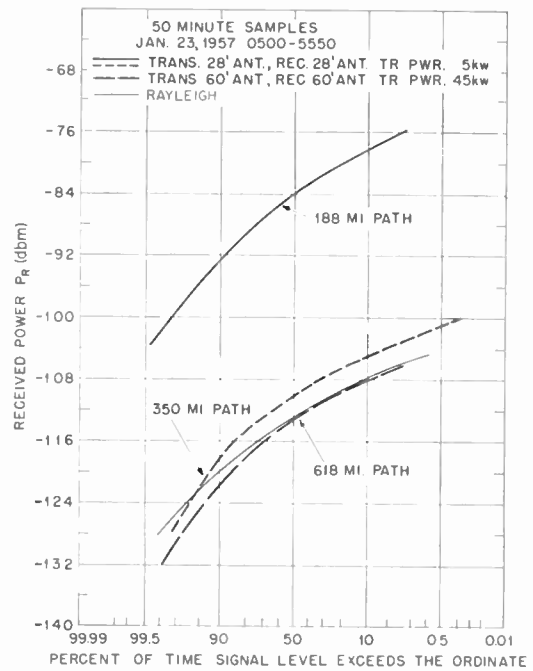


Fig. 14—Distributions of signal level observed for a 50-minute sampling period under typical winter conditions.

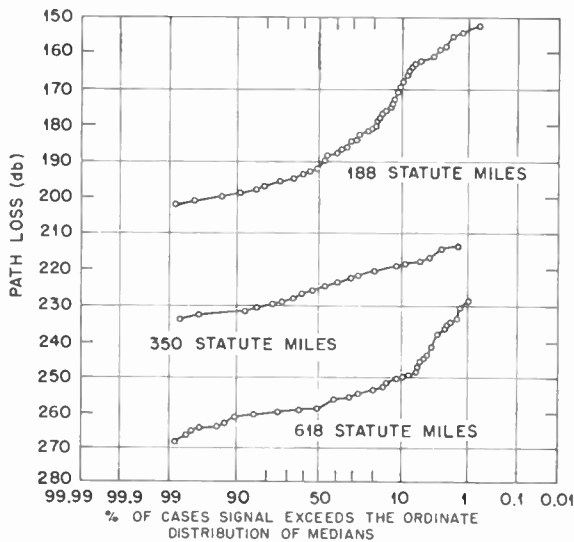


Fig. 13—Distributions of hourly median values observed at 400 Mc over paths 188 to 618 mi during a typical summer month.

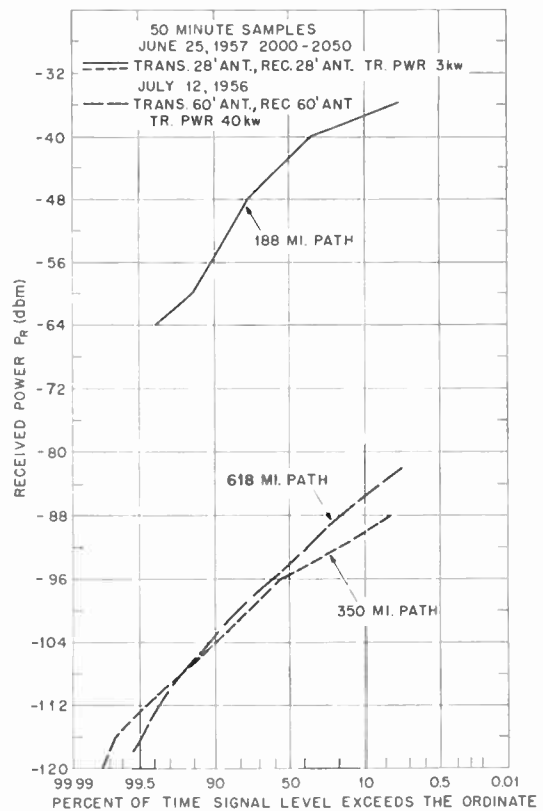


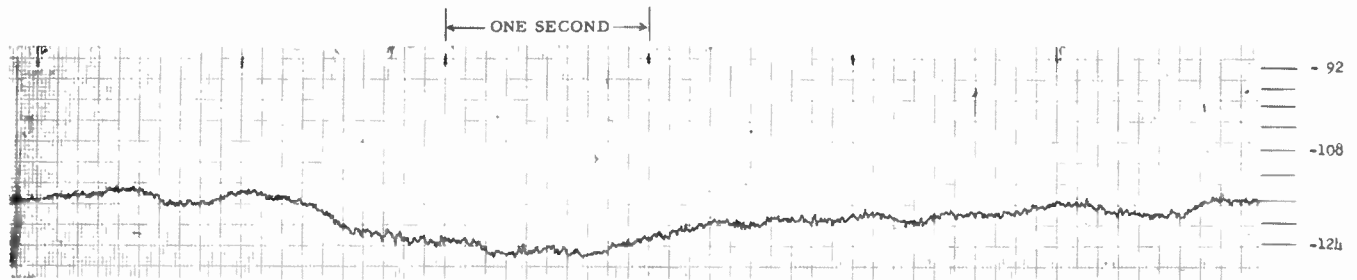
Fig. 15—Distributions of signal level observed for a 50-minute sampling period under typical summer conditions.

mi in length and show a greater departure from a Rayleigh distribution.

Although there is very little difference in the distributions of signal amplitude within the hourly periods observed at various distances, observations of samples of data recorded at fast chart speeds indicate an appreciable difference in the rate of fading for each path length. Typical samples indicating the fading observed at 188, 350, and 618 mi are shown in Fig. 16(a)–(c). An analysis of 30 samples of ten- to twelve-minute duration and evenly distributed through the January to July period indicates the following median fading rates at the indicated distances:

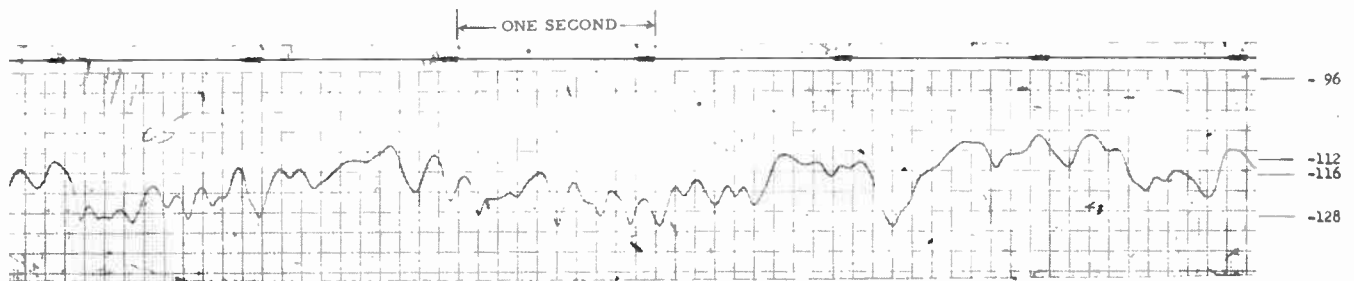
188 mi	0.1 cps
350 mi	0.4 cps
618 mi	0.2 cps.

There appears to be little difference in the fading rate at the 618-mi distance between a system using receiving antennas 60 ft in diameter and a system using antennas



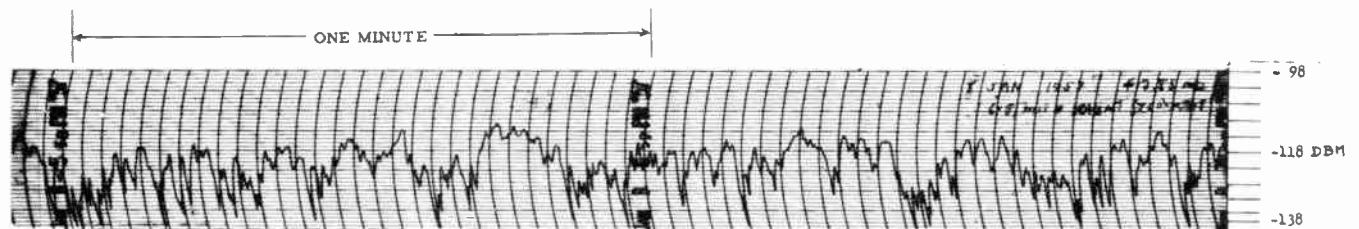
188 MILE PATH
417.05 MCPS
TRANS. 28' - RECV. 28'
FAST CHART SPEED 50MM/SEC.
6 SECOND SAMPLE
JAN. 8, 1957 TIME: 1957

(a)



350 MILE PATH
417.05 MCPS
TRANS. 28' - RECV. 28'
FAST CHART SPEED 50MM/SEC.
6 SECOND SAMPLE
JAN. 8, 1957 TIME: 1957

(b)



618 MILE PATH
412.85MCPS
TRANS. 60' - RECV. 28'
CHART SPEED: 25 MM/SEC.
TWO MINUTE SAMPLE
JAN. 8, 1957 TIME: 1758

(c)

Fig. 16—(a) Example of fading of signal observed over a 188-mi path at 400 Mc under typical winter conditions. (b) Example of fading of signal observed over a 350-mi path at 400 Mc under typical winter conditions. (c) Example of fading of signal observed over a 618-mi path at 400 Mc under typical winter conditions.

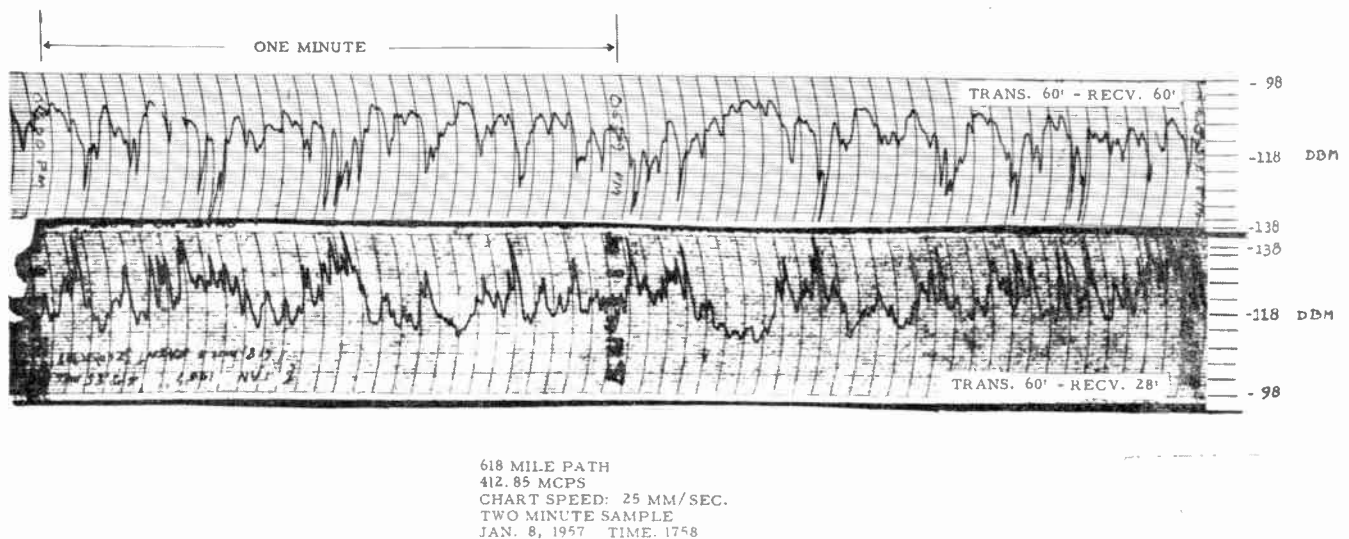


Fig. 17— Comparison of fading of 400-Mc signals received at 618 mi on a 28-ft and a 60-ft antenna.

28 ft in diameter. Fig. 17 shows a comparison of the fading observed on signals received over the 618-mi path obtained with the 28 ft and 60-ft diameter receiving antennas.

A more precise evaluation of the fading is obtained by computation of the autocorrelation function of samples of fading data 10 min or greater in duration. The autocorrelation functions for lag times out to 100 sec are shown in Fig. 18(a)–(c) on the next page. In order to show the details of the autocorrelation function in the neighborhood of the origin, portions of these same curves are shown in Fig. 19(a)–(c) with an expanded scale for the first ten seconds of lag time. Similarly, the autocorrelation functions were computed from data obtained over the 618-mi path using antennas 28 ft in diameter and 60 ft in diameter for both transmission and reception over the same path. Little difference is indicated for the differing size of antennas as shown by the curves in Fig. 20.

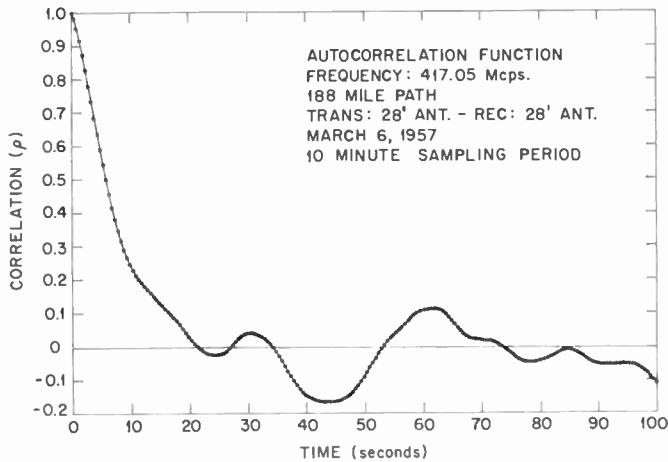
Further evidence of the effect of the size of the antennas on the rate of fading over a 618-mi path was obtained by comparing a signal received on a 60-ft antenna with that received on a small coaxially mounted corner-reflector antenna. The results of these measurements, as shown in Fig. 21, indicated very little difference in the fading of the signal received on the corner-reflector antenna with that received on the large 60-ft antenna.

The similarity of the fading observed on these two antennas, widely different in the sizes of their apertures, suggests that the effective angles of arrival of the signals propagated over the 618 mi are largely confined to angular dimensions equal to or less than the beamwidth of the 60-ft diameter antenna. (Half-power beamwidths $\approx 2.6^\circ$.)

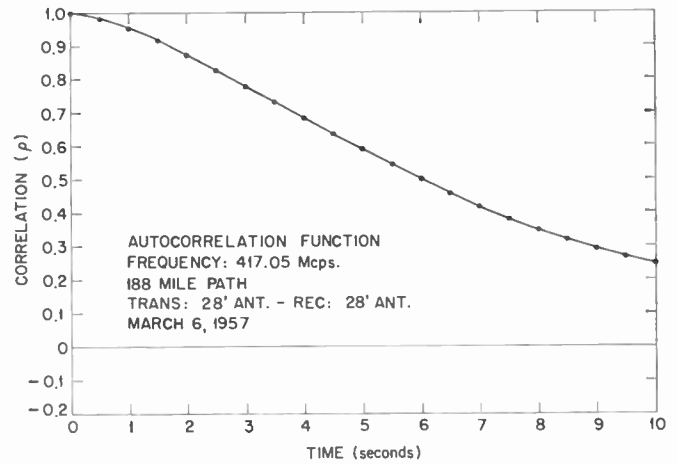
Measurements were also made to investigate the effect on the fading when the antennas were oriented off the great circle path. Using two feed horns with the 60-ft receiving antenna, two 2.8° beams were produced which could be directed by movement of each of the horns. In the first series of these measurements, the transmitting antenna was oriented along the great circle bearing and the two receiving beams were oriented $\pm 3^\circ$ off-path. The results indicated that the amplitude was about 16 db less for these positions than when the receiving antenna was oriented on the great circle path. An increase in the fading rate was also observed. It appeared that there was little correlation between the amplitude received on either beam for this antenna configuration.

Further measurements were made in which the transmitting and receiving antennas were moved off-path in azimuth by the same amount. The results of these measurements are shown in Fig. 22(a)–(c). A sample of the signals received for a two-minute period for both antennas oriented on course is shown in Fig. 22(a). The results of azimuthal movement of the beams off the path are shown in Fig. 22(b) and are characterized by a substantial increase in fading as well as a reduction in signal strength. Similar experiments were performed for angular movement of both transmitting and receiving antennas in elevation and the results are shown in Fig. 22(c) and indicate a less pronounced increase in fading. This pattern of variation of fading for angular movement in elevation and azimuth is similar to that observed at 3670 Mc over a much shorter path of 188 mi with highly directive antennas.⁵

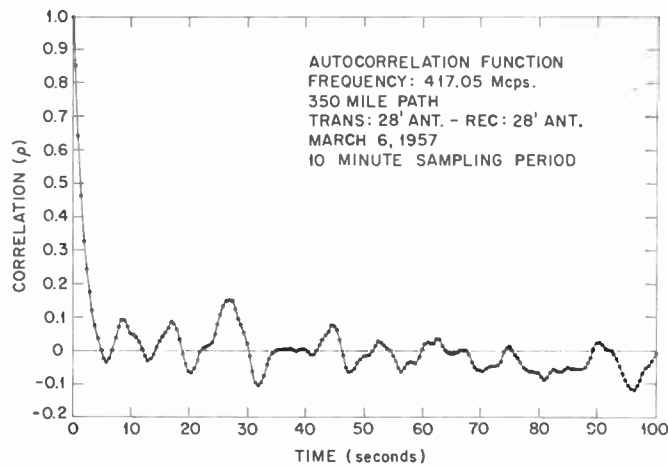
⁵ J. H. Chisholm, P. A. Portmann, J. T. DeBettencourt and J. F. Roche, "Investigations of angular scattering and multipath properties of tropospheric propagation of short radio waves beyond the horizon," Proc. IRE, vol. 43, pp. 1317–1335; October, 1955.



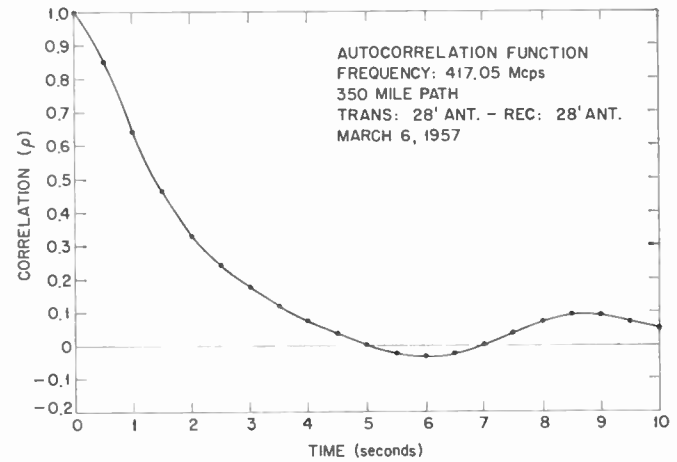
(a)



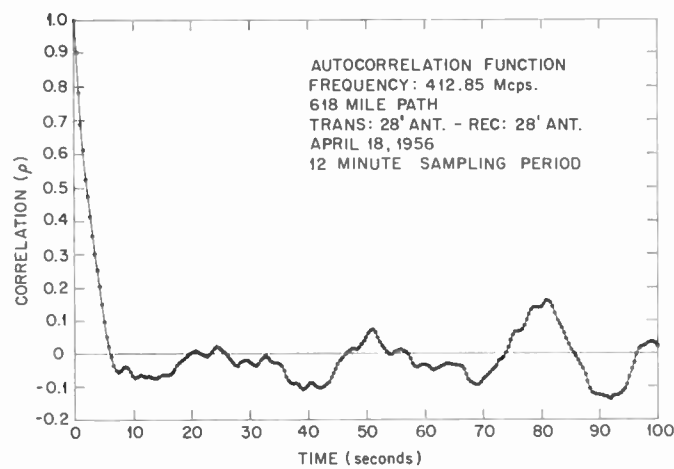
(a)



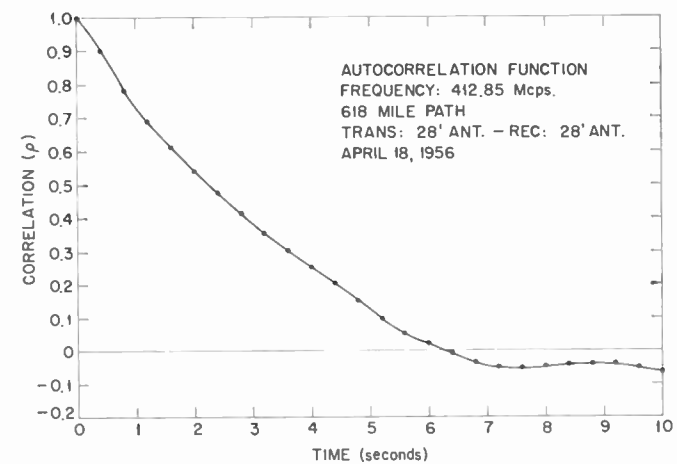
(b)



(b)



(c)



(c)

Fig. 18—Autocorrelation functions of fading of 400-Mc signals received over paths. (a) At 188 mi. (b) At 350 mi. (c) At 618 mi.

Fig. 19—Details of autocorrelation functions near the origin. (a) 188 mi. (b) 350 mi. (c) 618 mi.

Fig. 20 (left)—Autocorrelation functions of fading of 400-Mc signals received over a 618-mi path on systems using 28-ft antennas transmitting and receiving and using 60-ft antennas transmitting and receiving.

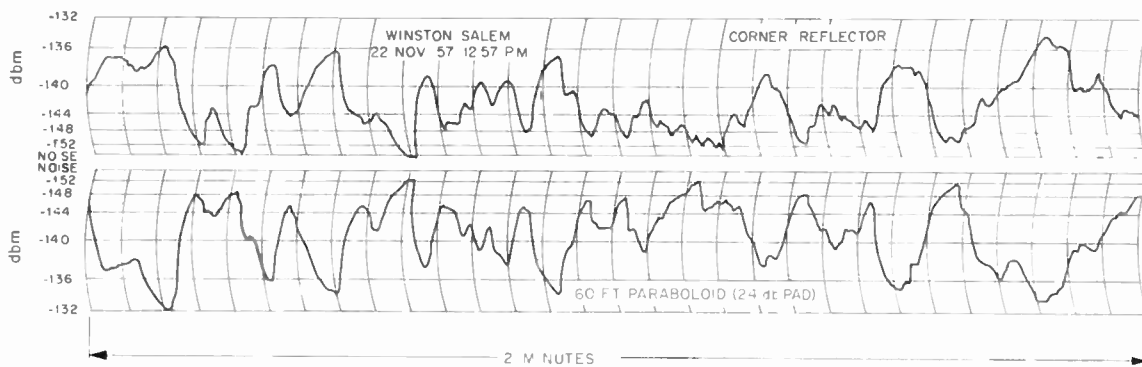
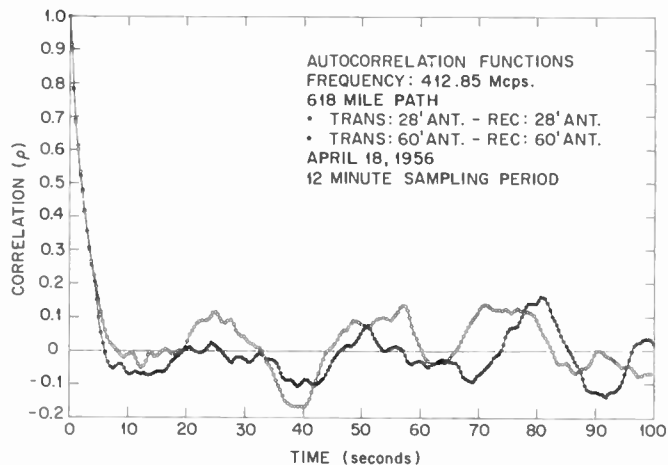


Fig. 21—Comparison of fading of 400-Mc signals received over 618-mi path on a 60-ft paraboloidal antenna and a small corner-reflector antenna mounted coaxially with the paraboloid.

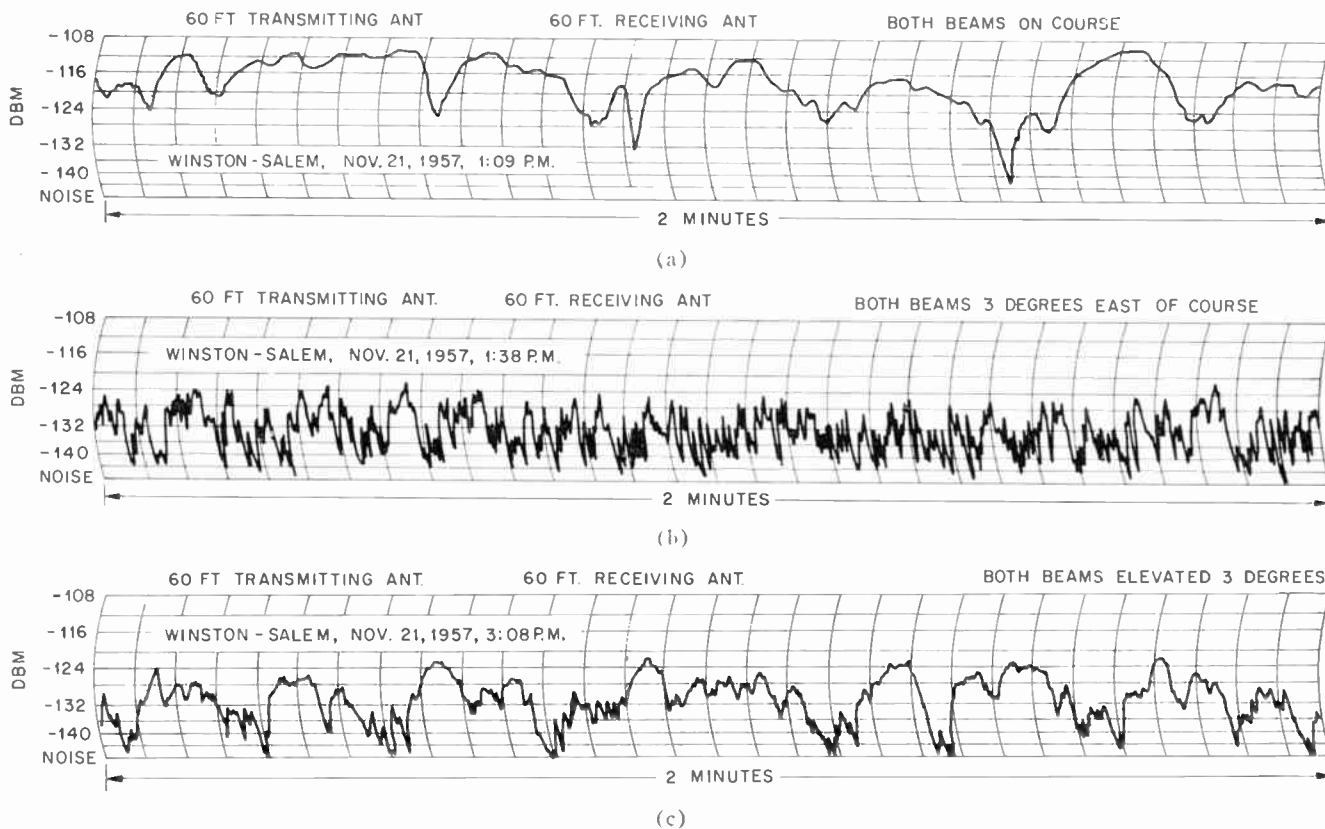


Fig. 22—Fading of 400 Mc signals received over a 618-mi path with the transmitting and receiving antennas oriented as follows: (a) On-path. (b) 3° east of course. (c) 3° elevated.

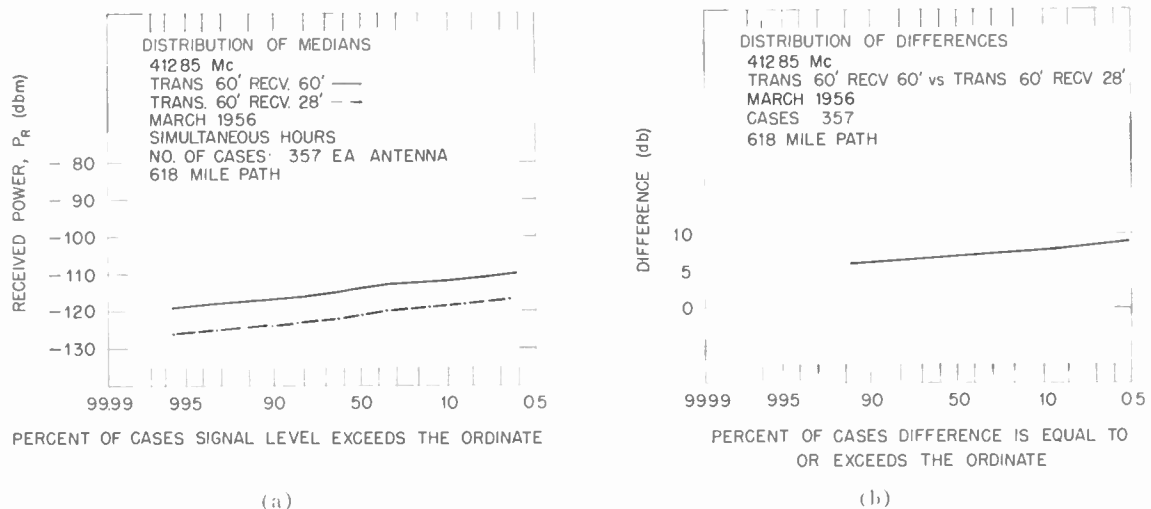


Fig. 23—(a) Distributions of hourly median values of signal levels received over a 618-mi path on a 60-ft and a 28-ft antenna. (b) Distribution of differences of hourly median values of 400-Mc signals received on a 28-ft and a 60-ft antenna.

ANTENNA PERFORMANCE OVER A 600-MI PATH

An important factor in evaluating the results of measurements of signal level obtained with highly directive antennas is the realized gain of the antenna system. Earlier theoretical analysis had predicted that at a distance of 600 mi and at a frequency of 400 Mc, the effective gain of a 60-ft diameter antenna would be from 2.5 to 10 db less than the measured plane wave gain.^{1,3,6,7} Measurements at Winston-Salem of transmissions from Round Hill over a twelve-month period simultaneously on a 28-ft receiving antenna and a 60-ft receiving antenna indicated that the median difference in the signals was 6.5 db which is the calculated plane wave difference in gain between the two antennas. The distribution of the signal levels received on each antenna for a typical month (for example, March, 1956) is shown in Fig. 23(a). The difference between the individual hourly medians of the two antennas was determined from these data. The distribution of these differences is shown in Fig. 23(b) indicating a small variability over a monthly period.

A subsequent series of measurements were made with 28-ft and 60-ft diameter antennas for both transmission and reception. These measurements were achieved simultaneously by use of two adjacent frequencies at 412.85 and 412.862 Mc. In order to utilize existing facilities, the system using the 60-ft antennas had a transmitter with a power output of 40 kw, and the system using the 28-ft antenna had a transmitter power output of only 12 kw. Distributions of signal levels received, using these two systems, are shown in Fig. 24 for a fifteen-minute sampling period. Fig. 24 indicates that the difference in the median values of received

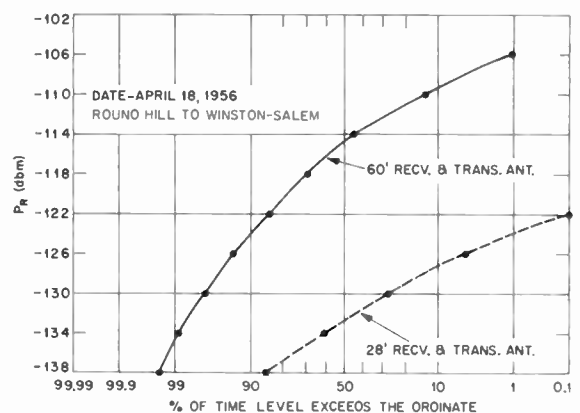


Fig. 24—Distribution of signal levels received for a fifteen-minute sampling period on systems using 60-ft to 60-ft combination and 28-ft to 28-ft combination.

signal was 18 db which is the same value as the difference in the computed antenna gains and the transmitter power of the two systems. The difference appears to decrease for the higher percentile values. Extension of the distribution curve for levels below -138 dbm was not possible because of the proximity of the signal level to the noise threshold of the receiving systems. The results were found to be the same over a series of tests during a day in which typical conditions of signal level and fading were experienced.

Comparison between the levels of signals received on a corner-reflector antenna and those received on a 60-ft antenna of transmissions from a 60-ft antenna indicates a difference of 24 db in the hourly median values which is also the same as the computed difference in gain of these two antennas. The results further indicate that the median plane wave gain of an antenna up to 25 wavelengths in diameter at 412 Mc is realized over paths 618 mi in length.

In order to investigate further the probable gain performance of antenna apertures in excess of 60 ft

⁶ H. G. Booker and J. T. deBettencourt, "A theory of radio transmission by tropospheric scattering using very narrow beams," *Proc. IRE*, vol. 43, pp. 281-292; March, 1955.

⁷ H. Staras, "Antenna-to-medium coupling loss," *IRE TRANS. ON ANTENNAS AND PROPAGATION*, vol. AP-5, pp. 228-231; April, 1957.

in diameter, a series of spatial correlation measurements were made over the 618-mi path using two corner-reflector receiving antennas spaced 100 ft and 700 ft along a line transverse to the great circle path. The results of these measurements are shown below as the average cross-correlation for each of the two spacings of the antenna:

Spacing	Average correlation coefficient
100 ft	0.5
700 ft	0.2

These data were further analyzed in terms of the cross-correlation function. These curves are shown in Fig. 25. It should be noted that the functions are normalized to the maximum value of the cross-correlation obtained for the 100-ft spacing. The 0.5 correlation coefficient for the 100-ft spacing indicated that antenna apertures considerably in excess of the 60-ft diameter parabolooids could be used effectively over this length of path.

In the summer of 1959, the AN/FRC-47(XD-1) tropospheric communications system between Sauratown Mountain and Millstone Hill was completed. This system employs truncated paraboloidal antennas with widths and heights of 120 ft. Systematic gain measurements were made to measure the performance of these antennas operating over a path comparable in distance and frequency to the previous Round Hill to Winston-Salem experimental system. The transmissions from a 120-ft antenna were received simultaneously on 16-ft and 120-ft diameter antennas. The measured plane wave gains of these antennas were found to be 21 db and 39.5 db, respectively. The signals received on each antenna were recorded over half-hour periods and the distributions determined. Typical distributions of the amplitude of signals received on each antenna for one of these half-hour periods are shown in Fig. 26. In this case the difference in the received signal levels was 19 db or within 0.5 db of the difference in the plane wave gains. A total of 59 of these half-hour runs was made over a seventeen-day period during the summer. The distribution of the differences in the median of the signal levels received with the 120-ft antenna and those received with the 16-ft antenna is shown in Fig. 27. The median difference of antenna gain observed over the 640-mi path was 19.6 db resulting in a median realized gain of the 120-ft antenna of 39.2 db. The apparent absence of severe gain degradation, observed in these measurements, indicates that, at a frequency of about 400 Mc, less than one decibel antenna-to-medium coupling loss is experienced when antennas up to 120 ft in diameter are used over paths up to 600 mi.

Antenna height gain measurements were made at the Winston-Salem terminal for signals received over the 618-mi path. The foreground of the antennas consists of a smooth grassy field with a gentle upward slope to a 10-ft elevation above the site elevation at a distance of 1000 ft where the ground slopes downward to thin woods

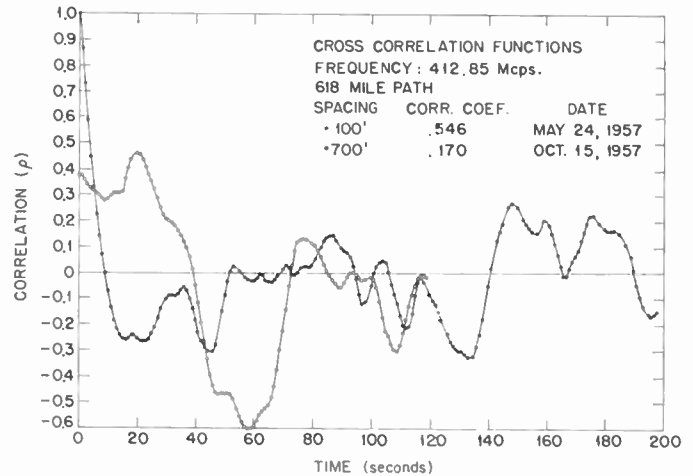


Fig. 25—Cross-correlation functions of signals received with corner-reflector receiving antennas spaced 100 ft and 700 ft transverse to the great circle path.

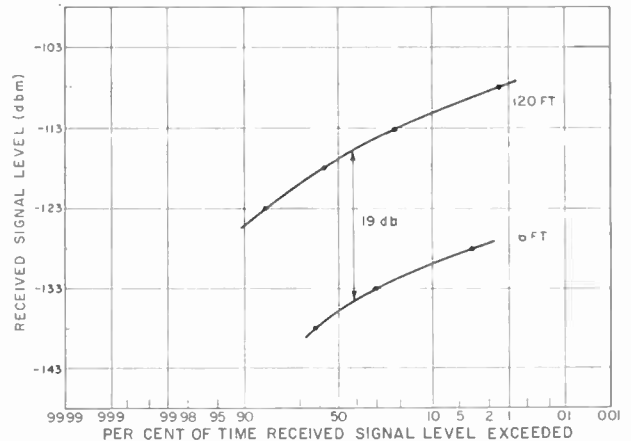


Fig. 26—Distribution of signal levels received on a 120-ft and a 16-ft antenna over the 640-mi path between Millstone and Sauratown.

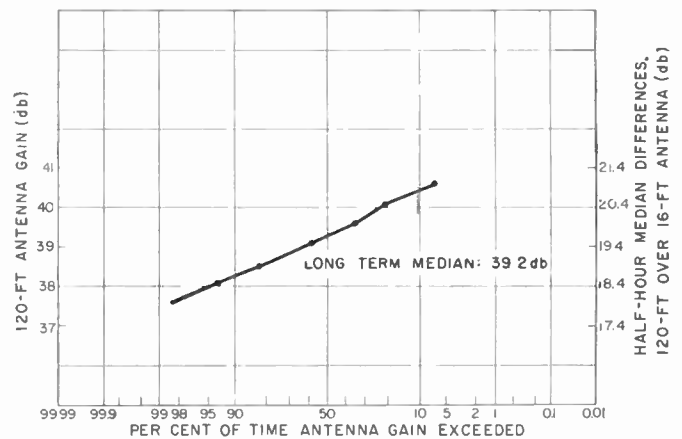


Fig. 27—Distribution of differences of the median value of signal levels observed on a 120-ft and a 16-ft antenna.

at a distance of 1500 ft. The measurements were accomplished with small identical corner-reflector antennas having gains of approximately 12 db above an isotropic antenna. The first series of measurements were made with heights of 10, 20, and 55 ft in January, 1957. Subsequent measurements were made in July, 1957, for heights of 25, 50, and 100 ft. In each series of measurements, the data were obtained by means of two simultaneous receiving systems with the received signal on the upper feed used for a fixed reference. These data are shown in Fig. 28, and the median value of the differences for the respective heights is plotted with the median level obtained from the antenna at the 50-ft height used as the zero decibel reference. These results indicate that a substantial height gain is achieved for the first ten wavelengths of height (approximately 25 ft) progressively decreasing to a small rate of height gain above 20 wavelengths. The data for July consist of measurements for successive hourly periods over a duration of two days, whereas the January data consist of measurements obtained from four to five hourly periods. The July data showed hour-to-hour variations in the differences ranging from less than 1-db height gain for the height increments to as much as 3 db in a few cases. The signal levels obtained during the July period on the fixed reference antenna at a height of 100 ft varied over a 25-db range. There does not appear to be any definite variation in the height gain associated with variation in the median signal levels.

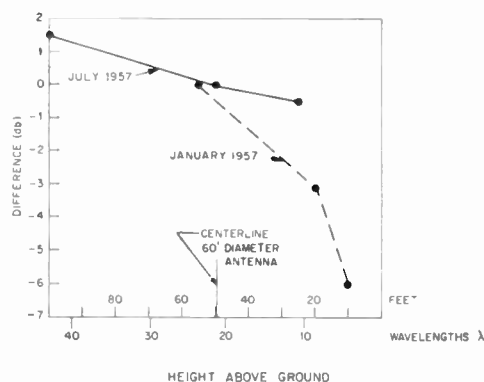


Fig. 28—Results of antenna height gain measurements obtained at the Winston-Salem site.

ANGULAR MEASUREMENTS OF SCATTERING

Attempts were made to measure the angular spread of the incoming signals in azimuth and elevation over the 618-mi transmission path in order to study the propagation mechanism and to evaluate further the effectiveness of antennas of various sizes. Measurements were made to determine the level of signals when the transmitting antenna was oriented off-path compared to the signal observed with the antenna oriented along the great circle path. Transmissions from the 60-ft antenna at Round Hill were received simultaneously on 60-ft and 28-ft diameter receiving an-

tennas as the transmitting antenna was rotated in azimuth and elevation. The geometry of the path is shown in Fig. 29(a). The signal level received in the off-path position was compared with that obtained with the antenna oriented along the path. The antennas were oriented back to the on-path position between each measurement to ensure that the conditions remained constant throughout the measurements. The results of the variation of signal level with azimuthal rotation are shown in Fig. 29(b). The solid curve indicates the levels received on the 60-ft diameter antenna, and the broken curve shows the levels received on the 28-ft diameter antenna. Since the two patterns, normalized to the level received on the 60-ft antenna when the transmitter was oriented on the great circle path, are essentially coincident, it may be concluded that the azimuthal spread of the received signals was less than the beamwidth of the larger antenna. Similar measurements were made with the transmitting antenna beam being varied in elevation. The curves in Fig. 29(c) show the variation in signal levels received on the 60-ft and 28-ft diameter antennas, normalized in the same manner as previously described, as the antenna was varied in elevation. As in the case of the azimuthal rotations, the signal level decreases with angular rotation closely following the antenna pattern of the transmitting antenna. These measurements in both azimuth and elevation indicate that the angular extent of the scattered signal is less than 2.8° (the antenna half-power beamwidth) when the signal levels are averaged over fifteen-minute sampling periods.

Some indication of the apparent instantaneous spread of the angle of arrival was determined from the variation in the signal level received on a fixed receiving antenna while the transmitting antenna was rotated in azimuth at a rate of 34° per sec. The results of these measurements are shown in Fig. 30(a)–(f). In each figure, the signal recorded is shown for that portion of each revolution of the transmitting antenna when the beam is oriented towards the receiving site. In some cases, the beam is fairly well maintained; in other cases nulls appear in the received pattern. Since the average fading rate observed on these signals was several tenths of a cycle per sec and the transmitting antenna traversed an angle equal to the beamwidth in about one tenth of a second, it is likely that the received pattern might have been altered by an occasional occurrence of a period of rapid fading coincident with the period of traverse of the transmitting antenna beam across the great circle path. These measurements are similar to the more rapid beam swinging measurements reported by Waterman.⁸ A quantitative interpretation is more difficult because of the wider beamwidths and limitation of the top speed of mechanical rotation of the large 60-ft transmitting antenna.

⁸ A. T. Waterman, Jr., "A rapid beam-swinging experiment in transhorizon propagation," IRE TRANS. ON ANTENNAS AND PROPAGATION, vol. AP-6, pp. 338–340; October, 1958.

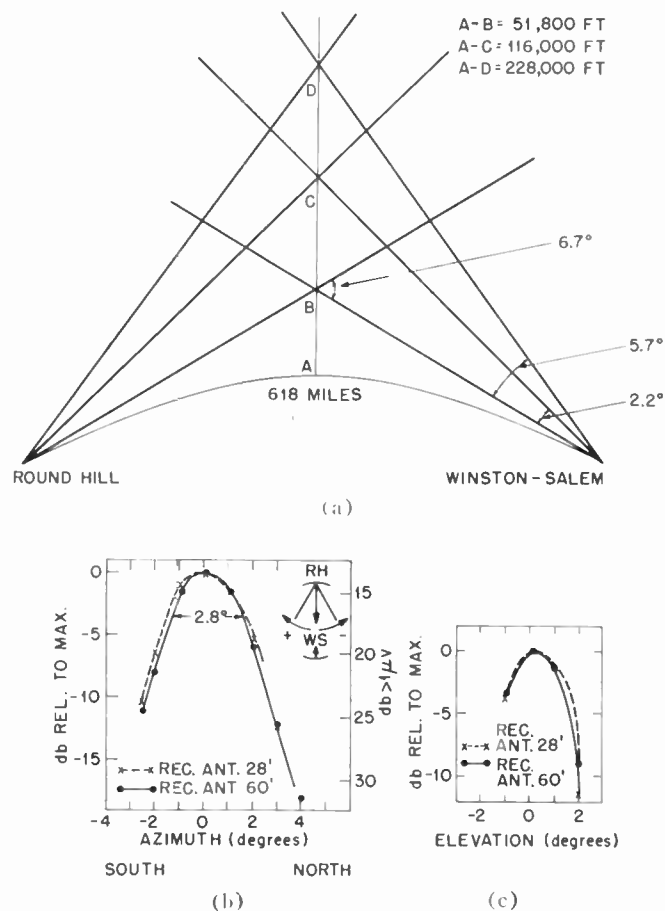


Fig. 29—Angular measurement of scattering obtained at Winston-Salem by rotation of a 60-ft diameter transmitting antenna at Round Hill. (a) Geometry of path indicating regions illuminated by the antenna beams. (b) Results of measurements of signals received with azimuthal rotation of transmitting antenna. (c) Results of measurements of signals received with rotation of transmitting antenna in elevation.

MULTIPATH MEASUREMENTS

A series of multipath delay measurements were made during August and September, 1959, over the Millstone Hill-Sauratown Mountain path. A 1- μ sec pulse was transmitted from Sauratown at a 20-kw level at 399 Mc with repetition intervals of 10 μ sec or 20 μ sec. At the Millstone receiving site, the received pulses were displayed on an oscilloscope. Pulses were received via more than one path; that is, some via shorter routes and some via longer routes, their pulses appearing earlier or later in time.

A block diagram of the equipment is shown in Fig. 31. The transmitter at Sauratown Mountain was keyed by a pulse generator synchronized to a 100-ke crystal standard. The received signals were mixed with a local oscillator to produce a 30-Mc IF. An echo line integrator improved the signal-to-noise ratio to give a usable display, since the train of pulses added up coherently in time over a fraction of a millisecond, whereas the noise did not. The pulse stream was then detected and displayed on a scope triggered by a second 100-ke standard.

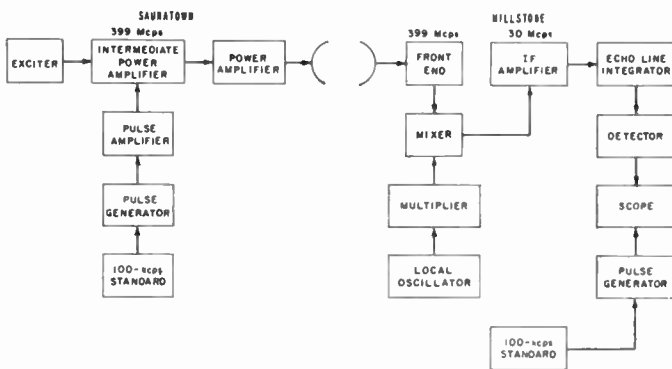


Fig. 31—Block diagram of the pulse system used for multipath delay measurements at 399 Mc over the Millstone-Sauratown path.

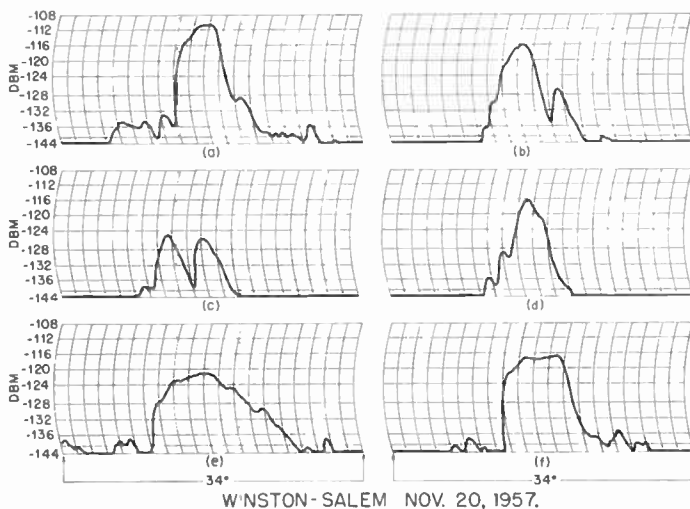


Fig. 30—(a)–(f) Measurements of signals received at Winston-Salem when the 60-ft transmitting antenna at Round Hill is rotated rapidly in azimuth

A display of received pulses obtained in these experiments is shown in Fig. 32. A pulse repetition interval of 20 μ sec was used for these data. The bandwidth of the transmitter and receiver distorted and widened the pulse but always by a constant amount; widening or smearing also occurred which was caused by propagation effects. In Fig. 32(a) two pulses are observed, suggesting two distinct paths with one pulse arriving 4 μ sec earlier than the other. The traces were photographed about a second apart with time proceeding downward. The amplitude scale is linear. Fig. 32(b) shows a variable time shift of an apparent two-path contribution. The photographs shown in Fig. 33(a) and (b) were made with transmitted pulses having repetition intervals of 10 μ sec. In Fig. 33(a), the first sequence shows a contribution which, in the succeeding sequences, increases in strength compared to that of the other relatively stable contributions. Fig. 33(b) shows

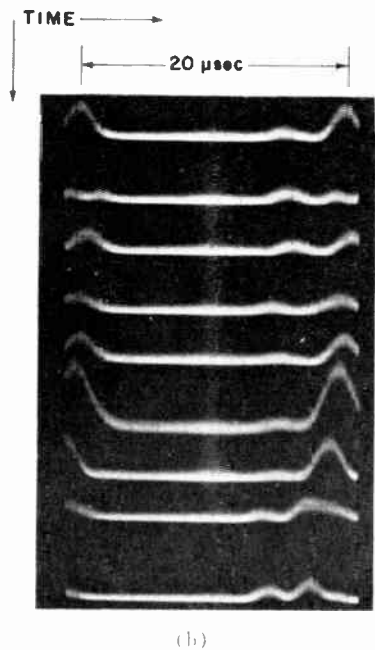
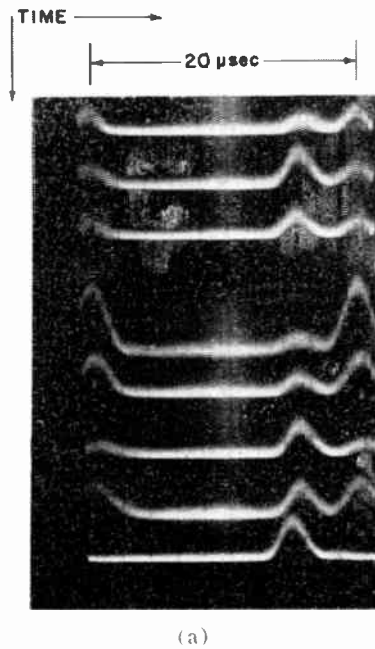


Fig. 32—(a) Photograph of display of transmitted pulses recorded on an oscilloscope at the Millstone receiving terminal. Pulses transmitted at $20\ \mu\text{sec}$ intervals indicating contribution from two apparent paths. (b) Photograph of display of transmitted pulses recorded on an oscilloscope at the Millstone receiving terminal. Pulses transmitted at $20\ \mu\text{sec}$ intervals indicating variable time shifts of two apparent paths.

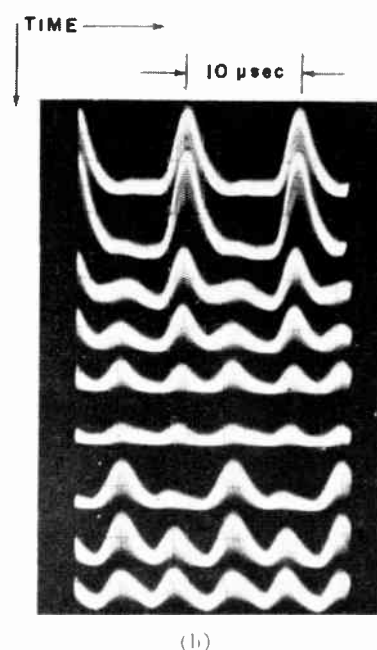
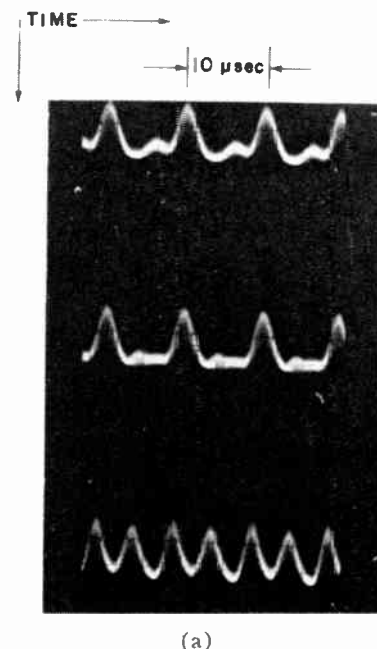


Fig. 33—(a) Photograph of display of pulses with $10\text{-}\mu\text{sec}$ repetition intervals showing a shift in time and build-up of pulses. (b) Photograph of display of pulses with $10\text{-}\mu\text{sec}$ repetition intervals showing pulses arriving stable in time varying alternately in amplitude.

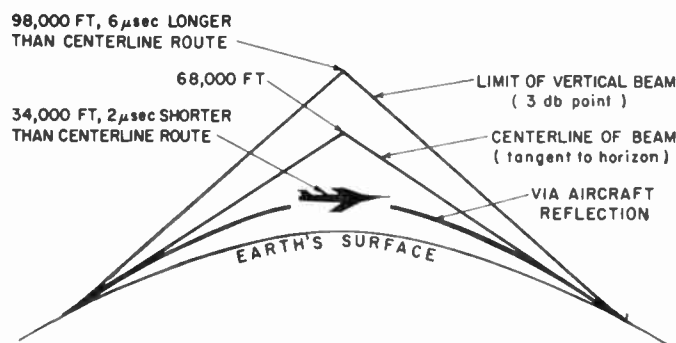


Fig. 34—Diagram showing various transmission paths between Winston-Salem and Millstone.

an example of two pulses relatively stable in time arrival, alternately varying in amplitude.

A diagram showing the various possible paths on a simple ray basis with the differential delays between discrete paths given in microseconds is shown in Fig. 34. The maximum delay between two paths displaced in azimuth (to the 3-db horizontal beamwidth point) is a small fraction of a microsecond.

The longest differential delay observed was about 8 μsec . Most of the time, the fundamental mode appeared with secondary modes shorter or earlier by up to 4 μsec and longer or later by up to 6 μsec . The major mode would shift in time by up to 2 μsec .

To place a "bench mark" in the sky, an aircraft was flown at midpath at altitudes between 28,000 and 36,000 ft, and the signal reflected from the plane was observed relative to signals via the natural modes. The pulse reflected from the aircraft had a characteristic amplitude fluctuation that permitted easy recognition. In all cases, the midpoint aircraft mode (known to be so by careful tracking of the aircraft and communication between aircraft, tracking station, and receiver site) arrived earlier than the major mode by up to 4 μsec with most modes occurring at about 2 μsec . Most of the time, no other natural mode signal was observed shorter or earlier than the aircraft-reflected mode, but on some few occasions natural modes were observed to arrive earlier than the signals reflected from the aircraft.

From these tests, it appears that the major mode arrives via a route along the center lines of both antennas plus or minus up to about 20,000 ft vertically or in azimuth at the midpoint. However, significant energy appears to be transmitted via modes with routes at least as low as 20,000 ft and at least as high as 90,000 ft when interpreted in terms of simple ray geometry.

FREQUENCY-SELECTIVE FADING MEASUREMENT

Frequency-selective fading measurements were made during the winter of 1956 to 1957 on the 618-mi path between the 60-ft antennas located at Round Hill and at Winston-Salem. The 50-kw FM transmitter was used

at Round Hill, and the receiving facility at Winston-Salem consisted of a pair of narrow-band recording receivers.

During the frequency selective fading measurements, the transmitter was frequency-modulated by tones at frequencies of 10, 20, 30, and 50 kc with a frequency deviation ratio of about 2.0 in order to produce maximum strength in the first sidebands. The two narrow-band, tunable recording receivers were used with a dual-channel pen recorder. A diagram of the equipment is shown in Fig. 35 (next page).

Fifteen-minute recordings were made of 2 frequencies separated 20, 40, 60, and 100 kc. Fig. 36 shows typical samples with 20-kc and 100-kc separations of the two sidebands. The recording scale is linear with voltage. The small, rapid variations are produced by receiver noise. Notice the appreciable lack of correlation when the signals are separated by 100 kc. Fig. 37 shows the correlation coefficients of rapid fading of signals received at various frequency separations. In order to provide the system designer with more specific data on the frequency-selective fading, the recordings were analyzed to obtain the distributions of the ratio of signal levels received at two frequencies. The results of this analysis are shown in Fig. 38.

This frequency-selective fading is believed to be further evidence of the presence of multipath propagation. The variations with time are most probably caused by small changes in the phase and amplitude of the various paths.

LIGHTNING INTERFERENCE

In general, it is considered that lightning has little effect on UHF communications. It is true, however, that the radio frequency spectrum of lightning extends into the UHF band. The energy levels are very low but are far from insignificant in relation to cosmic noise which, in the end, limits the useful gain of highly sensitive receivers at these frequencies. The results of observations made at Winston-Salem and Elberton (618 and 830 mi) show that lightning may cause some difficulty

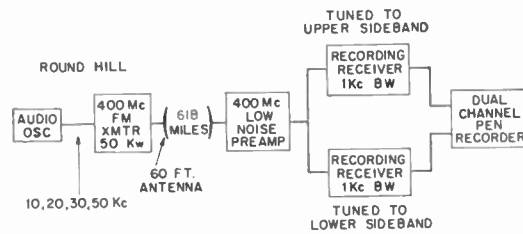


Fig. 35—Block diagram of equipment used in frequency selective fading measurement.

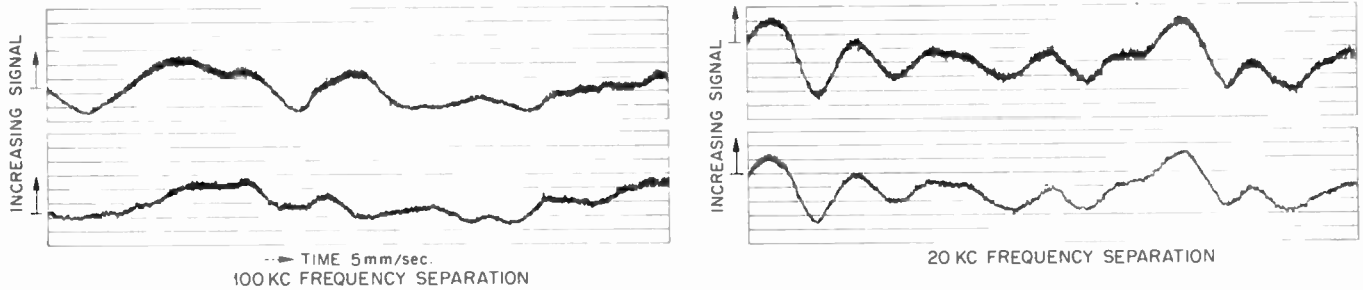


Fig. 36—Samples of fading of signal received on two channels separated in frequencies 100 kc and 20 kc

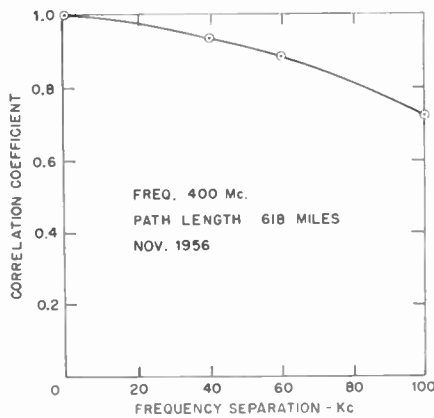


Fig. 37—Correlation coefficient of rapid fading vs frequency separation.

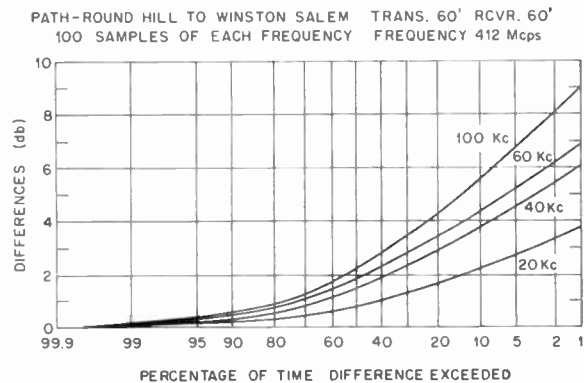


Fig. 38—Distribution of differences (db) in amplitude of signals received on two channels separated 20 kc-100 kc.

on marginal, long-distance tropospheric communication circuits.

On one occasion, lightning bursts caused by a storm located over Winston-Salem were recorded at Elberton, a distance of 210 mi. On May 30, 1956, high-speed graphic recordings were made of lightning bursts caused by several storms ranging from 125 to 225 mi distant from Winston-Salem along the axis of the receiving antenna beam. At that time, the transmitter was not in operation. Four of the more spectacular bursts recorded are shown in Fig. 39. Each graphic presentation is for a time period of five sec and shows the bursts that are received simultaneously with the system using the 28-ft and 60-ft antennas. The time constant of the system was approximately 10 msec. During many hours of recording at Winston-Salem, there was only one period when signal enhancements were observed that could be attributed to scattering of the transmitted signal from ionized lightning trails.

Several other investigators^{9,10} have reported results which appear to indicate that this phenomenon is possible.

In order to obtain some statistical values of the character of these noise bursts caused by lightning on an active day, the recordings obtained for May 30, 1956, were processed for distributions of the amplitudes and durations of the noise bursts. A distribution of the time durations of the noise bursts is shown in Fig. 40. The median burst length is 0.75 sec, and for 1 per cent of the time the duration exceeds 2 sec. The distribution of peak power levels for the noise bursts is given in Fig. 41 which shows 255 simultaneous cases for the 28-ft and 60-ft antennas.

⁹ D. R. Hay and T. R. Hartz, "Thunderstorm signals at very-high frequency and ultra-high frequency," *Nature*, vol. 175, pp. 949-950; May 28, 1955.

¹⁰ L. H. Bauer and W. A. Flood, "UHF forward scatter from lightning strokes," *Proc. IRE (Correspondence)*, vol. 45, p. 1743; December, 1957.

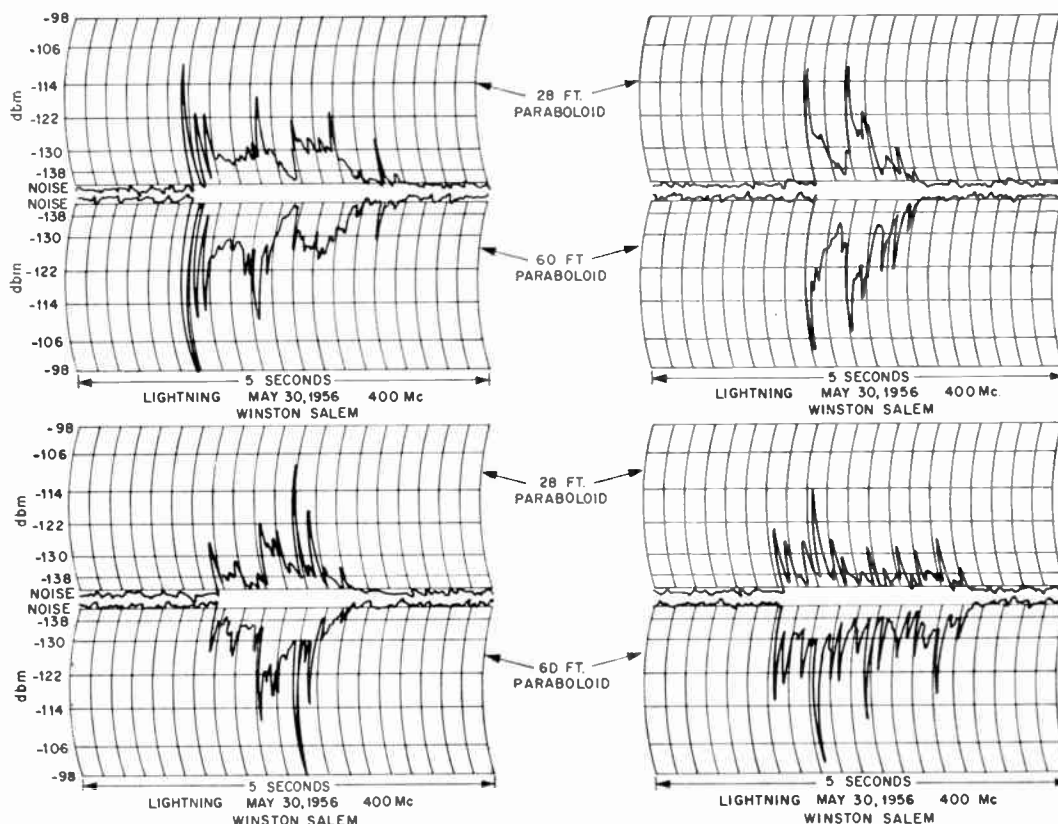


Fig. 39—Samples of lightning bursts recorded at Winston-Salem at 412 Mc.

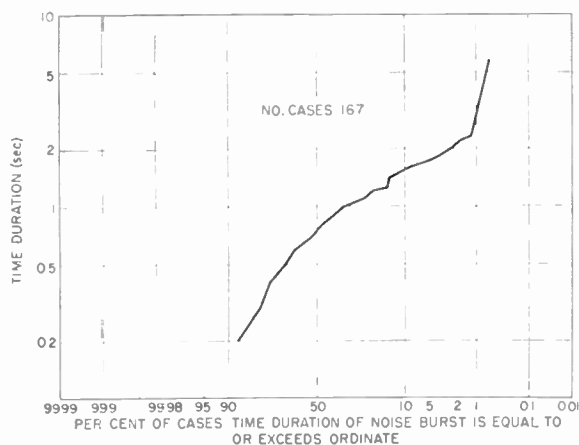


Fig. 40—Distribution of time durations of lightning bursts at 412 Mc caused by lightning observed at Winston-Salem on May 30, 1956.

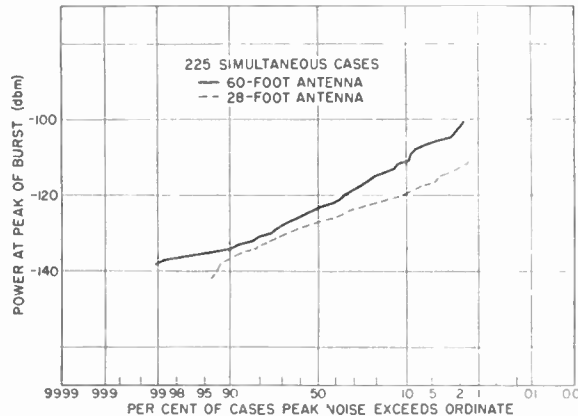


Fig. 41—Distributions of peak power of lightning bursts from lightning observed on a 28-ft and a 60-ft diameter antenna.

CONCLUSIONS

The results of these long-term experimental UHF measurements appear to provide new evidence of certain underlying patterns of radio propagation characteristics for these extended ranges. These characteristics have interesting implications to both the engineering of long-range communications systems and the physical validity of theoretical models of the propagation medium advanced by various workers. The practical extension of tropospheric communications systems to distances in excess of 500 mi beyond the radio horizon

depends critically upon an accurate knowledge of a number of separate, but interrelated, propagation characteristics. The use of very large transmitters and very large antenna systems for a practical communications system must inevitably be weighed against the bandwidth limitations of the propagation mechanism and efficiency of the large antenna systems at the extreme ranges. Practically all of the various theoretical models, advanced for explanations of the propagation mechanism and experimental measurements at lesser ranges, have indicated a progressive degradation in bandwidth and a decreasing efficiency of large antennas

as the propagation path is extended further beyond the radio horizon. These effects are inherent in the geometry of the ray paths from the antenna to the primary scattering or reflecting elements contained in the location of the common volume produced by the intersection of the portions of the antenna beams above their respective radio horizons.¹¹ This common volume progressively ascends into the stratosphere as the propagation path is lengthened beyond the range of 400 to 500 mi. Since the height of the tropopause varies between 10 and 14 km in height, it has been suggested that the signal level at distances in the region of 500 mi could be subject to large variations.¹¹ One of the unpredicted and relatively unexpected results of the signal level measurements for the 618- and 830-mi ranges was the small variations in the hourly median values during diurnal, monthly, and seasonal periods as contrasted to the variation observed at ranges of a few hundred miles. However, there appears to be a definite reversal of the trend of a decreasing rate of attenuation of the received signal level versus distance beyond 600 mi. While the progressive decrease in antenna performance with distance may be a contributing factor to the apparent increase in attenuation rate beyond 600 mi, the measured performance of 120-ft antennas, at the 600-mi distance, indicated relatively small gain losses. A drastic decrease in gain performance of the smaller 60-ft antenna at 830-mi would therefore be required to account for the large increase in attenuation observed over the longer path. It was not feasible to make comparisons of gain performance at the 830-mi distance utilizing small aperture antennas because of extremely weak signals. This trend implies a pessimistic forecast for practical tropospheric communications systems over paths having distances between radio horizons of 700 to 1000 mi in length.

The effective gain of the large 60- and 120-ft antennas, measured in the low UHF band in these experiments for the 600-mi range, belies some of the extrapolations of earlier theoretical results and experimental data. If these results are compared to similar gain studies¹² per-

formed at much shorter distances at 2000 Mc for antenna systems of comparable gain products of about 78 db (gain product of the 120-ft antennas at 400 Mc), it would appear that the antenna performance for a given aperture dimension in wavelengths and a given distance decreases with frequency and would appear to favor the longer wavelengths for operation of tropospheric communications systems at these extreme distances. Further experiments at extreme ranges at much higher frequencies than 400 Mc would be required to substantiate this apparent frequency trend of antenna performance as well as the possible existence of a frequency trend of the path loss vs distance.

The results of the pulse studies over the 640-mi path strongly suggest that discrete reflecting or scattering layers play a dominant role in the propagation process. It is believed that the variability of the relative time delays of the apparent discrete multipath contributions pose some interesting problems for further research into the physical nature of the propagation process, particularly with reference to the few cases of pulse signals which seem to arrive ahead or comparable in time with reference to scattering from an aircraft flying below the nominal radio horizon.

Although these measurements indicate the necessity for further research into the physical nature of the propagation mechanism and the necessity for further experimental measurements at higher frequencies at ranges of 600 mi and beyond, they have, nevertheless, demonstrated the feasibility of long-range tropospheric systems operating over ranges out to 600 mi.

ACKNOWLEDGMENT

The tropospheric scatter communications research program which is summarized in this paper was conducted from 1952 to 1956 under the supervision of Prof. W. H. Radford, Head, Communications-Division 3 of the MIT Lincoln Laboratory. Many individuals in the Communications Division contributed in the establishment of the experimental systems and conduct of the experimental measurements. In particular, grateful acknowledgment is made to A. J. Poté and Prof. R. R. Brown of the Lincoln Laboratory. Field engineering services and operation of the receiving sites which were performed largely by the Page Communications Engineers, Inc. and Westinghouse Electric Corporation are also acknowledged.

¹¹ H. G. Booker and W. E. Gordon, "The role of stratospheric scattering in radio communications," *Proc. IRE*, vol. 45, pp. 1223-1227; September, 1957.

¹² J. H. Chisholm, L. P. Rainville, J. F. Roche and H. G. Root, "Angular diversity reception at 2290 Mc over a 188-mile path," *IRE TRANS. ON COMMUNICATIONS SYSTEMS*, vol. CS-7, pp. 195-201; September, 1959.

Correspondence

The Use of a Paraboloidal Reflector of Small Focal Ratio as a Low-Noise Antenna System*

The recent developments in the design of low-noise amplifiers for very high frequencies have made it necessary to consider ways of reducing the other contributions to the input noise of a receiving system. One of these is ground radiation received in the "spillover" lobes of the antenna reception pattern and for a paraboloidal reflector of comparatively large focal ratio a typical value for the noise temperature attributable to ground radiation is 20°K. Jelley and Cooper,¹ for example, using a 60-ft reflector with $f/D=0.35$ quote (20 ± 5) °K at 1420 Mc, while more recently Schuster, Stelzreid and Levy² have achieved (17 ± 4) °K at 960 Mc using an 85-ft reflector with $f/D=0.43$. These are values measured with the antenna directed towards the zenith.

In attempts to minimize this contribution horn-reflector antennas and Cassegrain systems have been constructed. The former may give a ground noise no more than (2 ± 1) °K at 5650 Mc³ and for the latter 6°K has been reported at 960 Mc,⁴ this figure including ground radiation scattered from the reflector supports.

It is the purpose of this communication to point out that for a paraboloidal reflector with a conventional feed there may be very little ground contribution if the focal ratio is small. This fact emerges from experiments which have been carried out in connection with a survey at the Mullard Radio Astronomy Observatory of the galactic background radiation at 404 Mc,⁵ a survey in which particular attention was paid to calibration with thermal loads.

The antenna was a dipole and reflector combination supported by an axial tube at the focus of a paraboloidal reflector 27 ft in diameter and with $f/D=0.23$. Measurements of the reception pattern showed that 85 per cent of the power was concentrated into the main beam (defined as the region within 10° of the axis), 14 per cent was in other forward lobes and less than 1 per cent in the back lobes. The gain was calculated to be 27.4 db and the ratio of effective area to physical area 55 per cent.

The receiver was of the Dicke type with an electron beam parametric amplifier as the first stage. The rms noise fluctuations of the output were ± 0.2 °K and the zero drift was less than 1°K in a 12-hour period.

The determination of T_g , the noise temperature contribution from the ground, involved measurement of the variation of T_g with elevation by tracking several regions of sky from the horizon to the zenith. It was found that the observed changes of T_g could be accounted for by assuming a ground brightness temperature of 250°K in the vicinity of the antenna and 125°K for the distant ground seen at grazing incidence. Using this model the ground contribution at the zenith was computed as about 1°K, most of this being due to the zone between zenith angles 90° and 120°. This conclusion was confirmed by placing a wire netting screen 100-ft square under the antenna. This had the function of reflecting cold sky radiation into the antenna rather than ground radiation. It was raised at the edges so that only radiation from the distant ground could still reach the antenna. With the antenna beam in the zenith the addition of the screen caused no detectable change of output from a number of different points in the sky, therefore proving that the radiation from the area covered was certainly less than 0.5°K.

The ground contribution at the zenith was thus fixed as about 1°K. After allowance had been made for the changes in sky radiation in the sidelobes during the tracking experiment, the curve in Fig. 1 could be

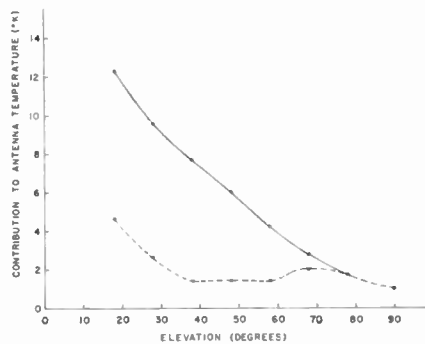


Fig. 1.

plotted (solid line). This gives the variation in the ground contribution with elevation, together with any variation in atmospheric noise with elevation. The figures given by Hogg⁶ suggest that the increase in atmospheric noise between elevations of 90° and 18° is 2°K. If allowance is made for this, it can be seen that down to an elevation of 18° the ground contribution is less than 10.5°K. The other curve in Fig. 1 (dashed

line) gives the observed variation of ground and atmospheric radiation when the screen is present and in this case the ground contribution remains less than 2.6°K.

To summarize, it is apparent that there is considerable advantage to be gained in a low-noise paraboloidal antenna system by 1) having the feed below the rim of the reflector, and 2) surrounding the antenna by a ground screen.

I. I. K. PAULINY-TOTH
National Radio Astronomy
Observatory
Green Bank, W. Va.
I. R. SHAKESHAFT
R. WIELEBINSKI
Mullard Radio Astronomy Observatory
Cavendish Laboratory
Cambridge, England

Effect of Mirror Alignment in Laser Operation*

While many of the operating parameters of lasers have been studied in many laboratories, the relatively important question of the effect of parallelism of plane end reflectors on laser operation has not been reported in detail. We have studied the effects of parallelism of external end mirrors on the threshold for laser action for a ruby laser. The uncoated ruby rod was mounted between the mirrors of a Hilger and Watts Fabry-Perot interferometer with its axis approximately normal to the mirrors and was excited by two U-shaped flash tubes. In this way the parallelism of the end mirrors could be varied without changing any of the other parameters of the laser system.

The end plates of the interferometer were aligned parallel to within an estimated error of 0.5 second of arc) using the method of multiple images of a mercury arc.¹ After the threshold for laser action was measured, the alignment was changed by adjustment of the end plates. The deviation from parallelism could be determined by the displacement of the multiple images. Data on the threshold energy as a function of parallelism are shown in Fig. 1. These data were obtained by rotating one mirror by various amounts about a fixed axis, starting at zero misalignment, going to a maximum misalignment in one direction, returning to zero, and going to maximum misalignment in the opposite direction. Data taken at a given point, when moving in one direction, agreed with that obtained at the same point going in the opposite direction.

* Received September 28, 1962.

¹S. Tolansky, "High Resolution Spectroscopy," Pitman Publishing Corp., New York, N. Y., ch. 9: 1947.

* Received September 17, 1962.

¹J. V. Jelley and B. F. C. Cooper, "An operational ruby maser for observations at 21 centimeters with a 60-foot radio telescope," *Rev. Sci. Instr.*, vol. 32, pp. 166-175; February, 1961.

²D. Schuster, C. T. Stelzreid, and G. S. Levy, "The determination of noise temperatures of large paraboloidal antennas," *IRE TRANS. ON ANTENNAS AND PROPAGATION*, vol. AP-10, pp. 286-291; May, 1962.

³R. W. DeGrasse, D. C. Hogg, E. A. Ohm, and H. E. D. Scovil, "Ultra-low-noise antenna and receiver combination for satellite or space communication," *Proc. NEC*, vol. 15, pp. 370-379; 1959.

⁴P. D. Potter, "Unique feed system improves space antennas," *Electronics*, vol. 35, pp. 36-40; June, 1962.

⁵I. I. K. Pauliny-Toth and J. R. Shakeshaft, "A survey of the background radiation at a frequency of 404 Mc/s," *Monthly Notices Roy. Astron. Soc.*, vol. 124, pp. 61-77; 1962.

⁶D. C. Hogg, "Effective antenna temperatures due to oxygen and water vapor in the atmosphere," *J. Appl. Phys.*, vol. 30, pp. 1417-1419; September, 1959.

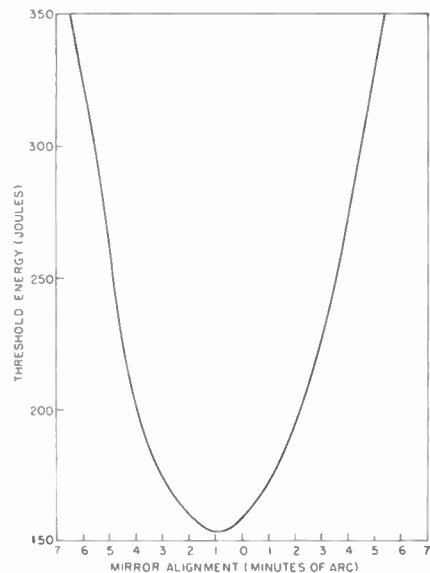


Fig. 1—Laser threshold energy vs mirror alignment.

The orientation of the axis of the ruby rod relative to the end plates is not significant, since changing the orientation by reasonably small amounts did not affect the data. The use of magnesium oxide reflectors around the flashtube-ruby configuration resulted in a diffuse illumination of the ruby, so that the threshold of laser action was characterized by emission from a considerable portion of the ruby face, rather than from a few active filamentary volumes.

The curve shows several interesting features. Over a range of about two minutes in mirror alignment, the threshold varies from its minimum value by only a few per cent. The threshold doubles only upon a displacement of about five minutes from the minimum position. These data show the threshold to be surprisingly insensitive to mirror alignment, and suggest that taking great care to polish laser rod ends to close parallelism is not necessary. The reason for this lack of sensitivity is presumably caused by the presence within the ruby of strains and optical inhomogeneities which make the path of the light in the ruby depart from a straight line trajectory. Making the end parallelism more perfect than the ruby does not improve the laser operation.

It is also interesting to note that the minimum threshold energy does not fall at the position of most exact alignment, but occurs at a misalignment of almost one minute of arc. We postulate that this amount of misalignment tends to correct the deviations of light rays in the ruby and is the position in which the end plates are most nearly optically parallel considering the presence of the crystal within the interferometer. These conclusions are qualitatively in agreement with the results of other workers² who found that an external mechanical stress on the ruby could compensate strains within the ruby and yield lowered thresholds and more symmetric emission patterns.

We have observed no dependence of the divergence of the laser output beam near

threshold on the alignment of the end plates.

These results may be of interest to investigators using Q-spoiled lasers with rotating mirrors or prisms, since the parallelism of the external mirrors required to yield laser action has not been previously defined. If, for example, a mirror rotates at 1500 revolutions per minute, it will pass from a position of 10-minute misalignment (where the laser should be "off") to zero misalignment (where the laser will be "on") in about 2×10^{-5} seconds, a time long compared to the duration of emission. The laser thus "turns on" slowly, a fact which should be considered in interpretation of the results using Q-spoiled lasers of this type.

J. F. READY
D. L. HARDWICK
Honeywell Research Center
Hopkins, Minn.

Electro-Optic Properties of Zinc Selenide*

The Pockels effect, or linear electro-optic effect, is an electric field induced, reversible change in the optic properties of piezoelectric crystals. The first general treatment of the effect was presented by Pockels.¹ More recently, Vlokh and Zheludev² published equations for the optic parameter changes for each of the twenty piezoelectric classes of crystal symmetry and for various directions of applied field. Kaminow³ and Watkins⁴ employed this effect in devices for amplitude modulation of light at frequencies up to 10 kMc.

Crystals of class $\bar{4}2m$ (V_d), such as KH_2PO_4 (KDP) and $\text{NH}_4\text{H}_2\text{PO}_4$ (ADP) are widely used for light modulation applications because of their large Pockels effect. The birefringence of these crystals severely limits the optical aperture and requires that the electric field be applied in the direction of light propagation for maximum effect. Crystals of the cubic class $\bar{4}3m$ (T_d) permit construction of a light modulator of wide angular aperture and application of the electric field perpendicular to the direction of light propagation. Recent work indicates that hexamethylenetetramine, $\text{N}_4(\text{CH}_2)_6$, of this crystal class has suitable properties for light modulator applications.⁵ Namba⁶ has reported the electro-optic properties of ZnS, but since single crystals of ZnS in the cubic modification are practically non-existent,

this material is of little practical value. Zinc selenide, ZnSe, crystallizes primarily in the zincblende structure⁷ and it was of interest to determine whether it possessed electro-optic properties similar to ZnS.

The crystals used in these measurements were mounted on a device designed for use on the stage of a polarizing microscope. With this device it was possible to apply electrodes to opposite faces of the crystal and perpendicular to the direction of propagation of the light. The crystal faces to which the electrodes were applied were silvered to assure a uniform electric field and the crystals were immersed in oil to prevent arcing across the surface of the crystal. In all cases the electric field was applied perpendicular to the 110 plane of the crystal. The wavelength of light used in all measurements was 547.5 m μ . The phase difference was measured using the polarizing microscope as a Senarmont compensator by inserting a properly oriented quarter-wave plate. The electric field was applied by means of a dc power supply capable of developing 15,000 volts.

The birefringence b , introduced by application of an electric field under these conditions is

$$b = n^3 r_{11} V d^{-1} \quad (1)$$

where n is the refractive index, r_{11} is the electro-optic constant, V is the voltage applied, and d is the crystal thickness in the direction of the applied field. The phase difference ϕ of the light components expressed in degrees is

$$\phi = 360\lambda^{-1} b l \quad (2)$$

where λ is the wavelength of light and l is the crystal thickness in the direction of light propagation. Combining (1) and (2), r_{11} may be calculated by means of (3)

$$r_{11} = (\phi \lambda d) / (360 n^3 l V) \quad (3)$$

from measured values of ϕ and V . Fig. 1 shows the phase difference of a ZnSe crystal as a function of the applied voltage. This sample of ZnSe showed a breakdown voltage lying between 5000 and 5500 volts so that measurements were taken to 4000 volts only. The value of r_{11} determined from the data of Fig. 1 is 4.82×10^{-8} cm/statvolt. These units were used in order that the coefficient may be compared to values already in the literature.

It was of interest to determine the new refractive indexes of ZnSe. Under the conditions that the measurements were taken, ZnSe becomes biaxial under application of the electric field with the principal refractive indices as follows:

$$\alpha = n + 1/2 n^3 r_{11} V d^{-1} \quad (4)$$

$$\beta = n \quad (5)$$

$$\gamma = n - 1/2 n^3 r_{11} V d^{-1} \quad (6)$$

The new indexes of refraction for the crystal used in Fig. 1 at 4000 volts are $\alpha=2.90$, $\beta=2.89$, and $\gamma=2.88$. This index change, 10^{-2} , is significant when compared to KDP where the change is of the order of 2×10^{-4} .

Due to its low breakdown voltage and low electro-optic coefficient, ZnSe is imprac-

⁷ D. C. Reynolds, Aeronautical Research Laboratory, Wright-Patterson AFB, suggested this material and kindly supplied the author with the crystals used in this work.

* Received September 20, 1962.

¹ F. Pockels, "Lehrbuch der Kristalloptik, B. G. Teubner, Leipzig, Germany, 1906.

² O. G. Vlokh and I. S. Zheludev, "Changes in the optical parameters of crystals caused by electric fields," *Soviet Physics - Crystallography*, vol. 5, pp. 368-380; November-December, 1960.

³ I. P. Kaminow, "Microwave modulation of the electro-optic effect in KH_2PO_4 ," *Phys. Rev. Lett.*, vol. 6, pp. 528-530; May, 1961.

⁴ M. C. Watkins, "Microwave Modulation of Light with ADP," presented at 18th Annual Nat'l Electronics Conf., Chicago, Ill.; Oct. 8, 1962.

⁵ R. W. McQuaid, "The Pockels Effect of Hexamethylenetetramine," to be published.

⁶ S. Namba, "Electro-Optical Effect of Zincblende," *J. Opt. Soc. Am.*, vol. 51, pp. 76-79; January, 1961.

² M. S. Lipsett and M. W. P. Strandberg, "Mode control in ruby optical lasers by means of elastic deformation," *Appl. Optics*, vol. 1, pp. 343-357; May, 1962.

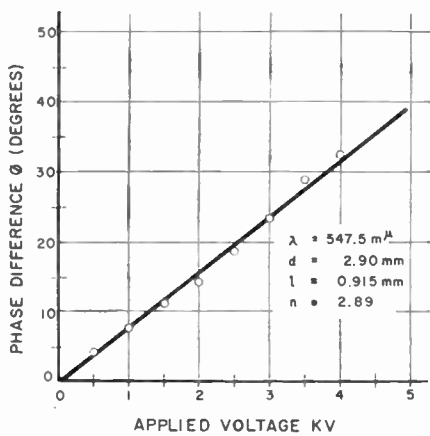


Fig. 1—Relation between phase difference and applied voltage as measured by the Senarmont compensator method.

tial as an optic modulator material. Zinc selenide may be of practical value in an application where a relatively large refractive index change is of interest.

RICHARD W. MCQUAD
Aircraft Armaments, Inc.
Cockeysville, Md.

On Power Dissipation in Semiconductor Computing Elements*

Landauer¹ has shown that the energy dissipated in a switching or logical operation must, for fundamental reasons, be several times larger than the thermal energy kT . The power dissipated in practical semiconductor devices is always many orders of magnitude greater than this. The present note represents an attempt to interpret these very large powers.

For the present purpose the power can be written roughly in the form V^2/R , where V is the voltage level at which the element operates and R is the resistance level. The voltage, V , in a practical nonlinear semiconductor circuit must be large enough so that the energy which an electron can obtain from the external voltage is larger than the thermal energy, that is $V > g_1 kT/q$. Here q is the electronic charge and g_1 is a number greater than one, its exact value depending on the reliability required.

First, consider relatively fast computers. Rapid and effective communication of an element with other elements must be provided. This means that the impedance level at which the element operates must be chosen to match some type of transmission line. The impedance of a transmission line, however, is the impedance of free space modified by various geometric factors and electric susceptibilities. For the present

order of magnitude estimates these modifying factors shall be neglected. Then, setting $g_1=5$ and $T=300^\circ\text{K}$, the power dissipated by a switching element turns out to be

$$P = (g_1 kT)^2 / q^2 Z_0 = 5 \times 10^{-3} \text{ w.} \quad (1)$$

Next consider slow computers. Here "slow" means that $v\tau$ (v =velocity of light and τ =time per operation) is large compared to the dimensions of the system. Then the problem of matching transmission lines is unimportant. The power in the expression V^2/R can be lowered by making R greater than Z_0 . The extent to which R can be increased is limited to values such that RC (C =capacitance of device and associated circuitry) is not greater than τ . C is generally somewhat larger than C_0 , a typical dimension of the system (in electrostatic units), $C=g_2^2 C_0$, say. Thus the minimum dissipation will correspond to $R=\tau/g_2 C_0$, which gives for the power

$$P = g_1^2 g_2 (kT)^2 C_0 / q^2 \tau. \quad (2)$$

This power can also be regarded as that used to charge a capacitance $g_2 C_0$ to a voltage $g_1 kT/q$ every τ sec.

Finally, the extension of the above considerations to very fast computer elements (very small τ) breaks down for various fundamental reasons. The first of these is the uncertainty principle. In order to circumvent the uncertainty principle it is necessary to require $V=g_3 h/q\tau$ where g_3 is similar to g_1 . Now the power is

$$P = (2.5 \times 10^{-32} \text{ wsec}^2) \tau^{-2}. \quad (3)$$

The powers given by (1)–(3) are summarized by Fig. 1. Suppose 1 cm is regarded as a conveniently attainable dimensional parameter, i.e., $C_0=1$ cm, and that g_2 is taken as 100. Then, starting with large τ at the right-hand side of the figure and proceeding to the left, the power dissipation is given by the dotted line labeled "100 μf ." As τ is made smaller the power increases in inverse proportionality to τ . When the dotted line intersects the horizontal full line labeled Z_0 , (2), the limitation imposed by the velocity of light on signal transmission is encountered, and τ can be further reduced only by making the device smaller, that is by reducing C_0 . If this reduction of size in proportion to the reduction in τ is carried out, the power is given by the line Z_0 until the quantum limitation is encountered.

It is also instructive to compare the energy dissipated per operation with Landauer's fundamental limitation.¹ The energy per operation, w , is obtained from the above formulas by multiplying the calculated powers by τ . The values of w/kT are plotted in Fig. 2. It is seen that the values of w/kT are very large. Analysis shows that the origin of these large values lies in the fact that many electrons are used for each operation. It is found that Landauer's result applies per electron; that is, that w/kT divided by the number of electrons which pass through the device in the time τ is of order of magnitude somewhat greater than one. In turn, the large number of electrons is required in order for the applied voltage to do enough work to create the necessary electromagnetic fields in the device.

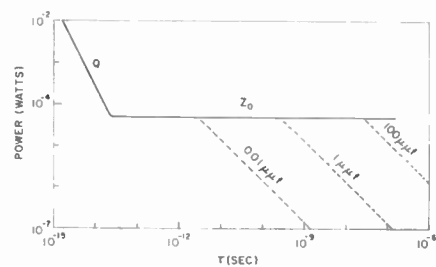


Fig. 1—Power dissipation in a computing element according to (2), (3), and (5). The dimensionless parameters g_1 and g_2 have been set equal to 5. The dotted lines are labeled with the value of $g_2^2 C_0$ in (3).

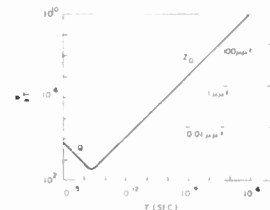


Fig. 2—Energy dissipated per operation in a computing element in the examples of Fig. 1. The energy is measured in units of kT .

The author is indebted to many colleagues for suggestions and criticisms, and particularly to R. W. Landauer, R. F. Rutz and F. H. Dill.

ROBERT W. KEYES
Thomas J. Watson
Research Center
IBM Corp.
Yorktown Heights, N. Y.

A Method of Switching Persistent Currents in Superconducting Coils*

The generation of magnetic fields by means of superconducting coils has received much interest recently. One of the design problems in any superconducting circuit is the heat leak to the helium bath through the incoming leads. This heat transfer is the result of both thermal conduction and Joule heating. By creating a closed superconducting path for the current in the coil, it is possible to disconnect the external power source thereby eliminating Joule heating in the leads except during the time necessary to initiate a persistent current. The material and diameter of the leads can, therefore, be chosen to keep the thermal conduction at a reasonably low value or, if necessary, a method could be devised for removing the leads entirely. Employing a persistent current also eliminates the problem of drift in the power supply.

The circuitry for switching the persistent current is shown in Fig. 1. The coil at the bottom represents the superconducting magnet. A piece of superconducting wire is spot-welded across the input leads

* Received August 29, 1962; revised manuscript received September 13, 1962.

¹ R. W. Landauer, "Irreversibility and heat generation in the computing process," *IBM J.*, vol. 5, pp. 183-191; July, 1961.

* Received September 13, 1962.

of the magnet forming a superconducting loop. Next a heater element is placed near a portion of the shorting wire. This will allow the wire to be brought out of the superconducting state by heating it above its critical temperature. If a current were passed through the heater at this time, a considerable amount of the liquid helium would be vaporized. To overcome this a glass sleeve with a small opening at each end is placed around the heater and shorting wire. The sequence of operation is as follows: First close switch *A*. This vaporizes the liquid in the glass sleeve and brings the portion of wire within the glass out of the superconducting state. There is now a small but finite resistance in parallel with the zero resistance of the magnet coil. Next close switch *B*. After the initial transient, all of the current will flow through the magnet coil. If the magnet coil is highly inductive, the time constant of this transient may be large. A simple method of decreasing this time constant is to lengthen the amount of wire brought out of the superconducting state. This may be easily accomplished by winding many turns of the wire around the

at the wire greater than its critical field. Methods of initiating the persistent current employing this principle and other methods employing pulsing techniques and dc transformers have previously been described.¹ Each of these may have certain advantages in specific cases. The method described in this note is simple in operation and construction and is particularly well suited to highly inductive devices.

In our experiments 5-mil diameter, silk covered niobium was used as the superconducting wire. The heater coil was ten turns of 20-mil diameter nichrome wire. A quarter of an ampere through the nichrome coil is sufficient to bring the niobium wire out of the superconducting state.

The author would like to acknowledge the many helpful discussions with J. T. Sibilian and J. J. Degan in this work.

M. D. BOSEFELD
Bell Telephone Labs., Inc.
Allentown, Pa.

¹R. F. Barron, "Superconductivity," *Machine Design*, p. 26; February 15, 1962.

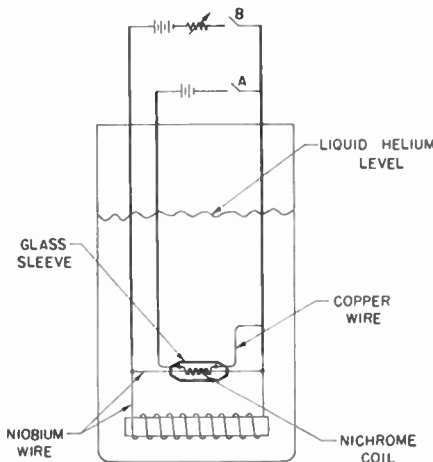


Fig. 1—Schematic representation of switching circuitry.

heater element. The rheostat is now adjusted to obtain the proper value of field. We next open switch *A*. The liquid flows back into the glass sleeve and quickly brings the wire back into the superconducting state. No current, however, will flow through the shorting wire at this time since there is no potential difference across the input leads of the magnet. If we now open switch *B*, the current in the magnet coil can no longer flow through the external circuitry and therefore switches to the zero resistance path of the superconducting short. Since there is no loss mechanism in the superconducting loop, the current will persist. To shut off the current it is merely necessary to close switch *A* and wait for the current to decay according to the L/R time constant of the closed loop.

In this method the shorting wire is brought out of the superconducting state by increasing its temperature above the critical value. Another way of quenching superconductivity is by generating a field

Varactor Frequency Doubler from 11.5 Gc to 23 Gc*

This note describes the performance of a frequency doubler, from 11.5 Gc to 23 Gc, which employs the epitaxial silicon varactor diode developed at Bell Telephone Laboratories. The best result obtained for the conversion loss (including circuit losses) is 3.7 db. The available output power is in excess of 200 mw. At 23 Gc, instantaneous bandwidths of 300 Mc and tuned bandwidths in excess of 1000 Mc have been obtained. This doubler, with a Western Electric 457A klystron, was originally designed as a pump source for parametric amplifiers.

The harmonic generator consists primarily of the diode and the input and output waveguide circuits. The diode is in the output guide and coupling between the two waveguides is accomplished by means of a coaxial line. This coaxial circuit also serves to hold the diode; at the same time, it supplies the dc bias and prevents the output power from feeding into the input waveguide.

The diodes used for this study are the epitaxial silicon diodes whose structure has already been reported.¹ The circuit parameters and total conversion loss (including circuit losses) for representative diodes are listed in Table I.

The variation of conversion loss with input power is shown in Fig. 1. In this case, only the bias is adjusted for minimum conversion loss. The data indicate no increase

in conversion loss up to 28 dbm of input power. This is the maximum power available from the klystron used. It is expected that the input power may be further increased without harm to the diode. It should be noted that the output power exceeded 200 mw during this experiment. The output power of third and fourth harmonics is sufficiently low that there is no measurable change in second harmonic output when a low-pass filter rejecting third and higher harmonics is inserted into the output circuit.

TABLE I

Diode	Total Capacity at Zero Bias*	Break-down Voltage at $-10 \mu\text{a}$	Dynamic Quality Factor† at 11.5 Gc	Conversion loss db
1	1.42	18	4.5	6.2
2	1.01	22	4.7	5.0
3	0.95	16.6	5.2	4.6
4	1.07	21.0	5.1	5.3
5	0.82	21.0	6.5	3.7
6	0.93	25	5.3	4.7

* Total capacity at zero bias includes 0.35 pf of package capacitance.

† The dynamic quality factor \bar{Q} is given by

$$\bar{Q} = \frac{Q}{\frac{2C_0}{C_1} - \frac{C_1}{2C_0}}, \quad \text{where } Q = \frac{1}{\omega C_0 R_S}$$

C_0 and C_1 are the coefficients of the capacitance $C = C_0 + C_1 \cos \omega t + \dots$, and R_S is the spreading resistance of the diode. The dynamic quality factors quoted here include the circuit losses of the doubler.

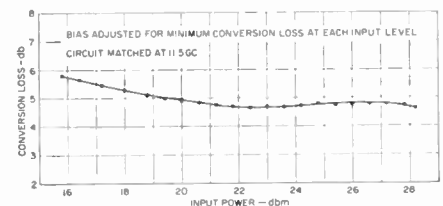


Fig. 1—Conversion loss vs input power for diode No. 3.

The harmonic generator described here was designed for a fixed single frequency application for which a high conversion efficiency was needed. However, the instantaneous 3-db bandwidth was more than 300 Mc at 23 Gc, and there appeared to be no change in bandwidth characteristics with increased input power as long as the bias voltage was adjusted for each individual input power level. With a simple adjustment of circuit and bias voltage, the bandwidth was expanded over 1000 Mc with an output power variation of ± 0.5 db.

Output powers much higher than 200 mw can be generated without degradation of the varactor diode. A diode using the present silicon mesa wafer, but in an improved package, should give greater conversion efficiency. It is anticipated that this harmonic generator can be modified without much difficulty to generate more than 10-mw power at 50 Gc.

M. UENOHARA
R. L. RULISON
C. H. BRICKER
Bell Telephone Labs., Inc.
Murray Hill, N. J.

* Received September 13, 1962.

¹K. M. Eisele and R. L. Rulison, "Low noise reactance amplification using refrigerated epitaxial silicon varactor diodes," *Proc. IRE (Correspondence)*, vol. 50, p. 1523; June, 1962.

An Electronically Variable Delay Line*

During experimental work on a low-noise crossed-field parametric amplifier, it was found that this tube could be used as an electronically variable delay line.

Fig. 1 shows a schematic drawing of the tube when used as a delay line. The tube resembles a Curcia coupler.¹ The RF energy is transferred to the fast cyclotron wave on the crossed-field beam in the input cavity. The modulated electron beam is slowed down and drifts at a low velocity over an appropriate length. In the output cavity the original beam velocity is re-established and the kinetic modulation is converted back to RF energy. The in- and output cavities are half-wave coaxial cavities with a resonance frequency equal to that of the cyclotron frequency of the electrons. The focussing dc electric field is set up between the positive center conductor and the negative tube envelope. The dc magnetic field is perpendicular to the drawing of the tube in Fig. 1.

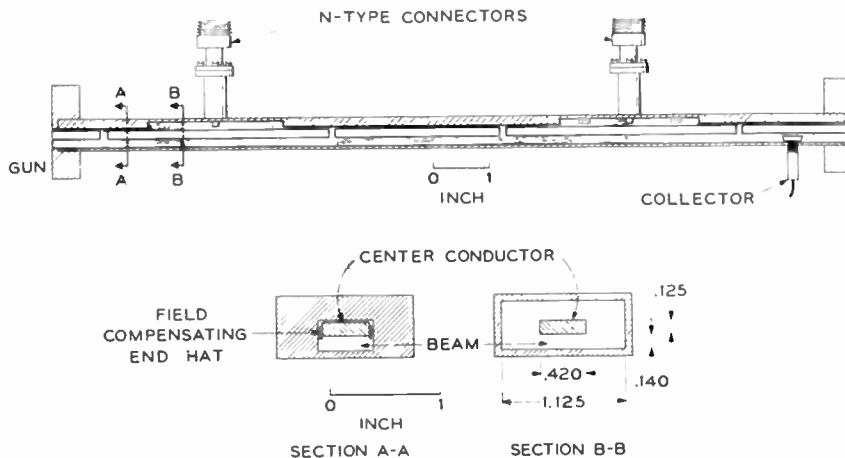


Fig. 1.

So that no direct RF leakage occurs between the in- and output cavities, the drift region has to be nonpropagating at the operating frequency. This is achieved by narrowing down the coaxial guide as shown in Section A, with only a $\frac{1}{4}$ -mil spacing between the center conductor and the tube envelope on the other side of the beam. The breaks in the center conductor also serve to decrease the leakage.

The group velocity for the fast cyclotron wave is equal to the beam velocity. Unlike longitudinal focussing the thermal velocities of the electrons do not determine the lower limit of the beam velocity, which is always given by the dc electric field over the dc magnetic field. Any excess energy over the drift energy will go into rotational motion of the electrons. This does not prevent the RF modulation from being transported on the beam without loss if electron-electron collisions can be neglected, and the field is uniform.

In one experiment the in- and output cavity beam voltages were fixed at 0.42 v. With a beam current of $4 \mu\text{a}$ from a space-charge-limited cathode, the bandwidth was 7 Mc. A change in the drift velocity in the drift region between the two cavities from 0.42 to 0.014 v (which corresponds to a voltage change between the positive and negative plates from 100 to 18) produced a change in the delay of an 100-ke RF pulse of $0.80 \pm 0.02 \mu\text{sec}$. The length of the drift region is 7.2 cm giving a theoretical change in the delay of $0.81 \mu\text{sec}$. The total measured delay of the pulse with the lower drift velocity in the drift region was $1.30 \pm 0.02 \mu\text{sec}$. The theoretical delay over the 19-cm length through the in- and output cavities at the higher drift velocity is $0.47 \mu\text{sec}$, giving a total theoretical delay of $1.28 \mu\text{sec}$. Of this time the electrons take $0.18 \mu\text{sec}$ to transverse either of the two cavities. We see that the total delay of the pulse is given by the time it takes the electrons to travel from the beginning of the input cavity to the end of the output cavity. The energy transfer from electromagnetic to kinetic energy in

the cavities takes place with the group velocity. The total loss of the coupler to a signal at 2000 Mc with the low beam velocity in the drift region was 3 db. This loss results from approximately 0.4-db line loss and 2.6-db cavity losses. Except for these resistive losses, the tube operates as a lossless coupler under these conditions. The pressure was 10^{-6} at the collector end of the tube.

It was possible to slow down the beam to a drift velocity corresponding to $3.4 \cdot 10^{-3}$ v and still operate the tube with a low loss of 4 db. This gives a beam velocity that is $1/9000$ times the velocity of light. The transit time of the electrons over 26 cm was 8 μsec . For minimum loss the collector current was $15 \cdot 10^{-9}$ a, which corresponds to a bandwidth of only a fraction of a megacycle at 2000-Mc signal frequency.

In the design of an actual delay line the bandwidth would determine the beam current and the beam voltage in the cavities. For a cavity made from a 50-ohm coaxial line and with a 4-mm separation between the sole and the center strip, a 40-Mc bandwidth at 2000-Mc signal frequency would require a current of $60 \mu\text{a}$ and a voltage of 1.8 v

under optimum design conditions. By stagger tuning the cavities the transmission loss may be traded for bandwidth. A broader bandwidth can be obtained by using distributed couplers.

To avoid loss to the signal in the velocity jumps the change in the dc velocity, *i.e.*, the electric or the magnetic field over one cyclotron orbit should be small. The maximum rate of change of the time delay is also determined by the adiabatic conditions. Thus a change in the delay by a factor of 10 would allow a 10-Mc time rate of change at 2000-Mc signal frequency.

A further investigation into the characteristics of crosses-field ultra-slow beams should be profitable. The primary interest in this device lies in its low loss, large bandwidth and rapid tuning rate at kilomegacycle frequencies.

J. W. KLÜVER
Bell Telephone Labs., Inc.
Murray Hill, N. J.

Tunnel Diode Audio-Frequency Noise*

For certain applications, we have found a useful evaluation of the noise of tunnel diodes to be the noise voltage of a diode biased at the point of maximum negative resistance. Such a measurement permits a quick rank ordering of diodes for noise with readily available laboratory equipment. The noise characteristics of tunnel diodes have been reported by a number of investigators, but data describing the audio frequency noise spectrum in the negative resistance region is scant [1]-[4].

A block diagram of the measuring scheme is shown in Fig. 1. Audio-frequency voltages appearing at A-A, whether noise or an arbitrary audio frequency from a signal source, may be considered as having been developed by a current passing through the parallel resistance consisting of the negative resistance of the tunnel diode and the two parallel resistors R_2 and R_3 comprising the load. The total resistance can be made arbitrarily large within limits of stability; hence, a voltage resulting from either the signal current or the noise current can be made large. This model is shown in Fig. 2, where I_n is the noise current source, $-g_d$ is the diode conductance, and g_L is the load conductance.

The effective amplification of the diode network is first established by introduction of an audio frequency of known amplitude as determined by the voltage drop across the fixed resistor R_1 . The output voltage across points A-A, maximized by adjustment of R_4 , establishes the point of maximum negative resistance. Next, resistor R_3 is adjusted for a convenient signal level with attention to distortion and switching instability. Finally, the oscillator or signal source is removed and the noise voltage is observed

* Received September 20, 1962; revised manuscript received September 26, 1962.

¹ C. L. Curcia, "The electron coupler," *RCA Rev.*, vol. 10, pp. 270-303; June, 1949.

* Received August 10, 1962; revised manuscript received, September 19, 1962.

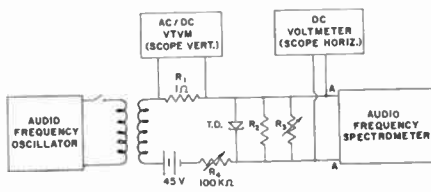


Fig. 1—Block diagram of noise measuring circuit.

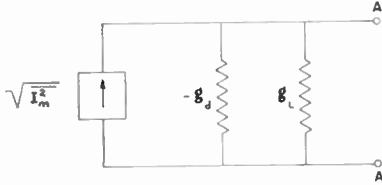


Fig. 2—Noise current source model in tunnel diodes.

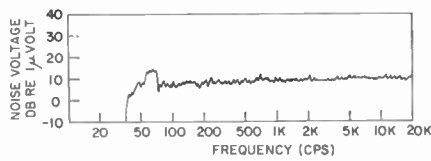


Fig. 3—Noise voltage of a GaAs tunnel diode (T1XA653); one third octave band analysis.

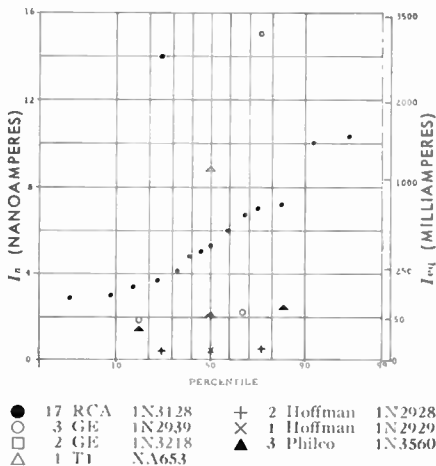


Fig. 4—Distribution of observed 1000-cps one-third octave band noise currents in groups of several diode types.

from which simple calculations permit the determination of the effective noise current source in the diode. Obviously, conditions for stability must be met in the measurement [3]. For example, with a 1N2939 (GE) it is possible to use a diode holding fixture, such as described in the literature [3] with a carbon resistor, R_2 , connected across the diode terminals and with the disk resistors omitted. The variable resistor, R_3 , consisted of a decade resistance box.

It was helpful to have an oscilloscope attached across R_1 and $A-A'$ for viewing the $I-V$ curve of the diode. Diodes with apparently smooth $I-V$ curves showed large noise values under some circumstances. Further investigation determined that there was, in fact, some switching of a random nature occurring and adjustment could be made to eliminate this switching in which case the noise reading reduced appreciably.

A typical one-third octave band spectrum analysis of a tunnel diode is given in Fig. 3. Ignoring the components introduced at 60 cycles power line frequency, the spectrum is seen to be approximately 1/f throughout the range.

The distribution of noise currents I_n in the third octave band centered on 1000 cps for a group of diodes is plotted on a probability scale graph in Fig. 4. A scale of equivalent shot noise current, I_{eq} , is shown for convenience: $I_{eq} = I_n^2 / 2q\Delta f$, where q is electronic charge and Δf is frequency bandwidth.

Assistance of R. C. Ose with some of the measurements is acknowledged.

M. D. BURKHARD

E. F. SIDOR

Industrial Research Products, Inc.

Franklin Park, Ill.

REFERENCES

- [1] M. D. Montgomery, "Excess noise in germanium and gallium-arsenide Esaki diodes in the negative resistance region," *J. Appl. Phys.*, vol. 32, pp. 2408-2410; November, 1961.
- [2] C. N. Berglund, "An Experimental Investigation of Noise in Tunnel Diodes," Rept. No. ESI-R-115, Mass. Inst. Techn., Cambridge, ASTIA Doc. No. AD263266; July, 1961.
- [3] Semiconductor Products Dept., General Electric Co., Liverpool, N. Y., "Tunnel Diode Manual," 1st ed., pp. 24-26; 1961.
- [4] A. Van der Ziel, "Noise aspects of low frequency solid state circuits," *Solid State Design*, vol. 3, pp. 39-44; March, 1962.

Focused Side Pumping of Laser Crystal*

One of the most efficient optical coupling arrangements to deliver light output from a flash lamp to a cylindrical laser crystal rod utilizes an elliptical reflecting cylinder.¹ The linear flash lamp and the laser crystal rod are placed at the two conjugate foci of the elliptical cross section. Under an idealized configuration of 1) large diameter reflecting cylinder, 2) lamp diameter approaching zero, and 3) laser rod diameter approaching zero, the pump flux incident at the laser rod surface will be constant and independent of direction of arrival. All the pump flux propagation vectors will intersect the laser rod axis but not necessarily at right angles. The pump flux is focused by the rod and may attain a high value at the rod center. Due to absorption, the flux will be attenuated in proportion to the depth into the rod.

In a recent paper, side pumping of a composite (dielectric-clad) laser rod using a source of diffused pump light has been treated.² An equation is given for the energy density within the composite rod, and a graph is presented for the case of a composite rod with an index of refraction of 1.76 and no attenuation. In the present paper only focused side pumping is considered as

found, for example, in an elliptical configuration. A full treatment of side pumping of a laser rod in an elliptical cylinder requires many factors which when considered fully will make the analysis beyond solution in closed form. Some of the elementary characteristics can be solved which will provide some qualitative insight into the more difficult problem. In the present simplified analysis it is assumed that all pump flux propagation vectors are normal to the laser rod axis and that the flux is constant and independent of direction of arrival.

At an air-dielectric interface a portion of the incident power P is reflected. The amount of power transmitted P' relative to P is given by $P'/P = 4n/(n+1)^2$ where n = index of refraction of the dielectric. If P_R is designated as the pump flux incident normal to the surface of a cylindrical laser rod of radius R , then the flux P_r due to focusing at some inner radius r is given by

$$\frac{P_r}{P_R} = \frac{P_r}{P_R'} \frac{P_R'}{P_R} = \frac{R}{r} \frac{4n}{(n+1)^2}$$

In this analysis scattering effects are considered to be negligible. If the pump flux is attenuated by the laser rod, then P_r is related to the incident flux by the following:

$$\frac{P_r}{P_R} = \frac{4n}{(n+1)^2} \frac{R}{r} e^{-\alpha(R-r)}$$

where α = absorption coefficient.

In an elliptical configuration, focused pump flux can arrive at each elemental volume in the laser rod from two diametrically opposite directions. Hence the total pump flux at any radius r comprises two components as given in the following equation:

$$\frac{P_r}{P_R} = \frac{4n}{(n+1)^2} \frac{R}{r} [e^{-\alpha(R-r)} + e^{-\alpha(R+r)}]$$

Contributions due to internal reflections are small and are neglected in this analysis. By factoring out the reflection loss at the air-dielectric interface, the following is obtained:

$$\frac{P_r}{P_R'} = \frac{2 \cosh \alpha R r'}{r' e^{\alpha R}}$$

where $r' \equiv r/R$. For convenience this equation is plotted in Fig. 1. If the rod is completely transparent, α and $\alpha R = 0$. The focussing action within the rod is depicted by the infinite value of P_r/P_R' at $r' = 0$. However, with a finite diameter of the lamp, the flux will become large but not infinite at the rod center. If $\alpha R = 0$, the intercept value of $P_r/P_R' = 2$ at $r' = 1.0$ and this is due to pump flux arriving from two opposite directions thereby doubling the value at the surface. As another example, if $\alpha R = 5$, $P_r/P_R' \approx 0.1$ at $r' = 0.2$ which infers that the rod surface and possibly the rod center will more likely exhibit laser action rather than the intervening region. In order to attain nearly uniform pump flux within the entire rod, a value of αR of about 2 offers a good compromise.

One of the criteria in considering the optical efficiency of an elliptical configuration is the one-way attenuation of the pump flux passing diametrically through the laser rod. Neglecting reflections at the air-dielectric interfaces, the one-way attenuation is $e^{-2\alpha R}$. The percentage of power absorbed as a function of αR is tabulated as follows:

* Received October 1, 1962.

¹ M. Ciftan, C. F. Luck, C. G. Shafer and H. Statz, "A ruby laser with an elliptical configuration," *Proc. IRE (Correspondence)*, vol. 49, pp. 960-961; May 1961.

² G. E. Devlin, J. McKenna, A. D. May and A. L. Schawlow, "Composite rod optical masers," *Appl. Optics*, vol. 1, pp. 11-15; January, 1962.

αR	0.50	0.75	1.00	1.25	1.50	2.0	3.0
Per cent absorbed	63.2	77.7	86.5	91.8	95.0	98.2	99.8

This shows that αR should be greater than unity to achieve high efficiencies. The value of αR for a typical $\frac{1}{4}$ -inch diameter, 0.05 per cent chromium-doped sapphire, is about 0.9 for blue pump flux.

Since pump flux arrives at each volume element in the laser rod from two opposite directions it is of interest to determine the fraction F of the total flux which comes from the nearer surface. This fraction can be shown to be equal to $F=1/(1+e^{-2\alpha r/r'})$. With αR and r' as parameters, curves of two values of F , viz 80 per cent and 90 per cent are plotted in Fig. 1. As expected, pump flux from the nearer surface makes a greater contribution particularly when αR is large.

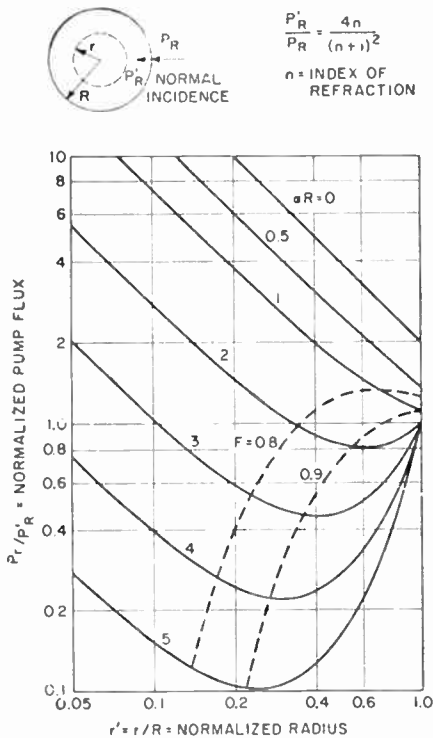


Fig. 1—Pump flux distribution inside a laser crystal.

The foregoing analysis was greatly simplified by assuming α to be a constant, and this assumption is valid if the pump flux is small. If the pump flux is large as required for laser action, population inversion of the active ions takes place and α will decrease from its initial value α_0 . The "penetration" of intense pump flux may be visualized qualitatively by referring to a curve of αR less than $\alpha_0 R$ to be applicable near the rod surface, and to slide upward the initial $\alpha_0 R$ curve to match $P_r/P_{r'}$ at an intermediate value of r' .

The fact that $P_r/P_{r'} = \infty$ at $r' = 0$ helps to explain the observation of a small central filament of laser action at threshold energy levels.³ It should be noted that at these low

³ Tyng Li and S. D. Sims, "Observations on the pump-light intensity distribution of a ruby optical maser with different pumping schemes," Proc. IRE (Correspondence), vol. 50, pp. 464-465; April, 1962.

energy levels, focusing in the laser rod is enhanced since the flash lamp discharge diameter is smaller than at higher energy levels.

K. TOMIYASU
General Engrg. Lab.
General Electric Co.
Schenectady, N. Y.

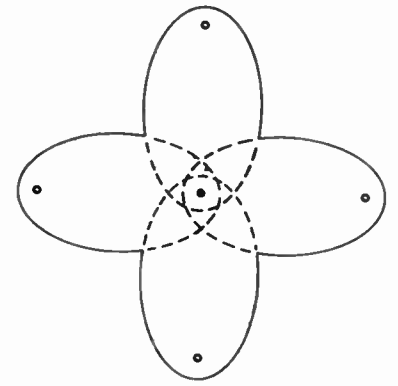


Fig. 4—Four ellipses confocal laser pumping configuration. (O, light source; ●, laser rod; —, reflecting wall; - - -, removed section of truncated ellipse.)

Efficiency of a Multiple Ellipses Confocal Laser Pumping Configuration*

The problem of optical pumping of a laser is one of focusing as much light as possible into a small volume. Probably the most interesting approach that has been made to this problem is through the use of the conjugate foci of an elliptical cylinder.¹ Except for reflectivity losses, this method provides for almost 100 per cent coupling between the light source and laser rod.

Recently, we have considered an optical pumping system which would make use of several light sources and several truncated elliptical cylinders, all sharing a common focus which would contain a laser rod. The configuration is as illustrated (Fig. 1). This is essentially the same configuration as described by Bowness, *et al.*²

An investigation of the expected improvement in ability to concentrate large amounts of light at the absorber has shown that the improvement is apparently non-existent. It was found that while large eccentricity in the ellipse increased the angle over which light would be gathered and focused in each of the truncated ellipses, it had the disadvantage of increasing the spread of the image. If the sources had been line sources instead of extended sources, this would not have been the case.

To provide some feel for the significance of the eccentricity we have tabulated the relationships between the semimajor axis, semiminor axis, the eccentricity, and the percentage of the light gathered when the ellipse is so truncated as to allow four light sources to pump one laser rod. The semimajor axis is taken as unit length.

Eccentricity	0.1	0.3	0.6	0.707	0.8
Semiminor Axis	0.95	0.84	0.63	0.54	0.45
Percentage Light Gathered	29	41	69	79	87

* Received October 8, 1962.

¹ M. Ciftan, C. F. Luek, C. G. Shafer, and H. Stutz, "A ruby laser with an elliptic configuration," Proc. IRE (Correspondence), vol. 49, pp. 960-961; May, 1961.

² C. Bowness, D. Missio, and T. Rogala, "A high-energy laser using a multi-elliptical cavity," Proc. IRE (Correspondence), vol. 50, pp. 1704-1705; July, 1962.

For a laser rod as small or smaller in diameter than the light source, the spread in the image reduces the total power gathered by the rod in proportion to the decrease in the optical power density. The appropriate integrals to allow for the two competing effects of light-gathering capability and image spread were evaluated approximately, through numerical techniques. It was found that the optical power density at the laser rod was proportional to the function $I(n, e)$ where n is the number of light sources used and e is the eccentricity of each of the truncated ellipses. This is tabulated as follows:

		$I(n, e)$				
		0.1	0.3	0.6	0.707	0.8
n	2	3.2	3.1	2.7	2.5	2.1
	4	3.2	3.1	3.1	3.1	3.0
	6	2.9	3.1	3.1	3.2	3.1

These are to be compared with the value for a single light source and a nontruncated ellipse of eccentricity $e=0.1$:

$$I(1, 0.1) = 3.0.$$

It seems, then, that there is no appreciable gain in going to the multiple source configuration, especially when considering the increase in total power required. We would suspect that the improvement reported by Bowness, *et al.* is simply due to using a lamp much smaller in diameter than the laser rod diameter. Presumably this same effect at least could be obtained by using a larger diameter, larger total light output lamp, in a single elliptical cavity with very low eccentricity.

D. L. FRIED
P. ELTGROTH
Information Systems Lab.
Space and Information Systems Div.
North American Aviation, Inc.
Torrance, Calif.

A 35.5-kMc Parametric Amplifier*

Parametric amplification and subharmonic oscillations with a varactor diode have been previously reported at frequencies as high as 30 kMc.¹ Experiments with these diodes at *X* band² indicate that they could be useful at even higher frequencies. To demonstrate this capability a degenerate, reflection-type, parametric amplifier was constructed to operate in the *Q*-band region.

The amplifier, as shown in Fig. 1, and sketched in Fig. 2, consists of two crossed waveguides machined from a silver block with the varactor mounted at the junction. One guide (*Q*-band) houses the signal cavity with tunable end plates. One of these plates has a small hole through which the signal is coupled. The smaller guide (*E*-band) provides for the 71-kMc pump power input

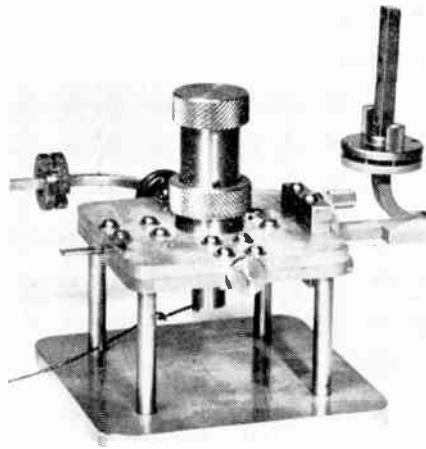


Fig. 1—Parametric amplifier.

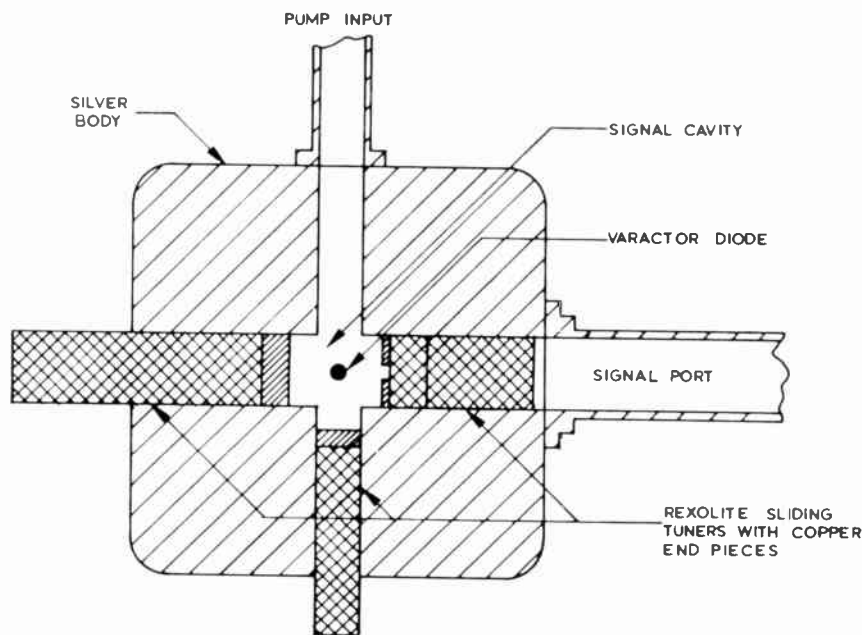


Fig. 2—Cross-section sketch of parametric amplifier.

and is terminated with a moveable short.

The point contact varactor diode was fabricated directly within the amplifier using an *N*-type, tellurium-doped, gallium arsenide crystal ($\rho=0.002 \Omega\text{-cm}$) and a 0.001-inch spring-tempered phosphor bronze whisker. The fabrication process is very similar to that described by Sharpless.³

Information on the device as an amplifier has not yet been obtained but subharmonic oscillations in a degenerate or quasi-degenerate mode have been induced at 35.5 kMc. The pump power is derived from a Raytheon QKK 865 klystron and based on its specifications, oscillations have been induced with as little as 5 mw of pump

power. As microwave components become available at higher pump frequencies, it is expected that these diodes can be made to operate even further up into the *Q*-band region.

GEORGE W. FITZSIMMONS
The Boeing Co.
Seattle, Wash.

Two Results in the Preliminary Design of Optimum Linear Systems*

Two results are presented here which may be used to advantage as short cuts in the preliminary design of optimum linear filters,

They are useful mainly when operations to be performed on the signal are specified in the time domain.

Let a signal $x(t)$, belonging to a stationary ergodic random process, consist of an information-carrying signal $s(t)$ along with additive noise $n(t)$. On passing $x(t)$ through a linear time-invariant physically realizable system with impulse response $h(t)$, the output is

$$y(t) = \int_0^{\infty} h(\tau)x(t-\tau)d\tau \quad (1)$$

where the lower limit of integration is zero rather than $-\infty$ due to the physically realizable nature of the system (*i.e.*, $h(t)=0$ for $t<0$). Now we are actually interested in performing a certain desired linear operation \mathcal{D} on the information signal $s(t)$ alone:

$$\mathcal{D}\{s(t)\} = \int_{-\infty}^{\infty} h_d(\tau)s(t-\tau)d\tau \equiv f_d(t) \quad (2)$$

where $h_d(t)$ is the corresponding desired impulse response of a system that is under no restriction of physical realizability. Then the mean-square error \mathcal{E} is given by the expected value of $|f_d(t)-y(t)|^2$, and by the well-known techniques of Wiener theory, \mathcal{E} is minimum if $h(t)$ satisfies the condition

$$\int_0^{\infty} h(\mu)R_{xx}(\tau-\mu)d\mu = \int_{-\infty}^{\infty} h_d(\mu)R_{xx}(\tau-\mu)d\mu, \quad \tau \geq 0. \quad (3)$$

In this equation $R_{xx}(\tau)$ and $R_{xx}(\tau)$ are the known auto- and cross-correlation functions, respectively. The right-hand side is known after h_d has been computed from (2). Thus (3) is a Wiener-Hopf equation which enables $h(t)$ to be determined.

Up to now $h(t)$ has been required to be zero for $t<0$. On removing this restriction, taking Fourier transforms of both sides of (3) with respect to τ and rearranging, we get for the optimum nonrealizable filter's transfer function

$$H_{OXR}(\omega) = \frac{\Phi_{xx}(\omega)}{\Phi_{xx}(\omega)} \cdot H_d(\omega) \quad (4)$$

where each Φ is the transform of the corresponding R or ϕ .

Thus the design procedure would usually require

- the determination of $h_d(t)$ from the specified operation $\mathcal{D}\{s(t)\}$ by the use of (2), and either
- the use of $h_d(t)$ in (3) to solve for $h(t)$ or
- the use of $H_d(\omega)$ in (4) to solve for the ONR filter, which leads to the optimum-realizable filter by following, say, the method of Bode and Shannon.¹

The results that simplify the procedure are based on the fact that one can obtain the end results, *viz.*, values for the right-hand

¹ H. W. Bode and C. E. Shannon, "A simplified derivation of linear least-square smoothing and prediction theory," *Proc. IRE*, vol. 38, pp. 417-426; April, 1950.

* Received July 5, 1962; revised manuscript received, September 17, 1962.

¹ B. C. DeLoach, "17.35 and 30-kMc parametric amplifiers," *Proc. IRE (Correspondence)*, vol. 48, p. 1323; July 1960.

² N. Houlding, "Measurement of varactor quality," *Microwave J.*, vol. 3, pp. 40-45; January, 1960.

³ W. M. Sharpless, "High-frequency gallium arsenide point-contact rectifiers," *Bell Sys. Tech. J.*, vol. 38, pp. 259-269; January, 1959.

* Received April 23, 1962; revised manuscript received May 14, 1962.

sides of (3) and (4), without having to determine $h_d(t)$ first. Thus it is shown below that

1) the Wiener-Hopf equation for the optimum linear filter can be expressed as

$$\int_0^\infty h(\mu)R_{xz}(\tau - \mu)d\mu = \mathfrak{D}\{R_{xz}(\tau)\}, \tau \geq 0 \quad (5)$$

2) the optimum nonrealizable filter has the transfer function

$$H_{ONR}(\omega) = \frac{\Phi_{xz}(\omega)}{\Phi_{xx}(\omega)} [e^{-j\omega t} \mathfrak{D}\{e^{j\omega t}\}] \quad (6)$$

Notice that the quantity within the large brackets is independent of t since the linear operation by \mathfrak{D} will leave an $e^{j\omega t}$ as the multiplier of $e^{-j\omega t}$.

The design procedure thus reduces to the obtaining of $H_{ONR}(\omega)$ from (6) and computation of $H_{on}(\omega)$ by the usual methods. The short cut is obviously useful when \mathfrak{D} is an operation specified in the time domain. If on the other hand the design requirement is already expressed in the frequency domain, i.e., H_d is given, then (4) can be used at once to get H_{ONR} . Two examples will illustrate the point.

A Servomechanism Problem

Let the desired output be a voltage proportional to the angular position of a shaft as also to the shaft's angular velocity. Thus with obvious notation

$$\mathfrak{D}\{s(t)\} = As(t) + B \frac{d}{dt}s(t) \quad (7)$$

where A and B are constants. Hence

$$\mathfrak{D}\{e^{j\omega t}\} = A e^{j\omega t} + B j\omega e^{j\omega t}$$

and from (6)

$$H_{ONR}(\omega) = \frac{\Phi_{xs}(\omega)}{\Phi_{xx}(\omega)} (A + B j\omega) \quad (8)$$

This represents a significant reduction in work as compared to the alternative procedure which requires calculation of h_d and H_{ONR} from (2) and (4).

Low-Pass Filter

Let it be desired to have a sharp cutoff in the frequency domain when $|\omega| \geq \omega_0$. Thus

$$H_d(\omega) = 1, \quad |\omega| \leq \omega_0 \\ = 0, \quad |\omega| \geq \omega_0 \quad (9)$$

In this case it is unnecessary to obtain \mathfrak{D} since (4) yields the result directly.

$$H_{ONR}(\omega) = \frac{\Phi_{xs}(\omega)}{\Phi_{xx}(\omega)} \cdot 1, \quad |\omega| \leq \omega_0 \\ = 0 \quad |\omega| \geq \omega_0 \quad (10)$$

Proofs

To prove result 1) we note from (2) that the defining equation for \mathfrak{D} when operating on $g(\tau)$ can be expressed as

$$\mathfrak{D}\{g(\tau)\} = \int_{-\infty}^\infty h_d(\sigma)g(\tau - \sigma)d\sigma$$

so that

$$\mathfrak{D}\{R_{xz}(\tau)\} = \int_{-\infty}^\infty h_d(\sigma)R_{xz}(\tau - \sigma)d\sigma, \quad (11)$$

which holds for all τ and therefore for $\tau \geq 0$.

Comparing the right-hand sides of (3) and (11) we find them equal if σ is replaced by μ so that $\mathfrak{D}\{R_{xz}(\tau)\}$ can be substituted for the former. Hence (5) holds and 1) is correct.

In order to prove result 2) we recall the definition

$$H_d(\omega) = \int_{-\infty}^\infty h_d(\tau)e^{-j\omega\tau}d\tau \quad (12)$$

Multiplying by $e^{-j\omega t}$ outside the integral sign and by $e^{+j\omega t}$ inside we get

$$H_d(\omega) = e^{-j\omega t} \int_{-\infty}^\infty h_d(\tau)e^{j\omega(t-\tau)}d\tau \quad (13)$$

A comparison with the defining equation (2) shows

$$\int_{-\infty}^\infty h_d(\tau)e^{j\omega(t-\tau)}d\tau = \mathfrak{D}\{e^{j\omega t}\} \quad (14)$$

Combining (13) and (14) we have the useful relation

$$H_d(\omega) = e^{-j\omega t} \mathfrak{D}\{e^{j\omega t}\} \quad (15)$$

and substitution in (4) yields result 2).

S. H. DURRANI
Elec. Eng. Dept.
University of New Mexico
Albuquerque, N. Mex.

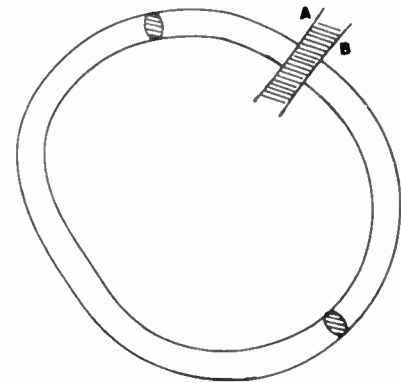


Fig. 1.

At low frequencies $e^{-j\omega R} \rightarrow 1$, which is equivalent to specifying a circuit which is small with respect to the wavelength. Integrating (1) around the surface of the circuit conductor from A to B (integration around the closed path is not possible since \bar{i} and σ are both zero in the dielectric) gives (see Fig. 1)

$$V_i = \int_A^B \frac{i(s) \cdot \bar{d}\bar{L}}{\sigma} + j\omega \int_A^B \bar{A} \cdot \bar{d}\bar{L} + \phi_B - \phi_A \quad (4)$$

where

$$\phi_B - \phi_A = \frac{Q}{C} = \frac{I}{j\omega C}$$

for time-harmonic dependence.

Then (4) is written as¹

$$V_i = I \left[R_s + j\omega L_s + j\omega L_e + \frac{1}{j\omega C} \right] \quad (5)$$

In this form one defines

$$L_e = \frac{1}{I} \int_A^B \bar{A} \cdot \bar{d}\bar{L} \quad (6)$$

If the path of integration is closed, then

$$\frac{1}{I} \oint \bar{A} \cdot \bar{d}\bar{L} = \frac{1}{I} \oint (\nabla \times \bar{A}) \cdot \bar{n} da \\ = \frac{\phi}{I} \triangleq L_e \quad (7)$$

However, (6) is not consistent with this definition.

The difficulty can be avoided by considering an imperfect capacitor as opposed to an ideal one; then the circuit law can be written as

$$\oint \bar{E}_i \cdot \bar{d}\bar{L} = \int_A^B \frac{i(s) \cdot \bar{d}\bar{L}}{\sigma_s} + \int_B^A \bar{E}_i \cdot \bar{d}\bar{L} + j\omega \oint \bar{A} \cdot \bar{d}\bar{L} + \oint \bar{C} \bar{V} \cdot \bar{d}\bar{L} \quad (8)$$

or

$$V_i = I(R_s + j\omega L_s) + \int_B^A \bar{E}_i \cdot \bar{d}\bar{L} + I(j\omega L_e) + 0 \quad (9)$$

One needs to consider the remaining integral from B to A . At any point in the dielectric

¹ E. C. Jordan, "Electromagnetic Waves and Radiating Systems," Prentice-Hall, Inc., New York, N. Y., 1st ed., pp. 381-388; 1960.

* Received April 20, 1962.

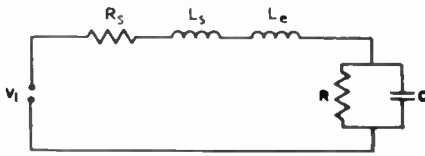


Fig. 2—Equivalent circuit.

medium the total current in the circuit can be expressed as

$$\bar{a}I = (\bar{i}_c + \bar{i}_p)A \quad (10)$$

where A is *not* necessarily the area of the electrodes but some function of the geometry; \bar{a} is a unit vector in the direction of the sum of the conduction and displacement current densities.

Now

$$\bar{a}I = (\sigma + j\omega\epsilon)\bar{E}^1 A \quad (11)$$

so that

$$\begin{aligned} \int_B \bar{E}^1 \cdot \bar{d}\bar{L} &= I \int_B \frac{\bar{a} \cdot \bar{d}\bar{L}}{(\sigma + j\omega\epsilon)A} \\ &= I \int_B \frac{(\sigma - j\omega\epsilon)\bar{a} \cdot \bar{d}\bar{L}}{(\sigma^2 + \omega^2\epsilon^2)A} \end{aligned} \quad (12)$$

which for a parallel plate capacitor becomes

$$I = \frac{(\sigma - j\omega\epsilon)d}{(\sigma^2 + \omega^2\epsilon^2)A} \quad (13)$$

This is recognized as the parallel impedance of an R and C where

$$R = \frac{1}{\sigma} \frac{d}{A}, \quad C = \frac{\epsilon}{d} \frac{d}{A} \quad (14)$$

The equivalent circuit for (8) is, then, as drawn in Fig. 2 without requiring an alternate definition of external inductance L_e .

ANTHONY J. FERRARO
Dept. of Elec. Engrg.
Pennsylvania State University
University Park, Pa.

Single-Sideband Modulation and Reception of Light at VHF*

In a previous note¹ the principles of single-sideband (SSB) light generation using electrooptic techniques were described. This work was an extension of the phasing method of SSB modulation² to optical frequencies. In the present letter we present a VHF version of this light modulator and then describe an optical analog of the phasing method of SSB reception.³

The SSB optical modulator contains two crystals of KH_2PO_4 (KDP) oriented with their "c" axes along the light propagation

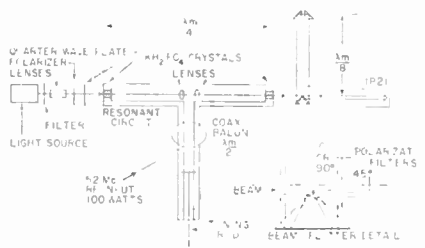


Fig. 1—Single-sideband optical modulator and receiver for VHF.

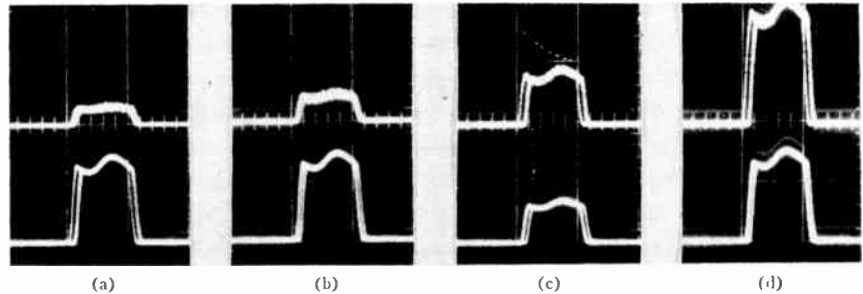


Fig. 2—Oscillograms of detector outputs.

direction and their "a" axes at 45° to each other. As shown in Fig. 1, the crystals are located in a 52-Mc (ω_m) resonant circuit driven by a VHF power source such that in-phase electric fields exist along their "c" axes. The required 90° phase difference¹ between the voltages on the two crystals is obtained by choosing the spacing between crystals to make the light transit time a quarter cycle at ω_m . A yellow beam from a zirconia arc lamp with a Corning CS 3-66 filter and a left-circular polarizer complete the modulator which is shown on the left in the figure. A multiplier phototube (RCA 1P21) with circuitry to filter out and rectify the 52-Mc component of anode current was used as a detector. Two outputs, proportional to the average (dc) intensity and RF component of intensity, respectively, were monitored.

As explained in the previous note,¹ the output light should consist of a left-circularly polarized carrier and a right-circularly polarized single sideband. It can be shown that the resultant polarization state has constant ellipticity with principal axes rotating at $\omega_m/2$ in a direction dependent on which sideband is present. Unwanted sideband suppression was checked by passing this light through a rotatable polarizer into the detector and noting the detector outputs. Constant dc and RF components of light at the detector as the polarizer was rotated through 360° were taken as proof of good suppression.

After alignment for good sideband suppression, the modulator served as a single-sideband light source for testing the phasing method of single-sideband reception. The optical receiver is shown at the right of Fig. 1. The light from the modulator is split into two beams by a prism, and each is filtered by a polarizer, the one in the diverted beam having its polarization axis horizontal or vertical, and the other with its polarization axis at 45° to the vertical. As shown in Fig. 1, the diverted beam travels an additional

quarter wavelength before entering the detector with the direct beam.

The phase of the RF intensity components differ by 90° in the two beams as a result of the different orientations of the polarizers, but because of the additional path of one beam, their phases at the detector differ by 0° or 180° . If the beam intensities are equal, complete cancellation of the RF intensity components occurs for that sideband having the 180° phase difference. The opposite sideband under the same

conditions has a 0° phase difference between the RF on the two beams at the detector and is received.

In Fig. 2 are shown a series of oscillograms taken under various conditions with the upper traces showing the level of the RF (52 Mc) intensity component and the lower traces showing the dc light level. A light chopper was used to show the base level with beam off in both traces. Fig. 2(a) indicates the RF signal due to noise with the modulator signal turned off; Fig. 2(b) is obtained at maximum rejection of the sideband produced by the modulator, and, as can be noted, the RF level is only slightly greater than for the case of Fig. 2(a). This small increase may be due to incomplete cancellation of the rejected sideband either in the modulator or receiver. Fig. 2(c) shows a case in which the diverted beam was blocked; the dc light level is halved, but the RF level increases markedly. In Fig. 2(d) the oscillogram is obtained with the receiver set to pass the generated sideband by rotating the plane polarizer in the diverted beam from the horizontal position used for Fig. 2(b) to the vertical position. Here the RF components in the two beams add as noted.

This receiving technique should be applicable to suppressed-carrier transmission provided both the suppressed carrier and reinserted carrier (local light oscillator beam) are coherent. The incoming signal and local oscillator could be circularly polarized, merged in a beam splitter to give two composite beams and processed as above. Other polarization combinations can be used, and, with some extra complexity, simultaneous upper and lower sideband reception is possible.

The authors acknowledge the help of Dr. E. M. Conwell in preparing this letter.

C. F. BUHRER
L. R. BLOOM
General Telephone and
Electronics Labs., Inc.
Bayside, N. Y.

* Received September 21, 1962.

¹ C. Buhrer, V. Fowler and L. Bloom, "Single-sideband suppressed-carrier modulation of coherent light beams," *Proc. IRE (Correspondence)*, vol. 50, pp. 1827-1828; August, 1962.

² Donald E. Norgaard, "The phase-shift method of single-sideband signal generation," *Proc. IRE*, vol. 44, pp. 1718-1735; December, 1956.

³ Donald E. Norgaard, "The phase-shift method of single-sideband signal reception," *Proc. IRE*, vol. 44, pp. 1735-1743; December, 1956.

Breakdown Voltage of GaAs Diodes Having Nearly Abrupt Junctions*

The data presented in this communication show the dependence of gallium arsenide breakdown voltage on resistivity and carrier concentration. The GaAs diodes used in this study were fabricated as follows: *N*-type GaAs crystal was grown horizontally on the 111 axis, sliced, lapped and polished. Slices were then Zn-diffused at 1000°C to a depth of approximately 6 to 20 microns. In subsequent operations small mesas (1 to 2 mils in diameter) were formed, the crystal was diced and etched down to a thickness of 3 mils, ohmic contacts were made to both sides of the junction, and the assembly was then etched, baked and encapsulated.

Because of the behavior of Zn diffusion in GaAs [1], junctions obtained by this technique were nearly abrupt. The abrupt nature of these junctions was established as follows: A diode was reverse-biased at -1 v and its quality factor was measured at 10 Gc [2]. The quality factor Q_r is given by

$$Q_r = \frac{1}{2\pi RC_f} \quad (1)$$

The bias was then increased and the quality factor was measured at the same frequency. Because the variation of the depletion-region thickness with voltage was negligible as compared to the thickness of the GaAs wafer, the diode series resistance R did not change. The only change occurred, therefore, in the junction transition capacitance C_r . The ratio of the quality-factor measurements at the voltages V_1 and V_2 in terms of the capacitance is given by

$$\frac{Q_1}{Q_2} = \frac{C_2}{C_1} \quad (2)$$

The junction capacitance varies with voltage in the following manner:

$$C_r = \frac{K}{(\phi - v)^n} \quad (3)$$

where K is a constant, V is the applied potential, and ϕ is the built-in junction potential. The value of n can be determined from (2) and (3) as follows:

$$n = \frac{\ln \frac{Q_1}{Q_2}}{\ln \left(\frac{\phi - V_1}{\phi - V_2} \right)} \quad (4)$$

The contact potential was determined for each diode by "curve-fitting" (3) on a log-log plot. The value of ϕ was found to vary from 1.0 v to 1.3 v depending on the resistivity of the GaAs pellet. The variation of the exponent n between 0.43 and 0.50 confirms the near-abrupt characteristics of the diodes under consideration.

N-type GaAs resistivity was measured by a Q meter technique, and breakdown voltage was defined as the voltage at a current of 20 μ a. Fig. 1 shows curves of breakdown voltage at 25°C as a function of crystal resistivity for both GaAs and silicon. For the same resistivity GaAs breakdown volt-

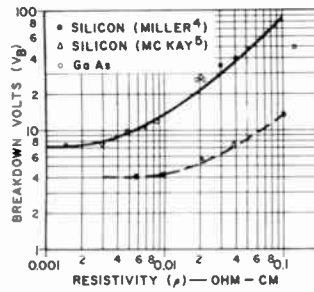


Fig. 1 - Breakdown voltage of GaAs and silicon step junctions as a function of wafer resistivity. Each point of the GaAs curve represents the median value as measured on a sample of at least 25 diodes.

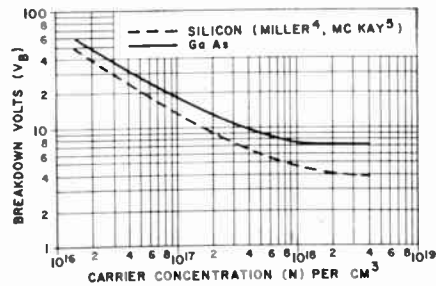


Fig. 2 - Breakdown voltage of GaAs and silicon step junctions as a function of net impurity concentrations.

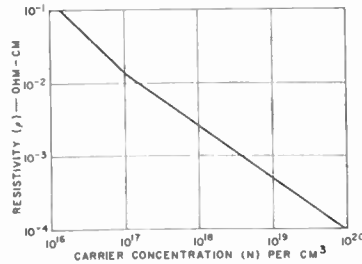


Fig. 3 - Carrier concentration as a function of resistivity in *n*-type GaAs.

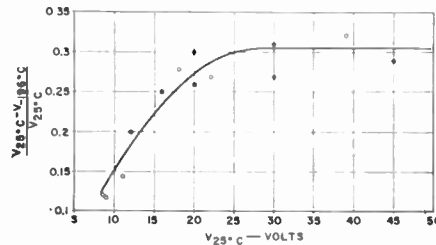


Fig. 4 - Relative changes of the breakdown ($V_1 - V_2$)/ V_1 between 25°C and -196°C as a function of the room temperature breakdown voltage V_1 .

age is always higher than that of silicon.

Fig. 2 shows the dependence of the GaAs breakdown voltage on the carrier concentration, and Fig. 3 shows resistivity as a function of concentration [3]. The general shape of the breakdown voltage curve for GaAs is similar to that of silicon and at low resistivities flattens considerably.

Breakdown voltages were also determined at liquid-nitrogen temperature

(-196°C). The relative changes of the breakdown ($V_1 - V_2$)/ V_1 are shown in Fig. 4 as a function of the room-temperature breakdown voltage V_1 . In all the diodes tested the breakdown voltage exhibited a positive temperature coefficient.

H. KRESSEL
A. BUCHER
L. H. GIBBONS, JR.
Semiconductor and Materials Div.
RCA
Somerville, N. J.

REFERENCES

- [1] F. A. Cunnell and C. H. Goeltz, "Diffusion of zinc in gallium arsenide," *J. Phys. and Chem. Solids*, vol. 15, p. 127; May, 1960.
- [2] R. I. Harrison, "Parametric diode Q measurements," *Microwave J.*, vol. 4, pp. 43-46; August, 1961.
- [3] J. Hillbrand, private communication; April, 1962.
- [4] S. L. Miller, "Ionization rates for holes and electrons in silicon," *Phys. Rev.*, vol. 105, p. 1246; February, 1957.
- [5] K. G. McKay, "Avalanche breakdown in silicon," *Phys. Rev.*, vol. 94, p. 877; May, 1954.

The O-Type Backward-Wave Oscillator Frequency Pushing*

The purpose of this correspondence is to disclose a general formula of the *O*-type backward-wave oscillator frequency pushing depending upon space charge and circuit loss. This equation was derived in order to investigate the transfer functions of microwave tubes. The derivation is based on the usual BWO model of Johnson.¹

It is assumed that 1) the phase-velocity conditions are satisfied, 2) the value of the interaction parameter C is small and the tube acts as a linear device. For large QC and $L=0$, it is well known that $b = \sqrt{4QC}$. This condition applies to the case of large QC and $L > 0$ after some modifications of Johnson's formula.¹ Then general characteristics of the frequency pushing can be summarized as follows:

- 1) In the region of small space charge and $L \geq 0$,

$$f_{st} - f = (CN)_{st} \cdot b_{st} [(I/I_{st})^{1/3} - 1] / (T_{bc})_{st} \quad (1)$$

- 2) In the region of middle space charge and $L \geq 0$,

$$= (CN)_{st} \cdot b_{st} [(I/I_{st})^{1/2} - 1] / 2(T_{bc})_{st} \quad (2)$$

- 3) In the region of large space charge and

$$f_{st} - f = (CN)_{st} \cdot b_{st} [(I/I_{st})^{1/2} - (I/I_{st})^{1/3}] / (T_{bc})_{st} \quad (3)$$

where

$$I_{st} = \text{Value of beam current to start the oscillation,}$$

* Received April 17, 1962.

¹ H. R. Johnson, "Backward-wave oscillators," *Proc. IRE*, vol. 43, pp. 684-697; June, 1955.

* Received May 31, 1962; revised manuscript received, June 7, 1962.

- I = Beam current operating value,
- $f_{s,t}$ = Frequency when $I = I_{s,t}$,
- f = Frequency for operating beam current,
- L = Total cold-circuit distributed loss in decibels,
- T_{bc} = Transit time of an electron and RF energy down the length of active portion of beam and circuit,
- b = Pierce's velocity parameter,
- N = Number of guide wavelength on circuit,
- C = Interaction parameter,
- $(CN)_{s,t}$, $b_{s,t}$, $(T_{bc})_{s,t}$ = Values of parameters when $I = I_{s,t}$.

TABLE I
THEORETICAL $(CN)_{s,t} \cdot b_{s,t}$

L	0	4	10	15	20
0	0.4781	0.4974	0.5290	0.5574	0.5881
0.25	0.5154	0.5453	0.5974	0.6472	0.7027
0.50	0.6117	0.6841	0.8034	0.8969	0.9865
0.75	0.8546	0.9309	1.0457	1.1559	1.2761
1.00	1.0182	1.1145	1.2828	1.4192	1.5564
1.50	1.3799	1.5025	1.7134	1.8950	2.0808

Values of $(CN)_{s,t} \cdot b_{s,t}$ can be easily shown in Table I from Johnson's results.¹ Good experimental confirmation is obtained with backward-wave oscillators. This further detail was reported elsewhere.²

ICHIRO SAKURABA
Faculty of Engrg.
Hokkaido University
Hokkaido, Japan

² I. Sakuraba, "Analysis of the O-type backward-wave oscillator frequency pushing," *J. Elec. Comm. Engrs. of Japan*, vol. 43, pp. 810-815; September, 1959.

Determination of Depletion Layer Thickness at Indium-Germanium Contacts with No Applied Voltage*

Electrochemical transistor technology makes possible a series of punch-through voltage measurements of a transistor as a function of metallurgical base width on a single piece of germanium. Such data, taken on transistors with homogeneous base material, provide a means for determining the depletion layer thickness for a given combination of materials, at a contact with no applied voltage. Such information is important when the metallurgical base width of a transistor, the punch-through voltage and the net dopant density are to be quantitatively related.

Fig. 1 shows the results of some measurements made for indium contacts on homogeneous N -type germanium of several val-

ues of resistivity. In the region where the applied voltage is sufficiently large to make the built-in voltage comparatively negligible, the slope can be used to calculate the dopant density.

$$N \approx K \left[\frac{dV_{PT}^{1/2}}{dW} \right]^2$$

where for germanium K is 2.7×10^{12} with the units of N in cm^{-3} , W in mils and V_{PT} in volts. The extrapolated line intercepts the abscissa axis at a value equal to the sum of the two equal depletion layer thicknesses.

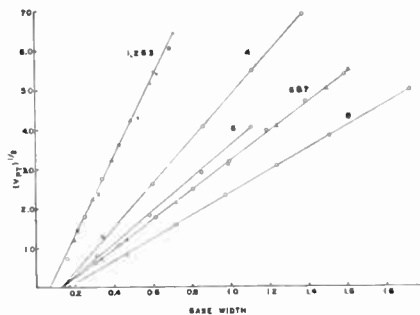


Fig. 1—The relationship between the square root of the punch-through voltage (volts) and the metallurgical base width (mils).

TABLE I

Sample Number	N , Calculated from Fig. 1 (cm^{-3})	N , Calculated from Resistivity Measurement (cm^{-3})	Single Depletion Layer Thickness with No Applied Voltage (mils)
1, 2 & 3	2.7×10^{13}	$2.5 - 3.1 \times 10^{13}$	0.035
4	8.4×10^{13}	5.5×10^{14}	0.065
5	4.6×10^{13}	5.5×10^{14}	0.065
6 & 7	3.7×10^{13}	3.0×10^{14}	0.070
8	2.2×10^{13}	3.0×10^{14}	0.080

Table I shows the values calculated from the data given in Fig. 1. Also shown are values of the net dopant density calculated from the measured values of resistivity made on the germanium wafer before being processed into a transistor, assuming a value of $3900 \text{ cm}^2/\text{volt-sec}$ for the mobility.

D. P. SANDERS
E. S. SCHLEGEL
Lansdale Div.
Philco Corp.
Lansdale, Pa.

WWV and WVVH Standard Frequency and Time Transmissions*

The frequencies of the National Bureau of Standards radio stations WWV and WVVH are kept in agreement with respect

to each other and have been maintained as constant as possible since December 1, 1957, with respect to an improved United States Frequency Standard (USFS). The corrections reported here were arrived at by means of improved measurement methods based on transmissions from the NBS stations WVV (60 kc) and WVVH (20 kc). The values given in the table are 5-day running averages of the daily 24-hour values for the period beginning at 1800 UT of each day listed.

The time signals of WWV and WVVH are also kept in agreement with each other. Since these signals are locked to the frequency of the transmissions, a continuous departure from UT2 may occur. Corrections are determined and published by the U. S. Naval Observatory. The time signals are maintained in close agreement with UT2 by properly offsetting the broadcast frequency from the USFS at the beginning of each year when necessary. This new system was commenced on January 1, 1960.

WWV FREQUENCY WITH RESPECT TO U. S. FREQUENCY STANDARD

1962	Parts in 10^{10} *
September 1	-129.7
2	-129.7
3	-129.7
4	-130.7†
5	-130.6
6	-130.6
7	-130.4
8	-130.3
9	-130.2
10	-130.1
11	-129.9
12	-129.8
13	-129.8
14	-129.7
15	-129.6
16	-129.6
17	-129.5
18	-129.4
19	-130.2†
20	-130.1
21	-129.9
22	-129.8
23	-129.7
24	-129.6
25	-129.6
26	-129.5
27	-129.5
28	-129.4
29	-129.3
30	-129.2
Monthly Mean:	-129.83

* A minus sign indicates that the broadcast frequency was below nominal. The uncertainty associated with these values is $\pm 5 \times 10^{-11}$.

† WWV frequency adjusted as follows:

September 4, -0.9×10^{-10} at 1800 UT
September 19, -0.8×10^{-10} at 1800 UT

Subsequent changes were as follows:

FREQUENCY OFFSET, WITH REFERENCE TO THE USFS

January 1, 1960, -150 parts in 10^{10}
January 1, 1962, -130 parts in 10^{10}

TIME ADJUSTMENTS, WITH REFERENCE TO THE TIME SCALE UT2

December 16, 1959, retardation, 20 milliseconds
January 1, 1961, retardation, 5 milliseconds
August 1, 1961, advancement, 50 milliseconds.

Adjustments were made at 0000 UT on the foregoing dates: an advancement means that the signals were adjusted to occur at an earlier time than before.

NATIONAL BUREAU OF STANDARDS
Boulder, Colo.

See "National standards of time and frequency in the United States," *Proc. IRE (Correspondence)*, vol. 48, pp. 105-106; January, 1960.

* Received April 2, 1962.

* Received October 24, 1962.

Prediction of Rise Time in Junction Transistors*

SUMMARY

This communication presents a generalized expression for rise time in junction transistors in applications where collector cutoff can be neglected. This expression includes a factor K determined by the impurity distribution in the base layer of the transistor. Experimental results are presented which verify the analysis.

INTRODUCTION

The existing rise-time relation¹ is suitable for alloy transistors; however, it is necessary to modify this equation to include the effects of the impurity distribution of the base region. This modification results in a generalized expression for rise time in junction transistors. It has been reported² that a factor K is determined by the impurity distribution in the base layer of the transistor. The following conditions prevail for various values of K :

- 1) $K=1$ for a retarding field in the base layer.
- 2) $K=0.82$ for uniform base layer.
- 3) $K<0.82$ for "built-in" fields in the base layer.

ANALYTICAL RESULTS

When Laplace transform notation is used, the common-emitter de current gain β_0 is given by

$$\frac{i_c(s)}{i_b(s)} = \frac{\beta_0 \exp\left(\frac{(K-1)s}{\sqrt{K}\omega_a}\right)}{\left(1 + \frac{s}{\omega_1}\right)} \quad (1)$$

β_0 =de common emitter current gain (db)
 $2\pi f_a = \omega_a$ =Radian frequency common base 3-db point (Mc). For a step input, (1) is modified as follows:

$$\frac{i_c(s)}{i_b(s)} = \frac{\omega_1 \beta_0 \exp\left(\frac{(K-1)s}{\sqrt{K}\omega_a}\right)}{s(s + \omega_1)} \quad (2)$$

The exponent of (2) can be rewritten in the following form:

$$\exp\left(\frac{(K-1)s}{\sqrt{K}\omega_a}\right) \cong 1 + \left[\frac{(K-1)}{\sqrt{K}}\right] \frac{s}{\omega_a}$$

Then

$$\frac{i_c(s)}{I_B \beta_0 \omega_1} = \left[\frac{1}{s(s + \omega_1)} + \frac{(K-1)}{\sqrt{K}\omega_a(s + \omega_1)} \right] \quad (3)$$

The inverse transform of (3) is given by

$$\frac{i_c(t)}{\omega_1 \beta_0 I_B} = \frac{1}{\omega_1} \left[1 - e^{-\omega_1 t} + \frac{(K-1)\omega_1}{\sqrt{K}\omega_a} e^{-\omega_1 t} \right] \quad (4)$$

* Received April 16, 1962.

¹ J. J. Ebers and J. L. Moll, "Large-signal behavior of junction transistors," Proc. IRE, vol. 42, pp. 1761-1772; December, 1954.

² D. E. Thomas and J. L. Moll, "Junction transistor short-circuit current gain and phase determination," Proc. IRE, vol. 46, pp. 1177-1184; June, 1958.

TABLE I
EXPERIMENTAL RESULTS

RCA Type	Common base cutoff frequency f_{cb} (Mc) (5v, 10 ma)	de Common base current gain α_0 (5v, 10 ma)	de Common emitter current gain β_0 (5v, 10 ma)	Common emitter gain bandwidth f_T (Mc) (5v, 10 ma)	K	Collector junction capacitance C_j (pF) (IV)	Rise time t_R nsec Meas ($I_C=10$ ma) ($I_B=3$ ma) ($R_L=220$)	Calculator
2N1708	485	0.9766	39.0	330	0.700	3.45	7.6	6.05
	495	0.9768	38.9	355	0.735	3.50	6.0	5.80
	445	0.9710	34.1	32.0	0.746	3.20	7.0	5.90
2N697	108	0.9785	44.1	90.5	0.86	28.4	28	29.1
	101	0.9821	52.8	84.5	0.84	30.2	28	31.5
	117	0.9912	120.0	101.0	0.87	26.6	22	25.6

Because

$$i_c(t_R) = \frac{0.9I_{cc}}{R_L} = 0.9I_C$$

I_B =base current (ma), I_C =collector current (ma),

$$t_R \omega_1 = \frac{1 - \frac{(K-1)\omega_1}{\sqrt{K}\omega_a}}{1 - \frac{0.9I_C}{I_B \beta_0}} \quad (5)$$

The rise time t_R is then given by

$$t_R = \frac{1}{\omega_1} \log_e \left[\frac{1 - \frac{(K-1)\omega_1}{\sqrt{K}\omega_a}}{1 - \frac{0.9I_C}{I_B \beta_0}} \right] \quad (6)$$

When $\omega_1 R_L C_c > 1$, ω_a is reduced. This is expressed as

$$\omega_1 = \frac{\omega_a \omega_c (1 - \alpha_0)}{\omega_c + \omega_a} \text{ and } \omega_c = \frac{1}{(R_L + r_e) C_c}$$

C_c =Collector junction capacitance (pf)
 α_0 =de common base current gain (db)
 R_L =Load resistance in ohms
 $r_e = 0.026/I_E$ at 25°C where I_E =emitter current (ohms).

For transistors with a retarding field in the base region the common emitter gain-bandwidth equals that of the common base. For $K<1$ the common base gain-bandwidth exceeds that of the common emitter.

$$\omega_a = \frac{\omega_T}{\alpha_0 K} \text{ and } K = \frac{f_3}{(1 - \alpha_0) f_a}$$

$\omega_T = 2\pi f_T$ =common emitter gain-bandwidth radian frequency (Mc).
 f_3 =common emitter 3-db point (Mc).

Thus, the expression for rise time becomes

$$t_R = \left[\frac{(R_L + r_e) C_c}{(1 - \alpha_0)} + \frac{\beta_0 K}{\omega_T} \right] \cdot \log_e \left[\frac{1 - \frac{(K-1)(1 - \alpha_0)\omega_c}{(\omega_c + \omega_1)\sqrt{K}}}{1 - \frac{0.9I_C}{I_B \beta_0}} \right] \quad (7)$$

When $K=1$, (7) reduces to the Ebers and Moll equation for rise time.

EXPERIMENTAL RESULTS

Experimental tests were performed on RCA 2N1708 and 2N697 transistors. Tests of f_{cb} and α_0 as functions of frequency were made on a General Radio Transfer Bridge,

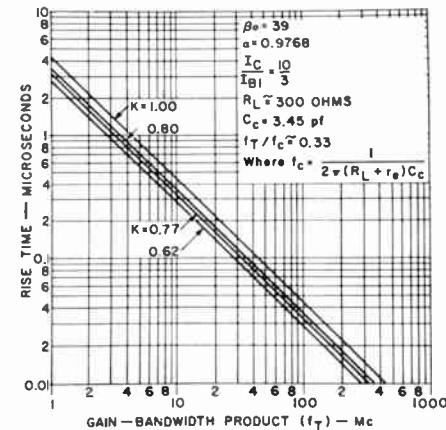


Fig. 1

tests of β_0 and α_0 on a Boonton Radio 275A test set, and tests of rise time on an HP Sampling Scope. Table I shows a cross section of the test results, and compares measured and calculated rise times.

CONCLUSIONS

The experimental results are in good agreement with calculations. Therefore, (7) can be very useful in predicting rise time for all types of transistors. Fig. 1 shows the gain-bandwidth product as a function of rise time with K as a parameter.

P. E. KOLK
Semiconductor and Materials Div.
RCA
Somerville, N. J.

Simplified Calculation of Unabsorbed Field Intensity on Overseas Transmission Circuits*

Unabsorbed field intensity is defined as the strength of a signal received at a distant point in the absence of ionospheric absorption. It depends upon the attenuation due to path length, or, in other words, on path attenuation. Adding an eventual ionospheric

* Received April 12, 1962.

absorption attenuation, the over-all signal attenuation is obtained.

Information on path attenuation is particularly important for analytical work on overseas propagation, as, for instance, the determination of the Lowest Usable High Frequency (LUF) and of the transmitting power required for a certain path. Approximate figures being sufficient for many applications, a simple logarithmic relation has been used, with different constants, by both the U. S. National Bureau of Standards¹ and H. Bremmer:²

$$\delta = \gamma \log D \quad (1)$$

where

- δ = attenuation in decibels
- D = distance in kilometers
- γ = constant = 22.0 or 25.0, respectively.

Together with results of his propagation studies and an analytical proof of his Chordal-Hop theory, the author published some years ago a new formula³ which yielded more correct data for normal types of transmission circuits investigated by him:

$$[D > 10^4 \text{ km}] \quad \delta \simeq 38.2\sqrt{\log D}. \quad (2)$$

According to the chordal-hop theory,³⁻⁵ a predominant mode of propagation consists of chordal hops along ionospheric layers without touching the earth's surface. Readers are also referred to a discussion, in these PROCEEDINGS, of echo-signal analysis with the aid of chordal-hop propagation.⁶ In the majority of cases, a ray is not supposed to touch ground between transmitter and receiver, and ground losses have thus been disregarded in (2). However, focussing has been taken into account.

The formula having been used successfully for comprehensive propagation studies,^{5,7} the author herewith intends presenting its derivation from basic relations.

Maxwell's field equations yield, in the practical system of units,

$$E = \frac{30\lambda I h}{\pi x^3} + j \frac{60 I h}{x^2} - \frac{120\pi I h}{\lambda x} \quad (3)$$

with

- E = field intensity in volts/m
- I = effective antenna current in amperes
- h = effective antenna height in meters
- x = distance from transmitter in meters
- λ = wavelength in meters.

¹ U. S. National Bureau of Standards, Washington, D. C., Circular 462; 1948.

² H. Bremmer, "Terrestrial Radio Waves," Elsevier, Amsterdam, The Netherlands; 1949.

³ H. J. Albrecht, "Further studies on the chordal-hop theory of ionospheric long-range propagation," *Arch. Meteorol. Geophys. u. Bioklimatol.*, vol. A2, pp. 84-92; 1959.

⁴ H. J. Albrecht, "Analysis of world-wide ionospheric propagation to and from Australia, 1953-54," *J. Wireless Inst. Austr.*, vol. 24, pp. 2-5; October, 1956.

⁵ H. J. Albrecht, "Investigations on great-circle propagation between Eastern Australia and Western Europe," *Geofis. pura e appl.*, vol. 38, pp. 169-180; 1957.

⁶ H. J. Albrecht, "Applying the chordal-hop theory of ionospheric long-range propagation to echo-signal delay," *Proc. IRE (Correspondence)*, vol. 49, pp. 356-357; January, 1961.

⁷ H. J. Albrecht, "Analysis of ionospheric paths in long-range propagation," *Indian J. Meteorol. Geophys.*, vol. 2, pp. 57-63; January, 1960.

Neglecting terms with x^3 and x^2 , and representing the power radiated by $P = 1579 (Ih/\lambda)^2$, (3) may be simplified to yield a reference signal at the reference distance of 1 km:

$$E_{(1 \text{ km})} \simeq 9.5 \times 10^{-3} \sqrt{P} \quad (4a)$$

or, expressed in decibels above $1/\mu\text{V/m}$

$$E_{(1 \text{ km})} \simeq 79.5 + 10 \log P. \quad (4b)$$

On the other hand, Försterling and Lassen published, in 1931, the following general expression for ionospheric propagation by "m" multiple hops between layer and earth's surface:⁸

$$E \simeq \frac{c_p |r|^{m-1} \cos \psi}{\sqrt{\Delta R m \sin \left(\frac{m\Delta}{R} \right)}} \quad (5a)$$

$$\Delta \simeq 2h_0 \tan \phi_0 + \frac{R}{R+h_0} \alpha' C \sin \phi_0 \ln \frac{1+\alpha' \cos \phi_0}{1-\alpha' \cos \phi_0} \quad (5b)$$

$$\alpha' = \frac{f/f_c}{1 - \frac{C}{\gamma_0} \frac{f^2}{f_c^2} \sin^2 \phi_0} \quad (5c)$$

where

- E = field strength at receiving point
- m = number of hops between ground and ionosphere
- ψ = transmission angle
- R = the earth's radius
- $|r|$ = reflection coefficient of the earth's surface
- ϕ_0 = angle of incidence at the layer
- c_p = constant depending upon transmitting power
- f = operating frequency
- f_c = critical frequency of the layer
- C = half thickness of the layer
- γ_0 = minimum height of ionosphere
- h_0 = height of reflection.

Emphasizing that we are interested in deriving a *simplified* expression of path attenuation, (5a) may be modified for the purpose of chordal-hop propagation; the constant c_p is given by (4a), $|r|$ and $\cos \psi$ equal unity while m denotes the number of ionospheric touching points. The average value of m can be obtained approximately from a range of possible values of layer height and minimum path height, i.e. lowest height of a ray path with respect to the earth's surface. Taking its limiting data as a layer height of 300 km with a minimum path height of 5 km and a layer height of 200 km with a minimum path height of 60 km, corresponding to values found in an analysis of the Australia-Europe transmission circuit, the average value of m is given by

$$\bar{m} \simeq 3.12 \times 10^{-4} D. \quad (6)$$

The objective of extreme simplification would permit us to substitute the numerical value of 0.7 for the sine function in (5a), thus restricting the validity of the simplified expression to distances larger than a minimum limit.

⁸ K. Försterling and H. Lassen, "Die Ionisation der Atmosphäre und die Ausbreitung der kurzen elektrischen Wellen (10-100 m) über die Erde," *Z. techn. Physik*, vol. 12, pp. 453-469 and pp. 502-527; 1931.

The signal intensity would thus amount to

$$E \simeq \frac{9.5 \times 10^3 \sqrt{P}}{\sqrt{44.6 \times 10^2 D}} \quad (7a)$$

or, in decibel form,

$$E \simeq 79.5 + 10 \log P - 36.5 - 10 \log D. \quad (7b)$$

Negative terms may be transformed by means of a square-root approximation and intensity becomes

$$E \simeq 79.5 + 10 \log P - 38.2\sqrt{\log D} \quad (8)$$

where the last term is identical to (2).

Eq. (8) is of practical usefulness for the determination of the signal intensity in the absence of ionospheric absorption. It should be noted, however, that the transmission term $79.5 + 10 \log P$ corresponds to ideal conditions. One method to account for frequency-dependent changes in this reference signal is the addition of a corrective term to the decibel expression. For short-wave calculations, the author has successfully used a term equal to $-0.02 f^2$, where f is the operating frequency in megacycles. With this in mind, (8) becomes

$$E \simeq 79.5 + 10 \log P - 0.02 f^2 - 38.2\sqrt{\log D}. \quad (9)$$

Applying the relation given in (2) and (9) in propagation calculations, much better agreement was found to exist with measured intensities. A further advantage has been noticed with LUF calculations which appear to display an improved accuracy when carried out with the new formula.

HANS J. ALBRECHT
c/o Schramberg-Sulgen
Württemberg, West Germany

Parameters of a Piezoelectric Crystal*

The four fundamental parameters capacitance C_1 , inductance L_1 , resistance R_1 and shunt capacitance C_0 of the equivalent electric circuit of a piezoelectric oscillator excited by electrodes which form a two-terminal network define the network shown in Fig. 1 completely, and all other parameters may be derived from them. It is generally assumed that the losses associated with C_0 can be neglected. This assumption

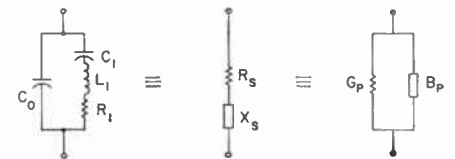


Fig. 1—Equivalent electric circuit of a piezoelectric vibrator near a resonance.

* Received April 16, 1962.

TABLE I
SOLUTIONS FOR THE VARIOUS CHARACTERISTIC FREQUENCIES SHOWN IN FIG. 2

Characteristic Frequencies	Meaning	Condition	Constituent Equation for Frequency	Root	57 IRE 14.A1[1]
$f_{\omega'}$	Frequency of Maximum Bp	$\frac{dBp}{d\omega} = 0$	$\Delta(1 - \Delta) - q(q - 1) = 0$	lower*	
f_m	Frequency of Maximum Admittance (Minimum Impedance)	$\frac{d Z }{d\omega} = 0$	$(\Delta^2 + q^2)^2 - 2q^2(\Delta + r) - 2\Delta r(1 - \Delta) - \Delta^2 = 0$	lower*	f_m
f_s	Motional (Series) Resonance Frequency	$X_1 = 0$	$\Delta = 0$		f_s
f_r	Resonance Frequency	$X_s = Bp = 0$	$\Delta(1 - \Delta) - q^2 = 0$	lower	f_r
$f_{\omega''}$	Frequency of Minimum Bp	$\frac{dBp}{d\omega} = 0$	$\Delta(1 - \Delta) - q(q + 1) = 0$	lower*	
f_u	Frequency of Maximum Phase	$\frac{d}{d\omega} \left(\frac{X_s}{R_s} \right) = \frac{d}{d\omega} \left(\frac{Bp}{Gp} \right) = 0$	$(2\Delta - 1)(\Delta + 2r) + (\Delta^2 + q^2) = 0$		
f_v	Frequency of Maximum X_s	$\frac{dX_s}{d\omega} = 0$	$\Delta(1 - \Delta) - q(q + 1) = 0$	upper*	
f_a	Antiresonance Frequency	$X_s = Bp = 0$	$\Delta(1 - \Delta) - q^2 = 0$	upper	f_a
$f_{p'}$	Parallel Resonance Frequency (Frequency of Maximum Resistance)	$\frac{dR_s}{d\omega} = 0$	$2(1 - \Delta)(\Delta + r) - q^2 = 0$		f_p
f_p	Parallel Resonance Frequency (Lossless)	$X_s \Big _{R_1=0} = \infty$	$\Delta = 1$		
f_n	Frequency of Minimum Admittance (Maximum Impedance)	$\frac{d Z }{d\omega} = 0$	$(\Delta^2 + q^2)^2 - 2q^2(\Delta + r) - 2\Delta r(1 - \Delta) - \Delta^2 = 0$	upper*	f_n
f_w	Frequency of Minimum X_s	$\frac{dX_s}{d\omega} = 0$	$\Delta(1 - \Delta) - q(q - 1) = 0$	upper*	

* Refers to real roots; complex roots to be disregarded.

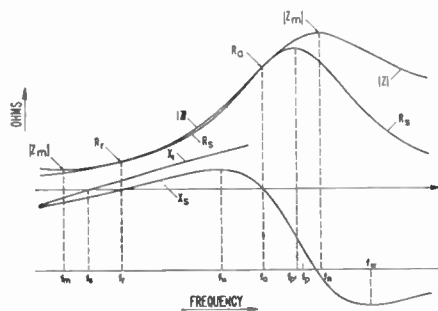


Fig. 2—Impedance $|Z|$, resistance R_s , reactance X_s and series arm reactance X_1 of a piezoelectric vibrator as a function of frequency. Z_m and Z_n denote minimum and maximum impedance, R_r and R_a the impedances at zero phase angle. For the meaning of the different frequencies, see Table I.

is valid for most crystals in practical use except for ferroelectric materials such as polarized barium titanate ceramics and others. The parameters of the equivalent electric circuit are characteristic constants for a given mode of motion of a particular specimen and functions of the orientation and dimensions of the electrodes.

In the IRE Standards [1] the equation for the impedance Z or admittance Y is presented in the form

$$Z = \frac{1}{Y} = \frac{1}{j} \frac{\omega_n}{\omega} \frac{R_1 Q}{r} \frac{1 + jQ \left(\frac{\omega}{\omega_n} - \frac{\omega_n}{\omega} \right)}{1 + jQ \sqrt{1 + r} \left(\frac{\omega}{\omega_p} - \frac{\omega_p}{\omega} \right)} \quad (1)$$

Using the generalized quantities

$$\Delta = \frac{\omega^2 - \omega_n^2}{\omega_p^2 - \omega_n^2} \quad \text{and} \quad q = \omega_n C_0 R_1,$$

this equation can be simplified [2]

$$Z = \frac{1}{Y} = jX_0 \frac{1 - jq}{1 - \Delta + jq} [2]. \quad (2)$$

Eq. (1) or its equivalent (2) defines the characteristic frequencies and conditions under which they occur; these are shown in Table I. The designation used in the IRE Standards [1] are also shown in this table.

For the purpose of defining the different characteristic frequencies, the impedance Z of the equivalent electric circuit, its resistive component R_s (resistance), its reactive component X_s (reactance) and the reactance X_1 of the L_1, C_1, R_1 branch are plotted as functions of frequency in Fig. 2. Z_m and Z_n denote the minimum and maximum impedance, respectively, and R_r, R_a the impedances at zero phase angle. This figure corresponds to the values $r=2, R_1=1 \Omega$ and $M=3$. For symbols used in this communication, see IRE Standards [1].

R. BECHMANN
A. D. BALLATO
U. S. Army Signal Res. and
Dev. Lab.
Fort Monmouth, N. J.

REFERENCES

- [1] "IRE Standards on Piezoelectric Crystals—The Piezoelectric Vibrator: Definitions and Methods of Measurement, 57 IRE 14.S1," Proc. IRE, vol. 45, pp. 353-358; March, 1957.
- [2] R. Bechmann and S. Ayers, "Thickness Modes of Plates Excited Piezoelectrically," Post Office Engrg. Dept., Dolis Hill, London, England, Res. Rept. 13471; May, 1952.

A General Expression for the Output of a Dicke-Type Radiometer*

There have been several analyses made of Dicke-type radiometers.¹⁻³ The results of an analysis⁵ are described here, which differ from the previous ones in that the effects of realizable filters, and asymmetrical rectangular modulation and demodulation are considered.

The analysis was done by representing Gaussian noise entering the radiometer as a Fourier series of sinusoidal waves, with random phase angles and amplitudes, and of fundamental period θ . This series was operated on by the various components of the radiometer, and then, at the output, θ was made to approach infinity. This method was

* Received March 29, 1962.
¹ S. J. Goldstein, "A comparison of two radiometer circuits," Proc. IRE, vol. 43, pp. 1663-1668, November, 1955; as corrected by D. G. Tucker, H. M. Graham, and S. J. Goldstein, Proc. IRE (Correspondence), vol. 45, pp. 365-366, March, 1957.
² L. D. Strom, "The Theoretical Sensitivity of the Microwave Radiometer, A Problem in Non-stationary Noise Analysis," Ph.D. dissertation, University of Texas, Austin; June, 1957.
³ W. Selove, "A dc comparison radiometer," Rev. Sci. Instr., vol. 25, pp. 120-122; February, 1954.
⁴ F. V. Bunkin and N. V. Karlov, "The sensitivity of radiometers," Zhur. Tekh., Fiz., vol. 25, pp. 430-435, March; pp. 733-741, April, 1955.
⁵ J. Knight, "Evaluation and Analysis of Radiometers," M.A.Sc. thesis, Dept. of Elec. Engrg., University of Toronto, Ontario, Canada; September, 1961.

originated by Bennet⁶ and was recently used by Green⁷ in an analysis of a somewhat similar system.

Consider the model as shown in Fig. 1, with a modulating waveform $f(t)$ as shown in Fig. 2. Then if a and b are the lengths of time the antenna is connected and disconnected respectively, one finds that

$$f(t) = C_0 + \sum_{m=1}^{\infty} C_m \cos(m\omega_q t + \beta_m) \quad (1)$$

where

$$C_0 = \frac{a-b}{a+b},$$

$$C_m = \frac{4}{m\pi} \sin \frac{m\pi a}{a+b},$$

$$\beta_m = \frac{m\pi a}{a+b},$$

and $\omega_q = 2\pi/a+b$ equals the fundamental angular frequency of $f(t)$.

It will be assumed that the integrator cutoff frequency is much lower than ω_q , that the harmonics of ω_q have negligible power at any frequency comparable with the IF bandwidth, and that the noise power input σ_N^2 and the signal power input σ_s^2 are stationary, ergodic Gaussian processes satisfying

$$\sigma_N^2 \gg \sigma_s^2.$$

With these assumptions the signal-to-noise ratio (SNR) is found to be

$$S/N = \frac{P_{dc}}{P_{ac}}$$

$$= \frac{2\pi\alpha \left\{ I(0) \right\}^2 \sum_{m=1}^{\infty} C_m^2 |H(m\omega_q)|^2 \cos^2 \delta_m \sigma_s^2}{16 \int_0^{\infty} |I(\omega)|^2 \sum_{m=1}^{\infty} C_m^2 |H(m\omega_q)|^2 \sigma_N^2 d\omega}$$

where

$I(\omega)$ is the integrator transfer function,
 $H(m\omega_q)$ is the transfer function of the band-pass filter at frequency $m\omega_q$,
 δ_m is the phase shift of this filter at frequency $m\omega_q$, and
 α is the effective input bandwidth of the radiometer defined by

$$\frac{\sigma_N^2}{2\pi\alpha} = \int_0^{\infty} G_s^2(\omega) d\omega. \quad (2)$$

where

$G_s(\omega)$ is the input power spectrum,
 P_{dc}/P_{ac} is the ratio of desired signal power which emerges as pure dc in this model, to the power in the random fluctuations of the output.

If we further assume that the phase-shift δ_m is negligible at all harmonics with appreciable power content, that $|I(0)|=1$, and if one sets

⁶ S. O. Rice, "Mathematical analysis of random noise," *Bell Sys. Tech. J.*, vol. 23, pp. 282-332, July, 1944; vol. 24, pp. 46-156, January, 1945. See sec. 3.4 and the comments after eq. (2.8-6).
⁷ P. E. Green, "The output signal-to-noise ratio of correlation detectors," *IRE TRANS. ON INFORMATION THEORY*, vol. IT-3, pp. 10-18, March, 1957; as corrected in *IRE TRANS. ON INFORMATION THEORY*, vol. IT-3, p. 82, June, 1958.

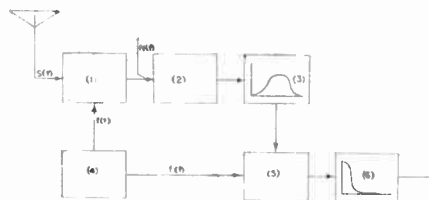


Fig. 1—Model of radiometer: (1) the modulator, (2) the square-law detector, (3) the band-pass filter with transfer function $H(\omega)$, (4) the rectangular wave generator, (5) the multiplier, and (6) the integrator with transfer function $I(\omega)$.

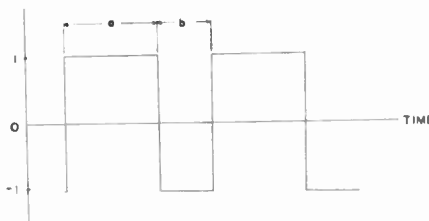


Fig. 2—The modulating function $f(t)$.

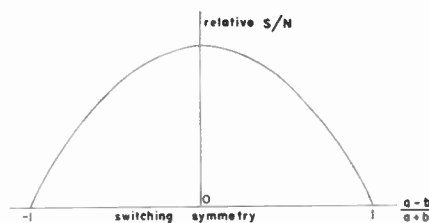


Fig. 3—A plot of switching symmetry against SNR.

$$\int_0^{\infty} |I(\omega)|^2 d\omega = \Gamma.$$

one obtains

$$S/N = \frac{P_{dc}}{P_{ac}} = \frac{2\pi}{16} \frac{\alpha}{\Gamma} \frac{\sigma_s^4}{\sigma_N^4} \sum_{m=1}^{\infty} C_m^2 |H(m\omega_q)|^2.$$

For an ideal band-pass filter, with characteristic

$$|H(m\omega_q)| = \begin{cases} 0 & \text{if } m \neq 0 \\ 1 & \text{if } m = 0 \end{cases}$$

one gets

$$S/N = \frac{P_{dc}}{P_{ac}} = \frac{\alpha \sigma_s^4}{2\Gamma \sigma_N^4} \left(\frac{a}{a+b} \right) \left(1 - \frac{a}{a+b} \right). \quad (3)$$

For a Dicke system with a reference source of power σ_R^2 one obtains

$$\frac{P_{dc}}{P_{ac}} = \frac{\alpha}{2\Gamma} \frac{(\sigma_R^2 - \sigma_s^2)^2}{\sigma_N^4} \left(\frac{a}{a+b} \right) \left(1 - \frac{a}{a+b} \right). \quad (4)$$

Note that this can no longer be considered as an SNR.

By removing the appropriate harmonics of $f(t)$, (3) can be transformed to give expressions in agreement with those of Strum,⁸ Galejs⁹ and Goldstein.¹

⁸ P. D. Strum, "Considerations in high sensitivity microwave radiometry," *Proc. IRE*, vol. 46, pp. 43-53, January, 1958; as corrected by R. S. Colvin, *Proc. IRE*, vol. 47, p. 2105, December, 1959.

⁹ J. Galejs, "Comparison of subtraction-type and multiplier-type radiometers," *Proc. IRE*, vol. 45, p. 1420-1422, October, 1957.

These equations allow one to evaluate proposals using asymmetrical switching. For example, in a Dicke radiometer no advantage is gained by leaving the input connected to the antenna for a longer period than to the reference source, as a plot of the SNR shows (Fig. 3).

Below meter wavelengths the reference source in a Dicke radiometer usually has a much higher noise temperature than the signal, thus radiometer gain variations are not as effectively removed as when the two are equal. It has been suggested that this might be corrected by keeping the reference source connected for a shorter part of the switching period, so that the average power was the same for both the signal and the reference source. Consider (4). We are no longer looking for a minimum P_{dc}/P_{ac} as when SNR was being considered, but rather for a null-balance obtained by changing the coefficients of σ_R^2 with respect to σ_s^2 to get $P_{dc}=0$. One sees, however, that changing the partial period a affects both σ_R^2 and σ_s^2 equally. $P_{dc}=0$ if $a=0$ or $a=1$, which is equivalent to saying that a bridge has a null-balance when its oscillator is shut off. Note however, from (2), that narrowing the input spectrum of the reference source decreases σ_R^2 and thus produces the desired result.

An intuitive idea of these results can be obtained from the Fourier series for a rectangular wave (1). The sum of the ac components are symmetrical about $(a-b)/(a+b)=0$ as shown in Fig. 3. Increasing the time during which the signal is connected, that is making $(a-b)/(a+b)>0$, actually decreases the power in these ac terms. The extra signal power goes into the dc term C_0 . This dc term is equivalent to the portion of the signal power which is unmodulated. The receiver noise is also unmodulated so both come out of the detector at zero frequency, and both are removed by the filter.

JOHN KNIGHT
 Dept. of Elec. Engrg.
 University of Toronto
 Toronto, Ontario, Canada

An Expansion for Log-Periodic Functions*

In the course of an investigation of the propagation of waves on a log periodically-loaded transmission line, a general representation for log-periodic functions has suggested itself. Such functions have the following property:

$$f(x) = f(x\tau). \quad (1)$$

That is, the function takes on the same values at intervals spaced according to a geometric series along the x axis.

$$f(x_0) = f(x_0\tau) = f(x_0\tau^2) = f(x_0\tau^3) = \dots \quad (2)$$

* Received May 9, 1962. Part of this work was supported through consultation with Sylvania Electric Products Co., Mountain View, Calif.

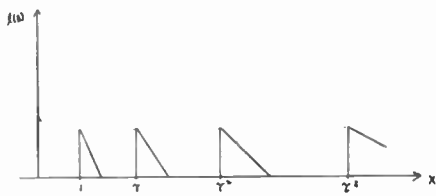


Fig. 1.

An example of such a function is shown in Fig. 1.

It is well known that a periodic function may be expanded in a Fourier series. Thus, if $p(y) = p(y+T)$, then

$$p(y) = \sum_{n=-\infty}^{\infty} c_n e^{i(2\pi n/T)y}. \quad (3)$$

The change of variables $x = e^{y/T}$ in (3) leads to a new series in which each term satisfies (1) with $T = \ln \tau$. This new series may then be used to represent an arbitrary log-periodic function

$$L(x) = \sum_{n=-\infty}^{\infty} a_n x^{j(n/a)}, \quad a = \frac{\ln \tau}{2\pi}. \quad (4)$$

It remains to find the formula for the coefficients a_n and to show that the representation is complete.

Let $u_n(x) = x^{j(n/a)}$. $u_n(x)$ is then a solution of the differential equation

$$x^2 u_n''(x) + x u_n'(x) + \left(\frac{n}{a}\right)^2 u_n(x) = 0. \quad (5)$$

The $u_n(x)$ are orthogonal over the period τ , that is, over any interval $b \leq x \leq b\tau$, with b arbitrary. The scalar product is complex and requires the weight function $1/x$.

$$\int_b^{b\tau} u_n(x) u_m^*(x) \frac{dx}{x} = \int_b^{b\tau} x^{j(n-a)x^{-j(m-a)}} \frac{1}{x} dx = \ln \tau \delta_{nm}. \quad (6)$$

If we multiply both sides of (4) by $x^{j(m/a)} dx/x$ and integrate over $(b, b\tau)$, we find with the aid of (6), that the coefficients in the expansion (4) are given by

$$a_m = \frac{1}{\ln \tau} \int_b^{b\tau} L(x) x^{-j(m/a)} \frac{dx}{x}. \quad (7)$$

Any function defined over an interval $(b, b\tau)$ which is square integrable over that interval may be expanded in the log-periodic series by means of (7). In as much as the interval $(b, b\tau)$ is finite and the series (4) contains all the eigenfunctions of (5) which satisfy the log-periodic boundary condition (1), we can reasonably expect that the representation is complete. It can also be shown directly that the series expansion of a square pulse converges, although not uniformly, and therefore, by superposition, the series for any piecewise continuous function should converge. Of course, any function defined only over the finite interval which is expanded according to (4) and (7) becomes a log-periodic function over all x . It is worth emphasizing, however, that for representations of functions over finite intervals (4) may be a convenient alternative to, say, a Fourier series

It is interesting to consider the limit of the sum (4) when τ is allowed to approach infinity. For this purpose it is convenient to rewrite (4) and (7) slightly.

$$L(x) = \frac{1}{\ln \tau} \sum_{n=-\infty}^{\infty} a_n x^{j(n/a)}$$

$$a_n = \int_1^\tau L(x) x^{-j(n/a)} \frac{dx}{x}. \quad (8)$$

Proceeding in a formal way, we write $j(n/a) = 2\pi n / \ln \tau = \nu_n$ and $a_n = \alpha(\nu_n)$. Then

$$\Delta \nu_n = \frac{2\pi j n}{\ln \tau} - \frac{2\pi j (n-1)}{\ln \tau} = \frac{2\pi j}{\ln \tau}. \quad (9)$$

Substituting into (8), we have

$$L(x) = \sum_{-\infty}^{\infty} \alpha(\nu_n) x^{\nu_n} \frac{\Delta \nu_n}{2\pi j}. \quad (10)$$

In the limit as $\tau \rightarrow \infty$, $\Delta \nu \rightarrow d\nu$, and the sum becomes an integral.

$$L(x) = \frac{1}{2\pi j} \int_{-\infty}^{\infty} \alpha(\nu) x^{\nu} d\nu$$

with

$$\alpha(\nu) = \int_1^\infty L(x) x^{-\nu} \frac{dx}{x}. \quad (11)$$

This is the "one-sided" Mellin Transform pair.¹

W. J. WELCH
Dept. of Elec. Engrg.
University of California
Berkeley, Calif.

¹ P. M. Morse and H. Feshbach, "Methods of Theoretical Physics," McGraw-Hill Book Co., Inc., New York, N. Y., pt. 1, p. 497; 1953.

Autocorrelation by Magnitude of the Difference*

For reasons of ease of implementation it is sometimes desirable to use functions other than the linear correlation function to examine data for coherence. One such function is the "comparison correlation function." This function may be written

$$C(X) = \overline{|f(x) - f(x+X)|}$$

where the multiplying operation of linear correlation is replaced by the indicated subtraction operation.

The comparison autocorrelation function may be readily calculated for a random pulse train such as the one shown in Fig. 1. The a_n 's are independent random variables having the same probability density function $H(a)$; and the interval lengths $(x_n - x_{n-1}) = \tau v_n$ are likewise independent random variables having the same probability density function $L(w)$.

* Received May 2, 1962. This communication presents a result of one phase of study sponsored by the Navigation and Guidance Laboratory ASD, Wright-Patterson Air Force Base, Ohio, under Contract AF33(616)-8407.

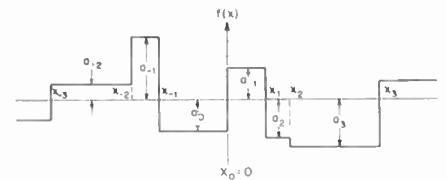


Fig. 4—A random pulse train.

The comparison autocorrelation function of $f(x)$ is then

$$C(X) = \overline{|a_n - a_{n+k}|} Q(X) + \overline{|a_n - a_{n+k}|} [1 - Q(X)],$$

where $Q(X)$ is the probability $f(x)$ has the same value in the interval X . The first term on the right accounts for the cases where a_n and a_{n+k} lie in the same interval and is therefore identically zero. The quantity $\overline{|a_n - a_{n+k}|}$ is the mean absolute value of the difference and will be designated ϵ_D . $C(X)$ then becomes

$$C(X) = \epsilon_D [1 - Q(X)].$$

The linear autocorrelation function of the function of Fig. 1 is

$$R(X) = \bar{a}^2 + \sigma_a^2 Q(X)$$

where σ_a^2 is the variance of the variable a , $(\bar{a}^2 - \bar{a}^2)$. It follows that $C(X)$ and $R(X)$ are related by the equation

$$C(X) = \frac{\epsilon_D}{\sigma_a^2} [\bar{a}^2 - R(X)].$$

For a Poisson distribution of the x_i 's which have a mean density of β points per unit x , it can be shown¹ that

$$Q(X) = e^{-\beta|X|}.$$

Substitution of this result in the equations for linear and comparison autocorrelation gives

$$R(X) = \bar{a}^2 + \sigma_a^2 e^{-\beta|X|},$$

$$C(X) = \epsilon_D [1 - e^{-\beta|X|}].$$

A second example of interest is one in which only two values of $f(x)$ are permitted. The two levels may then be assigned the values b and c .

For an assumed Poisson distribution of zero crossings it can be shown that²

$$R(X) = bc + \frac{(b-c)^2 [1 + e^{-\beta|X|}]}{4}$$

and

$$C(X) = \frac{|b-c|}{2} [1 - e^{-\beta|X|}].$$

Although derived independently these equations agree with the expressions for multi-level autocorrelations.

T. A. MARTIN
Goodyear Aircraft Corp.
Akron, Ohio

¹ H. M. James, N. B. Nichols, and R. S. Philips, "Theory of Servomechanisms," M.I.T. Rad. Lab. Ser. McGraw-Hill Book Co., Inc., New York, N. Y., vol. 25, pp. 300-303; 1947.

² T. A. Martin, "A Comparison Correlation Function for Digital Data: Correlation," Ph.D. Dissertation, Rensselaer Polytechnic Institute, Troy, N. Y., pp. 128-130; 1962.

Synchronous Wave Amplification in the Quadrupole Pump*

This communication explains some physical meaning of the synchronous wave amplification by describing beam patterns and electron orbits.

We already reported on the cyclotron wave amplification ($\omega_p - \beta_p v_0 = \pm 2\omega_c$) and the energy exchange ($\omega_p - \beta_p v_0 = \pm \omega_c$).¹ If the electron and pump wave velocities are equal, i.e., $\omega_p - \beta_p v_0 = 0$, there are also the exponential solutions. In the case of the clockwise pump, the x and y displacements are as follows:

$$\begin{aligned}
 x(z, t) = & (k\omega_c)^{-1} \{ -A_{e1}(0) \cosh \kappa z \\
 & \cdot \exp [j(\omega t - \beta_r z)] + A_{e2}(0) \sinh \kappa z \\
 & \cdot \exp [j\{(\omega - \omega_p)t - (\beta_r - \beta_{rp})z\}] \\
 & + A_{e2}(0) \cosh \kappa z \cdot \exp [j(\omega t - \beta_r z)] \\
 & - A_{e1}(0) \sinh \kappa z \\
 & \cdot \exp [j\{\omega + \omega_p)t - (\beta_r + \beta_{rp})z\}] \} \\
 y(z, t) = & j(k\omega_c)^{-1} \{ -A_{e1}(0) \cosh \kappa z \\
 & \cdot \exp [j(\omega t - \beta_r z)] + A_{e2}(0) \sinh \kappa z \\
 & \cdot \exp [j\{(\omega - \omega_p)t - (\beta_r - \beta_{rp})z\}] \\
 & - A_{e2}(0) \cosh \kappa z \cdot \exp [j(\omega t - \beta_r z)] \\
 & + A_{e1}(0) \sinh \kappa z \\
 & \cdot \exp [j\{\omega + \omega_p)t - (\beta_r + \beta_{rp})z\}] \}
 \end{aligned}$$

where $\kappa = \eta K / \omega_c v_0$, $\beta_{rp} = \omega_p / v_0$ and all other symbols are the same as those given by Siegman.²

Fig. 1 shows the beam patterns (snapshot) and the electron orbits in the case of positive energy synchronous wave amplification. In the plane $z=0$, the patterns (only shown in the black points to avoid complication) rotate counter-clockwise as time passes, showing that the input signal is a positive energy synchronous wave. As the rotating directions of signal and pump wave are opposite, idler wave becomes a negative energy synchronous wave regardless of values of ω and ω_p , and then the beam patterns are complicated by superposition of both waves. The electron orbit of a synchronous wave should increase without transverse velocity; however, when the idler frequency is different from the signal frequency, a phase difference occurs. Then the directions of increasing radii differ from each other, so that the resulting pattern becomes a little twisted.

Fig. 2 shows the case of negative energy synchronous wave amplification. In case $\omega > \omega_p$, the idler wave becomes the positive one and in case $\omega < \omega_p$, the negative one.

The particular case where $\omega_p = 0$ and $\beta_{rp} = 0$, means the dc pump where the signal and idler frequencies have the same frequency and opposite energy. Fig. 3 shows examples of positive energy synchronous wave amplification in the dc pump. As the amplitude increases, both patterns and orbits approach a plane.

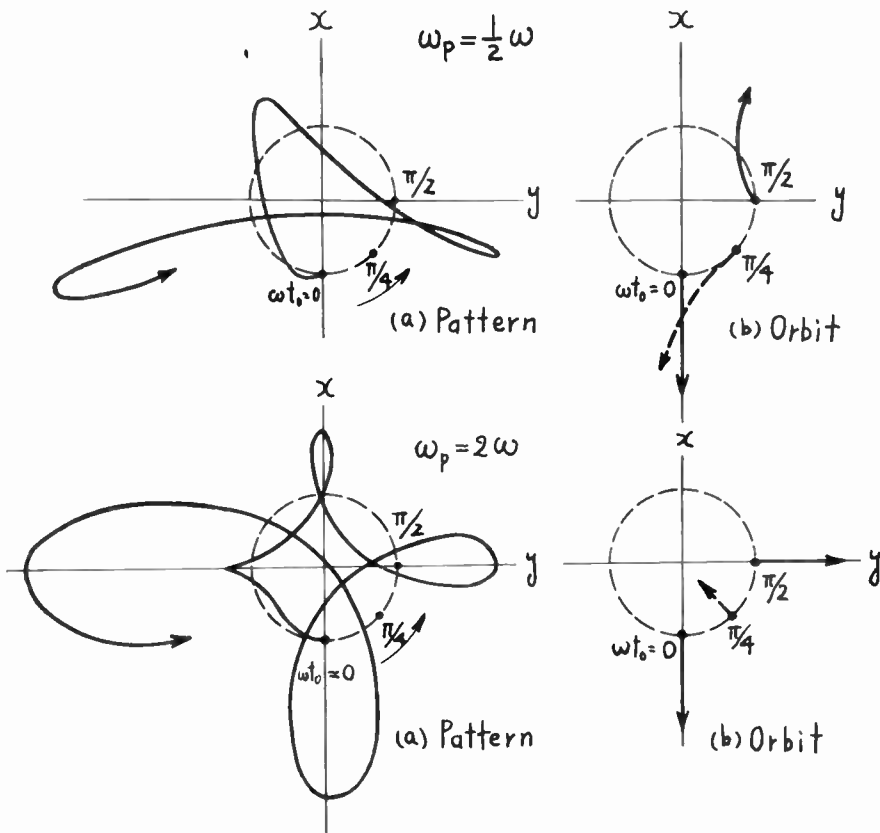


Fig. 1—Amplification of the positive energy synchronous waves in clockwise HF pump.

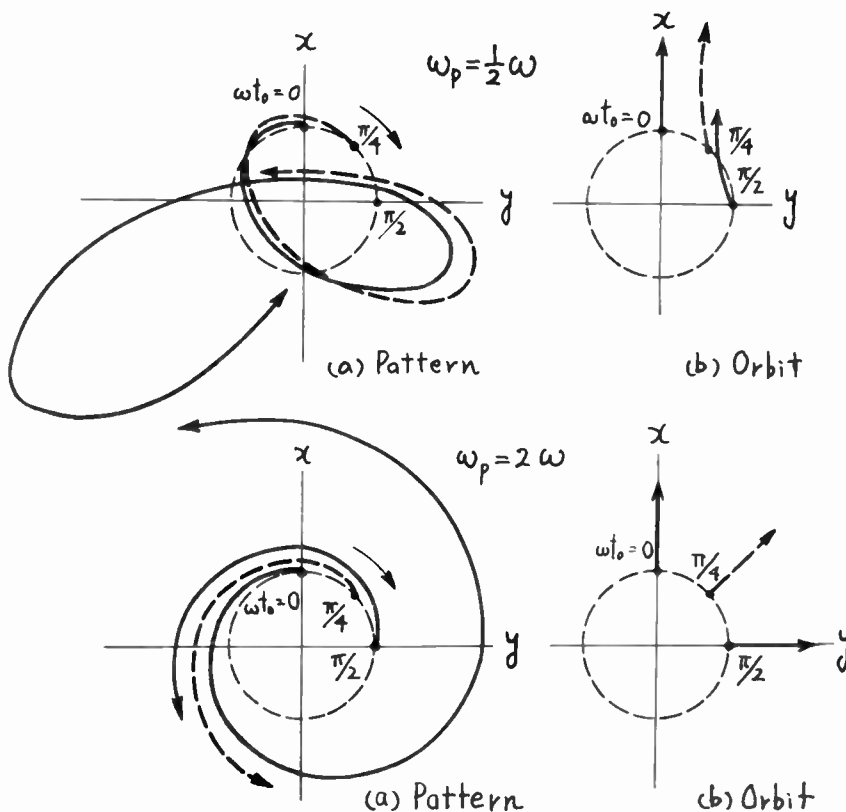


Fig. 2—Amplification of the negative energy synchronous waves in clockwise HF pump.

* Received April 6, 1962; revised manuscript received, April 20, 1962.

¹ K. Kakizaki and M. Otomo, "Analysis of transverse type electron beam parametric amplifiers," *J. Inst. Elec. Commun. Engrs. (Japan)*, vol. 44, pp. 1464-1473; October, 1961.

² A. E. Siegman, "DC pumped quadrupole amplifier," *Proc. IRE*, vol. 48, pp. 1750-1755; October, 1960.

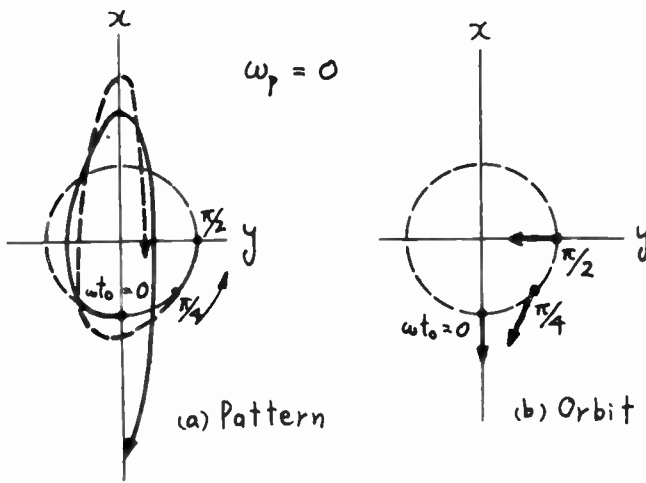


Fig. 3—DC pump amplification of the positive energy synchronous wave.

The behavior of electrons is similar to that of electric quadrupole focusing where electrons diverge in the x direction and converge in the y direction; the reverse is true in the case where the field is rotated by 90 degrees. In the parametric synchronous wave amplification, the quadrupole is equivalent to one section of dc focusing in case $\omega_p = 0$, and HF focusing in case $\omega_p \neq 0$.

K. KARIZAKI
Central Res. Lab.
Tokyo Shibaura Electric Co., Ltd.
Kawasaki, Japan

can be no change in the mean dc voltage and a parameter change must occur to compensate for this. This effect may be explained by considering the following example.

Consider the case of an abrupt junction diode connected as shown in Fig. 1.

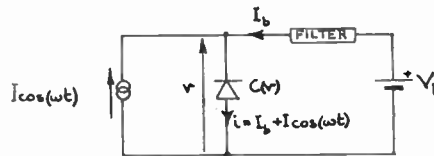


Fig. 1—Circuit of model discussed. The filter allows only dc and low-frequency transient charging currents to flow.

Resonant Frequency Shift Phenomenon in Parametric Amplifiers and Harmonic Generators that Use Current Driven Nonlinear Capacitors*

During an investigation into the behaviour of current driven (or shunt-type) harmonic generators using nonlinear capacitors, a considerable resonant frequency shift with changing current amplitude was observed. Existing small signal theories¹ fail to predict this phenomenon because they do not take account of the bias circuit.

If a sinusoidal current is passed through a nonlinear resistor a change in the mean dc voltage across the device occurs, and if an external conducting path is provided, a dc current will flow. In the case of an ideal nonlinear capacitor a similar dc voltage change would occur if no external current path were present. In practice a nonlinear capacitor always possesses some shunt conductance and an external bias is often applied, under these conditions, since no dc current can flow through a capacitor there

For the case of an abrupt junction diode the incremental capacitance $C(v)$ referred to the working point V_0 is given by

$$C(v) = C_0 \cdot V_0^{1/2} (\psi + v)^{-1/2} \quad (1)$$

where $V_0 = \psi + V_b$ and v is considered positive in the normal reverse direction. Now

$$i = \frac{dq}{dt} = \frac{dq}{dv} \cdot \frac{dv}{dt} = C(v) \cdot \frac{dv}{dt} \quad (2)$$

Since no dc current can flow through a nonlinear capacitor the bias current (I_b) will be zero, and the dc component of the diode voltage (v) must always equal the reverse bias voltage (V_b). In practice a small bias current will flow due to leakage current; however, this may be considered to be external to the nonlinear capacitor. Substituting for i and $C(v)$ in (2) gives

$$I \cos(\omega t) \cdot dt = C_0^{1/2} V_0^{-1/2} (\psi + v)^{-1/2} \cdot dv \quad (3)$$

Integrate (3)

$$\frac{I \sin(\omega t)}{\omega} + A = 2C_0^{1/2} V_0^{-1/2} (\psi + v)^{1/2} \quad (4)$$

Leeson¹ assumes that the constant of integration A is independent of the current amplitude I . In fact A is dependent on I as shown by the following analysis. Simplifying

(4) gives

$$v = \frac{I^2 [1 - \cos(2\omega t)]}{8\omega^2 C_0^2 V_0} + \frac{AI \sin(\omega t)}{2\omega C_0^2 V_0} + \frac{A^2}{4C_0^2 V_0} - \psi \quad (5)$$

As explained above the dc component of v must be V_b , hence the arbitrary constant A is given by

$$A^2 = 4C_0^2 V_0^2 - \frac{I^2}{2\omega^2} \quad (6)$$

Substituting for A in (5) gives

$$v = V_b + \frac{I}{\omega C_0} \sqrt{1 - \frac{I^2}{8\omega^2 C_0^2 V_0^2}} \cdot \sin(\omega t) - \frac{I^2}{8\omega^2 C_0^2 V_0} \cdot \cos(2\omega t) \quad (7)$$

The effective capacitance (C_e) is thus given by

$$C_e = \frac{C_0}{\sqrt{1 - \frac{I^2}{8\omega^2 C_0^2 V_0^2}}} \quad (8)$$

and not by C_0 as proposed by Leeson.

An estimation of the maximum value that C_e can attain (without conduction taking place) may be obtained if we assume that the absolute minimum value of v is $-\psi$. To do this it is necessary to obtain the maximum permissible value of I ; it can be shown from (7) that this value is given by

$$I_{max} = \omega C_0 V_0 \sqrt{\frac{8}{3}} \quad (9)$$

The corresponding value of capacitance $C_{e max}$ is given by

$$C_{e max} = \sqrt{\frac{3}{2}} \cdot C_0 \approx 1.23C_0 \quad (10)$$

Due to the fact that the minimum value of v cannot reach $-\psi$, an increase in effective capacitance of approximately 20 per cent of nominal must be expected when increasing the alternating current from zero amplitude to that value that just causes conduction on the peaks of the voltage excursion. If the diode is the only capacitive element present in a resonant circuit, a resonant frequency shift of up to 10 per cent can occur. The theoretical and measured resonant frequency shift characteristics obtained from an experimental series resonant circuit are shown in Fig. 2. The divergence of the two characteristics was due in part to the fact that the diode used did not possess a perfect abrupt junction and also to the fact that incomplete suppression of the second harmonic current led to measurement errors.

Obviously this change in effective capacitance is undesirable because it alters the frequency response of associated circuitry and also complicates measuring techniques. The effect may be reduced, but cannot be eliminated, by including external passive capacitors in the resonant circuits. Where possible the current amplitude should be held constant; for example, the pump amplitude of a parametric amplifier should be stabilized, to ensure that the system operates under its optimum conditions.

* Received April 16, 1962.
¹ For example, D. B. Leeson and S. Weinreb, "Frequency multiplication with nonlinear capacitors—a circuit analysis," Proc. IRE, vol. 47, pp. 2076-2084; December, 1959.

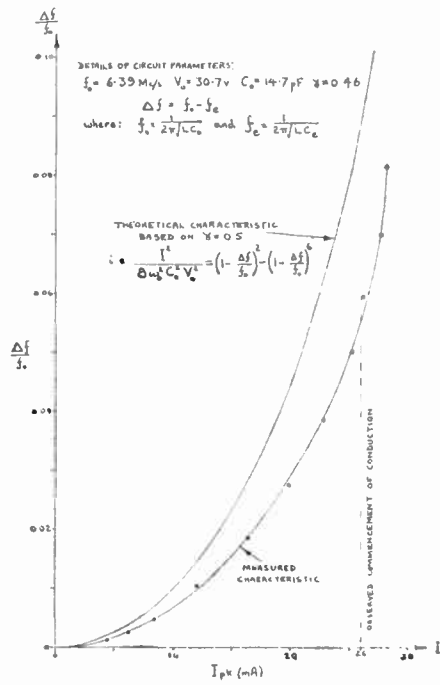


Fig. 2—Resonant frequency shift characteristic for a series tuned circuit employing a nonlinear capacitor as the only capacitive element.

This resonant frequency shift phenomenon may explain the frequency-dependent maximum efficiency condition for harmonic generators observed by Utsunomiya and Yuan.²

ACKNOWLEDGMENT

The author is indebted to the Directors of Ferguson Radio Corporation for permission to publish this paper.

G. C. LOWE
Ferguson Radio Corporation, Ltd.
Enfield, Middlesex, England

² T. Utsunomiya and S. Yuan, "Theory, design and performance of maximum efficiency variable reactance frequency multipliers," *Proc. IRE*, vol. 50, pp. 57-65; January, 1962.

Measurement of Effective Susceptibility of Magnetic Inks*

An important aspect of magnetic printing is the behavior of the iron-powder inks used under the influence of a magnetic field. The behavior of a magnetic ink particle depends on the forces applied to it, which in turn depends on the recorded field strength and the susceptibility of the particle. Also, susceptibility determinations are important because they tell us how to design the inks, how to select the ferrous ink materials, and how to control the ink properties during manufacture.

The dry powder ferromagnetic inks described here were prepared from a commer-

cial grade of iron powder, Hoeganaes Ancor EP 1024, 99 per cent Fe, nominal size: through 200 mesh. The particles were coated with resins, waxes, carbon black, or dyes, singly or in combination; typical concentrations were: iron powder 85-95 per cent by weight; coating material 5-15 per cent by weight. Coatings were applied by any of several methods, such as precipitation, solvent slurry coating, or fluidized bed coating.

The magnetization of a uniformly-magnetized homogeneous material may be expressed by $M = kH$, where k is the volume susceptibility. However, the magnetic field H is not wholly the applied field H_0 , but is reduced by the self-demagnetizing field D (due to shear) of the magnetized material. Thus $H = H_0 - D$. The demagnetizing field is proportional to the magnetization: $D = NM/4\pi$ where the constant of proportionality, N , is a function of the geometry alone.

We may thus rewrite $M = kH$ as $M = H_0 - (NM/4\pi)$ or

$$M = \frac{k}{1 + \frac{N}{4\pi} k} H_0$$

Now we can define an effective susceptibility as

$$k' = \frac{k}{1 + \frac{N}{4\pi} k}$$

If the susceptibility is very large (e.g., in a ferromagnetic material) and the product Nk is sufficiently greater than one, the effective susceptibility may be approximated by $k' = 1/(N/4\pi)$ regardless of the type of ferromagnetic material.

The expression for the demagnetization of most particle geometries is quite complex; however, the application of certain assumptions somewhat simplifies the problem. Let the shape of the iron particles of interest be approximated by prolate ellipsoids (the approximation is not unreasonable for the type of particle used in magnetic printing, as may be observed under a microscope). The demagnetization factor N may then be taken from curves constructed for prolate ellipsoids,¹ after determining the major to minor axis ratio, m , where the axes are those of the envelope containing the particle.

Generally, the particle is porous, and the m ratio of the envelope will not accurately identify the particle. Consider the particle as being composed of incremental bar magnets where the total cross-sectional area of magnetic material is given as: $A' = A(1-p)$, where A is the cross section of the envelope, and p is the porosity of the particle. The effective diameter is then $d' = d\sqrt{1-p}$. We now define an effective m ratio as

$$m' = \frac{L}{d'} = \frac{m}{\sqrt{1-p}}$$

This value m' must be used in determining the demagnetization for porous particles.

The size of the magnetic particles (about 40 microns) limits the methods of measurements by which it is feasible to determine

effective susceptibility. Torsion balances may be used,² but the approach is difficult and delicate. A simpler method is available, which gives the average effective susceptibility of a large number of particles.

The apparatus used is a modified Crittenden hysteresis loop tracer, where the sample of magnetic ink is placed into a tube (0.20 cm i.d., 80 cm long). The tube is vibrated to achieve maximum packing. The sample of ink is diluted with a Zn powder with about the same particle size and angularity as the iron powder. Fig. 1 shows the effect of decreasing the percentage (by volume) of iron on the bulk susceptibility of the iron powder. As the particles become spaced far apart, the susceptibility asymptotically approaches that of 2 per cent of iron (by volume). This asymptote is the susceptibility of a single particle, for the spacing is so large that the interaction between particles is negligible. That the effect is virtually independent of particle size (in the range of 30-150 microns) is shown in Fig. 2.

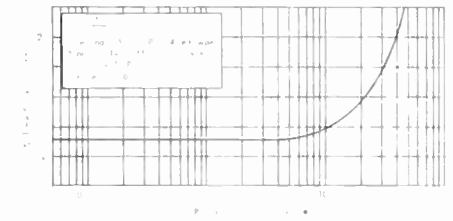


Fig. 1—Volume susceptibility of iron particles in a nonmagnetic diluent.

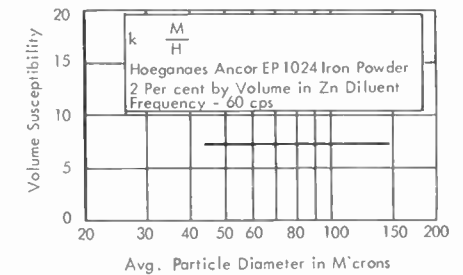


Fig. 2—Volume susceptibility of iron particles vs particle size.

Many samples of ink were prepared for experimental study; however, due to the extreme difficulty of measuring the density of the ink particles, and consequently the porosity, the deviation of the effective susceptibility, as obtained from the above equations from that obtained in the hysteresis curve tracer of diluted samples, were as low as ± 4 per cent and as high as ± 32 per cent.

Finally, we may draw the conclusions that the effective susceptibility of a ferromagnetic ink particle is inversely proportional to its self-demagnetization, N ; the effective m ratio and its porosity. The average susceptibility of ink particles is independent of particle size, over the range of 30 to 150 microns.

H. J. KUMP
IBM Computer Lab.
Components Div.
Poughkeepsie, N. Y.

* Received March 8, 1962; revised manuscript received, March 19, 1962.

¹ R. M. Bozorth, "Ferromagnetism," D. Van Nostrand & Co., New York, N. Y., p. 846; 1955.

² Bozorth, *Ibid.*, p. 858.

Minimum-Power FM Reception Using Frequency Feedback*

Enloe's two-threshold concept¹ has been used in formulating a generalized design procedure for designing FM feedback receivers for minimum-power reception. The key factor in this approach is the receiver closed-loop transfer function. The procedure consists of adjusting this transfer function to satisfy simultaneously three sets of conditions, as follows:

- 1) The two thresholds must be equal.
- 2) The common threshold power must be minimized.
- 3) The loop must be satisfactory from the standpoint of stability and transient response.

The receiver closed-loop transfer function, $H(s)$, relates VCO frequency (or phase) to the frequency (phase) of the received signal. It is made up, in part, of the post-discriminator filter, $F(s)$. The form of the latter and, therefore, of $H(s)$, may be chosen arbitrarily as long as the three conditions above can be met. The conditions would be met, in a given case, by appropriately adjusting the parameters (loop gain, filter time constants) of the selected transfer function.

The generalized design procedure owes its existence to the possibility of expressing the two thresholds in terms of $H(s)$. Thus, the two thresholds may be written,

feedback threshold power C_{TFB}

$$= (3.11)^2 n \int_0^\infty |H(j\omega)|^2 df \quad (1)$$

open-loop threshold power C_{TOL}

$$= 10\pi n \Delta f |1 - H(j\omega_b)| \quad (2)$$

where n =receiver noise power density, watts/cps; Δf =peak received carrier frequency swings, cps; and $f_b = \omega_b/2\pi$ =highest modulating (base-band) frequency.

Eq. (1) reflects the experimentally determined fact that feedback threshold occurs when total rms VCO phase perturbation due to input noise equals 1/3.11 radian. Eq. (2) assumes HF 3-dB bandwidth need be only twice the residual carrier frequency swing, $\Delta f|1 - H(j\omega_b)|$. In cases where this is not true (i.e., low index systems) a more complex threshold equation is required which, however, will still be a function of $H(s)$.

The design procedure then calls for adjusting $H(s)$ until the value of (1) equals that of (2) to satisfy condition 1) above. For condition 2), the smallest value of received power for which equality can be realized should be sought. Finally, loop stability, etc., must be maintained [condition 3).

The above will be illustrated by a simple example which is nevertheless of considerable practical interest. Specifically, let the filter, $F(s)$, be a simple RC low-pass section.

Then the closed-loop transfer function takes the form (Fig. 1)

$$H(s) = \frac{K}{(K + 1) + (\tau_1 + \tau_2)s + \tau_1\tau_2s^2} \quad (3)$$

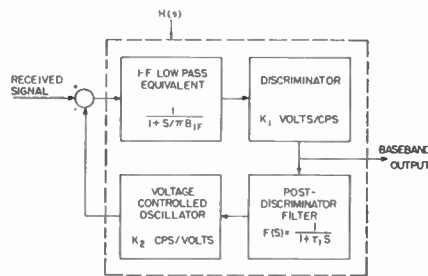
The $|1 - H(j\omega_b)|$ term in (2) becomes

$$|1 - H(j\omega_b)| = \left[\frac{(1 - \omega_b^2\tau_1\tau_2)^2 + (\tau_1 + \tau_2)^2\omega_b^2}{[(K + 1) - \omega_b^2\tau_1\tau_2]^2 + (\tau_1 + \tau_2)^2\omega_b^2} \right]^{1/2} \quad (4)$$

Eq. (4) is greatly simplified by proper choice of filter time constant, namely by letting $\tau_1 = 1/\omega_b^2\tau_2$. This also very nearly minimizes (4), thereby satisfying, for all practical purposes, the second of the above conditions. With this choice of τ_1 , (4) can be closely approximated by

$$|1 - H(j\omega_b)| \approx \frac{X}{K + 1} \quad (5)$$

where $X = (\omega_b\tau_2 + 1/\omega_b\tau_2)$.



$$H(s) = \frac{G(s)}{1 + G(s)} \quad G(s) = \frac{KF(s)}{1 + \tau_1 s + \tau_2 s^2}$$

$$\tau_2 = \frac{1}{\omega_b^2 \tau_1} \quad K = K_1 K_2$$

$$B_o = \left(\frac{K+1}{\tau_1 \tau_2} \right)^{1/2} \quad \xi = \frac{\tau_1 + \tau_2}{2[\tau_1 \tau_2 (K+1)]^{1/2}}$$

Fig. 1—FM receiver with frequency feedback.

The two thresholds now can be written

$$C_{TOL} = \frac{10\pi n \Delta f X}{K + 1} \quad (6)$$

and

$$C_{TFB} = \frac{(3.11)^2 \pi n f_m K^2}{2X(K - 1)} \quad (7)$$

Condition 1 is now satisfied by setting loop gain K to a value K_0 which equalizes (6) and (7). Using the approximation (3.11)² ≈ 10 , this is found to be

$$K_0 = X \left(\frac{2\Delta f}{f_b} \right)^{1/2} \quad (8)$$

The time constant, τ_2 , of the HF filter low-pass equivalent is found from the assumption that this filter bandwidth equals the residual HF swing, $\Delta f|1 - H(j\omega_b)|$. Solving for τ_2 , using (5) and (8) gives

$$\tau_2 \approx 1/\pi\sqrt{2\Delta f f_b} \quad (9)$$

That condition 3 is met can be verified by checking damping factor, ξ . Using the

relation given in Fig. 1, ξ is found to approach a minimum of about 0.35 for large modulation index.

In the above f_b and Δf are considered "given" quantities. As a numerical example, consider $f_b = 3$ Mc and $\Delta f = 60$ Mc, the values used in Enloe's sample design. Optimum loop gain K_0 proves to be 27 db; RC filter bandwidth, $1/2\pi\tau_1 = 0.95$ Mc; and HF 3-dB bandwidth = 19 Mc. Comparing the above HF bandwidth with Enloe's figure of 12.3 Mc, the present receiver is seen to have a threshold about 1.9-dB higher. This may be attributed to the more sophisticated base-band filtering used by Enloe.

The foregoing example illustrates a general procedure usable with loop transfer functions of arbitrary form. With more complex filtering the required computations, of course, are more involved, but the basic idea is the same. The value of the above approach lies in the direct link established between general design objectives (the three conditions stated at the outset) and fundamental circuit parameters such as gain and filter time constants, which must be adjusted to achieve these objectives. The link is established by expressing the two thresholds in terms of loop transfer function.

ROBERT E. HEITZMAN
Communications Div.
Hughes Aircraft Co.
Los Angeles, Calif.

A Method of Measurement and Display of Probability Functions of Ergodic Random Processes by Orthogonal Series Synthesis*

INTRODUCTION

With the growing importance of statistics in the fields of communication theory, vibration theory, acoustics, etc., a need has arisen for real time display of probability density functions and cumulative probability functions. Heretofore these displays have been carried out by one or two methods, both involving digitizing the range of the random signal into very narrow cells and employing counting or time measurement techniques. Both of these methods have a number of drawbacks. These are: 1) bandwidth limitations due to quantization, 2) counting or time-measuring accuracy, and 3) expense in performing these measurements using digital methods. The purpose of this communication is to introduce a new method of displaying probability density and cumulative probability distribution functions simultaneously and in real time by utilization of orthogonal series synthesis. The method was previously reported upon¹

* Received April 23, 1962.

¹ A. A. Wolf, "Some recent advances in the analysis and synthesis of nonlinear systems," *Trans. AIEE*, vol. 80, pp. 289-300; November, 1961.

* Received May 4, 1962; revised manuscript received May 28, 1962.

¹ L. H. Enloe, "Decreasing the threshold in FM by frequency feedback," *Proc. IRE*, vol. 50, pp. 18-30; January, 1962.

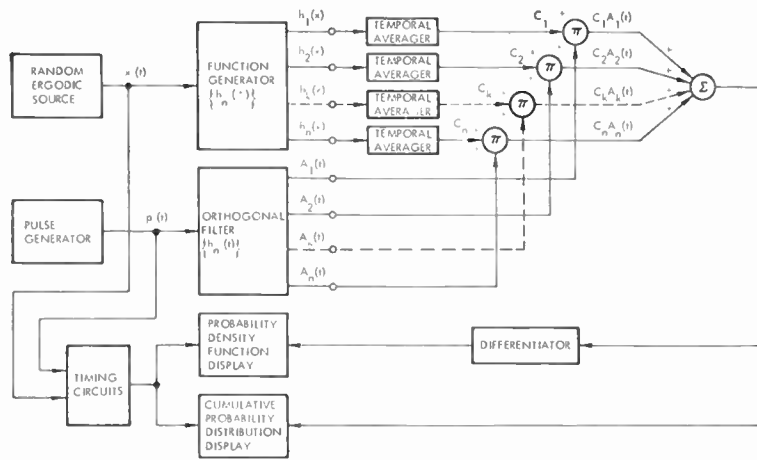


Fig. 1—Synthesis of probability functions by orthogonal components displayed in real time with $t > 0$ corresponding to x positive and negative.

in its application to the measurement and display of instantaneous² and short-term correlation functions in real time.

PRINCIPLE OF THE METHOD

The probability density function is synthesized as a linear combination of orthogonal functions with measured coefficients C_n . In this scheme an ergodic random process, $x(t)$, is applied as shown in Fig. 1 to a function generator whose outputs are a set of functions $\{h_n(x)\}$, $n=1, 2, \dots$, obeying the orthogonal relationship

$$\int_{-\infty}^{\infty} h_n(x)h_k(x)dx = \begin{cases} 1, & n = k \\ 0, & n \neq k \end{cases} \quad (1)$$

These functions are then time-averaged to give

$$C_n = \overline{h_n(x)} \quad (2)$$

Since the random process is ergodic,

$$\overline{h_n(x)} = E[h_n(x)] \quad (3)$$

in which the right side is the expected value of $h_n(x)$ defined by

$$E[h_n(x)] = \int_{-\infty}^{\infty} h_n(x)p(x)dx \quad (4)$$

Hence from (2), (3) and (4)

$$C_n = \int_{-\infty}^{\infty} h_n(x)p(x)dx \quad (5)$$

Eq. (5) is recognized as a linear integral equation of the Fredholm type, which has the solution

$$p(x) = \sum_{n=1}^{\infty} C_n h_n(x) \quad (6)$$

The quantities $\{C_n\}$ form a set which are statistics of the process $x(t)$ given by the temporal average, (2). If x is now displayed as a linear function of time, it is then obvious that the probability density function can be displayed in real time over the range of x .

If the display is to be done on a cathode-ray oscilloscope, then either a multiplex arrangement can be used to display both negative and positive x or dual beam arrangement may be used with timing circuits to shut the process off at the interface between the positive and negative parts of the sweep. The figure gives an implementation of this method in which it is shown that the orthogonal filter box generates impulse responses $h_n(t)$ which are orthogonal and have the same functional relation to t as the outputs of the function generator have with respect to x . Obviously in this method it is impossible to have an infinite number of orthogonal filter components in a physically realizable system. It has been found both theoretically and experimentally that in the integral-square sense the error produced can be made very small by truncating the series at some reasonable value of k . The error expression turns out to be given by³

$$e_N^2 = \int_{-\infty}^{\infty} p^2(x)dx - \sum_{l=1}^N C_l^2 \quad (7)$$

where e_N^2 denotes the integral square error produced by truncating the number of terms in the series to N terms.

It will be noticed in the figure that since the cumulative distribution function and the probability density function are related according to

$$P(\xi < x) = \int_{-\infty}^x p(\xi)d\xi = F(x) \quad (8)$$

where $F(x)$ is the cumulative distribution function and $p(x)$ is the probability density function; the display of both of these, therefore, can be obtained simultaneously.

CONCLUSIONS

The method presented in this communication has a number of advantages over standard methods for doing the same thing. Primarily, this is that the display of the probability density and cumulative prob-

ability distribution functions can be accomplished in real time as the process is examined. It is, of course, limited to ergodic⁴ processes in order to take advantage of the fact that the statistics C_n , which are obtained by the time averages, are equal to the same statistics obtained by probability averages as noted in (2) and (3). The accuracy of the method is given by (7) and it is possible by means of (7) to make the process adaptive such that the error can be minimized automatically as a function of the process being measured by maximizing the C_n^2 . This will be reported upon in detail in a later paper^{5,6} discussing the limitations and theoretical basis of the method. The display in real time is accomplished by means of orthogonal filters which are easily synthesized by RC active networks as reported elsewhere³ and the function generation is accomplished by well-known techniques using diodes and resistor networks.

A. A. WOLF
J. H. DIETZ
Emertron, Inc.
Silver Spring, Md.

⁴ A. A. Wolf, "On a Sufficient Test for Ergodicity in a Class of Stationary Random Processes," General Dynamics/Electronics, Tech. Rept. No. 5, April 12, 1961. (To be published in *Trans. AIEE* (1963).)

⁵ A. A. Wolf and J. H. Dietz, "A statistical theory of fault detection, parameter identification, and transmission characteristics, of linear and nonlinear systems," *J. Franklin Inst.*, (to be published 1963).

⁶ A. A. Wolf and J. H. Dietz, "Theory of Adaptive Correlation and Probability Function Systems," to be presented at the ASEE Winter General Meeting, New York, N. Y., 1963, (and to be published in *Trans. AIEE*).

Reflection Cavity Maser with Large Gain Bandwidth*

Measurements on a parallel configuration of two ruby reflection cavities at X band have shown voltage gain bandwidth products (GBP) of over 1700 Mc at a temperature of 4.2°K. The basic arrangement uses two silvered ruby cavities in a resonant coupling scheme recently described¹ but modified to allow adjustment of the coupling separately to each cavity. The cavity resonators were silvered and slotted as described by Cross,² and were operated through this investigation at the double pump angle for ruby (54.74°). (See Fig. 1.) Fig. 2 shows the range in GBP for a two-cavity pair with signal and pump frequencies nominally 9.255 Gc and 23.285 Gc, respectively. Assuming a $G^{1/2n} = k$ variation, the GBP may be written as $G^{1/2}B = k(G^{(n-1)/2n})$ where n is the number of resonant elements.

* Received April 13, 1962; revised manuscript received, April 23, 1962. This work was supported by the Bureau of Naval Weapons, Department of the Navy, under Contract NOrd 7386.

¹ J. J. Cook, L. G. Cross, M. E. Bair, and R. W. Terhune, "A low-noise X-band radiometer using maser," *Proc. IRE*, vol. 49, pp. 768-778; April, 1961.

² L. G. Cross, "Silvered ruby maser cavity," *J. Appl. Phys.*, vol. 30, p. 1459; September, 1959.

² A. A. Wolf, "On the significance of instantaneous and short-term correlation functions for a class of stochastic processes," *Proc. IRE (Correspondence)*, vol. 50; September, 1962.

³ A. A. Wolf and J. H. Dietz, "An adaptive correlator for underwater measurements," to be published in the *Trans. ISA*. Presented at the Fall Meeting of the Instrument Society of America, Los Angeles, Calif., Paper 90-LA-61; 1961.

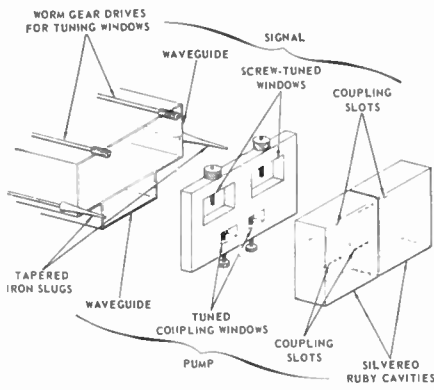


Fig. 1—Expanded view of two-cavity maser. Cavities and coupling plate are clamped to waveguide openings.

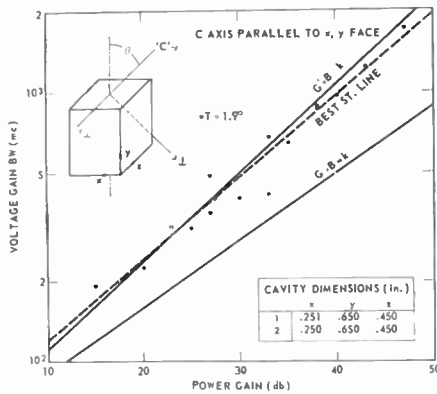


Fig. 2— $G^{1/2}B$ vs. G for two 0.05 per cent ruby cavities cut at $\theta = 90^\circ$.

For $n=2$, $G^{1/2}B = kG^{1/4}$ which has been verified for two resonant elements consisting of a coupling plate and one ruby resonance.³ For $n=3$, $G^{1/2}B = kG^{1/3}$ which is an improvement of $G^{1/3}$ over the nonresonant coupling case $n=1$. The experimental values obtained in two separate runs gave a least-squares fit with exponent 0.305 which is close to the expected improvement in GBP for three elements. The isolated point at 1.9°K shows very closely a $1/T$ dependence.

The problem of broad-band reflection cavity masers has received some attention mainly through the technique of combining the maser cavity resonance with suitable microwave structures.⁴ With two separate cavities, the dimensions may be selected to allow identical modes in each that are separated at X band by about 20–30 Mc. The two window coupling plate is then used to separately couple the modes into a wider composite resonance. In lieu of an exact method for computing the resonant frequencies of the ruby rectangular box, a semi-empirical approach has been used to es-

tablish a feel for the dimensions required to support a given mode.

Initially, one designates in the range of interest three frequencies corresponding to three lowest possible modes in the box, viz: f_{110} , f_{011} , and f_{101} . The coordinates of the box will determine which frequency is the lowest. Three equations of the form

$$f_{lmn}^2 = c^2/4 [l^2/\epsilon_x x^2 + m^2/\epsilon_y y^2 + n^2/\epsilon_z z^2]$$

are solved for the xyz dimensions. Here f_{lmn} is the resonant frequency of mode lmn , c the speed of light and ϵ_x , ϵ_y , ϵ_z the relative permittivities in the coordinate directions (taken ≈ 10 for the first trial). The observed frequencies of a test cavity are now used to calculate ϵ_x , ϵ_y , and ϵ_z which may then be used in the expression above to determine the dimensions of a new cavity having the desired operating frequency. The second cavity of the final pair may be designed by changing one dimension slightly. If this dimension is, say, z , then $dx = dy = 0$ and $df = \partial f/\partial z dz$ or $\Delta f = \partial f/\partial z \Delta z$. Since

$$\partial f/\partial z = -c^2 n^2/4f\epsilon_z z^3, \quad \Delta z = -4f\Delta\epsilon_z z^3/c^2 n^2$$

where f is the resonant frequency of the cavity before the z dimension is changed. For the second cavity the dimensional change is generally one or two mils. By restricting the cuts made in the boule to certain preferred directions, the effect on the mode picture of the ruby anisotropy may be minimized. The insert in Fig. 2 shows the relation between the box and crystal coordinates for the C axis parallel to the xy face. It may be shown that the dielectric tensor has the form

$$\begin{pmatrix} \epsilon_{\perp} \cos^2 \theta + \epsilon \sin^2 \theta & \frac{\sin 2\theta}{2} (\epsilon_{\perp} - \epsilon) & 0 \\ \frac{\sin 2\theta}{2} (\epsilon_{\perp} - \epsilon) & \epsilon_{\perp} \sin^2 \theta + \epsilon \cos^2 \theta & 0 \\ 0 & 0 & \epsilon_{\parallel} \end{pmatrix}$$

which for $\theta=0^\circ, 90^\circ$ becomes diagonal. For 90° , $\epsilon_{\parallel} = \epsilon_z \approx 11.5$ and $\epsilon_{\perp} = \epsilon_x = \epsilon_y \approx 9.5$.

A. W. NAGY
G. E. FRIEDMAN
Applied Physics Lab.
The Johns Hopkins University
Silver Spring, Md.

Let $f(t)$ be a function of the real variable t such that its Fourier transform $F(j\omega)$, defined by

$$F(j\omega) = \int_{-\infty}^{\infty} f(t) \exp(-j\omega t) dt, \quad (2)$$

is zero for $|\omega| > \pi$. Consider the integral

$$I = \int_{-\infty}^{\infty} f(t) \frac{\sin \pi(t-a)}{\pi(t-a)} dt. \quad (3)$$

I is in the form of a convolution integral so that I is found by taking the inverse transform of the product of the Fourier transforms of the factors of the integrand. Letting $\Phi(j\omega)$ be the Fourier transform of $(\sin \pi t)/(\pi t)$, we find that

$$\begin{aligned} \Phi(j\omega) &= 1, & |\omega| < \pi \\ &= 0, & |\omega| > \pi \\ F(j\omega)\Phi(j\omega) &= F(j\omega), & |\omega| < \pi \\ &= 0, & |\omega| > \pi. \end{aligned}$$

Then

$$\begin{aligned} I &= \frac{1}{2\pi} \int_{-\infty}^{\infty} F(j\omega)\Phi(j\omega) \exp(j\omega a) d\omega \\ &= \frac{1}{2\pi} \int_{-\pi}^{\pi} F(j\omega) \exp(j\omega a) d\omega \\ &= f(a) \end{aligned} \quad (4)$$

since, by hypothesis, $F(j\omega) = 0$ for $|\omega| > \pi$. $f(t)$ is assumed continuous at $t=a$.

By a simple scale change, one may get the more general formula

$$\int_{-\infty}^{\infty} f(t) \frac{\sin \pi b(t-a)}{\pi b(t-a)} dt = f(a)/b \quad (5)$$

for those functions $f(t)$ whose Fourier transforms $F(j\omega)$ are zero for $|\omega| > \pi b$.

HARRY URKOWITZ
Philco Scientific Lab.
Blue Bell, Pa.

A Low-Impedance Maxwell Bridge for Measuring Toroidal Magnetic Materials from 1 kc to 100 kc*

A specially designed Maxwell bridge (Fig. 1) extends the range of coaxial magnetic measurements several orders of magnitude lower in frequency and complex permeability. This bridge measures the quantities shown in Table 1 at frequencies from 1 kc to 100 kc using toroidal magnetic materials.

The effect of contact resistance upon the measurement is reduced as follows. The unknown arm is always closed. To insert a sample into this arm, the higher impedance product arm, B , and the detector branch are opened.

The unknown arm U (Fig. 1) is a shorted section of coaxial line. The product arms are special coaxial resistors while the parallel

The Sifting Property of a Common Function*

It is well known that the impulse function $\delta(t)$ has the "sifting" property; that is,

$$\int_{-\infty}^{\infty} f(t)\delta(t-a)dt = \frac{1}{2}[f(a+) + f(a-)] \quad (1)$$

for a function $f(t)$ which has no worse than an ordinary discontinuity at $t=a$. Other functions have the sifting property as well. One of these is the $\sin x/x$ function provided $f(t)$ is appropriately bandlimited.

* Received May 3, 1962; revised manuscript received, May 21, 1962.

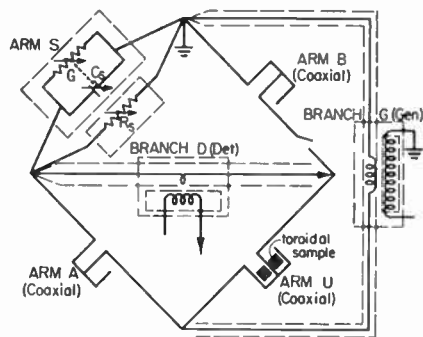


Fig. 1—Schematic of the low impedance Maxwell bridge for measuring toroidal magnetic materials from 1 kc to 100 kc.

are compared to data using other techniques (Fig. 2).

The equations for the inductance change (ΔL_u) and the resistance change (ΔR_u) due to the insertion of a sample into the unknown arm U are to a close approximation,

$$\Delta L_u = \Delta C_s R_A R_B$$

and

$$\Delta R_u = R_A R_B (\Delta G + \Delta G_s) - \omega^2 \Delta C_s K$$

where Δ refers to the change in a parameter with the sample in and with the sample out of the unknown coaxial arm U , ΔC_s is the capacitance change of the capacitance standard, ΔG is the conductance change of the capacitance standard,¹ ΔG_s is the con-

The authors thank W. A. Pittman for making most of the measurements and O. E. Holz and W. F. Clore for constructing the equipment.

A. L. RASMUSSEN
R. C. POWELL
Radio and Microwave Materials Sec.
Natl. Bur. Standards
Boulder, Colo.

REFERENCES

[1] A. L. Rasmussen and A. E. Hess, "R-F permeameter techniques for testing ferrite cores," *Elec. Manufacturing*, vol. 61, p. 86; May, 1958.
[2] C. A. Hoer and A. L. Rasmussen, "Exact equations for the radio frequency magnetic permeameter," to be published in *J. Res. NBS, C*.
[3] B. L. Danielson and R. D. Harrington, "A technique for reducing errors in permeability measurements with coils," *Proc. IRE*, vol. 48, pp. 365-366; March, 1960.

TABLE I

Quantity	Resolution	Range	Accuracy
Inductance	10 ⁻¹¹ henry	10 ⁻⁹ - 10 ⁻⁶ henry	± 1 per cent
Resistance	10 ⁻⁷ ohm	10 ⁻⁵ - 10 ⁻¹ ohm	± 5-10 per cent
Tangent δ	10 ⁻⁵	10 ⁻² - 10	± 5-10 per cent

* f = the frequency in kc.

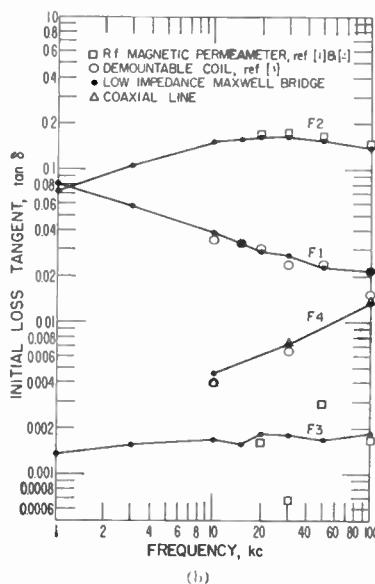
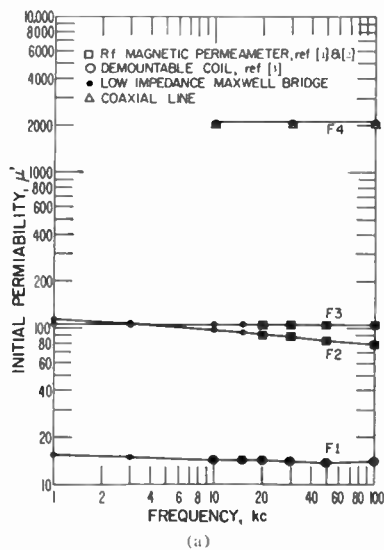


Fig. 2—Low impedance Maxwell bridge data accompanied by data using other techniques. Samples were toroidal ferrite cores. Other types of toroidal magnetic materials are measurable using this bridge.

arm is made up of commercially available components. The resistance of arm A is 0.1 ohm. The resistance of arm B can be changed to 10 ohms, 50 ohms or 100 ohms. The residuals of the product arms are evaluated but not compensated. The parallel standards arm S (Fig. 1) consists of a continuously adjustable capacitor 100 $\mu\mu\text{f}$ to 0.10 $\mu\mu\text{f}$ and a 111,110-ohm resistor with decade steps of one ohm. The triple-shielded generator and detector transformers (Fig. 1) are enclosed within the bridge itself. Two volts or less are applied to the bridge depending upon the sensitivity of the sample to RF magnetic-field strength. Toroidal magnetic materials with known inductances and negligible losses are used to calibrate the conductance changes of the capacitance standard and the impedances of the product arms.

Initial permeability (μ') and dissipation factor ($\tan \delta$) data obtained using the bridge

ductance change from the resistance standard R_s , R_A is the resistance of product arm A , R_B is the resistance of product arm B , ω is the angular frequency, and K is a calibration constant dependent on the impedances of the product arms.¹

The permeability (μ') is calculated using the equation, $\mu' = (\Delta L_u + L_a) / L_u$ where L_a = the equivalent air inductance of the space occupied by the magnetic core. For a core of rectangular section with a single turn, $L_a = 2 \cdot 10^{-7} h \cdot \ln b/a$ henries where h is the height in meters and b and a are the OD and ID, respectively.

The dissipation factor ($\tan \delta = \mu'' / \mu'$) the complex permeability being defined as $\mu^* = \mu' - j\mu''$) is calculated using the equation, $\tan \delta = \Delta R_u / \omega (\Delta L_u + L_a)$.

¹ Standard toroidal samples are used to obtain these calibration quantities.

Spurious Responses in Microwave Garnet Devices*

Above the saturation frequency the only troublesome spurious responses that are encountered in the design of single-crystal garnet resonators are the so-called magnetostatic modes¹ which are set up by inhomogeneities in the exciting RF magnetic fields. It should be noted that there are many applications where the spurious response is either too low in amplitude to cause difficulties or else can be tolerated. For example, in a multituned filter employing a series of cascaded garnet elements, the spurious response will generally be too weak to be of importance. The level of the strongest spurious response in a single-tuned filter can usually be kept at least 20 db below the main. Then, in a triple-tuned structure the spurious response will be at least 60 db down and will usually be greater than this. This is because the spurious responses will generally not couple as well as the main.^{2,3} Even for a single-tuned resonator the spurious may be ignored in some cases. For example, if the garnet filter is used as the input preselector of a superheterodyne receiver and there is only one spurious of consequence which is above the main response in frequency (a usual condition), then it is enough to choose the local oscillator to be below the signal to eliminate the undesirable effects.

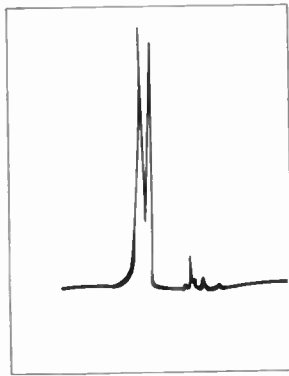
In cases where it is still advantageous to meliorate the intensity difference between main and spurious responses, it is necessary to consider the size and shape of the garnet crystals themselves in addition to the effect of coupling on the uniformity of the RF fields. Two factors play a role in this; first, it is never possible in practice to build RF structures that can achieve absolute uniformity of field so that the nonuniformity

* Received May 8, 1962.

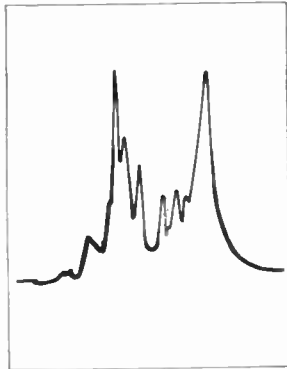
¹ L. R. Walker, "Ferromagnetic resonance: line structures," *J. Appl. Phys.*, vol. 29, pp. 318-323; March, 1958.

² P. C. Fletcher and I. H. Solt, Jr., "Coupling of the magnetostatic modes," *J. Appl. Phys.*, vol. 30, supp. no. 4, p. 181S; April, 1959.

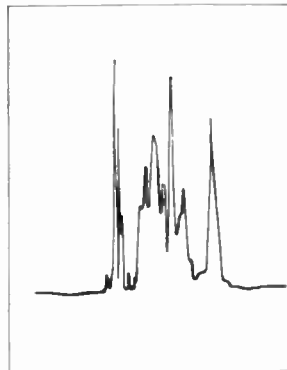
³ P. S. Carter, Jr., "Crystal garnet resonators," 1960 IRE INTERNAT'L CONVENTION RECORD, pt. 3, pp. 130-135.



(a)



(b)



(c)

Fig. 1—Spurious response as a function of sphere diameter at 14.0 kMc. (a) 0.040-in diameter YIG ball in a 0.059-in waveguide iris, frequency spread larger than that of (b) and (c). (b) 0.045-in diameter YIG ball in a 0.059-in waveguide iris. (c) 0.050 in diameter YIG ball in a 0.059-in waveguide iris.

“seen” by the garnet crystal will depend in part on its own geometry, and second, the characteristics of the spurious responses themselves are shape-dependent.¹

Some of our recent work with single-tuned K-band filters using single-crystal highly polished YIG spheres has pointed this up very clearly. Supposedly identical or similar YIG spheres obtained from various sources sometimes showed widely differing spurious spectra (Fig. 1). Pertinent data on four such YIG crystals is given in Table 1. Of particular interest are the two spheres (nos. 2, and 3) having identical diameters but widely differing spurious amplitudes. Linewidths and insertion losses

TABLE I

Sphere No.	Mean Diameter (2 planes)	Sphericity (2 planes) ^c	Main Response				Largest Spurious ^d	
			Linewidth at 14 gc (or) ^a	Frequency (gc)	Filter Insertion Loss (db)	Bandwidth (mc)	Frequency (gc)	db Below Main Response
1 ^a	0.0408	0.00010	2.0 ± 10%	13.95	2.5 ± 0.5	22 ± 2	13.85	11.0 ± 0.5
	0.0407	0.00005		16.50			2.0	
2 ^b	0.0500	0.00090	1.4 ± 15%	13.75	2.0	30	13.00	4.0
	0.0497	0.00035		16.45			1.5	
3 ^b	0.494	0.00015	1.5 ± 15%	13.75	2.8	31	13.00	8.0
	0.493	0.00005		16.50			1.5	
4 ^a	0.448	0.00050	3.5 ± 10%	12.5	2.0	22	13.0	23.0
	0.456	0.00030		18.0			2.0	

^a Single X-tal chip purchased; ground and polished at Loral.
^b Polished sphere purchased.
^c Difference between maximum and minimum diameters obtained by rotation about an axis in each of two perpendicular planes. Probable error is about ± 0.00005 inches.
^d Main spurious is approximately 700 Mc below main in all cases.

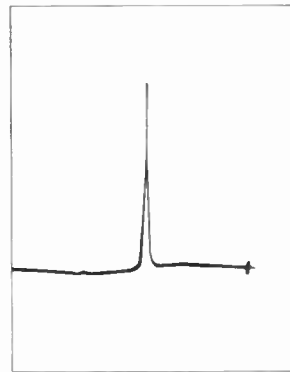


Fig. 2—Response of YIG no. 4 (Table I).

of both samples were the same within the experimental error. Nos. 1, 2 and 3 were then subjected to X-ray diffraction analysis, as well as measurements with the GE “goniostat” using a scintillation counter. All were found to be single-crystal YIG with no detectable impurities (lattice constants were 12.36A ± 0.01A). No detectable difference between the balls was found except possibly for differences in what was believed to be a thin amorphous surface layer which caused all balls to be poor diffractors of X rays. It is doubtful if this layer plays a significant role; it is probably associated with the polishing operation and its presence has been detected by others.⁴ The only significant difference found between the two 50-mil balls is the departure from sphericity of the one having the more prominent spurious spectrum. The data involving spheres (nos. 1 and 4), where greater polishing seems to enhance the spurious, is believed typical; these two spheres were originally part of the same crystal, polished for different lengths of time. It is conceivable that different surface irregularities effect the coupling between magnetostatic modes and degenerate spin waves differently and decrease the spin-spin relaxation time by a different amount for a particular magnetostatic mode than for the Kittel mode [Figs. 1(a) and 2].

In general, the magnitude of the spurious responses can be expected to increase with sphere diameter (Fig. 1). The most obvious reason for this is that the degree of RF field inhomogeneity can be expected to be greater

for samples whose physical extent in space is greater. However, there is another factor that comes into play. Fig. 1(c) shows the response of a YIG sphere in a waveguide iris of diameter only slightly larger than its own. The dense sets of spikes are probably higher magnetostatic modes excited by eddy currents induced in the iris wall and edges. The same sphere in a larger iris gave a much cleaner response. (A different structure was used to obtain (a), (b) and (c) of Fig. 1 than that used to obtain Table I.)

R. BLAU
 E. SULLIVAN
 M. SKRILL
 Loral Electronics Corp.
 New York, N. Y.

A Note on the Radiation Resistance and Field Strength of a Large Loop Antenna*

Imrie's note¹ is reviewed with interest since (except for differences in notation) his (6) represents a special case of the general solution for the “far-field” vector potential produced by a circular loop antenna with current

$$i(\phi, t) = I \left\langle \frac{\cos n\phi}{\sin n\phi} \right\rangle e^{i\omega t}$$

The general expression,

$$A = j^n \left[\frac{-j\mu I a}{4r} e^{i(\omega t - \beta r)} \right] \left\{ [R \sin \theta + \Phi \cos \theta] \cdot \frac{2n \left\langle \frac{\sin n\phi}{\cos n\phi} \right\rangle}{\beta a \sin \theta} J_n(\beta a \sin \theta) + \Phi \left\langle \frac{\cos n\phi}{\sin n\phi} \right\rangle \cdot [J_{n-1}(\beta a \sin \theta) - J_{n+1}(\beta a \sin \theta)] \right\}$$

* Received May 7, 1962.

¹ K. S. Imrie, “A note on the radiation resistance and field strength of large loop antennas,” *Proc. IRE*, vol. 50, p. 477; April, 1962.

¹ R. C. LeCraw (private communication).

has been derived both through an application of a limiting process² and a direct integration process.³ The direct integration process is based on an earlier work⁴ which clearly outlines the use of a power series expansion in terms of $(\beta a \sin \theta)$ for the derivation of the Sommerfeld integral expression for Bessel functions.

E. J. MARTIN, JR.
Midwest Research Institute
Kansas City, Mo.

²H. L. Knudsen, "The field radiated by a ring quasi-array of an infinite number of tangential or radial dipoles," Proc. IRE, vol. 41, pp. 781-789; June, 1953.

³E. J. Martin, Jr., "Radiation fields of circular loop antennas by a direct integration process," IRE TRANS. ON ANTENNAS AND PROPAGATION, vol. AP-8, pp. 105-107, January, 1960; "Correction," IRE TRANS. ON ANTENNAS AND PROPAGATION, vol. AP-8, p. 515, September, 1960.

⁴E. J. Martin, Jr., "An Approximation of the Helical Beam Antenna," M.S. thesis, University of Kansas, Lawrence, Kan.; 1956.

Optimum Cross-Correlation Radar System*

Some time ago R. L. Mattingly reported in a communication¹ that the conventional Dolph-Chebyshev design of linear arrays was inadequate in the radar case. He pointed out that if the *two-way pattern* is considered, one obtains the pattern $T_{2n}^2(u)$ where $T_n(u)$ is the Chebyshev polynomial of degree n and $u = u_0 \cos |\beta l \sin \theta|$ where

- β = phase constant in radians per meter
- l = element spacing in meters
- θ = angle measured from the normal to the array.

The constant u_0 is related to the sidelobe level ρ of the pattern $T_n(u)$ by the formula

$$\rho = 20 \log_{10} T_n(u_0). \quad (1)$$

Now as Mattingly indicated, the two-way pattern $T_{2n}^2(u)$ is a polynomial of degree $2n$ but is of course not the desired Chebyshev pattern of that degree, $T_{2n}(u)$. He recommended that the relation

$$T_{2n}(u) = 2T_n^2(u) - 1 \quad (2)$$

$$= 2 \left(T_n(u) - \frac{1}{\sqrt{2}} \right) \left(T_n(u) + \frac{1}{\sqrt{2}} \right)$$

be used to obtain a two-way pattern which is the optimum Chebyshev solution. To do this one simply transmits with, say, the pattern $T_n(u) - 1/\sqrt{2}$ and receives with the pattern $T_n(u) + 1/\sqrt{2}$. The two-way pattern is their product which by (2) yields the desired Chebyshev solution. Mattingly considered this to be the optimum design for the radar case.

However, with such a system the terminal voltage of the receiving antenna at

angular frequency ω and time t will be

$$V_{T1}(t, u) = \text{Re } T_{2n}(u)e^{j\omega t} \quad (3)$$

where Re indicates "the real part of . . ." If the usual square-law detector is used in the receiver the system output will be

$$P_M(u) = T_{2n}^2(u). \quad (4)$$

This represents an improvement over the conventional Dolph-Chebyshev system whose output is

$$P(u) = T_n^2(u) \quad (5)$$

but again the result is not in the form of a Chebyshev polynomial. Ideally we would have the output given by

$$P_0(u) = T_{2n}(u). \quad (6)$$

Such a pattern is not realizable with conventional antennas but can be obtained if a cross-correlation antenna system is used.

Consider the system shown in Fig. 1. The transmitter signal is divided into two equal parts and one part is shifted in frequency from ω to $\omega + \omega_1$, with $\omega_1 \gg \omega$. Then the two signals enter an aperture-weighting network which determines the transmitting patterns of the system. The two distinct transmitted signals are

$$V_{T1}(t, y) = \text{Re } A_1(u)e^{j\omega t}$$

$$V_{T2}(t, u) = \text{Re } A_2(u)e^{j(\omega + \omega_1)t} \quad (7)$$

where $A_1(u)$ and $A_2(u)$ are the field strength patterns of the two coincident antennas.

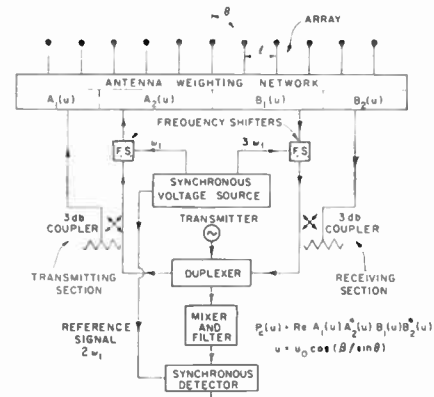


Fig. 1—Cross-correlation radar system.

When the system is in the receiving state there are two more distinct outputs with associated patterns $B_1(u)$ and $B_2(u)$. One of the signals is tagged with the modulation frequency $3\omega_1$. Then the two outputs in the presence of a single target in the u direction are given by

$$V_{R1}(t, u) = \text{Re } \left\{ A_1(u) + A_2(u)e^{j\omega_1 t} \right\} B_1(u)e^{j(\omega + 3\omega_1)t}$$

and

$$V_{R2}(t, u) = \text{Re } \left\{ A_1(u) + A_2(u)e^{j\omega_1 t} \right\} B_2(u)e^{j\omega t} \quad (8)$$

If these two voltages are multiplied and the low-frequency part is fed into a synchronous detector along with a reference signal at frequency $2\omega_1$, then the system output can

be shown to be proportional to

$$P_c(u) = \text{Re } A_1(u)A_2^*(u)B_1(u)B_2^*(u) \quad (9)$$

where * indicates the complex conjugate of the quantity.

In particular if we let

$$A_1(u) = T_n(u) + \left(\frac{1}{2} + \frac{1}{2\sqrt{2}} \right)^{1/2} \quad (10)$$

$$A_2(u) = T_n(u) + \left(\frac{1}{2} - \frac{1}{2\sqrt{2}} \right)^{1/2} \quad (11)$$

$$B_1(u) = T_n(u) - \left(\frac{1}{2} + \frac{1}{2\sqrt{2}} \right)^{1/2} \quad (12)$$

$$B_2(u) = T_n(u) - \left(\frac{1}{2} - \frac{1}{2\sqrt{2}} \right)^{1/2} \quad (13)$$

it can easily be shown that except for a constant factor

$$P_c(u) = P_0(u) = T_{2n}(u). \quad (14)$$

This is the *optimum power pattern* for the radar case in that for a given beamwidth it has the smallest sidelobes. A quantitative analysis of the three types of patterns showed that for large arrays ($n > 10$) and for identical beamwidths measured to the first null, the Mattingly pattern had a sidelobe improvement with respect to the conventional pattern of about 5 or 6 db while the correlation pattern's improvement was about 7 or 8 db. This is shown graphically in Fig. 2 where the improvement is plotted as a function of the sidelobe level of the conventional Dolph-Chebyshev array. In both cases improvement is greater when the original sidelobe level of the conventional array is high.

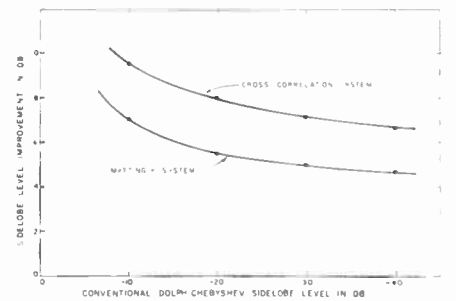


Fig. 2—Sidelobe level improvement of the Mattingly and cross-correlation radar patterns as a function of the conventional Dolph-Chebyshev sidelobe level.

This correlation system, it should be noted, involves only one *multiplicative* operation. Consequently it is linear in average power when the various target returns are mutually incoherent. Letting the average power reflected by the targets be given by the distribution $Q(u)$, the system output in their presence is

$$R_c(u_s) = \text{Re } \int B_1(u - u_s)A_1(u - u_s)A_2^*(u - u_s)B_2^*(u - u_s)Q(u)du \quad (15)$$

where u_s corresponds to the antenna beam direction. The corresponding output from a conventional system employing square-law detection is

$$R(u_s) = \int Q(u) |A(u - u_s)|^2 du \quad (16)$$

* Received May 11, 1962. This work was carried out under the sponsorship of the Wright Air Development Center, Contract AF33(616)-6079.

¹R. L. Mattingly, "Nonreciprocal radar antennas," Proc. IRE, vol. 48, pp. 795-796; March, 1960.

where $A(u)$ is the voltage pattern of the antenna. If the reflections are mutually coherent they can be represented by the complex function $q(u)$ which gives their amplitude and phase at the phase center of the antenna. The correlation system's output in this case is

$$R_c(u_s) = \text{Re} \int q(u)A_1(u - u_s)B_1(u - u_s)du$$

$$\int q^*(v)A_2^*(v - u_s)B_2^*(v - u_s)dv \quad (17)$$

and in the conventional case

$$R(u_s) = \left| \int q(u)A^2(u - u_s)du \right|^2 \quad (18)$$

which in reality is just a special case of the correlation radar system which results when $A_1(u) = A_2(u) = B_1(u) = B_2(u) = A(u)$.

ROBERT H. MACPHEE
Elec. Engrg. Dept.
University of Illinois
Urbana, Ill.

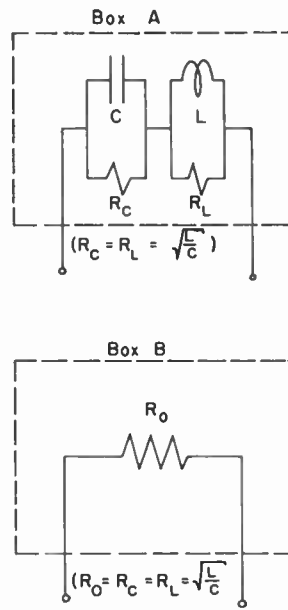


Fig. 1—Two black boxes enclosing two different linear circuits.

B are, respectively,

$$(G_r)_{\text{Box A}} = 2kR_0 \left[\frac{\omega^2 T_2 + (1/RC)^2 T_1}{\omega^2 + (1/RC)^2} \right], \quad (1)$$

and

$$(G_r)_{\text{Box B}} = 2kR_0 T_1. \quad (2)$$

Taking $T_2 = mT_1$, where $0 < m < 1$, we can rewrite (1) as

$$(G_r)_{\text{Box A}} = 2kR_0 T_1 - 2kR_0 T_1 \left[\frac{(1-m)\omega^2}{\omega^2 + (1/RC)^2} \right]. \quad (3)$$

The second term on the RHS of (3) is positive, but less than $2kR_0 T_1$. Hence,

$$0 < (G_r)_{\text{Box A}} < (G_r)_{\text{Box B}} = 2kR_0 T_1. \quad (4)$$

Thus, we have developed a measurement which solves our black box problem.

R. B. GOLDNER
Dept. of Elec. Engrg.
Mass. Inst. of Tech.
Cambridge, Mass.

Electron Ray Tracing*

Classical ray-tracing methods¹ do not yield correct position nor angle, even in a region of constant field. A method without this fault is proposed.

Let V_n and V_{n+1} be two adjacent equipotentials. Let P_n , N_n and θ_n be the point of incidence, the normal to V_n at P_n and the angle of incidence respectively, of the ray entering V_n . (See Fig. 1.)

Along the incident ray, lay off AP_n and use it as one unit. Project A onto N_n to obtain point B . With B as a center, draw an arc of radius $\sqrt{V_{n+1}/V_n}$ and let this arc meet with the parallel to N_n through A , at C . Project C onto N_n to obtain D . Extend line DC to E , so that $DC = CE$. Join EP_n to meet V_{n+1} at P'_{n+1} . Then the point P'_{n+1} is the first estimate of the point of incidence at V_{n+1} . The first estimate of the angle of incidence, θ'_{n+1} , is equal to the angle CBD .

Let the angle between N_n and N_{n+1} be δ . (See Fig. 2.) Lay off $GP_{n+1}' = DB - BP_n$. Construct $HG \perp GI'_{n+1}$.

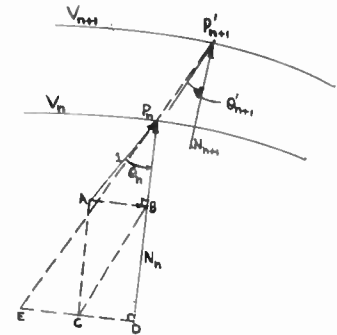


Fig. 1.

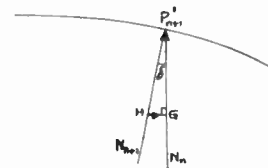


Fig. 2.

Let P_{n+1} and θ_{n+1} be the modified point of incidence and the angle of incidence, respectively. P_{n+1} can be obtained by the triangle EDP_n with the vector HIG added to the side DE to replace DE . Similarly, for θ_{n+1} , HIG is added to the side DC of the triangle CDB to replace DC .

In a constant field region, the unprimed values are the same as the primed values since δ is zero. Furthermore, the estimate yields correct values for both the point of incidence and the angle of incidence at V_{n+1} . This is so since the triangle EDP_n is proportional to the effective velocity vector diagram of the ray passing from V_n to V_{n+1} , and since the triangle CDB is proportional to the final velocity vector diagram of the ray at V_{n+1} .

In a nearly constant field, δ is not zero. To see that the unprimed values are better, note that the triangle HGP'_{n+1} is proportional to the final incremental-velocity vector diagram of the ray at V_{n+1} . Accordingly, θ_{n+1} is the angle of incidence of the ray at V_{n+1} . Also, P_{n+1} is better than P'_{n+1} since it is reasonable to assume a linear variation of the velocity component transversal to N_n . Or, an effective transversal velocity component of $\frac{1}{2}HIG$ can be assumed.

R. H. LEE
Autometric Corp.
Paramount Building
New York, N. Y.

* Received May 10, 1962.
¹ To enable us to make an open circuit noise measurement.

² J. C. Hancock, "An Introduction to the Principles of Communication Theory," McGraw-Hill Book Co., Inc., New York, N. Y.; 1961.

* Received May 8, 1962.
¹ O. Klemperer, "Electron Optics," Cambridge University Press, New York, N. Y.; 1953. See Circle Method, Parabola Method, Trigonometrical Method, etc.

Interesting Behavior of VA-99 as a Millimeter-Wave Amplifier*

The purpose of this communication is to report interesting behavior of a reflex klystron VA-99 when this is used as a millimeter-wave amplifier. The VA-99 amplifier indicated the highest gain and the lowest noise among all reflex klystron amplifiers ever tested at millimeter wavelengths.

The schematic diagram of the VA-99 amplifier test circuit is shown in Fig. 1. The amplifier circuit consists of a VA-99 reflex klystron, an H-plane tee and two EH tuners. Waveguide switches were used in measuring the insertion gain of the amplifier. The isolator and buffer attenuator were used for stabilization. The output of the circuit was observed by a RW-T R-B1 millimeter-wave superheterodyne receiver.

The VA-99 amplifier indicated relatively high gain and wide dynamic range at relatively high signal levels. Most reflex klystron amplifiers that were tested indicated saturation at about -30 dbm-input.¹ The VA-99 does not saturate even at -10-dbm input [Fig. 2(a)].

When the amplifier was adjusted for low-level input, it had extremely high gain [i.e., 25~34.9 db, Fig. 2(b)]. The bandwidth of the amplifier was approximately 30 Mc at high gain.

The RW-T R-B1 receiver output is shown in Fig. 3 with the sweep voltage applied to the horizontal axis. The bottom left is the input signal (-64 dbm) and the top left is the output (-41 dbm) of the VA-99 amplifier (23 db gain). The middle left in Fig. 3 shows the coexistence of oscillation and amplification at different frequencies by improper adjustment of repeller voltage. If supply voltage and circuit are poorly adjusted, reflex klystron amplifiers are noisy; proper adjustment and the right choice of tubes can make them very quiet^{2,3} as shown in Fig. 3.

Without the amplifier the input signal was decreased until it finally disappeared as shown in the bottom right (Fig. 3). When the VA-99 amplifier was in front of the RWT R-B1 receiver, the signal could be clearly seen as shown in the top right (Fig. 3) Using the amplifier, the RWT R-B1 receiver detected signals approximately 20 db below its tangential sensitivity. The tangential sensitivity of the VA-99 amplifier itself could not be measured because of the RWT R-B1 receiver noise.

As Ishii predicted^{2,3,4} and Brown explained,⁵ this reflex klystron did not generate much noise as is seen at the right in Fig. 3. The noise figure in this case was estimated at less than 5 db. The noiselessness of this

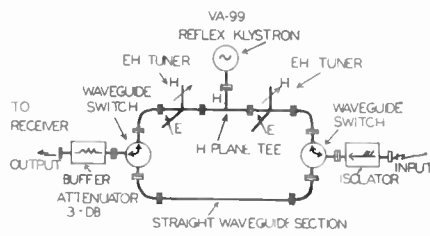
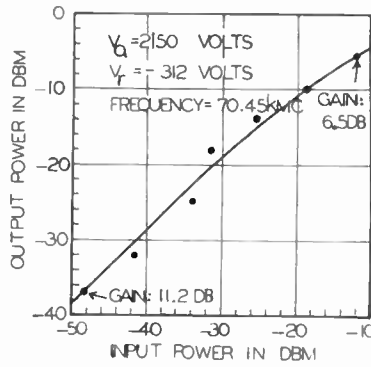
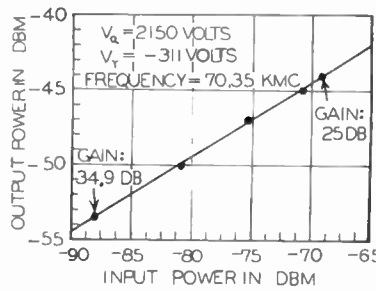


Fig. 1- Schematic diagram of VA-99 reflex klystron amplifier test circuit.



(a)



(b)

Fig. 2- Input-output relations of VA-99 amplifier. (a) High-level characteristic. (b) Low-level characteristic.

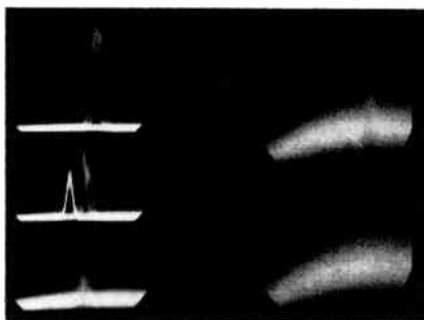


Fig. 3- Input and output display of VA-99 amplifier at 73.39 kMc. $V_a = 2200$ v. Top left: Amplified output (-41 dbm). $V_r = -319$ v. Middle left: Oscillation and amplification. $V_r = -314$ volts. Bottom left: Input (-64 dbm). Top right: Receiver output with VA-99 preamplifier. Bottom right: Receiver output without VA-99 preamplifier.

VA-99 amplifier is shown in Fig. 4. The top of Fig. 4 indicates the output of the RWT R-B1 receiver when its input is terminated. The bottom of Fig. 4 indicates the same output when the VA-99 amplifier is connected in front of the RWT R-B1 receiver. The VA-99 preamplifier had 26-db gain with its input terminated.



Fig. 4- Noise output of RWT R-B1 superheterodyne receiver without VA-99 preamplifier (top) and with VA-99 preamplifier (bottom).

The authors thank S. Krupnik, P. Vilmur, J. A. Stefancin and J. E. Billo for their assistance. The authors also thank R. G. Rockwell, Varian Associates, and Raytheon Company, Waltham, Mass., for contributing the klystron tubes.

K. ISHII
D. E. SCHUMACHER
K. R. KELLY
Dept. of Elec. Engrg.
Marquette University
Milwaukee, Wis.

A New Method to Find the Roots of a Fourth-Order Equation*

The roots of the fourth-order equation $f(z) = z^4 + A_1z^3 + A_2z^2 + A_3z + A_0$ (1) are known when the factorization

$$f(z) = (z^2 + y_1z + x_1)(z^2 + y_2z + x_2) \quad (2)$$

is known. The coefficients in (1) are assumed to be real and consequently the coefficients $y_{1,2}$ and $x_{1,2}$ in (2) are real, however as yet unknown. Depending on the polarity of the discriminants

$$d_i = y_i^2 - 4x_i, (i = 1 \text{ and/or } 2), \quad (3)$$

(1) has either

- (a) two pairs of conjugate complex roots ($d_i < 0$)
- (b) one pair of conjugate complex roots and two real roots ($d_1 < 0, d_2 > 0$) or
- (c) four real roots ($d_i > 0$), where no pairs are defined.

If one or both discriminants are zero, $f(z)$ has double roots.

Consider now the third-order equation

$$\phi(V) = V^3 - \phi_2V^2 + \phi_1V - \phi_0 = 0 \quad (4)$$

* Received May 10, 1962.

* Received May 9, 1962. This research was partly supported by a Frederick Gardner Cottrell grant to Marquette University, Milwaukee, Wis.

¹ K. Ishii, "On use of reflex klystrons for microwave and millimeter waves," *Proc. NEC*, vol. 16, pp. 744-752; 1960.

² Ishii, "Noise figure of reflex klystron amplifiers," *IRE TRANS. ON MICROWAVE THEORY AND TECHNIQUES*, vol. MTT-8, pp. 291-294; May, 1960.

³ K. Ishii, "Impedance adjustment effect on reflex klystron amplifier noise," *Microwave J.*, vol. 2, pp. 43-46; December, 1959.

⁴ D. M. Makurat, R. C. Hertel and K. Ishii, "The reflex klystron as an amplifier at 73 kMc," *Proc. IRE*, vol. 50, pp. 210-211; February, 1962.

⁵ F. W. Brown, "The noise figure of negative conductance amplifiers," *Proc. IRE*, vol. 49, pp. 520-521; February, 1961.

which can be factorized as

$$\phi(Y) = (Y - Y_1)(Y^2 - a_1Y + a_0). \quad (5)$$

In (4) the coefficients are also assumed to be real and consequently the coefficients a_0 and a_1 in (5) are real. We make (4) depending on (1) by defining

$$\phi_0 = A_3(A_1A_2 - A_0A_3) - A_1^2 \quad (6a)$$

$$\phi_1 = A_3^2 + A_1A_3 - 4A_0 \quad (6b)$$

$$\phi_2 = 2A_2 \quad (6c)$$

Depending on the polarity of the discriminant

$$\delta = a_1^2 - 4a_0 \quad (7)$$

(4) has in addition to the real root Y_1 either

(α) a pair of conjugate complex roots ($\delta < 0$) or

(β) two real roots Y_2 and Y_3 ($\delta > 0$).

It may also have a double real root ($\delta = 0$).

It can be proved that if $f(z)$ has the above property (b), then $\phi(Y)$ has the property (α) and its real root is

$$Y_1 = y_1y_2. \quad (8)$$

On the other side, if $f(z)$ has either the property (a) or the property (c), then $\phi(Y)$ has the property (β) where all three roots Y_1 , Y_2 and Y_3 are real. Depending on the polarity of the differences

$$\Delta_i = A_3^2 - 4Y_i \quad (i = 1, 2, 3) \quad (9)$$

$f(z)$ has the property (a) if only one of the differences is positive. This one is identical with the product y_1y_2 and has to be labelled as Y_1 according to (8). Eq. (1) has the property (c) if all the differences are positive. In this case any of the real roots of $\phi(Y)$ can be identified with the product y_1y_2 .

A real root of (4) can be found in first approximation by using a power table in evaluating $\phi(Y)$ for real numerical values of the variable Y in (4). The result can be brought to any desired accuracy by the well-known Newton Formula which is schematized in Horner's method. This root is called Y_1 in (5). With the linear root factor also, the quadratic residue polynomial in (5) is known. If δ defined in (7) is negative, the product y_1y_2 is known already. This product is also already known if δ and all the differences in (9) are positive. If δ and only one of the differences are positive, we have to make sure that the correct root is labelled as $Y_1 = y_1y_2$.

By the identity of (1) and (2)

$$y_1 + y_2 = A_3. \quad (10)$$

Eq. (10) and the correct definition of Y_1 according to (8) yield

$$2y_1 = A_3 + \sqrt{A_3^2 - 4Y_1} \quad (11a)$$

$$2y_2 = A_3 - \sqrt{A_3^2 - 4Y_1}. \quad (11b)$$

It can be shown that the two other coefficients in (2) are

$$x_i = \frac{y_1^3 - A_3y_1^2 + A_2y_i - A_1}{2y_i - A_3} \quad (12)$$

with $i = 1$ and/or 2.

The problem of finding the factorization (2), according to the described method, essentially boils down to the problem of finding one real root of (4) with its coefficients known by (6a, b, c) and its variable defined by (8). The further computation of the coefficients in (2) and of the actual root locations is a triviality. The technique seems to be remarkably easy. The method also works if $f(z)$ has double roots. The information given in this letter is sufficient to apply the method. Its derivation and proofs have recently been published by the author.¹ The content of this communication is one result of a root-finding technique for high-order polynomials on which the author is working at the present time. In his opinion it is worthwhile to be precommunicated. Here are three illustrative examples.

Example 1
Problem:
 $f(z) = z^4 - z^3 - 7z^2 - 13z + 4 = 0.$
 We derive
 $\phi(Y) = Y^3 + 14Y^2 + 46Y + 264 = 0.$
 A real root of $\phi(Y)$ has been found to be -12 . Therefore $\phi(Y) = (Y + 12) \cdot (Y^2 + 2Y + 22)$ with $\delta = 4 - 88 < 0$, and hence $\phi(Y)$ has the property (α) and $f(z)$ has the property (b). We identify immediately $Y_1 = -12 = y_1y_2$. By (11a, b), we find $y_1 = 3$ and $y_2 = -4$ and by (12), $x_1 = 4$ and $x_2 = 1$.

Example 2

Problem:

$$f(z) = z^4 - z^3 + 2z^2 - z + 15 = 0.$$

We derive

$$\phi(Y) = Y^3 - 4Y^2 - 57Y + 18 = 0.$$

A real root of $\phi(Y)$ has been found to be -0.31 . Hence $\phi(Y) = (Y - 0.31)(Y^2 - 3.69Y - 58.1)$ with $\delta = 13.62 + 232.4 > 0$. Therefore $\phi(Y)$ has the property (β) and $f(z)$ has the property (a) or (c); which one has to be decided by first solving the square equation $Y^2 - 3.69Y - 58.1 = 0$, and then by investigating the differences defined in (9). We find

Example 3

Problem:

$$f(z) = z^4 - 2z^3 - 13z^2 + 14z + 24 = 0.$$

We derive

$$\phi(Y) = Y^3 + 26Y^2 + 45Y - 72 = 0.$$

A real root of $\phi(Y)$ has been found to be $+1$. Hence $\phi(Y) = (Y - 1)(Y^2 + 27Y + 72)$. The roots of the residue square factor are -24 and -3 . The discriminant of this factor is $\delta = 729 - 288 > 0$, $\phi(Y)$ has the property (β) and $f(z)$ either the property (a) or (c). The differences (9) are

$$\phi(Y) = (Y - 0.31)(Y^2 - 3.69Y - 58.1)$$

$\Delta_1 = 4 - 4 = 0$
 $\Delta_2 = 4 + 96 = 100$
 $\Delta_3 = 4 + 12 = 16.$

$$\phi(Y) = (Y - 0.31)(Y + 6)(Y - 9.7).$$

Only $Y_1 = -6$ yields a positive difference and therefore $f(z)$ has the property (a). We proceed as in Example 1.

Example 3

Problem:

$$f(z) = z^4 - 2z^3 - 13z^2 + 14z + 24 = 0.$$

We derive

$$\phi(Y) = Y^3 + 26Y^2 + 45Y - 72 = 0.$$

A real root of $\phi(Y)$ has been found to be $+1$. Hence $\phi(Y) = (Y - 1)(Y^2 + 27Y + 72)$. The roots of the residue square factor are -24 and -3 . The discriminant of this factor is $\delta = 729 - 288 > 0$, $\phi(Y)$ has the property (β) and $f(z)$ either the property (a) or (c). The differences (9) are

$$\Delta_1 = 4 - 4 = 0$$

$$\Delta_2 = 4 + 96 = 100$$

$$\Delta_3 = 4 + 12 = 16.$$

The difference Δ_1 has to be counted as positive since the two others are positive and hence $f(z)$ has the property (c). No matter which one of the three real roots of $\phi(Y)$ we identify with y_1y_2 , we always get the result

$$f(z) = (z + 1)(z - 2)(z + 3)(z - 4).$$

KURT H. HAASE

Electronics Research Directorate
 AF Cambridge Research Labs.
 Office of Aerospace Research
 United States Air Force
 Bedford, Mass.

Systematic Matrix Inversion by Signal-Flow Graph*

Signal-flow graphs, since their first official appearance,¹ have resulted in a large number of papers giving elegant solutions to a number of problems involving systems of linear (differential or not) equations. In this case, the usefulness of flow graphs is based on greater human ability to identify and compute on patterns rather than to apply a pure algorithm.

Recently Leibowitz² has exposed the simple case of multiplication of second-order matrices with the help of flow graphs, this help being, however, minute since 2nd-order matrix multiplication is not a drawback for human limitations in applying rote or algorithms. The method exposed in Leibowitz's paper can, of course, be applied to a number of n th-order matrices, but the drawing complexities—crossed lines—will by no means facilitate the calculus for an engineer, even though he is fluent in flow-graph techniques.

The numerical inversion of a matrix is a pebble in almost every engineer's shoe. For flow-graph-minded people, what follows can be of some help in this respect.

A system of n -linear equations can be written as

$$\underline{x} = A\underline{y}. \quad (1)$$

with

$$\underline{x} = n \times 1 \text{ column matrix } \text{col}(x_1, x_2, \dots, x_n)$$

$$\underline{y} = n \times 1 \text{ column matrix } \text{col}(y_1, y_2, \dots, y_n)$$

$$A \triangleq [a_{ij}] = n \times n \text{ matrix, } i, j = 1, 2, \dots, n.$$

If A is a nonsingular matrix, the solution for \underline{y} is.

$$\underline{y} = A^{-1}\underline{x}. \quad (2)$$

In flow-graph terms, to solve system (1) corresponds to finding an equivalent system in which the x_i variables play the role of

* Received April 30, 1962.

¹ S. J. Mason, "Feedback theory—some properties of signal flow graphs," *Proc. IRE*, vol. 41, pp. 1144-1156; September, 1953.

² M. R. Leibowitz, "Feedback theory—further properties of signal flow graphs," *Proc. IRE*, vol. 44, pp. 920-926; July, 1956.

³ M. R. Leibowitz, "Visual matrix multiplication by flow graph," *Proc. IRE (Correspondence)*, vol. 50, pp. 211-212; February, 1962.

¹ K. H. Haase, "A New Method of Finding Roots of a Fourth-Order Polynomial with Real Coefficients," AF Cambridge Res. Labs., Bedford, Mass., Rept. No. AFCRL-62-44; January, 1962.

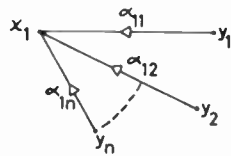
sources while the y_i are, at least, sinks. This is easy if we consider the two equivalent forms of the same algebraic expression

$$x_1 = \alpha_{11}y_1 + \alpha_{12}y_2 + \dots + \alpha_{1n}y_n \quad (3)$$

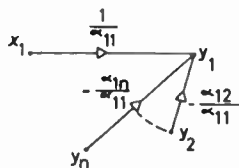
and

$$y_1 = \frac{1}{\alpha_{11}}x_1 + \left(-\frac{\alpha_{12}}{\alpha_{11}}\right)y_2 + \dots + \left(-\frac{\alpha_{1n}}{\alpha_{11}}\right)y_n \quad (4)$$

or the equivalence of their corresponding flow graphs:



Flow graph of (3).



Flow graph of (4).

When representing the linear system of (1) by a flow graph, α_{ij} will be the gain between node x_i and y_j .

The inversion of a second order matrix can be seen in Figs. 1 and 2.

By direct inspection (see Mason¹) of the flow graph in Fig. 2, and using Mason's notation, we obtain

$$\Delta = 1 - \frac{\alpha_{12}\alpha_{21}}{\alpha_{11}\alpha_{22}}$$

$$A^{-1} = \frac{1}{\Delta} \begin{bmatrix} 1 & -\alpha_{12} \\ -\alpha_{21} & 1 \end{bmatrix}$$

For the inversion of a 3rd-order matrix $[\alpha_{ij}]$, with $(i, j) = 1, 2, 3$ we refer to Figs. 3 and 4 where again by inspection we can obtain Δ and A^{-1} .

An important observation is that by inserting, in the triangle y_1, y_2, y_3 of Fig. 4, exactly this same figure (reduced in scale) defining a new relation

$$\underline{z} = B^{-1}\underline{y}$$

we find that the resultant flow graph is the flow graph of the inverse of the product of two matrices A and B

$$\underline{z} = B^{-1}\underline{y} = [B^{-1}A^{-1}]\underline{x} = [AB]^{-1}\underline{x}$$

Note that there will be no crossed lines in this resulting flow graph, which is an advantage when identifying the closed loops.

This last example was just for the love of art. Fig. 3 is not needed, since from the very beginning of this paper, [(3) and (4)], it is obvious that the inverse-matrix flow graph can be directly drawn with each y_i receiving a "contribution" of $1/\alpha_{ij}$ from x_j and of $(-\alpha_{ji}/\alpha_{jj})$ from each other y_j .

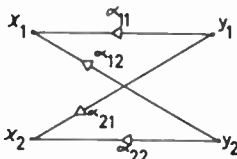


Fig. 1 $\underline{x} = A\underline{y}$.

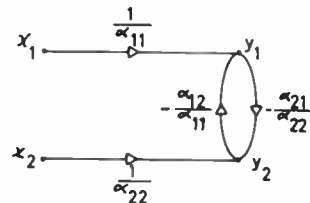


Fig. 2 $\underline{y} = A^{-1}\underline{x}$.

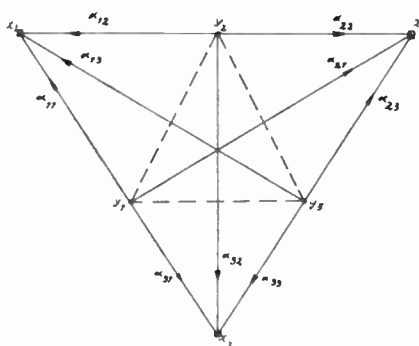


Fig. 3 $\underline{x} = A\underline{y}$.

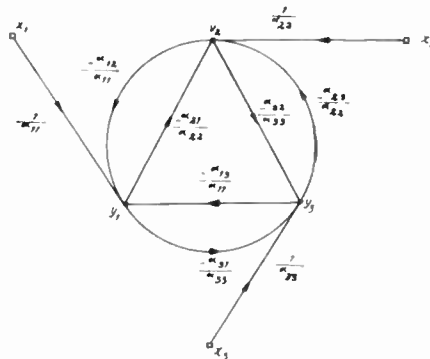


Fig. 4 $\underline{y} = A^{-1}\underline{x}$.

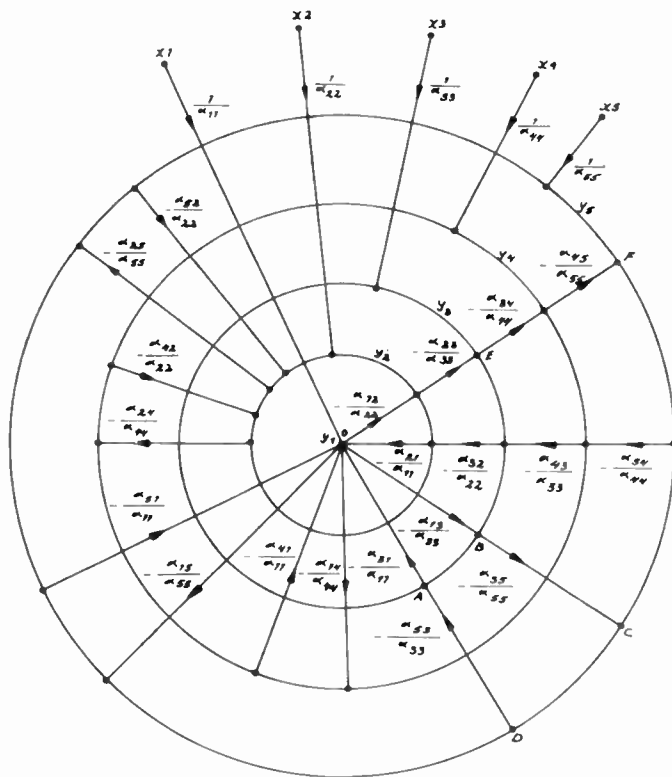


Fig. 5—Modified flow graph of the inverse of a 5th-order matrix.

By using this observation we can easily obtain the general flow graph of the inverse of an n th-order matrix. This is exemplified in Fig. 5, where the nodes y_i ($i \neq 1$) have been substituted by circumferences.

A 5th-order matrix is taken to illustrate this new method of drawing a flow graph. In this figure, the beginning or end of branches is represented by a heavy dot. Other crossings have no mean.

This particular way of drawing a signal-flow graph is crucial for our aim of simplifying the "reading" of a flow graph, since all the closed loops are now recognized as closed path contours of sectors (like AOB, DOF, etc.) and ring sections (like ABCD, AEFD, etc.).

JEAN-PAUL JACOB
IBM Nordiska Lab.
Stockholm, Sweden

A DC-Pumped Amplifier Using Space-Periodic Magnetic Field*

The dc-pumped cyclotron-wave amplifier described by a number of authors¹⁻³ amplifies the fast cyclotron wave in a periodic electrostatic quadrupole array. The quadrupole field introduces coupling between the positive-energy fast cyclotron wave and the negative-energy slow cyclotron wave, resulting in exponential growth and, therefore, amplification.

In addition to this mechanism there are basically two other possible dc-pumping schemes for transverse waves, each involving interaction between one positive-energy wave and one negative-energy wave as listed below.⁴

Waves Coupled in the dc Pump	dc Pump Structure
Cyclotron-Cyclotron	Periodic electric or magnetic quadrupole
Cyclotron-Synchronous	Periodic electric or magnetic fields of rotational symmetry
Synchronous-Synchronous	Straight electric or magnetic quadrupoles

Bass⁵ has described an amplifier based on the second pumping scheme, involving cyclotron-synchronous coupling by means of a pump consisting of an electrostatic ring system. This communication describes the basic features and experimental results of a similar amplifier using a magnetostatic pump.

As shown in Fig. 1 the input and output couplers are of the Cuccia type. The pump consists essentially of an array of five kovar disks introducing a ripple on the axial magnetic field. Provided the periodicity equals the cyclotron wavelength, the ripple introduces cumulative coupling between the fast cyclotron signal wave originating from the input coupler and the appropriate synchronous wave. The resulting amplitude growth is illustrated in Fig. 2, showing the trajectory of an individual electron in the pump field.

If A_1 , A_2 , and A_0 represent the wave amplitudes of the fast cyclotron wave and the synchronous wave before and after the pump, respectively, the interaction is described by the following relations:⁶

$$A_1^0 = A_1^i \cosh \alpha z + A_2^i \sinh \alpha z \quad (1)$$

$$A_2^0 = A_2^i \cosh \alpha z + A_1^i \sinh \alpha z \quad (2)$$

where $\alpha z = \pi N$, $B_1/2B_0$. The relative ripple is B_1/B_0 and the number of cyclotron wavelengths in the pump is N , in our case

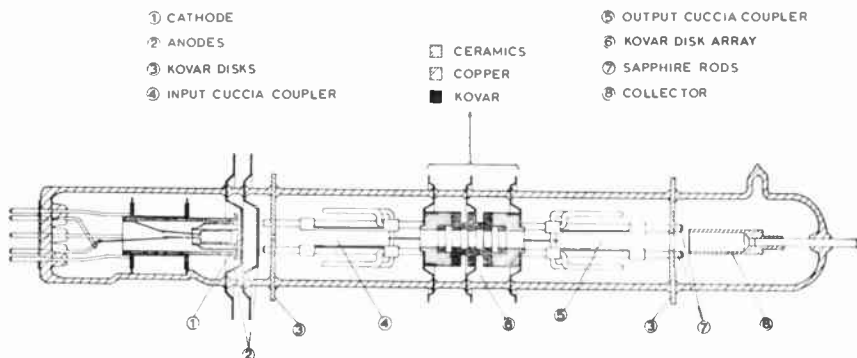


Fig. 1—Cross section of the dc-pumped amplifier.

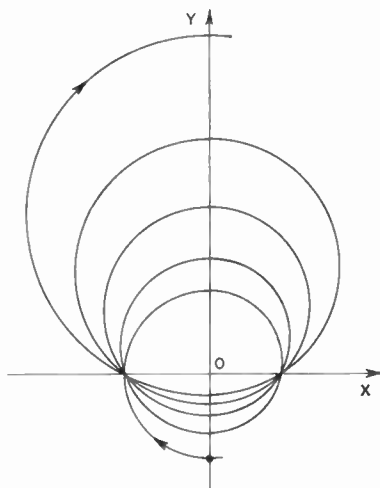


Fig. 2—Trajectory of an electron in the pump.

$B_1/B_0=0.209$ and $N=5$. Hence $\alpha z=1.64$, yielding a theoretical electronic gain of 8.5 db. The tube was operated at 28 V and 0.4 ma beam current at a frequency of 730 Mc. Fig. 3 shows the measured small-signal gain plotted vs frequency. The agreement with theory is good.

Saturation, which occurred at 0.7-mw RF power at 9-mw dc beam power, was not caused by beam interception which varied only a few per cent up to full saturation.

Undesired beam expansion and interception in the pump structure were avoided by means of a special focusing scheme which, in principle, can be applied to any dc-pumped tubes, but not to RF-pumped tubes. The principle is based on the fact that the relation between output and input amplitudes is given by (1) and (2) for all signal frequencies from zero to infinity. In particular, by considering the beam as made up of an assembly of filamentary beams carrying waves of zero frequency, the beam expansion in the pump is described by the same set of equations, provided space-charge forces are small. By using a dc beam characterized by $A_1+A_2=0$, (1) and (2) reduce to

$$A_1^0 = A_1^i e^{-\alpha z} \quad A_2^0 = A_2^i e^{-\alpha z} \quad (3)$$

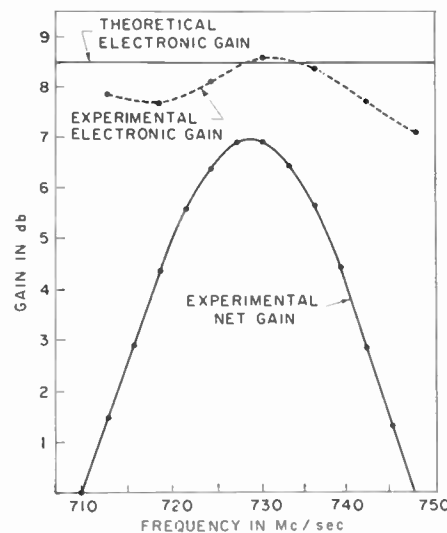


Fig. 3—Experimental and theoretical gain plotted vs frequency.

Under these circumstances the beam cross section decreases exponentially with z . The required condition is satisfied by a dc beam in which the individual electrons rotate in circles intersecting the axis; the beam is therefore heavily scalloped. This was obtained by having zero magnetic flux at the cathode and beam space charge considerably below the Brillouin value. The correct phase between A^1 and A^2 was obtained by locating the maximum beam scallop at the entrance to the pump structure by means of the dc voltage. The focusing action could be verified by observation of the intercepted current which was negligible at the correct scallop position.

The suggested focusing method can, in principle, be applied to all types of dc-pumped tubes by providing the correct type of dc beam, and possibly help overcome undesired beam expansion which is one of the major obstacles in obtaining high gain in these tubes.

T. WESSEL-BERG
Microwave Laboratory
Stanford University
Stanford, Calif.
K. BLÖTEKJÆR
Norwegian Defense Research Estab.
Bergen, Norway

* Received May 27, 1962; revised manuscript received, June 15, 1962.

¹ E. L. Gordon, "A transverse field traveling wave tube," *Proc. IRE (Correspondence)*, vol. 48, p. 1158; June, 1960.

² A. E. Siegman, "The dc pumped quadrupole amplifier—a wave analysis," *Proc. IRE*, vol. 48, pp. 1750-1755; October, 1960.

³ J. C. Bass and M. G. F. Wilson, "Cyclotron wave interaction in spatially periodic electrostatic quadrupole fields," *J. Electronics*, vol. 11, pp. 125-134; August, 1961.

⁴ K. Bløtekjær and T. Wessel Berg, "Some aspects of cyclotron wave amplification in time-periodic and space-periodic fields," *Record Internat'l Congr. Microwave Tubes*, Munich, Germany, June, 1960, Friedr. Vieweg and Sohn, Braunschweig, pp. 372-382; Germany, 1961.

⁵ J. C. Bass, "Microwave amplification in electrostatic ring structures," *Proc. IRE (Correspondence)*, vol. 49, pp. 1424-1425; September, 1961.

A New Precision Low-Level Bolometer Bridge*

Reisener and Bix¹ have presented an interesting method for the measurement of low-level RF power. I have been using an alternative system which I believe has some advantages over that described. The block diagram is shown in Fig. 1.

The method employs as the reference power a 1-Mc signal modulated by a square wave at a suitable audio frequency. The reference signal is fed to the bolometer in the off-periods of the unknown power which is chopped by the same square wave in anti-phase. Power measurement is effected by adjustment of the level of the 1-Mc signal to achieve a null on the output meter at which setting the unknown power equals the 1-Mc reference power. The 1-Mc power is very easily found from a knowledge of bolometer resistance and 1-Mc applied voltage.

Reisener and Bix use a dc pulse in place of the 1-Mc pulse used here. This makes necessary a bridge circuit which is not required if an RF reference is used. The bridge circuit is needed to discriminate between the square wave of reference power which is used to maintain the bolometer resistance constant and the square wave at the same frequency, which exists due to modulation of the bolometer resistance at unbalance and which contains the information necessary to balance the unknown and reference power.

As a detector of small powers the bridge circuit is less sensitive than that shown here. This can be seen by reference to equivalent circuits [Fig. 2(a) and (b)] where

- I = Bolometer bias current.
- ΔR = Change in bolometer resistance due to RF power.
- $\overline{V_{NR}}^2$ = Mean-square-noise voltage of resistance R .
- $\overline{V_{NB}}^2$ = Mean-square-noise voltage of bolometer.
- $\overline{V_{NA}}^2$ = Mean-square-noise voltage of amplifier referred to input.
- R_L = Resistance presented to the circuit by the amplifier.

If, as is the case in practice, $R_L \gg R \gg \Delta R$, then for Fig. 2(a)

$$\frac{P_{sig}}{P_{noise}} \propto \frac{(I\Delta R)^2}{\overline{V_{NB}}^2 + 3\overline{V_{NR}}^2 + 4\overline{V_{NA}}^2}$$

for Fig. 2(b)

$$\frac{P_{sig}}{P_{noise}} \propto \frac{(I\Delta R)^2}{\overline{V_{NB}}^2 + \overline{V_{NA}}^2}$$

The bridge method is as sensitive as the RF injection method only in the extreme case where bolometer noise swamps all other noise. The RF injection method is likely to show the greatest advantage in sensitivity when cooled and evacuated bolometers are used. The smallest quantity of power which can be measured with a given accuracy is, of course, proportional to the minimum detectable power.

* Received May 21, 1962.
 1 W. C. Reisener and D. L. Bix, "A new precision low-level bolometer bridge," *Proc. IRE*, vol. 50, pp. 39-42; January, 1962.

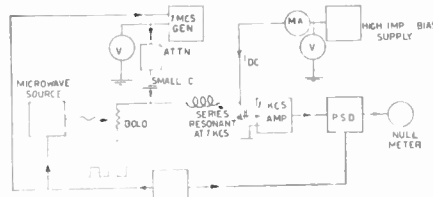


Fig. 1.

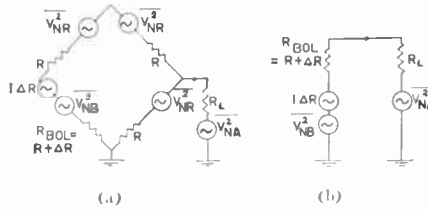


Fig. 2.

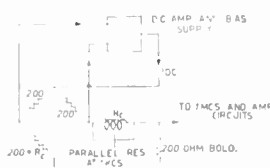


Fig. 3.

The RF injection system also eliminates a major practical difficulty of the bridge system, *viz.*, that to achieve balance a small differential signal must be amplified by the ac amplifier in the presence of large signals appearing on both inputs in phase.

The effective time during which bolometer drift can introduce an error is the square-wave period for the RF injection system, whereas for the bridge system it is the delay time of the dc servo amplifier, which is significantly longer.

The measurement system of Fig. 1 suffers two drawbacks. First, three meter readings are required to determine power after a null has been obtained. Second, long-term drifts may affect the bolometer match to the unknown power. These disadvantages can be eliminated as shown in Fig. 3 by the addition of a bridge and servo system for the bolometer bias supply which is used solely to maintain the bolometer resistance constant over periods which are long compared to the square-wave frequency. A match to the unknown power is thus ensured during the whole of the measurement process and since the bolometer resistance is fixed the only meter reading required once a null has been achieved is that of 1-Mc voltage. The parallel resonant circuit in Fig. 3 isolates the bridge from the remainder of the measurement circuitry at the square-wave frequency and thus in no way affects sensitivity.

In practice the simpler system has functioned adequately for laboratory use and the extra complication of a bridge and servo loop has not been found worthwhile.

Q. V. DAVIS
 Royal Radar Establishment
 Malvern, Worcestershire, England

An Unexpected Effect in an Experimental Transverse Wave Tube*

The present letter is concerned with a rather surprising effect observed in an experimental tube designed to study magnetostatic pumping of cyclotron waves. The tube employs two parallel-plate couplers (Cuccia couplers) separated by a metallic drift tube of 59-mm length and 2.6-mm inner diameter. The tube was intended for investigation of periodic magnetostatic pump structures applied external to the drift tube, which is part of the vacuum envelope, but the effect discussed here was observed while carrying out preliminary tests in the absence of pump fields. The theoretical transmission loss due to circuit losses in the resonant couplers was one-to-two db, which in general agreed well with the measured values. However, under certain circumstances gain was observed and when the conditions were optimized, gain in excess of 30 db was obtained. An experimental gain-vs-frequency response is shown in Fig. 1. The dc potential of the couplers and the drift tube was 25.5 volts. The collector current was 600 μ A and the drift-tube current 140 μ A. It should be pointed out that gain was also observed with no current intercepted on the drift tube. In Fig. 1 the solid line represents the net gain and the dotted line the electronic gain, which to a certain extent is frequency-dependent. This may be due to the attenuation caused by axial velocity spread.

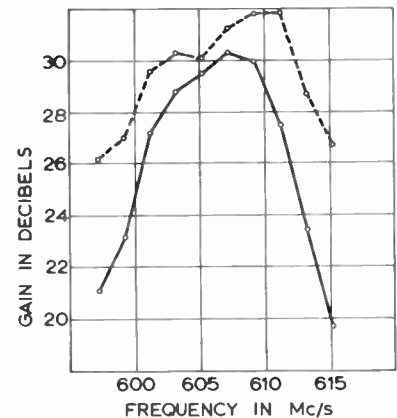


Fig. 1.

The observed gain is not predicted by any of the existing theories of transverse waves, and it seems necessary to look for effects which have not been paid attention to. In the following we shall describe an effect which possibly is involved in the amplification mechanism, although the theory presented here does not give an entirely satisfactory explanation.

The electron beam represents a space charge which induces an image charge in the surrounding drift tube. If the beam is not concentric with the drift tube, the field due

* Received May 14, 1962; revised manuscripts received May 24, 1962 and August 9, 1962.
 The research reported in this communication has been sponsored by Rome Air Dev. Ctr., Air Force Systems Command, Griffiss AFB, Rome, N. Y., monitored by the European Office, Office of Aerospace Research.

to the image charge acts on the electrons and may under certain circumstances cause growth of the transverse beam waves.

The following discussion is based on the assumption that the dc beam performs a helical motion due to small imperfections in the gun region. This is justified experimentally by the fact that higher gain was obtained if the dc beam was deflected by means of a transverse magnetic field produced by an external coil. We shall consider a very simplified model, assuming a filamentary beam performing a helical motion with a frequency ω_1 at a constant distance r_0 from the center of the drift tube. The transverse RF displacement is considered as a small perturbation of the dc motion. An approximate expression for the electric field at the beam position is given by

$$E_x = -\frac{Kr_0}{a^2 - r_0^2} \cos \phi - \frac{Ka^2}{(a^2 - r_0^2)^2} x - \frac{Kr_0^2}{(a^2 - r_0^2)^2} (x \cos 2\phi + y \sin 2\phi) \quad (1)$$

$$E_y = -\frac{Kr_0}{a^2 - r_0^2} \sin \phi - \frac{Ka^2}{(a^2 - r_0^2)^2} y - \frac{Kr_0^2}{(a^2 - r_0^2)^2} (y \sin 2\phi - x \cos 2\phi) \quad (2)$$

where

$$K = I_0 / (2\pi\epsilon_0 v_0) \quad (3)$$

and

$$\phi = \omega_1 z / v_0 \quad (4)$$

In these equations, a is the drift tube radius, I_0 is the dc beam current, v_0 is the axial beam velocity, z is the axial position, and x and y represent the transverse RF displacement.

The first terms on the right-hand sides of (1) and (2) are dc terms, causing the dc rotational frequency ω_1 to be lower than the cyclotron frequency ω_c . The second terms have a similar effect on the RF motion. Since the two terms are of different magnitude, ω_1 is different from the natural frequency ω_2 of the RF motion.

The remaining terms represent a periodic field equivalent to that produced by a quadrifilar helix. This field gives rise to cyclotron wave amplification, provided the periodicity of the field is correct for cumulative interaction. The required synchronization condition would be satisfied if the two frequencies ω_1 and ω_2 were equal. As mentioned above, this is not the case, and it appears that the propagation constants for the waves are all purely imaginary, *i.e.*, no amplification occurs. Therefore, the simple filamentary beam model does not explain the observed gain. We still have the possibility that space charge effects in a finite diameter beam may cause the two frequencies ω_1 and ω_2 to coincide. Assuming that this is true, a theoretical gain of 32 db is obtained for r_0 equal to 0.9 mm, *i.e.*, the beam center is 0.4 mm from the drift-tube wall. These values seem quite reasonable since the nominal radius of the beam is 0.4 mm, and a large fraction of the beam is intercepted on the drift tube.

To conclude, two items have been discussed in the present letter, namely, the experimentally observed amplification of cy-

clotron waves in a drift tube and a suggested mechanism for amplification due to image charges in the drift-tube wall. Further theoretical and experimental investigations are required in order to determine whether this is the correct explanation for the observed gain.

The authors are indebted to Mr. Magne Sørensen, who contributed to the success of the work by making the tube.

K. BLÖTEKJÆR
Microwave Laboratory
Stanford University
Stanford, Calif.

B. MALSNES
A. NORDHOTTEN
Norwegian Defence Res. Estab.
Bergen, Norway

Microwave Measurement of Conductivity and Dielectric Constant of Semiconductors*

Measurement of semiconductor parameters at microwaves have been reported by several authors.¹⁻⁵ In some of the reported measurements,¹⁻³ the samples were put inside a waveguide and the semiconductor parameters were obtained by measuring the attenuation and phase-shift of the transmitted signal. Essentially the same method has been described in detail recently by Jacobs, *et al.*,⁶ for evaluating the conductivity of a semiconductor sample assuming the value of the dielectric constant. Other workers obtained the semiconductor parameters⁷ by putting a small sample inside a cavity and determining the resonant frequency and Q of the loaded cavity. In the present communication a microwave method is proposed for measuring both the conductivity and dielectric constant of semiconductor crystals having conductivities lower than $1 \text{ } \Omega/\text{m}$. The method is similar to that used for low-loss dielectrics.⁷

The experimental arrangement for the proposed method is shown in Fig. 1. The sample is shaped to fit inside a waveguide and the rear surface is shorted by a copper

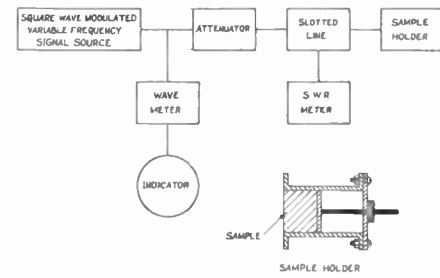


Fig. 1—Schematic diagram showing the experimental arrangement.

plunger. The dielectric constant and conductivity of the sample is obtained by locating a quarter wave frequency for the guide section loaded with the semiconductor and measuring the VSWR at that frequency.

The phase constant, attenuation constant and the wave impedance of the semiconductor loaded guide are given respectively by

$$\beta_s = \frac{2\pi}{\lambda_1} \left[K_s - \left(\frac{\lambda_1}{\lambda_0} \right)^2 \right]^{1/2} \quad (1)$$

$$\alpha_s = \frac{\sigma_0}{2} \sqrt{\frac{\mu_0}{\epsilon_0}} \frac{1}{\sqrt{K_s - (\lambda_1/\lambda_0)^2}} \quad (2)$$

$$\frac{Z_s}{Z_0} = \frac{[1 - (\lambda_1/\lambda_0)^2]^{1/2}}{[K_s - (\lambda_1/\lambda_0)^2]^{1/2}} \quad (3)$$

where $\sigma_0/\omega k_s \epsilon_0 \ll 1$. The symbols have their usual meaning. It should be noted that the approximation $\sigma_0/\omega k_s \epsilon_0 \ll 1$, is valid for all semiconductor samples having σ_0 lower than $1 \text{ } \Omega/\text{m}$.

Hence if the length of the sample be such that it is an odd multiple of a quarter wavelength K_s can be evaluated from the relation

$$K_s = \left(\frac{\lambda_1}{\lambda_0} \right)^2 + \left[\frac{\lambda_1(2n+1)}{4l} \right]^2 \quad (4)$$

The unknown integer n in the above equation may be eliminated by locating the next quarter-wave or half-wavelength frequency.

The measurement of the VSWR at the quarter-wave frequency also enables one to evaluate σ_0 . The relation giving σ_0 in terms of VSWR is

$$\sigma_0 = 2 \sqrt{\frac{\epsilon_0}{\mu_0}} \frac{\sqrt{K_s - (\lambda_1/\lambda_0)^2}}{l} \cdot \coth^{-1} \left[\frac{\sqrt{K_s - (\lambda_1/\lambda_0)^2}}{\sqrt{1 - (\lambda_1/\lambda_0)^2}} \cdot \frac{1}{\gamma} \right]$$

where l is the length of the sample and γ is the VSWR at the quarter-wave frequency. It should be noted that the accuracy in the measurement of σ_0 is limited by the accuracy of the measured value of γ . In this method by properly choosing l , γ may conveniently be arranged to be of the order of 1 where the accuracy of its measurement would be maximum.

The quarter-wave frequency may be conveniently located by measuring the VSWR at different frequencies. The frequency at which it is minimum corresponds to a quarter-wave frequency.

Measurement of the dielectric constant and conductivity of a silicon sample having a conductivity of $0.7 \text{ } \Omega/\text{m}$ were made by thi

* Received May 28, 1962.

¹ T. S. Benedict and W. Shockley, "Microwave observation of the collision frequency of electrons in germanium," *Phys. Rev.*, vol. 89, pp. 1152-1153; March, 1953.

² T. S. Benedict, "Microwave observation of the collision frequency of holes in germanium," *Phys. Rev.*, vol. 91, pp. 1565-1566; September, 1953.

³ F. D. Altroy and H. Y. Fan, "Polarization of impurities in germanium," *Phys. Rev.*, vol. 100, p. 1260; November, 1955.

⁴ J. M. Goldley and S. C. Brown, "Microwave determination of the average masses of electrons and holes in germanium," *Phys. Rev.*, vol. 98, pp. 1761-1763; June, 1955.

⁵ T. Stubbs, "Measurements of the temperature variation of the effective mass of the free carriers in silicon, with 3 cm. wavelength," *State Inst. for Tech. Res.*, Helsinki, Finland, Publ. 42; 1958.

⁶ H. Jacobs, F. A. Brand, J. D. Meindl, M. Benanti and R. Benjamin, "Electrodeless measurement of semiconductor resistivity at microwave frequencies," *Proc. IRE*, vol. 49, pp. 928-932; May, 1961.

⁷ C. A. Montgomery, "Technique of Microwave Measurements," M.I.T. Rad. Lab. Ser., McGraw-Hill Book Co., Inc., New York, N. Y., vol. 11, p. 625; 1947.

method. The value of K_s was obtained to be 11.5 and the value of σ_0 agreed to within 10 per cent of the dc value.

It may be noted that the proposed method requires comparatively simple experimental arrangement, namely a SWR detector and a variable-frequency signal source only. The temperature control may also be conveniently introduced by enclosing the sample holder inside a bath. A detailed description of the method for measuring the conductivity and dielectric constant at different temperatures and the experimental results will be published later.

The authors wish to express their appreciation of the constant encouragement received from Prof. J. N. Bhar and their thanks to other colleagues of the laboratory for their kind cooperation.

B. R. NAG
S. K. ROY
Inst. of Radiophysics and Electronics
University of Calcutta
Calcutta, India

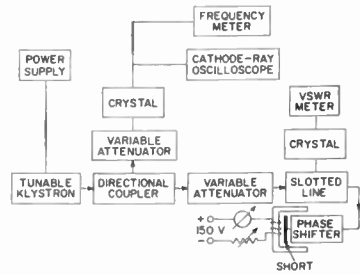


Fig. 1—Cold-test circuit.

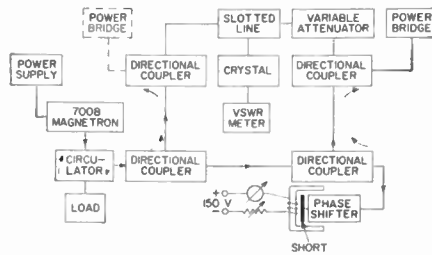


Fig. 2—High-power test setup.

Reciprocal Ferrite Phase-Shifter Measurements*

The results of high-power (spin-wave) experiments on microwave ferrites are generally published in the form of $y=f(h)$, where y is the loss component of permeability or susceptibility and h is the microwave magnetic field. Similar results for the real component of the complex permeability can also be plotted but are rarely published. These graphs represent important intrinsic characteristics of the ferrites but unfortunately mean little to the general microwave practitioner who prefers to see graphs of phase shift and attenuation in a given geometry. It must be realized, however, that phase shift cannot be entirely ascribed to the real, and loss to the imaginary component of the complex permeability.

In the course of some experiments on reciprocal phase shifters it was found convenient to plot their behavior in the form of Smith charts, in which the two components mentioned above can easily be recognized. The experiments were performed at 9 Gc in rectangular large X-band waveguide. The test circuits for low- and high-power measurements are shown in Figs. 1 and 2, respectively. In the latter case the incident power was determined by replacing the ferrite phase shifter with a solid short.

The difference in behavior between the MgMn ferrite "Ferramic R1"¹ and the Ni ferrite "Airtron C3P50"² is striking. The former exhibits an obvious increase of its loss component in higher microwave fields, while the reactive component remains almost constant, as shown in Fig. 3. The magnitude of the RF field was calculated at about 30 oersteds for the maximum power

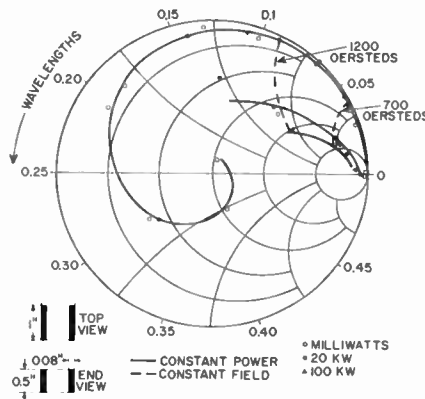


Fig. 3—Phase-shifter characteristics with Ferramic R1.

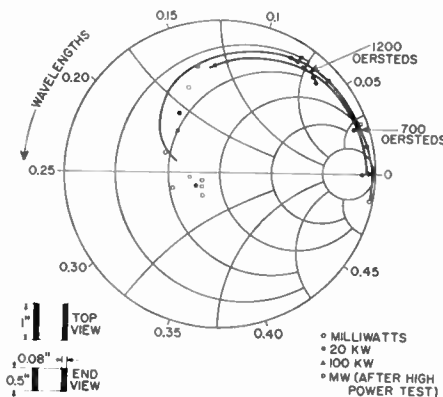


Fig. 4—Phase-shifter characteristics with Airtron C3P50.

input of 100 kw. In the case of the Ni ferrite, on the other hand, the two components of the complex permeability seem to have switched roles. Fig. 4 shows that at 1200 oersteds the loss component experiences little change with increasing power, while the phase-shifting ability is noticeably reduced. At 700 oersteds neither component exhibits a significant change. Because of this unexpected behavior the phase shifter was cold-tested again after the high-power experiments; no significant deviation from the original results were observed.

Although the graphs of Figs. 3 and 4 do not represent intrinsic material characteristics it is felt that such a presentation conveys more information to the microwave engineer than the usual susceptibility plots. If some standard configuration could be agreed upon, the Smith-chart presentation should be quite sufficient for most power applications of ferrites.

MAX J. SCHINDLER
Electron Tube Div.
RCA
Harrison, N. J.

Hilbert Transforms and Positive-Real Functions*

In a recent communication¹ Papoulis has given a proof of the angle constraint for positive-real functions along the lines of that which Bayard attributes to Leroy.² The method is based upon the Hilbert transform and consequently bypasses the lengthy arguments based upon Schwarz's lemma.

Since the proof based upon the Hilbert transform is less general than that using Schwarz's lemma, it is of interest to know the limitations of the first method. For instance, the Hilbert transform method cannot be directly applied to the positive-real functions

$$F(p) = p,$$

$$F(p) = +\sqrt{p},$$

$$F(p) = \sum_{m=1}^{\infty} [p/(m!)] / [p^2 + (1/m)^2].$$

In contrast, the Schwarz's lemma proof holds for all positive-real functions.

To see the limitations, we realize that the Hilbert transform proof rests upon equations (5) and (6) of Papoulis

$$R(\omega) = \int_{-\infty}^{\infty} R(y)\delta(\omega - y)dy \quad (5)$$

$$F(p) = \frac{1}{\pi} \int_{-\infty}^{\infty} \frac{R(y)}{p - jy} dy. \quad (6)$$

* Received June 11, 1962; revised manuscript received, June 25, 1962.
¹ A. Papoulis, "Hilbert transforms and positive-real functions," Proc. IRE (Correspondence), vol. 50, p. 470; April, 1962.
² M. Bayard, "Théorie des réseaux de Kirchhoff," Editions de la Revue d'Optique, Paris, France, p. 259; 1954.

* Received May 16, 1962.
¹ Indiana General Co., Kearsby, N. J.
² Airtron Div. of Litton Industries, Morris Plains, N. J.

For (5) to be valid we require $R(y)$ to be a distribution, and for (6) to be valid we require that $R(y)$ and $X(y)$ be distributions which can be convoluted with $1/\omega$ and

$$R(\omega) = \lim_{\substack{\sigma \rightarrow 0 \\ \sigma > 0}} \operatorname{Re} F(p), \quad X(\omega) = \lim_{\substack{\sigma \rightarrow 0 \\ \sigma > 0}} \operatorname{Im} F(p)$$

where the limit is taken in the distributional sense.³ For this we assume, along with Papoulis, that $\operatorname{Re} p > 0$ and that the imaginary constant at infinity, which generally occurs in (6), is zero, since we are interested in positive-real $F(p)$.

The limitations placed upon the Hilbert transform proof are then

- 1) $R(\omega)$ and $X(\omega)$ be distributions defined by the above limit, and
- 2) $R(\omega)$ and $X(\omega)$ be convolvable with $1/\omega$.

If these restrictions are satisfied, the proof given by Papoulis is valid. (F need not be rational.) Note that the three functions given above don't satisfy these restrictions. The beauty of the proof of Papoulis lies in the interpretation of (6) as a convolution, to which engineering concepts such as the impulse response can be applied.

It should be emphasized that the real part of $F(p) = K/(p - j\omega_0)$ is undefined. If in this latter expression one approaches $j\omega_0$ by letting $0 < \sigma \rightarrow 0$, then one gets $R(\omega) = K\pi\delta(\omega - \omega_0)$ for the "real part." However, if one approaches $j\omega_0$ by letting $0 > \sigma \rightarrow 0$, then one gets $-K\pi\delta(\omega - \omega_0)$ as the "real part." If one lets $\sigma \rightarrow 0$ through both positive and negative σ , then an indeterminate expression results.³

By using Schwarz's lemma, one easily shows that, $\angle =$ angle of,

$$|\angle F(p)| \leq |\angle p| \quad \text{in } \operatorname{Re} p > 0$$

if $F(p)$ is any positive-real function; conversely if $F(p)$ is analytic in $\operatorname{Re} p > 0$ and satisfies this constraint, it is positive-real.⁴ We wish to point out that if $F(p)$ is a symmetric, positive-real, $n \times n$ matrix,⁵ then $\bar{x}F(p)x$ is a positive-real scalar for every real n -vector x ; $\text{tild} =$ transpose. Consequently an $n \times n$, symmetric matrix, $F(p)$, is positive-real if and only if

- 1) $F(p)$ is analytic in $\operatorname{Re} p > 0$
- 2) $|\angle \bar{x}F(p)x| \leq |\angle p|$ in $\operatorname{Re} p > 0$ for every real n -vector x .

We also wish to point out that, as Prof. Kuh has suggested, the angle constraint for nonreciprocal networks is still unknown. In this latter connection, Belevitch has some interesting results which are soon to appear.⁶

R. W. NEWCOMB
Dept. of Elec. Engrg.
Stanford University
Stanford, Calif.

³ R. W. Newcomb, "Hilbert Transforms—Distributional Theory," Stanford Electronics Lab., Stanford University, Calif., Tech. Rept. No. 2250-1, p. 2; February, 1962.

⁴ D. F. Tuttle, Jr., "Network Synthesis," John Wiley and Sons, New York, N. Y., vol. 1, pp. 115-121; 1958.

⁵ D. C. Youla, L. J. Castriota, and H. J. Carlin, "Bounded real scattering matrices and the foundations of linear passive network theory," IRE TRANS. ON CIRCUIT THEORY, vol. CT-6, pp. 102-124; March, 1959. (See p. 122, def. 21; note that $F(p)$ need not be rational.)

⁶ V. Belevitch, private correspondence; May 2, 1962.

Selectivity and Sensitivity in Functional Blocks*

The problem of obtaining a narrow band-pass (*i.e.*, selective) frequency response without inductance has long been of interest. The main area of application of such selective networks has been at low frequencies where the inductors that would be required

$$S_x^{r\mu} = \frac{ds_p}{s_p} \cdot \frac{x}{dx} = \frac{(d\sigma_p + jd\omega_p)}{(\sigma_p + j\omega_p)} \cdot \frac{x}{dx} = \frac{(\sigma_p d\sigma_p + \omega_p d\omega_p) + j(\sigma_p d\omega_p - \omega_p d\sigma_p)}{\sigma_p^2 + \omega_p^2} \cdot \frac{x}{dx} \quad (2)$$

are undesirably large. Presently a selective network is being sought that can be built into a solid functional block where appreciable inductance is not obtainable. The purpose of this communication is to point out the seriousness of the sensitivity to component variations which is inherent and unavoidable in most of the solutions that are being proposed. Although this sensitivity has been known for years,¹⁻³ it is often either ignored or else treated as something which can be overcome by some slight refinement.

This discussion pertains to all linear networks which achieve selectivity by using an active element to counterbalance losses in the remainder of a feedback loop. Included are all amplifiers using an RC null circuit or phase shifter in the feedback path and all of the various forms of simulated inductance in negative resistance devices where feedback is inherent in the bilateral negative resistance.³⁻⁹ The resonant response of such networks is dominated by a conjugate pair of simple poles of the transfer function lying very close to the $j\omega$ axis. If a Q of 10 is arbitrarily accepted as the lower boundary for "selective" response, the Q resulting from a pair of poles at $x_p = \sigma_p \pm j\omega_p$ is

$$Q = \frac{\omega_p}{-2\sigma_p} \quad (1)$$

The selective region of the s plane for which $Q \geq 10$ then extends only $\tan^{-1} -\sigma_p/\omega_p \approx 3^\circ$ to the left of the $j\omega$ axis. Any error in a

component which causes the poles to move to the left of their desired location causes loss of selectivity, while a small error to the right causes loss of bandwidth. Of course the network becomes self-oscillatory if the poles touch the $j\omega$ axis.

It is not difficult to show quantitatively how sensitive Q is. The sensitivity of the dominant pole is given by

This sensitivity may be evaluated from the characteristic equation of the network and is equal to the percentage variation in the pole caused by a 1 per cent error in some element, x . The Q sensitivity is then

$$\begin{aligned} S_x Q &= \frac{dQ}{Q} \cdot \frac{x}{dx} = \frac{\omega_p d\sigma_p - \sigma_p d\omega_p}{-\sigma_p \omega_p} \cdot \frac{x}{dx} \\ &= 2 \frac{\omega_p}{-2\sigma_p} \cdot \frac{\omega_p d\sigma_p - \sigma_p d\omega_p}{\omega_p^2} \cdot \frac{x}{dx} \\ &\approx -2Q \operatorname{Im} S_x^{r\mu} \quad \text{for } \omega_p \gg -\sigma_p \quad (3) \end{aligned}$$

The real part of the pole sensitivity results in a radial motion of the pole which changes the resonant frequency but does not affect Q . On the other hand, the Q sensitivity is the imaginary part of the dominant pole sensitivity magnified by a factor of $2Q$.

If (2) and (3) are evaluated for any passive selective network (which must be absolutely stable) such as an LC tank circuit, the imaginary part of the pole sensitivity is found to be inversely proportional to Q . Therefore, the Q sensitivity is independent of Q and is not excessive.

However, it can be shown that the imaginary part of the pole sensitivity of an active feedback network which achieves selectivity by approaching the verge of oscillation does not change appreciably across the narrow selective region. Therefore, the higher the Q that is achieved, the more sensitive Q is to element variations. As an example, if a standard parallel- T null circuit is used in the feedback path of a high-gain amplifier to obtain selectivity, the imaginary parts of the pole sensitivities for the various elements range from $\frac{1}{2}$ to $\frac{1}{3}$. To attain a Q of 50 within ± 10 per cent would then require that the components in the null circuit maintain tolerances of about ± 0.1 per cent over the entire range of operating conditions. Similar conclusions apply to all other ways of achieving selectivity by using either an active feedback loop or negative resistance.

Although these concepts are not new to circuit theorists, they do not seem to have been fully appreciated by those who are seeking solutions to the solid-state tuning problem. A realistic approach to selectivity requires an understanding of the related problems of sensitivity. The desired selectivity must not only be attained, but also maintained within reasonable limits. On this basis a proposed solution is worthy of continued investigation only if the associated tolerances are likely to be achievable.

W. E. NEWELL
Research and Development Ctr.
Westinghouse Electric Corp.
Pittsburgh, Pa.

* Received May 14, 1962.
¹ H. Fleisher, "Low-Frequency Feedback Amplifiers," in G. E. Valley, Jr. and H. Wallman, "Vacuum Tube Amplifiers," M.I.T. Rad. Lab. Ser., McGraw-Hill Book Co., Inc., New York, N. Y., vol. 18, ch. 10; 1948.
² S. W. Punnett, "Audio frequency selective amplifiers," *J. Brit. IRE*, vol. 10, pp. 39-59; February, 1950.
³ N. S. Nagaraja, "Effect of component tolerances in low frequency selective amplifiers," *J. Indian Inst. Sci.*, vol. 37, sec. B, pp. 324-337, October, 1955; vol. 38, sec. B, pp. 81-92, April, 1956.
⁴ J. M. Brown, "A Transistorized Negative Feedback High-Q Filter," Polytechnic Inst., Brooklyn, N. Y., Res. Rept. R-664-58, PIB-592; January 13, 1959.
⁵ W. D. Fuller and P. S. Castro, "A microsystems bandpass amplifier," *Proc. Nat'l Electronics Conf.*, vol. 16, pp. 139-151; 1960.
⁶ B. T. Murphy and J. D. Husher, "A frequency-selective amplifier formed in silicon," *Proc. Nat'l Electronics Conf.*, vol. 16, pp. 592-599; 1960.
⁷ M. Schuller and W. W. Gartner, "Inductive elements for solid state circuits," *Electronics*, vol. 33, pp. 60-61; April 22, 1960.
⁸ H. G. Dill, "Inductive semiconductor elements and their application in band pass amplifiers," *IRE TRANS. ON MILITARY ELECTRONICS*, vol. MIL-5, pp. 239-250; July, 1961.
⁹ H. A. Stone and R. M. Warner, "The field-effect tetraode," *Proc. IRE*, vol. 49, pp. 1170-1183; July, 1961.

The Majority Decision Element as a Null Detector*

The possibilities inherent in the null-zone reception of binary transmissions have been explored in considerable detail.¹⁻⁶ It has been shown that even for unidirectional systems, null-zone reception is capable of increasing the information rate. More importantly, it has been shown to provide a useful decision mechanism for decision-feedback systems. These treatments were based on null-zone detectors which, in the uncoded case, consisted of dividing the possible received signals into three zones, 1, 0, and ϕ . For the coded case the detectors were based on the properties of the code. This brief presentation considers the use of multiple receptions and a majority decision element as a null detector.

Consider an uncoded binary symmetric communication system in which N replicas of the same binary signal are received either by using N different receivers and a single transmission, or by using one receiver and N repetitions. A binary decision is made on each replica and the N decisions comprise a N -digit word which is processed by a majority decision element.

The majority decision element considered here is one with a null region. For each N -digit word input, a ternary output results. If the number of ones (or zeros) present in the input word exceeds the number of zeros (or ones) in the input word by more than a width-setting K , a one (or zero) is generated at the output. If the difference is equal to or less than K , a null output is obtained. Since K can assume only integral values, the null region is "quantized." This principle of operation is illustrated in Fig. 1.

In order for the output of the majority decision element to be in error, more than $(N+K)/2$ of the N binary digits must be incorrect. If the number of incorrect binary digits, j , is bounded by

$$(N-K)/2 \leq j \leq (N+K)/2,$$

a null symbol is generated by the majority decision element as an indication that the inputs are sufficiently ambiguous to warrant withholding a decision or, in the case of a feedback system, to warrant requesting further information.

For convenience consider the case in which the probability of each binary decision being in error is independent of the correctness of the other decisions. Let all

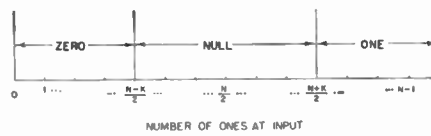


Fig. 1—Decision zones of the majority decision element.

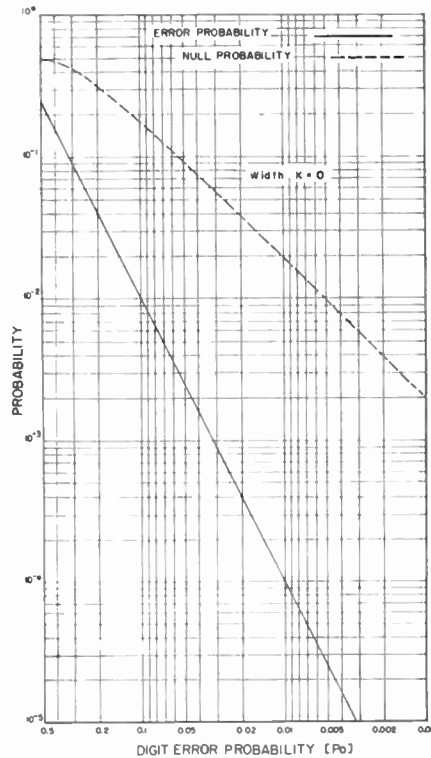


Fig. 2—Performance of the majority decision element as a null detector; two-digit input.

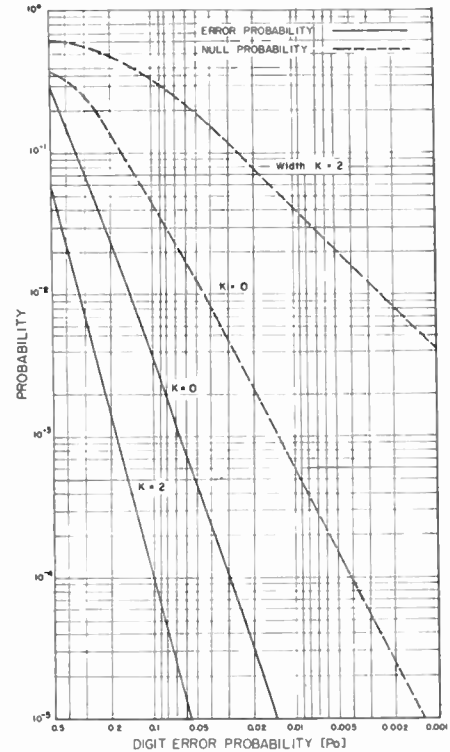


Fig. 3—Performance of the majority decision element as a null detector; four-digit input.

these error probabilities have the same value p_0 . Then the probability of incorrectly accepting a digit is

$$p = \sum_{j \geq (N+K+1)/2} \binom{N}{j} p_0^j (1-p_0)^{N-j} \quad (1)$$

and the probability of rejection is

$$u = \sum_{j \geq (N-K)/2} \binom{N}{j} p_0^j (1-p_0)^{N-j}. \quad (2)$$

The allowable values of K are

$$K = N-2, N-4, \dots, 0. \quad (3)$$

It is interesting to note that as p_0 approaches one half, the probability of accepting an incorrect digit is 2^{-N} , provided the null width is set at the maximum allowable value $N-2$. This improvement in reliability is a consequence of the redundancy introduced by the multiple receptions and decision processes.

The performance of a decision-feedback system using the majority decision element as a null detector is given in Figs. 2 and 3. These curves also apply to unidirectional systems in which repeats are not requested but the nulls are printed out. One practical application of these results is to those communication systems in which the signals are masked primarily by receiver front-end

noise. By using parallel receivers and a majority decision element as a null detector, significant reductions in error probability are obtained.

The author wishes to thank L. S. Schwartz of New York University, N. Y., for suggesting this study.

ROBERT C. SOMMER
College of Engineering
New York University
New York, N. Y.

Some Combinations of Noise Signals*

Consider two independent Gaussian noise signals, N_1 and N_2 , each with rms value σ_0 and probability density function

$$\phi_0(x) = \frac{1}{\sqrt{2\pi\sigma_0^2}} \exp\left(-\frac{x^2}{2\sigma_0^2}\right). \quad (1)$$

* Received May 21, 1962.

* Received May 11, 1962.
¹ F. J. Bloom, S. S. L. Chang, B. Harris, A. Hauptschein, and K. C. Morgan, "Improvement of binary transmission by null zone reception," *Proc. IRE*, vol. 45, pp. 963-975; July, 1957.
² B. Harris and K. C. Morgan, "Binary symmetric decision-feedback systems," *Trans. AIEE*, vol. 38 (*Commun. and Electronics*), pp. 436-442; September, 1958.
³ B. Harris, A. Hauptschein, and L. S. Schwartz, "Optimum decision-feedback systems," 1957 IRE NATIONAL CONVENTION RECORD, pt. 2, pp. 3-10.
⁴ B. Harris, A. Hauptschein, K. C. Morgan, and L. S. Schwartz, "Binary communication feedback systems," *Trans. AIEE*, vol. 40 (*Commun. and Electronics*), pp. 960-969; January, 1959.
⁵ B. Harris, A. Hauptschein, K. C. Morgan, and L. S. Schwartz, "Binary decision-feedback systems for maintaining reliability under conditions of varying signal strengths," *Proc. NEC*, vol. 13, pp. 126-140; October, 1957.
⁶ S. S. L. Chang, B. Harris, and K. C. Morgan, "Cumulative binary decision-feedback systems," *Proc. NEC*, vol. 14, pp. 1044-1057; October, 1958.

The cumulative distribution function of N_1 is

$$P\{|N_1| < x\} = \frac{1}{2} \left(1 + \operatorname{erf} \frac{x}{\sqrt{2}\sigma_0} \right) \quad (2)$$

where

$$\operatorname{erf} z = \frac{2}{\sqrt{\pi}} \int_0^z \exp(-y^2) dy.$$

The density function of a full-wave rectified noise signal $|N_1|$ is given by

$$p_1(x) = \begin{cases} 2\phi_0(x), & x \geq 0 \\ 0, & x < 0 \end{cases} \quad (3)$$

and its distribution function is

$$P\{|N_1| < x\} = \begin{cases} \operatorname{erf} \frac{x}{\sqrt{2}\sigma_0}, & x \geq 0 \\ 0, & x < 0 \end{cases} \quad (4)$$

The density function, f_a , of the sum of two statistically independent rectified noise signals, $|N_1| + |N_2|$, is given by the convolution of p_1 with itself. Thus

$$f_a(x) = \begin{cases} p_a(x), & x \geq 0 \\ 0, & x < 0 \end{cases}$$

where

$$\begin{aligned} p_a(x) &= 4 \int_0^x \phi_0(y)\phi_0(x-y) dy \\ &= \frac{2}{\pi\sigma_0^2} \exp\left(-\frac{x^2}{4\sigma_0^2}\right) \int_0^x \exp\left[-\frac{\left(y-\frac{x}{2}\right)^2}{\sigma_0^2}\right] dy. \end{aligned}$$

Hence

$$f_a(x) = \begin{cases} 4\phi(x) \operatorname{erf} \frac{x}{2\sigma_0}, & x \geq 0 \\ 0, & x < 0 \end{cases} \quad (5)$$

where

$$\phi(x) = \frac{1}{\sqrt{2\pi}\sigma_0} \exp\left(-\frac{x^2}{2\sigma_0^2}\right), \quad \sigma = \sqrt{2}\sigma_0$$

and

$$P\{|N_1| + |N_2| < x\} = \begin{cases} \operatorname{erf}^2 \frac{x}{2\sigma_0}, & x \geq 0 \\ 0, & x < 0 \end{cases} \quad (6)$$

It is interesting to note from (4) and (6) that the distribution function of the sum of the absolute values of two independent normally distributed random variables (with zero means and equal variances) is equal to the square of the distribution function of the absolute value of the sum of the same two random variables

$$P\{|N_1| + |N_2| < x\} = [P\{|N_1 + N_2| < x\}]^2.$$

The density function, f_b , of the sum of a rectified noise signal and a Gaussian noise signal $|N_1| + N_2$, is given by the convolution

of p_1 with ϕ_0 . Thus

$$\begin{aligned} f_b(x) &= 2 \int_{-\infty}^{\infty} \phi_0(y)\phi_0(x-y) dy \\ &= \frac{1}{\pi\sigma_0} \exp\left(-\frac{x^2}{4\sigma_0^2}\right) \int_{-x-2\sigma_0}^{\infty} \exp(-u^2) du. \end{aligned}$$

Hence

$$f_b(x) = \phi(x) \left[1 + \operatorname{erf} \frac{x}{2\sigma_0} \right] \quad (7)$$

and

$$P\{|N_1| + N_2 < x\} = \frac{1}{4} \left[1 + \operatorname{erf} \frac{x}{2\sigma_0} \right]^2 \quad (8)$$

The density function, f_c , of the difference of two rectified noise signals, $|N_1| - |N_2|$, is given by the convolution of $p_1(x)$ with $p_1(-x)$. Thus

$$f_c(x) = \begin{cases} p_c(x), & x \geq 0 \\ 2f_b(x), & x < 0 \end{cases}$$

where

$$\begin{aligned} p_c(x) &= 4 \int_x^{\infty} \phi_0(y)\phi_0(x-y) dy \\ &= 2f_b(x) - p_a(x). \end{aligned}$$

Hence

$$f_c(x) = 2\phi(x) \left[1 - \operatorname{erf} \frac{|x|}{2\sigma_0} \right] \quad (9)$$

and

$$P\{|N_1| - |N_2| < x\} = \begin{cases} \frac{1}{2} \left[1 + 2 \operatorname{erf} \frac{x}{2\sigma_0} - \operatorname{erf}^2 \frac{x}{2\sigma_0} \right], & x \geq 0 \\ \frac{1}{2} \left[1 + 2 \operatorname{erf} \frac{x}{2\sigma_0} + \operatorname{erf}^2 \frac{x}{2\sigma_0} \right], & x < 0. \end{cases} \quad (10)$$

The density functions (1), (3), (5), (7), and (9) are illustrated in Fig. 1.

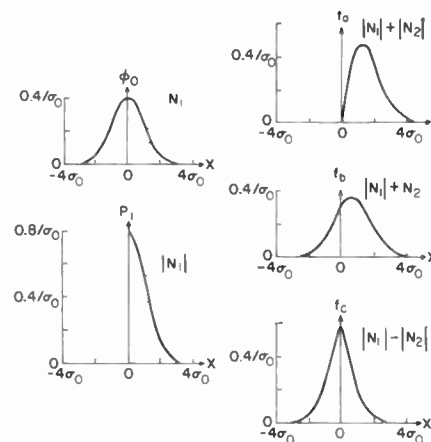


Fig. 1—Probability density functions for some combinations of noise signals.

KENNETH ABEND
Philco Scientific Lab.
Blue Bell, Pa.

Bounds on the 3-Positions Experiment Integral*

It is known that the 3-positions experiment integral¹⁻³

$$P_3(a) = \int_{-\infty}^{\infty} \phi(t-a) [\Phi(t)]^2 dt \quad (1)$$

where

$$\begin{aligned} \Phi(t) &= \int_{-\infty}^t \phi(x) dx \\ &= \frac{1}{\sqrt{2\pi}} \exp\left(-\frac{t^2}{2}\right), \end{aligned} \quad (2)$$

is bounded below^{2,3} for all a (and approximated^{2,3} for large a) by

$$P_3(a) \geq 2\Phi\left(\frac{a}{\sqrt{2}}\right) - 1. \quad (3)$$

Using²⁻⁴

$$P_2(a) = \int_{-\infty}^{\infty} \phi(t-a) \Phi(t) dt = \Phi\left(\frac{a}{\sqrt{2}}\right) \quad (4)$$

we obtain

$$\begin{aligned} 0 < \int_{-\infty}^{\infty} \phi(t-a) \left[\Phi(t) - \Phi\left(\frac{a}{\sqrt{2}}\right) \right]^2 dt \\ = P_3(a) - \left[\Phi\left(\frac{a}{\sqrt{2}}\right) \right]^2. \end{aligned} \quad (5)$$

Combining with

$$\begin{aligned} \left[\Phi\left(\frac{a}{\sqrt{2}}\right) \right]^2 - \left[2\Phi\left(\frac{a}{\sqrt{2}}\right) - 1 \right] \\ = \left[\Phi\left(\frac{a}{\sqrt{2}}\right) - 1 \right]^2 > 0 \end{aligned} \quad (6)$$

it is seen that

$$P_3(a) > \left[\Phi\left(\frac{a}{\sqrt{2}}\right) \right]^2 > 2\Phi\left(\frac{a}{\sqrt{2}}\right) - 1, \quad (7)$$

giving an even tighter lower bound on P_3 .

Letting

$$\begin{aligned} \operatorname{erf} x &= \frac{2}{\sqrt{\pi}} \int_0^x \exp(-t^2) dt \\ &= \frac{1}{2} \left(1 + \operatorname{erf} \frac{x}{\sqrt{2}} \right). \end{aligned} \quad (8)$$

* Received May 21, 1962.

¹J. L. Lawson and G. F. Uhlenbeck, "Threshold Signals," M.I.T. Rad. Lab. Ser., McGraw-Hill Book Co., Inc., New York, N. Y., p. 171; 1950.

²R. H. Urbano, "Analysis and Tabulation of the M Positions Experiment Integral and Related Error Function Integrals," AF Cambridge Res. Ctr., Electronic Res. Directorate Rept. No. TR-55-100, ASTIA Doc. No. AD 79394; April, 1955.

³C. W. Helstrom, "The comparison of digital communication systems," IRE TRANS. ON COMMUNICATIONS SYSTEMS, vol. CS-8, pp. 141-150; September, 1960.

⁴G. Lieberman, "Quantization in coherent and quadrature reception of orthogonal signals," RCA Res., vol. 22, p. 464; September, 1961.

we obtain

$$P_3(a) = \Phi\left(\frac{a}{\sqrt{2}}\right) - \frac{1}{4} \left[1 - \int_{-\infty}^{\infty} \phi(x-a) \operatorname{erf}^2 \frac{x}{\sqrt{2}} dx \right] \quad (9)$$

Using^{5,6}

$$1 - \exp\left(-\frac{x^2}{2}\right) < \operatorname{erf}^2 \frac{x}{\sqrt{2}} < 1 - \exp\left(-\frac{2x^2}{\pi}\right) \quad (10)$$

the inequality

$$1 - \frac{1}{\sqrt{2}} \exp\left(-\frac{a^2}{4}\right) < \int_{-\infty}^{\infty} \phi(x-a) \operatorname{erf}^2 \frac{x}{\sqrt{2}} dx < 1 - \sqrt{\frac{\pi}{4+\pi}} \exp\left(-\frac{2a^2}{4+\pi}\right) \quad (11)$$

is obtained. Hence

$$\Phi\left(\frac{a}{\sqrt{2}}\right) - \frac{1}{4\sqrt{2}} \exp\left(-\frac{a^2}{4}\right) < P_3(a) < \Phi\left(\frac{a}{\sqrt{2}}\right) - \frac{1}{4} \sqrt{\frac{\pi}{4+\pi}} \exp\left(-\frac{2a^2}{4+\pi}\right) \quad (12)$$

or

$$\Phi\left(\frac{a}{\sqrt{2}}\right) - 0.17678e^{-0.25a^2} < P_3(a) < \Phi\left(\frac{a}{\sqrt{2}}\right) - 0.16575e^{-0.29a^2} \quad (13)$$

The upper bound of (13) is always a close approximation for $P_3(a)$, while the lower bound of (7) is close for $a \gg 1$. These bounds are illustrated in Fig. 1.

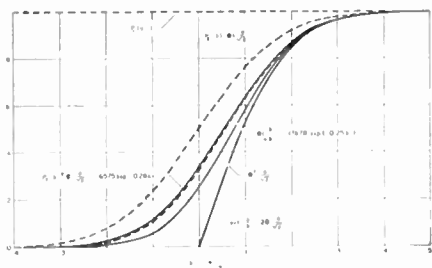


Fig. 1—Bounds for the 3-positions experiment integral.

KENNETH ABEND
Philco Scientific Lab.
Blue Bell, Pa.

On the Two-Generator Method (e_n, i_n) of Noise Characterization*

A system of noise measurement first proposed by Rothe¹ has been gaining popularity recently as a method for noise characterization of transistors at low frequencies. The form of Rothe's system most often used replaces the noisy fourpole with a noiseless fourpole plus a series-input voltage generator and a parallel-input current generator.

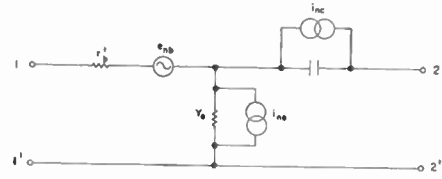


Fig. 1— e_{nb} =equivalent thermal noise voltage generator for r_b' , i_{nb} =equivalent shot noise current generator for the emitter junction, i_{nc} =equivalent shot noise current generator for the collector junction.

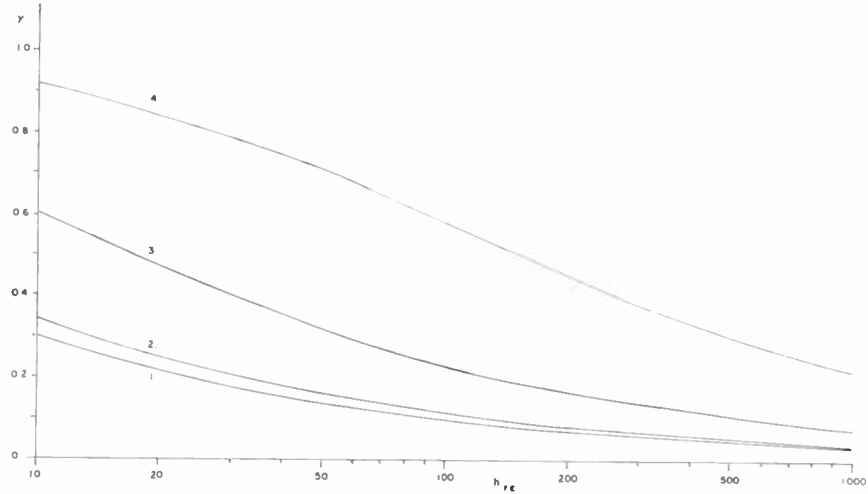


Fig. 2—Noise correlation factor γ vs h_{FE} with r_b'/r_e as a parameter. Assume $\alpha = 1$. 1) $r_b'/r_e = 0$, 2) $r_b'/r_e = 1$, 3) $r_b'/r_e = 10$, 4) $r_b'/r_e = 100$.

The noise figure can be computed by (1) from e_n and i_n if the correlation factor, γ , is known. The usual assumption is that γ is equal to one.²

$$F = 1 + \frac{1}{4kT\Delta f} \left[i_n^2 R_G + \frac{e_n^2}{R_G} + 2\gamma e_n i_n \right] \quad (1)$$

Obtaining the noise figure may be quite important since it does give a direct index of noise performance. The assumption that $\gamma = 1$ can only be justified in regions where it is known that one type of noise dominates, e.g., in the LF region. However, in the plateau region where the noise figure is flat, $\gamma \neq 1$, and may be much less than one. Consider Fig. 1 which is a good noise model of a transistor in this region.

In order to determine the equivalent short-circuit voltage generator, e_n , at the input, we short-circuit terminals 1-1'. The output noise at terminals 2-2' will contain noise from all three generators. Next, terminals 1-1' are open-circuited to determine the equivalent noise current generator, i_n . In this case the noise originating in r_b' will be absent from the output. Since the noise in r_b' is not correlated with the other two generators, the correlation between e_n and i_n

will always be less than one and is usually considerably less than one.

Perhaps a more elegant demonstration of this can be made by equating Neilson's³ noise-figure expression to the noise figure based on the alternate system.

$$F = 1 + \frac{1}{4kT\Delta f} \left[i_n^2 R_G + \frac{e_n^2}{R_G} + 2\gamma e_n i_n \right] = 1 + \frac{r_b'}{R_G} + \frac{r_e}{2R_G} + \frac{(r_b' + r_e + R_G)^2}{2\alpha_0^2 R_G r_{hFE}} \quad (1)$$

(Neilson's equation is in a simple form for the plateau region.)

Letting $R_G \rightarrow 0$, we can solve for e_n^2 , and

$$e_n^2 = 4kT\Delta f \left[r_b' + \frac{r_e}{2} + \frac{(r_e + r_b')^2}{2\alpha_0^2 r_{hFE}} \right] \quad (2)$$

Similarly, for i_n , let $R_G \rightarrow \infty$

$$i_n^2 = \frac{2kT\Delta f}{\alpha_0^2 r_{hFE}} \quad (3)$$

We can now insert these two expressions for e_n^2 and i_n^2 in (1) and solve for γ .

$$\gamma = \frac{\frac{r_b'}{r_e} + 1}{\sqrt{\left[\frac{2r_b'}{r_e} + 1 \right] [\alpha_0^2 h_{FE}] + \left[\frac{r_b}{r_e} + 1 \right]^2}}$$

This is shown graphically in Fig. 2.

* Received May 12, 1962; revised manuscript received, May 18, 1962.

¹ H. Rothe, "Theory of noisy fourpoles," IRE TRANS. ON ELECTRON DEVICES, vol. ED-1, pp. 258-268; December, 1954. See also, H. Rothe and W. Dahlke, "Theory of noisy fourpoles," PROC. IRE, vol. 44, pp. 811-818; June, 1956.

² A. E. Sanderson and R. G. Falks, "A simplified noise theory and its application to the design of low-noise amplifiers," IRE TRANS. ON AUDIO, vol. AU-9, pp. 106-108; July-August, 1961.

³ E. G. Neilson, "Behavior of noise figure in junction transistors," PROC. IRE, vol. 45, pp. 957-963; July, 1957.

⁵ G. Polya, "Remarks on computing the probability integral," Proc. Berkeley Symp. on Mathematical Statistics and Probability, University of California Press, Berkeley, Calif., p. 63; 1949.

⁶ J. T. Chu, "On bounds for the normal integral," Biometrika, vol. 42, pts 1 and 2, p. 263; June, 1955.

As would be expected, γ strongly depends on the ratio of r_h' to r_e . At low emitter currents, ($i_e \gg r_h'$),

$$\gamma \cong \frac{1}{(\omega_e^2 h_{FB} + 1)^{1/2}}$$

So, γ is small at small emitter currents. Thus the assumption that $\gamma = 1$ is not valid in the region where transistors are often most useful.

HARRY F. COOKE
Central Res. Lab.
Texas Instruments, Inc.
Dallas, Tex.

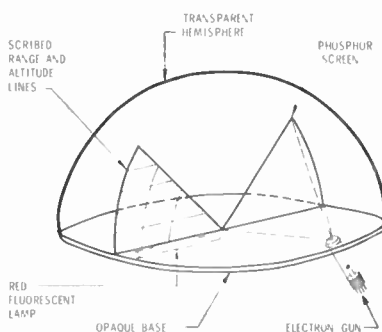


Fig. 1—Monochrome 3-D display.

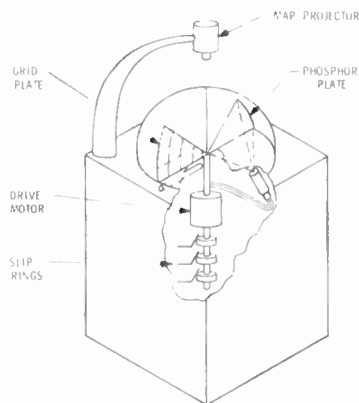


Fig. 2—Display mechanical assembly.

3-D Display System*

Recently a new family of three-dimensional displays employing rotating planes have been developed. As a radial xy plane is rotated at high speed, spots of light are rapidly gated on and off and the targets appear to hover in the contained cylinder.

Two variations have been publicized:

1) A rotating reflective xy plane upon which are projected spots of light from an external source: To get full circular coverage the external light sources must surround the display or else rotate with the vane. Furthermore, the lights must be repetitively gated on for a few microseconds and also deflected on the xy plane.

2) A rotating electroluminescent panel acting as the xy plane: A cross-conductor matrix causes intersections to glow when the appropriate circuits are energized. Although this arrangement has many advantages there are disadvantages such as

- a) Insufficient brightness of electroluminescent panels,
- b) Limited resolution because each matrix conductor must be brought out through a slip ring and brush.

CBS Laboratories has proposed a 3-D display employing a rotating cathode-ray tube that overcomes the problems inherent in the other devices.¹

As shown in Fig. 1, the cathode-ray tube employs a single electron gun positioned to excite a range-height ($x-y$) phosphor plane within a transparent hemisphere. The entire tube is rotated at 30 rps and each target is flashed on at a 30-times-per-second rate. The electron beam is positioned to unique points on the range-height plane and gated on momentarily in accordance with incoming information. Targets appear as moving or hovering spots of green light within the hemisphere. Transparent phosphors are used to eliminate the spatial haze generated by standard phosphors.

* Received June 1, 1962; revised manuscript received, July 13, 1962.

¹ Described in a proprietary proposal CLD-136, to the Federal Aviation Agency for airport traffic control; May 12, 1961.

Above the hemisphere is the small optical map projector. Within the enclosure, the tube is supported by a shaft driven by an 1800-rpm motor.

A converter is needed to translate the radar information to a form usable in the display. Whereas the PPI radar views the target once every revolution of the antenna, 30 times per second. We proposed to use digital circuitry and magnetic core shift registers to store the range-height information.

Actually, the 3-D cathode-ray tube is not complicated because there are no moving parts relative to the tube itself. Dynamic balancing is important and the hemisphere should be optically nondistorting. Since the spot diameter to be generated on the phosphor screen is of the order of 1/16 inch, a sophisticated electron gun is unnecessary.

Advantages of the CBS Laboratories 3-D display are

- 1) High resolution limited only by spot size and deflection accuracy.
- 2) Bright display.
- 3) Potential for full color operation.

A. A. GOLDBERG
CBS Laboratories
Stamford, Conn.

A second plane, oriented 180° with respect to the phosphor plane, serves as a 3-D reticle. Range-height calibration markings are etched on the surface of the glass and edge lighted by a red light from beneath. This light can be continuous or stroboscopic. Slip-rings carry the deflection signals and low voltages to the electron gun. High voltage is generated in a small package fastened to the bottom and rotating with the tube, thus eliminating the need for high-voltage slip rings.

Color is added information that can be used in a number of ways. For air traffic control, colors can be assigned to airplanes as a function of priority to land or for identification. Targets can be made any color in the spectrum with the proposed display.

The color 3-D display is similar to the monochrome display except that separate red, green and blue phosphor range-height planes are excited by separate electron guns. Each gun is gated on when its plane is located correctly for the target. Overlapping sequential combinations of primary colors provide a great variety of tints.

A map can be projected on the flat base of the display as an aid to interpreting the azimuth direction and position of targets. This is accomplished with a small optical projector, positioned directly above and on the axis of the rotating hemisphere as shown in Fig. 2. Slides can be changed automatically to accommodate different radar ranges.

As shown in Fig. 2, the 3-D hemisphere is mounted atop a four-foot enclosure with the balance of the cathode-ray tube hidden.

“Egg Crate” Reflector Surface for Large Paraboloids*

With parabolic reflectors of area equal to a large playing field now being planned to operate in winds that may reach gale force, the problem of finding ways of reducing the pressure differences between the back and front of the reflector surface in a manner acceptable electrically is becoming an important economic one.

It has been conclusively demonstrated, by Jet Propulsion Lab. tests on model paraboloidal aerials in a wind tunnel [1], that perforation of the surface to provide air flow between the back and front of the reflector is effective in reducing the maximum forces and moments on the aerial structure.

The purpose of this communication is to point out that a cellular mesh made up of short lengths of waveguide has electrically ideal properties and offers attractive transparency to the flow of air between the front and back faces of the reflector.

Electrically at frequencies below the cutoff frequency the fields corresponding to waveguide propagation in a waveguide are attenuated exponentially according to the formula

$$L = 54.5 \frac{d}{\lambda_c} \left[1 - \frac{\lambda_c^2}{\lambda^2} \right]^{1/2} \text{ decibels}$$

where λ_c = cutoff wavelength, λ = operating wavelength and d = guide length. Hence for $\lambda = 1.5\lambda_c$, $L = 40.6 \text{ db}/\lambda_c$ length of waveguide.

* Received June 18, 1962.

A square cellular "egg crate" made of sheet metal is an aggregate of waveguides. If these panels are made of depth four times the cell width, when subjected to a normal incident wavefront on its front face it will act as a reflector, and the leakage between the front and back faces through the reflector would be 81 db for an operating wavelength three times the wall side, and would increase proportionally as the depth is increased.

The mechanics of reflection is as follows: the air space impedance to the progress of a wavefront in the cell is very high, hence the front edges of the sheet metal forming the cellular mesh collect and reflect the incident electrical wavefronts. Hence we must add to the above attenuation that corresponding to the reflecting mesh against a space of reactive impedance equal to the entry impedance of the waveguide. A similar mismatch will occur at the back ends of the waveguide where they discharge into the air. These losses add to the electrical effectiveness of the screen, but to determine them is a difficult problem, related to that discussed by Kieburz and Ishimaru [4].

The determination of the air resistance of a structure with the egg crate reflector surface is a complex one, only likely to be satisfactorily solved by wind tunnel tests.

However, in a perforated panel, decisive factors in keeping the resistance to the flow of air low for a given area of air passage is to keep the perimeter of the air passage low. The waveguide cellular structure proposed has the double advantages of large air passage area (approaching 100 per cent) with relatively low perimeters of air passage per unit area. Further most of the loss of head will be at the entrance and exit to the mesh, and it is considered that increasing the depth of the mesh to provide very high attenuation will not add substantially to the resistance to air flow. Although these proposals will greatly increase the area of sheet metal used in the reflector, over-all weight need not increase significantly as the cellular structure can be made strong and rigid with very thin sheet metal, and saving in structural steel due to force and moment reduction should be considerable.

In conclusion it is considered that whether used as panels in an existing surface or as a complete reflecting surface the egg crate type panel offers attractive possibilities in effecting economy in the cost of large paraboloidal reflector installations. The author thanks his colleagues at the Jet Propulsion Lab., Pasadena, Calif., for useful discussions, and the University of Adelaide for study leave.

E. O. WILLOUGHBY
Jet Propulsion Lab.
Calif. Inst. of Tech.
Pasadena, Calif.

Origin of the Word "Radio"*

Evidence of early thoughts on the best nomenclature for the new communication technique is to be found in the Correspondence column of *The Electrician*, January 21, 1898. There, J. Munro writes:

"Sir: *Wireless telegraphy* is not a bad technical term; but if a more scientific name be desirable, would not Radio-telegraphy or Ray Telegraphy be preferable to *Space Telegraphy*, which Dr. Lodge employs in his interesting lectures? Perhaps someone will suggest a good term. Yours etc."

Apparently no one has thought of a better!
E. F. GOODENOUGH
Marconi's Wireless
Telegraph Co. Ltd.
Baddow Res. Labs.
Chelmsford, Essex, England

* Received May 28, 1962.
See "Poles and Zeros," *Proc. IRE*, vol. 49, p. 1373; September, 1961; and L. Espenschied, "Origin of the word, radio," *Proc. IRE*, (*Correspondence*), pp. 327-328; March, 1962.

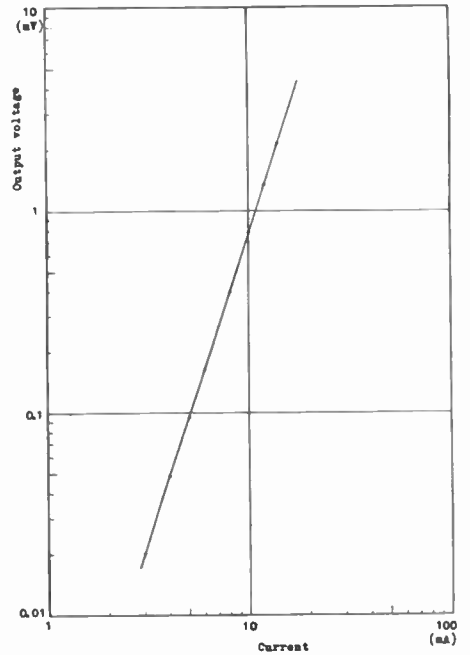


Fig. 1—Characteristics of a cubic device for $Y = AX^3$.

Function Generator for $Y = AX^3 + BX^2 + CX + D$, Employing the Galvanomagnetic Effects in Semiconductors*

The Hall effect in semiconductors has been utilized to multiply two electrical quantities, control current and magnetizing current, and thus provides a useful means as a square analog device. A semiconductor analog device reported here is an application of the magnetoresistance effect in semiconductors and can be used as a cubic element in an analog computer. Furthermore, simultaneous application of the Hall effect and the magnetoresistance effect in a semiconductor piece provides a rather simple and accurate analog device for any cubic equation.

As is well known, the electric resistance of a semiconductor containing high-mobility carriers shows an increase proportional to the square of the magnetic induction when $\mu B \ll 1$ in mks units.

Therefore, if a current I which energizes the magnet is passed through the semiconductor piece, the increase in the voltage drop across the semiconductor becomes proportional to I^3 .

An experimental result obtained with the use of a Halltron¹ is shown in Fig. 1, where the slope is just 3.0.

Fig. 2 is a practical circuit for the combination of the magnetoresistance effect and the Hall effect in a semiconductor and gives an analog output for any $Y = AX^3 + BX^2 + CX + D$, where the bridge should be

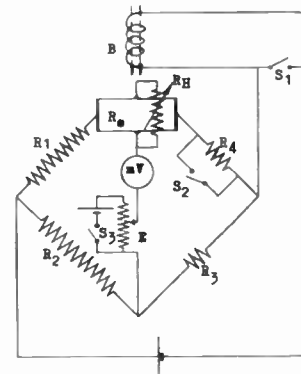
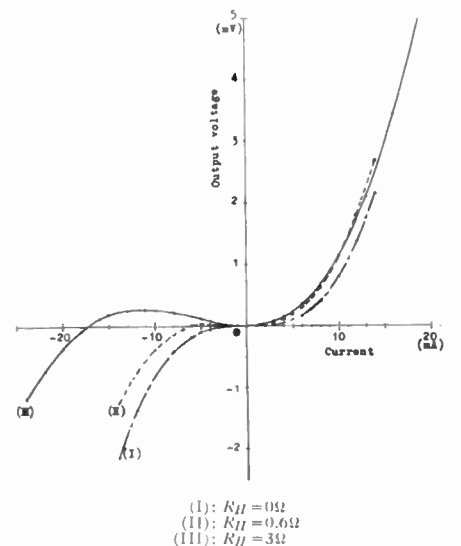


Fig. 2—Analog device for $Y = AX^3 + BX^2 + CX + D$.



(I) $R_H = 0\Omega$
(II) $R_H = 0.6\Omega$
(III) $R_H = 3\Omega$

Fig. 3—Characteristics of an analog device for $Y = AX^3 + BX^2$.

* Received May 31, 1962; revised manuscript received June 7, 1962.

¹ Made by Ohio Semiconductors, Div. of Tecumseh Products Co., Columbus, Ohio.

[1] "Advanced Antenna System," Jet Propulsion Lab., Calif. Inst. of Tech., Pasadena, Calif., Space Programs Summary No. 37-14, vol. 1, p. 119; April 1, 1962.

[2] "Reference Data for Radio Engineer," IIT and Co., New York, p. 628; 1956.

[3] L. G. Huxley, "Principles and Practice of Wave Guides," Cambridge University Press, New York, N. Y.; 1958.

[4] R. B. Kieburz and A. Ishimaru, "Scattering by a periodically apertured conducting screen," *IRE TRANS. ON ANTENNAS AND PROPAGATION*, vol. AP-9, p. 506; Nov., 1961.

balanced in advance with shorting S_1 and S_2 and opening S_3 .

The values of the constants A and B can be controlled to a large extent by varying the resistance R_2 and R_3 in holding the bridge condition.

Another method of controlling the values for A and B is to adjust a variable resistance, R_H , connected to the Hall terminals as shown in Fig. 2. The connection of a load resistance R_H to the Hall terminals tends to increase the magnetoresistance and to decrease the Hall effect effectively. Consequently the smaller the load resistance R_H , the bigger the value for A and the smaller the one for B , or vice versa. The connection of the output terminal to either of the Hall terminals decides the sign of B . Thus any values for A and B can be obtained. The values for C and D can also be controlled easily.

Experimental results of the analog device for $Y = AX^3 + BX^2$ are shown in Fig. 3, where the Halltron and the magnetic circuit MCI were used. The semiconductor element is of InAs polycrystal and has an input impedance of 1.6Ω at zero magnetic induction. The influence of the load resistance R_H on the characteristics can clearly be seen.

With an error of less than 1 per cent, accuracy in these analog devices seems to be good enough for practical application, and the temperature dependency could be compensated with appropriate connection of thermistors.

Further investigations into the mechanism and the characteristics are in progress.

S. KATAOKA

H. YAMADA

Electrotechnical Lab.

Nagata-cho, Chiyoda-ku,

Tokyo, Japan

bias and this measurement was then repeated at different frequencies. The varactor was mounted in a coaxial line holder and the reactance of the varactor at a particular bias was tuned out with a short-circuited stub in series with the varactor. A plot of the impedance locus follows a constant resistance circle which gives the value of the equivalent series resistance of the diode normalized to the characteristic impedance of the transmission line. It is seen that the resistance R_s is essentially independent of bias in the bias range limited by $\pm 10 \mu\text{a}$ of conduction current. Fig. 2 shows the variation in R_s with frequency for several types of varactors. At low frequencies the equivalent series resistance increased considerably, thus decreasing the Q of the varactor from its expected value based on high-frequency measurements.

Sawyer² and Eng³ have noted the effect of increasing resistance at low frequencies on germanium diodes and have concluded that it is due to surface effects which are dependent on the atmosphere surrounding the varactor junction. If this is the case the effect should not be limited to germanium varactors alone. The measured data shows the same effect for diffused mesa and epitaxially constructed varactors, for gallium arsenide, as well as for silicon varactors.

It is of interest to consider the effect that a nonconstant resistance will have on the operation of a parametric amplifier having a low signal frequency and a high output frequency. A lower sideband up-converter amplifier whose unwanted frequencies are all open-circuited at the diode terminals is assumed. R_{s1} is taken as the equivalent series resistance of the varactor at the signal frequency ω_1 and similarly R_{s2} at the idler frequency ω_2 . Following the analysis of Uenohara⁴ the power gain of the amplifier from ω_1 to ω_2 is

$$G_{21} = \frac{4 \frac{R_g R_L}{(R_{s2})^2} \tilde{Q}_1^2}{\left| \left(1 + \frac{Z_{11}^*}{R_{s1}} \right) \left(1 + \frac{Z_{22}}{R_{s2}} \right) - \tilde{Q}_1 \tilde{Q}_2 \right|^2}$$

where

Z_{11} = impedance seen by the varactor at ω_1 and $\text{Re}(Z_{11}) = R_g + R_1$

Z_{22} = impedance seen by the varactor at ω_2 and $\text{Re}(Z_{22}) = R_L + R_2$

R_L = load resistance at ω_2

R_g = generator internal impedance

\tilde{Q}_1 and \tilde{Q}_2 = dynamic quality factors of the varactor at ω_1 and ω_2 , respectively, and are assumed known.

\tilde{Q}_1 is known so that if

² D. E. Sawyer, "Surface-dependent losses in variable reactance diodes," *J. Appl. Phys.*, vol. 30, pp. 1689-1691, November, 1961.

³ S. T. Eng, "Characterization of microwave variable capacitance amplifiers," *IRE TRANS. ON MICROWAVE THEORY AND TECHNIQUES*, vol. MTT-9, pp. 11-21, January, 1961.

⁴ M. Uenohara and K. Kurokawa, "Minimum noise figure of the variable-capacitance amplifier," *Bell Sys. Tech. J.*, vol. 40, pp. 695-722; May, 1961.

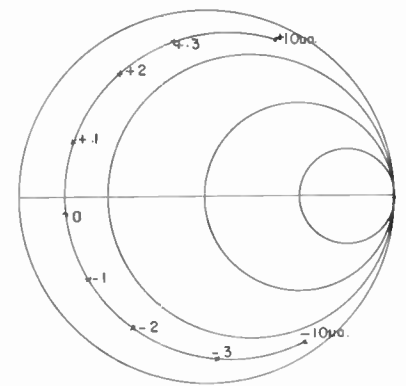


Fig. 1—Smith diagram. Varactor impedance vs bias.

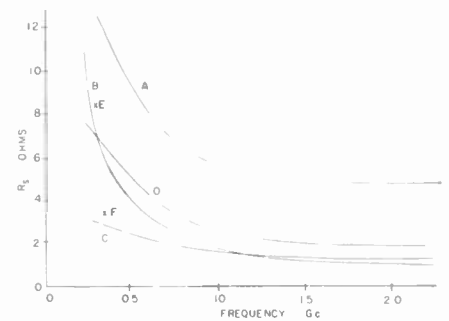


Fig. 2. Equivalent series resistance vs frequency. A and B—Microwave Associates silicon diffused mesa varactors (A—MA 450 11R, B—MA 450 FR); C—Sylvania D 4075 II silicon epitaxial varactor; D—Northern Electric NE 42 silicon epitaxial varactor; E, and F—Texas Instruments XD 502 gallium arsenide diffused mesa varactor (E—measured, F—calculated).

$$\left(\frac{Z_{11}^*}{R_{s1}} \right) \quad \text{and} \quad \left(\frac{Z_{22}}{R_{s2}} \right)$$

are chosen to best utilize this value of \tilde{Q}_1 appreciable gain can be obtained.

Noise considerations of the amplifier yield a noise figure given by

$$F = 1 + \frac{T_1 R_1 + T_g R_g}{T_g R_s} + \frac{T_L R_L + T_1 R_1 + T_s R_{s2}}{T_g R_s \tilde{Q}_1^2} \left| 1 + \frac{Z_{11}^*}{R_{s1}} \right|^2$$

where T_1 , T_s , T_g and T_L are the temperatures of R_1 , R_s , R_g and R_L , respectively. Normally the last term is insignificant but if \tilde{Q}_1 is degraded due to an increased resistance R_{s1} the term will become significant. In addition, the term $T_s R_{s1}$ contributes a greater value than usual if R_{s1} is higher than expected. As a result the noise figure of the amplifier increases somewhat when the series resistance of the varactor varies with frequency but the gain can be made independent of R_{s1} by a proper choice of impedance ratios

$$\left(\frac{Z_{11}^*}{R_{s1}} \right) \quad \text{and} \quad \left(\frac{Z_{22}}{R_{s2}} \right)$$

It should be noted that any effects due to the nonconstant resistance are negligible above 1000 Mc for the varactors measured.

The author wishes to acknowledge the many helpful suggestions of Prof. J. L. Yen under whose supervision this investigation

Frequency Dependence of the Equivalent Series Resistance of Varactor Diodes and its Effect on Parametric Amplification*

In most applications the equivalent circuit representation of a varactor diode consists of a series connection of a resistance R_s and a voltage-dependent capacitance.¹ This communication discusses the results of measurements made in the UHF range to determine R_s as a function of frequency and the effect of a nonconstant R_s on the operation of a lower sideband up-converter parametric amplifier.

To determine the equivalent series resistance of a varactor at different frequencies, the varactor impedance was first measured at a specific frequency as a function of

* Received June 4, 1962.

¹ L. A. Blackwell and K. L. Kotzebue, "Semiconductor-Diode Parametric Amplifiers," Prentice Hall, Englewood Cliffs, N. J., 1961.

was performed. Acknowledgments are also due J. Zaleski who performed many of the measurements. Appreciation is extended to Texas Instruments, Sylvania Electric and Northern Electric for supplying sample varactors.

The varactor measurements described in the foregoing were taken using ordinary slotted line techniques. At low frequencies the Q of the diode normally increases and since the voltage across the junction is Q times the incident voltage when series resonating the diode, the voltage across the junction can become quite high; a large voltage swing across the junction could lead to harmonic generation or oscillations and power loss at these frequencies. This effect would be interpreted as an increase in the equivalent series resistance of the varactor. Hence measurements in the lower frequency ranges could be inaccurate unless a low enough measuring power level is used.

Measurements made in the above manner at 320 mc were checked using the following method. The signal was fed into the probe of a slotted line which was connected to the diode under test at one port of the slotted line section. The power level incident on the varactor diode was less than -70 dbm. The signal from the remaining port of the slotted line was then fed through a circulator for isolation amplified by a 320 mc low noise amplifier, mixed to a 30 mc i.f. and then amplified and detected in a normal manner. Results on several varactors were identical to previous results for which a power level of -20 dbm at the varactor was used.

It then appears that reasonably high signal levels could be used in the measurement of varactor characteristics at low frequencies without sacrificing accuracy. However, the use of a radiometer for measurement at low frequencies guarantees good accuracy.

Acknowledgments are due J. D. McNeill for making possible the taking of these measurements using the Radio Observatory's radiometer. Acknowledgements are also due Dr. A. Uhler, Jr., of Microwave Associates for suggesting remeasurement of the varactors at low frequencies.

L. D. BRAUN
Radio Astronomy Project
Dept. of Elec. Engrg.
University of Toronto
Toronto, Can.

A Stability Chart for Linear Discrete Systems*

A linear discrete system is considered to be stable if all the roots of its characteristic equation lie inside the unit circle in the z -plane.¹ Thus the stability problem reduces mathematically to obtain the necessary and sufficient condition for the roots of the following real polynomial to lie inside the unit circle:¹

$$F(z) = a_0 + a_1z + a_2z^2 + \dots + a_{n-k}z^{n-k} + \dots + a_nz^n, \quad \text{with } a_n > 0. \quad (1)$$

* Received June 11, 1962.
¹ E. I. Jury, "Sampled-Data Control Systems," John Wiley and Sons, Inc., New York, N. Y., 1958.

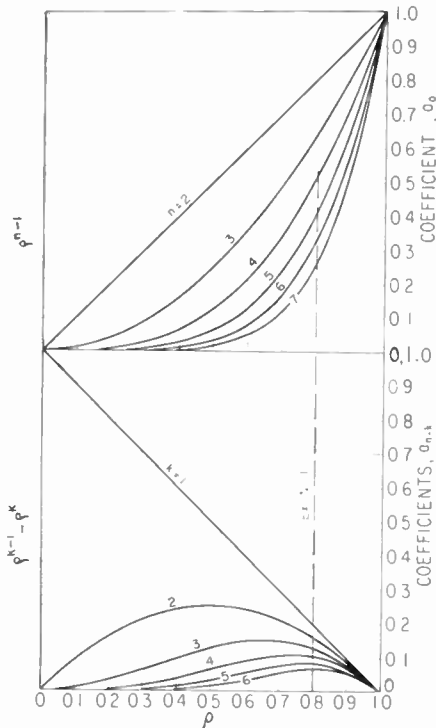


Fig. 1—Stability chart for linear-discrete systems.

Three methods of analytic test for stability, namely the determinant,² the table³ and the division⁴ methods, have been recently introduced. All of these tests involve certain algebraic calculations which can be simplified considerably for a quick test of stability of the polynomial of (1). The purpose of this note is to introduce a chart (Fig. 1) which can be used in some cases to determine a quick stability test. It should be noted that this chart does not include the necessary and sufficient conditions for the roots of (1) to lie inside the unit circle, but it does give these conditions for certain classes of polynomials.

The calculation of this chart is based on the material from a recent article by Wilf⁵ which introduces the "minimax" principle. This method gives precisely the largest root of another equation which dominates the form of (1). This maximum root is given by several relationships, but for our discussion the following one is used:⁵

$$|z| \leq \rho + \max_{1 \leq k < n} \left\{ \left| \frac{a_{n-k}}{a_n} \right| \rho^{-(k-1)} \right\}, \quad \rho > 0 \quad (2)$$

and for $k = n$

$$|z| \leq \frac{|a_n|}{|a_n|} \frac{1}{\rho^{n+1}}, \quad \rho > 0. \quad (3)$$

² E. I. Jury, "A simplified stability criteria for linear discrete system," *Proc. IRE*, vol. 50, pp. 1493-1500; June, 1962.

³ E. I. Jury and Jean Blanchard, "A stability criteria for linear discrete system in a table form," *Proc. IRE (Correspondence)*, vol. 49, pp. 1947-1948; December, 1961.

⁴ E. I. Jury, "A stability criterion for linear discrete system using a simple division," *Proc. IRE (Correspondence)*, vol. 79, p. 1948; December, 1961.

⁵ H. S. Wilf, "Perron-Frobenius theory and the zeros of polynomials," *Proc. Am. Math. Soc.*, vol. 12, pp. 247-250; April, 1961.

For the development of the stability chart we require that $|z|=1$ and for the application of the method, ρ should lie between zero and unity. If we let $a_n=1$ we obtain from (2) and (3)

$$|a_{n-k}| \leq \rho^{k-1} - \rho^k, \quad k = 1, 2, \dots, n-1 \quad (4)$$

and

$$\left| a_0 \right| \frac{1}{\rho^{n+1}} \leq 1 \quad \text{or} \quad |a_0| \leq \rho^{n+1}. \quad (5)$$

By letting

$$y = \rho^{k-1} - \rho^k \quad (6)$$

and

$$y_1 = \rho^{n+1} \quad (7)$$

we obtain the chart for different values of k as a function of ρ and also for different values of n . The maximum of the curves is given by

$$y_{\max} = \frac{(k-1)^{k-1}}{k^k}. \quad (8)$$

The chart is designed for systems up to $n=7$ and could be extended for higher order systems.

Examples:

To illustrate the application of the chart we test the following polynomials for stability:

a) $F(z) = z^4 + 0.2z^3 + 0.01z^2 + 0.03z - 0.024. \quad (9)$

From the chart we find that for certain range of values of $\rho < 0.8$ the inequalities of (4) and (5) are satisfied, and hence the system has all its roots inside the unit circle. The roots of (9) are

$$z_1 = -0.5, \quad z_2 = 0.3, \quad z_{3,4} = \pm j0.4 \quad (10)$$

b) $F(z) = z^4 - 0.8z^3 + 0.31z^2 - 0.128z + 0.024. \quad (11)$

In this case no value of ρ between zero and unity satisfies (4) and (5) and hence the chart is not suitable for obtaining information on the roots of $F(z)$. However, in this case the system is stable and the roots are

$$z_1 = 0.5, \quad z_2 = 0.3, \quad z_{3,4} = \pm j.4. \quad (12)$$

Although a general statement on the relative use of the chart is not accurately feasible, if the roots are equally scattered among the four quadrants of the unit circle the chart is then quite effective to determine stability. Furthermore, the use of the chart in quick design for stabilizing an unstable system should not be overlooked.

In conclusion, it should be pointed out that the chart is very useful for a quick check of stability of linear discrete systems. A similar chart cannot be calculated for the continuous case in the s plane; however, by use of bilinear transformation which maps the left half of the s plane into the unit circle, one can also in certain cases use the chart for a quick check of stability of linear continuous systems.

ACKNOWLEDGMENT

The author gratefully acknowledges the assistance of T. Pavlidis in the calculations of the stability chart.

E. I. JURY
Dept. of Electrical Engineering
University of California
Berkeley, Calif.

Contributors



William F. Bodtmann was born in Union City, N. J., on December 26, 1922. From 1937 to 1961 he attended Monmouth College, West Long Branch, N. J., where he studied mathematics and physics.

He has been with the Bell Telephone Laboratories, Inc., since 1941 except for a period from 1942 to 1944 when he served in the Army Air Corps, attaining the rank of Second Lieutenant. After returning to the Laboratories, he assisted in research on delay-measuring equipment and components for microwave radio systems. His recent work has been in research on light route microwave radio relay systems and frequency compression demodulators for use with satellite communication systems.



James H. Chisholm was born in Byron, Ga., on February 8, 1913. He received the B.S.E.E. degree from the Georgia Institute of Technology, Atlanta, in 1934.

He was associated with the Masonite Corporation, until his entry into active service with the Signal Corps in 1941. From 1941 to 1946 he served as a Signal Officer with the U. S. Air Force, where he was engaged in the development and operation of air defense systems.

In 1947 he joined the Central Radio Propagation Laboratory of the National Bureau of Standards, Boulder, Colo., where he was engaged in research in tropospheric propagation. In 1951 he joined the M.I.T. Lincoln Laboratory, Lexington, Mass., and since 1955 has been group leader of the Radio Propagation Group.



Nick Holonyak, Jr. (S'51, A'55-M'59) was born in Zeigler, Ill., on November 3, 1928. He received the B.S. degree in electrical engineering, in 1950, the M.S. degree, in 1951, and the Ph.D. degree, in 1954, from the University

of Illinois, Urbana.

While a graduate student at the University of Illinois, he was a Teaching Assistant, a Research Assistant in microwave tubes and semiconductor electronics, and held the

Texas Instruments Fellowship in transistor physics. He joined the transistor development department of Bell Telephone Laboratories, Murray Hill, N. J., in 1954, and worked on diffused-impurity silicon devices. He was inducted into the U. S. Army in 1955 and served with the Signal Corps at Fort Monmouth, N. J., and in Japan. In 1957 he joined the Advanced Semiconductor Laboratory of the General Electric Company, Syracuse, N. Y., and has been involved in studies of power and signal $p-n-p-n$ devices, tunnel diodes, halide transport and epitaxial growth of intermetallic compounds and compound mixtures, double injection and deep impurity level effects and junction luminescence.

Dr. Holonyak is a member of the American Physical Society, the Mathematical Association of America, Sigma Xi, Eta Kappa Nu, Tau Beta Pi, Pi Mu Epsilon, and Phi Kappa Phi.



Ivars Melngailis (M'59) was born in Riga, Latvia, on November 13, 1933. He received the B.S., M.S., and Ph.D. degrees in electrical engineering from Carnegie Institute of Technology, Pittsburgh, Pa., in 1956,

1957, and 1961, respectively. During the academic year 1957-1958 he studied physics at the University of Munich, Germany, under a Fulbright Fellowship.

In 1958-1959 he was Instructor in Electrical Engineering at Carnegie Institute of Technology and in 1960 a Project Engineer studying low temperature electrical properties of germanium. At present he is a member of the Applied Solid-State Physics Staff at the M.I.T. Lincoln Laboratory, Lexington, Mass., engaged in research on electrical and magnetic phenomena in semiconductors and semiconductor devices.

Dr. Melngailis is a member of Tau Beta Pi, Eta Kappa Nu.



Norman H. Meyers (SM'59) was born in Buffalo, N. Y., on February 11, 1931. He received the B.E.E. degree from Rensselaer Polytechnic Institute, Troy, N. Y., in 1952, and the M.S. and Sc.D. degrees in electrical

engineering from the Massachusetts Institute of Technology, Cambridge, in 1954 and 1957, respectively.

He remained at M.I.T. as an Assistant Professor of Electrical Engineering, from 1957 to 1958, and did research in the classical electrodynamics of moving media. From 1958 to 1961 he was a member of the Research Laboratory Staff of International Business Machines Corporation, Yorktown Heights, N. Y., where he managed a group engaged in the study of thin-film superconducting components and circuits. He is currently attending the Harvard Graduate School of Business Administration, Boston, Mass., where he expects to receive the M.B.A. degree in June, 1963.

Dr. Meyers is a member of Tau Beta Pi, Eta Kappa Nu, Sigma Xi, and the Scientific Research Society of America.



Walter E. Morrow, Jr. (S'48, A'41) was born in Springfield, Mass., on July 24, 1928. He received the S.B. and the S.M. degrees from Massachusetts Institute of Technology, Cambridge, in 1949 and 1951, respectively.

Since 1951 he has been associated with the M.I.T. Lincoln Laboratory, Lexington, Mass., first as a Staff Engineer, and more recently as a Group Leader. While at Lincoln Laboratory he has done research and development on transistor circuit design, VHF ionospheric scatter communication systems, and UHF tropospheric scatter communications systems.



Burt E. Nichols (M'57) was born in Newton, Mass., on January 2, 1923. He received the B.S.E.E. degree from Cornell University, Ithaca, N. Y., in 1944.

He was a USNR Officer following his attendance at the

Massachusetts Institute of Technology Radar School, Cambridge, in 1945. In 1951 he went to Rome, Italy, as an Engineer attached to the Air Force Military Assistance Advisory Group at the American Embassy. Working with the Italian Air Force, he assisted in setting up an electronics school for training with American radar and radio equipment which was given to the Italian Air Force under the mutual aid program. In 1954 he returned to the United States and joined the staff of the M.I.T. Lincoln Laboratory, Lexington, Mass., in the communica-

tions systems engineering group where he is presently employed, working with the development of the SSB system for the UHF tropospheric scatter communications systems.

❖



Robert H. Rediker (A'53-SM'58) was born in Brooklyn, N. Y., on June 7, 1924. He received the B.S. degree in electrical engineering, in 1947, and the Ph.D. degree in physics, in 1950, from the Massachusetts Institute of

Technology, Cambridge.

During 1950-1951, he was a Research Associate in cosmic rays in the Physics Department of M.I.T. In 1951 he became a staff member at the M.I.T. Lincoln Laboratory, Lexington, Mass., where he worked on transistorized computer circuits. During the academic year 1952-1953, he was on the staff of the Physics Department of Indiana University, Bloomington. Since June, 1953, he has been engaged in semiconductor device research at the M.I.T. Lincoln Laboratory where he now heads the Applied Solid-State Physics group.

Dr. Rediker is a member of the American Physical Society and Sigma Xi.

❖



James F. Roche (M'52) was born in Lynn, Mass., on July 27, 1923. He received the B.S.E.E. degree from the University of Rhode Island, Kingston, in 1943.

From 1943 to 1946 he served with the Signal Corps, primarily with the Radio Propagation Unit. He became a Civilian Engineer with the Signal Corps in 1946 and was engaged in radio wave propagation studies pertaining to Army communication circuits. In September, 1951, he joined Aeronautical Radio Inc., Washington, D. C., as a frequency and radio wave propagation engineer. From 1953 to 1960 he was a member of the staff of the M.I.T. Lincoln Laboratory, Lexington, Mass., where he was engaged in radio wave propagation research. He joined the Engineering Staff at Raytheon Company, Waltham, Mass., in 1960. In January, 1962, he joined the Systems Projects Laboratory of Sylvania Electronic Systems Amherst Laboratories, where he is

continuing work in the field of radio propagation research.

Mr. Roche is a registered professional engineer in the District of Columbia and a member of Commission II URSL.

❖



Clyde L. Ruthroff (M'56) was born in Sioux City, Iowa, on February 4, 1921. He received the B.S. degree in electrical engineering, in 1950, and the M.A. degree in 1952, from the University of Nebraska, Lincoln.

From 1939 to 1946 he served in the U. S. Navy. He then worked as a Central Office Craftsman for the Long Lines Department of the American Telephone and Telegraph Company until 1952. Since 1952, he has been with the Bell Telephone Laboratories, Inc., where he has concentrated on radio research with emphasis on FM problems and transistor circuits for microwave components and systems.

Mr. Ruthroff is a member of Sigma Xi.

❖



Alfred E. Teachman (A'27-A'39-SM'49) was born in New Bedford, Mass., on July 23, 1904. He received his technical education at Eastern Radio Institute, Boston, Mass., National Radio Institute, and Capitol Radio Engineering Institute, Washington, D. C., from which he graduated in 1924, 1928, and 1934, respectively.

Between periods of education and self-study he was engaged in radio service work and was a Consultant to Weston Electrical Instrument Corporation, on the design of radio service test equipment. He developed one of the earliest forms of radio noise signal generators and in 1936 described its use in the testing of radio receivers. During this period he was also actively interested in the detection and elimination of radio noise and developed several forms of noise reducing antennas. In 1937 he joined the Columbia Broadcasting System, WEEI in Boston, where he was promoted to Studio Supervisor and then to Maintenance and Construction Supervisor.

Commissioned in the Air Corps during World War II, most of his service was performed at Aircraft Radio Laboratory, Wright Field, Ohio, where he was in charge

of the radio noise research unit and was responsible for numerous developments in the art of shielding, filtering and bonding. He was Chairman of the Army-Navy Committee on radio noise filters. From 1953 to 1958 he was a staff member of M.I.T. Lincoln Laboratory, Lexington, Mass., where he was engaged in a study of ionospheric distortion of the far-field pattern of a highly directional array in the lower broadcast frequencies. Later he was Project Leader in an experimental investigation of 400-Mc tropospheric propagation over great distances both over land and over water. From 1958 to 1960 he was with Page Communications Engineers, Inc., Washington, D. C., as Project Manager for research and development contracts, and Project Engineer for the tropospheric path loss tests preliminary to extending the DEW LINE communication system over the Greenland Ice Cap to Iceland. He was an Engineer with Jansky & Bailey, Alexandria, Va., from 1960 to 1961, and in 1962 was a Consultant in Washington, D. C. Recently he joined the Philco Corporation, as a Senior Engineering Specialist in the new Systems Technology Center, Arlington, Va.

Mr. Teachman is a charter member of the Professional Group on Broadcast Transmission and a Past President of Capitol Radio Engineering Institute Alumni Association. He is the author of many published articles and papers.

❖



Stephen Yando was born in New York, N. Y., on June 7, 1923. He received the B.E.E. degree from the Cooper Union Institute of Technology, New York, N. Y., in 1943, and the M.E.E. degree from the Polytechnic Institute of Brooklyn, N. Y., in 1956.

From 1943 to 1952 he obtained a broad experience in electronic systems and components at the Sperry Gyroscope Company, Mackay Radio and Telegraph Company, Hazeltine Electronics Corporation, Press Wireless Manufacturing Company and Amperex Electronic Corporation. From 1952 to 1958 he was engaged in microwave and television system research and development at the Bayside Laboratories of Sylvania Electric Products Inc., Bayside, N. Y. Since 1958 his field of interest has been electroluminescent display devices. Initially started by Sylvania this work has been supported since 1960 by its successor, the General Telephone & Electronics Laboratories, Inc., Bayside, where he is presently employed.

Mr. Yando is a member of the G. T. & E. chapter of the Research Society of America.

Books

Introduction to Radar Systems, by Merrill I. Skolnik

Published (1962) by McGraw-Hill Book Co., Inc., 330 W. 42 St., New York 36, N. Y. 636 pages+12 index pages+ix pages+references by chapter. Illus. 6 $\frac{1}{2}$ ×9 $\frac{1}{2}$. \$14.50.

This is an excellent book for anyone engaged in the radar profession. The best review of the book is in the Preface, wherein the author clearly outlines the organization and the subject matter covered. Using many of the author's own words: "This book presents a unified approach to the systems aspect of radar. Although the subject is of particular interest to the specialist in the radar field, it will also be of interest to civilian and military users of radar, designers, operations analysts, students, managers, as well as engineers and scientists in related fields."

"Radar Systems Engineering," MIT Radiation Laboratory Series, Vol. 1, has been a standard systems engineering reference book since it was published in 1947. This new book provides an excellent updating of this important subject, and within the restraints of security classification and convenient size, it is remarkably complete and current. The book is divided into four general areas covering the basic characteristics of radar, subsystems and components, signal processing and applications.

The accuracy of the historical data is indicative of the completeness of reference research. The definition of systems engineering and the examples of typical radar projects in Chapter 13 should go a long way towards clearing up the general misuse of this title. In most cases the "introduction" to each element of the subject is adequate with numerous references, and the resulting reference chain, providing for any depth of penetration desired. There are some areas that might provoke disagreement, but in this lively profession, this is a healthy situation. The chapter on antennas is perhaps the most lengthy one in the book, numbering about ninety pages. By contrast, the four and one-half pages covering displays is indeed "treated lightly." The many references, while extremely useful, may not always be available; however, for most purposes, the systems engineers will find that this book will stand alone, and will certainly stand out on the bookshelves of the profession.

I. L. McNALLY
Raytheon Company
Wayland, Mass.

Control System Theory: Feedback Engineering, by Gladwyn Lago and Lloyd M. Benningfield

Published (1962) by Ronald Press Co., 15 E. 26 St., New York 10, N. Y. 493 pages+5 index pages+xii pages+6 appendix pages. Illus. 6 $\frac{1}{2}$ ×9 $\frac{1}{2}$. \$12.00.

This book should more properly be titled "Linear Control System Theory," since it is carefully limited to a discussion of linear systems at an introductory level most useful in classroom teaching of linear control system theory. The contents of the book

are essentially the same as that of a fair number of other books written for the same purpose: Laplace transform, electric circuits, electromechanical and mechanical systems, simple control system analysis, stability, frequency response in terms of Nyquist and Bode diagrams, transient and steady-state relationships, and root locus. The material included on hydraulic and pneumatic systems, network synthesis, direct synthesis, and analogue computers is not so uniformly found in other texts. Since the authors avoided almost all discussion of nonlinearities, no material was included on describing functions, phase-space analysis, or relay control systems. Also omitted was discussion of carrier type systems, except by very oblique reference, and of sampled data systems.

The book seems carefully written, and in most cases, it is only when the authors feel constrained to introduce a complex topic in a brief and simple fashion that an incomplete treatment is given. Examples are used very freely to carry along the logic of the presentation, and must be covered for proper understanding. This generous use of examples should greatly help those engaged in self-study.

It is to the disadvantage of the reader that the over-all quality of the print is not the best, and the examples are set off in smaller type. The figures used with the examples are designated by a complex numbering scheme without captions, and reference to them is buried in the small print of some example. Eyes tire.

The examples probably will not suffer from technological obsolescence, since the authors have taken little advantage of the opportunity to present an insight into the nature of real systems. There are no missile dynamics, no sun trackers, no feedback accelerometers.

The text considers the control system only as a device intended to specify an input-output relationship in the absence of disturbances. The companion problem of reducing the system sensitivity to disturbances in the form of undesired inputs or system parameter changes is not considered. As a consequence, the initiated will finish this book with a good understanding of only one aspect of the problem.

In summary, the book is plain fare, competently written to cover the input-output relationship in linear feedback control systems. The format could be improved.

A. M. HOPKIN
University of California
Berkeley, Calif.

Microminiaturization: Proceedings of the AGARD Conference, G. W. A. Dummer, Ed.

Published (1962) by Pergamon Press, Inc., 122 E. 55 St., New York 22, N. Y. 352 pages+ix pages+3 index pages+references by chapter. Illus. 10×6 $\frac{1}{2}$. \$15.00.

In July 1961, a Conference on Microminiaturization as applied to electronics was

held in Oslo, Norway, for the Avionics Panel of the Advisory Group for Aeronautical Research and Development (AGARD) of NATO. This book presents six British, three French, and sixteen American papers by experts in the field. The three French papers, still untranslated, highlight the international flavor of the book.

The coverage of the three main systems of microminiaturization—micromodules, thin film circuits, and integrated semiconductor circuits—ranges from broad survey papers to details of developmental applications. Discussion by conference participants provides additional perspective.

The papers on micromodules include systems based on the 0.310 inch square microelement; an 0.450 inch circular microelement; 0.500 inch square parts of varying thicknesses stacked horizontally; 0.030 inch thick "dot" type parts; metal and glass encased assemblies of small parts; 0.500 inch square individually sealed multi-elements wafers with tab connections; and small parts assembled to substrates in flat 1.6×0.8×0.15 inch modules.

Deposition of thin film circuitry is discussed in terms of resistive and capacitive films formed by anodization of sputtered tantalum; chemical deposition of electrodeless nickel resistors and electroplated copper conductors; vacuum deposition of nichrome resistors, chromium-gold or chromium-copper conductors, and silicon-monoxide capacitors; vacuum deposition of multilayered thin films using aluminum for conductors, nichrome for resistors, and silicon monoxide for capacitors and insulation; nickel-iron magnetic films; and tin and lead cryotron memory films with silicon monoxide insulation.

The papers on integrated single crystal semiconductor circuit fabrication provide a broad coverage of this approach to the design and processing of both passive and active elements. These include diffused *p-n* junction resistors, depletion layer variable resistors, *p-n* junction variable capacitors, *n-p-n* type ac capacitors, *p-i-n'* diode type fixed capacitors, shaped distributed rc networks, *p-n* junction diodes, and diffused transistors. An extensive treatment of circuit design, fabrication and application of semiconductor networks of various types is also given.

In this fast moving field, the book provides a definitive record of the 1961 status of the various competing and complementary approaches and technologies. For those specialists actively engaged in the field, the book gives a quick look at paths some others are following. For development engineers throughout the electronics industry, a careful evaluation of the various approaches and capabilities discussed can provide valuable guidance for the selection of appropriate microminiaturization techniques for advanced equipment designs.

ROBERT A. GERHOLD
U. S. Army Electronics Research
and Development Laboratory,
Fort Monmouth, N. J.

The Age of Electronics, Carl F. J. Overhage, Ed.

Published (1962) by McGraw-Hill Book Co., Inc., 330 W. 42 St., New York, N. Y., 212 pages+6 index pages+ix pages. Illus. 6 X 9. \$7.95.

As the first decade of operation of the Lincoln Laboratory at the Massachusetts Institute of Technology was drawing to a close, a series of lectures was conceived of as a fitting mark of this decennial occasion. The eight lectures comprising the series were presented at M.I.T. during the winter of 1961-1962. "The Age of Electronics" is comprised of these eight lectures substantially as presented, and an introductory first chapter outlining broadly the fields covered in the ensuing eight. This first chapter is by Carl F. J. Overhage, Director of the Lincoln Laboratory since 1957.

The book has its value not so much in what it says alone, but rather through the insight provided into the thinking and personalities of the eight outstanding contemporary scientists chosen as the lecturers. The lectures were directed to the technical staff of the Laboratory and their peers who attended as guests, thus providing a technically intellectual audience without specific scientific orientation. The lectures are not highly theoretical but tend to be historical and philosophical, as each is seen through the eyes of a scientist intimately identified with his subject.

The chapter entitled "Maxwell, Hertz, and Lorentz" lays the scientific background upon which the very existence of the technologies of the ensuing seven chapters is based. This heritage of European science, laid down largely in the first half of the past century, is placed before the reader by Hendrik B. G. Casimir, a recognized European scientist, who studied with Ehrenfest, Bohr, and Pauli, and is now Director of the Philips Research Laboratories.

Lloyd V. Berkner, President of the Graduate Research Center of the Southwest, and IRE Past President, presents in Chapter Three the basic principles of communications from the concepts of information theory, through the properties and limitations of various transmission media. Insight also is presented regarding the receiving, interpretation, and retention capabilities of animate communicants, including man.

Radar, its inception and development, is reviewed in the next chapter by Ivan A. Getting, who participated intimately in that development while at M.I.T. and later through direction of research and development of radar tubes at Raytheon. He is now President of Aerospace Corporation. His chapter, which is largely historical, tends to point up the origins and consequences of important developments.

There is a bit of spicy philosophy regarding computers and their use in scientific research contained in the fifth chapter by Stanislaw M. Ulam, Research Advisor at the Los Alamos Scientific Laboratory. The limitation now imposed on science by the lack of adequate knowledge about non-linear transformation is discussed in light of the use of large computers.

Remote from our terrestrial environment lies the vastness of the universe, about which intriguing new clues are being added through scientifically directed use of radio

astronomy. The course of this fascinating development is outlined in the chapter by Edward G. Bowen, Chief, Division of Radio Physics, The Commonwealth Scientific and Industrial Research Organization, Sidney, Australia.

William Shockley, formerly with the Bell Telephone Laboratories and now Director, Shockley Transistor, Unit of Clevite Transistor, was co-winner of the Nobel Prize for his part in the work culminating in the transistor. In his own engaging way, he reviews the nature of conduction in semiconductors, starting with his now familiar analogy to the closely parked jeeps and continuing through field effects and surface states to the transistor of today.

While Professor of Physics at Columbia University, Charles H. Townes, who is now Provost at M.I.T., foresaw the use of stimulated emission of radiation in a nonequilibrium system as a means of generating and amplifying microwave and ultramicrowave power. Particularly interesting is that portion of his chapter relating to the steps of conception that led to the maser.

"Satellite Relays," which is the final chapter, deals with a subject of high current interest. The man whose name has perhaps been most closely associated with the rise of this new technology is John R. Peirce, Executive Director, Research, Communications Principles Division of the Bell Telephone Laboratories. His chapter deals extensively with Telstar and its terrestrial acouterments both as a technical development and as a communications transmission medium. His intimate identification with the science underlying the communications industry lends much to his historical review and his recounting of the meticulous detail in which the program has been carried out.

There are, of course, some shortcomings in the book. It is all too short to do justice to the historical development and the basic sciences underlying the eight subjects covered. Then too, the technical level of the presentations varies considerably through this does not detract from the insight into the scientific personalities of the authors.

ROBERT M. BOWIE
General Telephone &
Electronics Laboratories
New York, N. Y.

Linear Vacuum-Tube and Transistor Circuits, by Alfred J. Cote, Jr. and J. Barry Oakes

Published (1961) by McGraw-Hill Book Co., Inc., 330 W. 42 St., New York 36, N. Y., 402 pages+9 index pages+XXVI pages. Illus. 6 X 9. \$10.75.

It is the intent that this book present a unified basic approach to the analysis and synthesis of vacuum-tube and transistor linear circuits, emphasizing the device similarities and differences. The eleven chapters with title and contents are as follows:

Chapter 1. Preliminary Considerations: Ideal elements, symbols and equations, Ideal and practical active elements, Terminology and conventions, Static characteristics and bias. The concepts of device transfer characteristics are introduced and transvoltage, transcurrent, transadmittance, and transimpedance are defined.

Chapter 2. Two-Port Theory: Equations, Interconnection, Input and output immit-

tances, Power transfer, Two-ports of particular interest, Negative immitances, Stability criteria, Poles and zeros.

Chapter 3. Vacuum-Tubes and Transistors as Two-Ports: Equivalent circuits, matrix representation, Low-frequency properties, Input and output admittances, Transfer quantities.

Chapter 4. Effect of Frequency on Active Element Performance: Transcurrent, Transvoltage, Active element pairs, Duality and Analogy.

Chapter 5. Passive Two-Port Networks: Filters, Normalization, Mathematical approximations, Interstage filter.

Chapter 6. Cascaded Stages: Basic cascade configuration, Higher order filters, Practical cascaded amplifiers, RC coupled cascade, Transformer coupled cascade, Video amplifiers, Compensation.

Chapter 7. Bandpass Cascades: Overall design, Selection of active element, Representation of Active Element, Neutralization, Selection of coupling networks.

Chapter 8. Feedback Configurations: Basic feedback equation, Feedback circuits, Stability, Nyquist plot, Properties and application of feedback.

Chapter 9. Feedback Oscillators: Basic configurations, Frequency, Stability. Some of the limitations of the linear approximation are mentioned.

Chapter 10. Two-Port Stability and Power Gain: Power flow, Analysis of power flow, Power input and power output surfaces, Forward power gain, Charts and overlays.

Chapter 11. Matrix Analysis of Networks: Network graph, Elements of branch, Reduction of branches to general form, Network matrices, Nodal network equations, Mesh network equations, Node-pair network equations, Loop network equations.

Throughout the book two-port network theory is used. A more descriptive title would be: "Two-Port Network Theory with Emphasis on Linear Active Circuits." The Preface states the intention that this book be used as a text by senior undergraduate or graduate electrical engineering students. Obviously, to use it effectively in an undergraduate curriculum will require more than ordinary adjustment of other courses, to avoid duplication and to incorporate essential supplemental material.

As background, the authors recommend: electrical physics, electrical network equations, passive filter theory, physics of vacuum-tubes and transistors.

To this list, I would add an elementary electronic circuits course to impart greater feeling for such things as characteristic curves, basic circuits, element selection, operating point, and load lines. To round out the electronics knowledge of the undergraduate additional courses should be included on non-linear processes, analysis, and circuits.

This book is very impressive in the range and scope of its coverage. Numerous examples illustrate application of the various topics. For those seeking greater depth each chapter contains a generous reference list. Though its immediate adoptability as an undergraduate text can be questioned, it should be of interest in graduate electronics

courses and as a basis for self-study by practicing engineers. Its lucid presentation of many modern techniques will also make it a valuable reference.

IAN O. EBERT
Michigan State University
East Lansing, Mich.

The Dynamics of Automatic Control Systems, by E. P. Popov

Published (1962) by Addison-Wesley Publishing Co., Inc., Reading, Mass. 757 pages+xiii pages+3 bibliography pages. Illus. 64×10. \$10.75.

In recent years, many books on elementary control theory have been published. Unfortunately, many of them essentially have been rearrangements of the material in previously published textbooks. Consequently, new books on fundamental control theory have not been received with great enthusiasm. Nevertheless, this book on basic control theory by Popov should be of interest to the novice or expert, especially if the reader is not acquainted with Russian contributions to control theory.

For example, the book places special emphasis on the study of stability, and the methods of Mikhailov, Vyshnegradskii, Liapunov, Krylov-Bogoliubov, are developed in detail and are compared with the methods of Hurwitz and Nyquist. Of course, many more Russian contributions are described, and a summary of Russian work and interest in automatic control is given in the short Chapter IV entitled, "Some Problems in the Theory of Automatic Regulation." It is interesting to learn that the Russian Vyshnegradskii founded the theory of automatic regulation in 1876, and I. I. Polzunov developed the first automatic regulator in 1765. The author admits that he has not included a complete history of automatic control and that he has not reflected the work of foreign authors. Thus, to the Western reader, it may seem strange not to find in this historical section the names of Watt, Maxwell, Hazen, or Minorski and their early work in automatic control, but it may be just as strange for the Russian reader of a book written in the West not to find the names of Vyshnegradskii or Polzunov.

The book itself is clearly written in spite of the translator's warning that his direct translation of the Russian text preserves much of the Russian sentence structure which is not always the same as it would be if originally written in English. In fact, the Translator, A. D. Booth, notes that the book will be "of interest to English readers in showing the meticulous detail into which Russian engineers and students are led when discussing these subjects."

Although elementary, the book is not based on the use of operational calculus or the theory of functions of a complex variable. The first chapter of 29 pages describes the concept of automatic control, and many examples are given to illustrate the meaning of linear, discontinuous, and sampled data control systems.

The next chapter discusses "Transients in Automatic Regulation Systems," beginning with a clarification of linearity and its meaning in a physical system. Various forms of nonlinearities are described including saturation, discontinuities, and hysteresis. In ad-

dition, emphasis is given to the fact that all linear systems are not described by ordinary differential equations, and that linear systems also include variable parameters, distributed parameters, transport lag, and sampled data. Transient responses for linear systems are described as solutions to differential equations; a relatively long discussion is devoted to the significance and determination of initial conditions; and the significance of errors and stability is introduced. Forced oscillations lead to the frequency response concept and to the use of the Fourier series. The next section is concerned with the transient responses and stability of nonlinear systems, and detailed comparisons are made between the response characteristics of linear and nonlinear systems.

This chapter ends quite significantly by introducing the concept of transforming an n th order differential equation into a system of n first-order differential equations, and this in turn provides an introduction to the concept of phase space on which modern advanced control theory is based. Liapunov's concept of stability is given and the use of phase trajectories in phase space is illustrated through the phase plane, first with linear systems, then with nonlinear systems, the latter providing a basis for discussing stability in the "small" and in the "large." Thus the foundations for advanced control theory currently being studied is introduced quite thoroughly at the beginning of this book. It should be noted that none of the recent books on basic control theory written in this country have introduced these important concepts.

The book continues with discussions of "Methods of Improving the Regulation Process," (Chapter III) essentially a discussion of system structures. After Chapter IV, previously mentioned, Part II begins with "Linearization and Transformation of the Differential Equations of an Automatic Regulation System." Linearization techniques are described which lead to more detailed discussions of frequency responses and their asymptotic representations. Methods of "Setting up Equations of Linear Automatic Regulation Systems" are described in Chapter VI and various "Stability Criteria for Ordinary Linear Systems" are given in Chapter VII.

These ideas are expanded into the "Choice of Structure and Parameters of Ordinary Linear Automatic Regulation Systems from the Stability Condition" in Chapter VIII using Vyshnegradskii's stability criterion, and this leads to approximate criteria of the quality of transient responses in Chapters IX and X.

Part III describes "Special Linear Automatic Regulation Systems" with derivation of equations containing delay and distributed parameters in Chapter XI, and an investigation of their stability in Chapter XII which is based mainly on the Mikhailov stability criterion. Part III ends with Chapter XIII, describing the equations and stability of sampled data systems.

The next part of the book discusses "Non-Linear Automatic Regulating Systems," starting with the derivation of equations in Chapter XIV, and continuing with stability studies in Chapter XV using phase

trajectories and the Andronov point transformation method and the method of isoclines. Also included in this chapter is a fine introduction of Liapunov's direct method and its applications. The introduction is quite detailed in spite of its brevity. For example, the method of obtaining dv/dt is described in detail and several illustrations are given. The limitations and difficulties in using the Liapunov stability theorem, because it is a sufficient but not necessary condition for stability, are discussed in detail. Liapunov's theorem is extended to the study of instability of nonlinear systems and the works of Aizerman and Lur'e are introduced.

The difficulties of obtaining exact solutions to stability problems lead to a discussion of the approximate method of Krylov and Bogoliubov and its variations, in Chapter XVI. Approximate methods are used to determine stability of systems containing several types of nonlinearities, and the chapter ends with a description of the methods developed by Gol'dfarb (describing function method), Bulgakov, and Lur'e.

Part IV ends with Chapter XVII, on the subject of "Self Oscillations in the Presence of External Force and Forced Oscillation on Non-Linear Systems." This includes a description of the approximate methods of Pospelov, Gol'dfarb, and Tsytkin, the latter for relay systems only.

The last part of the book contains two chapters on obtaining the response of a system to various inputs and disturbances to verify that the structures and parameters have been chosen properly. Approximate methods of Bashkirov for linear systems including time-variable parameters and for non-linear systems are given in Chapter XVIII, and analytic solutions and frequency methods are described in Chapter XIX. Nearly ten pages of this chapter are devoted to the Laplace transform and its use in obtaining a system response. The book ends rather abruptly with Solodovnikov's method of trapezoidal frequency characteristics and a bibliography of 51 references, all Russian, except one by Lauer, Lesnick, and Matson ("Servomechanism Fundamentals," McGraw-Hill Book Co., Inc., 1947).

As illustrated by this detailed review, this book is basic but different from the many that have been published. In fact, it is in many ways more basic and meaningful than most of the current elementary texts, because it leads directly and logically to an understanding of techniques used in advanced control theory.

Nevertheless, the book does have some deficiencies, especially for students in this country. For example, very little reference is made to the works of Western authors who have made significant contributions similar to those of the Russian works, which are not easily obtained. Another difficulty is that the author naturally uses symbols and terminology which have not been developed or used in this country, and sometimes assumes that the reader is more familiar with mathematical notations than the ordinary engineer is in this country. Another minor defect is that the book has no Index.

Although this book may not be used as a classroom text in this country because of

its lack of conformity to the usual control course organization and terminology, it should prove to be a valuable reference for those who are interested in obtaining a clear and basic introduction to modern control theory and Russian contributions to automatic control.

GEORGE S. AXELBY
Westinghouse Electric Corp.
Baltimore, Md.

Physical Electronics, by C. L. Hemenway, R. W. Henry and C. Caulton

Published (1962) by John Wiley and Sons, Inc., 440 Park Ave. S., New York 16, N. Y. 364 pages+12 index pages+xiv pages+16 appendix pages+references by chapter+problems and answers. Illus. 6×9½. \$8.25.

There was a time, about thirty years ago, when the electronic engineer could be reasonably proficient in his field with only a minimum of knowledge of the behavior of electrons outside of his circuits. True, a few engineers were concerned with the dynamics of electrons in cathode ray tubes and magnetrons, but on the whole, if you knew Ohm's law, circuit theory, and had a smattering of Maxwell's theory, you were fairly well equipped for the times.

In the short span of three decades, new needs and the expanding technology to meet them have produced a bewildering variety of new electron devices, most of them depending on an intimate knowledge of the behavior of electrons in various strange environments such as super-conductors, semi-conductors, plasmas, and the like.

In the thirties these were provinces belonging to the physicists. Now, however, the devices coming out of them have now so permeated the field of electronics that the competent engineer must master at least the fundamental physical processes that underlie them. There is need, then, for a book such as "Physical Electronics" which gathers all of the diverse fields together in terms of the basic physics involved. This is an ambitious program, but one in which the authors have succeeded admirably.

The first three chapters cover the elements of quantum mechanics and statistical mechanics. The concept of the "Fermi level," which is so important for an understanding of transistors, is developed carefully and lucidly.

The next four chapters are devoted to the "classical electron devices," a new name for the lowly vacuum tube. In these the student is given a brief review of the fundamentals of the interactions between electrons and fields in a vacuum.

Chapter 8 takes up the behavior of assemblies of particles undergoing collisions, and the Boltzmann and Einstein relations for equilibrium conditions, and diffusion under nonequilibrium conditions are derived. In Chapter 9 this theory is applied to

gaseous processes, and Chapter 10 treats gaseous devices. Chapter 11 considers the liquid state and plasmas, and if this chapter is short, it is because, as the authors state, there is a large gap in our real knowledge of these states.

Chapter 12 picks up the solid state, with a discussion of the band theory of solids. This chapter is rather hard going. One regrets that the authors did not include in their list of suggested references that excellent small treatise of Rice and Teller on "The Structure of Matter," where the band theory is treated with great skill.

Chapters 13 and 14 take up semiconductor and semiconductor devices, respectively. Only the fundamental theory is treated, but this is done in excellent fashion. Electron and hole concentrations are derived, using the Fermi distribution developed in Chapter 3, and the calculation of the Fermi level is explained in detail. Under devices, the characteristics of *p-n* junctions are developed, leading to the theory of the junction transistor. Depletion-layer capacitance, Zener diodes, and tunnel diodes are also discussed.

Chapter 15, on the physics of electron beams again reverts to the classical devices, with an introduction to coupled mode theory in klystrons. The book closes with Chapter 16, an excellent introduction to the theory of modern amplifiers. The interaction between electron beams and slow wave structures is extended, with emphasis on power flow and coupled mode theory, using the several varieties of TWT as examples. Parametric amplifiers are explained very well, and the discussion includes Weiss's delightfully simple quantum mechanical derivation of the Manley-Rowe relations. Masers are treated only briefly.

The book has adequate appendices covering the symbols used in the text, selected physical constants, vector relationships, and some fundamental relationships of electromagnetism. Well formulated and instructive problems (some of them with answers) are given at the end of each chapter. The reader is reminded by this reviewer that the ability to work the problems is a useful check on his understanding of the theory.

While the book is designed specifically for a junior or senior level course in electrical engineering or physics, it should be invaluable as a review for the busy practicing engineer who feels that he has skipped or forgotten some of the physics of the devices with which he works daily.

C. W. CARNAHAN
Menlo Park, Calif.

RECENT BOOKS

Dummer, G. W. A., and Robertson, J. Mackenzie. *British Miniature and Sub-miniature Valves Data Annual, 1962-*

1963. Pergamon Press, Inc., 122 E. 55 St., New York 22, N. Y. \$30.00. Representative ranges of miniature and sub-miniature valves, with those having B9A bases setting the upper size limit, and details of many special types.

Editors of *Fortune*. *The Space Industry: America's Newest Giant.* Prentice-Hall, Inc., Englewood Cliffs, N. J. \$4.95. Study of many aspects of the business of Space.

Jackson, John D. *Mathematics for Quantum Mechanics* W. A. Benjamin, Inc., 2465 Broadway, New York 24, N. Y. \$4.75.

Presents the mathematical background necessary for an understanding of quantum mechanics.

Kuratowski, K. *Introduction to Set Theory and Topology.* Addison-Wesley Publishing Co., Inc., Reading, Mass. \$6.50. Textbook for students at the advanced undergraduate or graduate level, covering basic material from the theory of sets and functions, and fundamental topics in topology.

Physical Society of Japan. *Proceedings of the International Conference on Magnetism and Crystallography.* Physical Society of Japan, University of Tokyo, Tokyo, Japan. Contains 308 papers presented at the Conference held in 1961, and discussions.

Pollack, Harvey. *Experimental Electronics for Young People.* John F. Rider Publisher, Inc., 116 W. 14 St., New York 11, N. Y. \$3.45. For the 12-16 year age group. Teaches electronics through a series of 49 experiments, including diagrams.

Smith, R. A. *Wave Mechanics of Crystalline Solids.* John Wiley and Sons, Inc., 440 Park Ave. S., New York 16, N. Y. Aims to treat the fundamental theory of wave motion in solids, both that of the lattice, and of the electrons, in as elementary a way as is possible.

Summer, W. *Ultra-Violet and Infra-Red Engineering.* John Wiley and Sons, Inc., 440 Park Ave. S., New York 16, N. Y. \$7.50. Discusses some practical aspects of infrared and ultraviolet emission, as well as engineering and manufacturing applications of these radiations to chemistry, biology, and processing in general.

Susskind, Charles. *The Encyclopedia of Electronics.* Reinhold Publishing Corp., 430 Park Ave., New York 22, N. Y. \$19.50.

Walsh, John E. *Handbook of Nonparametric Statistics.* D. Van Nostrand Co., Inc., 120 Alexander St., Princeton, N. J. \$15.00. Presentation of a large number of nonparametric probability information procedures of practical significance in scientific research.

Scanning the Transactions

LANGUAGE—Information theoreticians would be the first to admit that the English language has no exclusive claim to information-carrying capacity. The September, 1962 issue of the IRE TRANSACTIONS ON INFORMATION THEORY bears witness to this by including three papers in French. This is the first time full-length papers have been published in a major IRE publication in a language other than English. In view of the international character of the Institute, it is not inappropriate that this "first" has occurred. An additional point of interest is that this issue, which contains the papers presented at the 1962 International Symposium on Information Theory held in Belgium, was printed in the Netherlands.

PERT has two definitions. The first, that of lexicographers, says the word means bold, saucy, lively. The second, the specialized definition of engineering managers (who spell it PERT but pronounce it pert), states that it refers to a management control tool for defining and integrating what must be done to accomplish program objectives on time. In this usage, PERT is also the acronym for "Program Evaluation and Review Technique." We are here concerned with the second definition, noting in passing, however, that the first definition might have some relevancy in that PERT is still somewhat controversial and open to lively and bold discussion.

PERT was developed several years ago to deal with a specific problem: the creation of the U. S. Navy's Polaris weapon system. It met with surprising success in this application. Since that time, a quantity of words verging on the illimitable has been written about this management technique. This prolixity of PERT prose often results because not everyone is looking at the same thing—or the same way at the same thing. It has been proposed that one of the most basic impediments to a common understanding of the technique is the belief that it is a tool for performing the classical functions of planning and control. This it is not, says one writer. He proposes that it is rather a tool for aiding project *decision making*, something distinct from classical planning and control. He states that "it helps the project manager decide, in a dynamic environment full of technical breakthroughs, unanticipated problems, and customer- and contractor-generated design changes, how he should be using his resources today to secure the best chance for successful, economical project completion." In his paper, he gives a description of the general framework of the decision-making process; applies this framework specifically to the R and D project management problem; shows the relationship of standard PERT information outputs to the decision-making framework; and demonstrates in detail the use of slack-path analysis to provide useful additional information for project management. (R. E. Thompson, "PERT-Tool for R and D Project Decision Making," IRE TRANS. ON ENGINEERING MANAGEMENT, September, 1962.)

BEETHOVEN created his magnificent works without the benefit of the modern scientific tools of mathematical analysis and synthesis. It is doubtful if, had they been available, his creative spirit would have found it necessary or desirable to invoke their aid. In retrospect, however, it is interesting to analyze mathematically his and other great music in an attempt to gain a modicum of objective insight into its genius—without implying that artistic value is something which can be measured. A recent paper presents the results of a study of the statistical properties of music written during the last four and a half centuries, thus covering the works of such diverse

composers as Bach, Mozart, Beethoven, and the contemporary artists. The statistical distributions of pitch and intervals appearing in the various works were determined. One conclusion, not too surprising to those who look with something less than favor on it, was that modern classical music has a strong random nature (noise?) to it. (W. Fucks, "Mathematical Analysis of Formal Structure of Music," IRE TRANS. ON INFORMATION THEORY, September, 1962.)

A PULSE MODULATION technique has been developed which differs from, and has several advantages over, existing methods. Capable of operating with a high degree of precision and overcoming certain bandwidth problems associated with other techniques, the modulator appears to hold excellent possibilities for a variety of applications in control systems and data transmission. It can be used wherever dc or low-frequency information is to be amplified or transduced.

The modulator converts a dc-input signal into a pulse train with constant amplitude, but with both the pulse frequency and width varied in such a way that the ratio of the pulse "on-time" to the total time is linearly proportional to the magnitude of the dc-input signal. The information is thus contained in the pulse train as relative time and is independent of pulse amplitude. This means that the amplitude characteristics of any amplifying devices which follow are relatively unimportant, and amplification may be performed by nonlinear devices. A significant advantage is that the pulse train requires only limited bandwidth for transmission over a complete range of duty ratios, whereas pulse-width and pulse-frequency modulation require infinite bandwidth. Demodulation of the pulse train, to yield a dc output proportional to the dc input, can be accomplished by a device with low-pass frequency characteristics so as to reject the periodic components to a satisfactory degree. This pulse-rate technique has been studied and is discussed in detail in a recent paper. Appropriate modulating circuits are presented with complete analyses and test data. (R. A. Schaefer, "A New Pulse Modulator for Accurate DC Amplification with Linear or Nonlinear Devices," IRE TRANS. ON INSTRUMENTATION, September, 1962.)

LIGHT MODULATION—The developer of an efficient technique for the modulation of light may not have the world beat a path to his door, as is predicted for the proverbial inventor of a better mouse trap, but he will indeed receive the gratitude of those waiting to exploit the untapped potentials of optical communications. A step in this direction has been made in a proposed scheme to improve wide-band light modulation using the electro-optic effect. Modulation by this means requires a traveling-wave type of reaction. If electro-optic material is lossy at the microwave modulation frequencies, the modulating field is strongly attenuated and low modulation efficiency results. In the proposed technique, instead of using one waveguide containing the active material, as is usually the case, two waveguides are used which are continuously coupled so that power is fed throughout the entire length of the guide containing the electro-optic material. By the stratagem of suitably tapering the coupling and the appropriate propagation constant, an analysis shows that the modulation efficiency can be significantly increased. (I. P. Kaminow, R. Kompfner, and W. H. Louisell, "Improvements in Light Modulators of the Travelling-Wave Type," IRE TRANS. ON MICROWAVE THEORY AND TECHNIQUES, September, 1962.)

Abstracts of IRE Transactions

The following issues of TRANSACTIONS have recently been published, and are now available from The Institute of Radio Engineers, Inc., 1 East 79 Street, New York 21, N. Y., at the following prices. The contents of each issue and, where available, abstracts of technical papers are given below.

Sponsoring Group	Publication	IRE Members	Libraries and Colleges	Non-Members
Communications Systems	CS-10, No. 2	\$2.25	\$3.25	\$4.50
Component Parts	CP-9, No. 3	2.25	3.25	4.50
Education	E-5, No. 2	2.25	3.25	4.50
Electronic Computers	EC-11, No. 4	2.25	3.25	4.50
Engineering Management	EM-9, No. 3	2.25	3.25	4.50
Microwave Theory and Techniques	MTT-10, No. 5	2.25	3.25	4.50
Space Electronics and Telemetry	SET-8, No. 3	2.25	3.25	4.50

Communications Systems

VOL. CS-10, No. 2, JUNE, 1962

Editorial—(p. 151)

Techniques for Incoherent Scatter Communication—Donald P. Harris (p. 154)

Special radiometric-detection procedures are appropriate when communication signals are severely distorted by a rapidly fluctuating, noisy, time-dispersive channel. This paper presents a performance analysis of some digital communication techniques that can be used when most other techniques fail. Error-probability expressions are derived and evaluated for a wide range of possible operating conditions. Effective use of available signal power is found to be possible on badly behaved channels, provided there is sufficient bandwidth available for the optimization of performance.

The Influence of Fading Spectrum on the Binary Error Probabilities of Incoherent and Differentially Coherent Matched Filter Receivers—P. A. Bello and B. D. Nelin (p. 160)

Previous derivations of the influence of fading on the error probabilities of binary data transmission systems have assumed that the fading rate is so slow that fluctuations within a bit may be ignored. This slow fading assumption is removed in the present paper which derives general expressions for the binary error probabilities of incoherent and differentially coherent matched filter receivers employing post-detection diversity combining. In the analysis it is assumed that the transmitted signals occupy a bandwidth much smaller than the coherence bandwidth of the medium so that "flat" fading may be assumed. In addition, it is assumed that the amplitude and phase fluctuations produced by the medium have the same statistical character as those of narrow-band Gaussian noise.

The general analytical results are specialized to the cases of frequency shift keying using incoherent detection, and phase shift keying using differentially coherent detection, and to the cases of exponential and Gaussian fading correlation functions. For these special cases, signal-to-noise degradation curves are given as a function of fading bandwidth. The

PSK system is degraded more rapidly with increasing fading bandwidth than is the FSK system. Curves are given which show the error probabilities and corresponding fading bandwidths for which the noncoherent FSK and the differentially coherent PSK systems break even. For lower error probabilities or higher fading bandwidths, the FSK system becomes superior to the PSK system in the sense of being able to provide the same error probability with less signal-to-noise ratio.

The existence of an irreducible error probability is demonstrated for the incoherent and differentially coherent matched filter receivers. Thus, in general, an increase in transmitted signal power cannot reduce the error probability below a certain value depending upon the fading spectrum and order of diversity. Theoretical curves of irreducible error probability are given for the incoherent FSK and differentially coherent PSK systems.

An important result of the analysis is that the shape of the fading spectrum can make a significant difference in the amount of signal-to-noise degradation.

The results of the analysis also indicate that care must be exercised in employing a "slow fading" assumption since, if low bit error probabilities are desired, significant degradations in performance can occur even though the fading rate is quite low relative to the data rate.

Comparative Performance of Digital Data Transmission Systems in the Presence of CW Interference—Frank G. Splitt (p. 169)

During the last decade there has been a considerable amount of work done on the analysis of digital data transmissions in an interference environment. With few exceptions, the type of additive interference considered is normal noise. This paper treats the case where the interference consists of CW that falls within the pass band of the receiver. The results obtained can also be utilized to ascertain system performance in the presence of interference from similar systems and for certain classes of interrupted CW (ICW) interference.

The performance of differential phase-shift, coherent phase-shift, amplitude-keyed, frequency-shift and time-shift binary digital data

transmissions is determined. The average digit error probability is taken as the measure of system performance. The element of uncertainty involved in the CW interference analysis is due to random variation in the phase angle between the signal and interference. The performance of systems employing angle modulation is found to be independent of this phase angle for certain values of the interference frequency. In general, it is shown that the digit error probability varies as the arc cosine of a function of the signal-to-interference ratio, the function being dependent on the system under consideration.

It is shown that, of the systems investigated, coherent phase-shift keying is the best transmission technique in the face of CW interference. The digit error probability in a differential phase-shift-keyed transmission is found to be a sensitive function of the frequency of the interfering tone, and depending on this frequency, can be quite different from that obtained in a coherent phase-shift-keyed transmission. Frequency-shift keying is found to exhibit the lowest threshold of the noncoherent systems considered, while time-shift keying is found to give an improvement of approximately 4 db over a simple amplitude-keyed system.

Theoretical Diversity Improvement in Multiple Frequency Shift Keying—Peter M. Hahn (p. 177)

Multiple frequency shift keying (MFSK) is a modulation suitable for transmitting digital data under fading conditions. A quantitative analysis of MFSK-with-diversity is presented.

The MFSK signals on the several diversity channels are presumed to be perturbed independently by Rayleigh fading and additive white Gaussian noise. Also, it is assumed that fading is slow and that envelope, cross-correlation (matched filter) detection is used.

The diversity combining method is chosen so that the receiver performs a likelihood-ratio test in deciding which one of K frequencies was transmitted. This optimum combining method is to square and add the detected outputs of corresponding filters from each diversity channel.

Theoretical error probability as a function of signal-energy-per-bit received is derived, and curves are plotted for two-, four-, and eight-frequency MFSK-with-diversity. Bandwidth requirements, as a function of type and order of diversity, are determined.

Eight-frequency MFSK with triple diversity has a 21.8-db advantage over simple FSK for transmitting 6-bit characters with a 0.001 error probability.

On the Optimum Performance of N-ary Systems Having Two Degrees of Freedom—R. W. Lucky and J. C. Hancock (p. 185)

A digital transmission system with n possible transmitted symbols is considered. If the time between transmitted symbols is T_b seconds and the bandwidth is W , the n possible symbols correspond to n vectors in a $2WT_b$ dimensional signal space. This paper considers the theoretical properties of a class of digital systems where the signal space is two-dimensional. Such systems are both amplitude- and phase-modulated. Approximate expressions are derived for the average probability of error for these systems as a function of the placement of the n symbol vectors in the two-dimensional signal space. Optimum placements are then given which minimize this probability of error for a given average or peak power SNR constraint. It is shown that the optimum channel structure is a function of the alphabet size n , and the type of power constraint, as well as the SNR. In general the optimum system is a phase-modulated system for low SNR's and for alphabet sizes $n \leq 16$ in the high SNR region. The performance of this optimum system in terms of channel capacity and probability of error is then compared with the performance of one-dimensional systems, AM-only and PM-only, in a complete set of curves for both peak and average power.

TV Broadcast from an Earth Satellite—Richard G. Gould (p. 193)

This paper considers the need for and the feasibility of direct continental TV broadcast to conventional home receivers from an orbiting stationary satellite. Among the factors considered are time and language differences of the potential audience, the lack of suitable programming material, and frequency allocation problems. Required transmitter and primary power have been calculated for several coverage situations on both a VHF and a UHF channel. These powers are significantly above previous estimates published elsewhere, and above the power capability of even the proposed SNAP 8, 60-kw nuclear reactor except for coverage of limited areas on the ground.

AFC for Frequency Hopping Systems—T. J. Rey and H. C. Pascual (p. 202)

An AFC system has been developed for stabilizing the frequency of a voltage-tunable oscillator near any one of many discrete frequencies. A delay line takes the place of the conventional cavity in the discriminator. The discrete steps correspond to the electrical length of the delay line, e.g., 2 Mc in the S-band system reported herein. Slow frequency fluctuations inherent in the oscillator are reduced; a stabilization factor of 100 has been achieved in a system for jumping frequency rapidly by stepping the tuning voltage. The nature of the hysteresis loops and means for their reduction are discussed. The system is significant for improving the stability and the spectrum of wide-band tunable oscillators as used in frequency hopping apparatus.

A Carrier-Operated Echo Suppressor and Control Device—T. F. Benewicz (p. 208)

Of the numerous distortions affecting high quality facsimile reception, noise and echo represent the most troublesome offenders.

This paper describes a device which fills the critical need for suppression of noise and echo currents on two-way multipoint facsimile networks.

Laboratory test data as well as operational performance results, gathered during field trials of two prototype units, are presented.

Additional applications for the device, including TONLOC, disabling of companders during picture transmission, and possible application to data transmission systems are discussed.

Correspondence—(p. 214)

Contributors—(p. 223)

Component Parts

VOL. CP-9, NO. 3, SEPTEMBER 1962

Information for Authors—(p. 87)

Who's Who in PGCP—A. M. Okun, Member, Administrative Committee—(p. 88)

Wire-Coupled Crystal Mechanical Filter—Tasuku Yuki (p. 89)

A general discussion of a wire-coupled crystal mechanical filter and its problem on the design and fabrication is followed by a detailed description of transducer-coupler-transducer system named the two-element type, which is the simplest construction of electromechanical filters.

This filter is composed of quartz crystals as the transducers and resonators and fine wires as the couplers. The theoretical possibilities of this construction are discussed by the longitudinal-vibration type and its nature is examined by the several experiments. Then, a filtering characteristic of a flexural-vibration type filter is illustrated as an example of filters constructed by the other vibration modes.

The limits of usable frequency ranges are approximately from 10 to 1000 kc in view of their fabrication easiness and the preferred fractional bandwidths are from 0.05 to 3 per cent.

Processes for Fabricating a Planar P-N-P Silicon Transistor—A. P. LaRoque, R. S. Yatsko, A. Rogel, R. Jackson, and V. Rible (p. 96)

Processes and techniques required for fabrication of experimental planar *p-n-p* silicon transistors have been developed and demonstrated as feasible. Processes involved include material preparation, antimony base diffusion, boron emitter diffusion, oxide masking, photoresist techniques, simultaneous gold metalizing of emitter and base regions, collector alloy contact and basing and thermocompression bonding. Initial transistors have typical dc Beta values of 35 to 40 and F_T values as high as 250 Mc.

Processes described have also been used in preliminary fabrication of solid-state microcircuit passive components.

A Figure of Merit for the Design of Inductance Coils Having Low Distributed Capacitance—Bradford Howland (p. 102)

The performance of an inductor is often significantly compromised by the combined effects of series resistance and distributed capacitance. For a given inductance value and coil configuration, it is always possible to vary the absolute size and/or turns count so as to reduce one residual parameter at the expense of an increase in the other. The ratio $M=L/RC^2$ is unaffected by these transformations and is proposed as a figure of merit characterizing the particular coil design. Measurements of M for sample coils of a number of commonly used types are given; they provide lower limits to the performance attainable with available magnetic materials.

A Study of Design Parameters in the Vaporization Cooling of Electronic Components—Victor Asch (p. 105)

Vaporization cooling has already been established as one of the most effective methods of removing heat from electronic components. In this paper, the author briefly reviews the

principles involved, reports his findings on the effects of varying certain design variables on system performance, and presents a method of predicting system behavior.

The design variables considered are: the proximity of components to each other, the position of components, the effect on components of impinging bubble flow, and the use of a wetting agent. System performance is evaluated by considering the relationship between heat flux and surface-to-liquid temperature difference.

The Optimum Design of the Toroidal Resonator—T. R. O'Meara (p. 115)

The optimum design of a class of toroidal resonators which are capacitively loaded and therefore short in wavelengths is considered. The possibility of including magnetic cores with various types of air gaps is included and it is shown that below a certain critical size, which is a function of the magnetic merit factor, the net Q may be improved with the optimum material and the optimum air gap. Even without magnetic cores these resonators obtain a higher Q per unit volume than any other known electrical resonator.

Solid-State Physical Phenomena and Effects: Part IV—Edwin J. Scheibner (p. 119)

This is the fourth in a series of articles dealing with phenomena of the solid state. Nineteen solid-state phenomena and physical effects are described. This group of phenomena includes primarily the resonance effects, that is, those effects which can be described in terms of discrete energy levels rather than energy bands.

Correspondence—(p. 142)

Contributors—(p. 143)

Education

VOL. E-5, NO. 2, JUNE, 1962

Editorial—John G. Brainerd (p. 55)

Introduction to the Proceedings of the Workshop on Systems Engineering—Richard B. Kershner (p. 57)

System Theory—William H. Huggins (p. 61)

General System Theory—L. A. Zadeh (p. 63)

Models and Model Construction—William K. Linvill (p. 64)

Values and Measures of Effectiveness—Martin N. Ernst (p. 68)

Human Factors Engineering and Research in Telephone Systems Engineering—John E. Karlin (p. 71)

Computers and Simulation in Systems Engineering—R. W. Hamming (p. 76)

Mathematical Programming in Systems Engineering—Ronald A. Howard (p. 78)

Feedback and Systems Engineering—John G. Truxal (p. 82)

Relation of Engineering Economy to Systems Engineering—Gerald J. Matchett (p. 85)

Probability and Statistics in Systems Work—I. S. Reed (p. 87)

Considerations in Engineering Electronic Systems—Harold D. Ross, Jr. (p. 92)

The Use of Communication Theory Concepts in the Analysis of Metropolitan Systems—John W. Dyckman (p. 97)

Queue Theory—R. E. Machol (p. 99)

Systems Engineering and Research at Case Institute of Technology—H. R. Nara (p. 105)

Systems Engineering Department, College of Engineering, University of Arizona—A. Wayne Wymore (p. 108)

Systems Engineering at the Moore School of Electrical Engineering—Ralph M. Showers (p. 113)

The Systems Analysis and Design Program—John Staudhammer (p. 115)

The Air Force Institute of Technology—
T. L. Regulinski (p. 117)
Systems Engineering in Interdisciplinary
Curricula—The Program at Carnegie Institute
of Technology—Walter R. Reitmar (p. 119)
Contributions—(p. 122)
Contributors—(p. 140)

Electronic Computers

VOL. EC-11, No. 4, AUGUST, 1962

A Simplified Procedure for the Realiza-
tion of Linearly-Separable Switching Func-
tions—C. L. Coates, R. B. Kirchner, and
P. M. Lewis, II (p. 447)

A previous paper gives a procedure for the testing and realization of linearly-separable switching function, *i.e.*, functions which can be realized by a single threshold component. That procedure can be considerably simplified, particularly when the given function is symmetric in sets of two or more variables. The simplifications arise due to a reduction of the number of functions in the function tree in view of the coefficient ordering.

Although this procedure was derived with the aim of reducing the amount of computation below that required for straightforward solution of the simultaneous inequalities that define the problem, the resulting method has some interesting relationships to that due to Winder.

The Diagnosis of Asynchronous Sequential
Switching Systems—S. Seshu and D. N. Freeman (p. 459)

This paper considers the problem of automatically testing a sequential switching circuit. It is assumed that the sequential circuit is non-clocked in order that the same automatic tester may be used for a wide class of circuits. The program for the tester is to be generated by an IBM 7090 computer from the logical description of the circuit to be tested. The specific problem considered here is to write a program for the 7090 in order to accomplish this purpose. A method of solution and a brief description of the program are given and a worked example is supplied.

A Programmed Algorithm for Assigning
Internal Codes to Sequential Machines—
D. B. Armstrong (p. 466)

A relatively fast procedure for assigning codes to the internal states of a sequential machine is described, which leads to a reasonably economical logical realization of the machine in many cases. The method is applicable to both completely and incompletely specified state tables, and permits the use of redundant internal variables if desired.

An algorithm which implements the method approximately, and which is nonnumerative, has been programmed for the 7090 computer. The program handles problems with up to 100 internal states and 30 input symbols, or 3000 total states. It has performed a problem of maximum size in 120 seconds.

Although fast, the method sometimes fails to attain truly economical logic in cases where where unusually simple realizations are known to exist (*e.g.*, the shift register). More comprehensive methods are now known, which in principle can produce better results, but which will be far more tedious to execute. They will be reported separately.

The Reduction of Redundancy in Solving
Prime Implicant Tables—I. B. Pyne and E. J. McCluskey, Jr. (p. 473)

This paper is primarily concerned with finding, in the most efficient possible way, the set of all solutions to a cyclic prime implicant table. (A solution is a set of rows such that every column contains at least one marked entry in a

row belonging to the set and such that no row can be deleted from the set without destroying this property.) Extensive use is made of the relationship between this and the problem of efficiently reducing a Boolean frontal function from the form of a product of sums of single literals to a sum of products. The transformation methods commonly in use today have the disadvantage that they tend to introduce duplicate and redundant products. (A redundant product includes at least one row which can be removed, and the remaining rows will still constitute a solution.) Several methods which appreciably reduce the number of such redundancies are presented. One of these methods (called row branching), applies repeatedly the algebraic transformation

$$f = \alpha f(\alpha=1) + f(\alpha=0)$$

where α is the Boolean variable corresponding to a row of the table, and f is the function corresponding to the given table. The mechanism by which a redundant solution is generated is described.

The paper includes other useful transformation procedures such as, for example, a tabular method in which redundancies are avoided systematically at each step. In a final section, the tables themselves are discussed as algebraic entities, and their algebraic properties employed to solve an example by factoring the table into a "sum" of tables each of which has a single solution. Illustrative examples and theorem proofs are included.

Control Units for Sequencing Complex
Asynchronous Operations—Antonio Grasselli (p. 483)

Sequential circuits techniques for the synthesis of digital-computer-control units are investigated. The assumption is made that the operations to be controlled are complex sequences of asynchronous events linked by precedence relations. An algorithm for the synthesis of the control unit flow table from the list of precedence statements is given.

Sign Detection in Nonredundant Residue
Systems—Nicholas Szabó (p. 494)

The problem of sign determination in non-redundant residue systems is investigated. A general theorem is derived establishing necessary conditions for sign detection, and the use of this theorem is demonstrated through specific examples. It is shown that for a particular system organization these same conditions are also sufficient for sign detection. An implementation of this last system is presented for four moduli.

Division and Overflow Detection in Residue Number Systems—Y. A. Keir, P. W. Cheney, and M. Tannenbaum (p. 501)

Residue arithmetic has some intriguing characteristics which could possibly be exploited in a special purpose, or even a general purpose, computer. However, simple mechanizations of the operations of division and overflow detection are not inherent in the structure of a residue number system. Methods of handling these operations are discussed in this paper. In the first section, a relatively straightforward division process is presented whose execution time is comparable to those of existing binary machines. The next section shows how the division process can be cut short under certain conditions. The amount of equipment required for this is not insignificant; however, this equipment can also be used to speed up the normal division procedure and to detect multiplicative overflow. The multiplicative overflow detection scheme proposed in the concluding section has the following desirable features:

- 1) It does not require a redundant number system.
- 2) It is compatible with the division process and requires no special circuitry.

- 3) It is faster than the brute-force approaches which either require residue division or essentially check the residue multiplication by a multiplication in a more conventional number system.

Encoding and Decoding for Cyclic Permutation Codes—Peter G. Neumann (p. 507)

Maximum-likelihood encoding and decoding procedures are presented for cyclic permutation error-correcting codes. These procedures take advantage of the cyclic permutation structure, and are applicable to all such codes. On the other hand, familiar parity-checking procedures are applicable only to those few cyclic permutation codes which are group codes. A comparison of the two different procedures for the group code case shows that they are roughly comparable in complexity.

Computer Multiplication and Division Using Binary Logarithms—John N. Mitchell, Jr. (p. 512)

A method of computer multiplication and division is proposed which uses binary logarithms. The logarithm of a binary number may be determined approximately from the number itself by simple shifting and counting. A simple add or subtract and shift operation is all that is required to multiply or divide. Since the logarithms used are approximate there can be errors in the result. An error analysis is given and a means of reducing the error for the multiply operation is shown.

Design of Computer Circuits Using Linear Programming Techniques—G. H. Goldstick and D. G. Mackie (p. 518)

A step-by-step procedure is presented for formulating circuit synthesis problems in a manner amenable to solution using linear programming. A method of systematizing component value determination using linear programming is explained. The design equations and conditions required to synthesize a diode-coupled inverter and a design procedure for achieving an optimum circuit are presented. The Simplex Method is used to determine component values such that power dissipation is minimized.

Pulse Generator with Logarithmic Spacing—James L. Farrell (p. 531)

In this paper a circuit is developed which provides a train of uniform pulses logarithmically spaced in time. As applied to computing the system offers new methods for calculating products, quotients, powers, and roots. A pulse-interval error of less than one per cent (rms) was obtained with an experimental circuit.

The Simulation of Cognitive Processes, II: An Annotated Bibliography—P. L. Simmons and R. F. Simmons (p. 535)

A Method for Evaluating Stieltjes Integrals on the Analog Computer—T. C. Anderson (p. 552)

A technique for performing Stieltjes integration on an analog computer is developed. The particular class of integrator functions considered consists of those functions of bounded variation with a finite number of jump discontinuities. The desired results are achieved through the use of analog logic and memory circuits and an example given showing an application of the method.

Flight Simulation of Orbital and Re-Entry Vehicles—L. E. Fogarty and R. M. Howe (p. 555)

The three translational and three rotational equilibrium equations for an orbital vehicle subject to aerodynamic and jet reaction forces are derived using a modified flight-path axis system for the translational equations. The dependent variables of the system are horizontal velocity component, vertical velocity component, and flight-path heading angle. The resulting equations are shown to have advantages for

computer mechanization over alternative axis systems for the translational equations. Complete equations for determining vehicle orientation, instantaneous latitude and longitude, angle of attack, angle of sideslip, aerodynamic forces and moments, etc., are presented. Modifications in the translational equations which allow direct solution by an analog computer are also given. Analog computer mechanization of these equations in both real and fast time is described, including a novel technique for division which preserves favorable multiplier scaling. Specific machine results are presented which demonstrate accurate solution of close-satellite trajectories, including re-entry from satellite altitudes to sea level. With no change in circuit or scaling the same computer mechanization yields zero-drag orbits which close within several hundred feet of altitude.

An Analog Computer Realization of the Euclidean Tools—Robert E. Keller (p. 564)

The compass and straightedge of Euclidean geometry offer many computational possibilities. Their analog computer realization as described here was developed for the study of the kinematics of machinery, but may be useful in several other areas. For the particular case discussed it was necessary to realize these tools without the use of special electronic devices and to make them available for simultaneous use at an arbitrary number of locations. Low operating frequencies were acceptable. The realization utilizes dynamic computing equipment to generate a reference circle or line, and simple logic in the utilization of the reference. The system may be extended to function generation and multiplication.

Correction to "Parametric Techniques for Eliminating Division and Treating Singularities in Computer Solutions of Ordinary Differential Equations"—Arthur Hausner (p. 570)

Correction to "Two-Level Correlation of an Analog Computer"—C. L. Becker and J. V. Wait (p. 578)

Correspondence—(p. 571)

Contributors—(p. 580)

Reviews of Books and Papers in the Computer Field—(p. 583)

Abstracts of Current Computer Literature—(p. 591)

PGEC News—(p. 607)

Notices—(p. 607)

Engineering Management

VOL. EM-9, NO. 3,

SEPTEMBER, 1962

About This Issue—The Editor (p. 101)

Announcement of Transactions Awards 1960-1961—(p. 103)

Optimum Allocation of Research/Engineering Manpower Within a Multi-Project Organizational Structure—A. A. McGee and M. D. Markarian (p. 104)

An analytic technique has been formulated which permits the management of an organization engaged in a number of research and engineering projects to allocate available technical manpower among and within projects. The technique has value as a device to determine in detail where men with specific skills may be best utilized and as a tool to gage the impact of proposed additional workload on available manpower resources and projects in progress. The technique makes use of the basic network analog to designate the sequence and interaction of the detailed activities making up each project. Judgments must be made by engineering management of the minimum essential manning and maximum productive manning required for each network activity to obtain the time-manpower function and its range of feasible values. The scheduled time for comple-

tion of each project must be stated as well as the total available manpower by skill, by time period. An integer solution is attained which is compatible with the available manpower constraint and which represents a practical economic optimum. The technique used is an iterative method suitable for computer computation.

The Role of Project Management in Scientific Manufacturing—Keith Davis (p. 109)

A survey was made of various types of project management organizations used to achieve some measure of managerial unity. Four principal types were identified.

The project expeditor achieves unity of communication, the project coordinator gets unity of control, the project confederation achieves unity of direction, and project general management accomplishes the ultimate unity of command. Furthermore, project management may disregard existing levels and functions in superimposing its own structure on the existing organization.

Project organization requires a project manager with considerable role adaptability. He must balance technical solutions with time, cost, resource, and human factors. He is an integrator and a generalist, rather than a technical specialist; and he devotes most of his management time to the functions of planning and control. Both the project manager and his superiors may need to give more emphasis to the management aspects of his job. To be an effective project manager, the technical man needs to be intellectually sophisticated in the field of management and also to have an attitude which gives some priority to the management aspects of his job.

A Look at Network Planning—Thomas V. Sobczak (p. 113)

The evolution of network planning techniques is described. The main lines of development and the variations around them are indicated. Those discussed include: Critical Path, PERT, PEP, CPM, LESS, PACT, SPEC-TROL, and SCANS. A table is presented of areas within industrial or military organizations where such techniques are in operation or appear suitable for application.

PERT—Tool for R and D Project Decision Making—Robert E. Thompson (p. 116)

The question of whether PERT is of significant value to project managers will not be resolved until the technique is understood to be a tool for a newly recognized function rather than a new tool for an old function. The newly recognized function is decision making as opposed to the old function of planning and control. The need for the performance of the new function arises from the dynamic and complex character of modern R and D projects. PERT as a decision-making tool can best be understood within the framework of the decision-making process. The decision-making framework indicates that assumptions must continuously be made in four areas. The information needed to develop these assumptions constitutes the information necessary for decision making. The information obtained by PERT provides a portion of this information.

SCANS—System Description and Comparison with PERT—B. L. Fry (p. 122)

The name SCANS is an acronym derived from Scheduling and Control by Automated Network System. The system is based upon the network techniques developed for PERT and might well be considered to be one of the many versions of PERT which have evolved since its introduction.

Although SCANS is described as an automated system and as a man-machine system, it is the men in the system who perform the most important functions of planning, decision making, and control. The machines only perform the functions which would have to be

delegated to clerical and computational personnel if the machines were not available. SCANS is not intended to be a substitute for the human mental process. It can only hope to facilitate this process and improve its effectiveness by providing the best information in an efficient format at the time it is required.

The Applicability of PERT as a Management Tool—John G. Barnby (p. 130)

This paper discusses the environment in which analytical methods of program evaluation and review (PERT, PEP) are most useful. The conditions under which these techniques are most applicable are discussed. A number of limitations are pointed out. Aspects of the cost of using these techniques are discussed.

Activity Costing—Key to Progress in Critical Path Analysis—Roderick W. Clarke (p. 132)

Realization of the full potential of critical path techniques involves six essential aspects. These are 1) network planning, 2) time and resource planning, 3) optimum scheduling and allocation, 4) progress reporting, 5) analysis and control of progress, and 6) statistical analysis to improve time and resource planning. All of these aspects are not currently being employed and thus full benefits are not accruing to the user. The principal reason for this is the lack of data on which to base time-cost trade-off relationships. This in turn is due to the present structure of accounting and control systems which do not relate costs with the work accomplished.

Several efforts employing enumerative cost models are currently in existence or under development which largely overcome the shortcomings of present accounting and control systems. The enumerative cost model collects cost by network activity and compares actual expenditure and schedule progress with that planned in order to determine program status in an accurate and unambiguous fashion. In addition, this type of model will provide the raw materials for construction of the time-cost relationships required for optimization provided that the non-comparability of activities problem can be overcome.

Probabilistic Forecasting of Manpower Requirements—K. S. Packard (p. 136)

The use of the probability of a successful proposal in manpower forecasts is discussed. Formulas for the expected requirements and the standard deviation are presented. An illustrative example of the use of these formulas is given.

The Razor's Edge of Support System Management—J. W. Vick Roy (p. 138)

Two costly mistakes are frequently made in the management of the support program for a major weapon or space system: 1) Considerations of support requirements are neglected until it is too late to accomplish a reasonably scheduled minimum cost program. 2) In an ardent effort to avoid the first mistake, hardware and software programs are promulgated before support concepts or prime system design have been adequately frozen. The purpose of this paper is to illuminate these pitfalls and indicate how they may be avoided.

About the Authors—(p. 141)

Affiliated Societies—IRE Professional Group on Engineering Management—(p. 143)

Microwave Theory and Techniques

VOL. MTT-10, NO. 5,

SEPTEMBER, 1962

Broad-Band TEM Diode Limiting—R. V. Garver and J. A. Rosado (p. 302)

The bandwidths of two types of limiters operating below diode resonance and one type

of limiter operating at diode resonance are calculated. A 2.5-Ge base-band limiter was made providing a low power insertion loss of less than 1 db, a limiting threshold of 10 mw, and a high power isolation of greater than 20 db. A 0.9- to 1.3-Ge matched limiter was made having a VSWR of less than 1.2 for all power levels. The burnout power of these two limiters was calculated to be about 10 watts incident CW power or 1500 watt-microsecond incident pulse energy. Using the diode resonance the calculations indicate that it is possible to make a 5-Ge limiter with 15 per cent bandwidth, less than 1-db power insertion loss, a limiting level of 10 mw, and greater than 20-db isolation at high power. The bandwidths derived for diode limiting are equally applicable to switching.

Improvements in Light Modulators of the Traveling-Wave Type—I. P. Kaminow, R. Kompfner, and W. H. Louisell (p. 311)

Wide-band modulation of light by means of the electro-optic effect requires a traveling-wave type of interaction, with the modulation field traveling with the same phase velocity as the light in some suitably proportioned structure. If electro-optic material is lossy at the modulation frequencies, the modulating field is strongly attenuated with a resultant low-modulation efficiency.

A scheme is analyzed here in which power is continuously fed into the light-carrying guide to make up for the attenuation as the wave progresses down the guide. By suitably tapering the coupling and the uncoupled propagation constant, the electric field can be maintained constant in the light-carrying guide and the "coupled" propagation constant in this guide can be maintained in synchronism with the light wave, thereby increasing the modulation efficiency.

Electromagnetic Waves in Waveguides with Wall Impedance—Kaneyuki Kurokawa (p. 314)

A variational expression for the propagation constant of the waves in waveguides with inhomogeneous media and with wall impedance is presented. Using this expression, the shift of the propagation constant due to the wall impedance is calculated. It is also clarified how the removal of degeneracy takes place. Then the same problem is discussed using another approach, a perturbation method. The result is identical with that of the variational principle, as is to be expected. In the final section, taking degenerate TEM modes as an example, it is shown that appropriate choices of field configuration are necessary when the formula for an attenuation constant derived from the conservation of energy is applied to degenerate modes.

A Three-Cavity Circularly Polarized Waveguide Directional Filter Yielding a Maximally Flat Response—Robert L. Williams (p. 321)

A directional filter is a completely matched four-port device which exhibits directional properties and a filter-like frequency characteristic. This paper extends work previously done on a single-cavity narrow-band circularly polarized waveguide directional filter to the case of three cavities connected in cascade with an overall bandwidth greater than 1 per cent. Analysis of the filter leads to a relationship between the two inner coupling factors and the two outermost coupling factors for a maximally flat response. The results obtained from an experimental filter using the design approach discussed herein compare favorably with the theoretical filter response. Directivity and band-elimination filter characteristics are discussed.

Power Transmission Through General Uniform Waveguides—Walter K. Kahn (p. 328)

The problem of transmitting electromagnetic power through a dissipative waveguide in an optimal fashion is examined. At any frequency the problem is reduced to a weighted eigenvalue problem in which the maximum efficiency appears as the eigenvalue and the required excitation is specified by the corresponding eigenvector. Numerical results are presented.

Further Considerations on Fabry-Perot Type Resonators—William Culshaw (p. 331)

An integral equation valid for Fabry-Perot type resonators with reflectors of arbitrary curvature and spacing is derived, and equations for the planar, confocal, and spherical geometries are considered further. A numerical iteration method is used to solve the equations, and the properties of the various solutions for the different kernels are discussed. Results show that the confocal type has the lowest diffraction loss, and that the losses in the planar- and spherical-type geometries are identical, as are the normal mode field distributions over the reflectors, apart from a change in sign of the phase angle. Variational methods are applied to give results for the eigenvalues of the planar geometry with great facility, particularly for cases where the eigenvalues are closely spaced. Some potential uses and the respective merits of the resonators are briefly mentioned.

Stepped-Impedance Transformers and Filter Prototypes—Leo Young (p. 339)

Quarter-wave transformers are widely used to obtain an impedance match within a specified tolerance between two lines of different characteristic impedances over a specified frequency band. This paper gives design formulas and extensive tables of designs, most of which were especially derived so that an integrated account could be presented for the first time. Numerous examples are given. Only homogeneous, synchronous transformers and filters are included in this paper, but a short bibliography on related topics is appended.

The theory is also applied to band-pass filters, by showing how to convert quarter-wave transformers into half-wave filter prototypes. The theoretical and numerical results presented are applicable to the design of impedance transformers, direct-coupled cavity filters, short-line low-pass filters, optical anti-reflection coatings and interference filters, acoustical transformers, branch-guide directional couplers, TEM-mode coupled-transmission-line directional couplers, and other circuits. These applications have been or will be dealt with in separate papers; this paper gives the basic theory and some of the numerical data required for these applications.

In-Line Waveguide Calorimeter for High-Power Measurement—M. Michael Brady (p. 359)

The static in-line calorimeter measures the temperature rise in the walls of a waveguide caused by the attenuation of microwave power flowing through the waveguide. It is simple and inexpensive and can be constructed so that it will fit on waveguide already existing in a microwave system. The device should be reliable because it uses no active circuitry. In addition, few mechanical problems are encountered in its use because the existing waveguide need not be altered. The theory of the device is developed, and two experimental S-band calorimeters using stainless steel waveguide and resistance-wire bridge temperature indicators are described. The measured sensitivity and time constant for both units fall within the experimental error of confirming the theoretically predicted figures.

Scattering of Surface Waves by Discontinuities on a Unidirectionally Conducting Screen—S. R. Seshadri (p. 367)

It is shown that a plane screen consisting of closely-spaced parallel wires which are sepa-

rated from one another and which are such that the radius of the wires and the spacing between them are small in comparison to wavelength, can support a surface wave, the spread of whose field components depends only on the angle which the direction of propagation makes with the direction of the wires. The problem of radiation from a discontinuity in such a semi-infinite waveguide is studied for the following three types of discontinuities: 1) when the waveguide terminates in empty space, 2) when it terminates at another such semi-infinite waveguide having different propagation characteristics, and 3) when it terminates at a perfectly conducting half-plane. In each case, the power reflection coefficient, where applicable the power transmission coefficient, the loss of power due to radiation, and its angular distribution are evaluated. The motivation for this investigation is briefly indicated.

Surface Waves on Radially Inhomogeneous Cylinders—A. Vigants and S. P. Schlesinger (p. 375)

A characteristic equation and a cutoff equation are derived for higher order surface-wave modes on lossless isotropic cylinders with arbitrary radial permittivity variation. The derivation, based on the use of the fundamental matrix of a set of differential equations, reduces analytical work and results in expressions well suited for digital computer evaluation of surface-wave eigenvalues and mode spectra. The theory is applied in an investigation of HE_{21} and EH_{21} mode propagation for a particular set of models for the radially varying permittivity. Typical results showing eigenvalue variation, dispersion characteristics and radial field variation, including experimental verification of dispersion characteristics, are shown. The method of analysis can be extended to anisotropic cylinders with permittivity a function of both radius and frequency.

A Plasma Controlled Directional Coupler—Jack Willis (p. 383)

A new type of waveguide directional coupler is described which has a discharge tube as the coupling element in the common narrow wall between the guides. The use of the discharge tube allows continuous control of the amount of coupling between the guides. The theory of the coupler is given with curves for designing such a coupler. The paper describes the results obtained from a 3-db coupler. Measurements were made at a frequency of 450 Mc, of VSWR, noise output, and switching speed. These show a VSWR of the order of 1.3 over the control range, and an excess noise temperature with a peak of 20,000°K at one value of control current. The coupler is capable of switching up to speeds of 1000 cps.

Correspondence—(p. 389)

Contributors—(p. 404)

Space Electronics and Telemetry

VOL. SET-8, No. 3,

SEPTEMBER, 1962

Delay Variations in Telemetry Filters—K. L. Berns (p. 199)

The significance of filter delay characteristics in telemetry applications is discussed, and fundamental terms are defined. Suggested methods of delay measurement are presented, and experimental results are given. Recommendations are offered regarding filter specifications.

A Telemetering System by Code Modulation— $\Delta\Sigma$ Modulation—H. Inose, Y. Yasuda, and J. Murakami (p. 204)

A communication system by code modulation is described which incorporates an inte-

gration process in the original delta modulation system and is named delta-sigma modulation after its modulation mechanism. It has an advantage over delta modulation in dc level transmission and stability of performance, although both require essentially an equal bandwidth and complexity of circuitry. An experimental telemetry system employing delta-sigma modulation is also described.

Phase-Lock Loop Frequency Acquisition Study—J. P. Frazier and J. Page (p. 210)

The ability of a phase-lock loop using a proportional plus integral control filter to acquire a noisy signal when the local oscillator is being swept was determined empirically by means of a low-frequency, GEISE model of such a system.

The effects of the damping factor and natural frequency on the frequency acquisition properties of linear loops (as distinguished from a loop in which the IF signal is limited) are considered in this study. In addition, consideration is given to a loop in which the IF signal is "hard" limited and the loop designed to maximize the sweep rate under the constraint that the probability of acquisition is equal to or greater than 90 per cent for a given SNR.

The rms phase jitter in the output signal was measured as a method of verifying the standard analytic approach to predicting phase jitter.

The results of the study are as follows:

- 1) The range of damping factors from 0.5 to 0.85 yields near optimum acquisition performance.
- 2) Although a drop in loop gain produces lower phase jitter for a given $(S/N)_{IF}$, it degrades the over-all ability of the loop to acquire and track a signal.
- 3) A "hard" limiter in the IF can be effectively used as a gain control to enhance loop performance.
- 4) Using an empirical formula derived from experimental results, the VCO sweep

rate for 90 per cent probability of acquisition can be predicted accurately, given the $(SNR)_{IF}$ and loop parameters.

Message Compression—H. Blasbalg and R. Van Blerkom (p. 228)

Two general classes of operations for the purpose of compressing the output of a message source are considered: (1) Entropy-reducing (ER) transformation, and (2) Information-preserving (IP) transformation (redundancy removal). The type (1) transformation, when acceptable, can yield substantial compression gains in telemetry applications while the type (2) transformation can yield substantial gains for certain types of source statistics.

A new concept, adaptive coding, is introduced. It is shown that for quasi-stationary source statistics it is possible to obtain estimates of the statistics and to use these subsequently for efficient coding. A general statistical measure for monitoring the efficiency of the adaptive procedure is presented and a decision rule, based on this statistic, for updating the coding is defined. It is shown that the statistical estimates need not be precise since the coding efficiency remains reasonably insensitive to small errors; hence, only violent changes in the source statistics must be detected.

A number of configurations for performing adaptive and nonadaptive compression are discussed in detail. Some of these procedures, such as predictive coding, are well known while others are new. In particular, a practical configuration is presented for compressing the output of many sensors which have the statistical structure; no changes in the signal for relatively long time intervals and very rapid changes for relatively short time intervals. It is concluded that this approach has the advantage over variable rate commutation procedures in that short message bursts can always be detected without increasing the communications channel capacity.

The problem of buffer overflow is considered in general and specifically, in the multiple sensor compression system configuration. Here it is shown that buffer overflow can be controlled simply by degrading the fidelity of the sensor outputs gradually and under control. In general, it is concluded that the buffer design problem is just another difficult problem in designing an efficient telemetry system. It is, however, a poor excuse for eliminating compression from telemetry system design without giving it proper consideration. In short, compression is a possible trade-off among the theoretical channel parameters and practical considerations which can influence the over-all system performance and which deserves consideration.

Experimental Optimization and Evaluation of Telemetry Systems—W. F. Link and C. D. Eatough (p. 239)

A careful laboratory program to experimentally optimize and evaluate four telemetry systems in wide use (FM-FM, PAM-FM, PDM-FM and PCM-FM) has been concluded as part of a general study of problems in the telemetry field. Each of the four systems was implemented in the laboratory and the system under test was modulated by random signal sources typifying actual data. Broad-band random noise was then introduced at the RF and the various system parameters were optimized to obtain the lowest threshold for stated performance. Having optimized the parameters in this manner, performance against other types of interference was also measured. For each system an accurate error comparator was designed which repetitively sampled the system input and output and compared the samples for error.

The information obtained on internal parameter optimization and over-all performance for each system is extremely useful to systems design as well as to evaluation and comparison of the systems.

Contributors—(p. 247)

Announcement

Abstracts and References to be Discontinued

THE IRE has been advised by the compilers and publishers of Abstracts and References that this service is being discontinued at the end of 1962. For PROCEEDINGS readers this will mean that this feature will make its final appearance in the January, 1963, issue. The Annual Index for 1962 will be published as usual as Part 2 of a subsequent issue.

Abstracts and References has appeared in the PROCEEDINGS since June, 1946, by special arrangement with two organizations in England: the Radio Industrial Organization of the Department of Scientific and Industrial Research, the compilers, and Hiffe Electrical Publications, Ltd., publishers of *Electronic Technology*, from which Abstracts and References are reprinted. We are indebted to both organizations for making this valuable service available to the IRE and its members during an important period of rapid literature growth. In particular we wish to express our thanks to Hugh S. Pocock, Chairman of Hiffe Electrical Publications, Ltd. and W. T. Cocking, Editor of *Electronic Technology*, for their close cooperation these many years.

An alternative source of information on radio and electronics engineering literature is available in the well known abstracting journal *Electrical Engineering Abstracts*, published by the Institution of Electrical Engineers of London. By special arrangement with the IEE, IRE members may subscribe at a reduced price as indicated below.

Electrical Engineering Abstracts has been published by the Institution of Electrical Engineers for 64 years and forms Section B of a double publication, *Science Abstracts*, of which Section A is *Physics Abstracts*, published by the IEE in association with the American Physical Society and the Institute of Physics and Physical Society of London.

Electrical Engineering Abstracts, which is broader in scope than Abstracts and References, currently pub-

lishes about 15,000 abstracts a year of an average length of 120 words. *Physics Abstracts* is even larger, publishing about 25,000 abstracts a year. Together, the two publications cover the field of physics, electrical engineering, radio and electronics. Nearly a thousand journals are regularly scanned for material of possible value, more than half of them being foreign-language journals; they include all those formerly covered by Abstracts and References.

The proportion of pages in *Electrical Engineering Abstracts* devoted to the subjects of interest to IRE members (electronics, electromagnetic wave, radio-communication, data processing, etc.) exceeds 75 per cent in most issues. The abstracts are classified under 89 separate chapter headings, arranged in six sections of which four are directly concerned with radio engineering.

While a comprehensive coverage of the physical subjects which have an increasing interest for electronics engineers—semiconductor physics, spectral emission, electron-atom collisions, and so on—is given by *Physics Abstracts*, a large selection of abstracts on these and similar subjects is printed also in *Electrical Engineering Abstracts*, so that the electronics engineer is given references, not only to the engineering literature, but to a useful amount of physics literature as well.

Electrical Engineering Abstracts is published monthly. The normal annual subscription rate, which includes Author and Subject indexes (total size in 1963 estimated to be 2000 pages) is £14 (\$39). By a special arrangement with the IEE, however, members of any grade of the IRE and AIEE can subscribe to *Electrical Engineering Abstracts* at the privilege rate of £10.10.0. or \$30. Members who wish to subscribe should send their names and addresses, with payment in dollars or sterling, to The Secretary, The Institution of Electrical Engineers, Savoy Place, London, W.C.2, England.

—The Editor

Abstracts and References

Compiled by the Radio Research Organization of the Department of Scientific and Industrial Research, London, England, and Published by Arrangement with that Department and *Electronic Technology*, Dorset House, Stamford St., London S.E. 1, England

NOTE: The Institute of Radio Engineers does not have available copies of the publications mentioned in these pages, nor does it have reprints of the articles abstracted. Correspondence regarding these articles and requests for their procurement should be addressed to the individual publications, not to the IRE.

The Index to the Abstracts and References published in the PROC. IRE from February, 1961 through January, 1962 is published by the PROC. IRE, June, 1962, Part II. It is also published by *Electronic Technology* and appears in the March, 1962, issue of that Journal. Included with the Index is a selected list of journals scanned for abstracting with publishers' addresses.

Acoustics and Audio Frequencies	2539
Antennas and Transmission Lines	2539
Automatic Computers	2540
Circuits and Circuit Elements	2540
General Physics	2541
Geophysical and Extraterrestrial Phenomena	2543
Location and Aids to Navigation	2545
Materials and Subsidiary Techniques	2545
Mathematics	2548
Measurements and Test Gear	2548
Other Applications of Radio and Electronics	2548
Propagation of Waves	2549
Reception	2549
Stations and Communication Systems	2549
Subsidiary Apparatus	2550
Television and Phototelegraphy	2550
Tubes and Thermionics	2550
Miscellaneous	2551

The number in heavy type at the upper left of each Abstract is its Universal Decimal Classification number. The number in heavy type at the top right is the serial number of the Abstract. DC numbers marked with a dagger (†) must be regarded as provisional.

UDC NUMBERS

Certain changes and extensions in UDC numbers, as published in PE Notes up to and including PE 666, will be introduced in this and subsequent issues. The main changes are:

Artificial satellites:	551.507.362.2	(PE 657)
Semiconductor devices:	621.382	(PE 657)
Velocity-control tubes, klystrons, etc.:	621.385.6	(PE 634)
Quality of received signal, propagation conditions, etc.:	621.391.8	(PE 651)
Color television:	621.397.132	(PE 650)

The "Extension and Corrections to the UDC," Ser. 3, No. 6, August, 1959, contains details of PE Notes 598-658. This and other UDC publications, including individual PE Notes, are obtainable from The International Federation for Documentation, Willem Witsenplein 6, The Hague, Netherlands or from The British Standards Institution, 2 Park Street, London, W. 1, England.

A list of organizations which have available English translations of Russian journals in the electronics and allied fields appears at the end of the Abstracts and References section.

ACOUSTICS AND AUDIO FREQUENCIES

- 534.14-8:537.311.33 3557
Amplification of Ultrasonic Waves in Piezoelectric Semiconductors—D. L. White. (*J. Appl. Phys.*, vol. 33, pp. 2547-2554; August, 1962.) The technique necessary for amplification is discussed and extension to higher frequencies and more general operating conditions is considered. See 1 of January (Hutson, *et al.*).
- 534.231:534.88 3558
Space/Time Correlation in Spherical and Circular Noise Fields—M. J. Jacobson. (*J. Acoust. Soc. Am.*, vol. 34, pp. 971-978; July, 1962.) The cross-correlation of the noise field of an infinite number of white-noise sources is examined as a function of time delay, wavelength between correlation points and frequency.
- 534.232 3559
Determination of the Parameters of a Piezoelectric Transducer from the Decay of Resonant Vibrations—M. Redwood. (*J. Acoust. Soc. Am.*, vol. 34, pp. 895-902; July, 1962.) The theory of the method and its limitations are discussed. It is particularly suitable for rapid measurements on transducers with low coupling coefficients ((0.4).
- 534.232.089.6 3560
Shock-Wave Transducer Calibration—R. E. Ziemer and R. F. Lambert. (*J. Acoust. Soc. Am.*, vol. 34, pp. 987-988; July, 1962.) "The use of a shock-wave technique to obtain a frequency-response calibration of a small lead zirconate-titanate transducer is described. The response curve is obtained through numerical Fourier transformation of the recorded response to a shock-wave excitation. Sources of error and agreement with other methods of calibration are discussed."
- 534.417.089.6 3561
Hypophone Calibration in a Vibrating Column of Liquid—F. Schloss and M. Strasberg. (*J. Acoust. Soc. Am.*, vol. 34, pp. 958-960; July, 1962.) The procedure has advantages over usual laboratory methods for the calibration of small low-sensitivity hydrophones: pressures up to 1000 dyn cm² can be produced.
- 534.61-14 3562
A Test Sound Source for Wide-Band Microphones for the Measurement of Pressure Impulses in Liquids—W. Eisenmenger. (*Acustica*, vol. 12, no. 3, pp. 165-172; 1962. In German.)
- 534.782 3563
Verification of the Properties of an Artificial Mouth by the Method of the Thresholds of Audibility, Intelligibility and Perception—

G. Ibba. (*Alta Frequenz*, vol. 31, pp. 127-133; March, 1962.) The ability of an artificial mouth to reproduce speech is assessed on the basis of subjective tests.

621.395.61:621.382.23 3564
Experimental Tunnel-Diode Electromechanical Transducer Elements and their Use in Tunnel-Diode Microphones—E. S. Rogers. (*J. Acoust. Soc. Am.*, vol. 34, pp. 883-893; July, 1962.) The theory of a tunnel-diode transducer is developed and circuits for operation of variable-resistance or modulated negative-resistance microphones are analyzed.

621.395.616 3565
Investigations on a Condenser Microphone with Cardioid Characteristic—B. Weingartner. (*Acustica*, vol. 12, no. 3, pp. 158-165; 1962. In German.) Deviations from the desired frequency response curve and directivity pattern near the lower and upper frequency limits are studied with reference to theoretical and experimental data. A method of improving low-frequency response is indicated.

621.395.625.3:681.84.083.84 3566
The Measurement of Modulation Noise—E. Belger. (*Rundfunktech. Mitt.*, vol. 6, pp. 152-154; June, 1962.) Modulation noise caused by inhomogeneities in the coating of magnetic recording tape is considered. The masking of this noise by the useful sound is investigated and a filter compensating for the masking effect is proposed to facilitate the measurement of noise.

ANTENNAS AND TRANSMISSION LINES

621.372.2 3567
Matrices and Equivalent Circuits of Three-Wire Transmission Lines—M. Soldi. (*Alta Frequenza*, vol. 31, pp. 219-225 and 359-374; April and June, 1962.) Detailed theoretical treatment of three-wire transmission lines for use as high-frequency circuit elements. The theory is extended to cover transmission lines with any number of conductors.

621.372.2 3568
The Change of Shape of Steep-Fronted Pulses by Multiple Reflections along a Transmission Line—D. Seitzer. (*Arch. elekt. Übertragung*, vol. 16, pp. 263-270; June, 1962.) Further investigation of the effects of irregularities in a homogeneous line on the shape of a step-voltage waveform. See also 360 of February.

621.372.2:621.318.57:537.312.62 3569
Low-Impedance Transmission System for Driving Cryogenic Circuits—D. J. Dumin. (*Rev. Sci. Inst.*, vol. 33, pp. 715-720; July

1962.) The possible advantages of driving cryotron circuits with a low-impedance transmission system are discussed. Although losses are higher a reduction in the signal coupled between cables in a cryotron system is possible when low-impedance cable is used. A note is given on low-impedance pulse generator design.

621.372.22 3570

Circuit Arrangements at the Output of Short Distributed Inhomogeneous Lossy Lines—W. Jutzl. (*Z. angew. Phys.*, vol. 14, pp. 365–369; June, 1962.) Output matching conditions and circuits are discussed.

621.372.832.8 3571

On Some Design Problems of a Star-Type Ferrite Circulator—S. J. Lewandowski. (*J. Inst. Telecommun. Engrs., India*, vol. 8, pp. 103–106; March, 1962.) Theory developed by Auld (26 of 1960) was used as a basis for an experimental investigation of the circulator. Modifications were made to improve the wide-band operation.

621.372.851:621.385.632.19 3572

Diaphragm-Loaded Waveguides as Delay Lines—A. Fiebig. (*Arch. elekt. Übertragung*, vol. 16, pp. 283–290; June, 1962.) The advantages are discussed of diaphragm-loaded waveguide for use as delay-line systems in traveling-wave tubes operating at extremely high frequencies. The design of a multiple-beam delay line and experimental investigations are described.

621.372.852.22 3573

Modes in Rectangular Guides Loaded with Magnetized Ferrite—G. Gerosa. (Proc. IRE, vol. 50, pp. 1826–1827; August, 1962.) The analysis given shows that one of the modes found by Seidel and Fletcher (757 of 1960) does not exist.

621.372.852.323 3574

High-Power Resonance Isolators—F. W. Smith. (Proc. IRE, Pt. B, vol. 109, pp. 420–429; September, 1962.) A method is described for improving the power-handling capacity of resonance-absorption isolators. Performance data are given on X-band isolators for handling powers > 2 kW with 25 per cent load reflection, which maintain their low-power characteristics.

621.372.853:537.56 3575

Coupling of Modes between a Slow-Wave Plasma Mode and a Helix—S. F. Paik. (*J. Appl. Phys.*, vol. 33, pp. 2468–2473; August, 1962.) Propagation characteristics of a transmission system consisting of a plasma column and coaxial helix are analyzed. Results are compared with those obtained by Bulgakov *et al.* (*Z. Tekh. Fiz.*, vol. 30, pp. 840–850; July, 1960.)

621.396.67:621.396.621.22:621.397.62 3576

Communal Aerials for Television Reception in Adjacent Channels—H. Licht. (*Rundfunktech. Mitt.*, vol. 6, pp. 145–151; June, 1962.) The design of antenna installations suitable for the reception of transmissions in adjacent frequency channels within a given band is discussed, allowing for the problems arising from differences in signal level and direction of incidence at the antenna. Particular care is needed in the adjustment of receivers.

621.396.67:621.396.946 3577

The Importance of 'Cold' Aerials for Space Communications—A. Fournier and P. Chavance. (*Rev. tech. Comp. fran., Thomson-Houston*, no. 36, pp. 45–53; June, 1962.) The equivalent noise temperature of antennas is considered and, in particular, Cassegrain and horn-reflector antennas are compared.

621.396.67.095(204):621.396.944 3578

Dipole Radiation in a Conducting Half-Space—R. K. Moore and W. E. Blair. (*J. Res.*

NBS, vol. 65D, pp. 547–563; November/December, 1961.) Theoretical investigation of the problem of communication between aerials submerged in a conducting medium such as sea water. The analysis is given in terms of a dipole radiating in a conducting half space separated by a plane boundary from a dielectric half space.

621.396.673 3579

Measurements of Low-Angle Radiation from a Monopole—A. C. Wilson. (*J. Res. NBS*, vol. 65D, pp. 641–645; November/December, 1961.) Determination, by scale model techniques, of the effectiveness of a ground system of long-wire radials to obtain low angles of radiation. Measurements were made at 400 Mc with a base-driven vertical monopole and a target transmitter antenna at a distance of 200 λ .

621.396.674.3 3580

Transient Response of a Dipole Antenna—S. P. Morgan. (*J. Math. Phys.*, vol. 3, pp. 564–565; May/June, 1962.) The current excited by a step-function voltage across an infinitesimal centre gap is derived using a double Fourier transformation.

621.396.674.3:551.510.535 3581

The Impedance of a Short Cylindrical Dipole in the Ionosphere—E. N. Bramley. (*Planet-Space Sci.*, vol. 9, pp. 445–454; August, 1962.) Theoretical expressions are obtained for the dipole impedance in a) an isotropic conducting medium, b) a magneto-ionic medium, and are used to calculate numerical values for an antenna in the ionosphere.

621.396.677.3.012.12 3582

Phased-Array Coordinate Transformations—J. H. Best. (*Microwave J.*, vol. 5, pp. 51–54; July, 1962.) A three-dimensional presentation is needed to show the radiation pattern of planar phased arrays adequately. Plotting power contours on a spherical coordinate system is the most practical way of doing this. The particular advantages and the transformation formula for three such systems are given.

621.396.677.43 3583

Rhombic Aerial Design: Two-Tiered Array—F. J. Norman. (*Electronic Tech.*, vol. 39, pp. 337–346; September, 1962.) Field measurements of parameters indicate that the theoretical directivity patterns are achieved in practice. Graphical procedures for determining the gain and the shape of the main lobe and minor lobes are given.

621.396.677.7 3584

Radiation from a Magnetic Line Dipole Source of Finite Width—L. W. Zelby. (Proc. IRE, vol. 50, pp. 1848–1849; August, 1962.) Analysis to determine the conditions for launching a surface wave.

621.396.677.85 3585

Electromagnetic Scattering from Radially Inhomogeneous Spheres—R. J. Garbacz. (Proc. IRE (*Correspondence*), vol. 50, p. 1837; August, 1962.) The equations for the spherical Luneberg lens given by Tai (130 of 1961) are used as a basis of a method of determining scattering patterns which is suitable for high-speed computer calculation.

AUTOMATIC COMPUTERS

681.142 3586

Improved Electronic Differentiator has Low Noise Factor—N. D. Diamantides. (*Electronics*, vol. 35, pp. 46–47; July, 1962.) A 2:1 improvement in noise factor is achieved using the circuit configuration described which incorporates an extra amplifier, providing a time delay, and avoids a series input capacitor.

661.142:621.318.134 3587

The Measurement and Reduction of Noise in Coincident-Current Core Memories—P. Cooke and D. C. Dillstone. (Proc. IEE, Pt. B, vol. 109, pp. 383–389; September, 1962.)

661.142:621.382.2/.3 3588

Transistor-Diode Static Switching Units—J. F. Young. (*Electronic Eng.*, vol. 34, pp. 595–599; September, 1962.) The advantages of replacing resistors by diodes in the input of transistor NCR circuits are noted and operating conditions are discussed.

CIRCUITS AND CIRCUIT ELEMENTS

621.372.413:537.312.62 3589

Measurements on Two Nb Superconductive RF Cavities—L. Rinderer, J. Rüfenacht, and A. Susini. (*Phys. Lett.*, vol. 2, pp. 119–120; September, 1962.) The construction of the cavities, which are tuned to 270 Mc, is described and results of measurements made on them are given.

621.372.44 3590

Dependence of Parametric Element Non-linearity on Tuning Circuit—G. H. B. Thompson; A. L. Helgesson. (Proc. IRE (*Correspondence*), vol. 50, pp. 1845–1846; August, 1962.) Comment on 45 of January and author's reply.

621.372.44 3591

Varactor Charge-Voltage Expansions for Large Pumping Conditions—A. L. Helgesson. (Proc. IRE (*Correspondence*), vol. 50, pp. 1846–1847; August, 1962.) The results given earlier (45 of January) are extended to high-level pumping.

621.372.5/6 3592

Narrow-Band R.F. Networks—A. Susini. (*Electronic Tech.*, vol. 39, pp. 357–361; September, 1962.) A simplified treatment using the pole-zero approach.

621.372.54:621.315.212 3593

V.H.F. Notch Filters: T-Type Coaxial-Line Construction—W. Wharton and R. E. Davies. (*Electronic Tech.*, vol. 39, pp. 332–336; September, 1962.) The theory of the T-type coaxial notch filter first described by Sosin (1162 of 1953) is presented and design curves for practical filters are given.

621.372.55 3594

A Technique for Equalizing Parabolic Group Delay—R. M. Kurczok. (Proc. IRE (*Correspondence*), vol. 50, p. 1840; August, 1962.) A technique applicable to RF and HF amplifier chains is outlined in which all-pass equalizing networks are avoided by using single- and double-tuned circuits in alternate coupling networks.

621.372.56.018.756 3595

Attenuators for High-Frequency Pulses—H. L. Stadler. (*Rev. Sci. Instr.*, vol. 33, p. 761; July, 1962.) A note on the design of an asymmetric H attenuator.

621.373:621.372.2:621.372.44 3596

Tunnel Diode Loaded by a Shorted Transmission Line—M. H. Steward; J. Nagumo and M. Shimura. (Proc. IRE (*Correspondence*), vol. 50, pp. 1830–1833; August, 1962.) Correction and comment on 3669 of 1961 with authors' reply.

621.373:621.372.44:681.142 3597

Amplitude Limiting and Hysteresis of Parametron Oscillations—E. Völcker. (*Elektronik*, vol. 11, pp. 1–4, 47–49, 117–120 and 262–265; January, February, April and September, 1962.) Theoretical treatment of various modes of operation of the parametron [see e.g., 3588 of 1959 (Goto)].

- 621.373.421.11 3598
Design of Temperature-Compensated Tuned Circuits—O. Schweib. (*Electronic Tech.*, vol. 39, pp. 347-352; September, 1962.) Formulas are given from which variable tuned circuits can be designed to cover a prescribed frequency range with a given maximum temperature coefficient.
- 621.373.52 3599
Designing Class-C Transistor LC Oscillators—P. Laakmann. (*Electronics*, vol. 35, pp. 42-45; July, 1962.) An analysis with an example of design illustrating the advantages of the earthed-collector Hartley circuit.
- 621.374.4:538.569.4 3600
Resonant Harmonic Generation in Ruby—C. M. Kellington. (*Phys. Rev. Lett.*, vol. 9, pp. 57-58; July, 1962.) An experiment is described in which harmonic generation occurs in a medium which is resonant with respect to both the fundamental and the harmonic.
- 621.374.4:621.372.44 3601
Generation of Harmonics with Varactor Diodes—G. B. Stracca. (*Alta Frequenza*, vol. 31, pp. 134-149; March, 1962.) The analysis is given for an ideal varactor diode used as a harmonic generator at high signal levels. Experimental results are compared with the theoretical characteristics. For English version see *ibid.*, Stracca, vol. 31, pp. 291-307; May, 1962.
- 621.374.4:621.372.44 3602
Analysis of Frequency Multipliers with 'Varactor' Diodes—M. Vadjjal and C. Dragone. (*Alta Frequenza*, vol. 31, pp. 150-157; March, 1962.) The general analysis given is applied to the calculation of load and source impedance for optimum output from the frequency multiplier.
- 621.374.4:621.372.44 3603
Similarity Considerations for Varactor Multipliers—A. Uhlir, Jr. (*Microwave J.*, vol. 5, pp. 55-59; July, 1962.) A dimensional analysis of the performance of varactors as harmonic generators shows that a better equivalent circuit is needed to represent the varactor at VHF.
- 621.374.4:621.382.23 3604
A Tunnel-Diode Wide-Band Frequency-Doubling Circuit—J. H. Burbo. (*Proc. IRE (Correspondence)*, vol. 50, p. 1850; August, 1962.) Methods of stabilizing the circuit described by Neu (767 of March) are mentioned.
- 621.375.4 3605
Output Impedance Compensation of Common-Emitter Stage—S. S. Hakim. (*Electronic Tech.*, vol. 39, pp. 353-356; September, 1962.) By shunting the output of a common-emitter stage with a series R_L circuits it is possible to maintain the impedance purely resistive for frequencies up to about $f_a/5$.
- 621.375.4.012.8 3606
Analytical Investigation of the Hybrid- π Equivalent Circuit of a Transistor as an Amplifier at Radio Frequencies—V. Banfi. (*Alta Frequenza*, vol. 31, pp. 210-218; April, 1962.)
- 621.375.4.018.78:621.372.632 3607
Experimental Investigations and Calculations on Distortion and Mixing Processes in Transistor Stages at Low Frequencies—J. S. Vogel and M. J. O. Strutt. (*Arch. elekt. Übertragung*, vol. 16, pp. 291-295; June, 1962.) An accurate method for computing the distortion effects in transistor circuits with low source and load impedance is given. See also 2892 of 1961.
- 621.375.43.024 3608
Thermal Negative Feedback in a Transistor Amplifier for Direct Current—G. Paimi and O. Svelto. (*Alta Frequenza*, vol. 31, pp. 206-209; April, 1962.) An experimental amplifier is described in which negative feedback at extremely low frequencies is produced by thermal effects.
- 621.375.9:538.569.4 3609
General Considerations on the Three-Level Solid-State Microwave Maser—M. Bidault. (*Rev. tech. Comp. franç. Thomson-Houston*, no. 36, pp. 55-109; June, 1962.) Operation of the maser is summarized and the physical properties of maser materials and related microwave components are reviewed.
- 621.375.9:538.569.4 3610
Operation of a Travelling-Wave Maser in a Transverse-Field Superconducting Electromagnet—W. G. Nilsen. (*J. Appl. Phys.*, vol. 33, pp. 2522-2523; August, 1962.) A 6-Gc traveling-wave maser showed a net gain of 30 db with 3-db bandwidth of about 20 Mc.
- 621.375.9:538.569.4:621.3.018.41(083.74) 3611
Ammonia Maser on the 3.2 Line as a Frequency Standard: Part I—K. Shimoda and N. Kohno. (See 3812.)
- 621.375.9:621.372.44 3612
Investigation of an Experimental Travelling-Wave Parametric Amplifier—R. Mavaddat and F. J. Hyde. (*Proc. IEE, Pt. B.*, vol. 109, pp. 405-413; September, 1962.) The effect of mismatch at source and load is investigated. The signal gain obtainable with the experimental amplifier was of the order of 10 db, and the bandwidth approximately 3 Mc with the double-channel noise factor < 1.1 at mid-band (6.7 Mc).
- 621.375.9:621.372.44 3613
Some Properties of Parametric Systems with Great Depth of Modulation: Part I—Theory—J. B. Gunn. (*Solid-State Electronics*, vol. 5, pp. 181-204; July/August, 1962.) The behavior of a resonant system in which the resonance frequency is varied slowly and periodically, and the practical limitations of its performance as an amplifier are discussed.
- 621.375.9:621.372.44 3614
Parametric Amplifiers using Diodes: Type TH.D.20—M. Baril. (*Rev. tech. Comp. franç. Thomson-Houston*, no. 36, pp. 111-127; June, 1962.) Two low-noise amplifiers, one for the range 1250-1350 Mc and the other for 3100 Mc, are described.
- 621.375.9:621.372.44:621.385.6 3615
Graphical Expressions of Synchronous Conditions in the Transverse-Type Electron-Beam Parametric Amplifier—K. Kakizaki. (*Proc. IRE*, vol. 50, pp. 1850-1851; August, 1962.)
- 621.375.9:621.382.23 3616
Design of a Series-Tuned Negative-Resistance Amplifier—J. C. Paul. (*Semiconductor Prod.*, vol. 5, pp. 29-35; June, 1962.) Analytical and graphical design procedures are presented for a low-level low-noise tunnel-diode preamplifier for 3 Mc which together with the bias supply can be built into a very small unit.
- 621.375.9:621.382.23 3617
Noise Figure of Moody and Wacker's Broad-Band Tunnel-Diode Amplifier—A. van der Ziel. (*Proc. IRE (Correspondence)*, vol. 50, p. 1844; August, 1962.) See 2141 of 1961.
- 621.375.9:621.382.23 3618
Nonlinear Distortion in Tunnel-Diode Amplifiers—R. M. Kurzrok and A. Newton. (*Proc. IRE (Correspondence)*, vol. 50, pp. 1853-1854; August, 1962.) An approximate theoretical analysis.
- 537.311:061.3 3620
Report on the Symposium on Electronic Tunnelling in Solids, Philadelphia, 1961—E. O. Kane. (*J. Phys. Chem. Solids*, vol. 23, pp. 173-180; January/February, 1962.) A summary of the proceedings of the meeting 30th-31st January. References are given to published material.
- 537.311.33 3621
Density Matrix Approach to a Simple Hot-Electron Problem—A. Hasegawa and J. Yamashita. (*J. Phys. Chem. Solids*, vol. 23, pp. 875-880; July, 1962.) A transport theory of non-ohmic conductivity in semiconductors is developed in a form which is closely related to the Kohn-Luttinger theory of ohmic conductivity.
- 537.311.33 3622
Impurity Effects on the Plasma Oscillation of an Electron Gas—Y. H. Ohtsuki. (*Progr. theor. Phys.*, vol. 27, pp. 1082-1083; May, 1962.) The effects of impurities on the oscillation damping factor are calculated.
- 537.311.33:538.63 3623
A Possible Origin of A.C. Current through Oscillating Cylindrical Electron-Hole Plasma—T. Misawa. (*Jap. J. Appl. Phys.*, vol. 1, pp. 67-69; July, 1962.) Glicksman (1197 of April) proposed unstable helical perturbations in carrier density as an origin. It is argued that ac current will only result if the specimen is cylindrically asymmetric, or in an inclined magnetic field.
- 537.312.62 3624
The Solution of a Transition Problem in a Superconducting Strip—W. Liniger. (*J. Math. Phys.*, vol. 3, pp. 578-586; May/June, 1962.)
- 537.312.62:535.215:621.318.57 3625
Radiation-Induced Transport of Magnetic Flux along a Superconducting Sheet—J. F. Marchand and J. Volger. (*Phys. Lett.*, vol. 2, pp. 118-119; September, 1962.) The normally conductive area formed by a spot of light on a sheet of superconducting material is probably due to a local heating effect. Flux from a magnet near the sheet can be isolated in such an area and transported about the sheet by moving the illuminated region, a procedure which can be regarded as the action of a flux pump. The flux can be "set" at any point by switching off the light source.
- 537.525 3626
Build-Up of Electron Density in Neon-Argon Gas Discharges in Pulsed Microwave Fields—M. Kumagai and T. Tsukishima. (*J. Phys. Soc. Japan*, vol. 17, pp. 1204-1205; July, 1962.)
- 537.525:621.391.822 3627
Radio-Frequency Noise of an Immersed Langmuir Problem—R. D. Sears and J. J. Brophy. (*J. Appl. Phys.*, vol. 33, pp. 2583-2587; August, 1962.) The spectrum of noise from 50 kc to 10 Mc in a cold-cathode Ne discharge is examined.
- 537.56 3628
Transport Phenomena in a Nonuniform Slightly Ionized Gas—S. Zivanovic and M. S. Sodha. (*Progr. theor. Phys.*, vol. 27, pp. 1128-1136; June, 1962.) Solution of Boltzmann's equation gives electric and thermal currents in varying electric and static magnetic fields. The electron energy distribution is non-Maxwellian if gradients occur in n_e and v .
- 537.56 3629
Containment of Plasmas by High-Frequency Electric Fields—M. Ericson, C. S. Ward,

- S. C. Brown, and S. J. Buchsbaum. (*J. Appl. Phys.*, vol. 33, pp. 2429-2434; August, 1962.) A cylindrical plasma column was produced in hydrogen by a microwave electric field crossed with a static magnetic field. Under certain conditions the plasma appeared as a stable cylindrical column with diameter as small as $\frac{1}{4}$ that of the discharge tube. The experimentally observed properties of this "constricted" discharge can be explained by treating the plasma as a compressible dielectric medium.
- 537.56** **3630**
Electron Temperature in Partially Ionized Gases Subject to Intense A.C. Fields—S. Viswanathan. (*J. Appl. Phys.*, vol. 33, pp. 2481-2483; August, 1962.) A strong electric field applied to a plasma produces electrons with a temperature considerably higher than the temperature of the neutral gas in the plasma.
- 537.56:537.533** **3631**
The Interaction of Charged-Particle Beams with Plasma—Ya. B. Fainberg. (*Atomnaya Energiya*, vol. 11, pp. 313-335; October, 1961. English translation, *J. Nuclear Energy, Pt. C*, vol. 4, pp. 203-220; June, 1962.) Instability and nonlinear effects in beam-plasma interaction are discussed with reference to the acceleration of charged particles and the generation and amplification of microwaves. 79 references.
- 537.56:537.533** **3632**
Electromagnetic Properties of a Plasma-Beam System—J. Neufeld. (*Phys. Rev.*, vol. 127, pp. 346-359; July, 1962.) A continuation of earlier work on the interaction of an electron beam with a cold plasma (see e.g., 2154 of 1961 (Neufeld and Doyle)), and an extension to the case of a thermal plasma.
- 537.56:537.533** **3633**
Properties of a Plasma Created by an Electron Beam—P. Hedvall. (*J. Appl. Phys.*, vol. 33, pp. 2426-2429; August, 1962.) The beam and plasma were confined by an axial magnetic field. Types of oscillation that occurred are discussed.
- 537.56:538.566** **3634**
Experimental Two-Beam Excitation of Plasma Oscillations—M. J. Kofoed. (*Phys. Fluids*, vol. 5, pp. 712-720; June, 1962.) Further tests made since the previous paper (3057 of 1960) are described and an expression is derived which gives the ratio of phase velocity to electron beam velocity for the production of strong oscillations.
- 537.56.08:537.533** **3635**
Microwave Probing of Ionized-Gas Flows—R. G. Jahn. (*Phys. Fluids*, vol. 5, pp. 678-686; June, 1962.) A transverse microwave beam device is described and a technique is outlined for examining the build-up of ionization behind a strong shock wave in A.
- 538.114** **3636**
Use of Green Functions in the Theory of Ferromagnetism—R. A. Tahir-Kheli and D. ter Haar. (*Phys. Rev.*, vol. 127, pp. 88-100; July, 1962.) **Part 1**—General Discussion of the Spin-S Case—Green's functions, decoupled by a simple procedure are applied to the problem of a lattice at each site of which is a spin $S(S=\frac{1}{2}, 1, 3/2, 2, 5/2, 3)$. The magnetization at low, high and sub-Curie-point temperatures is obtained using the Heisenberg Hamiltonian. **Part 2**—Dyson Spin Waves—Using the Dyson Hamiltonian both with and without the interaction term, the magnetization, spin specific heat and spin-wave dispersion are obtained for low temperatures. The effect of higher-order decoupling is also considered. The results for cubic lattices agree reasonably with other theories; the decoupling seems to be more exact for larger S.
- 538.3** **3637**
A General Method of Representation of Electromagnetic Fields—G. Borgiotti. (*Alla Frequenza*, vol. 31, pp. 226-234; April, 1962.) The method is based on simple properties of vector space and Fourier transforms. Various types of representation are obtained by changing the vector basis of reference of the two-dimensional space considered. For English version see Borgiotti, *ibid.*, vol. 31, pp. 285-293; May, 1962.
- 538.311** **3638**
The Electromagnetic Field of a Straight Current-Carrying Insulated Wire with Bare Ends Laid Parallel to the Surface in Sea-Water in Three-Layer Space: Air, Water, Earth—H. Buchholz. (*Arch. Elektrotech.*, vol. 47, pp. 80-105 and 133-148; June and July, 1962.) **Part 1**—The D.C. Case. **Part 2**—The A.C. Case for any Frequencies.
- 538.56:531.6** **3639**
Direct Transmission of Mechanical Energy by Means of Electromagnetic Waves—G. Latmiral and G. Franceschetti. (*Alla Frequenza*, vol. 31, pp. 78-81; February, 1962; In English.) The ponderomotive forces and torques exerted on a dipole by a linearly or circularly polarized wave are calculated. The amount of mechanical energy that can be directly transmitted from a transmitting to a receiving antenna is shown to be the energy equivalent of the Doppler effect.
- 538.561:537.56** **3640**
Microwave Radiation from a Magneto-plasma—S. Miyoshi. (*J. Phys. Soc. Japan*, vol. 17, pp. 1206-1207; July, 1962.) Difficulty in measuring the electron density of the plasma [see 3336 of 1961 (Hirshfield and Brown)] is overcome by using an interferometer in the 8-mm- λ region.
- 538.566:537.56** **3641**
Electromagnetic Waves in a Bounded, Anisotropic Plasma—K. A. Graf and M. P. Bachynski. (*Canad. J. Phys.*, vol. 40, pp. 887-905; July, 1962.) A theoretical study of the interaction of a plane EM wave with a flat uniform free-space/plasma interface in a static magnetic field. Values are listed of the attenuation and phase constants for each of the two possible waves in the plasma.
- 538.569.4:535.853** **3642**
Use of Travelling-Wave Helices in E.S.R. and Double Resonance Spectrometers—R. H. Webb. (*Rev. Sci. Instr.*, vol. 33, pp. 732-737; July, 1962.) The use of a traveling-wave helix for concentrating microwave fields is discussed, with special attention to its application for electron spin resonance and Overhauser effects.
- 538.569.4:538.221** **3643**
Ferrimagnetic Resonance with Orthogonal and Parallel Pumping—R. M. White and E. Schlömann. (*J. Appl. Phys.*, vol. 33, pp. 2437-2438; August, 1962.) The threshold of nonlinear absorption due to unstable growth of certain spin waves is calculated for the case of an RF field applied orthogonally to the dc field, with another RF field of twice the frequency simultaneously applied parallel to the dc field.
- 538.569.4:538.222** **3644**
Magnetic Resonance with Strong Radio-Frequency Fields in Solids—I. Solomon and J. Ezratty. (*Phys. Rev.*, vol. 127, pp. 78-87; July, 1962.) Redfield's proposal of a spin temperature in the rotating frame is verified independently of a relaxation theory. The technique gives a usable signal in solids for which the ordinary absorption signal is almost undetectable.
- 538.569.4:621.375.9:535.61-15** **3645**
Infrared Spectroscopy using Stimulated-Emission Techniques—C. K. N. Patel, W. R. Bennett, Jr., W. L. Faust, and R. A. McFarlane. (*Phys. Rev. Lett.*, vol. 9, pp. 102-104; August, 1962.) Optical maser oscillation has been obtained in each of the noble gases; and a total of 14 transitions have been observed in the wavelength range 1.5-2.2 μ .
- 538.569.4:621.375.9:535.61-15** **3646**
Optical Maser Emission from Trivalent Praseodymium in Calcium Tungstate—A. Yariv, S. P. S. Porto, and K. Nassau. (*J. Appl. Phys.*, vol. 33, pp. 2519-2521; August, 1962.)
- 538.569.4:621.375.9:535.61-2** **3647**
Optical-Pumping Cavity Construction Technique—R. H. Itronik, R. C. Jones, and C. J. Bronco. (*Rev. Sci. Instr.*, vol. 33, pp. 776-777; July, 1962.) A technique for constructing elliptical reflectors of any size by use of simple machine settings is described.
- 538.569.4:621.375.9:535.61-2** **3648**
Optical Mixing of Coherent and Incoherent Light—A. W. Smith and N. Braslau. (*IBM J. Res. Dev.*, vol. 6, pp. 361-362; July, 1962.) The signal from a ruby maser has been mixed with quite broad and relatively weak spectral lines of a mercury lamp, using a KDP crystal 0.6 cm thick.
- 538.569.4:621.375.9:535.61-2** **3649**
Theoretical Considerations on Millimetre-Wave Generation by Optical Frequency Mixing—J. R. Fontana and R. H. Pantell. (*Proc. IRE*, vol. 50, pp. 1796-1800; August, 1962.) The conversion efficiency obtainable with different types of nonlinear media is considered. Nonlinear passive resistive elements may have efficiencies up to 25 per cent, regardless of frequency ratio, and a diode characteristic would give optimum results.
- 538.569.4:621.375.9:535.61-2** **3650**
Microwave Photomixing of Optical Maser Outputs with a p-i-n-Junction Photodiode—H. Inaba and A. E. Siegman. (*Proc. IRE (Correspondence)*, vol. 50, pp. 1823-1824; August, 1962.) Experimental results are given on the operation of a photodiode as a mixer in an optical superheterodyne system using microwave-modulated light.
- 538.569.4:621.375.9:535.61-2** **3651**
Optical Harmonic Frequency Ratio Measurements—I. D. Abella. (*Proc. IRE (Correspondence)*, vol. 50, pp. 1824-1825; August, 1962.) Simultaneous observation of the fundamental and second harmonic produced by a high-intensity ruby maser does not indicate discrepancies in the expected frequency ratio, within experimental limits and allowing for purely instrumental shifts.
- 538.569.4:621.375.9:535.61-2** **3652**
Single-Sideband Suppressed-Carrier Modulation of Coherent Light Beams—C. F. Bührer, V. J. Fowler and L. R. Bloom. (*Proc. IRE*, vol. 50, pp. 1827-1828; August, 1962.) The electro-optic effect on KDP crystals [see also 3430 of 1961 (Kaminow)] is used in the modulator described, which has been tested at AF for modulating the light produced by a gas laser.
- 538.569.4:621.375.9:535.61-2** **3653**
A Total-Reflection Solid-State Optical-Maser Resonator—L. Bergstein, W. Kahn, and C. Shulman. (*Proc. IRE*, vol. 50, p. 1833; August, 1962.) The configuration proposed uses total internal reflection for the light beam in the resonator and frustrated total reflection via a coupling prism for the output coupling. The system may be used to support two mutually independent resonance waves traveling in opposite directions.
- 538.569.4:621.375.9:535.61-2** **3654**
A Method for Calibration of Laser Energy

Output—A. L. Glick. (Proc. IRE (*Correspondence*), vol. 50, p. 1835; August, 1962.) The energy output is calibrated by attenuating the laser beam with neutral filters and directing it into a phototube; the current produced is then integrated.

538.569.4:621.375.9:535.61-2 3655

Generation and Radiation of Ultramicrowaves by Optical Mixing—O. P. Gandhi. (Proc. IRE, vol. 50, pp. 1929-1830; August, 1962.) The nonlinear mixing system discussed provides for the generation of the beat frequency between laser beams operating at different temperatures, and for the highly directional radiation of these microwaves.

538.569.4:621.375.9:535.61-2 3656

Direct Observation of Longitudinal Modes in the Output of Optical Masers—R. C. Duncan, Jr., Z. J. Kiss, and J. P. Wittke. (*J. Appl. Phys.*, vol. 33, pp. 2568-2569; August, 1962.) Modes were observed in U:CaF₂ and ruby masers with a high-resolution spectrometer. Mode spacings are in reasonable agreement with theory.

GEOPHYSICAL AND EXTRA-TERRESTRIAL PHENOMENA

523.16 3657

The Solar Wind—E. N. Parker. (*J. Res. NBS*, vol. 65D, pp. 537-542; November/December, 1961.) A concise review of the theory of interplanetary plasmas, fields, and cosmic-ray variations, based on the solar-wind model of interplanetary dynamical processes.

523.164 3658

A System of Digital Analysis for Radio Astronomy using a Fully Steerable Telescope—C. G. T. Haslam, J. G. Davies, and M. I. Large. (*Monthly Notices Roy. Astron. Soc.*, vol. 124, pp. 169-178; June, 1962.)

523.164 3659

Intense Shell Sources of Radio Emission—H. van der Laan. (*Monthly Notices Roy. Astron. Soc.*, vol. 124, pp. 179-187; June, 1962.) Observational evidence for the existence of shell sources is cited and conditions under which such sources might be formed are outlined.

523.164.3 3660

A Survey of the Anticentre Region of the Galaxy at 237 Mc/s—R. D. Davies and C. Hazard. (*Monthly Notices Roy. Astron. Soc.*, vol. 124, pp. 147-154; June, 1962.)

523.164.3 3661

Faraday Rotation of Polarized Galactic Radio Emission—R. Wiebeleski and J. R. Shakeshaft. (*Nature*, vol. 195, pp. 982-983; September, 1962.) Polarization measurements at 408 Mc of radiation from certain areas of the sky have revealed a small linearly polarized component. Variations of the direction of the phase of polarization of this component are found to be related to the Faraday rotation angle of the ionosphere. Outside the ionosphere its direction tends to be perpendicular to the galactic plane.

523.164.3 3662

10-cm Observations of Venus near Superior Conjunction—F. D. Drake. (*Nature*, vol. 195, p. 894; September, 1962.) Results confirm earlier observations in indicating little difference between surface temperatures of the illuminated and dark hemispheres of the planet.

523.164.3 3663

Measurements of the Polarization and Angular Extent of the Decimeter Radiation from Jupiter—D. Morris and G. L. Borge. (*Astrophys. J.*, vol. 136, pp. 276-282; July, 1962.)

523.164.3 3664

A Possible Explanation for Jovian Decimeter Bursts—S. E. Strom and K. M. Strom. (*Astrophys. J.*, vol. 136, pp. 307-309; July, 1962.) Signals from weak RF sources occulted by Jupiter are focused by the Jovian atmosphere close to the earth's orbit. A correlation is shown between burst length and the apparent speed of Jupiter against the star background.

523.164.3 3665

Microwave Spectrum of Saturn—F. D. Drake. (*Nature*, vol. 195, pp. 893-894; September, 1962.) Results of observations at 10 cm λ on Saturn, combined with those of Cook, *et al* (135 of 1961), indicate that the emissions are almost entirely of thermal origin.

523.164.32 3666

Characteristics of Type III Radio Bursts—J. M. Malville. (*Astrophys. J.*, vol. 136, pp. 266-275; July, 1962.) Observations of the drift rate, duration, and frequency range of Type III bursts between 580 and 8 Mc are discussed.

523.164.32 3667

Association of Centimetre-Wave Bursts with Different Spectral Types of Metre-Wave Bursts of Solar Radio Emission—M. R. Kundu. (*J. Geophys. Res.*, vol. 67, pp. 2695-2706; July, 1962.) A statistical analysis is made of the characteristics of cm- λ bursts associated with different spectral types of m- λ burst in the range 100-580 Mc.

523.165 3668

Some Features of the Response of Neutron Monitors to Low-Energy Particles Incident on the Top of the Atmosphere—W. Webber. (*Canad. J. Phys.*, vol. 40, pp. 906-923; July, 1962.) Comparison of primary particle flux above the atmosphere with that recorded by neutron monitors at sea level shows that low-energy primaries contribute more to sea-level measurements than was previously thought.

523.165 3669

Observation of the Van Allen Radiation Regions during August and September 1959: Part 4—The Outer-Zone Electrons—R. L. Arnoldy, R. A. Hoffman and V. R. Winekler. (*J. Geophys. Res.*, vol. 67, pp. 2595-2612; July, 1962.) A report of Explorer VI data obtained when the count-rate time variations and the geomagnetic activity were low. Part 3: 1534 of May (Hoffman, *et al.*).

523.165 3670

Forbush Decreases produced by Diffusive Deceleration Mechanism in Interplanetary Space—H. Laster, A. M. Lenchev, and S. F. Singer. (*J. Geophys. Res.*, vol. 67, pp. 2639-2643; July, 1962.) A Forbush decrease is explained in terms of a diffusive deceleration mechanism in turbulent interplanetary magnetic plasma clouds. Cosmic rays lose energy in an inverse Fermi mechanism and by betatron action in the weakening magnetic field of an expanding cloud.

523.165 3671

Detection of the Radiation Anomaly above the South Region of the Atlantic Ocean at Heights of 310-340 km.—L. V. Kurnosova, T. N. Kolobyanina, V. I. Logachev, L. A. Razorenov, I. A. Sirotkin, and M. I. Fradkin. (*Isk. Sput. Zemli*, No. 8, pp. 90-93; 1961, English Translation, *Planet-Space Sci.*, vol. 9, pp. 513-516; August, 1962.)

523.165 3672

An Extremely Intense Electron Flux at 1000-Kilometre Altitude in the Auroral Zone—B. J. O'Brien and C. D. Laughlin. (*J. Geophys. Res.*, vol. 67, pp. 2667-2672; July, 1962.) An intense flux of dumped electrons at 1000 km altitude was observed with Injun I. No variation in flux was detected by Explorer XII at several earth radii on the same magnetic shell.

tion in flux was detected by Explorer XII at several earth radii on the same magnetic shell.

523.165:523.75 3673

Measurement of the Intensity of Charged Particles after the Chromospheric Flare of the 7th July 1958—E. V. Gorchakov and G. A. Bazilevskaya. (*Isk. Sput. Zemli*, No. 8, pp. 84-86; 1961, English translation, *Planet-Space Sci.*, vol. 9, pp. 507-509; August, 1962.) Satellite data showed a marked ionization increase between the eruption and the subsequent magnetic storm.

523.165:523.75 3674

The Flux of Heavy Nuclei in the July 10, 1959, Flare—S. Biswas. (*J. Geophys. Res.*, vol. 67, pp. 2613-2615; July, 1962.) Emulsion measurements are given for the range 150-500 Mev per nucleon.

523.165:523.75 3675

The Measurement of the Cut-Off Rigidity at Minneapolis using Solar Protons and α Particles from July 10, 1959, Flare—P. S. Freier. (*J. Geophys. Res.*, vol. 67, pp. 2617-2626; July, 1962.) The solar beam at Churchill (not affected geomagnetically) is compared with the magnetically controlled flux at Minneapolis.

523.165:523.75 3676

Gamma Rays from the Solar-Cosmic-Ray-Produced Nuclear Reactions in the Earth's Atmosphere and Lower Limit on the Energy of Solar Protons observed at Minneapolis—P. D. Bhavsar. (*J. Geophys. Res.*, vol. 67, pp. 2627-2637; July, 1962.)

523.165:550.38 3677

The Magnetic Field of the Quiet-Time Proton Belt—S. I. Akasofu, J. C. Cain, and S. Chapman. (*J. Geophys. Res.*, vol. 67, pp. 2645-2647; July, 1962.) The magnetic field of a model proton belt, which is analogous to that measured by Explorer XII, is computed numerically. The equatorial magnetic field at the earth's surface due to this belt is about 38 γ .

523.165:550.385.4 3678

Geomagnetic-Storm Effects on Charged Particles—T. Obayashi. (*J. Geomag. Geoelect.*, vol. 13, Nos. 1/2, pp. 26-32; 1961.) The change in geomagnetic cut-off, for a model in which the magnetic storm is equivalent to an impressed uniform field, is calculated; it compares favorably with observations of cosmic rays and ionospheric absorption.

523.165:550.385.4 3679

Cosmic-Ray Threshold Rigidities during the Magnetic Storm of November 12, 1960—C. J. Hatton and P. L. Marden. (*Phil. Mag.*, vol. 7, pp. 1145-1156; July, 1962.) During the storm the magnetic threshold rigidity for particles reaching the earth was lowered all over the world. That this reduction was anisotropic in longitude is explained by streaming solar plasma drawing out the geomagnetic lines of force on the night side of the earth.

523.165:551.594.5 3680

Distribution in Space of the Earth's Outer Radiation Belt and the Auroral Zones—E. V. Gorchakov. (*Isk. Sput. Zemli*, pp. 81-83; 1961.) English translation, *Planet-Space Sci.*, vol. 9, pp. 503-505; August, 1962.) The boundary of the belt and the position of maximum intensity within it located by satellite, indicate that outer-belt particles are not the cause of auroras.

523.5+551.594.5:621.396.677 3681

Some Radar Observations of Meteors and Aurorae at 300 and 500 Mc/s using a Large Radio Telescope—D. Barber, H. K. Sutcliffe and C. D. Watkins. (*J. Atmos. Terr. Phys.*, vol. 24, pp. 585-607; July, 1962.) **Part 1**—Observations of Meteors (pp. 585-597). **Part 2**—Observations of the Aurora Borealis (pp.

599-607).—The observations were made with a high-power transmitter installed on the Jodrell Bank 250-ft radio telescope.

523.746.5 3682

A Quick Method for Estimating the Stage of the Sunspot Cycle—W. B. Chadwick. (*J. Res. NBS*, vol. 65D, pp. 637-640; November/December, 1961.) The method given is based on the maximum median hourly value of foF2 for each month as observed at Washington, D.C. Regression equations and standard errors are also included.

523.75 3683

The Solar Geophysical Events of November 1960—T. Obayashi. (*J. Geomag. Geoelect.*, vol. 13, nos. 1/2, pp. 11-25; 1961.)

523.75:523.165:550.385.4 3684

Solar Magnetic Cloud Producing Cosmic-Ray Storm, Magnetic Storm and Type VI Solar Radio Outburst—Y. Kamiya. (*J. Geomag. Geoelect.*, vol. 13, nos. 1/2, pp. 33-41; 1961.) An analysis of several years' data shows that eruptions on the sun accompanied by Type IV RF emission are the cause of the cosmic-ray storms at the earth. Magnetic storms are greatest when produced by flares near the sun's central meridian, but the intensity of cosmic-ray storms is independent of the heliographic longitude of the eruption.

550.37 3685

The Solar and Lunar Daily Variations of Earth Currents Near the Magnetic Equator—R. Hutton. (*J. Atmos. Terr. Phys.*, vol. 24, pp. 673-680; August, 1962.) One conclusion from a detailed study of equatorial earth currents is that they are enhanced by the electrojet.

550.385.4+551.594.5 3686

On the Bennett-Hulburt Hypothesis of the Origin of Magnetic Storms and Aurorae—V. C. A. Ferraro and D. M. Willis. (*Astrophys. J.*, vol. 136, pp. 288-303; July, 1962.) A detailed analysis and criticism of the Bennett-Hulburt hypothesis (126 of 1955). The currents in solar streams are shown to be several orders of magnitude smaller than those of even minor magnetic storms.

550.385.4:523.75 3687

Dependence of Interval between Flare and Associated Sudden-Commencement Storm on Prestorm Conditions—M. W. Haurwitz. (*J. Geophys. Res.*, vol. 67, pp. 2979-2982; July, 1962.) The time delay between a sudden commencement and its "parent" flare is least for those s.c.'s which have been preceded by high magnetic activity.

550.385.4:523.75 3688

On the Choice of Condition to Apply at the Boundary of the Geomagnetic Field in the Steady-State Chapman-Ferraro Problem—J. R. Spreiter and B. R. Briggs. (*J. Geophys. Res.*, vol. 67, pp. 2983-2985; July, 1962.) A previous discrepancy in the boundary condition applicable to the steady-state Chapman-Ferraro problem is resolved, and a previous paper (1541 of May) is amended.

551.507.362.1/2 3689

The Study of the Ionosphere and Interplanetary Gas by means of Artificial Earth Satellites and Space Rockets (Methods and some Results of Radio Investigations)—Ya. L. Alpert. (*Isk. Sput. Zemli*, no. 7, pp. 125-169; 1961, English translation, *Planet Space Sci.*, vol. 9, pp. 391-433; July, 1962.) Measurements made since 1953 by rocket and satellite techniques are discussed. 49 references.

551.507.362.1 3690

A Review of Upper-Atmosphere Rocket Research in Japan—K. Maeda and K. Hiaro. (*Planet Space Sci.*, vol. 9, pp. 355-369; July,

1962.) A description of the launching facilities, rocket equipment and results of the current research program, with a note on future plans.

551.507.362.2 3691

Satellite Orbit Perturbations due to Radiation Pressure and Luni-solar Forces—R. R. Allan. (*Quart. J. Mech. Appl. Math.*, vol. 15, pt. 3, pp. 283-301; August, 1962.) A vectorial method is used to determine the perturbations of the orbit assuming that the perturbing body remains fixed during one revolution of the satellite.

551.507.362.2 3692

The Influence of Lunar and Solar Attraction on the Motion of an Artificial Earth Satellite—A. V. Egorova. (*Isk. Sput. Zemli*, no. 8, pp. 46-56; 1961, English translation, *Planet Space Sci.*, vol. 9, pp. 479-490; August, 1962.) The perturbations are determined using Lagrange's planetary equations and taking the orbit of the perturbing body as the reference plane.

551.507.362.2 3693

General Solution of the Problem of the Motion of an Artificial Satellite in the Normal Field of the Earth's Attraction—E. P. Akseonov, E. A. Grebenikov, and V. G. Demin. (*Isk. Sput. Zemli*, no. 8, pp. 64-71; 1961, English translation, *Planet Space Sci.*, vol. 9, pp. 491-498; August, 1962.) The motion of a satellite in an oblate potential field is studied using generalized coordinates and Lagrange's equations of motion. The method of an independent variable is used for the integration.

551.510.535+523.164.32 3694

Scattering and Conversion Cross-Sections in Inhomogeneous Plasma—M. H. Cohen. (*J. Geophys. Res.*, vol. 67, pp. 2729-2739; July, 1962.) A general scattering theory is developed for a magnetic-field-free plasma, allowing for both transverse and longitudinal waves. Special features of the cross-section formula are discussed and ionospheric incoherent-scatter experiments and solar RF bursts are considered quantitatively.

551.510.535 3695

Corpuscular Heating of the Upper Atmosphere—H. K. Paetzold. (*J. Geophys. Res.*, vol. 67, pp. 2741-2744; July, 1962.) Satellite drag data are used to examine the dependence of temperature on solar activity. Two-thirds of the energy influx originates from ultraviolet radiation and one-third from interplanetary corpuscles.

551.510.535 3696

Upper Atmosphere Turbulence Determined by means of Rockets—J. E. Blamont and C. de Jager. (*J. Geophys. Res.*, vol. 67, pp. 3113-3119; July, 1962.) Paper presented at a symposium on fundamental problems in turbulence, Marseilles, September 4-9, 1961. The results discussed are based on investigations with the aid of Na vapor trails at heights between 80 and 120 km.

551.510.535 3697

D-Region Ionization by Solar X Rays—E. G. Poppoff and R. C. Whitten. (*J. Geophys. Res.*, vol. 67, pp. 2986-2988; July, 1962.) By using the X-ray spectra reported by Kreplin (4097 of 1961) it is shown that X rays can make an important contribution to ionization in the range 70-90 km, at least during periods of sunspot maximum.

551.510.535 3698

Electron Cooling in the D Region—A. Dalgarno and R. J. Moffett. (*Planet Space Sci.*, vol. 9, pp. 355-369; July, 1962.) A theoretical treatment for N₂ and O₂ from which the mean rate of electron energy loss is calculated for gas temperatures in the range 100-1000°K.

551.510.535 3599

The Reflection Characteristics of a Patchy

Sporadic-E Layer—J. D. Whitehead. (*J. Atmos. Terr. Phys.*, vol. 24, pp. 681-684; 1962.) An explanation is given of the insensitivity of foEs and fBEs to gain changes of an ionosonde; fBEs is the better measure of the peak electron density in the layer.

551.510.535 3700

The Thermal Balance of the Ionospheric F Region—C. H. Cummack. (*J. Atmos. Terr. Phys.*, vol. 24, pp. 691-699; August, 1962.) Heating of the F region by ionizing radiation, and cooling by conduction and radiation, are considered. When simplifications are made, the equations can be solved to give the variation of temperature with height and local time.

551.510.535 3701

Lunar Variations of Spread-F—B. V. Krishnamurthy and B. R. Rao. (*J. Atmos. Terr. Phys.*, vol. 24, pp. 742-743; August, 1962.) Harmonic analysis of spread-F indices at Waltair yields small lunar diurnal and semi-diurnal components.

551.510.535 3702

Vertical Transport of Electrons during Pre-sunrise F-Layer 'Splitting'—P. Bandyopadhyay and S. K. Chatterjee. (*Indian J. Phys.*, vol. 36, pp. 124-128; March, 1962.) An extension of earlier work (501 of 1960). The observed splitting of the layer is associated with a strong upward movement of the upper part of the layer and also with low values of magnetic K index.

551.510.535 3703

Ionospheric Drift Measurement—E. Harnischmacher. (*Arch. tech. Messen*, pp. 147-150; July, 1962.) Various methods are summarized including those based on fading, meteor echoes and fluctuations of noise from radio stars.

551.510.535:550.382 3704

Study of the Geomagnetic Anomaly during Sunspot Maximum—C. S. R. Rao. (*J. Atmos. Terr. Phys.*, vol. 24, pp. 729-737; August, 1962.) Critical-frequency and N(h) data obtained for a number of stations during September, 1957 and March, 1958, are used to study the geomagnetic anomaly in the F2 region.

551.510.535:550.385 3705

Intensification of the Earth's Magnetic Field by Turbulence in the Ionosphere—H. K. Moffatt. (*J. Geophys. Res.*, vol. 67, pp. 3071-3073; July, 1962.) Paper presented at a symposium on fundamental problems in turbulence, Marseilles, September 4-9, 1961. The problem of ionospheric turbulence is treated for the case of a large-scale weak magnetic field applied to the system. Large fluctuations may arise for magnetic Reynolds number $\gg 1$.

551.510.535:551.594.5 3706

Electron Precipitation accompanying Ionospheric Current Systems in the Auroral Zone—J. R. Bascus and R. R. Brown. (*J. Geophys. Res.*, vol. 67, pp. 2673-2680; July, 1962.) Magnetic bays developing out of quiet conditions are examined to obtain information on current systems. Links with the auroral morphology of Davis (1570 of May) are suggested.

551.510.535:551.594.5 3707

Time, Height, and Latitude Distribution of D Layers in the Subauroral Zone and their Relation to Geomagnetic Activity and Aurora—A. Pedersen. (*J. Geophys. Res.*, vol. 67, pp. 2685-2694; July, 1962.) Observations of echoes in the range 60-90 km at stations in northern Sweden during disturbed periods.

551.510.535:621.3.087.4 3708

Design of Panoramic Ionospheric Recorders—L. H. Heiser and L. D. Wilson. (*J. Res. NBS*, vol. 65D, pp. 629-636; November/

December, 1961.) Design aspects are discussed and the technical data of a transportable ionosonde are summarized (see 3709 below).

551.510.535:621.3.087.4 3709
An Electronically Scanned Panoramic Ionospheric Recorder—L. D. Wilson. (*Aust. J. Appl. Sci.*, vol. 13, pp. 89-97; June, 1962.) Linear or logarithmic sweeps of variable duration for the frequency range of 0.1-20 Mc or any part of that range may be made. The transmitter which operates normally at 5.5 kW \pm 1 dB, has a subsidiary amplifier to boost the output to 44 kW \pm 3 db. See 517 of February (Heisler and Wilson).

551.510.535:621.396.674.3 3710
The Impedance of a Short Cylindrical Dipole in the Ionosphere—Bramley. (See 3581.)

551.510.535(98):523.75 3711
Characteristics of Solar Energetic Particles which Excite Polar-Cap Blackouts—K. Simno. (*J. Geomag. Geoelect.*, vol. 13, pp. 1-10; 1961.) The association of S and G types of pca event (see 2977 of 1961) with flare position, geomagnetic disturbance and solar RF bursts is examined.

551.510.536 3712
'Scale Frequency' of the Exosphere—R. L. Dowden. (*Nature*, vol. 195, pp. 984-985; September, 1962.) The parameter "scale frequency" is defined in terms of the whistler nose frequency and the gyro-frequency. Applications to theoretical studies on a model or real exosphere are noted.

551.594.5 3713
A Comparison of Auroral-Zone X-Ray Observations from Periods with Different Levels of Solar Activity—R. R. Brown. (*J. Geophys. Res.*, vol. 67, pp. 2681-2684; July, 1962.) The comparison shows a decline in the frequency of events with solar activity.

551.594.5:523.165 3714
A Charge Separation Mechanism for the Production of Polar Auroras and Electrojets—J. W. Kern. (*J. Geophys. Res.*, vol. 67, pp. 2649-2665; July, 1962.) Charge separation in the geomagnetically trapped radiation is invoked to explain some observed phenomena associated with polar auroras and electrojet current systems.

551.594.5:550.385.4 3715
Large-Scale Auroral Motions and Polar Magnetic Disturbances: Part 2—The Changing Distribution of the Aurora during Large Magnetic Storms—S. I. Akasofu. (*J. Atmos. Terr. Phys.*, vol. 24, pp. 723-727; August, 1962.) During the great magnetic storms of September 23, 1957, and February 11, 1958, the northern border of auroral activity moved southwards leaving the usual region of most frequent aurorae deserted. Part 1: 198 of 1961.

551.594.6 3716
A further Note on Terrestrial Extremely-Low-Frequency Propagation in the Presence of an Isotropic Ionosphere with an Exponential Conductivity/Height Profile—J. Galejs. (*J. Geophys. Res.*, vol. 67, pp. 2715-2728; July, 1962.) Various electron-density data, particularly those relating to the night-time ionosphere are examined with reference to the elf wave analysis of 147 of January.

551.594.6 3717
Duration and Spacing of Sferic Pulses—R. F. Linfield and C. A. Samson. (*Proc. IRE*, vol. 50, pp. 1841-1842; August, 1962.) Report on an analysis of waveforms of atmospherics recorded simultaneously at two stations.

551.594.6:539.16 3718
Sudden Enhancement of Atmospherics associated with High-Altitude Nuclear Explosions—M. K. Das Gupta and A. K. Sen. (*J. Atmos. Terr. Phys.*, vol. 24, pp. 739-740; August, 1962.)

Atmospheric noise records at 120 kc show sudden enhancement effects associated with the Russian high-altitude nuclear explosions of 1961.

551.594.6:551.510.536 3719
On the Origin of "Very-Low-Frequency Emissions"—H. Unz. (*J. Atmos. Terr. Phys.*, vol. 24, pp. 685-689; August, 1962.) The magneto-ionic theory for drifting plasma is applied to the theory of the origin of VLF emissions. The frequency at which there will be interaction, and possibly amplification, between two different streams of electrons is found. Physical phenomena are explained by interaction between several streams of electrons of different plasma frequency and different velocity.

551.594.6:621.391.82 3720
On the Spectrum of Terrestrial Radio Noise at Extremely Low Frequencies—(See 3848.)

LOCATION AND AIDS TO NAVIGATION

621.396.93.029.45 3721
The Use of V.L.F. Transmissions for Navigation—C. Powell. (*J. Inst. Nav.*, vol. 15, pp. 277-288; July, 1962. Discussion.) A survey of proposed VLF navigational aids, their expected performance and installation problems. The accuracies required are discussed together with other methods of providing the facilities needed for modern navigation.

621.396.932/.933:621.391.812.63.029.45 3722
Effects of the Ionosphere of V.L.F. Navigational Aids—W. T. Blackband. (*J. Res. NBS.*, vol. 65D, pp. 575-580; November/December, 1961.) The feasibility of basing worldwide navigational aids on VLF transmissions is discussed. Preliminary aircraft measurements show that fixes obtained are internally consistent to within one nautical mile at ranges between 5000 and 6000 miles.

621.396.962.3 3723
The Echo Noise Ratio Obtainable in Radar by means of Pulse Compression—V. Palermo; U. Tiberio. (*Alta Frequenza*, vol. 31, p. 235; April, 1962.) Comment on 1581 of May and author's reply.

621.396.967.2:621.396.65 3724
Radio-Relay Networks for the Elbe and Weser Shore-Based radar Systems—H. J. Kramer. (*Philips Telecommun. Rev.*, vol. 23, pp. 130-146; July, 1962.) Radar signals are relayed in the 7-Gc band from radar stations to operational centres. Frequency-diversity reception methods are used. See 1530 of 1961 (le Compte, et al.).

MATERIALS AND SUBSIDIARY TECHNIQUES

535.215:546.817-31 3725
Overshoot in Photoconductivity of Lead Oxide—K. E. Haq. (*J. Appl. Phys.*, vol. 33, pp. 2606-2612; August, 1962.) Overshoot is due to build-up of space charge in the bulk of the material. It is only observed in the range -50 to +70°C.

535.37:537.226 3726
Dielectric Anomalies in Zinc Sulphide and Cadmium Sulphide Excited by Light—T. Fujimura and K. Kamiyoshi. (*Sci. Rep. Res. Inst. Tohoku Univ., Ser. A.*, vol. 13, pp. 466-476; December, 1961.) Details of experiments on the Debye effect in ZnS phosphors and anti-Debye effect in CdS phosphors are given. Results are interpreted in terms of a two-layer model [162 of 1952 (Koops)].

537.227 3727
Domain Walls Caught in Sudarés in Rochelle Salt Crystal—K. Ohi and T. Nakamura. (*J. Phys. Soc. Japan*, vol. 17, p. 1195;

July, 1962.) Simultaneous observation of both sudarés and ferroelectric domains under direct and alternating fields is reported.

537.227:546.431'824-31 3728
Some Observations on Switched Single-Crystal Barium Titanate—D. S. Campbell. (*Phil. Mag.*, vol. 7, pp. 1157-1166; July, 1962.) Results are given for various polarization states of an etched single crystal.

537.227:546.431'824-31:539.12.04 3729
Radiation Damage on BaTiO₃ Single Crystal—S. Hayawaka and H. Ikushima. (*J. Phys. Soc. Japan*, vol. 17, pp. 1198-1199; July, 1962.) Experimental note on the effect of γ irradiation.

537.227:546.431'824-31:539.23 3730
Electron-Optical Studies of Barium Titanate Single-Crystal Films—M. Tanaka, N. Kitamura, and G. Honjo. (*J. Phys. Soc. Japan*, vol. 17, pp. 1197-1198; July, 1962.)

537.227:621.318.57 3731
Increase in Dielectric Constant during Switching in Barium Titanate and Triglycine Sulphate—E. Fatuzzo. (*J. Appl. Phys.*, vol. 33, pp. 2588-2596; August, 1962.) Measurements at frequencies up to 2 Gc reveal two relaxation levels, one previously measured by Landauer, et al., (3759 of 1956) and a new one at much higher frequencies; 100 Mc for triglycine sulphate and above 2 Gc for BaTiO₃.

537.228.1/2 3732
Piezoelectric Properties of Triglycine Sulphate—T. Ikeda, T. Tanaka, and H. Toyoda. (*Jap. J. Appl. Phys.*, vol. 1, pp. 13-21; July, 1962.) Induced piezoelectricity and electrostrictive effects are examined for temperature dependence, and influence of irradiation.

537.228.1 3733
Rotating Disk of Piezoelectric Crystals—H. S. Paul. (*Aust. J. Appl. Sci.*, vol. 13, pp. 98-106; June, 1962.) The mechanical stresses and electric field developed in the disk are calculated.

537.228.1:538.222 3734
The Generation of Microwave Phonons for Studying the Spin-Lattice Interaction—P. H. Carr and M. W. P. Strandberg. (*J. Phys. Chem. Solids*, vol. 23, pp. 923-937; July, 1962.) Phonon packets were produced by the piezoelectric effect and their interaction with paramagnetic impurities in quartz was studied.

537.228.1:549.514.51 3735
Higher-Order Temperature Coefficients of the Elastic Stiffnesses and Compliances of Alpha-Quartz—R. Bechmann, A. D. Ballato, and T. J. Lukaszek. (*Proc. IRE*, vol. 50, pp. 1812-1822; August, 1962.) The frequency/temperature characteristics of AT-, BT-, CT- and DT-cut crystals are considered on the basis of new calculations of elasticity and temperature coefficients. For German version see *Arch. elekt. Übertragung*, vol. 16, pp. 307-313; June, 1962. (Bechmann).

537.228.2 3736
Investigations on Ceramic Electrostrictive Materials as a Function of their State of Polarization—K. Fehér and W. Schmidt. (*Acustica*, vol. 12, pp. 173-179; 1962. In German.) A method is described for measuring the intrinsic energy inherent in polarized ceramic materials. An "electrostriction constant" is determined from measurements on BaTiO₃ specimens.

537.311.32 3737
Electrons and Holes in Bismuth—A. L. Jain and S. H. Koenig. (*Phys. Rev.*, vol. 127, pp. 442-446; July, 1962.) An examination of recent data shows that there are three electron ellipsoids and one light-hole ellipsoid in momentum space for Bi.

- 537.311.33 3738
Quantitative Measurements of Semiconductor Homogeneity from Plasma Edge—D. F. Edwards and P. D. Maker. (*J. Appl. Phys.*, vol. 33, pp. 2466–2468; August, 1962.) This method based on the position of the plasma edge is an order of magnitude more sensitive than previous ones. A demonstration with an InAs sample is described.
- 537.311.33 3739
Dipole Scattering from Ion Pairs in Compensated Semiconductors—R. Stratton. (*J. Phys. Chem. Solids*, vol. 23, pp. 1011–1017; July, 1962.) Scattering cross-sections for unscreened and screened dipoles are derived and compared with those for point charges. Electron mobility is calculated for electron scattering by dipoles only and the combined effects of dipoles, point charges and vibrations are considered.
- 537.311.33 3740
Scattering of Charge Carriers from Point Imperfections in Semiconductors—T. Morimoto and K. Tani. (*J. Phys. Soc. Japan*, vol. 17, pp. 1121–1128; July, 1962.) A calculation of the scattering is made using the Born approximation and taking account of strain scattering due to point defects. A considerable interference effect is found between the Coulomb scattering and the scattering due to lattice distortion. This could explain the difference in electron mobilities between Sb-doped and As-doped Ge.
- 537.311.33 3741
Effect of Surface Recombination on the Law of Decrease of Excess Minority Carriers in a Semiconductor—A. Fortini. (*J. Phys. Radium*, vol. 23, pp. 273–276; May, 1962.) The total number of excess carriers at a given time is computed for optical excitation of a semi-infinite and finite one-dimensional crystal.
- 537.311.33 3742
Space-Charge-Layer Width and Capacitance of Symmetrical Step Junctions—C. C. Wang. (*Proc. IRE (Correspondence)*, vol. 50, pp. 1838–1839; August, 1962.) For step junctions the inductance effect noted at high forward bias voltages is associated with the drop of quasi-Fermi levels in the neutral regions in which the corresponding carriers are majority carriers.
- 537.311.33 3743
The Dielectric Constant of a Semiconductor as related to the Intrinsic Activation Energy—C. F. Cole, Jr. (*Proc. IRE (Correspondence)*, vol. 50, pp. 1856; August, 1962).
- 537.311.33:519.4 3744
Group Theory and the Energy Band Structure of Semiconductors—A. Nussbaum. (*Proc. IRE*, vol. 50, pp. 1762–1781; August, 1962.) The concepts of group theory are explained and applied to the determination of band structure in Te.
- 537.311.33:535.215 3745
Observation of Photovoltaic Oscillations in Semiconductors—L. Gold. (*J. Phys. Soc. Japan*, vol. 17, p. 1193; July, 1962.) A theory is given to explain oscillations observed by Kikuchi and Abe (2013 of June).
- 537.311.33:535.215 3746
Theory of Photoelectric Emission from Semiconductors—E. O. Kane. (*Phys. Rev.*, vol. 127, pp. 131–141; July, 1962.) The variation of yield with energy near threshold is found for a general band structure, and for several production and scattering mechanisms. The distributions of the emitted carriers in energy and direction are also calculated.
- 537.311.33:537.228.1 3747
Current Saturation in Piezoelectric Semiconductors—R. W. Smith. (*Phys. Rev. Lett.*, vol. 9, pp. 87–90; August, 1962.) Observations of current saturation in CdS are reported. It is believed to be due to saturation of the shift velocity of electrons.
- 537.311.33:537.312.9 3748
Resistance of Elastically Deformed Shallow *p-n* Junctions—W. Rinder. (*J. Appl. Phys.*, vol. 33, pp. 2479–2480; August, 1962.) The resistance of diffused and alloyed junctions was found to be highly sensitive to stress under both forward and reverse bias.
- 537.311.33:538.614 3749
Oscillatory Interband Faraday Rotation and Voigt Effect in Semiconductors—Y. Nishina, J. Kolodziejczak, and B. Lax. (*Phys. Rev. Lett.*, vol. 9, pp. 55–57; July, 1962.) Results of experiments on thin Ge samples in fields up to 90 kG at room temperature are shown graphically.
- 537.311.33:538.614 3750
Faraday Effect in Semiconductors—I. M. Boswarwa, R. E. Howard and A. B. Lidiard. (*Proc. Roy. Soc. (London), A*, vol. 269, pp. 125–141; August, 1962.) Calculations are carried out on the Faraday rotation in semiconductors due to four kinds of electron transition. The dependence of these on frequency is studied.
- 537.311.33:538.63 3751
Galvano-thermodynamic Effects in Degenerate Semi-conductors and Semimetals with Nonparabolic Band Shapes: Part 2—General Theory—T. C. Harman and J. M. Honig. (*J. Phys. Chem. Solids*, vol. 23, pp. 913–922; July, 1962.) A general theory of galvano-thermodynamic phenomena has been derived for a band with spherically symmetric energy surfaces. The magnitudes of all 560 effects can be predicted from a small number of measurements.
- 537.311.33:539.12.04 3752
Radiation Effects in Semiconductors—G. Wertheim. (*Nucleonics*, vol. 20, pp. 47–50; July, 1962.) The effects of irradiation are (a) ionization, which has a temporary effect and (b) displacements, which cause permanent damage.
- 537.311.33:[546.28+546.289] 3753
Diffusion of Vacancies during Quenching of Ge and Si—J. Melngailis and S. O'Hara. (*J. Appl. Phys.*, vol. 33, pp. 2596–2601; August, 1962.) The concentrations of vacancies trapped in growing Ge and Si dendrites, and in Ge slabs cooled by radiation are calculated. Dislocation loops are unlikely to form in growing dendrites.
- 537.311.33:[546.28+546.289] 3754
Transport Phenomena in Germanium and Silicon—G. E. Tauber. (*J. Phys. Chem. Solids*, vol. 23, pp. 7–18; January/February, 1962.) Matrix elements are calculated for warped energy surfaces, such as occur in Ge or Si, using the appropriate transition probabilities derived by Ehrenreich and Overhauser (1131 of 1957). The general results are applied to the evaluation of the transport quantities for acoustic and optical scattering.
- 537.311.33:[546.28+546.289] 3755
Diffusion of Interstitial Impurities in Germanium and Silicon—R. A. Swalin. (*J. Phys. Chem. Solids*, vol. 23, pp. 154–156; January/February, 1962.) Treatment of diffusion relative to the structure of the diamond lattice, and the development of a semi-empirical equation relating the activation energies to properties of the solute.
- 537.311.33:546.28 3756
Boron-Induced Dislocations in Silicon—D. F. Miller, J. E. Moore, and C. R. Moore. (*J. Appl. Phys.*, vol. 33, pp. 2648–2652; August, 1952.) Effects of gradual increase in B density in Si are described. At 8×10^{18} atoms cm^{-3} , lattice stress is sufficient to induce edge dislocation generation from loop interaction.
- 537.311:546.28 3757
Diffusion of Phosphorus in Silicon from the Azeotrope of Phosphorus Pentoxide and Water—R. P. Lothrop. (*J. Appl. Phys.*, vol. 33, p. 2656; August, 1962.)
- 537.311.33:546.28 3758
***n*-Type Conversion of Thermally Oxidized Si Surface**—H. Edagawa, Y. Morita, S. Makawa, and Y. Imishi. (*J. Phys. Soc. Japan*, vol. 17, pp. 1190–1191; July, 1962.) Results of measurements on oxidized Si junctions suggest that *n*-type conversion is due to imperfections at the Si-SiO₂ interface or in the bulk of SiO₂ film.
- 537.311.33:546.28 3759
Resistivity Changes in Quenched *p*-Type Silicon—W. H. Shepherd. (*J. Phys. Chem. Solids*, vol. 23, pp. 161–163; January/February, 1962.) Some observations on the effect described by Kirvaldige and Zhukov (2669 of 1961).
- 537.311.33:546.28 3760
Field-Effect Measurements on High-Resistivity *p*-Type Silicon—D. Gerlich. (*J. Phys. Chem. Solids*, vol. 23, pp. 837–842; July, 1962.) The distribution of the fast surface states is found to vary with the chemical treatment.
- 537.311.33:546.28 3761
Changes in Silicon under Intensive Bombardment with 50-KeV to 100-keV Electrons—H. Hora. (*Z. angew. Phys.*, vol. 14, pp. 9–12; January, 1962.) A change from *n*- to *p*-type material was observed with a 50-kev beam of intensity 9×10^{22} electrons/cm². This is attributed to Frenkel defects caused by surface effects. For results obtained with Si films see 1608 of May.
- 537.311.33:546.28:535.215 3762
Direct and Indirect Excitation Processes in Photoelectric Emission from Silicon—G. W. Gobeli and F. G. Allen. (*Phys. Rev.*, vol. 127, pp. 141–149; July, 1962.) Atomically clean surfaces, with various degrees of sample doping, have been studied. The results indicate volume excitation processes, both direct and indirect, and agree with Kane's theory (3746 above). A direct escape depth for excited electrons is determined.
- 537.311.33:546.28:535.215 3763
Work Function, Photoelectric Threshold, and Surface States of Atomically Clean Silicon—F. G. Allen and G. W. Gobeli. (*Phys. Rev.*, vol. 127, pp. 150–158; July, 1962.) The results indicate that the surface atom density and surface state density are almost equal for all available degrees of chemical doping.
- 537.311.33:546.28:621.391.822 3764
1/f Noise from Vacuum-Cleaned Silicon—A. U. MacRae. (*J. Appl. Phys.*, vol. 33, pp. 2570–2572; August, 1962.) Elimination of the slow surface states by surface cleaning in high vacuum did not appreciably affect the observed 1/f noise. The noise may be due to some process in the space-charge region.
- 537.311.33:546.289 3765
Direct Observation of Dislocation Looks in Arsenic-Doped Germanium—G. E. Brock and C. L. Aliotta. (*IBM J. Res. Dev.*, vol. 6, pp. 372–374; July, 1962.) Dislocation loops can be produced easily in *n*-type Ge, the impurity-vacancy interaction being important in their formation. Loop formation does occur during annealing of bulk Ge.
- 537.311.33:546.289 3766
Behaviour of Germanium in Gallium Arsenide—L. J. Viehand and T. Seidel. (*J. Appl.*

Phys., vol. 33, pp. 2414-2415; August, 1962.) "The amphoteric behavior of Ge in GaAs has been studied quantitatively for small variations in melt composition around the maximum melting point."

537.311.33:546.289 3767
Nuclear Spin-Lattice Relaxation Time in Germanium—B. J. Wyluda. (*J. Phys. Chem. Solids*, vol. 23, pp. 63-65; January/February, 1962.) Measurements were made on *n*-type Ge samples of resistivity from 30 to 0.01 $\Omega \cdot \text{cm}$ at 295°, 77.2° and 20°K

537.311.33:546.289 3768
Galvanomagnetic Properties of Grain Boundaries in Germanium Bicrystals from 1.25 to 240°K—G. Landwehr and P. Handler. (*J. Phys. Chem. Solids*, vol. 23, pp. 891-906; July, 1962.) Hall effect, magneto-resistance and conductivity of wide angle grain boundaries have been measured.

537.311.33:546.289 3769
Epitaxial Vapour Growth of Single-Crystal Ge—M. Takabayashi. (*Jap. J. Appl. Phys.*, vol. 1, pp. 22-29; July, 1962.) Perfect crystals are made by thermal decomposition of GeI₂. The purity is comparable to the best melt-grown Ge.

537.311.33:546.289 3770
Recombination of Electrons and Donors in *n*-Type Germanium: Part 2—G. Ascarelli and S. Rodriguez. (*Phys. Rev.*, vol. 127, pp. 167-169; July, 1962.) The theory indicates that at liquid-He temperatures impact recombination is more important than the alternative mechanism studied (a two-stage transition) for electron concentrations greater than a given value. For lower concentrations the reverse is true. Part 1: 1328 of April.

537.311.33:546.289 3771
Magnetic Susceptibility of Weakly Interacting Donors in Germanium—D. H. Damon and A. N. Gerritsen. (*Phys. Rev.*, vol. 127, pp. 405-413; July 15, 1962.)

537.311.33:546.289 3772
Surface Storage and Recombination of Carriers in Germanium between 90 and 300°K—K. H. Beckmann and D. Geist. (*Z. angew. Phys.*, vol. 14, pp. 352-358; June, 1962.) The results are analyzed of conductivity and lifetime measurements on *n*-type Ge rods of thickness 0.1 and 1.5 mm and subjected to various forms of thermal, mechanical and chemical treatments.

537.311.33:546.289:538.569.4 3773
Measurements of Relaxation Time in Germanium by the Cyclotron Resonance—M. Fukui, H. Kawamura, I. Imai, and K. Tomishima. (*J. Phys. Soc. Japan*, vol. 17, pp. 1191-1192; July, 1962.)

537.311.33:546.289:539.23 3774
Effect of the Temperature of Formation on the Crystallinity and Electricity Properties of Germanium Films on Fluorite—R. L. Schalla, L. H. Thaller, and A. E. Potter, Jr. (*J. Appl. Phys.*, vol. 33, pp. 2554-2555; August, 1962.)

537.311.33:546.48-31 3775
Semiconductivity and Thermoelectric Power of Cadmium Oxide—E. F. Lambs, and F. C. Tompkins. (*Trans. Faraday Soc.*, vol. 58, pp. 1424-1438; July, 1962.) Wright's equations for fully degenerate semiconductors agree well with experimental results, but Wagner's theory of conduction-electron concentration was irreconcilable with measurements at different oxygen pressures.

537.311.33:546.48'241 3776
Behaviour of Gold in Cadmium Telluride Crystals—I. Teramoto and S. Takayanagi. (*J. Phys. Soc. Japan*, vol. 17, pp. 1137-1141; July, 1962.) The experimentally determined diffusion

coefficient for temperatures above 600°C is $D = 67 \exp(-2.0\text{eV}/kT) \text{ cm}^2 \text{ sec}^{-1}$. Below 400°C, the observed effects are explained by a model involving the segregation of Au atoms to dislocations.

537.311.33:546.48'241 3777
Phase Equilibria in the System Cd-Te—M. R. Lorenz. (*J. Phys. Chem. Solids*, vol. 23, pp. 939-947; July, 1962.) The results provide a foundation for a basic investigation of the semiconductor properties of CdTe.

537.311.33:546.681'18 3778
Some Electrical Properties of *p*-Type Gallium Phosphide—R. J. Cherry and J. W. Allen. (*J. Phys. Chem. Solids*, vol. 23, pp. 163-165; January/February, 1962.) Results of Hall-effect and resistivity measurements are discussed.

537.311.33:546.681'18:535.376 3779
Injection Electroluminescence at *p-n* Junctions in Zinc-Doped Gallium Phosphide—J. Starkiewicz and J. W. Allen. (*J. Phys. Chem. Solids*, vol. 23, pp. 881-884; July, 1962.) The effect on the spectrum of doping with different amounts of Zn and O₂ is shown and discussed.

537.311.33:546.681'19 3780
Diffusion, Solubility and Electrical Behaviour of Li in GaAs Single Crystals—C. S. Fuller and K. B. Wolfstirn. (*J. Appl. Phys.*, vol. 33, pp. 2507-2514; August, 1962.)

537.311.33:546.681'19 3781
Preparation and Characterization of High-Resistivity GaAs—R. W. Haisty, E. W. Mehal, and R. Stratton. (*J. Phys. Chem. Solids*, vol. 23, pp. 829-836; July, 1962.)

537.311.33:546.681'19 3782
Recombination Radiation Emitted by Gallium Arsenide—R. J. Keyes and T. M. Quist. (*Proc. IRE*, vol. 50, pp. 1822-1823; August, 1962.) Measurements of emitted radiation intensity on diffused GaAs diodes biased in the forward direction indicate that at 77°K the efficiency in converting injected holes into photons of energy close to the band gap may be as high as 85 per cent for these diodes. Data on spectral distribution and speed of response for this radiation are given.

537.311.33:546.682'86 3783
Indium Antimonide—a Review of its Preparation, Properties and Device Applications—K. F. Hulme and J. E. Mullin. (*Solid-State Electronics*, vol. 5, pp. 211-247; July/August, 1962.) Aspects of InSb research are covered in which physics, chemistry and metallurgy are involved. 196 references.

537.311.33:546.682'86:539.23 3784
Annealing Effects in Evaporated InSb Films—E. B. Dale and G. Senecal. (*J. Appl. Phys.*, vol. 33, pp. 2526-2530; August, 1962.)

537.311.33:546.817'241 3785
Free-Carrier Absorption in *p*-Type PbTe—H. R. Riedl. (*Phys. Rev.*, vol. 127, pp. 162-166; July, 1962.) Infrared absorption at 4-28 μm was studied at several temperatures in samples with different carrier density. There is additional absorption at intermediate wavelengths, compared with that in *n*-type PbTe.

537.311.33:546.87'24'22 3786
Anisotropy of the Electrical Conductivity and the Seebeck Coefficient of Bi₂Te₃—H. H. Soonpa, (*J. Appl. Phys.*, vol. 33, pp. 2542-2546; August, 1962.)

537.311.33:546.873'241 3787
Effects of Heavy Deformation and Annealing on the Electrical Properties of Bi₂Te₃—J. M. Schultz, J. P. McHugh, and W. A. Filler. (*J. Appl. Phys.*, vol. 33, pp. 2443-2450; August, 1962.) Deformation causing nonbasal slip in Bi₂Te₃ changes the material from *p*- to

n-type and reduces its resistivity by forming an excess of negative carriers. Annealing eventually removes the extra carriers and the material becomes *p* type again. A model is given to account for the observed results.

537.312.62 3788
Critical Fields of Thin Superconducting Films: Part 1—Thickness Effects—A. M. Toxen. (*Phys. Rev.*, vol. 127, pp. 382-386; July, 1962.)

537.312.62 3789
Critical Field of Thin Superconducting Shapes—J. J. Hauser and E. Helfand. (*Phys. Rev.*, vol. 127, pp. 386-390; July, 1962.)

537.312.62 3790
Multiphonon Effects in Tunnelling between Metals and Superconductors—J. M. Rowell, A. G. Chynoweth, and J. C. Phillips. (*Phys. Rev. Lett.*, vol. 9, pp. 59-61; July, 1962.)

537.312.62 3791
Synthetic High-Field, High-Current Superconductor—C. P. Bean, M. V. Doyle, and A. G. Pincus. (*Phys. Rev. Lett.*, vol. 9, pp. 93-94; August, 1962.) A note on the preparation and properties of a filamentary structure made by pressing Hg into porous Vycor glass.

537.312.62 3792
Tunnelling into Superconductors—J. Bardeen. (*Phys. Rev. Lett.*, vol. 9, pp. 147-149; August, 1962.) The use and justification of the semiconductor model is discussed in the light of the method of deriving the tunnelling current of Cohen, *et al.* (2743 of August).

537.312.63 3793
Phenomenological Theory of Superimposed Films of Normal and Superconducting Metals—D. H. Douglass, Jr. (*Phys. Rev. Lett.*, vol. 9, pp. 155-159; August, 1962.) A modification of Cooper's model (3475 of 1961) is proposed, which removes certain inherent difficulties.

537.323:546.863'873'241 3794
Lattice Parameters in the System Antimony Telluride-Bismuth-Telluride—W. R. Bekkedre and O. J. Guentert. (*J. Phys. Chem. Solids*, vol. 23, pp. 1023-1025; July, 1962.) Lattice spacings and unit cell volumes were found over the complete range of composition.

538.221:538.569.4 3795
Nuclear Magnetic Resonance of Fe⁵⁷ in α -Fe₂O₃—M. Matsuura, H. Yasuoka, A. Hirai, and T. Hashii. (*J. Phys. Soc. Japan*, vol. 17, pp. 1147-1154; July, 1962.)

538.221:539.23 3796
Shape-Sensitive Uniaxially Magnetized Domains in Ni-Fe Films—O. W. Mueckenhirn, M. H. Monnier, and P. J. Besser. (*J. Appl. Phys.*, vol. 33, pp. 2632-2635; August, 1962.) Properties of shape-sensitive films and factors influencing their production are described. A hypothesis correlating these factors with the film properties is proposed.

538.221:539.23 3797
Domain Structure in Single-Crystal Thin Films of Iron—Y. Gondo. (*J. Phys. Soc. Japan*, vol. 17, pp. 1129-1136; July, 1962.) Observations of the structure of Fe films evaporated on to MgO cleavage surfaces are discussed.

538.221:539.23 3798
The Temperature Dependence of the Magnetization of Very Thin Iron Films—H. Mayer and D. Stükel. (*Naturwiss.*, vol. 49, pp. 277; June, 1962.) A note on measurements of saturation magnetization as a function of temperature in the range 180-590°K, on Fe films of thickness 10-120Å.

538.221:539.23 3799
The Influence of the Manufacturing Conditions on the Magnetic Properties of Electro-

lytically Produced Permalloy Films—A. Politycki and H. Gotthard. (*Z. angew. Phys.*, vol. 14, pp. 363-365; June, 1962.)

538.221:539.23:621.318.57 3800
Partial-Switching Processes in Thin Magnetic Films—W. Dietrich. (*IBM J. Res. Dev.*, vol. 6, pp. 368-371; July, 1962.) The partial switching which occurs when rapidly rising field pulses with amplitudes just beyond the rotational threshold are applied to the film, is ascribed to inhomogeneities. An unexpected creep effect is also reported.

538.221:621.318.12 3801
The Stability of Permanent Magnets—H. Vial. (*Elektrotech. Z., Ed. B.*, vol. 14, pp. 467-468; August, 1962.) The demagnetization of alnico and Ba-ferrite permanent magnets due to temperature fluctuations and external fields can be minimized by a process of artificial aging.

538.221:621.318.134 3802
Square-Loop Ferrites containing Cadmium—A. Bragiński, W. Ciastoń, J. Kulikowski, and S. Makolagwa. (*Proc. IEE, Pt. B*, vol. 109, pp. 380-382; September, 1962.) A comparative investigation of Mn ferrites containing Cd and Zn with or without additions of Mg. The preparation of Cd ferrites may be facilitated by applying high oxygen pressure at peak sintering temperature to reduce Cd volatilization.

538.221:621.318.134 3803
The Inclusion of α -Fe₂O₃ in Mn Ferrite Single Crystals and its Influence on Dislocation Density—H. Burger and I. Hanke. (*Z. angew. Phys.*, vol. 14, pp. 40-43; January, 1962.)

538.221:621.318.134:538.569.4 3804
Observation of Domain Wall Resonances in Ferrimagnetic Oxides—E. L. Boyd, J. I. Budnick, L. J. Bruner, and R. J. Blume. (*J. Appl. Phys.*, vol. 33, pp. 2484-2485; August, 1962.)

538.222:546.824-31 3805
A Study by Static Magnetic Techniques of Rutile Single Crystals after Various External Treatments—K. G. Srivastava. (*Phys. Lett.*, vol. 2, pp. 143-144; September, 1962.) A note on the effects of thermal quenching, electron bombardment and X rays.

539.23:546.48'221 3806
Rectification and Space-Charge-Limited Currents in CdS Films—J. Dresner and F. V. Shalleross. (*Solid-State Electronics*, vol. 5, pp. 205-210; July/August, 1962.) The variation of electrical properties with different methods of preparation is discussed.

539.232 3807
A Study of the Structure of Evaporated Lithium Fluoride—D. S. Campbell, D. J. Stirling, and H. Blackburn. (*Phil. Mag.*, vol. 7, pp. 1099-1116; July, 1962.) A report of an investigation of the effect of different evaporation rates on the initial stages of growth of a non-metallic material. LiF deposits on carbon are in the form of discrete crystalline islands.

548.0:537.311.33 3808
Use of Modified Free-Energy Theorems to Predict Equilibrium Growing and Etching Shapes—R. J. Jaccodine. (*J. Appl. Phys.*, vol. 33, pp. 2643-2647; August, 1962.) A construction for equilibrium shape of an etching crystal gives results in good agreement with those obtained by experiment.

621.357.7:539.23 3809
Method for Controlling Multicomponent Sputtering—W. R. Sinclair and F. G. Peters. (*Rev. Sci. Instr.*, vol. 33, pp. 744-746; July, 1962.) A method for sputtering simultaneously from electrically independent electrodes is described.

MATHEMATICS

517.432.1:621.317:621.372.5 3810
The Determination of the Input Function for Linear Systems with Known (Measured) Output Function—E. G. Woschni. (*Hochfrequenz und Elektroak.*, vol. 71, pp. 110-114; June, 1962.) Application of operational calculus to the problem of determining the true variation of a measured quantity from the output function distorted by the transfer system quadrupoles.

517.941:621.391.812.63 3811
The Nonsingular Embedding of Transition Processes within a More General Framework of Coupled Variables—Heading. (See 3837.)

MEASUREMENTS AND TEST GEAR

621.3.018.41(083.74):621.375.9:538.569.4 3812
Ammonia Maser on the 3.2 Line as a Frequency Standard: Part 1—K. Shimoda and N. Kohno. (*Jap. J. Appl. Phys.*, vol. 1, pp. 5-13; July, 1962.) Frequency stability within a few parts in 10¹⁰ at 24 Gc is reported.

621.3.018.41(083.74):621.396.712 3813
World-Wide V.L.F. Standard-Frequency and Time-Signal Broadcasting—A. D. Watt, R. W. Plush, W. W. Brown, and A. H. Morgan. (*J. Res. NBS*, vol. 65D, pp. 617-627; November/December, 1961.) Limitations in the stability of received signals are discussed, including path phase distortion, carrier-to-noise and envelope delay variations, with regard to the accuracy of clock synchronization and frequency calibrations.

621.317.3:538.632 3814
A New Technique for Measuring Hall-Effect Coefficient—H. Hamer. (*Semiconductor Prod.*, vol. 5, pp. 35-36; June, 1962.) A general description of a method which discriminates strongly against ohmic drop and stray induced potentials. An alternating magnetic field and constant current are used.

621.317.331:537.311.33 3815
Four-Point Probe for Measuring the Resistivity of Small Samples—J. K. Kennedy. (*Rev. Sci. Instr.*, vol. 33, pp. 773-775; July, 1962.) A device is described based on the method originally described by Valdes (1502 of 1954) but modified to be more suitable for small samples.

621.317.335.3 3816
A Method of Measuring Static Dielectric Constant especially of Materials with Long Relaxation Times—L. N. Clarke. (*Aust. J. Appl. Sci.*, vol. 13, pp. 81-88; June, 1962.) The method is based on the measurement of charge using a high-gain dc amplifier connected as an integrator. The measurement time can be extended to several hours by using the integrator as a null detector of charge. Typical curves of charge and discharge as a function of time are given for four types of capacitor.

621.317.335.3:621.372.413 3817
Modified Method of Measuring Dielectric Constants—J. K. Sinha. (*J. Inst. Telecommun. Engrs., India*, vol. 8, pp. 93-102; March, 1962.) A modification to a method developed by Sinha and Brown (664 of 1961) permits measurements to be made on samples of length $<\lambda/2$.

621.317.337:621.372.413 3818
A Technique for the Measurement of Q —J. K. Sinha and S. Sundaram. (*J. Inst. Telecommun. Engrs., India*, vol. 8, pp. 79-82; March, 1962.) Consistent and reliable measurements of Q factors of the order of 20000 have been made on X-band cavity resonators by observation at an IF of about 30 Mc.

621.317.352.029.6:621.372.852.3 3819
An Absolute Microwave Attenuator—P. F. Mariner. (*Proc. IEE, Pt. B*, vol. 109, pp. 415-

419; September, 1962.) The construction and method of operation of a rotary attenuator are described, and the errors that may arise in its use are analysed. Results are given for a 3-cm- λ attenuator which has been compared with a precision piston attenuator operating at 60 Mc.

621.317.382:538.63 3820
Sensitivity of a Magnetoresistance Wattmeter—S. Kataoka. (*Proc. IRE (Correspondence)*, vol. 50, pp. 1849-1850; August, 1962.) A comparison is made between the magnetoresistance device (1657 of May) and a Hall-effect wattmeter.

621.317.44 3821
Highly Sensitive Static Magnetic Field Detector—D. J. Dumin. (*Proc. IRE (Correspondence)*, vol. 50, p. 1825; August, 1962.) The operation of the detector described is based on the diamagnetic properties of superconductors.

621.317.7:535.215 3822
Apparatus for Measuring the Temperature Dependence of Photo-Hall Effects in High-Resistivity Photoconductors—H. E. MacDonald and R. H. Bube. (*Rev. Sci. Instr.*, vol. 33, pp. 721-723; July, 1962.) A description of apparatus for the measurement of the Hall effect in illuminated samples with mobility as low as 0.1 cm²/v. sec, over the temperature range 77-450°K.

621.317.7:621.391.822 3823
Standard Noise Sources—P. A. H. Hart. (*Philips Tech. Rev.*, vol. 23, pp. 293-309; July, 1962.) Resistor, saturated-diode and gas-discharge sources are discussed. The most suitable frequency ranges for each type are considered.

621.317.733.029.64:538.569.4 3824
A Microwave Bridge with Superheterodyne Reception for Electron-Spin-Resonance Measurements in the X Band—H. Seidal. (*Z. angew. Phys.*, vol. 14, pp. 21-22; January, 1962.)

OTHER APPLICATIONS OF RADIO AND ELECTRONICS

621.362:621.387 3825
Extended-Space-Charge Theory in Low-Pressure Thermionic Converters—R. G. McIntyre. (*J. Appl. Phys.*, vol. 33, pp. 2485-2489; August, 1962.) An analysis is given of the low-pressure Cs-filled plasma diode.

621.362:621.387 3826
Origin of the Oscillations in a Low-Pressure Thermionic Converter—P. Mazur. (*J. Appl. Phys.*, vol. 33, p. 2653; August, 1962.) By integrating the Vlasov equation, it is shown that the stationary states previously believed to be the cause of small current oscillations, do not exist in just that region of the I/V characteristic where the oscillations are observed.

621.362:621.387.143 3827
The Direct Conversion of Heat into Electrical Energy by means of Rare-Gas-Filled Thermionic Valves—W. Bloss. (*Z. angew. Phys.*, vol. 14, pp. 1-9; January, 1962.) Description of a thermionic converter based on the plasmatron principle [e.g., 1108 of March (Pfender and Bloss)].

621.375.9:621.372.44:621.313.13 3828
Parametric Machines—D. J. Hamrahan; H. E. Stockman. (*Proc. IRE (Correspondence)*, vol. 50, pp. 1844-1845; August, 1962.) Comment on 2751 of 1961 and author's reply.

621.385.833 3829
An Arrangement for the Magnetization of Objects in Electron Microscopes—E. Fuchs and W. Liesk. (*Optik. Stuttgart*, vol. 19, pp. 307-310; June, 1962.) The method described facilitates the investigation of magnetic struc-

tures in the presence of external fields and incorporates a system of automatic compensation for the image movement due to the magnetic field changes.

621.385.833 **3830**
Display Method for the Investigation of Ceramic Surfaces by Electron Microscope—E. Sterk, M. Tardos, and V. Szántó. (*Naturwiss.*, vol. 49, pp. 277-278; June, 1962.) The method described is suitable for the investigation of the fine structure of ferrite surfaces.

621.385.833 **3831**
The Optimum Resolving Power of the Electron Microscope—M. L. De. (*Naturwiss.*, vol. 49, pp. 296-297; July, 1962. In English.) A modified expression for minimum spherical aberration is discussed.

621.385.833 **3832**
Change of the Electron-Microscope Image Contrast at the Transition Amorphous-Crystalline and Liquid-Crystalline—L. Reimer. (*Naturwiss.*, vol. 49, pp. 297-298; July, 1962.) Possible applications of the contrast changes are suggested with reference to results obtained with In.

621.387.462:537.311.33 **3833**
Semiconductor Nuclear Radiation Detectors—G. Dearnaley. (*J. Brit. IRE*, vol. 24, pp. 153-170; August, 1962.) The mode of operation, methods of preparation and characteristics of various detectors are described, together with the requirements for pulse amplification. 70 references.

PROPAGATION OF WAVES

621.391.812.3 **3834**
Transit-Time Fluctuations of Waves—R. S. Brown. (*J. Atmos. Terr. Phys.*, vol. 24, pp. 669-671; August, 1962.) An evaluation of the mean square value of the fluctuation of transit time about the average caused by inhomogeneities of refractive index.

621.391.812.623 **3835**
Obstacle Gain and Shadow Loss—G. H. Grenier. (*Microwave J.*, vol. 5, pp. 60-69; July, 1962.) A practical method of determining path losses to within several db is given, using simple "knife-edge" analysis as the first approach.

621.391.812.63 **3836**
Study of Radio Wave Propagation in Sweep-Frequency Pulse Transmission Tests in Japan—Y. Aono. (*J. Radio Res. Labs, Japan*, vol. 9, pp. 125-200; March, 1962.) The experimental procedure, observational results and analysis for propagation paths of 1090 and 1840 km are given. Vertical-incidence soundings were made simultaneously with the oblique measurements.

621.391.812.63:517.941 **3837**
The Nonsingular Embedding of Transition Processes within a More General Framework of Coupled Variables—J. Heading. (*J. Res. NBS*, vol. 65D, pp. 595-616; November/December, 1961.) Mathematical treatment of reflection and coupling processes for plane EM waves propagated in an inhomogeneous horizontally stratified anisotropic ionosphere.

621.391.812.63:551.510.535:523.75 **3838**
The Effect of a Solar Flare on the Frequency of High-Frequency Ground Back-Scatter—G. H. Barry and P. R. Widess. (*J. Geophys. Res.*, vol. 67, pp. 2707-2714; July, 1962.) Fixed-azimuth back-scatter radar equipment operating at 25 Mc was used to investigate the ionospheric effects of a Glass 2 flare. The observed sudden frequency shift of ground back-scatter is attributed to a rapid change in ionization density in a nondeviative layer 40-100 km thick.

621.391.812.63.029.45/51 **3839**
Ionospheric Reflection Processes for Long Radio Waves: Part 3—B. S. Westcott. (*J. Atmos. Terr. Phys.*, vol. 24, pp. 701-713; August, 1962.) Formulas derived earlier are applied to the case of a sech² ionospheric profile, and the results are compared with those previously obtained for an exponential profile. Part 2: 3497 of October.

621.391.812.63.029.45 **3840**
Attenuation Coefficients for Propagation at Very Low Frequencies (VLF) during a Sudden Ionospheric Disturbance (S.I.D.)—E. T. Pierce. (*J. Res. NBS*, vol. 65D, pp. 543-546; November/December, 1961.) Atmospheric-noise records for the frequency range 3.5-50 kc are analyzed. The onset of sid conditions has little effect on attenuation between about 12 and 20 kc, but causes a decrease in attenuation above this range and a pronounced increase below 12 kc. An improved atmospheric noise recorder is proposed which is capable of discriminating between source effects and propagation influences.

621.391.812.63.029.45 **3841**
Magneto-ionic Duct Propagation Time (Whistler Mode) versus Geomagnetic Latitude at 4 kc/s—C. V. Greenman. (*Proc. IRE*, vol. 50, p. 1852; August, 1962.) Simplified analysis showing that a graph of the propagation time as a function of geomagnetic latitude of origin may have a flat portion or one of negative slope.

621.391.812.631 **3842**
Very-Low-Frequency Effects from the November 10, 1961, Polar-Cap Absorption Event—H. F. Bates. (*J. Geophys. Res.*, vol. 67, pp. 2745-2751; July, 1962.) Changes in amplitude and phase are observed on the polar VLF transmission from Rugby, U.K., to College, Alaska.

621.391.814.2 **3843**
Propagation of Electromagnetic Step Functions over a Conducting Medium—P. E. Mijnaerds. (*J. Appl. Phys.*, vol. 33, pp. 2556-2564; August, 1962.) "A theoretical treatment is presented of the behaviour of various components of the electromagnetic field generated by a horizontal electric dipole, embedded in a homogeneous conducting half-space, and excited by a step-function current."

RECEPTION

621.396.621:534.76 **3844**
Simple Decoders (Adaptors) for Use with the F.C.C. Stereo V.H.F. Broadcasting System—G. D. Browne. (*Mullard Tech. Commun.*, vol. 6, pp. 360-367; August, 1962.) Two simple types of decoder operating from the discriminator of a normal FM receiver are described in which low- and high-pass filters are avoided. For a similar description see *Wireless World*, vol. 68, pp. 487-491; October, 1962.

621.396.666:621.396.65 **3845**
A Method of I.F. Switching for a Microwave Diversity System—D. R. Bester. (*J. Brit. IRE*, vol. 24, pp. 171-179; August, 1962.) High-speed diode switches operating at the IF of 70 Mc are used.

621.391.8:621.372.632:621.372.44 **3846**
Parametric-Converter Performance on a Beyond-the-Horizon Microwave Link—J. Harvey. (*Ilec. Commun.*, vol. 37, pp. 230-237; 1962.) A report of comparative measurements on noise and error rate over a quadruple-diversity link of the White Alice system equipped with two parametric and two normal receivers.

621.391.812.3 **3847**
Distribution of Echo Amplitudes from an Undulating Surface—J. D. Whitehead. (*J.*

Atmos. Terr. Phys., vol. 24, pp. 715-721; August, 1962.) The amplitude distribution is calculated for waves reflected at normal incidence from a reflector whose curvature has a Gaussian distribution. Application to SW radio communication is briefly discussed.

621.391.82:551.594.6 **3848**
On the Spectrum of Terrestrial Radio Noise at Extremely Low Frequencies—H. R. Raemer. (*J. Res. NBS*, vol. 65D, pp. 581-593; November/December, 1961.) A theory of the radio-noise frequency spectrum is presented and the results are compared with those of measurements of the spectrum given in 688 of 1961 (Balser and Wagner). See also 2985 of 1961.

621.391.821 **3849**
Reliability of Atmospheric Radio Noise Predictions—J. R. Herman. (*J. Res. NBS*, vol. 65D, pp. 565-574; November/December, 1961.) Measured noise values at five frequencies between 0.013 and 10 Mc obtained at four measuring stations are compared with C.C.I.R. predictions. Reasons for discrepancies are discussed.

621.391.821 **3850**
Atmospheric Radio Noise Studies based on Amplitude-Probability Measurements at Slough, England during the International Geophysical Year—C. Clarke. (*Proc. IEE, Pt. B*, vol. 109, pp. 393-404; September, 1962.) Measurements of amplitude-probability distributions in a power bandwidth of 370 cps are presented for frequencies of 24 and 135 kc, and 11 and 20 Mc. Diurnal and seasonal variations of noise power and average value of the noise envelope are derived, and measured values of noise power are compared with C.C.I.R. predictions.

STATIONS AND COMMUNICATION SYSTEMS

621.396.43:551.507.362.2 **3851**
An Interconnecting Telecommunication Network using Stationary Satellites—P. Deiman and P. Chavance. (*Rev. tech. Comp. franç. Thomson-Houston*, pp. 7-42; June, 1962.) Specially designed modulation techniques are suggested to simplify the ground stations required.

621.396.65.029.64 **3852**
Research on Radio Relay Systems having a Very High Transmission Capacity (2700 Telephone Channels or the Equivalent)—F. Carassa. (*Alta Frequenza*, vol. 31, pp. 82-95; February, 1962. In English.) Report on design studies and experimental investigations for a telephony and television relay system operating at 6 Gc.

621.396.712:621.3.018.41(083.74) **3853**
World-Wide V.L.F. Standard-Frequency and Time-Signal Broadcasting—Watt, Plush, Brown, and Morgan. (See 3813.)

621.396.74.029.62(43) **3854**
V.H.F. Transmitters in the German Federal Republic and the Soviet-Occupied Zone—(*Rundfunktech. Mitt.*, vol. 6, pp. 176-179; June, 1962.) Lists and a map of transmitter locations give the position as at April, 1962. For similar data on short-wave and long- and medium-wave transmitters see *ibid.*, vol. 6, pp. 180-184; June, 1962.

621.396.97:534.76 **3855**
Stereophonic Broadcasting Systems—G. D. Browne. (*Mullard Tech. Commun.*, vol. 6, pp. 346-359; August, 1962.)
Part 1—The Mullard System (pp. 346-354).
Part 2—The F.C.C. System (pp. 355-359).

SUBSIDIARY APPARATUS

- 621.314.63 3856
Impedance and Rectifying Characteristics of Silicon p - n Junctions with Surface Inversion Layer—O. Jäntschi. (*Solid-State Electronics*, vol. 5, pp. 219-259; July/August, 1962. In German.) Impedance measurements have been made on three rectifiers prepared from p -type material of different resistivity. The thickness of the space-charge region and the channel conductivity are determined from the equivalent circuit, and the total surface charge and the surface potential are calculated.

TELEVISION AND PHOTO-TELEGRAPHY

- 621.397.62:621.396.67:621.396.621.22 3857
Communal Aerials for Television Reception in Adjacent Channels—Licht. (See 3576.)
- 621.397.7(43) 3858
The Television Networks of the German Federal Republic and the Soviet-Occupied Zone—(*Rundfunktech. Mitt.*, vol. 6, pp. 157-175; June, 1962.) Tabulated data on television transmitters as at April 1, 1962, with maps showing their location and that of television links.

TUBES AND THERMIONICS

- 621.382:539.12.04 3859
Radiation Effects in Semiconductor Devices—J. W. Easley. (*Nucleonics*, vol. 20, pp. 51-56; July, 1962.) The effects of radiation described in 3752 after the characteristics of semiconductor devices. Illustrative examples are given.
- 621.382:539.23 3860
Current Voltage Characteristic of Tunnel Junctions—H. P. Knauss and R. A. Breslow. (*Proc. IRE (Correspondence)*, vol. 50, p. 1834; August, 1962.) Note on a hysteresis effect in the I/V characteristics observed in an $\text{Al-As}_2\text{O}_3\text{-Cu}$ junction at room temperature.
- 621.382.2 3861
The Characteristics of a Semiconductor p - n Junction at High Current Densities—E. Rocher. (*Z. angew. Phys.*, vol. 14, pp. 347-352; June, 1962.) The static and dynamic characteristics of a Ge diode are obtained and the results analysed with reference to Stafeev's theory (e.g., 1417 of 1960). At high current levels the forward inductance is suddenly reduced which results in a negative-resistance section of the dynamic characteristic.
- 621.382.23 3862
A Two-Term Analytical Approximation of Tunnel-Diode Static Characteristics—A. Ferenczi and W. H. Ko. (*Proc. IRE*, vol. 50, pp. 1852-1853; August, 1962.) A simple two-term exponential approximation is given and its accuracy is determined in comparison with actual characteristics.
- 621.382.23 3863
Simple Method for Calculating the Tunneling Current of an Esaki Diode—J. Karlovský. (*Phys. Rev.*, vol. 127, p. 419; July, 1962.) Assuming that the distances between the Fermi level and the band edges E_1 and E_2 on both sides of the junction do not exceed $2kT$, the Fermi function is approximated by a straight line.
- 621.382.23 3864
Reversible Degradation Effects in GaSb Tunnel Diodes—W. N. Carr. (*Solid-State Electronics*, vol. 5, pp. 261-263; July/August, 1962.) Degradation effects are measured and discussed in relation to a theory of diffusion of impurities [TRANS. ON ELECTRON DEVICES, vol. ED-8, p. 428; September, 1961. (Gold and Weisberg)].

- 621.382.23 3865
InSb Diodes with Normal Barrier Capacitance—M. T. Minamoto and C. M. Allen. (*Solid-State Electronics*, vol. 5, pp. 263-266; July/August, 1962.) Results are presented which show better agreement with normal theory than those of Lee and Kaminsky (622 of 1961).
- 621.382.23 3866
Pressure Dependence of the Characteristics of InSb Esaki Diode—Y. Ōmura and M. Wakatsuki. (*J. Phys. Soc. Japan*, vol. 17, pp. 1207-1208; July, 1962.) Characteristics of InSb tunnel diodes are measured at hydrostatic pressures up to 11000 kg cm^{-2} .
- 621.382.23:537.533.7 3867
Electron-Beam Microanalysis of Germanium Tunnel Diodes—M. I. Nathan and S. H. Moll. (*IBM J. Res. Dev.*, vol. 6, pp. 375-377; July, 1962.) Small regions of solid specimens are excited by a finely focused beam of high-energy electrons. An X-ray spectrometer is used to observe the characteristic emission lines of the atoms in the sample. Results of a quantitative analysis of impurities in tunnel diodes are given.
- 621.382.23:539.12.04 3868
Neutron Irradiation of Zener Diodes—J. K. D. Verma. (*J. Phys. Soc. Japan*, vol. 17, p. 1203; July, 1962.) Irradiation apparently augmented both field emission and avalanche breakdown effects. The changes produced in the diode characteristic are illustrated.
- 621.382.23:621.318.57 3869
A Broad-Band Ku Crystal-Diode Switch—K. W. Beck and J. J. Rowley. (*Proc. IRE (Correspondence)*, vol. 50, pp. 1847-1848; August, 1962.) The switch described can operate in the frequency range 12-17 Gc with a minimum bandwidth of 2 Gc.
- 621.382.3 3870
The Static Characteristics of Transistors—E. Köhler and H. G. Schulz. (*Nachricht.*, vol. 12, pp. 168-172, 218-221, and 266-271; May-July, 1962.) Summary of the main results of theoretical and experimental investigations of the static characteristics of transistors, including operation outside the normal working range.
- 621.382.3:621.317.61 3871
The Measurement of the Characteristics of Transistors: Parts 1-3—R. Paul. (*Nachricht.*, vol. 12, pp. 163-167, 213-217, and 260-265; May-July, 1962.) A series of papers reviewing measurement techniques, with numerous references.
- 621.382.323 3872
Thermal Noise in Field-Effect Transistors—A. van der Ziel. (*Proc. IRE*, vol. 50, pp. 1808-1812; August, 1962.) The noise figure of field-effect transistors is governed by thermal noise of the conducting channel. Expressions are derived for the equivalent output noise generator and for the equivalent noise resistance of the device.
- 621.382.323 3873
Silicon Field-Effect Transistor with Internal Epitaxial Channel—G. C. Onodera, W. J. Corrigan, and R. M. Warner, Jr. (*Proc. IRE (Correspondence)*, vol. 50, p. 1824; August, 1962.) A technique for the fabrication of field-effect devices is described which meets the requirements of good reproducibility.
- 621.382.333.3 3874
Dynatron-Type Negative Resistance Observed in the Collector-Voltage Saturation Region of the Junction Transistor—O. Nakahara. (*Jap. J. Appl. Phys.*, vol. 1, pp. 30-40; July, 1962.) Experimental results are compared with theoretical calculations, assuming appreciable conductivity modulation of the

base resistance in the saturation region, and with similar phenomena in field-effect transistors.

- 621.382.333.4 3875
Inductance from a Field-Effect Tetrode—P. J. Etter and B. L. H. Wilson. (*Proc. IRE (Correspondence)*, vol. 50, pp. 1828-1829; August, 1962.) Bias conditions are proposed for a field-effect tetrode acting as gyrator to simulate an inductance of very high Q value. A suitable design for the gyrator is given.
- 621.383.292 3876
Continuous-Channel Electron Multiplier—G. W. Goodrich and W. C. Wiley. (*Rev. Sci. Instr.*, vol. 33, pp. 761-762; July, 1962.) Electron multiplication by secondary emission is achieved in small tubular dynodes and used to amplify very weak currents.
- 621.383.42:621.311.69 3877
The Efficiency of Selenium Photocells at Low Illumination Levels—W. Dürr. (*Z. angew. Phys.*, vol. 14, pp. 88-91; February, 1962.) Comparative measurements of efficiency for sunlight and for monochromatic light of $\lambda = 577 \text{ m}\mu$ on Se and Si photocells.
- 621.383.5 3878
Storage of Photoelectric Signals in n - p Junctions—G. A. Boutry, F. Desvignes, and M. Robert. (*J. Phys. Radium*, vol. 23, pp. 262-264; April, 1962.) A theoretical and experimental note on biasing effects at low temperature with application to the observation of extremely weak photoelectric signals ($\sim 10^{14} \text{ A}$) and the realization of an infrared scanning tube.
- 621.383.5 3879
Silicon Surface-Barrier Photocells—E. Ahlstrom and W. W. Gärtner. (*J. Appl. Phys.*, vol. 3, pp. 2602-2606; August, 1962.) Data are given on photocurrent as a function of light intensity, reverse-bias voltage and temperature, and on open-circuit photovoltage as a function of light intensity, wavelength and temperature.
- 621.383.52 3880
A High-Speed Point-Contact Photodiode—L. U. Kibler. (*Proc. IRE*, vol. 50, pp. 1834-1835; August, 1962.) Brief description of a Ge p - i - n junction photodetector suitable for wide-band operation at frequencies up to 50 Gc. Tests were carried out with a He-Ne gas maser.
- 621.383.52:621.391.64 3881
New Infrared-Generating Diode Transmits Television over Modulated Light Ray—T. Maguire. (*Electronics*, vol. 35, pp. 24-25; July, 1962.) Zn-diffused GaAs diodes can be used to transmit television signals, although the output is not coherent.
- 621.385.032.212.3 3882
The Construction of a Stable Field Cathode—Z. Hájek and L. Eckertová. (*Naturwiss.*, vol. 49, p. 201; May, 1962.) Stable currents and repeatable results were achieved with cold cathodes of the type $\text{Al-Al}_2\text{O}_3$ -metal (e.g., Ag, Au, Pt). The requisite conditions for such operation are summarized and advantages over the porous type of cathode [e.g., 350 of 1960 (Skelleet, et al.)] are mentioned.
- 621.385.032.213.13 3883
The Space-Charge-Neutralized Hollow Cathode—A. L. Eichenbaum. (*RCR Rev.*, vol. 23, pp. 230-245; June, 1962.) Cs vapour in an electron-emissive cylinder can be used to produce either electron beams of high current density at moderate temperatures or beams of moderate density at low temperatures.
- 621.385.032.213.23 3884
Role of Carburization in the Suppression of Emission from Barium-Activated Tungsten

- and Molybdenum Surfaces**—E. S. Rittner and R. Levi. (*J. Appl. Phys.*, vol. 33, pp. 2336–2340; July, 1962.) Emission inhibition due to carburization [see 3977 of 1961 (Levi and Rittner)] results from greatly reduced activator coverage of the surface of the carbide relative to that of the metal, because of much weaker adsorption forces.
- 621.385.032.213.23** 3885
Field-Emission Studies on Kinetics of Barium Oxide on Tungsten—K. Noga. (*J. phys. Soc. Japan*, vol. 17, pp. 950–961; June, 1962.) Studies of the absorption of BaO on W are reported. The mean dipole moment of the adsorbed molecule is estimated. At temperatures above 800°C the oxide reacts chemically with W with an activation energy of approximately 3.3 ev.
- 621.385.2:537.24** 3886
Microparticles Diodes—C. Maisonnier and M. Haegi. (*J. Appl. Phys.*, vol. 33, pp. 2474–2478; August, 1962.) The motion of a group of small conducting spheres located between two parallel plates is investigated theoretically for space-charge-limited flow and a more realistic model is proposed. Experimental apparatus used to check theoretical predictions is described.
- 621.385.2.029.6** 3887
Measurements of the Frequency Dependence of the Admittance of Plane-Parallel Space-Charge Diodes in the Transit-Time Region—F. Seifert. (*Nachricht. Z.*, vol. 15, pp. 263–266; June, 1962.) Measurements are carried out at frequencies in the range 300–600 Mc on modified disk-seal diodes with cathode/anode spacings of 1.45 and 2 mm.
- 621.385.3.012:681.142** 3888
The Calculation of Accurate Triode Characteristics using a Modern High-Speed Computer—O. H. Schede, Sr. (*RCA Rev.*, vol. 23, pp. 246–284; June, 1962.) The classical space-current solution is shown to be inadequate for modern close-spaced thermionic valves. A computer is programmed to calculate complete I/V characteristics from basic input data, with corrections for space-charge effects and initial electron velocities.
- 621.385.6** 3889
Electrokinetic Vortex Beams—H. W. König. (*Arch. elekt. Übertragung*, vol. 16, pp. 271–282; June, 1962.) The characteristics of vortex beams are derived theoretically with particular emphasis on energy relations. See also 1099 of March (Riedler).
- 621.385.6:537.533** 3890
Axial Quasi-Brillouin Streams—M. H. Miller. (*J. Appl. Phys.*, vol. 33, pp. 2247–2248; July, 1962.) "A non-laminar model for axially uniform electron streams is postulated and conditions for which the model is consistent with physical requirements are derived. The character of the current density profiles permitted by the model are discussed." For analysis of rectilinear flow see 330 of January.
- 621.385.6:621.391.322** 3891
Some Results from the Measurements of the Noise Parameters in Electron Beam—S. Saito and Y. Fujii. (*Proc. IRE*, vol. 50, pp. 1706–1707; July, 1962.) Description of the experimental determination of these parameters by a direct method of measurement [1067 of 1969 (Saito)].
- 621.385.6.032.269.1** 3892
Electron Guns for Forming Solid Beams of High Perveance and High Convergence—R. D. Frost, O. T. Purl, and H. R. Johnson. (*Proc. IRE*, vol. 50, pp. 1800–1807; August, 1962.) Two methods of design are described and data are given of three types of electron gun developed by these techniques.
- 621.385.62:537.13** 3893
A 5-Mc/s Klystron Amplifier using Positive Ions—M. R. Gavin, K. Chandra, and L. J. Lloyd. (*Nature*, vol. 195, p. 988; September, 1962.) Certain experimental difficulties encountered in investigating design principles of microwave klystrons are avoided by substituting positive ions for electrons and operating at a much lower frequency.
- 621.385.62.3** 3894
Optimum R.F. Field Distribution of Monotron Cavities—K. Blotekjaer and B. Grung. (*J. Electronics and Control*, vol. 12, pp. 441–459; June, 1962.) Mathematical analysis relating to the design of monotron oscillators for maximum negative small-signal electronic conductance. The optimum field distribution is shown in a number of graphs for various d.c. gap transit angles and space-charge densities.
- 621.385.623.2** 3895
Optimization of R.F. Voltage Amplitudes and Gap Spacing of Generalized Floating-Drift-Tube Oscillators—K. Blotekjaer. (*J. Electronics and Control*, vol. 12, pp. 461–499; June, 1962.) A detailed analysis of a monotron oscillator with an interaction region comprising a number of narrow gaps separated by drift tubes. The conditions for maximum conversion efficiency are determined.
- 621.385.624** 3896
Klystron Frequency Multipliers: Effect of D.C. Velocity Spread on Performance—L. Solymar and P. V. Schefer. (*Electronic Tech.*, vol. 39, pp. 362–364; September, 1962.) A theoretical treatment is given based on large-signal ballistic theory applied to a model consisting of two discrete electron beams.
- 621.385.63** 3897
The Beam Miser—a Unique Depressed Collector for Crossed-Field Travelling-Wave Tubes—J. M. Osepchuk. (*Microwave J.*, vol. 5, pp. 75–78; July, 1962.) A 30 per cent increase in the power output of standard M-type backward-wave oscillators has been achieved by the addition of a collector internally connected to the cathode so as to reduce the anode current for a given beam current.
- 621.385.63** 3898
Power Carried by the Helitron Waves on an E-Type Filamentary Electron Beam—I. Sakuraba. (*Proc. IRE*, vol. 50, p. 1839; August, 1962.)
- 621.385.63:621.375.9:621.372.44** 3899
Partition Effects in Transverse Electron-Beam Waves—P. A. H. Hart. (*J. Appl. Phys.*, vol. 33, pp. 2401–2408; August, 1962.) Theory is presented concerning the attenuation of the original beam waves, the fast, the slow, and two synchronous waves, and the generation of noise waves if part of the beam is intercepted. See also 1833 of 1960 (Siegmant).
- 621.385.63:621.375.9:621.372.44** 3900
Transverse Electron-Beam Noise Described by Filamentary Beam Parameters—K. Blotekjaer. (*J. Appl. Phys.*, vol. 33, pp. 2409–2414; August, 1962.) The equivalence of the physical noisy beam and the theoretically equivalent modulated filamentary beam is demonstrated. The frequency components of the equivalent filamentary beam modulation are calculated.
- 621.385.63:621.375.9:621.372.44** 3901
Graphical Expressions of Synchronous Conditions in the Transverse-Type Electron-Beam Parametric Amplifier—K. Kakizaki. (*Proc. IRE (Correspondence)*, vol. 50, pp. 1850–1851; August, 1962.)
- 621.385.64** 3902
Electron Trajectories in a Magnetron—C. G. Lehr, J. W. Lotus, I. Silberman, and R. C. Gunther. (*J. Electronics and Control*, vol. 13, pp. 89–122; August, 1962.) The problem of electron trajectories in an oscillating magnetron was investigated by numerical analysis using Hartree's method of self-consistent fields. The trajectories so obtained do not converge to a self-consistent result until the requirement of space-charge-limited cathode emission is dropped.
- 621.385.832** 3903
Charging Processes due to Returning Secondary Electrons in Homogeneous Storage Layers of Charge Storage Tubes—W. Harth. (*Z. angew. Phys.*, vol. 14, pp. 12–20; January, 1962.) Investigation of the charging mechanism using a double-beam storage tube with a mesh-type collector grid at a variable distance from the storage target. The effect on the resolving power of storage tubes is discussed.
- 621.385.832** 3904
The Deflection Errors of Cylindrical Electrostatic Simultaneous Deflection Systems—F. Schäff, W. Harth, and E. Dommaschek. (*Z. angew. Phys.*, vol. 14, pp. 507–512; August, 1962.) The deflection characteristics and aberrations of a cylindrical "deflection" system [See e.g., 2591 of 1956 (Schlesinger)] are calculated.
- 621.387:621.362** 3905
Extended-Space-Charge Theory in Low-Pressure Thermionic Converters—McIntyre. (See 3825.)
- 621.387:621.362** 3906
Origin of the Oscillations in a Low-Pressure Thermionic Converter—Mazur. (See 3826.)
- 621.387.143:621.362** 3907
The Direct Conversion of Heat into Electrical Energy by means of Rare-Gas-Filled Thermionic Valves—Bloss. (See 3827.)

MISCELLANEOUS

- 621.39:061.4** 3908
National Radio Show Review.—(*Wireless World*, vol. 68, pp. 475–482; October, 1962.) An analysis of design trends with reference to equipment seen at the exhibition at Ears Court, London, August 22–September 1, 1962.
- 621.396:523.55** 3909
Space Research and Telecommunications—(*Tech. Mitt. PTT*, vol. 40, pp. 250–280; August, 1962.) The text is given of the following papers presented at a convention held in Basle on November 17, 1961:
a) Space Research—M. Golay (pp. 251–257. In French)
b) Plasma Physics—F. Lüdi (pp. 257–268. In German)
c) Maser and Laser: their Physical Principles and Possible Applications—B. Elschner (pp. 268–273. In German).
d) Telecommunications with the Aid of Artificial Earth Satellites—W. Klein (pp. 173–286. In German).

Translations of Russian Technical Literature

Listed below is information on Russian technical literature in electronics and allied fields which is available in the U. S. in the English language. Further inquiries should be directed to the sources listed. In addition, general information on translation programs in the U. S. may be obtained from the Office of Science Information Service, National Science Foundation, Washington 25, D. C., and from the Office of Technical Services, U. S. Department of Commerce, Washington 25, D. C.

PUBLICATION	FREQUENCY	DESCRIPTION	SPONSOR	ORDER FROM:
Acoustics Journal (Akusticheskii Zhurnal)	Quarterly	Complete journal	National Science Foundation—AIP	American Institute of Physics 335 E. 45 St., New York 17, N. Y.
	Monthly	Complete journal	National Science Foundation—MIT	Instrument Society of America 313 Sixth Ave., Pittsburgh 22, Pa.
Automation and Remote Control (Avtomatika i Telemekhanika)	Monthly	Abstracts only		Office of Technical Services U. S. Dept. of Commerce Washington 25, D. C.
Journal of Abstracts, Electrical Engineering (Reserativnyy Zhurnal: Elektronika)	Monthly	Abstracts of Russian and non-Russian literature		Office of Technical Services U. S. Dept. of Commerce Washington 25, D. C.
Journal of Experimental and Theoretical Physics (Zhurnal Eksperimentalnoi i Teoreticheskoi Fiziki)	Monthly	Complete journal	National Science Foundation—AIP	American Institute of Physics 335 E. 45 St., New York 17, N. Y.
Journal of Technical Physics (Zhurnal Technicheskoi Fiziki)	Monthly	Complete journal	National Science Foundation—AIP	American Institute of Physics 335 E. 45 St., New York 17, N. Y.
Proceedings of the USSR Academy of Sciences: Applied Physics Section (Doklady Akademii Nauk SSSR: Otdel Prikladnoi Fiziki)	Bimonthly	Complete journal		Consultants Bureau, Inc. 227 W. 17 St., New York 22, N. Y.
Radio Engineering (Radiotekhnika)	Monthly	Complete journal	National Science Foundation—AIEE	Royer & Roger, Inc. 41 E. 28 St., New York 16, N. Y.
	Monthly	Abstracts only		Office of Technical Services U. S. Dept. of Commerce Washington 25, D. C.
Radio Engineering and Electronics (Radiotekhnika i Elektronika)	Monthly	Complete journal	National Science Foundation—AIEE	Royer & Roger, Inc. 41 E. 28 St., New York 16, N. Y.
	Monthly	Abstracts only		Office of Technical Services U. S. Dept. of Commerce Washington 25, D. C.
Solid-State Physics (Fizika Tverdogo Tela)	Monthly	Complete journal	National Science Foundation—AIP	American Institute of Physics 335 E. 45 St., New York 17, N. Y.
Telecommunications (Elektrosviaz')	Monthly	Complete journal	National Science Foundation—AIEE	Royer & Roger, Inc. 41 E. 28 St., New York 16, N. Y.
	Monthly	Abstracts only		Office of Technical Services U. S. Dept. of Commerce Washington 25, D. C.
Automation Express	10/year	A digest: abstracts, summaries, annotations of various journals		International Physical Index, Inc. 1909 Park Ave., New York 35, N. Y.
Electronics Express	10/year	A digest: abstracts, summaries, annotations of various journals		International Physical Index, Inc. 1909 Park Ave., New York 35, N. Y.
Physics Express	10/year	A digest: abstracts, summaries, annotations of various journals		International Physical Index, Inc. 1909 Park Ave., New York 35, N. Y.
Express Contents of Soviet Journals Currently being Translated into English	Monthly	Advance tables of contents of translated journals		Consultants Bureau, Inc. 227 W. 17 St., New York 22, N. Y.
Technical Translations	Twice a month	Central directory in the U. S. of translations available from all major sources in the U. S.	OTS and Special Libraries Assoc.	Superintendent of Documents U. S. Gov't Printing Office Washington 25, D. C.